STAR
1436

NASA Conference Publication 2331

The 1983 Goddard Space Flight Center Battery Workshop

(NASA-CP-2331) THE 1983 GODDARD SPACE FLIGHT CENTER BATTERY WORKSHOP (NASA) 548 p HC A23/MF A01 CSCL 10C
N84-33668 THRU N84-33704
Unclas
G3/33 20531

Proceedings of a workshop held at
NASA Goddard Space Flight Center
Greenbelt, Maryland
November 15-17, 1983

NASA

NASA Conference Publication 2331

The 1983 Goddard Space Flight Center Battery Workshop

D. Baer and G. Morrow, *Editors*
Goddard Space Flight Center
Greenbelt, Maryland

Proceedings of a workshop held at
NASA Goddard Space Flight Center
Greenbelt, Maryland
November 15–17, 1983

NASA
National Aeronautics
and Space Administration

Scientific and Technical
Information Branch

1984

PREFACE

This document contains the proceedings of the 16th Annual Battery Workshop held at Goddard Space Flight Center, Greenbelt, Maryland on November 15 to 17, 1983. The Workshop was attended by manufacturers, users and government representatives interested in the latest results in battery technology as they relate to high reliability operations and aerospace use. The subjects covered included Advanced Energy Storage Programs, Lithium Cell Technology, Nickel Cadmium Technology, Testing and Flight Experience, and Metal Hydrogen Technology.

PRECEDING PAGE BLANK NOT FILMED

INTRODUCTION

David Baer
Goddard Space Flight Center

On behalf of George Morrow and myself, I would like to take this opportunity to welcome everyone to the Goddard Space Flight Center. We anticipate that this year's workshop will be beneficial, and we hope everyone enjoys their stay in the Washington area.

This year we have returned to the old format with the exception that we requested a camera-ready copy of the papers be provided for the proceedings. This was done, however, for economic reasons; not because we are making this a more formal conference. We would like to keep this workshop as informal as possible, and we still encourage questions and comments from the audience.

The first session, Advanced Energy Storage Programs, is a new topic which will hopefully give the people in the battery community some insight into the Energy Storage technology being considered for future applications.

Since the first session is relatively short, the second session on Lithium Cell Technology will begin mid-morning and continue for the remainder of our first day. The second day's sessions will address Nickel Cadmium Technology followed by Testing and Flight Experience in the afternoon. The first topic on Thursday morning is Metal Hydrogen.

We hope that this year's workshop is as informative as those in the past and that everyone will participate by asking questions and offering comments.

PRECEDING PAGE BLANK NOT FILMED

PAGE IV INTENTIONALLY BLANK

PREVIOUS BATTERY WORKSHOP PROCEEDINGS PUBLICATIONS

For your information, we have included a list of the acquisition numbers for all Battery Workshop proceedings since 1970. Copies of previous publications are available upon request. The document numbers and the addresses are as follows:

Year	Contents	Document Number
1982	Workshop	83N35230
1981	Workshop	82N20402
1980	Workshop	81N21493
1979	Workshop	80N20820
1978	Workshop	79N28669
1977	Workshop	79N21565
1976	Workshop	77N21550
1975	Workshop	76N24704
1974	Workshop	75N16976
1973	Workshop (1st day)	75N15152
	Workshop (2nd day)	75N17808
1972	Workshop (1st day)	73N21956
	Workshop (2nd day)	73N21957
1971	Workshop (Volume 1)	72N27061
	Workshop (Volume 2)	72N27062
1970	Workshop (1st day)	71N28659
	Workshop (2nd day)	71N28672

NASA may contact:

NASA Scientific and Technical Information Facility (STIF)
P.O. Box 8757
BWI Airport
Baltimore, Md., 21240
(301) 859-5300

All other interested parties contact:

National Technical Information Services (NTIS)
U.S. Department of Commerce
Springfield, Va., 22161
(703) 487-4600

PRECEDING PAGE BLANK NOT FILMED

PAGE vi INTENTIONALLY BLANK

CONTENTS
1983 GSFC Battery Workshop

Co-Chairmen: David A. Baer
George W. Morrow
Goddard Space Flight Center

Page

PREFACE iii

INTRODUCTION v

PREVIOUS BATTERY WORKSHOP PROCEEDINGS PUBLICATIONS vii

SESSION I

TOPIC: ADVANCED ENERGY STORAGE PROGRAMS

Chairman: F.E. Ford, Goddard Space Flight Center 1

INERTIAL ENERGY STORAGE FOR SPACECRAFT
G. Ernest Rodriguez, Goddard Space Flight Center .... 3 ✓D1

DISCUSSION 18

REGENERATIVE HYDROGEN-OXYGEN FUEL CELL-ELECTROLYZER SYSTEMS FOR ORBITAL ENERGY STORAGE
D. W. Sheibley, NASA/Lewis Research Center .... 23 ✓D2
Presentor, O. Gonzalez, NASA/Lewis Research Center

DISCUSSION 39

PRECEDING PAGE BLANK NOT FILMED

PAGE viii INTENTIONALLY BLANK

SESSION II

TOPIC: LITHIUM CELL TECHNOLOGY

Chairman: G. Halpert, Jet Propulsion Laboratory 43

CHARGE CONTROL INVESTIGATION OF RECHARGEABLE LITHIUM CELLS
B. Otzinger, Rockwell International
R. Somoano, Jet Propulsion Laboratory .... 45 ✓D3

DISCUSSION 60

PERFORMANCE AND SAFETY CHARACTERISTICS OF LITHIUM - MOLYBDENUM DISULFIDE CELLS
J. A. Stiles, Moli Energy Limited .... 65 ✓D4

DISCUSSION 83

CHARACTERIZATION OF OPEN CIRCUIT VOLTAGE AND CAPACITY AS A FUNCTION OF TIME
P. W. Krehl and R. C. Stinebring, Wilson Greatbatch, Ltd. .... 87 ✓D5

DISCUSSION 96

CHARACTERIZATION OF GLASS FIBER SEPARATOR MATERIAL FOR LITHIUM BATTERIES
S. Subbarao and H. Frank, Jet Propulsion Laboratory .... 97 ✓D6

DISCUSSION 107

KINETICS OF OPEN CIRCUIT PROCESSES IN UNDISCHARGED Li/SOCl$_2$ CELLS
L. D. Hansen, Brigham Young University
H. Frenks, Jet Propulsion Laboratory .... 109 ✓D7

RELATED STUDIES IN LONG TERM LITHIUM BATTERY STABILITY
R. J. Horning and D. L. Chua, Honeywell Power Sources Center .... 117 ✓D8

DISCUSSION 128

TESTING OF CANDIDATE BATTERIES FOR GLOBAL POSITIONING SYSTEM
J. A. Barnes, F. C. DeBold, R. F. Bis, S. Buchholz, P. Davis, and L. A. Kowalchik, Naval Surface Weapons Center .... 129 ✓D9

DISCUSSION 136

RESERVE Li/SOCl$_2$ BATTERY SAFETY TESTING
C. T. Dils and K. F. Garoutte, Honeywell Power Sources Center . . . . 139 ✓D10

DISCUSSION 148

PERFORMANCE AND SAFETY TO NAVSEA INSTRUCTION 9310.1A OF LITHIUM-THIONYL CHLORIDE RESERVE BATTERIES
J. C. Hall, Atlus Corporation . . . . 149 ✓D11

HIGH RATE DISCHARGE STUDIES OF LI/SO$_2$ BATTERIES
J. A. Barnes, S. Buchholz, R. Frank Bis, F. C. Debold, and L. A. Kowalchik, Naval Surface Weapons Center . . . . 159 ✓D12

DISCUSSION 164

SHUNT DIODE DESIGNS IN Li/CF SHUTTLE BATTERIES
D. Miller and R. Higgins, Eagle-Picher Industries, Inc. . . . . 171 ✓D13

SESSION III

TOPIC: NICKEL CADMIUM TECHNOLOGY

Chairman: C. Badcock, The Aerospace Corporation 183

SEPARATOR QUALIFICATION FOR AEROSPACE NICKEL-CADMIUM CELLS
M. J. Milden, The Aerospace Corporation . . . . 185 ✓D14

DISCUSSION 192

ELECTROCHEMICALLY DEPOSITED CADMIUM ELECTRODE FOR USE IN SEALED Ni-Cd CELLS
W. H. Houston and T. A. Edgar, Eagle-Picher Industries, Inc. . . . . 199 ✓D15

DISCUSSION 220

SECOND PLATEAU VOLTAGE IN NICKEL-CADMIUM CELLS
K. L. Vasanth, Bowie State College . . . . 223 ✓D16

DISCUSSION 240

PREDICTION OF BATTERY LIFE AND BEHAVIOR FROM ANALYSIS OF VOLTAGE DATA
P. P. McDermott, B-K Dynamics, Inc. . . . . 245 ✓D17

DISCUSSION 259

PREDICTION MODEL FOR THE LIFE OF NICKEL-CADMIUM BATTERIES IN GEOSYNCHRONOUS ORBIT SATELLITES
J. H. Engleman, M. B. Zirkes-Falco, R. S. Bogner, and D. F. Pickett, Jr., Hughes Aircraft Company .... 263 ✓D18

DISCUSSION 273

Ni/Cd BATTERY LIFE EXPECTANCY IN GEOSYNCHRONOUS ORBIT
R. J. Broderick, GTE Satellite Corporation .... 275 ✓D19

NICKEL CADMIUM CHARGE CONTROL CONCEPTS
R. M. Sullivan, Johns Hopkins University Applied Physics Laboratory .... 291 ✓D20

DISCUSSION 305

SESSION IV

TOPIC: TESTING AND FLIGHT EXPERIENCE

Chairman: J. Harkness, Naval Surface Weapons Center.... 307

DEEP RECONDITIONING TESTING FOR NEAR EARTH ORBITS
F. E. Betz and W. L. Barnes, Naval Research Laboratory .... 309 ✓D21

DISCUSSION 322

IN-FLIGHT PERFORMANCE OF A SIX AMPERE-HOUR NICKEL-CADMIUM BATTERY IN LOW EARTH ORBIT
J. K. McDermott, Martin Marietta Denver Aerospace .... 325 ✓D22

RCA SATCOM BATTERY IN-ORBIT PERFORMANCE UPDATE AND ACCELERATED LIFE TEST RESULTS
S. J. Gaston and S. F. Schiffer, RCA-Astro-Electronics .... 341 ✓D23

DISCUSSION 350

PERFORMANCE OF THE IUE SPACECRAFT BATTERIES AFTER 70 MONTHS
S. E. Tiller, NASA/Goddard Space Flight Center .... 353 ✓D24

DISCUSSION 365

MANAGEMENT AND PERFORMANCE OF APPLE BATTERY IN HIGH TEMPERATURE ENVIRONMENT
M. S. Suresh, A. Subrahmanyam and B. L. Agrawal, ISRO Satellite Centre .... 367 ✓D25

COMPARISON OF STANDARD AND HEART-PACER TYPE 3RD ELECTRODES IN DESIGN VARIABLE CELLS
G. W. Morrow, NASA/Goddard Space Flight Center . . . . 385 ✓D26

DISCUSSION 398

SPECIAL TEST METHODS FOR BATTERIES
S. Gross, Boeing Aerospace Company . . . . 401 ✓D27

DISCUSSION 417

EMU BATTERY/MODULE SERVICE TOOL CHARACTERIZATION STUDY
C. F. Palandati, NASA/Goddard Space Flight Center . . . . 419 ✓D28

SESSION V

TOPIC: METAL HYDROGEN

Chairman: L. Thaller, NASA/Lewis Research Center 433

PRELIMINARY SILVER-HYDROGEN CELL TEST RESULTS
C. Lurie, TRW Space and Technology Group . . . . 435 ✓D29

DISCUSSION 445

LONG LIFE NICKEL ELECTRODES FOR A NICKEL-HYDROGEN CELL: CYCLE LIFE TESTS
H. S. Lim and S. A. Verzwyvelt, Hughes Research Laboratories . . . . 449 ✓D30

DISCUSSION 462

FACTORS AFFECTING NICKEL-OXIDE ELECTRODE CAPACITY IN NICKEL-HYDROGEN CELLS
P. F. Ritterman, COMSAT . . . . 463 ✓D31

DISCUSSION 471

POSITIVE ELECTRODE FABRICATION FOR BIPOLAR Ni-H_2 CELLS
T. Edgar, Eagle-Picher Industries, Inc . . . . 473 ✓D32

DISCUSSION 492

BIPOLAR NICKEL-HYDROGEN BATTERIES FOR AEROSPACE APPLICATIONS
C. W. Koehler and G. V. Ommering, Ford Aerospace and Communications Corporation
N. H. Puester and V. J. Puglisi, Yardney Electric Corporation . . . . 495 ✓D33

DISCUSSION 503

TEST RESULTS OF A TEN CELL BIPOLAR NICKEL-HYDROGEN BATTERY
R. L. Cataldo, NASA/Lewis Research Center .... 507 ✓ D34

DISCUSSION 520

FAILURE ANALYSIS OF NICKEL-HYDROGEN CELL SUBJECTED TO SIMULATED LOW EARTH ORBIT CYCLING
V. C. Mueller, McDonnell Douglas Astronautics Company .... 523 ✓D35

DISCUSSION 536

COMPARATIVE PERFORMANCE ASSESSMENT OF INTELSAT V NICKEL HYDROGEN AND NICKEL CADMIUM BATTERIES
D. Cooper and A. Ozkul, International Telecommunications Satellite Organization .... 539 ✓D36

DISCUSSION 555

LIST OF ATTENDEES 557

SESSION I

ADVANCED ENERGY STORAGE PROGRAMS

Chairman: F. E. Ford
Goddard Space Flight Center

N84
33669

UNCLAS

N84 33669

INERTIAL ENERGY STORAGE FOR SPACECRAFT

G. Ernest Rodriguez
Goddard Space Flight Center

ABSTRACT

The feasibility of inertial energy storage in a spacecraft power system is evaluated on the basis of a conceptual integrated design that encompasses a composite rotor, magnetic suspension, and a permanent magnet (PM) motor/generator for a 3-kW orbital average payload at a bus distribution voltage of 250 volts dc. The conceptual design, which evolved at the Goddard Space Flight Center (GSFC), is referred to as a "Mechanical Capacitor." The baseline power system configuration selected is a series system employing peak-power-tracking for a Low Earth-Orbiting application. Power processing, required in the motor/generator, provides potential alternative that can only be achieved in systems with electrochemical energy storage by the addition of power processing components. One such alternative configuration provides for peak-power-tracking of the solar array and still maintains a regulated bus, without the expense of additional power processing components. Precise speed control of the two counterrotating wheels is required to reduce interaction with the attitude control system (ACS) or alternatively, used to perform attitude control functions. Critical technologies identified are those pertaining to the energy storage element and are prioritized as composite wheel development, magnetic supension, motor/generator, containment, and momentum control. Comparison with a 3-kW, 250-Vdc power system using either NiCd or NiH_2 for energy storage results in a system in which inertial energy storage offers potential advantages in lifetime, operating temperature, voltage regulation, energy density, charge control, and overall system weight reduction. The key disadvantages are attitude control interface and launch constraints. A hardware development program is required to verify analytical assumptions used to perform feasibility studies. The objective of this program is to develop an integrated magnetically suspended reaction wheel capable of performing energy storage and momentum/torque functions.

INTRODUCTION

Energy storage and conversion have been and will continue to be key elements in developing earth applications and science-oriented spacecraft. Most spacecraft flown to date utilize photovoltaic technology for energy conversion and electrochemical technology for energy storage. Performance improvements of these technologies, as well as the search for new ones, are constantly pursued through various research and development programs. An attractive alternative to electrochemical energy storage is inertial energy storage. The development and applications of composite materials in super flywheels has aroused considerable interest in spacecraft power system applications because of the potential high energy density capability. The concept of inertial energy storage for a photovoltaic powered spacecraft encompasses various basic elements, which are:

- flywheel spinning at an angular velocity ω
- flywheel supported by a shaft and bearings
- motor/generator to convert available electrical energy from the photovoltaic source to mechanical energy and/or to convert stored mechanical energy in the flywheel to electrical energy for the spacecraft load
- a suitable fixed platform for the integration of the spinning assemblies.

These basic elements are configured as shown in Figure 1 for illustrative purposes. The energy stored in this system can be quantitized by the familiar equation:

$$E = \frac{1}{2} I \omega^2$$

where I = moment of inertia
ω = angular velocity.

PRECEDING PAGE BLANK NOT FILMED

Assessment of inertial energy storage for spacecraft power systems has been the subject of study at GSFC in task 4 under the NASA Research and Technology Objective and Plan (RTOP) titled "Advanced Power System Technology" (506-55-76). This task was initiated to develop concepts, perform feasibility analysis, design, develop and demonstrate high overall system efficiency and reliability in a spacecraft power system, and evolved from the development at GSFC of the "Mechanical Capacitor" (References 1 through 5).

INITIAL GUIDELINES

Initial guidelines for the assessment of inertial energy storage for spacecraft are well documented in Reference 6. These guidelines were based on a Low Earth Orbit mission, typically 60 min sun, 30 min eclipse, sized for payload power in the range of 2.5 kW to 25 kW (orbital average), with modularity in mind to allow for growth potential. Initial studies were to concentrate on a power system sized for an operational load of 2.5 kW at 90% duty cycle, and a peak of 7.5 kW at 10% duty cycle. This corresponds to an orbital average load of 3 kW. Target driven mass estimates were 115 kg for the solar array, (based on 56 W/kg technology) 115 kg for the storage element, (based on 22 Whr/kg energy storage density), and 70 kg for power conditioning components (based on 43 W/kg technology), for which the total mass estimate is 300 kg, representing 10 W/kg power system technology.

POWER DISTRIBUTION

Ac/dc power distribution was a power system issue under consideration at the beginning of the study effort. The energy conversion process within the motor/generator involves ac voltage/current generation, and as such, the feasibility of ac power distribution was investigated. The basis for the investigation was not power distribution per se, but rather the interconnection of the source, energy storage element and load. This is illustrated in Figure 2, where two approaches are considered. These two approaches are simply conversion of the source to ac to match the energy storage element, or conversion of the storage element to dc to match the source.

Conversion of the storage element to dc was the method selected for the following reasons:

- allows simple method of paralleling modules
- allows speed control of individual wheels as a simple method of momentum management
- allows for a simple and effective way to achieve high efficiency (in/out) and a regulated bus.

The inherent ac voltage/current generation within the motor/generator is of insufficient power quality (variable voltage and frequency) for ac power distribution. In addition the corresponding low frequency would result in higher mass (transformer) penalties at the user interface than can be achieved with state-of-the-art 20 kHz power conditioning equipment.

POWER SYSTEM CONFIGURATION

Most spacecraft power system configurations can be categorized into two basic types:

- series system
- shunt system.

Series/shunt applies to the power processing element that is used to control the solar-array power. Although combinations or variations of these two are used for mission-unique applications, generally, the series system is used in LEO missions and the shunt system is used in GEO missions. The series element allows maximum extraction of solar-array power (peak-power-tracking) as the array temperature (and thus array power) undergoes large temperature excursions, typical of LEO, and provides a means for keeping the excess array power distributed on the array when not required by the spacecraft load. In GEO missions, the array temperature remains constant during the extended sunlight periods, and the shunt element provides an efficient means for transferring the array power to the spacecraft load by shunting only what is in excess.

A unique characteristic of the inertial energy storage system is that the power conditioning electronics required for the motor/generator inherently provide a means for charge and discharge control over the design speed range of the flywheel, and thus additional power conditioning elements are not required as in an electro-chemical storage system. For a LEO mission, the series system configuration would be the same for either an electrochemical or inertial storage system, but for GEO the charge and discharge regulators (required for a regulated bus) in an electrochemical based system could be eliminated in an inertial storage system. The additional losses incurred by the charge/discharge regulator result in a combined in/out efficiency of about 65% whereas for the inertial system the efficiency would be more like 80%. This, however, is not a serious penalty because of the long sunlit/eclipse duty ratio but could result in a mass penalty. Detailed system comparisons have not been performed for the GEO mission.

Alternative system configurations can be realized with the inertial energy storage elements. One such system, shown in Figure 3, utilizes the motor control electronics to peak power track the array and the generator electronics to regulate the bus voltage. This would require additional motor/generator windings and electronics, but the net savings in mass and efficiency may still be significant over the baseline series system. Further detailed trade-off studies are necessary for evaluating this configuration.

DOE FLYWHEEL TECHNOLOGY PROGRAM

Flywheel development, prompted by the energy shortage and stimulated by an organized effort of the DOE, resulted in many approaches brought to the testable model stage. The DOE Flywheel Technology program concentrated on the development of the composite rotors, sized at approximately 500 watt hours, and primarily intended for vehicular application. High strength fibers are used at the outer periphery for high energy density and various schemes were devised to interface the outer rim with an inner disk. Several of the rotors developed are shown in Figures 4 and 5.

The Laurence Livermore National Laboratories (LLNL), under contract with the DOE, narrowed their selection to three promising candidates:

- the cruciform spokes by Ganet-Air Research
- the laminated disk and rim by LLNL & GE
- the woven spiral by AVCO Corporation.

These three designs were tested at the conclusion of the DOE program. Of the three designs, only the spiral weave design exhibits a desirable form factor providing an essential monolithic "thick rim" with adequate volumetric efficiency and an ID/OD ratio sufficiently low to support an integral motor/generator at an acceptable stress level. Unfortunately, development problems were encountered in the fabrication of this design. Of the three designs tested, the hybrid GE design performed quite satisfactorily, exhibiting a higher burst energy than expected and demonstrated 10^4 cycles.

An alternative design not tested is the "best rim" design reported in Reference 4. This design utilizes various concentric graphite epoxy rims which are pre-stressed, thus allowing a smaller ID/OD ratio that can be achieved by only one rim.

GSFC CONCEPTUAL FLYWHEEL DESIGN

The conceptual design of an integrated flywheel energy storage system for spacecraft power application is depicted in Figure 6. This design consists of two counter-rotating wheels (for momentum cancellation) suspended magnetically at the inner radius of the "thick rim" composite rotor, and including an integral permanent magnet, ironless armature, brushless dc motor/generator. Stationary components would include the stator windings for the motor/generator, control windings for the magnetic suspension, and the necessary electronics. Most of the heat would be generated within the stationary housing, and thus heat extraction is not a serious problem. This design approach is a radical departure from the configuration shown in Figure 1, but represents an attempt to eliminate the problems of power transmission through shafts, reduce gyroscopic loads on shaft bearings, and maximize high energy density potential of the rim with high volumetric efficiency by utilizing the volume of the "hole" in the middle. Critical technologies associated with a successful design of this integrated flywheel design are the following:

- thick rim composite rotor
- magnetic suspension of rotating mass
- high efficiency motor/generation employing permanent magnet, ironless aramature, brushless dc motor technology
- M/G electronics to provide for motor/generator interface and speed control
- safe containment of the rotating mass.

BENEFITS COMPARISON

A comparison study was conducted to evaluate the benefits/merits of an inertial storage power system with an electromechanical storage system. This study was conducted by performing a "point" design for a NiCd, NiH_2 and inertial energy storage based systems. The system configuration selected for all three is the series system employing a peak power tracker series element. Results of this point design are tabulated in Table I for comparison. The inertial energy storage system exhibits potential improvements in all categories, with the important note that care must be taken to ensure attitude control system compatibility. The high momentum inherent in energy storage wheels requires careful control and thus provides an attractive alternative approach to combine attitude control functions with the energy storage wheels.

INTEGRATED ATTITUDE CONTROL ENERGY STORAGE

An attractive concept for combining the functions of energy storage and attitude control functions was described by Henry Hoffman at the Integrated Flywheel Technology Workshop at GSFC on August 2, Reference 7. Theoretically, one wheel only provides energy storage and impacts the attitude control system; two wheels provide energy storage and one-axis attitude control; three wheels provide energy storage plus two-axis attitude control; and four wheels provide energy storage and three-axis attitude control. Thus, a minimum of four wheels are required to perform four functions; energy storage and 3-axis control. More than four wheels provide for redundancy configuration and modularity. A conceptual drawing of the required four wheel in a tetrahedral configuration (no axis colinear) is illustrated in Figure 7. The fundamental control law for any given number of wheels with non-colinear axis is given as:

$$\begin{pmatrix} X_1 & X_2 & X_3 \cdots\cdots X_N \\ Y_1 & Y_2 & Y_3 \cdots\cdots Y_N \\ Z_1 & Z_2 & Z_3 \cdots\cdots Z_N \\ \omega_1 & \omega_2 & \omega_3 \cdots\cdots \omega_N \end{pmatrix} \begin{pmatrix} T_1 \\ T_2 \\ T_3 \\ \vdots \\ T_N \end{pmatrix} = \begin{pmatrix} T_X \\ T_Y \\ T_Z \\ \dot{E} \end{pmatrix}$$

CONCLUSIONS

The application of inertial energy storage for a spacecraft power system relies on the key characteristics of the energy storage element. Power distribution (ac versus dc), power system configuration, performance, and system compatibility have been evaluated on the basis of the conceptual flywheel system design (developed at GSFC and referred to as the "Mechanical Capacitor") consisting of two counterrotating composite rotors, suspended magnetically at the inner diameter and accelerated/decelerated by a PM brushless, ironless dc motor/generator contained within the stationary inner volume. This energy storage element exhibits characteristics similar to those of an electrochemical energy storage element, which makes it an almost one-for-one replacement. Ac power distribution is not found to be advantageous since the inertial energy storage element does not exhibit the desirable characteristcs required by an ac power distribution system. The power system configuration selected is identical with state-of-the-art systems using electrochemical energy storage. A unique system configuration identified incorporates the main functions of power conditioning within the energy storage element, reducing the system component count from three to two, namely solar array (1) and energy storage (2). Performance is highlighted as long lifetime (20 to 30 years), high temperature waste heat rejection, simple state-of-charge detection and control, inherent high-voltage implementation, high-pulse power capability, higher energy density (Wh/kg) than NiCd, and higher volumetric density than NiH_2 (Wh/m^3). These features, although potential, make inertial energy storage a significant improvement over electrochemical systems. Compatibility with other systems is found to be adequate, with the recognition that momentum disturbance to the attitude control systems must be precisely controlled or alternatively used for attitude control as well.

Self-discharge, or energy storage efficiency, containment, and launch restrictions are three areas that require careful consideration in the intended application. For example, in LEO applications the self-discharge of the inertial energy storage element does not significantly affect the overall system performance. In unmanned vehicles, containment requirements would be less demanding than in manned vehicles. Spacecraft acquisition during launch may require electrochemical energy storage in a launch mode in which the energy storage wheels must be "locked."

Combined application of inertial energy storage and attitude control functions has been the focus of attention in two reported studies, one by NASA/Langley Research Center (LaRC) in 1974 (Reference 8) and the other by the European Space Agency (ESA) in 1978 (Reference 9). Both reports find the combined functions to be feasible and result in conceptual designs and methods to accomplish the objective. The NASA/LaRC study effort progressed to the development of inertial energy storage hardware using titanium for the wheel and conventional bearings. The ESA study has not proceeded to the development of hardware but identifies the merits of magnetic bearings and composite rotors. In either case, the subject of inertial energy storage for spacecraft application remains a "study" effort, and until competitive hardware is developed, its application will remain on paper. Since the inertia required for energy storage is significantly larger than that required to perform attitude control functions, a conservative program (and lower risk) to undertake is to develop the fundamental inertial energy storage hardware. Once developed, the hardware application will follow, for if it is to be used in power systems, it must be controlled, and if it must be controlled, it should be used for attitude control as well.

The mechanical capacitor conceptual design considered in this feasibility study is based on three key technologies, two of which are well developed and have been demonstrated, but yet remain to be used in flight hardware. These two technologies, magnetic bearings and dc PM ironless armature, brushless motors, ideally suited for use in momentum wheels for attitude control, do not exist in the list of flight-approved hardware. Conventional bearings and ac motors, presently used in most momentum wheels, do not offer the high performance required for an inertial energy storage system to be competitive with electrochemical systems. Conceivably, if a flywheel system as conceptually described can be successfully demonstrated, it would facilitate or encourage the use of these two technologies in momentum wheels. On the other hand, if these two technologies existed in present flight hardware, a significant data base would have been available to substantiate the feasibility of inertial energy storage. However, the key single most critical technology is the high-speed composite rotor, which, although significant progress has been achieved within the last two years, requires further development, verification, and system implementation.

In terrestrial applications, inertial energy storage becomes competitive over electrochemical systems from a "maintenance free" consideration. Similarly, in spacecraft applications, long lifetime is the key advantage of inertial energy storage over electrochemical storage. To realize this, successful integration of the critical technologies identified must be pursued.

During the last few years, flywheel technology was supported primarily by the Department of Energy, and is now terminated. Recent results obtained by the General Electric Company under this program are very encouraging in that they support the assumptions used for energy density capability in this study. In addition, results on cyclic testing have verified 10^4 cycles, which is one order-of-magnitude improvement over past performances and approaches the potential cycle life of 10^5 cycles referenced in this report.

RECOMMENDATIONS

Significant potential advantages of inertial energy storage for spacecraft power systems as identified warrant the development of hardware to a proof of principal stage. To accomplish this, a sizable commitment in resources is required to demonstrate a complete power system. At a minimum, the development of a suitable composite rotor should be pursued with less risk involved at the expense of a longer time span in achieving the proof of principal hardware. Magnetic suspension and motor/generator development should be accomplished together, following demonstration of a successful rotor design. Verification of the fundamental energy storage function would occur when the rotor, suspension, and PM motor/generator are integrated as one. After the energy storage function has been demonstrated, the next step would be attitude control compatibility verification. The development and demonstration of a complete power system would be the final phase.

The following program has been suggested and recommended to OAST. The objective of the program is to develop a prototype magnetically suspended reaction wheel to perform both energy storage and one axis attitude control of momentum and torque. This program is based on negligible return from further paper studies and the need to verify analytical study assumptions.

The following system technologies and goals are recommended:

- high energy density composite hubless rotor with an ID/OD ratio of ≈ 0.5 yielding a maximum operational energy density of 50 W hr/kg and an energy storage capacity of 1.6 kw hr (75% DOD)
- magnetic suspension of the hubless rotor to yield low standby power consumption and low high-speed losses at 40 KRPM
- permanent magnet, ironless armature, brushless dc motor/generator with 3ϕ stator windings sized for a 2.5 kw nominal power rating, peak 7.5 kW at 250 Vdc, and yielding better than 95%
- power conditioning electronics for the motor/generator, yielding a power efficiency of better than 95% and capable of providing speed control for both bus regulation and momentum control
- integration of the above to perform in a LEO space environment corresponding to 10^5 charge/discharge cycles at 75% DOD.

REFERENCES

1. Kirk, J. A., P. A. Studer, and H. E. Evans, *Mechanical Capacitor*, NASA/GSFC TN D-8185, November 1975.

2. Michaels, T. D., E. W. Schliebin, and R. D. Scott, *Design Definition of a Mechanical Capacitor*, Final Report, NASA/GSFC, May 1977.

3. Scott, R. D., *Mechanical Capacitor Energy Storage System*, RCA, Advanced Technology Laboratories, Final Report, NASA CR-170613, February 1978.

4. Kirk, James A., "Flywheel Energy Storage–I Basic Concepts," *Int. J. Mech. Sci.*, Vol. 19, January 1977, pp. 223-231.

5. Kirk, James A., "Flywheel Energy Storage–II Magnetically Suspended Super Flywheel, "*Int. J. Mech. Sci.*, Vol. 19, January 1977, pp. 233-245.

6. Slifer, Luther W., Jr. *Initial Guidelines and Estimates for a Power System with Inertial (Flywheel) Energy Storage*, NASA/GSFC TM 82134, December 1980.

7. Integrated Flywheel Technology, *Proceedings of Workshop,* Aug. 2,3, 1983, NASA Conference Publication 2290.

8. Notti, J. E., A. Cormack III, and W. C. Schmill, *Integrated Power/Attitude Control System (PACS) Study*, Vols I & II, NASA Contract Report, NASA CR-3383, April 1974.

9. Guyen, N., H. Nahia, and Marian Francois, *Study of System Implications of High Speed Flywheels as Energy Storage Devices on Satellites*, MATRA Note No. 30/1020, ESA Contract No. 3261/77/NL/AK, October 1978.

Table I

BENEFITS COMPARISON

(For 3 kW, 250 Vdc LEO S/C Power System)

	NICD (SOA)	NIH_2 (Projected)	Flywheel (Projected)
Lifetime (yr)	5	5	20
DOD (%)	25	40	75
*Energy Density (W hr/kg)	5.5	13.9	17.6
*Volumetric Energy (kW hr/m^3)	8.2	7.2	20.8
Voltage Regulation (±%)	14	14	2
Thermal Constraint (°C)	0 to 20	0 to 20	−25 to +50
High Voltage	Many series cells	Many series cells	Easily accommodated (M/G design)
Charge Control	Complicated	Pressure sensing may simplify	Wheel speed affords easy detection and control
Launch Constraint	None	None	Wheels locked
Compatibility with ACS and structure	No interaction	No interaction	Critical – differential speed control required – balance Benefit – perform ac function

*Usable

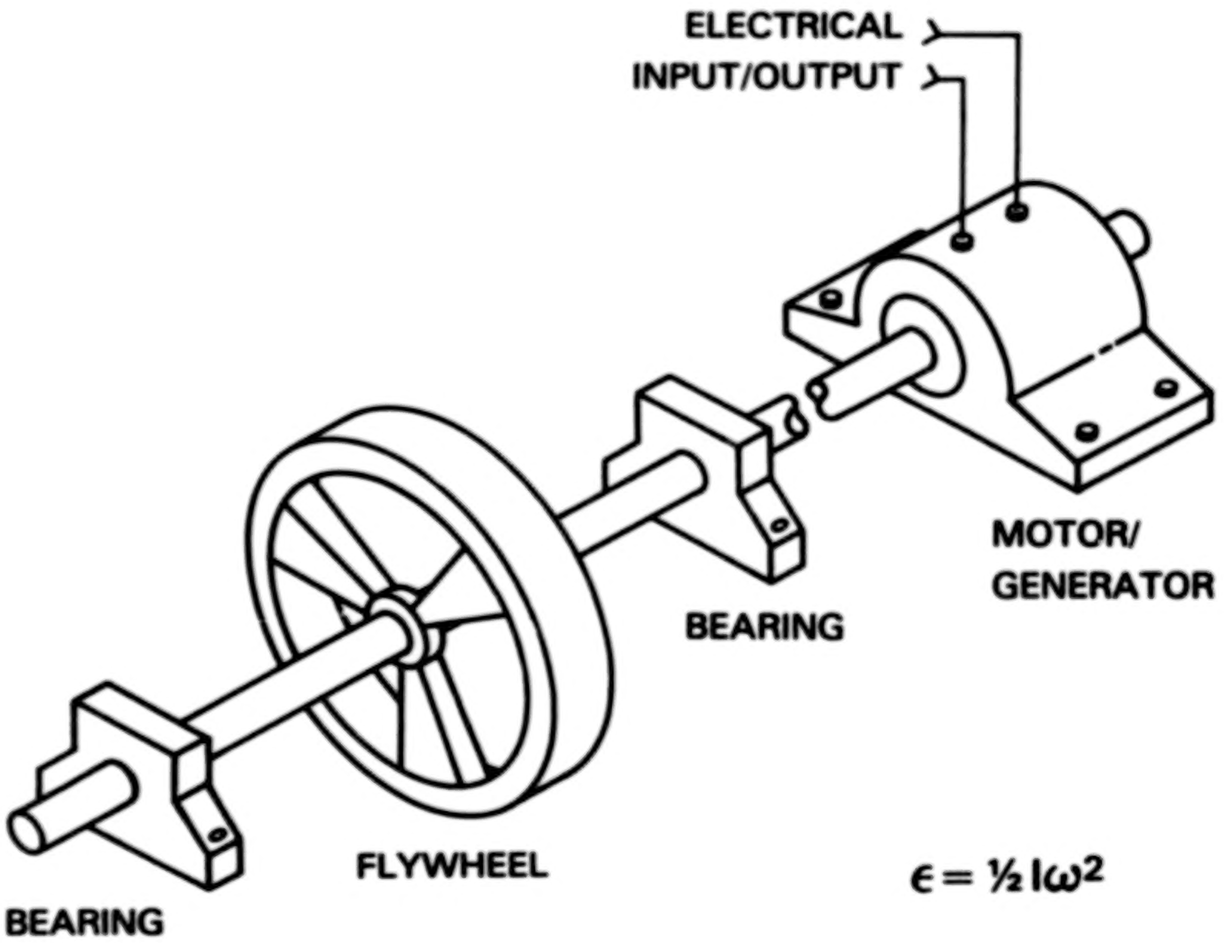
ELECTRICAL
INPUT/OUTPUT
MOTOR/
GENERATOR
BEARING
FLYWHEEL
BEARING

$$\epsilon = \frac{1}{2} I\omega^2$$

Figure 1. Inertial Energy Storage Element

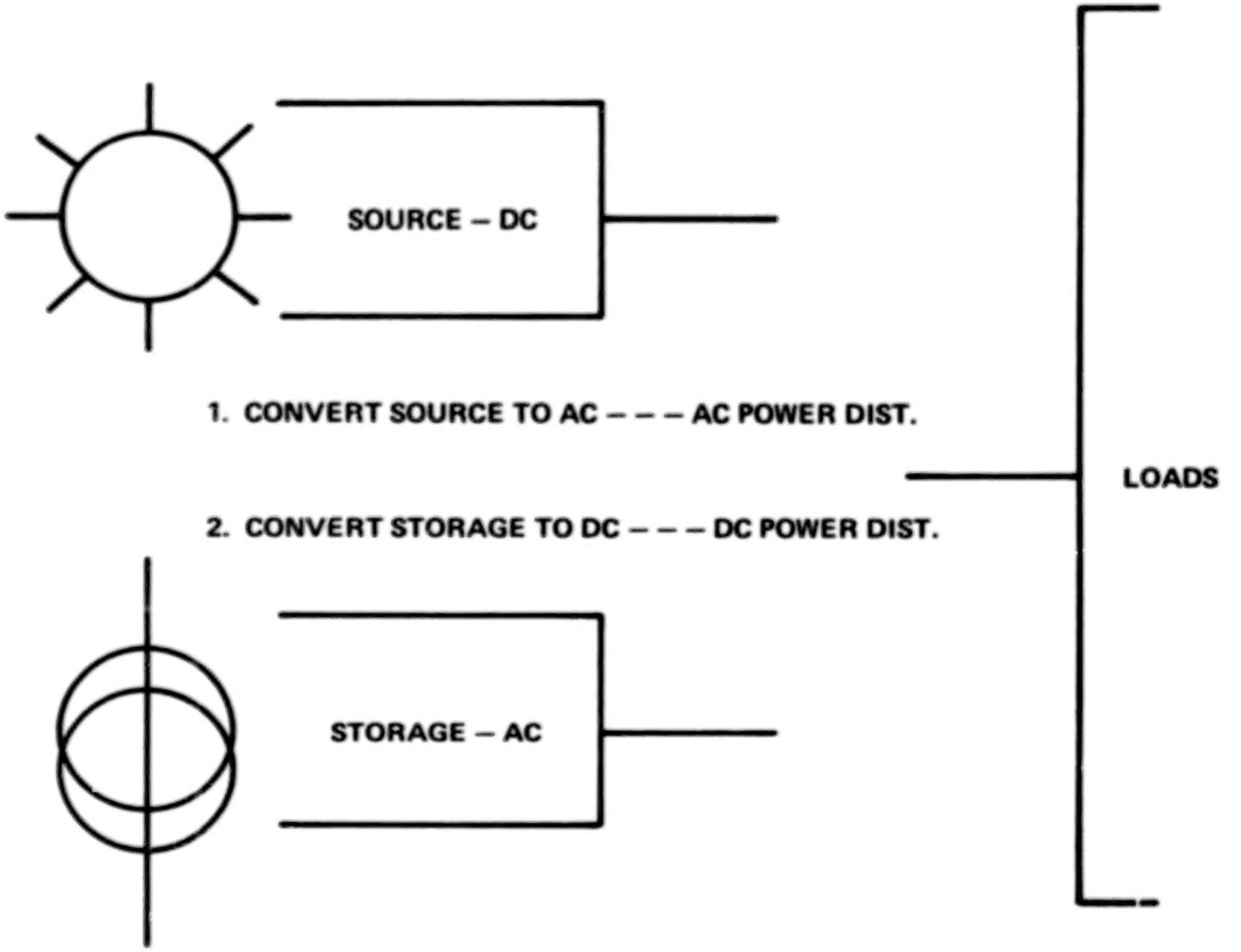
SOURCE – DC
1. CONVERT SOURCE TO AC – – – AC POWER DIST.
2. CONVERT STORAGE TO DC – – – DC POWER DIST.
STORAGE – AC
LOADS

Figure 2. Power System Distribution Alternatives

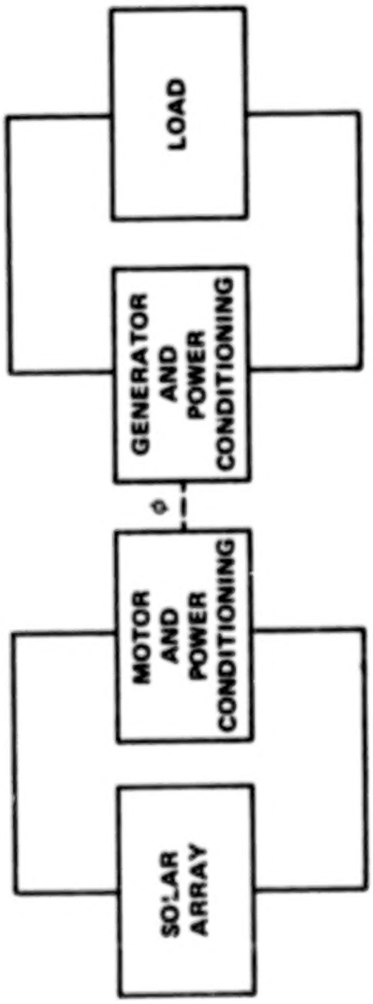
SOLAR ARRAY
MOTOR AND POWER CONDITIONING
φ
GENERATOR AND POWER CONDITIONING
LOAD

Figure 3. Peak-power-tracker, Regulated Bus System

ORIGINAL PAGE IS
OF POOR QUALITY

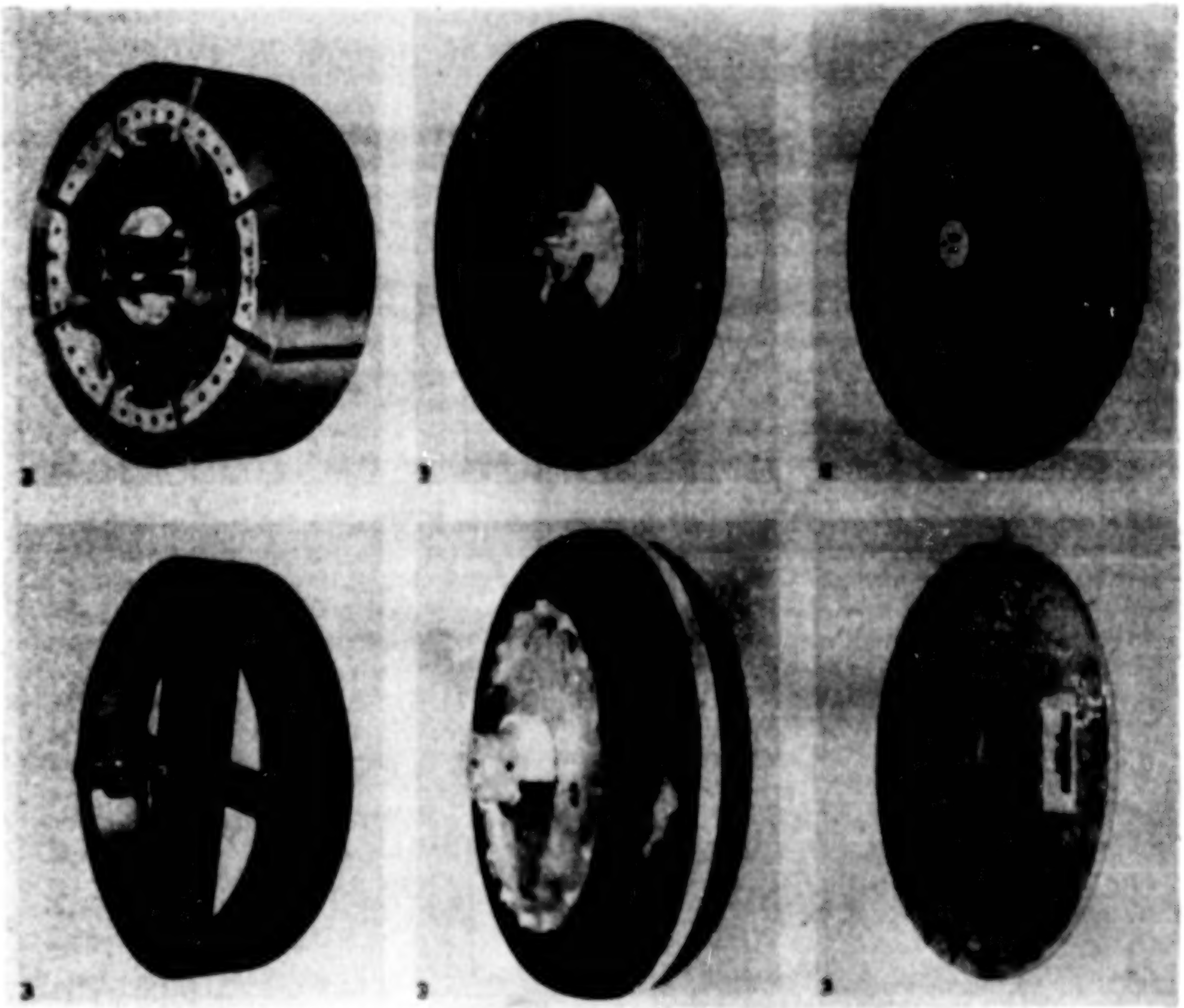

Figure 4. Composite Rotor Designs, DOE/LLNL

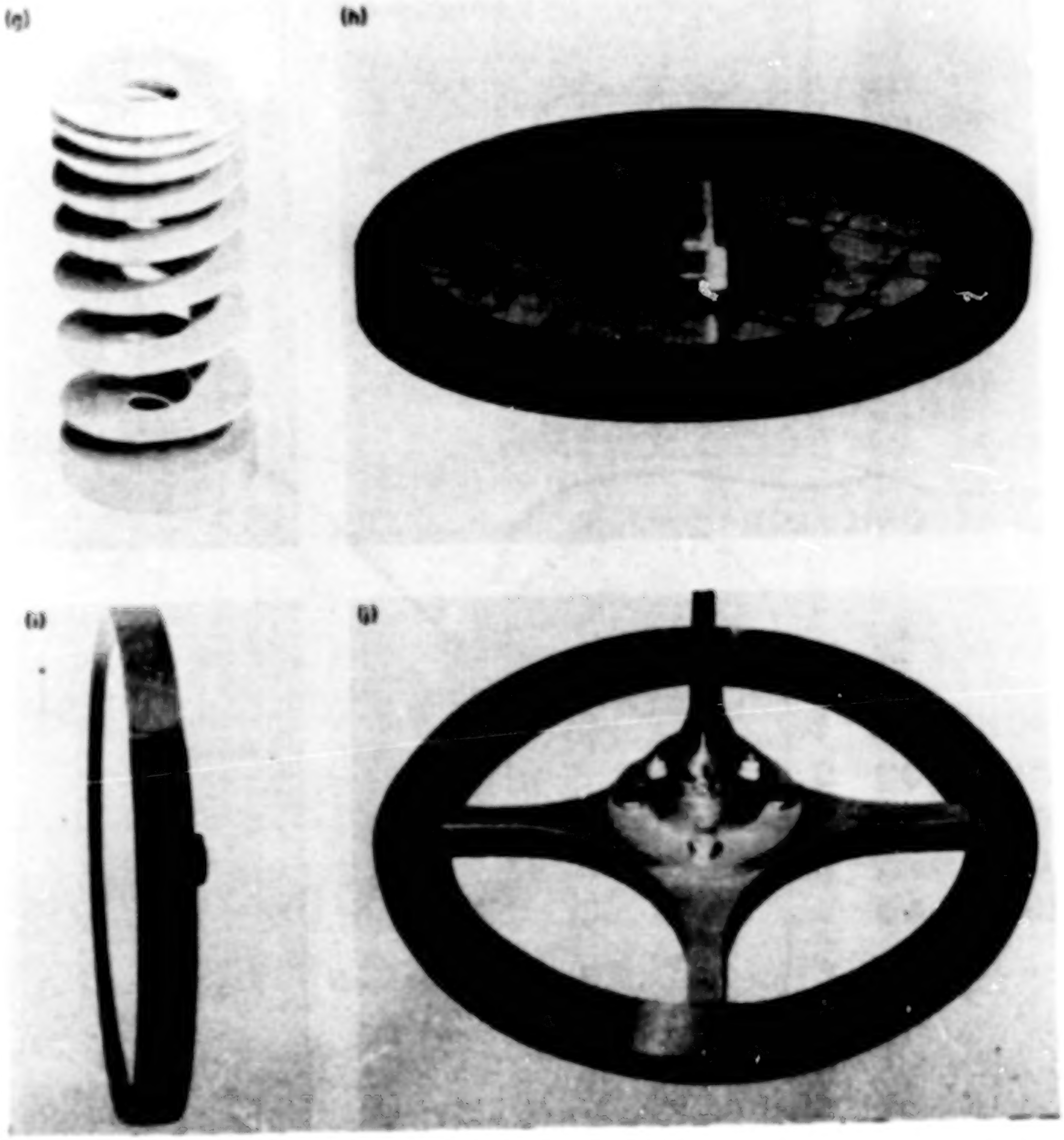

Figure 5. Composite Rotor Designs, DOE/LLNL

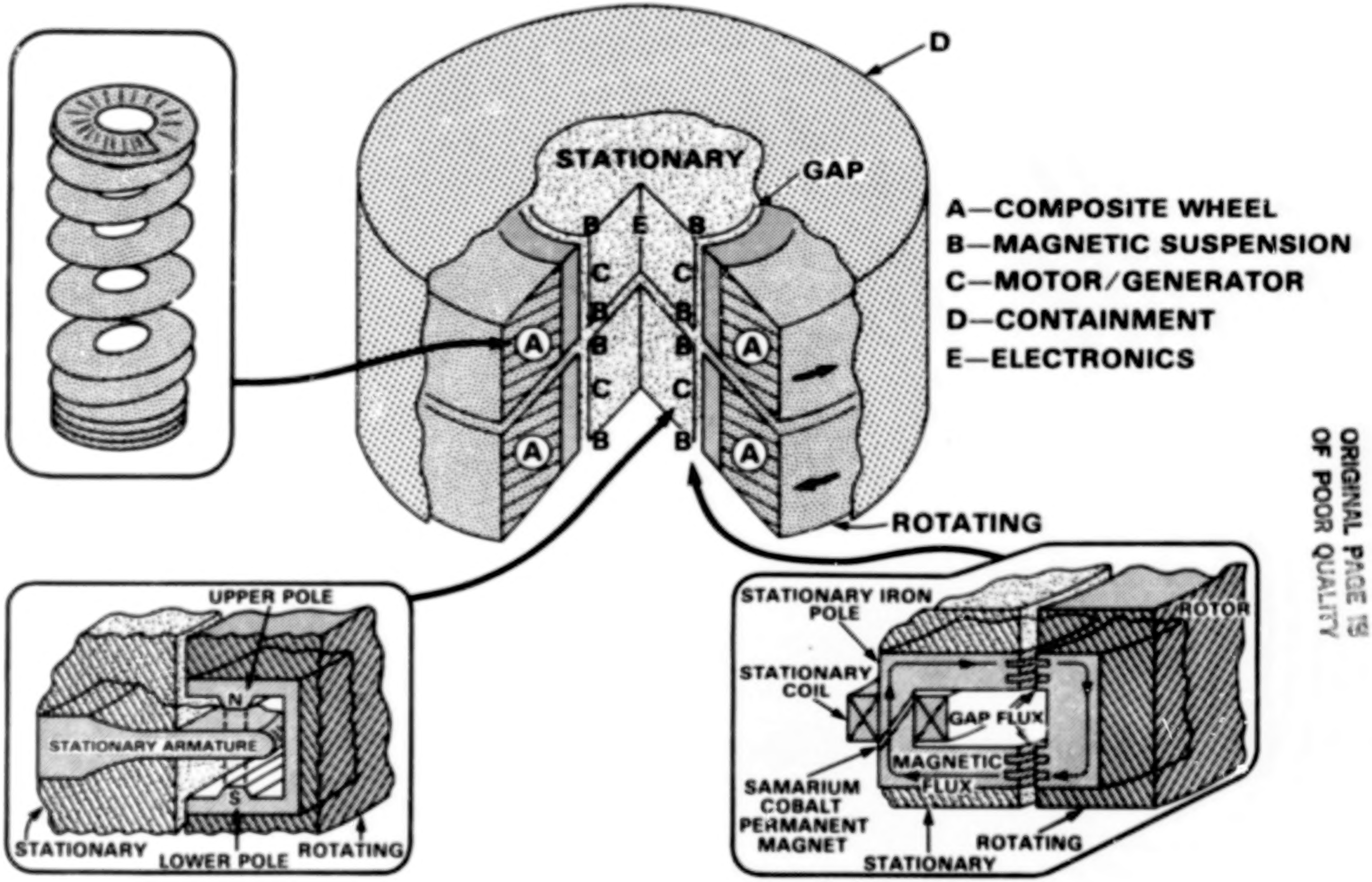

D
STATIONARY
GAP
B
E
C
A
ROTATING
A—COMPOSITE WHEEL
B—MAGNETIC SUSPENSION
C—MOTOR/GENERATOR
D—CONTAINMENT
E—ELECTRONICS
UPPER POLE
N
S
STATIONARY ARMATURE
STATIONARY
LOWER POLE
ROTATING
STATIONARY IRON POLE
STATIONARY COIL
GAP FLUX
MAGNETIC FLUX
SAMARIUM COBALT PERMANENT MAGNET
ROTOR
ROTATING
STATIONARY

Figure 6. Conceptual Spacecraft Power System Flywheel Design

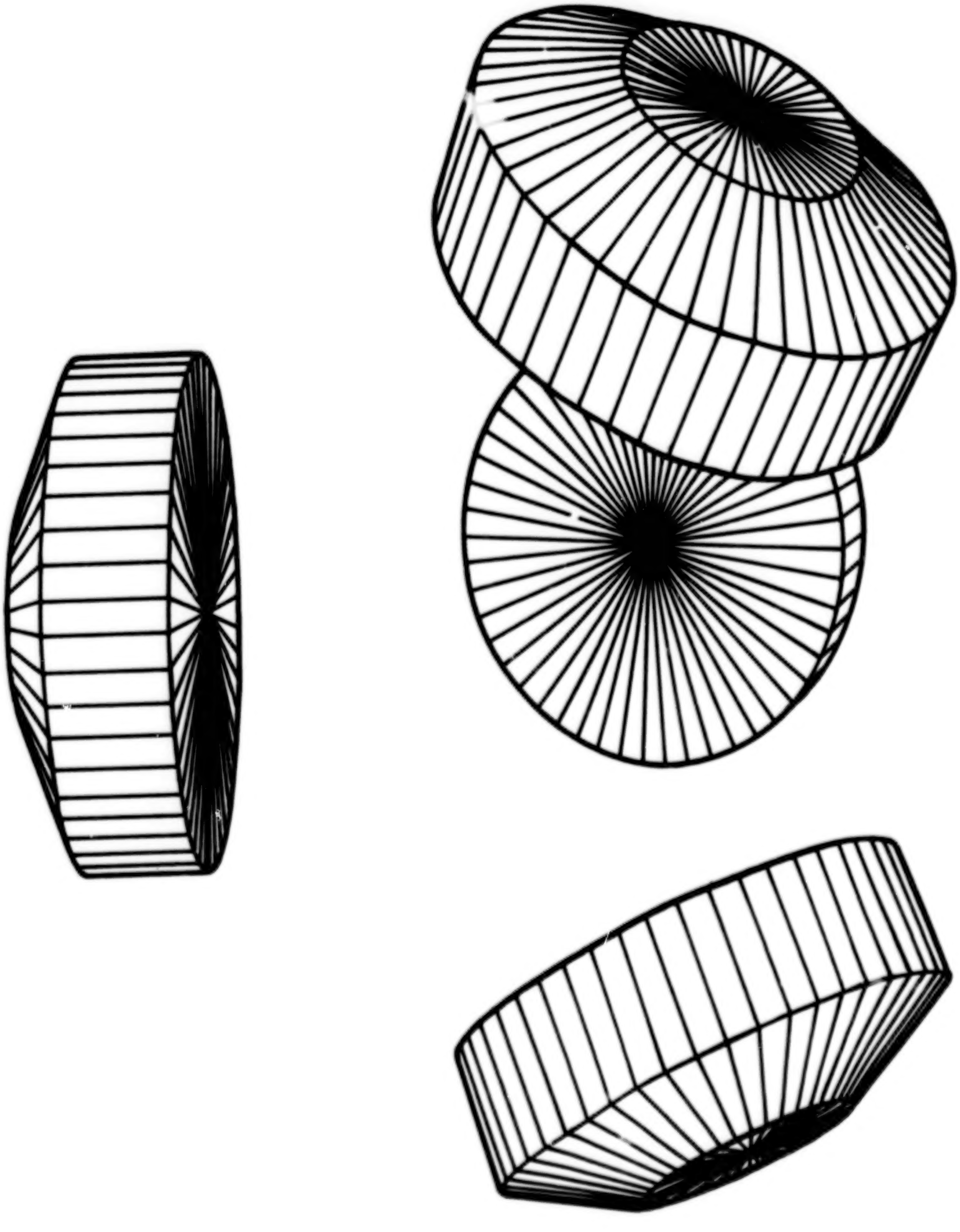

Figure 7. Four Wheel Tetrahedral Configuration for 3-axis Control and Energy Storage

SESSION I

DISCUSSION

Q. Galassi, Hughes Aircraft: When you figured out the number of storage devices you needed, did you base your analysis on a three axis vehicle versus a spin-stabilize vehicle?

A. Rodriguez, GSFC: Well, no. We're not talking about a spin-stabilized vehicle. It's just for a typical three axis control vehicle.

Q. Galassi, Hughes Aircraft: If you did do any analysis on a spin stabilized, if you put it at the center of spin or the axis, could this be also used in that capacity and that type of vehicle?

A. Rodriguez, GSFC: Oh, yes I'm sure it could be.

Q. Somoano, JPL: What is it exactly that limits the cycle life?

A. Rodriguez, GSFC: Well, one of the things that limits it is the stress. The wheel is the fiber composites at this point in time, the stress is an unknown item. The wheel that was tested at Lawrence-Livermore that GE developed, for example, that wheel was tested for 10^4 cycles. So, we know that wheel capability is up to that point you can do that. 10^5 cycles is, as I have demonstrated here, a limit that we think can be achieved. But it is just basically stress-fatigue of the material - just up and down, up and down, and it wears out. If it wasn't for that, we could perhaps conceive a much greater lifetime.

Q. Milden, Aerospace: How much and how long - how much would it cost to have flight quality hardware, thing number one, thing number two - how long would it take to get flight quality hardware?

A. Rodriguez, GSFC: That's a tough question. We anticipate about four to five years before we have a proof-of-concept type of a unit because we're talking about a rather unique approach in here where you have two systems that are interacting that need to be resolved. There's a lot of interactions going on. In terms of how much, I'm not quite sure whether you're addressing the actual cost once the design is developed or to develop that design. Could you perhaps clarify.
I don't visualize the flywheel system itself as any more costly than typical electrochemical systems to date. But in terms of developing, of course, there's a considerable development cost.

Q. Question inaudible.

A. Rodriguez, GSFC: Okay. In the conceptual design that we have, the wheels rotate around 30-40 thousand revolutions per minute. That's your max speed.

Q. George, MSFC: The question of speed brings to mind the diameter that you're talking about. The earlier effort on a magnetically suspended wheel, if I remember correctly, was rather large - six feet in diameter and it was humming along about 7,000 rpm's. What are you talking about here?

A. Rodriguez, GSFC: Well, the wheel that we have - a conceptual design for the time being is 20 inches outside diameter, 10 inches inside diameter. So the magnetic suspension would occur perhaps at a diameter of 10 inches. I think you might be talking about the AMCD that was developed at Langley? Goddard? It is a 5½ foot diameter wheel. However that wheel was principally for momentum control. It's a little bit different concept but still the same basic fundamentals are there. You have the magnetic suspension at three different points on that wheel. I believe you're right. It's about 3,000-4,000 rpm's. We're talking about a much smaller wheel.

Q. Miller, McDonald-Douglas: I was wondering what is the principal failure mode of such a wheel? Is it disintegration? And if it is, how do you get this past your safety people?

A. Rodriguez, GSFC: The failure mode of the wheel depends on the wheel design itself. You can design them in different modes. One of the attractive features is that if you design in such a way that the outer fibers begin to fail first, then you have what we call a safe containment. It doesn't blow up or it doesn't fragmentize like a metallic wheel does. So we feel that the containment issue is easier handled with this kind of a design.

Q. Miller, McDonald-Douglas: In other words it kind of eliminates from the outer edge?

A. Rodriguez, GSFC: Yes, correct.

Q. Gross, Boeing: Ernie, what did you calculate the power consumption for the magnetic bearings to be for this design?

A. Rodriguez, GSFC: Let's see, I remember there is a number that Dave Eisenhower published in the paper and I don't recall the exact number. I think it's 1/10th of a watt per pound or something of that nature. If you check with me later, I'll give you a reference on that article and you can look it up. It's pretty well documented.

ORIGINAL PAGE IS
OF POOR QUALITY

Q. Colburn, Lockheed: It appears you're mixing together an attitude control system and a power system and the common ground is the static reaction wheels or momentum storage wheels. Have you done any analysis on the requirements of a reaction wheel used in an attitude control loop versus what the power system requirements are? It seems to me, you made the assumption that these two common pieces of hardware are compatible in two somewhat different roles. Have you investigated that any?

A. Rodriguez, GSFC: Well, we really haven't gotten into the attitude control function in a whole lot of detail. But, I believe I could say that, yes, we looked at it. The energy storage wheel that we're talking about here has a momentum capacity of roughly 9,000 newton meters/seconds and the typical reaction wheel that is used, let's say, on the MMS spacecraft as, for example, is only 20 newton meters/ seconds. So, you're talking about two orders of magnitude difference just in momentum. So, the point is that the wheel is needed for energy storage not for attitude control . The attitude control system doesn't need a wheel anywhere near this size. We need it for energy storage for the power system and, as long as it's there, then why not use it for the attitude control system function? The other area that we looked at is the task capability of the wheel and we really haven't gotten into that too much, but I think you can perform both the momentum control and the task capabilities that are required by the attitude control system by sizing the wheel for energy storage. Oh yes, one of the things that happened this summer - we had a flywheel technology workshop here at Goddard where it was primarily attended by colleagues within NASA and DOE. But the two items that were considered there were the attitude control and energy storage functions as a system.

Q. Question inaudible.

A. Rodriguez, GSFC: Okay. That's a good question. Did everybody hear the question, he wants to know how does the magnetic bearings compare with what I'm talking about here and the system that the Lincoln Labs designed, I believe. A fellow by the name of Milner, I think, designed a system that was a one kilowatt-hour wheel. If you looked at my earlier view graph where I had a shaft and a motor and bearing and that kind of a concept - that's the kind of concept that Lincoln Labs designed. They essentially had a wheel hanging on the end of a shaft, and then they had magnetic bearings to support that shaft and that mass, and a permanent magnet-motor generator to turn the whole shaft. So essentially the elements that I'm talking about they have designed but in a different configuration. One of the things that I think Phil Studer emphasizes with the magnetic suspension is that when you try to design magnetic bearings where you're going to have to have at least two on the end of a shaft, you're going to get into some pretty stiff problems because of tasks

A. Rodriguez, GSFC (Con't): on those bearings. So what he is proposing is that the magnetic bearing be in the center of a wheel rather than out on the ends of a shaft. Move the bearings towards the center. Maybe that wasn't too clear in the concepts that I showed here. You can do it either way. Now I showed perhaps the magnetic suspension on the top and bottom portion of the inside of the rim but you could also put it right in the center. The concept then is to move the magnetic bearings toward the center.

Q. Koehler, Ford: In the case of a multi-wheel system, if one wheel fails does that mean an immediate failure of the satellite?

A. Rodriguez, GSFC: Well, yes with the minimum four wheel system that I proposed - yes. If you had failure with the one wheel you would loose some control and it most likely would be failure of the mission depending on the particular mission in mind. But the approach to have redundancy would be to have more than four wheels. So your minimum requirement is four wheels.

Q. Roth, NASA HQ: I'm just wondering for the uninitiated, what are you doing here that's different specifically from what's been done in the past? I mean we've kind of been beating around all that.

A. Rodriguez, GSFC: Well I believe what's been done in the past if you're referring to the IPAX that Langley developed.

Q. Roth, NASA HQ: Anything over the last 10 or 20 years. What makes this stand out or makes it unique from any of the other work?

A. Rodriguez, GSFC: Basically it doesn't exist. There is no hardware that utilizes a composite wheel for the high energy density - number one. There is no system that I know of that uses the magnetic bearings that I just talked about. There is no motor generator design that I'm aware of in this kind of a system. So those three things exist independently by themselves, but they don't exist in an integrated system. And I believe that for a spacecraft application, you have to have all these three things integrated. The design of the motor generator is not a straight-forward design. The design of the magnetic bearings is not straight-forward. They all have to be interleagued because the rotating dynamics of that mass makes them involve each other quite extensively. So I believe that's perhaps why we're all at where we're at, because basically the technology is there, it just has to be put together.

Q. Jagielski, GSFC: Ernie, you were talking about the power density of the flywheel. Was that specifically for just one flywheel - just for one single axis, and if you were talking about redundancy how would that alter the power density of the flywheel system?

A. Rodriguez, GSFC: Yes, I talked about a power density of say 2½ kilowatts - 7½ kilowatts. That would be for a pair of wheels. That was our original concept when we got into the study, and that is signed for a payload - spacecraft payload of 3 kilowatts. Now if you have a different application where the power is higher or lower then you would have to size your wheels accordingly. Does that answer your question Jim?

N84
33670

UNCLAS

D2

N84 33670

REGENERATIVE HYDROGEN-OXYGEN FUEL CELL - ELECTROLYZER SYSTEMS FOR ORBITAL ENERGY STORAGE

Dean W. Sheibley
National Aeronautics and Space Administration
Lewis Research Center
Cleveland, OH 44130

INTRODUCTION

Fuel cells have played a major role in spacecraft power generation. The Gemini and Apollo programs used fuel cell power plants as the primary source of mission electrical power, with batteries as the backup. The current NASA use for fuel cells is in the orbiter program. Here, low temperature alkaline fuel cells provide all of the on-board power with no backup power source. Three power plants per shipset are utilized. The original fuel cell power plant configuration contained two 32-cell substacks connected in parallel. This configuration was flown on STS-1 through STS-8. Starting with STS-9, a three substack configuration (three 32-cell substacks connected in parallel) will be used to obtain longer life and better voltage performance.

Fuel cells will continue to have a major role in space power generation and storage. With the addition of an electrolysis capability, the regenerative fuel cell system is expected to provide multikilowatt-hour energy storage capability for large orbiting spacecraft which are dependent upon photovoltaic solar arrays for primary power. These future space applications will require one to two orders of magnitude greater power (up to 250 kW) than has been needed up to now. These applications include unmanned platforms in low-earth orbit (LEO) and geosynchromous orbit (GEO), and a permanently manned space operations center in LEO. All of NASA's capabilities have complimentary military interest for surveillance, command, and weapons applications in space.

The main thrust of the OAST fuel cell technology program in NASA since 1979 has been focused on LEO energy storage applications. The effort is a combined program conducted by Johnson Space Center (JSC) and Lewis Research Center (LeRC). The goal is to demonstrate functional feasibility of regenerative fuel cell (RFC) systems, both acidic and alkaline, in breadboard test article configurations by 1984. At that time, an engineering model will be built for a technology readiness demonstration by early 1987. The engineering model system will be supported by long term endurance testing of multiple cell stacks of full size hardware tested toward a goal of 40,000 hours.

Although the overall efficiency (50-60 percent) of the integrated hydrogen-oxygen fuel cell-electrolyzer system is not as high as the nickel-cadmium and nickel-hydrogen battery systems, point design comparisons of the RFC with these battery systems yield results which, from a total system standpoint, show the RFC to have the best effective energy density, minimum weight, and the greatest projected life before subsystem replacement over a 10-year period. In addition, the RFC is the only near-term energy conversion/storage system that offers the potential advantages of full integration with life support, space manufacturing, and station-keeping propulsion systems.

RECENT STUDIES

Previous design studies (1, 2, 3) on orbital energy storage systems for LEO have evaluated weight optimized 100 kW systems based on launch weight and weight to orbit over a 5 to 10 year period. The weights included fuel cell and electrolyzer components, reactant gases and tanks, radiators, and solar array. Electrical efficiency ranged from 36 to 50 percent. The recent Boeing study (4) compares the RFC energy storage system with other energy storage systems optimized for efficiency. This optimization is achieved by reducing current density, thereby improving electrical efficiency to approximately 60 percent for the RFC systems. The optimization increases the weight of fuel cell and electrolyzer components, but greatly reduces the weight and area of the solar array, which on weight optimized systems accounted for approximately 70 percent of the total system weight. Reduction of solar array reduces orbital drag which reduces the fuel requirement for altitude maintenance of the spacecraft. Thus, it becomes obvious that all impacted areas of the vehicle must be properly treated in comparison studies to identify the genuinely optimized concept.

COMPONENT TECHNOLOGY DEVELOPMENT

There are four technology requirements common to energy storage systems for LEO:

1. increased life; 40,000 hours (5 years) has been established as a goal,
2. increased reliability; a minimum 2-year life on components,
3. increased efficiency; greater than 50 percent overall electrical efficiency,
4. higher voltage; an apparent optimum voltage range exists between 100V to 240V.

The combined JSC-LeRC program has focused upon improving fuel cell-electrolyzer component life, and electrical efficiency. The requirements of increased reliability, and higher voltage will be formally addressed as part of the engineering model development effort.

Regenerative Fuel Cell Feasibility Demonstrations

The feasibility demonstration of regenerative fuel cells has focused upon improving fuel cell-electrolyzer component life and electrical efficiency. A 5-year (40,000 hour) life has been established as a goal with an overall electrical efficiency goal for the storage subsystem of 60 percent in a voltage range of 100 to 200 volts. Both the acid (SPE) and alkaline RFC systems are to be evaluated at JSC using breadboard test articles with periodic up-grading of component and system technology.

Acid (SPE) Breadboard System

The acid breadboard was delivered to the Johnson Space Center on February 1, 1983. The breadboard consists of a fuel cell subsystem for power generation, an electrolysis subsystem for H_2-O_2 generation, a reactant storage subsystem, and a remote control console. The remote control console allows for individual operation of the fuel cell and electrolysis subsystems, operation of both subsystems simultaneously, and for the operation of the two subsystems in a cyclic mode. The remote control console also automatically monitors the subsystems and will shut down the breadboard safely if any parameters go out of limits. A sketch of the acid regenerative fuel cell breadboard system is shown in Figure 1. The system is located in the Thermal Test Area (TTA) at JSC.

The initial objective of demonstrating the feasibility of using a RFC as an energy storage subsystem for a LEO energy storage system has been accomplished with the breadboard having accumulated 1025 LEO cycles as of September 20, 1983. Several of these cycles have been acquired with the solar power station

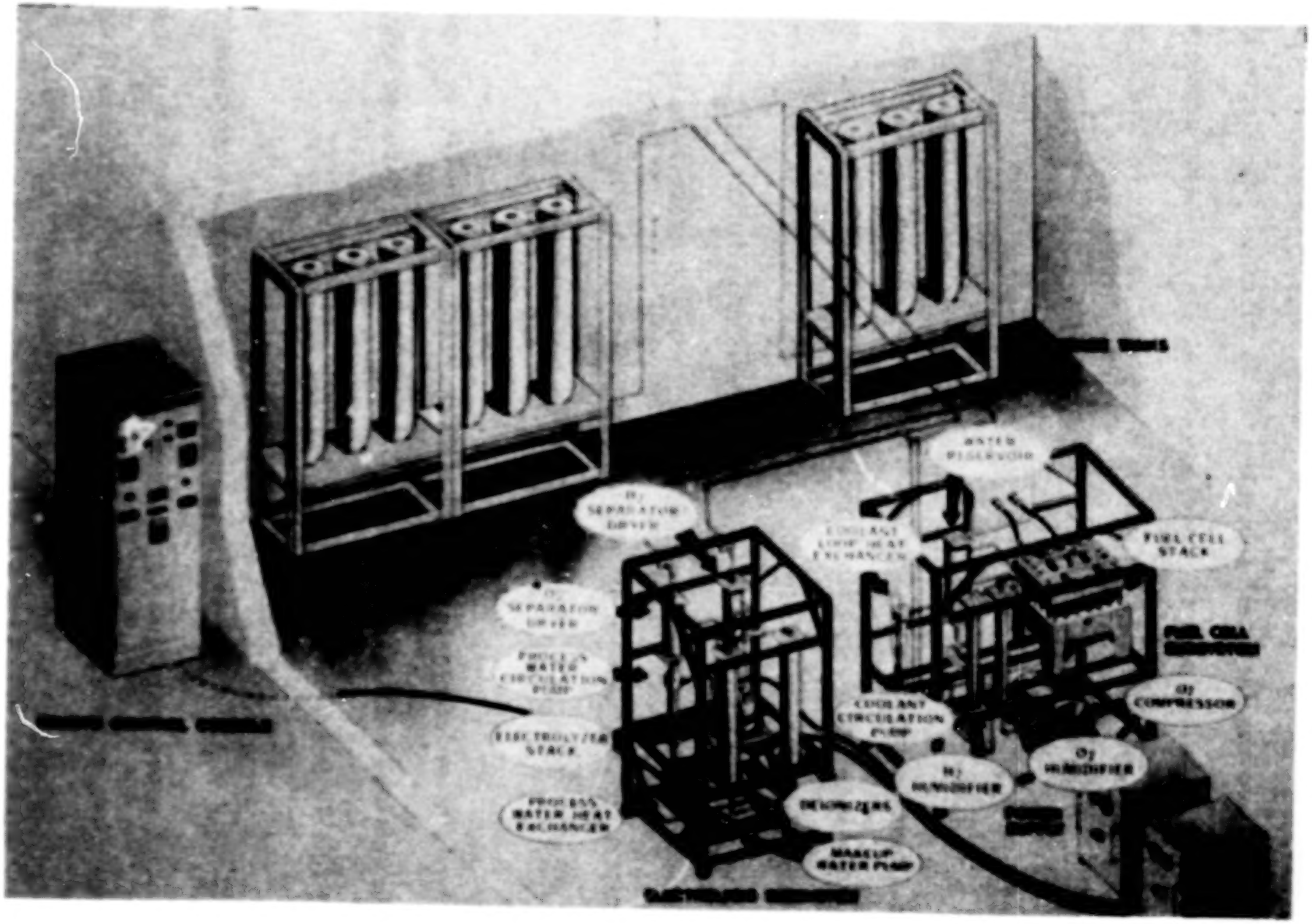
H_2 SEPARATOR DRYER
O_2 SEPARATION DRYER
PROCESS WATER CIRCULATION PUMP
ELECTROLYZER STACK
PROCESS WATER HEAT EXCHANGER
COOLANT LOOP HEAT EXCHANGER
WATER RESERVOIR
FUEL CELL STACK
O_2 COMPRESSOR
COOLANT CIRCULATION PUMP
O_2 HUMIDIFIER
H_2 HUMIDIFIER
DEIONIZERS
MAKEUP WATER PUMP

Figure 1. Breadboard regenerative fuel cell energy storage system.

connected directly (no power conditioning equipment used) to the electrolysis subsystem. The LEO cycle consists of running the electrolysis subsystem for 54 minutes, and the fuel cell subsystem for 36 minutes. The electrolysis unit consists of 22 cells (0.23 ft^2) and operates at the following parameters; 24 amps, 36 volts, and 73° F. The gas is stored at 130 psia for the H_2 and 115 for the O_2. The fuel cell consists of eight cells (1.1 ft^2) operating at 112 amps, 6.5 volts, 160° F. The LEO cyclic mode is a closed loop operation.

The following findings have been observed about the acid system. No measurable water loss has been found, however, apparently four percent more gas is produced than is consumed. This is mostly due to the diffusion of the gases across the SPE membrane. There has been no permanent cell performance degradation detected in either the fuel cells or electrolysis cells. Also, the remote control console is working very well and is shutting the system down whenever tolerance limits are reached.

A synopsis of endurance test data base supporting the acid RFC is shown in Figure 2, along with the projected efficency of the total storage system and the major technology problems associated with the system.

Future plans for the acid RFC breadboard include continued operation in the LEO cyclic mode, operation for 30 days of a scaled-down version of a Space Station power profile, and open-ended testing of both the fuel cell and electrolysis subsystems to establish a better endurance data base. The breadboard will also be utilized as a test bed for advanced cell and component development verification.

Alkaline Breadboard System

The alkaline RFC breadboard is scheduled for delivery at JSC in early January 1984. It will integrate a 30-cell alkaline electrolysis unit (0.1 ft^2) with an Orbiter fuel cell power plant (#708). The 30-cell electrolyzer unit (1.5 kW nominal) will be replaced in April 1984 with a 6-cell 1 ft^2 electrolyzer unit (3 kW nominal) which is considered full size hardware for the space station mission. It also provides a better power match with the 4.5 kW Orbiter power plant.

The alkaline RFC is supported by endurance testing of the electrolyzer and fuel cell components. Electrolysis endurance testing has surpassed 23,000 hours (September 20, 1983) in the LEO regime with 0.1 ft^2 single cells at 180° F, 150 ASF, at ambient pressure with no voltage degradation. Figure 3 shows cell voltage vs. time for a cell containing a "SUPER" anode catalyst.

A complete electrolysis subsystem containing a 6-cell stack of 1 ft^2 cells, and the controller is scheduled to begin a 20,000 hour endurance test in April 1984.

A fuel cell stack of 6 cells (Orbiter-size hardware) has accumulated 8600 hours of LEO cycle endurance testing with a voltage degradation rate of less than 1 microvolt/hour. A plot of average cell voltage vs. time is shown in Figure 4. A minimum endurance test goal of 20,000 hours is anticipated. The 6-cell stack is operating at 200 ASF, 60 psia, and 140° F.

ENDURANCE TESTING (LIFE)

FUEL CELL:	>40000 hr IN SUBSCALE CELLS 2000 hr CONTINUOUS TEST AT 180° F, 60 psia IN 1.1 ft^2 CELLS
ELECTROLYZER:	45000 hr IN 0.23 ft^2 CELLS (NAVY OXYGEN GENERATION PROGRAM) CONTINUOUS TESTING AT 1000 ASF, 120° F
INTEGRATED SYSTEM:	DELIVERED TO JSC FEB. 1983. SIMULATED ORBITAL TESTING STARTED IN APRIL, 1983. - 1540 hr, 1025 CYCLES (SEPT. 20, 1983)

PROJECTED EFFICIENCY (TOTAL STORAGE SYSTEM)

WEIGHT OPTIMIZED 100 kW SYSTEM 48%
OPTIMIZED FOR EFFICIENCY (LOW CURRENT DENSITY) 64%

TECHNOLOGY PROBLEMS

HYDROGEN DIFFUSION THROUGH MEMBRANE (INHERENT PROBLEM)

HYDROGEN EMBRITTLEMENT OF NIOBIUM COLLECTOR DURING LONG TERM USE

Figure 2. Acidic (SPE) fuel cell - electrolyzer system for orbital energy storage.

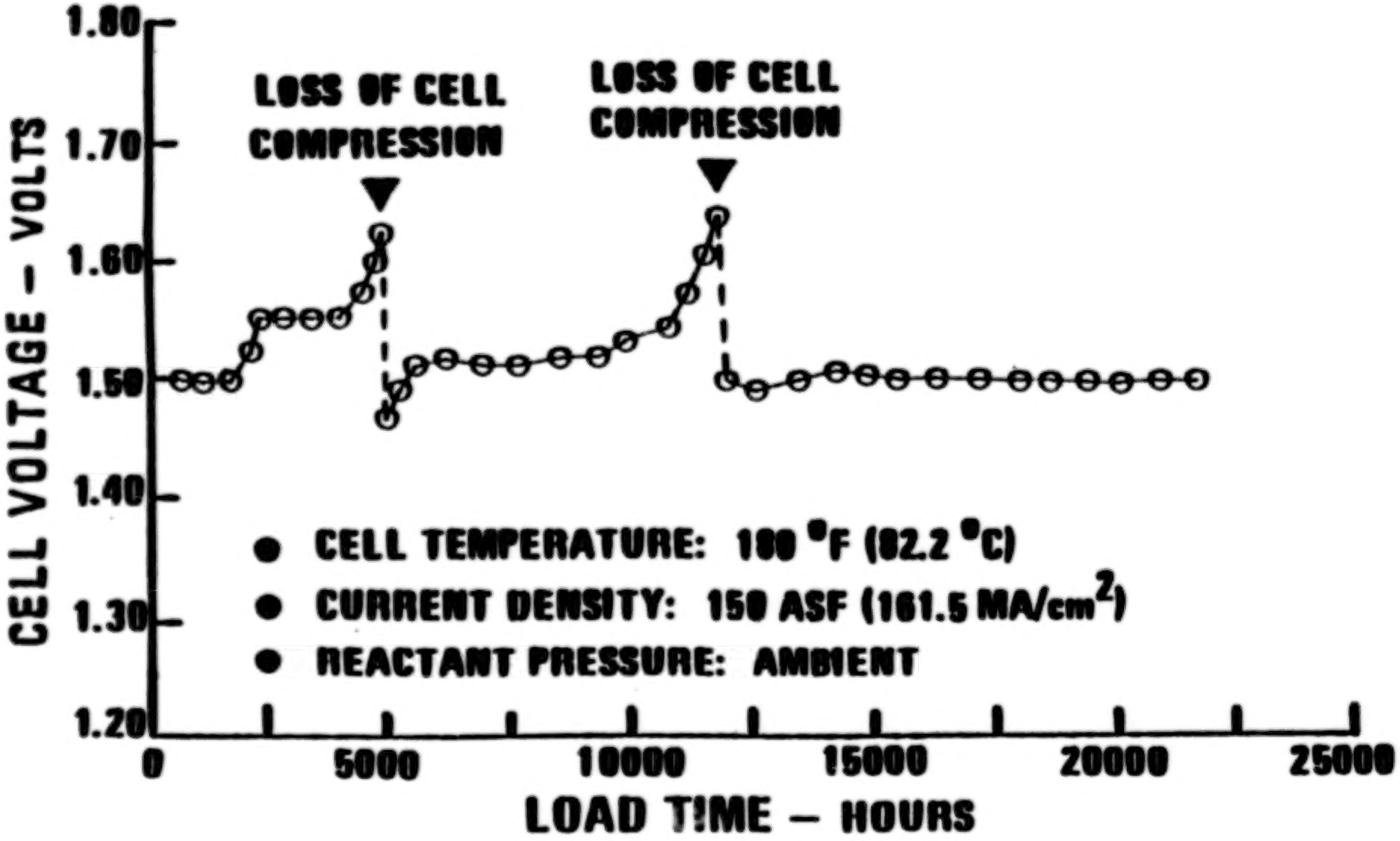

- **Successfully completed 21600 hours of testing**
- **Performance remains stable**

Figure 3. Super anode cell endurance.

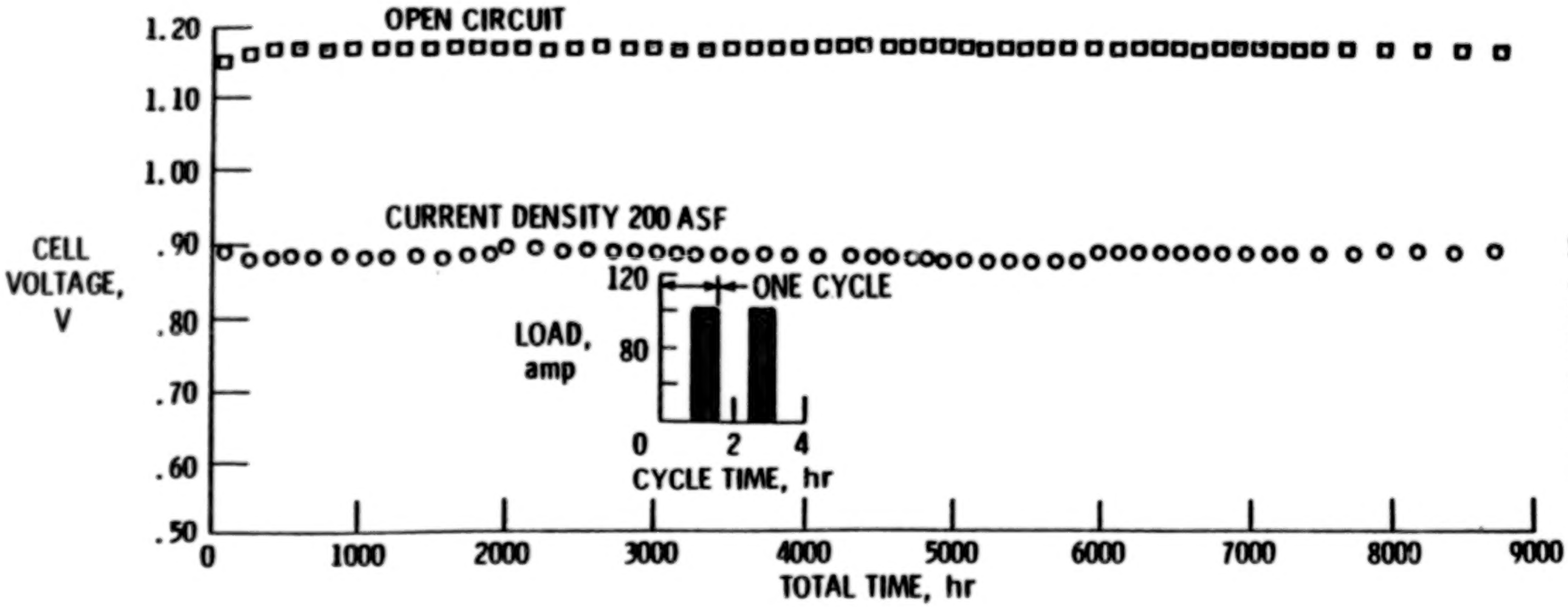

Figure 4. NASA Lewis six-cell stack long term endurance test - successfully completed 8600 hr (5733 cycles) of cyclical operation, performance remains stable, less than 1.0 microvolts per hr voltage reduction.

- ENDURANCE TESTING

  FUEL CELL:
  - TWO 10000 hr CONTINUOUS TESTS AT 100 ASF IN ORBITER SIZE STACKS DURING DEVELOPMENT PROGRAM FOR SHUTTLE
  - 1390 hr AT 200 ASF LEO CYCLIC REGIME TESTING CONFIRMED OPERATION IN CYCLIC MODE
  - 6 CELL STACK (ORBITER SIZE COMPONENTS) STARTED ON LEO CYCLIC ENDURANCE TEST IN SEPT. 1982; 8250 hr (5167 SIMULATED ORBITAL CYCLES) AS OF SEPT. 20, 1983; GOAL 20 000 hr BY MARCH, 1985; 200 ASF, 140^{0} F, 60 psia

  ELECTROLYZER:
  - 23 000 hr ACCUMULATED (SEPT. 20, 1983)) IN LEO CYCLIC MODE AT 150 ASF, 180^{0} F, AMBIENT PRESSURE IN 0.1 ft^2 CELLS; VOLTAGE STABLE NEAR INITIAL VOLTAGE
  - SCALE UP TO 1ft^2 UNDERWAY; ENDURANCE TESTING TO START MARCH, 1984

- PROJECTED EFFICIENCY (TOTAL STORAGE SYSTEM)
  - WEIGHT OPTIMIZED 100 kW SYSTEM: 50%
  - OPTIMIZED FOR EFFICIENCY: 66%

- TECHNOLOGY PROBLEMS
  - VOLTAGE DEGRADATION DUE TO CARBONATE (FROM ELECTRODE FRAME MATERIALS)
  - ASBESTOS MATRIX INSTABILITY ABOVE 220^{0} F

Figure 5. Alkaline fuel cell - electrolvzer system for orbital energy storage.

A synopsis of the endurance test data base for the alkaline RFC is shown in Figure 5, along with projected system electrical efficiency and the major technology problems currently being work on in the technology program.

POINT DESIGN COMPARISON

A 60 kW point design comparison was made for an energy storage system for a manned space station in low earth orbit. The design compared two battery systems, Ni/Cd and bipolar Ni/N_2, and the H_2-O_2 RFC system. A list of design requirements are shown in Figure 6. A significant factor in the design was the redundancy requirement imposed on the system, which resulted in two storage modules on each of three main power buses. The configuration also required the system to provide full power with two modules failed. This requirement increases the depth of discharge on the batteries, while increasing the current density of the fuel cell and electrolyzer. The results of the design are given in Figure 7. The RFC has the highest effective energy density, and the lowest weight. Based on current life projections, the Ni/Cd battery system would require replacement in 5 to 6 years, the bipolar Ni/H_2 battery system in 3 to 4 years, and the RFC system in 7 to 8 years. The Ni/Cd life projection was based upon 16 percent DOD for six battery modules (increasing to 25 percent DOD for four modules) and an operating temperature of 10° C. The bipolar nicke hydrogen life was estimated based upon 50 percent DOD for six battery modules (75 percent DOD for four modules) and an operating temperature of 30° C. The RFC estimate of 7 to 8 years was based upon the estimated voltage degradation rate of the fuel cells derived from the carbonate conversion time dependent model from the Orbiter qualifcation programs. The

DESIGN REQUIREMENTS

POWER:	AVERAGE - 60 KW PEAK - TBD EMERGENCY - SEPARATE SYSTEM
CONFIGURATION:	
	- 6, 10-KW MODULES - 2 MODULES ON EACH OF 3 BUSES - 4 MODULES, ABLE TO CARRY FULL POWER (15 KW/MODULE)
VOLTAGE:	120V
ORBIT:	NOMINAL - 270 N.M. RANGE - 200-300 N.M.
TIME:	CHARGE - 58.8 MIN. DISCHARGE - 35.7 MIN.
LIFE:	10 YEARS

Figure 6. 60-KW point design comparison of nickel-cadmium,bipolar nickel-hydrogen and regenerative fuel cell energy storage subsystems.

DESIGN RESULTS

CHARACTERISTIC	NI/Cd	B.P. Ni/H_2	RFC
EFFECTIVE ENERGY DENSITY	3.3 wh/kg	14.9 wh/kg	17.8 wh/kg
ROUND TRIP ELECTRICAL EFFICIENCY (END OF LIFE)	70%	70%	56%
TOTAL STORAGE SUBSYSTEM WEIGHT	11 050 kg	2408 kg	2023 kg
TOTAL STORAGE SUBSYSTEM VOLUME	120 ft^3	115 ft^3	203 ft^3
REQUIRED STORAGE SUBSYSTEM REPLACEMENTS FOR 10-YEAR LIFE	1	2	1
HEAT REJECTION: REQUIREMENT (MAXIMUM)	27 kW	30 kW	38 kW
TEMPERATURE	10^0 C	30^0 C	60^0 C
NUMBER OF CONTROLLABLE UNITS	4320	6	F.C. 6 E. 6

Figure 7. 60-KW point design comparison of nickel-cadmium, bipolar nickel-hydrogen and regenerative fuel cell energy storage subsystems.

RFC parameters selected were 140° F operating temperature, a full cell current density of 135 ASF, and an electrolyzer current density of 150 ASF.

From the standpoint of overall system autonomous control, the number of controllable units greatly favor the RFC and bipolar Ni/H_2 battery storage systems. The level of autonomous control is greatly simplified in controlling 6 to 12 subsystems as compared to 4320 individual 50 ampere/hour Ni/Cd cells.

Concluding Remarks

Fuel cells have found application in space since Gemini. Over the years technology advances have been factored into the mainstream hardware programs. Performance levels and service lives have been gradually improving. More recently, the storage application for fuel cell-electrolyzer combinations has been receiving considerable emphasis. The regenerative system application described here is part of a NASA Fuel Cell Program which has been developed to advance the fuel cell and electrolyzer technology required to satisfy the identified power generation and energy storage need of the Agency for space transportation and orbital applications to the year 2000.

REFERENCES

1. Trout, J. Barry, "Energy Storage for Low Earth Orbit Operations at High Power", Proceedings of AIAA/NASA Conference on Advanced Technology for Future Space Systems, May 8-10, 1979, Hampton, VA.

2. "Electrochemical Cell Technology for Orbital Energy Storage", Contract NAS 9-15831, General Electric Direct Energy Conversion Programs, Report ECOES-12, November 19, 1979.

3. R.E. Martin, "Electrochemical Energy Storage for an Orbiting Space Station", Contract NAS 3-21293, United Technologies Corp., Report NASA CR-165436, December 1981.

4. "Analysis of Regenerative Fuel Cells", Contract NAS 9-16151, Report D180-27160-1, Boeing Aerospace Co., August 1982.

Q. McDermott, Martin Marietta: On the Shuttle and on the Gemini you showed 2 and 3 fuel cells. Is that a redundancy system we're looking at there?

A. Gonzalez, NASA/Lewis Research Center: For the Shuttle? Yes.

Q. McDermott, Martin Marietta: I noticed first it was 2, then it went to 3. Is that because of increased load requirements or is it that they have gone from having 2 redundant fuel cells.

A. Gonzalez, NASA/Lewis Research Center: They've gone up for redundancy.

COMMENT

Gross, Boeing: I'd like to make a couple of comments on things that came out of our looking at this regenerative fuel cell system. There are two very interesting attributes of regenerative fuel cell systems. One is that, though I noticed in this study that you showed - you had a separate emergency power system, but, as it turns out, the regenerative fuel cell system has a very excellent capability to provide emergency power because you already have the fuel cells you already have all the hardware. All you need to do to provide emergency power is to increase the size of the hydrogen and oxygen tanks and the gasses, and this can come fairly inexpensively, and for manned space applications you can easily convince yourself that you ought to have a very large emergency power capability. The second point is that when you design the regenerative fuel cell system for high energy efficiency and for long life, you operate at relatively low current densities. Now, this allows a fair number of failures before you run into any trouble. You can merely increase the current density on the non-failed units when this happens and it can operate and tolerate a fairly large number of failures very successfully.

COMMENT

Gonzalez, NASA/Lewis Research Center: You're right. With the emergency system which was not included in this study, this requirement came from the space station office and they still haven't determined what peak emergency requirements will be. That's why they were not included. But it could be included in a fuel cell system without really increasing the weight of the system or the volume of the system too much.

Q. Orin, Ford: For the design that you're showing for the fuel cell system, you're showing that the efficiency is about 56% and there is an added heat rejection requirement. How much mass is associated with those two factors?

A. Gonzalez, NASA/Lewis Research Center: With the heat rejection requirement? I really cannot tell you.

Q. Van Ommering, Ford: How about the efficiency reduction compared to nickel cadmium and nickel hydrogen.

A. Gonzalez, NASA/Lewis Research Center: No. This is the power system only. When you go to the total energy storage system then the efficiency will play a role in it because it will affect the size of the power array system and the fuel consumption for keeping it in orbit. But this is only the energy storage system and it doesn't include any other subsystem with it. These numbers will have to be included into further studies which include the total power system instead of the energy storage system which is what this includes in it. So that's why it doesn't reflect it.

Q. Roth, NASA HQ: With regard to the technical problems that you mentioned before going through the membrane and so on - just how significant are these problems and what does it really take to resolve them so that this becomes a truly useable system?

A. Gonzalez, NASA/Lewis Research Center: It is a useable system. The SB system has gas diffusion through the membrane. This decreases the overall efficiency of the system. But, if you operate it at a low pressure like this system has been operated - up to 120 PSI then you won't really suffer any great penalty in the overall efficiency and you can still achieve your 60% efficiency of the total energy storage system. For the alkaline subsystem, the carbonation problem is with the frame materials and these are trying to be replaced. The matrix instability is already being taken care of. The asbestos is being replaced with PKT separator.

Q. Rodriguez, GSFC: Could you comment on the voltage regulation of the regenerative fuel cell perhaps in the percentage of the charge and discharge?

A. Gonzalez, NASA/Lewis Research Center: I don't understand the question.

Q. Rodriguez, GSFC: Well, does the fuel cell voltage vary as it's being charged or discharged?

A. Gonzalez, NASA/Lewis Research Center: No.

Q. Rodriguez, GSFC: It does not vary at all?

A. Gonzalez, NASA/Lewis Research Center: No. It varies with life. That's the voltage variance that you would see, less than one microvolt per hour, but not during the cycle.

ORIGINAL PAGE IS
OF POOR QUALITY

A. Rodriguez, GSFC: Thank you.

Q. Yen, JPL: You mentioned about you have this hydrogen embarkment of a nyobium phylactis. How serious is this problem and do you have any idea what is the chemical nature of this problem?

A. Gonzalez, NASA/Lewis Research Center: The seriousness of the problem, I already mentioned that, over the 40,000 hours, it didn't show up but it is known that it will happen with time. I cannot really tell you what the chemical mechanism for it is.

A. Yen, JPL: I see.

A. Gonzalez, NASA/Lewis Research Center: I can give you the contacts to find it out.

A. Yen, JPL: Alright, thank you.

COMMENT

Ford, GSFC: Just to make a couple of comments. When you're talking about advanced energy storage systems, in looking at the next ten years, one of the things that's going to become very important is not just the life but the life cycle cost. And I think just to make the point that as you think of these systems you have to look at that. If you talk about life cycle cost, you talk about the initial investment plus the cost to replace it and that replacement cost is a function of the ultimate life and one of the things that I think we've got to face is that the present systems that we've been using in the past, while they perform quite nicely for most of the applications, do not seem consistent with the long life that we are being asked to look into for the future systems. This is one of the things that prompted us to start looking elsewhere - the flywheel. Other cost factors that came out of these - and these studies are very difficult as Sid can vouch for as other people have tried to undertake these things, it's very difficult to get your arms around all these parameters and compare apples and apples. In most cases we find out the technologist in a given field advocates his technology and out of lack of total knowledge of the other areas tends to sell short the other technologies - not intentionally but just the fact that in some cases the information is not available. I think it behooves us though, to realize that we've got to look at the system aspect. We're no longer just talking about component technology as with the flywheel. The flywheel will get across at least every major subsystem. The solar array will be impacted by the round-trip efficiency, provided we use solar arrays for power generation. So a 10% loss in round trip efficiency will have significant impact on the size of the array. The size of the

Ford, GSFC (Con't): array affects the amount of fuel it takes to keep it in-orbit because of drag. What we're really saying is that we're going to have to become more system oriented rather than component technologist, which we still have to be. We're going to have to start considering the system related problem. And that's really how the future is going to be met would it be an electrolysis fuel cell, flywheel, batteries or something out there we haven't even talked about yet. So I challenge you to put on your hats and start thinking system - related problems as well as component related problems. And with that, unless there are any comments or further comments we will close this session. Are there any other comments? Would anybody like to make any additional statements at this time?

SESSION II

"LITHIUM CELL TECHNOLOGY"

Chairman: G. Halpert
Jet Propulsion Laboratory

N84
33671

UNCLAS

D3

N84 33671

CHARGE CONTROL INVESTIGATION OF RECHARGEABLE LITHIUM CELLS*

Burton Otzinger
Rockwell International

Robert Somoano
Jet Propulsion Laboratory

ABSTRACT

An ambient temperature rechargeable Li-TiS_2 cell has been cycled under conditions which simulate aerospace applications. A novel charge/discharge state-of-charge control scheme was used, together with tapered current charging, to overcome deleterious effects associated with end-of-charge and end-of-discharge voltages. The study indicates that Li-TiS_2 cells hold promise for eventual synchronous satellite-type applications. Problem areas associated with performance degradation and reconditioning effects are identified.

INTRODUCTION

Ambient temperature rechargeable lithium cells hold promise as advanced energy sources for future space applications. The Li-TiS_2 couple, with a nonaqueous electrolyte, is the best known ambient temperature system. A battery of this type is of interest due to its expected high energy density (> 100 Wh/Kg) and long life (up to 10 years). However, Li-TiS_2 cell research and technology are in an early development stage with only hand or custom made cells available. In order to further the development of this battery type and assess the state-of-the-art, a cycle life study of a Li-TiS_2 laboratory cell was conducted. The cell was developed at JPL and tested at Rockwell. This paper summarizes the results of this study.

EXPERIMENTAL

Recent cycle life tests conducted at JPL with constant current charge (1 mA/cm^2) to 3 volts and discharge (2mA/cm^2) to 1.6 volts (100% depth-of-discharge) provided up to 750 cycles with 30% of theoretical capacity remaining at conclusion of the test (see figure 1). The cathode limited cells utilized a $LiAsF_6$/2MeTHF electrolyte and were of ~ 0.40 mAhr capacity. The tests were voluntarily terminated at the 30% capacity level. Capacity decline, especially during the early stages of cycle life, and cathode deactivation were identified as important problem areas

---

*A portion of this work represents one phase of research performed by the Jet Propulsion Laboratory, California Institute of Technology sponsored by the National Aeronautics and Space Administration, Contract NAS7-918.

PRECEDING PAGE BLANK NOT FILMED

ORIGINAL PAGE IS
OF POOR QUALITY

These full charge/discharge results were so encouraging that it seemed appropriate to initiate cycle life tests that would simulate and allow evaluation of the cell for an aerospace application. It was decided to conduct the cycle life testing based on synchronous satellite discharge parameters. Low Earth Orbit (LEO) and many other aerospace applications require a capability of a one-hour or greater discharge rate. The time available for charge is at least 22.8 hours in synchronous orbit operation. It was decided, however, to charge using a taper charge method with a maximum starting current of about the 2.5 hour rate. This should produce a charge time of about four hours allowing the acquisition of four maximum depth-of-discharge (DOD) cycles per day. The taper charge parameters selected would result in full charge cut-off at 2.64 volts with approximately 10 ma charge current flowing. The maximum DOD for synchronous orbit operation is generally in the 50% to 70% range of battery rated capacity in ampere-hours. It was therefore decided to start cycling the cell at 70% DOD until the end-of-discharge (EOD) voltage decayed to approximately 1.7 volts, and then reduce the DOD to 60% until 1.7 volts is reached again, and finally reduce the DOD to 50% and cycle the cell to test termination when 1.6 volts is reached. The EOD voltage was maintained above 1.7 volts during the early cycle testing, because earlier investigation by JPL indicated that accelerated degradation takes place when the Li-TiS_2 cell is discharged to a cut-off of 1.6 volts versus 1.7 volts.

The test parameters described for the cycle test of the cell at synchronous orbit rates and typical maximum DOD are similar to those used in the battery industry for accelerated life cycling of cells/batteries. Similar cycle testing of JPL cells at Rockwell over the past two years provided data indicating that the onset of end-of-life was characterized by a reduction in taper charge current at the 2.64 volt cut-off with successive cycling and a reduction in the elapsed time for charging. The result of reduced charge time and current due to degraded charge acceptance capability was to reduce subsequent discharge capacity and EOD voltage.

It was decided to evaluate a novel charge/discharge state-of-charge (SOC) control scheme designed to overcome some of the deleterious factors leading to the degradation noted above. Where 70% DOD cycling normally takes place between 100% SOC and 30% SOC, the scheme to be evaluated positions the cycling to take place between 90% SOC and 20% SOC, and maintains that position as long as possible. After the cell SOC is established at 20%, the computer controls the SOC by restoring the ampere-hours equivalent to a 70% DOD, and then maintains the SOC range with a charge to discharge (C/D) ratio of one on a coulombic or ampere-hour basis. This approach is made possible by the fact that the Li-TiS_2 couple has a coulombic cycling efficiency close to 100%. This scheme eliminates over-charge and results in a charge completion at a voltage considerably below the 2.64 volt full-charge value. Since both over-charge and excessive charge voltage are factors associated with electrochemical degradation in cell operation, their reduction should contribute to increased cycle life.

In addition, the reconditioning value of charging a degraded cell at a low (30 hour) rate using constant current charge to a voltage cut-off was examined.

CELL AND TEST INSTRUMENTATION DESCRIPTION

The Li-TiS_2 test cell was fabricated at JPL and is an experimental prototype of their own design. The design details are described in table I.

The cycle life tests were conducted in the battery test laboratory at Rockwell, Seal Beach, California. A block diagram of the battery test station with the test cell instrumentation interface is shown in figure 2. The test cell, was contained in a steel pipe safety enclosure, and the enclosure was maintained in an exhaust hood that provided a flow of air over the test cell area to the outside of the building. The temperature of the cell was monitored on its top between the terminals and an additional thermocouple was located on the enclosure baseplate, since the bottom of the cell was in contact with the baseplate for improved heat removal.

RESULTS

Two important variables that result from the application of charge/discharge parameters to control cycle life testing are the end-of-charge voltage (EOCV) and end-of-discharge voltage (EODV). The EOCV with a fixed ampere-hour input reflects the energy level required to store the capacity selected. The ideal response would be a constant EOCV with successive cycles. An increasing EOCV with cycling indicates a capacity degradation process that results in the required voltage increase to store the fixed capacity at a greater energy level. After maximum EOCV is reached, as limited by charge control parameter selection, the capacity stored and available on the subsequent discharge decreases rapidly with further cycling. The EODV indicates the energy level at which the capacity selected for discharge is developed with a given load current. A decreasing EODV is related to degradation processess that increase polarization factors and/or decrease available capacity. Minimum operational EODV is selected based on acceptable system undervoltage and maximum depth-of-discharge degradation effects. For the purposes of this cycle life test, 1.6 volts was selected as the system undervoltage value and 1.7 volts selected as the minimum acceptable cycling voltage. An EODV value below the 1.6 volt system undervoltage limit would signal cell failure and end of the cycle life test. A history of the EOCV and EODV values obtained during the 143 cycles of the cycle life tests are shown in the data plots of figure 3. An Annotation of the Cycle Life Testing shown in figure 3 is provided in table II. The cycle life test can be considered as four consecutive parts. The first part consists of cycles 1 thru 3 where the cell capacity and 20% state-of-charge (SOC) voltage were established.

The results of cycling at 70% DOD are covered by the second part of the life cycle test, cycles 4 thru 84. The first and last cycle performance at 70% DOD is provided in the charge/discharge data plots, figures 4-7. The effectiveness of a reconditioning method consisting of a low rate, constant current charge was tried during the second part of cycling in cycles 61, 66, 72 and 73. In the cycle 61 charge, the ampere-hour return was limited to the 70% DOD value removed, and therefore accounts for the low EOCV shown in figure 3. The reconditioning charge was not successful as indicated by a lack of improvement in the cycle 61, EODV. In cycle 66 the reconditioning charge was cut off at 2.61 volts and the ampere-hour input allowed to increase correspondingly. Again, the cycle 66 discharge showed a negligible improvement in EODV value. It was decided to try two consecutive reconditioning charges in cycles 72 and 73. Since cycle 72 showed little effect with the charge voltage cut-off at 2.7 volts, it was increased to 2.80 volts in cycle 73. The result was again disappointing and testing of the reconditioning procedure abandoned. The charge to discharge ratio (C/D) in ampere-hours was increased for the first time from one to 1.015 in cycle 75 to compensate for possible degraded efficiency and thereby prevent the EODV from droping below 1.7 volts. It can be seen in figure 2 that soon after the C/D ratio increase the cell was being charged to the 2.64 volt taper charge limit. At this time the state-of-charge positioning was back to the normal 100% to 30% SOC range.

The results of cycling at 60% DOD are covered by the third part of the cycle life test, cycles 85 thru 105. The improvement in EODV in cycle 80, after a 9 hour open-circuit stand, due to a computer malfunction, led to consideration of an open circuit stand period as a "reconditioning" method. The first open circuit recondition period was tried after cycle 85 discharge. The resulting improvement in cycle 87 EODV was surprisingly good. In cycle 89 thru test completion, a one hour delay after each discharge was included to take advantage of any small reconditioning effect that might be gained.

The results of cycling at 50% DOD are covered by the fourth and last part of the cycle life test, cycles 106 thru 143. The extended open circuit stand period was tried in cycles 129 and 138 as described in table II. The reconditioning effect in cycles 129 and 138 was clearly evident, but of short duration over subsequent cycles. It is theorized that the effect is due to reduction of a temporary polarization condition in the electrolyte and/or TiS_2 plate structure due to relatively high discharge/charge current density operation.

CONCLUSIONS

The results of this cycle life study, together with those carried out at JPL, demonstrate that ambient temperature Li-TiS_2 laboratory cells can be cycled extensively. The potential for eventual use of a secondary lithium battery is very good, especially for synchronous satellite-type applications. There are certainly problems that must be solved, such as capacity decline, and scale-up/systems issues to be addressed. Our understanding of the fundamental processes and degradations modes in rechargeable lithium cells must improve substantially.

Our accelerated cycle life study, using progressive DOD decrease, 70%, 60%, 50%, has provided a good set of baseline data to be used for future test data comparison. The state-of-charge control scheme evaluated shows good promise as a means of extending cycle life, and provides, in the EOCV data, a possible graphic indication of progressive cell degradation during the cycle life test. The EOCV reflects the potential of the TiS_2 electrode, and a rapid rise is the EOCV is ostensibly due to problems at the cathode. A similar correlation between lithium transport in the cathode and capacity decline has been noted in the JPL cycle life studies (ref. 2). Low rate constant current charging as a reconditioning method is not effective. However, periods of open circuit stand after discharge may provide a reconditioning effect. The result may be due to reduction of temporary polarization conditions caused by operation at relatively high current density. Clearly, more work must be done to assess the effects of stand, self discharge, and reconditioning.

REFERENCES

1. Yen, S.P.S., Shen, D.H., and Somoano, R. B.: Elastomeric Binders for Electrodes. J. Electrochem. Soc., Vol. 130, No. 5, May, 1983, pp. 1107-1109.

2. Shen, D. H., Yen, S.P.S., Carter, B. J., and Somoano, R. B.: Lithium Diffusion in Secondary Lithium/TiS_2 Cells. Proceedings of the Lithium Battery Symposium, Fall meeting of the Electrochemical Society, Oct., 1983.

Table I

Description of JPL Li-TiS_2 Cell

Configuration	Cylindrical - plates spiral wound
Capacity:	
Analytical	0.63 Ampere-hours
Rated	0.48 Ampere-hours to 1.7 Volts
Voltage:	
Open Circuit	2.7 Volts
Load (Ave.)	2.0 Volts at C/3 rate
Number of Plates	2
Plate Area	77.4 square cm
Positive Plate	TiS_2 on Ni Exmet-Elastomeric binder (ref. 1); no conductive diluent.
Negative Plate	Li Foil pressed on Ni Exmet
Electrolyte	(1.5M) $LiAsF_6$-2Methyl THF
Separator	2 Layers of Celgard 2400
Case Material	Stainless Steel
Size	2.3 cm diameter by 6.4 cm long
Weight	85 Grams

Table II

Annotation for Cycle Life Test

CYCLE	NOTE
1	To verify full charge at 2.64 volts and obtain rated capacity discharge.
2	To verify maximum start current, charge cut-off and rated capacity.
3	To determine voltage at 20% State-of-Charge (S.O.C.) cut off.
4	To determine voltage with 70% rated capacity return to 90% S.O.C.
23	High End-of-Discharge (EOD) voltage because computer malfunction caused 9 1/4 hour open circuit period during discharge.
61	First recondition charge (0.336 A-H return at 0.015 amperes).
66	Second recondition charge (0.396 A-H return at 0.015 ampere to 2.61 volts; and 0.384 A-H discharge).
72	Third recondition charge (0.387 A-H return at 0.015 amperes to 2.7 volts; and 0.384 A-H discharge).
73	Fourth recondition charge (0.387 A-H return at 0.015 amperes to 2.8 volts; and 0.384 A-H discharge).
75	Changed charge to discharge (C/D) ratio from 1 to 1.015 (0.336 A-H to 0.341).
78	Changed C/D from 1.015 to 1.03 (0.341 A-H to 0.346).
80	High EOD voltage because computer malfunction caused 9 hour open circuit period during discharge.
85	Changed discharge from 70% depth-of-discharge (D.O.D.) to 60% with 1.035 C/D ratio.
86	First open circuit stand recondition of $85^{1/2}$ hours between Cycle 85 EOD and Cycle 86 charge.
89	Started one hour delay after each discharge and start of next charge.
106	Changed discharge from 60% D.O.D. to 50% with 1.013 C/D ratio.

Table II

Annotation for Cycle Life Test (Cont.)

CYCLE	NOTE
109	Started one hour delay after each charge and start of next discharge.
119	Changed discharge cut-off voltage to 1.6 volts from 1.7 volts.
129	Open circuit stand recondition of $18^{1/2}$ hours between Cycle 128 E.O.D. and Cycle 129 charge.
138	Open circuit stand recondition of 74 hours between Cycle 137 discharge and Cycle 138 charge.

ORIGINAL PAGE IS
OF POOR QUALITY

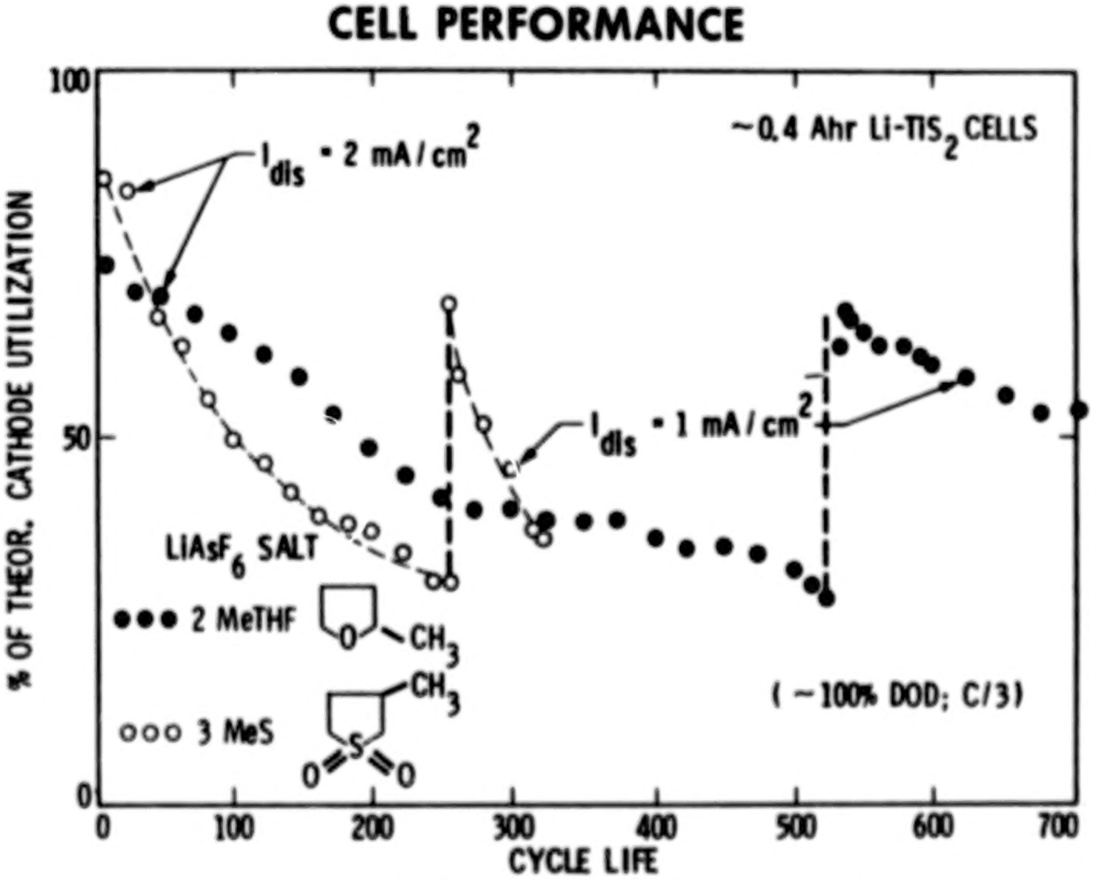

- LONGEST CYCLE LIFE REPORTED
- CAPACITY DECLINES WITH CYCLE LIFE - TWO DIFFERENT RATES
- LiAsF$_6$/2MeTHF YIELDS LONGER LIFE CYCLE THAN LiAsF$_6$/3MeS

Figure 1. Cycle life of a Li-TiS$_2$ cell.

ORIGINAL PAGE IS
OF POOR QUALITY

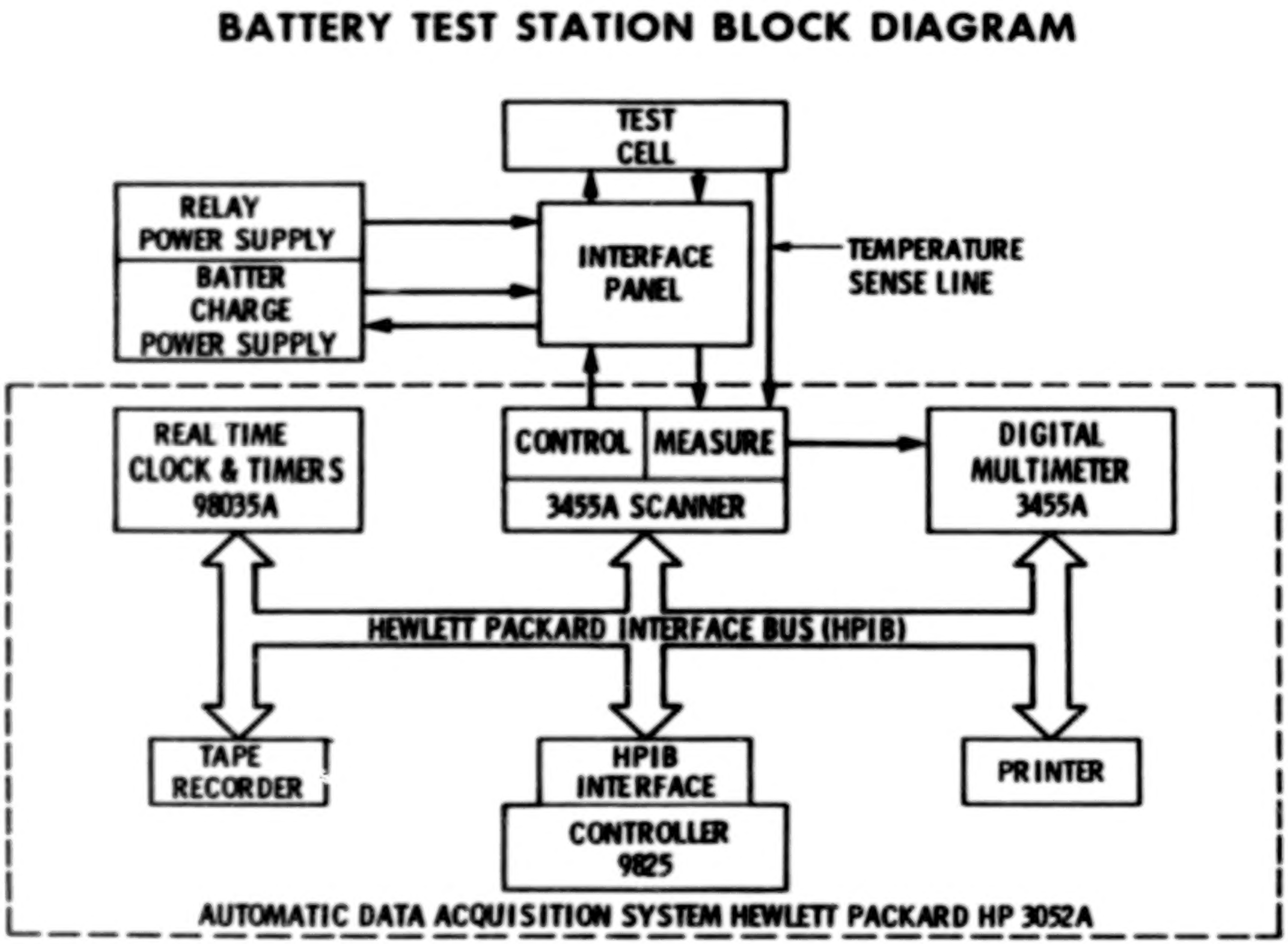
BATTERY TEST STATION BLOCK DIAGRAM
TEST CELL
RELAY POWER SUPPLY
BATTER CHARGE POWER SUPPLY
INTERFACE PANEL
TEMPERATURE SENSE LINE
REAL TIME CLOCK & TIMERS 98035A
CONTROL
MEASURE
3455A SCANNER
DIGITAL MULTIMETER 3455A
HEWLETT PACKARD INTERFACE BUS (HPIB)
TAPE RECORDER
HPIB INTERFACE
CONTROLLER 9825
PRINTER
AUTOMATIC DATA ACQUISITION SYSTEM HEWLETT PACKARD HP 3052A

Figure 2. Battery Test Station Block Diagram.

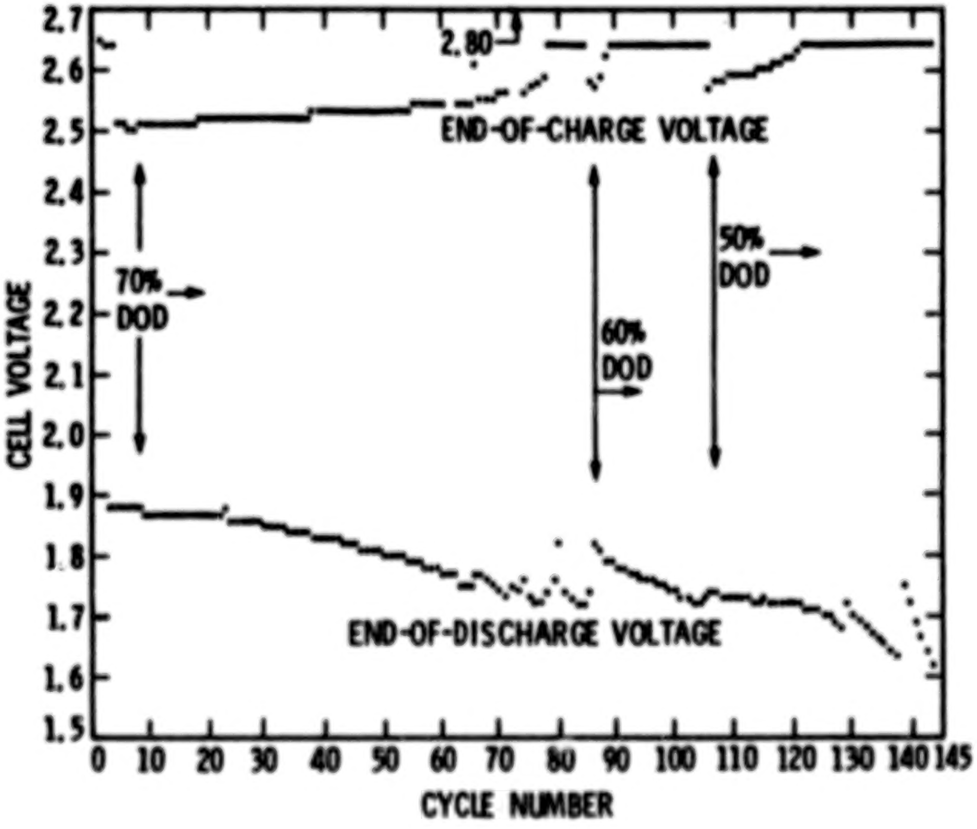

CELL END-OF-CHARGE AND
END-OF-DISCHARGE VOLTAGE VERSUS CYCLE
($Li/LiAsF_6$-2 MeTHF/TiS_2)

Figure 3. Cycle life test: End of charge and end of discharge voltage versus cycle.

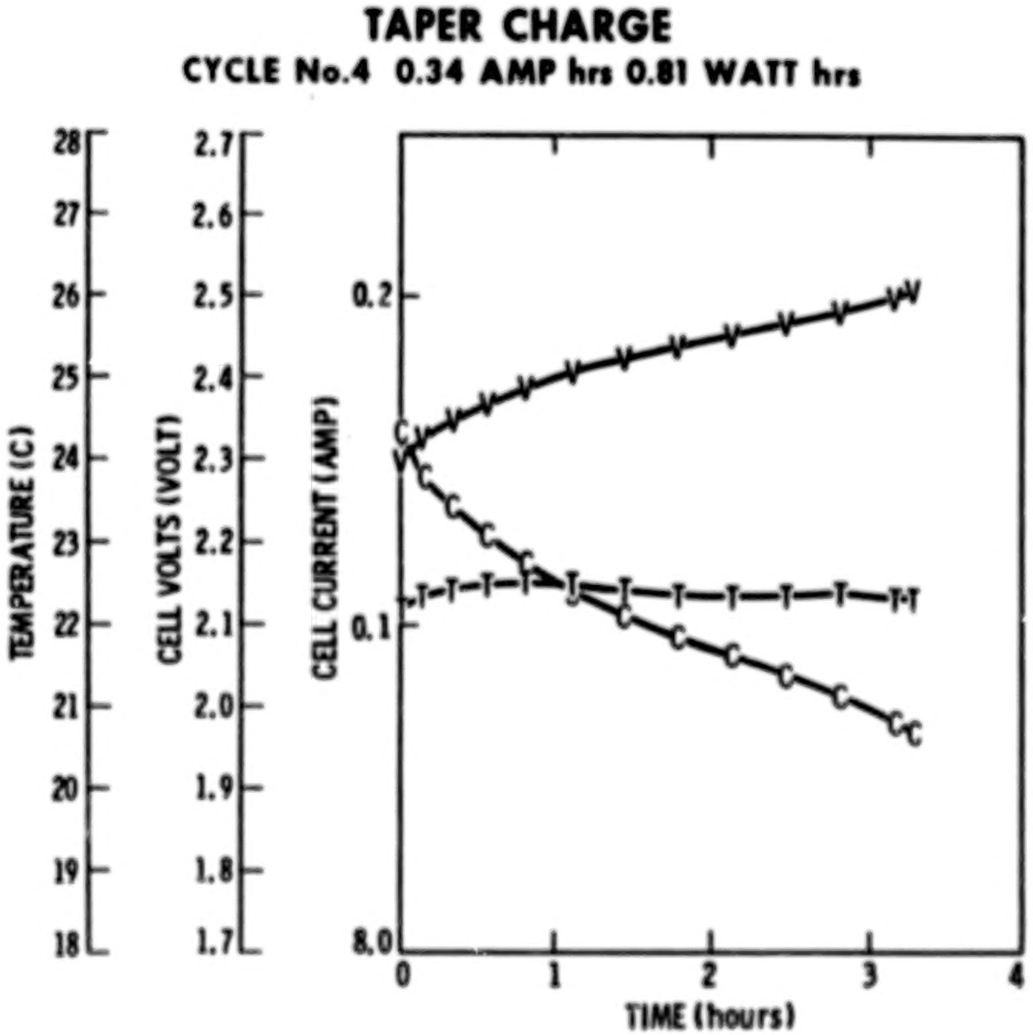

Figure 4. Charge Performance, Cycle No. Four.

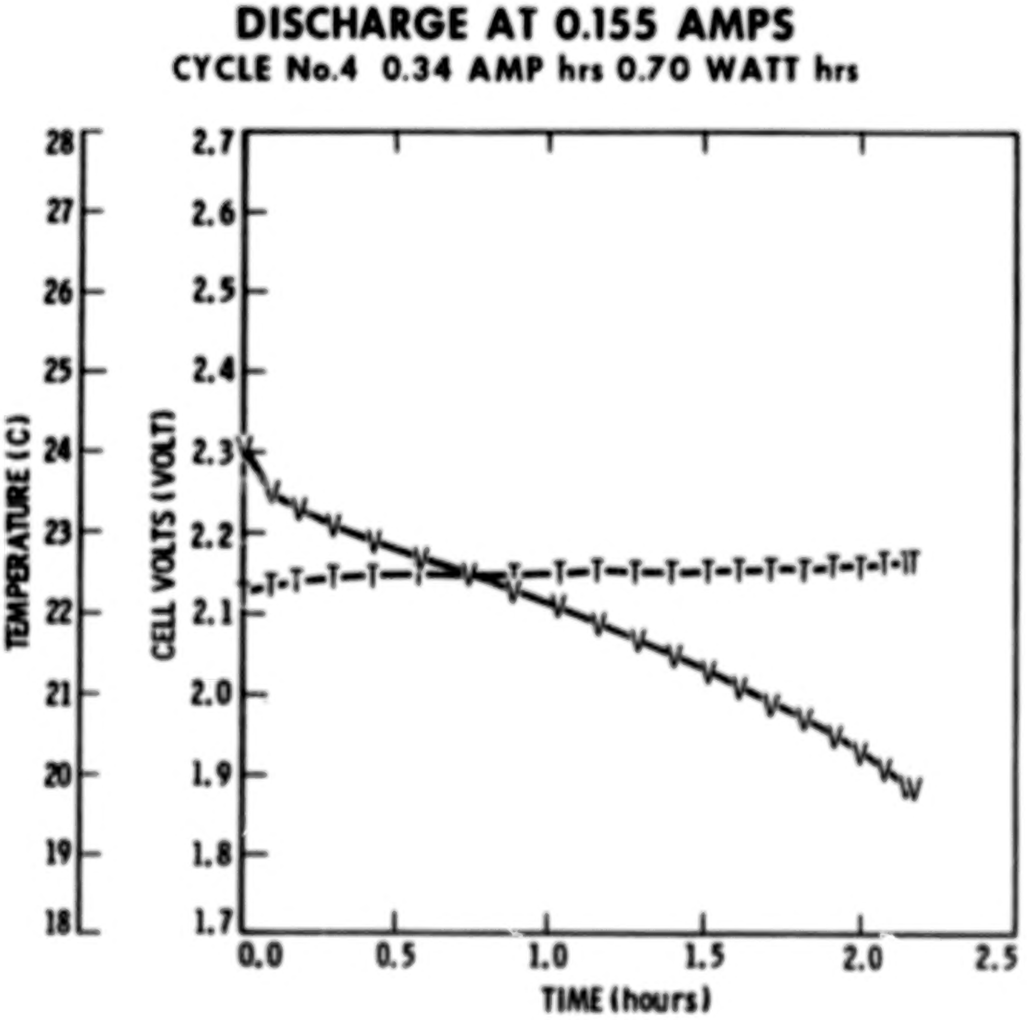

Figure 5. Discharge Performance, Cycle No. Four.

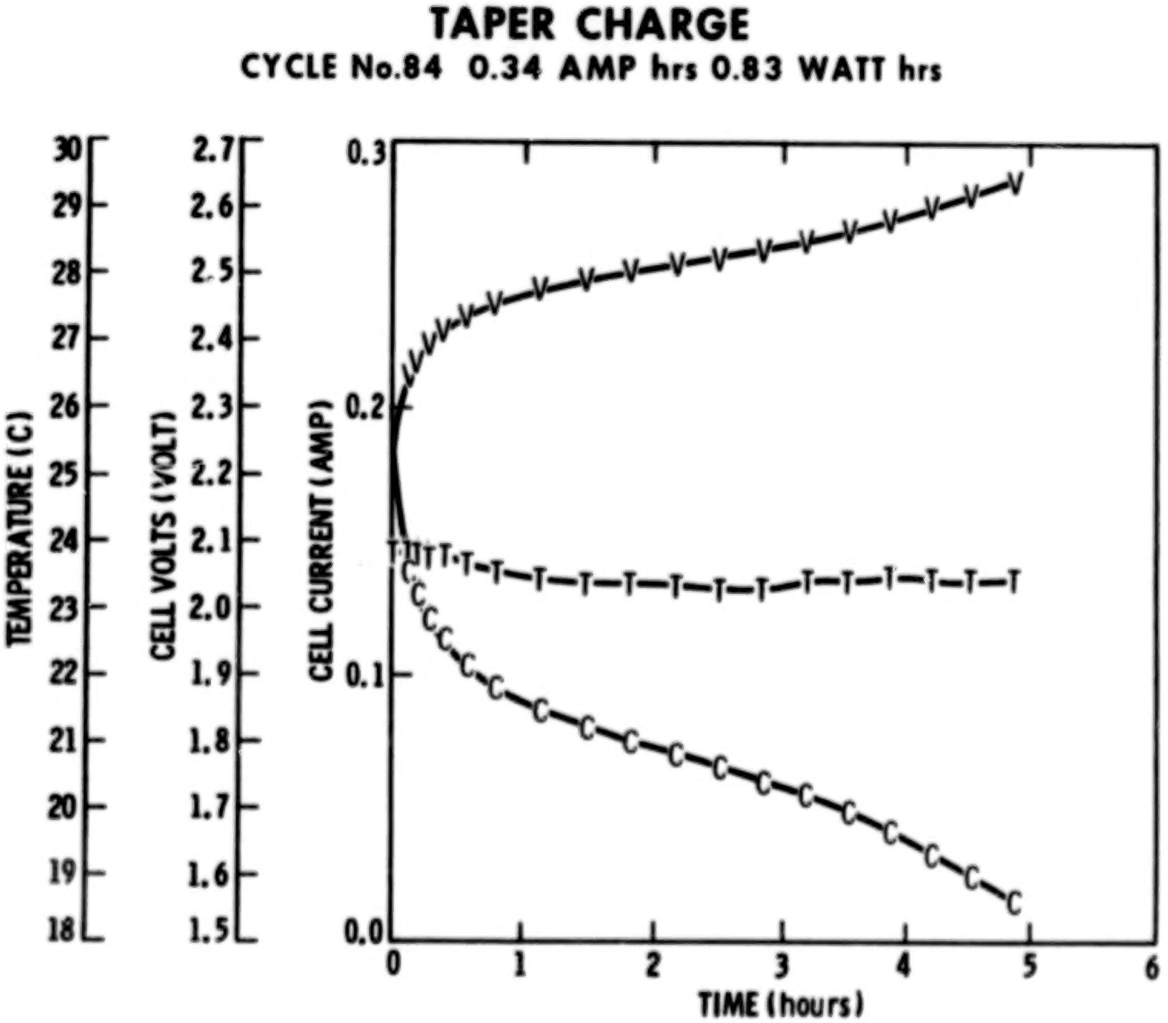
TAPER CHARGE

CYCLE No.84 0.34 AMP hrs 0.83 WATT hrs

Figure 6. Charge performance, cycle no.84.

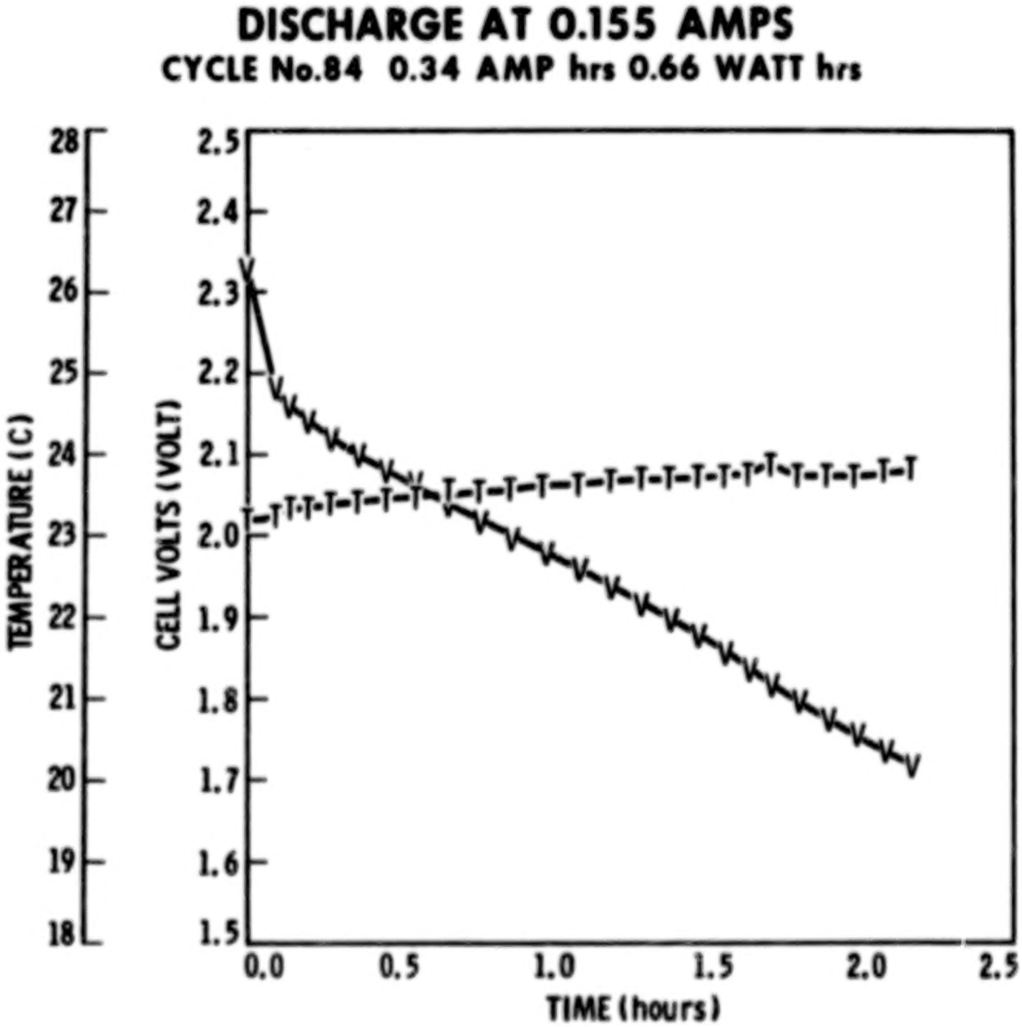

Figure 7. Discharge performance, cycle no.84.

SESSION II

DISCUSSION

Q. Ritterman, COMSAT: You mentioned, I think you showed that the area of the electrode is about 80 square centimeters and you've got a current density of 2 milliamps per square centimeter. That's not your normal geosynchronous rate of discharge as say opposed to 10 or 12 milliamps per square centimeter. You've got roughly 12 square inches of area. It'll give you half an ampere of capacity. Is that particular to this laboratory cell or is this the way lithium cells are designed?

A. Otzinger, Rockwell International: No. It's just this particular cell. I think in the future they're planning on doubling that area. They really didn't try to do that. What you're saying I guess in effect is that what we're running like a three-hour rate and for synchronous you'd like to see more like a two hour rate.

A. Ritterman, COMSAT: It's more than that. Two milli-amps per square centimeter is like I think a 410 discharge rate in NI-CD. I'm saying that probably you have to get a thicker electrode in order to make this thing feasible on the weight basis. So that your current density is lower than you would normally see. Two milliamps is lower than you'd normally see in geosynchronous discharge. It's something like 10 or 12 milli-amps per square centimeter.

A. Otzinger, Rockwell International: Well, like I said, I think that we're still early in the game and I think that it can be dealt with.

Q. Ritterman, COMSAT: Do you have any data on thicker electrodes?

A. Otzinger, Rockwell International: No.

Q. Ritterman, COMSAT: Does JPL have any data?

A. Otzinger, Rockwell International: The indication is no - by movement of the head.

Q. Galassi, Hughes Aircraft: On one of your graphs you had a change in slope on your percent cathode utilization.

A. Otzinger, Rockwell International: Yes.

Q. Galassi, Hughes Aircraft: You said you're investigating?

A. Otzinger, Rockwell International: Yes.

Q. Galassi, Hughes Aircraft: Is your cathode subject to pitting and therefore exposing more surface area causing change in slope?

A. Otzinger, Rockwell International: I think that Dr. Somoano should answer that question.

A. Somoano, JPL: When we used to use a teflon binder in our TIST cathodes yes, we had a problem with chemical integrity. Since we've been using the elastime binders the cathodes look very well. We don't see any profound pitting it all.

Q. Dudley, European Space Agency: You mentioned you had an excess of lithium in the anode. Can you tell us roughly how much this documetric excess is and whether the loss is mechanical or a reaction with the electrolyte?

A. Otzinger, Rockwell International: There is about a five to ten percent excess lithium and we think the loss is reactive with the electrolyte which is the major problem.

Q. Allvey, Saft America, Inc.: This is more of the same question actually. Your original curve showed this loss of capacity down to about 50%. And I was actually wondering whether the cathode remained the limiting effect all throughout?

A. Otzinger, Rockwell International: Yeah that's a very good question. We've taken these cathodes out of cells after several hundreds of cycles and put them in cells with fresh lithium, fresh electrolyte salt and so forth and found no improvement whatsoever in capacity. So we do think the cathode is being deactivated. However, it's very likely that problems with the lithium anode are giving rise to products that may be compromising the performance of the cathode. For example after many hundreds and hundreds of cycles we find some kind of entity permanently intercolated - irreversably intercolated in the TIS 2. And these may be some of the degradation products of the lithium electrolyte reaction.

Q. Harkness, NWSC: Bert, on your charge you mentioned on the taper charge - was it set up where the hardware was programmed as the cell voltage reached a certain point that the constant current would be stepped down? Or was that inefficiency in the power supply setting on a voltage limit to where it tapered early and then the voltage tapered on up to the charge voltage that you wanted?

A. Otzinger, Rockwell International: Let me see if I understand. We set up the taper charge parameters and they stayed in place. And then we superimposed the state of charge control parameters on top of that. And so that, when we started to go higher, eventually it got to where the state of charge of 70% we're putting in was greater than the capacity that was available in the cell - or it was getting there. And so it reached then as a final value, the constant voltage value that was set as part of the taper charge scheme. So you had really two charge control methods super imposed. We of course, would like to keep it out of control of the taper charge. We're just using the advantages of the taper charge method of putting in a relatively low rate of charge at the end, gain reducing the stress on a cell. That, of course is the one claim to fame of a taper charge. That's the only reason people do it. They can put a lot in when the cell is fully discharged and it wants to absorb a lot of charge and then put a lot less in at the end when it doesn't want to be taking a lot of charge on.

Q. Question inaudible.

A. Otzinger, Rockwell International: Okay that was the last one I showed. Cycle 84? Yeah, well I think what you're printing out is the fact when we are running out of capacity - then so, yes, you would drop down rather abruptly because you're running out of capacity.

COMMENT

Gross, Boeing: Since the purpose of this investigation was to obtain baseline information, I would think it would be worthwhile to conduct a further set of charge control investigations using lithium limited designs. For, after all, that's probably what you will ultimately want to have in a cell design, either by starting initially or eventually moving toward as a lithium electrode degrades.

Otzinger, Rockwell International: I guess we agree with you Sid.

Q. Myer, AT&T Bell Labs: We found that in order to get to anywhere near the practical densities of a lithium cell, that is higher than nickel cadmium, we had to reduce the amount of excess lithium substantially. And, under those conditions, the lithium became limiting electrode. My question is under those conditions would any of these charge control parameters be the same and do you have work in progress to look at the cycle life of the lithium electrode?

A. Somoano, JPL: That's a very good point. We've not looked at lithium limited electrodes and this is something we plan to do this fiscal year to initiate. I have no idea how the charge control procedures

A. Somoano, JPL (Con't): would be and I might mention also, for higher energy density, we need to go to something other than TIS 2. It's merely a vehicle right now to assess the state-of-the art in electrolyte problems.

N84
33672

UNCLAS

D4

N84 33672

PERFORMANCE AND SAFETY CHARACTERISTICS OF LITHIUM-MOLYBDENUM DISULFIDE CELLS

J.A. Stiles, Moli Energy, LTD

I. INTRODUCTION

Moli Energy Limited (Moli) has, during the past five years, developed a technology base that is leading to the commercialization of a new family of electrochemical batteries. These batteries utilize the phenomenon of intercalation in a lithium-molybdenum disulfide system.

The molybdenum disulfide electrode, which had been examined by other investigators and rejected as being an unlikely candidate for practical use, has been thoroughly investigated by Moli. The underlying causes of the early failures were carefully analysed and the results utilized to create modifications in the molecular structure of the material. The consequent results are dramatic improvements in the utility of the material as an electrode active material. In addition Moli has developed a practical lithium electrode, which vastly reduces the problem of limited reversibility encountered in other developmental secondary lithium cells.

The first product under development is a C cell, utilizing a sprially wound 'jelly roll' electrode configuration. The C cell, in its non-optimized developmental form, has demonstrated attractive characteristics. These include:

1. High Rate Capability

Sustained drain rates of several amperes at a cell voltage above 1.3 volts have been demonstrated.

2. Inherent Safety Below 180°C

A wide variety of electrical and thermal abuse tests have been conducted which show that the cells are resistant to venting or rupture, provided that the cell temperature does not exceed 180°C.

3. Wide Ambient Temperature Operating Range

Sustained drain rates of at least 1 ampere at a cell voltage above 1.3 volts can be maintained over the temperature range from -15°C to +75°C. Lower drain rates can still be maintained at temperatures below -15°C.

PRECEDING PAGE BLANK NOT FILMED

4. Very Low Self-Discharge

Microcalorimetric measurements indicate a charge retention time in excess of 5 years.

5. Moderately High Energy Density

Energy densities range from 72 watt-hours per kilogram for a C cell to 150 watt-hours per kilogram for larger cells scheduled for future development.

6. State of the Art Cycle Life for Lithium Batteries

A cycle life in excess of 100 cycles with an 80% depth of discharge has been demonstrated. Cycle life testing on smaller cells indicates that 600 cycles with a similar depth of discharge will be achievable with optimization of the cell design.

7. Intrinsically Low Materials and Manufacturing Costs

Cost analysis has indicated that Moli cells will ultimately be cost competitive with currently marketed rechargeable cells.

II. EXPERIMENTAL CELLS

Extensive data has been collected on small-scale, starved-electrolyte cells. Figure 1 shows a schematic representation of the cell construction. These cells were fabricated with electrode capacities per unit area and electrode spacings representative of those contemplated for full-size large cells. Cycle life tests were conducted in such a manner as to demand constant average power from a cell during every useable cycle.

A single cycle sequence entails charging a cell at constant current to a preset voltage value and then discharging it at constant current to a lower preset voltage value. Based on these tests, the cycle life is defined as the number of successive cycles that can be obtained using the defined cycle sequence until the discharge time is reduced to one-half of that of the first discharge. The depth of discharge is determined by an appropriate choice of cycle sequence parameters. Figure 2 shows charge and discharge profiles for a typical small-scale cell. Figure 3 shows discharge curves as a function of cycle number. Figure 4 shows how the defined cycle life varies as a function of depth of discharge. Finally, Figure 5 shows the realizable capacity at various, uninterrupted, constant current drain rates.

III. DEVELOMENTAL CELLS

Initial developmental work at Moli was directed towards fabrication and performance evaluation of jelly roll cells in 1/2C-size cans. These cells were fabricated using machine-produced electrodes. Figure 6 shows the delivered charge from one of these cells over 320 cycles.

More extensive data has been obtained on developmental C cells. These cells were dry-room-fabricated using machine-produced electrodes in batches of 5 to 10 cells. Considerable quantities of performance and testing data have been accumulated.

1. Performance Data

A number of performance tests on non-optimized C cells have been conducted. The jelly roll construction of these cells is shown schematically in Figure 7. Figure 8 shows typical charge and discharge curves for C cells. Figure 9 shows the cell capacity available as a function of drain rate at temperatures of 22°C (72°F) and -12°C (+10°F). Figure 10 shows the cycling performance of a batch of consecutively fabricated cells. The cells functioned for 115 cycles and 145 cycles with an 85% depth of discharge. The limited cycle life, as compared to that obtained for the small-scale, flat-plate cells, can be attributed to specific shortcomings in the C cell design and fabrication procedure. It is anticipated that cycle life can be extended substantially through improvements in the electrode design.

2. Abuse Testing Data

To date a variety of electrical abuse tests have been conducted.

Figure 11 shows the evolution with time of the current and cell surface temperature for a C cell subjected to a short-circuit test. The cell was initially at an ambient temperature of 22°C and the short resistance was 20 mΩ. The

ORIGINAL PAGE IS
OF POOR QUALITY

cell delivered current until the cell temperature reached approximately 140°C, at which time the current dropped substantially and the cell temperature began to fall again. No venting of the cell occurred.

The drop in cell current is not associated with a complete discharge; rather it is attributed to the separator porosity being substantially reduced at 140°C. Tests on other cells have revealed that the sharpness of the current reduction at 140°C is increased if the cells are insulated to minimize heat loss and at the same time reduce the temperature gradient within the cells.

The resistance of the C cells to forced discharge and to overcharge is summarized in Table 1. The tests were conducted at constant current using a fully charged cell as a reference point. Thus, a 300% overcharge is defined as that condition where a cell has received a charge equal to three times its nominal capacity beyond the normal, fully charged state. A 400% forced discharge is defined as a constant current drain until the charge extracted from the cell exceeds the nominal capacity of the cell by 300%.

The results presented in Table 1 are for cells deep cycled 10 times before they were overcharged or force-discharged. As these results show, for overcharge rates of C/3 or less and for forced discharge not exceeding 250% there was no venting with flame or ejection of cell contents. For abuse outside of these limits, ejection of cell contents or venting with flame sometimes occurred.

Table 2 shows similar overcharge and forced discharge results for cells which were first deep cycled until they lost 50% of their deliverable capacity. In this case the overcharge results were unchanged over those obtained after 10 cycles, but the cells could not be force-discharged to 250% without venting with flame. However, it was noted that venting did not occur until the cells were driven into voltage reversal to about -4 volts. A silicon diode (such as 1N4005) connected across the cells so as to limit voltage reversal to less than -1 volt was found to reliably prevent venting in these cases.

Connection of a C cell to an AC mains circuit with a 15-ampere circuit breaker caused the circuit breaker to open. Additionally, tabs within the cell vaporized to cause the cell to be open-circuited. However, there was no visible deformation of the cell.

IV. CONCLUSIONS

The lithium-molybdenum disulfide system offers attractive characteristics including high rate capability, successful operation up to 75°C, a very low self-discharge rate, a good cycle life, and safety characteristics which compare favourably to those of other lithium cells. Moreover, the materials and manufacturing costs for the system can be effectively controlled, so the cells should ultimately be competitive with currently marketed rechargeable cells.

Table 1

DEVELOPMENTAL C CELLS
(NON-OPTIMIZED)

ELECTRICAL ABUSE TESTS
CONDUCTED ON CELLS AFTER 10 CYCLES AT 20°C

	C/100 RATE	C/10 RATE	C/5 RATE	C/3 RATE	C RATE
OVERCHARGE--150%	0	0	1	1	X
OVERCHARGE--300%	0	0	1	1	X
FORCED DISCHARGE--250%	0	0	0	0	0
FORCED DISCHARGE--400%	0	X	X	X	X

0 = NO CELL DEFORMATION
1 = SLIGHT DEFORMATION OR MILD VENTING
X = VENT WITH FLAME OR EJECTION OF CELL CONTENTS
INC. = TEST INCOMPLETE

Table 2

DEVELOPMENTAL C CELLS
(NON-OPTIMIZED)

ELECTRICAL ABUSE TESTS
CONDUCTED ON CELLS CYCLED TO ½ CAPACITY AT 20°C

	C/10 RATE	C/5 RATE	C/3 RATE	C RATE
OVERCHARGE--150%	0	0	0	INC.
OVERCHARGE--300%	0	0	0	INC.
FORCED DISCHARGE--250%	X	X	X	INC.
FORCED DISCHARGE--400%	X	X	X	INC.
FORCED DISCHARGE*--250%	0	INC.	0	INC.
FORCED DISCHARGE*--400%	0	INC.	0	INC.

*WITH DIODE PROTECTION (1N4005 SI DIODE)

0 = NO DEFORMATION
X = VENT WITH FLAME OR EJECTION OF CELL CONTENTS
INC. = TEST INCOMPLETE

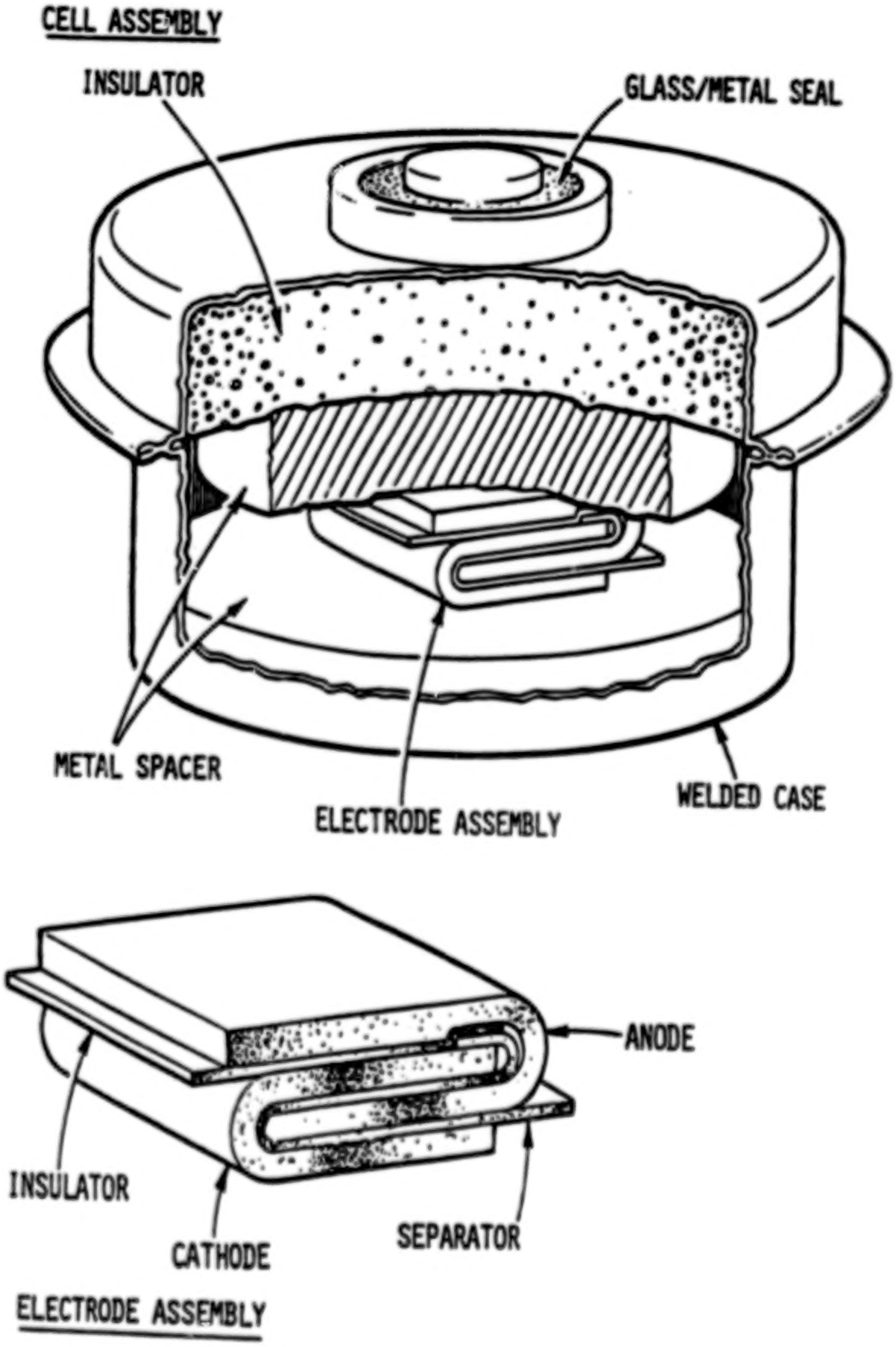
CELL ASSEMBLY
INSULATOR
GLASS/METAL SEAL
METAL SPACER
ELECTRODE ASSEMBLY
WELDED CASE
ANODE
INSULATOR
CATHODE
SEPARATOR
ELECTRODE ASSEMBLY

Figure 1.

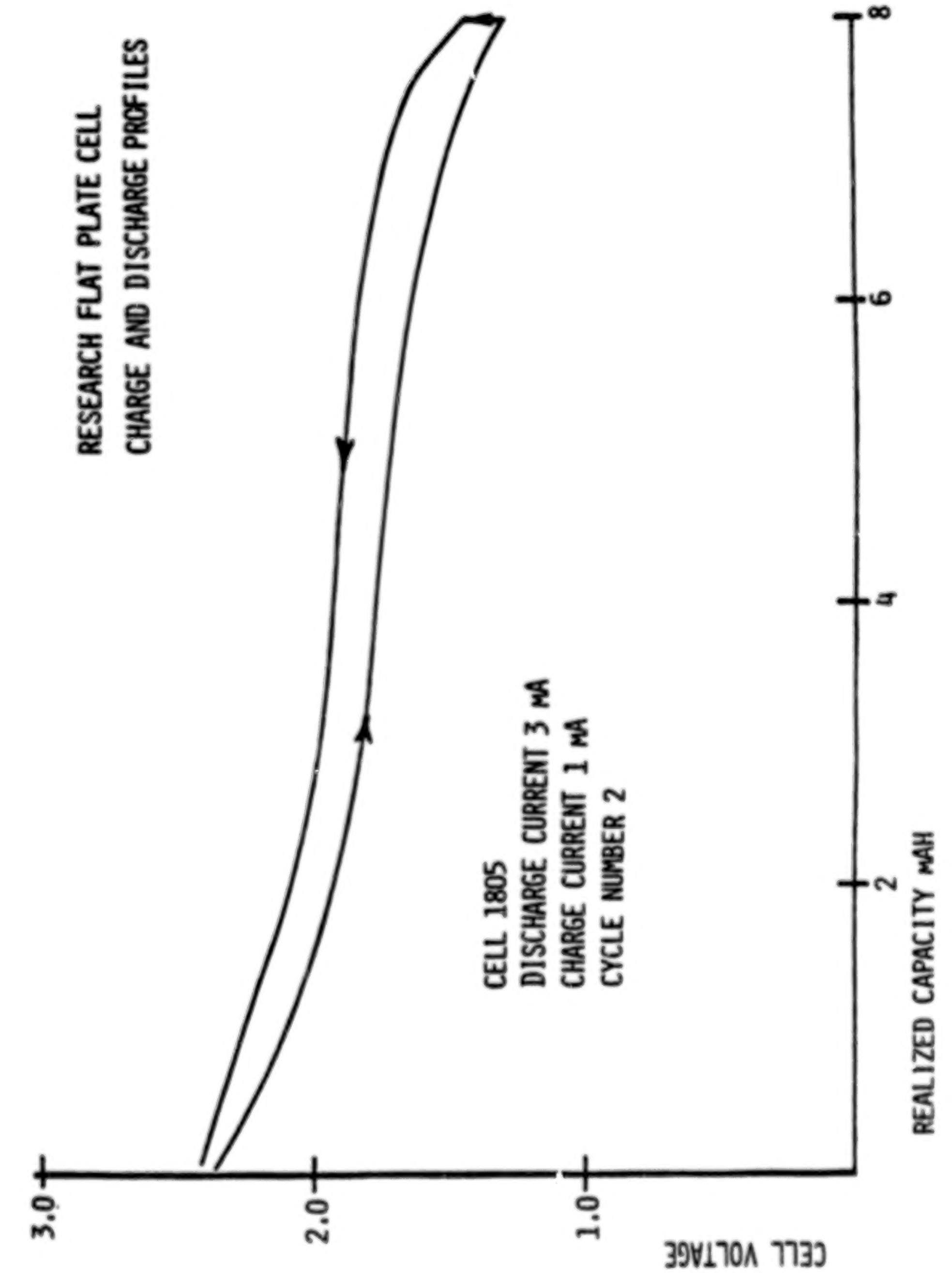

RESEARCH FLAT PLATE CELL
CHARGE AND DISCHARGE PROFILES

CELL 1805
DISCHARGE CURRENT 3 mA
CHARGE CURRENT 1 mA
CYCLE NUMBER 2

Figure 2

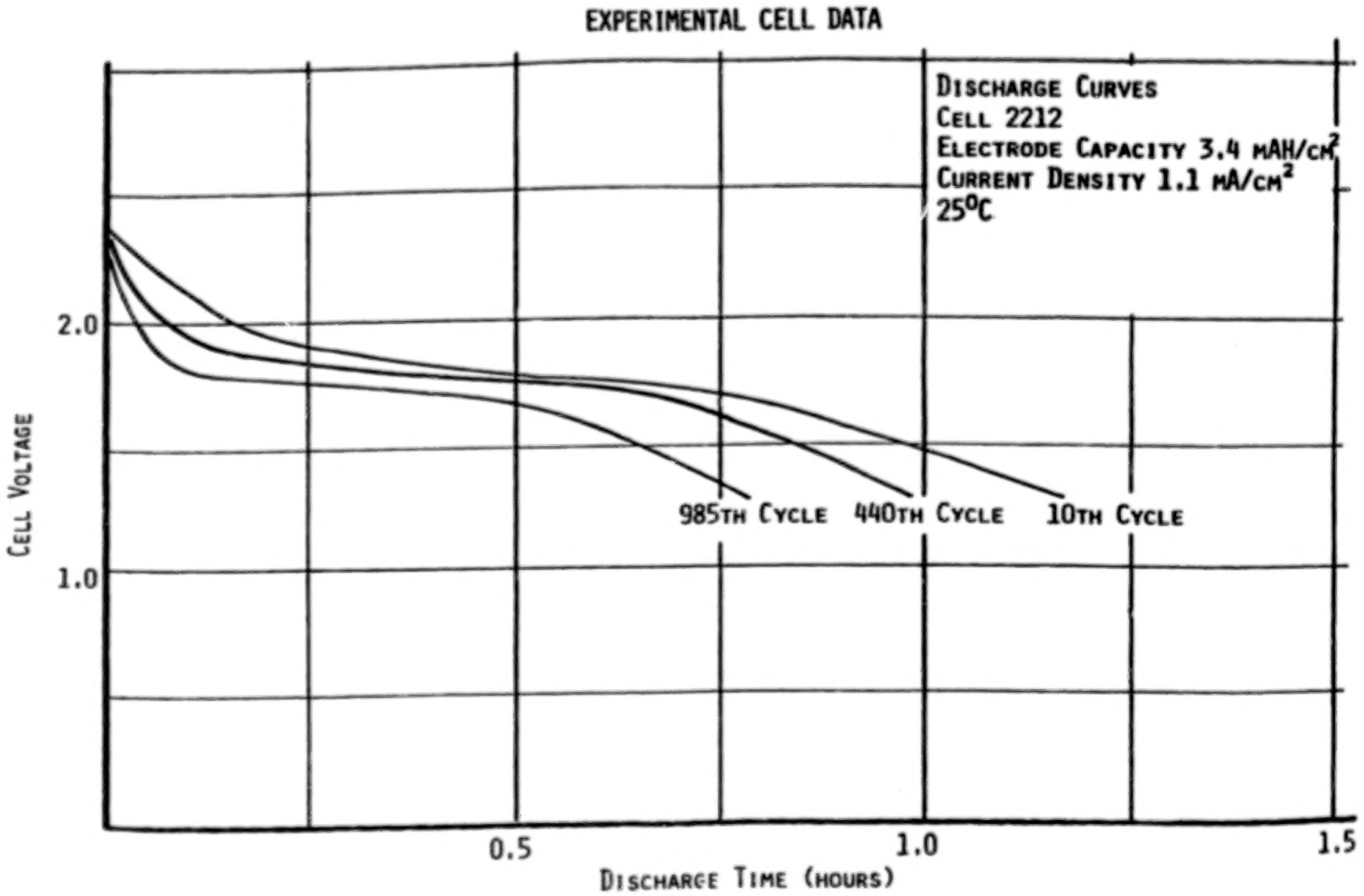
EXPERIMENTAL CELL DATA
Discharge Curves
Cell 2212
Electrode Capacity 3.4 mAH/cm²
Current Density 1.1 mA/cm²
25°C
2.0
1.0
Cell Voltage
985th Cycle
440th Cycle
10th Cycle
0.5
1.0
1.5
Discharge Time (hours)

Figure 3

ORIGINAL PAGE IS
OF POOR QUALITY

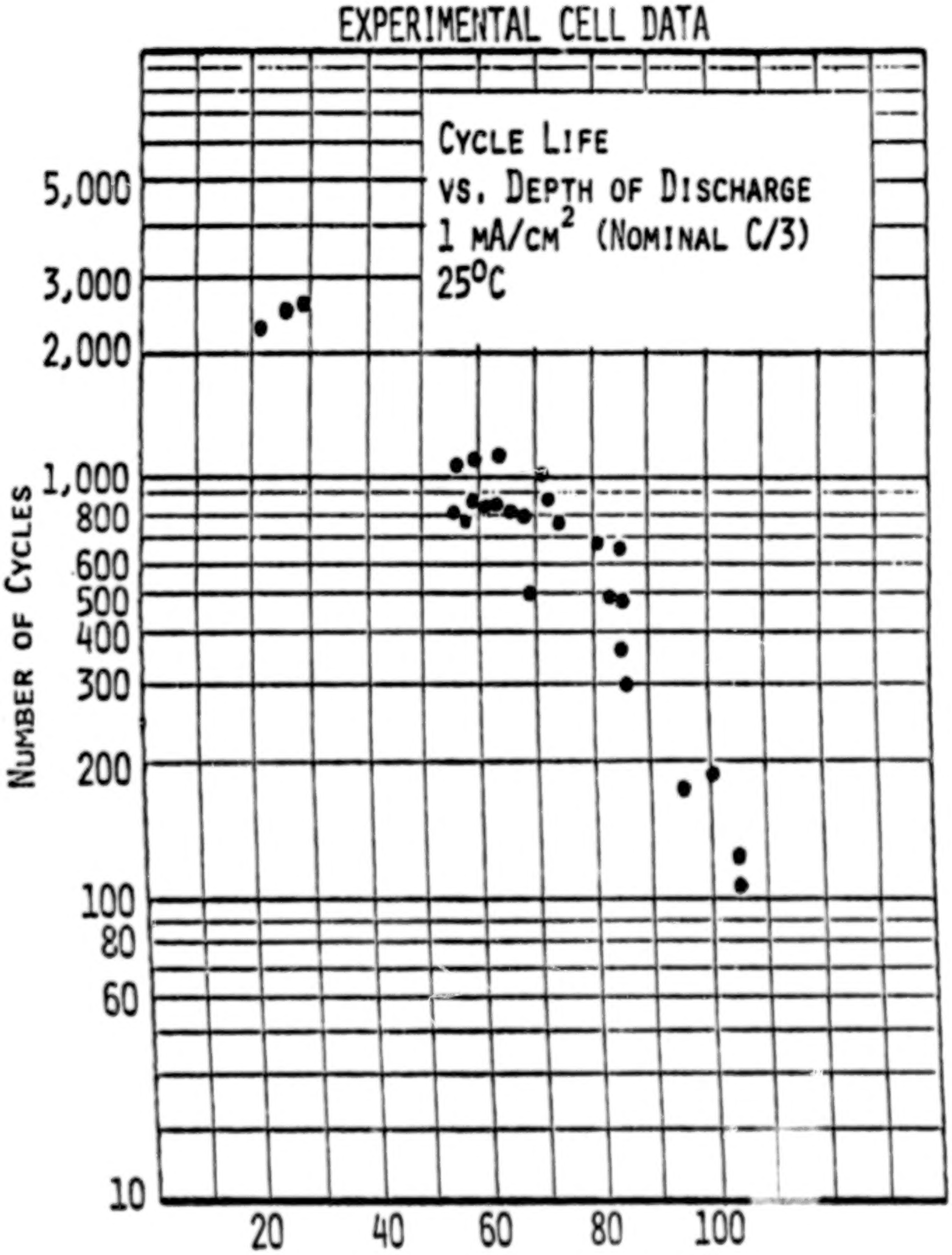

Figure 4

ORIGINAL PAGE IS
OF POOR QUALITY

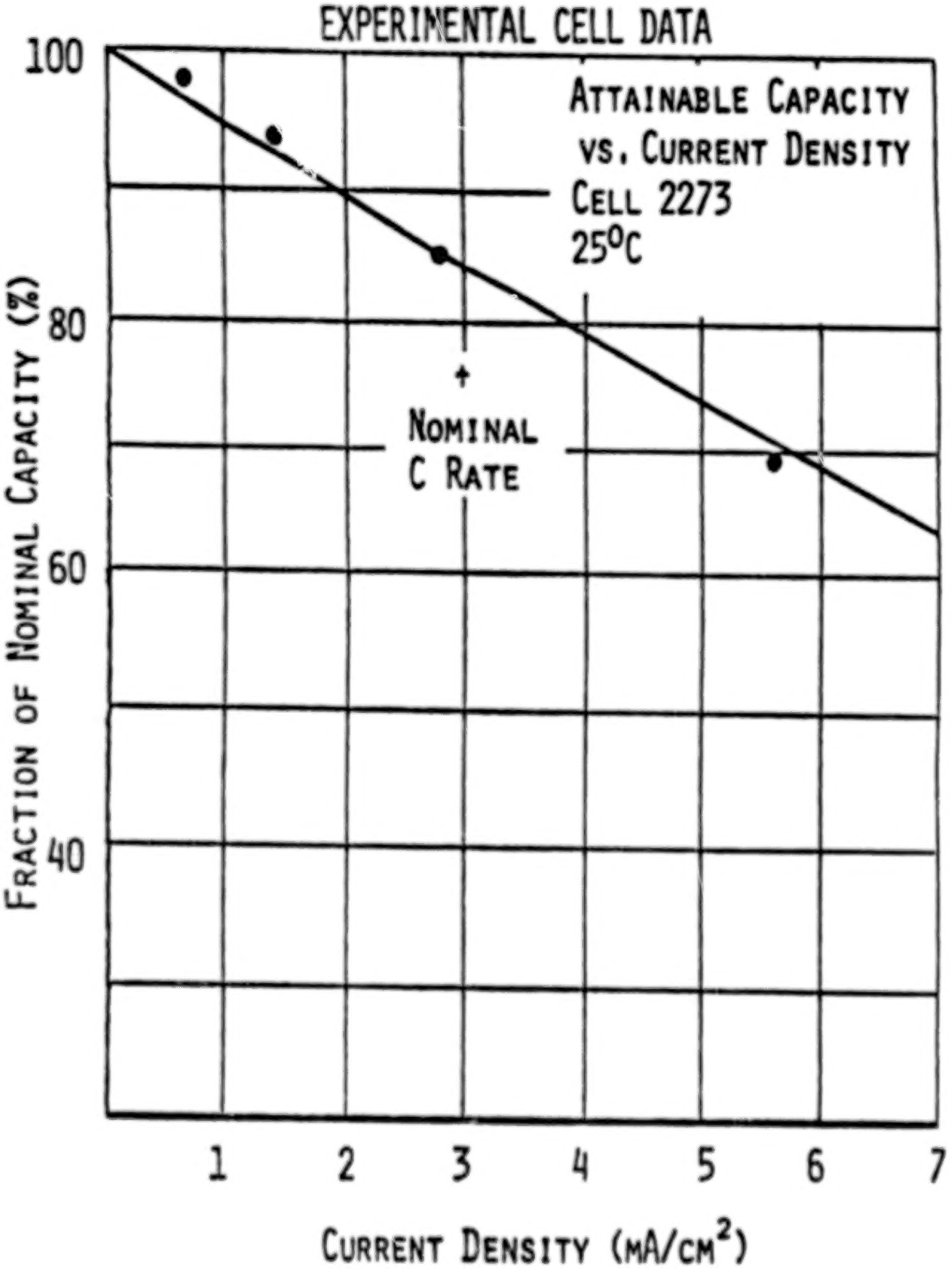

Figure 5

ORIGINAL PAGE IS
OF POOR QUALITY

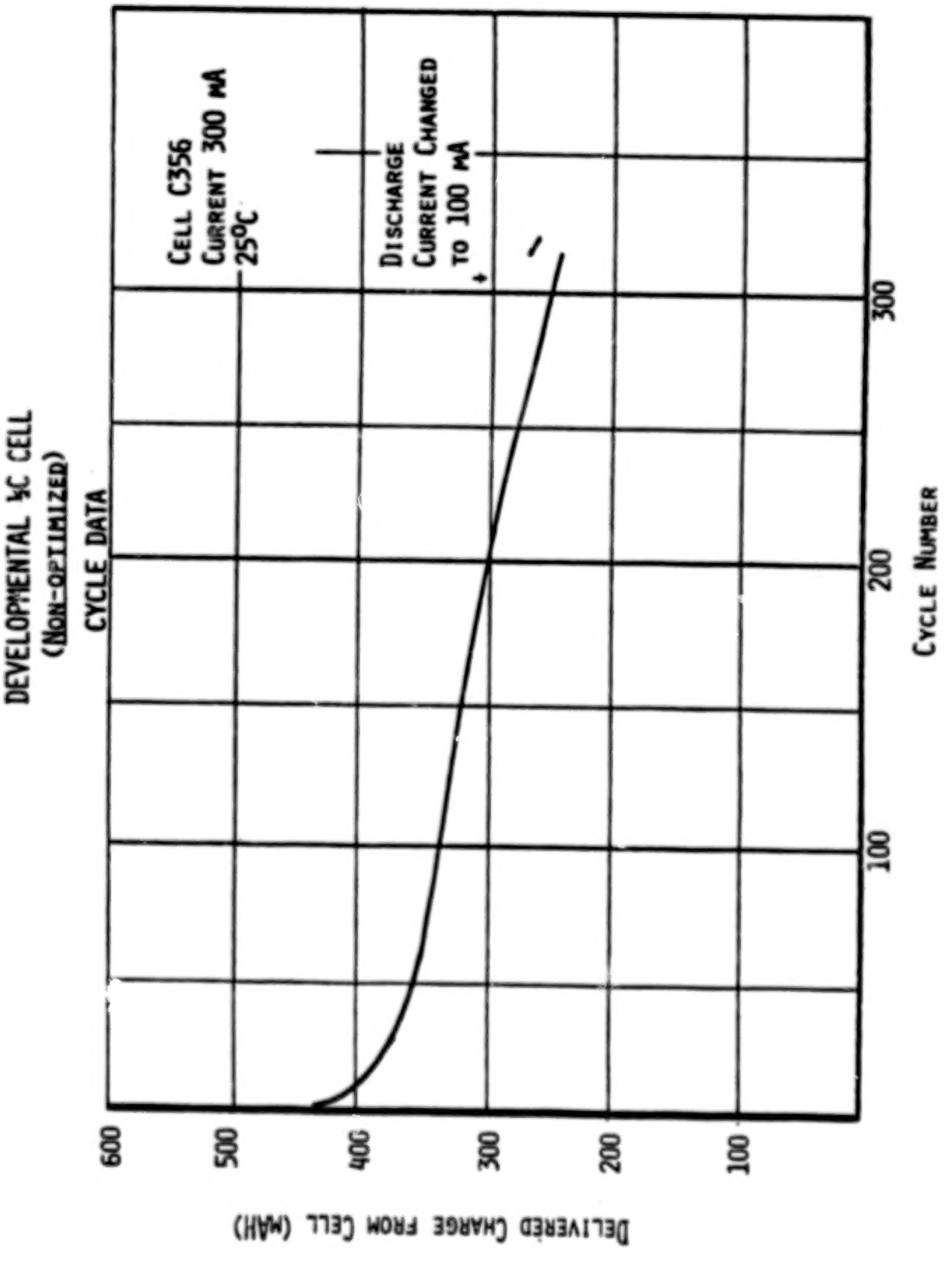

Figure 6

ORIGINAL PAGE IS
OF POOR QUALITY

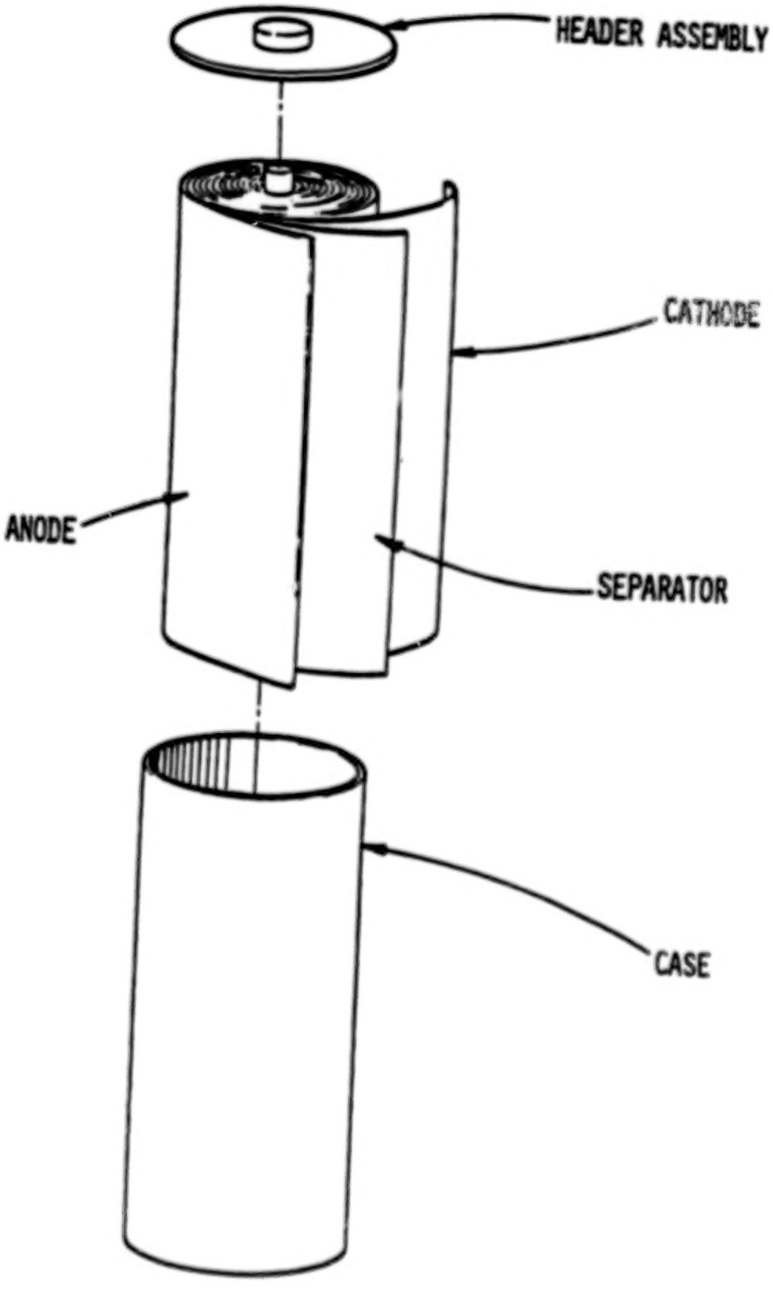
HEADER ASSEMBLY
CATHODE
ANODE
SEPARATOR
CASE

Figure 7

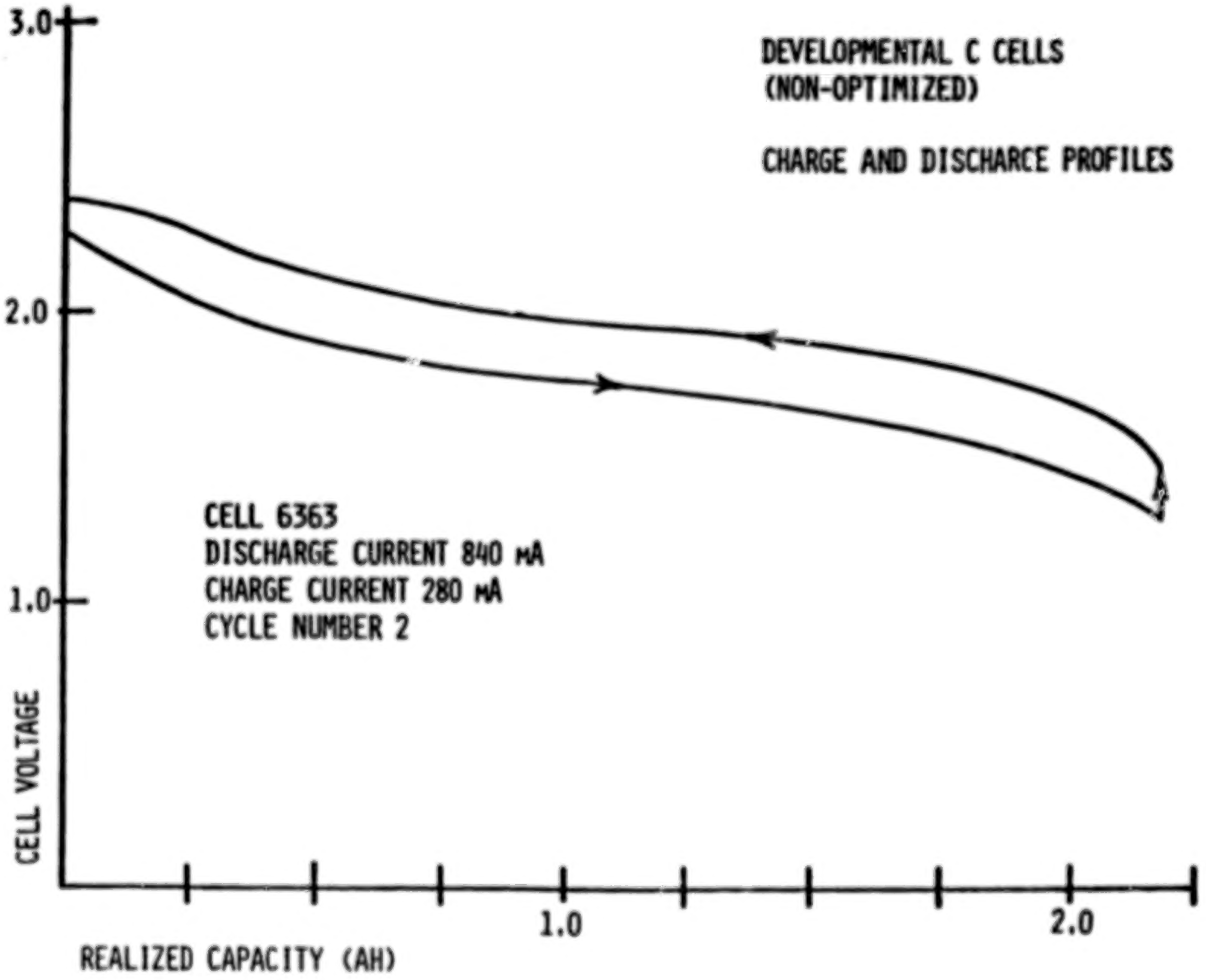
DEVELOPMENTAL C CELLS
(NON-OPTIMIZED)
CHARGE AND DISCHARCE PROFILES
CELL 6363
DISCHARGE CURRENT 840 mA
CHARGE CURRENT 280 mA
CYCLE NUMBER 2
3.0
2.0
1.0
CELL VOLTAGE
1.0
2.0
REALIZED CAPACITY (AH)

Figure 8

ORIGINAL PAGE IS
OF POOR QUALITY

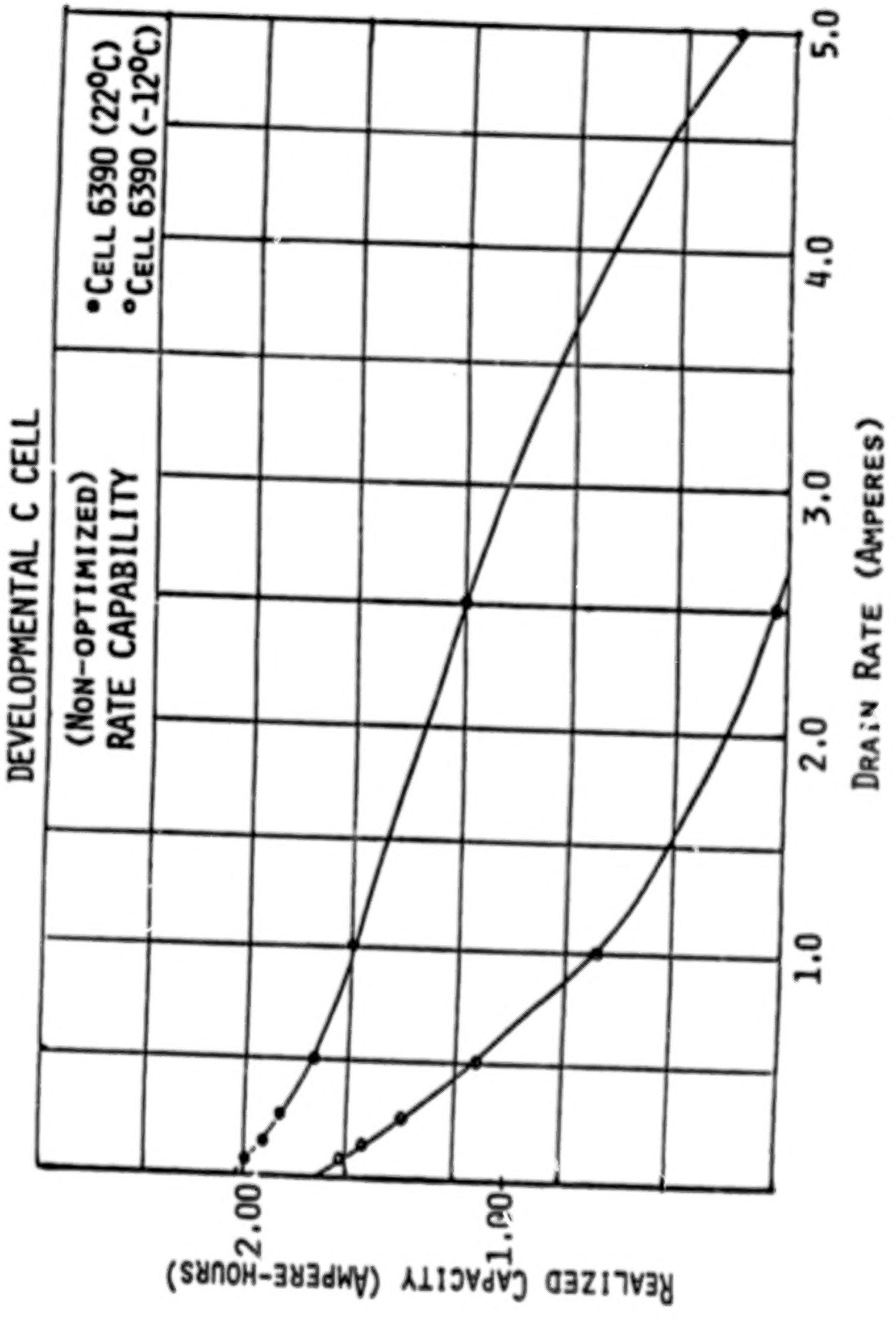

Figure 9

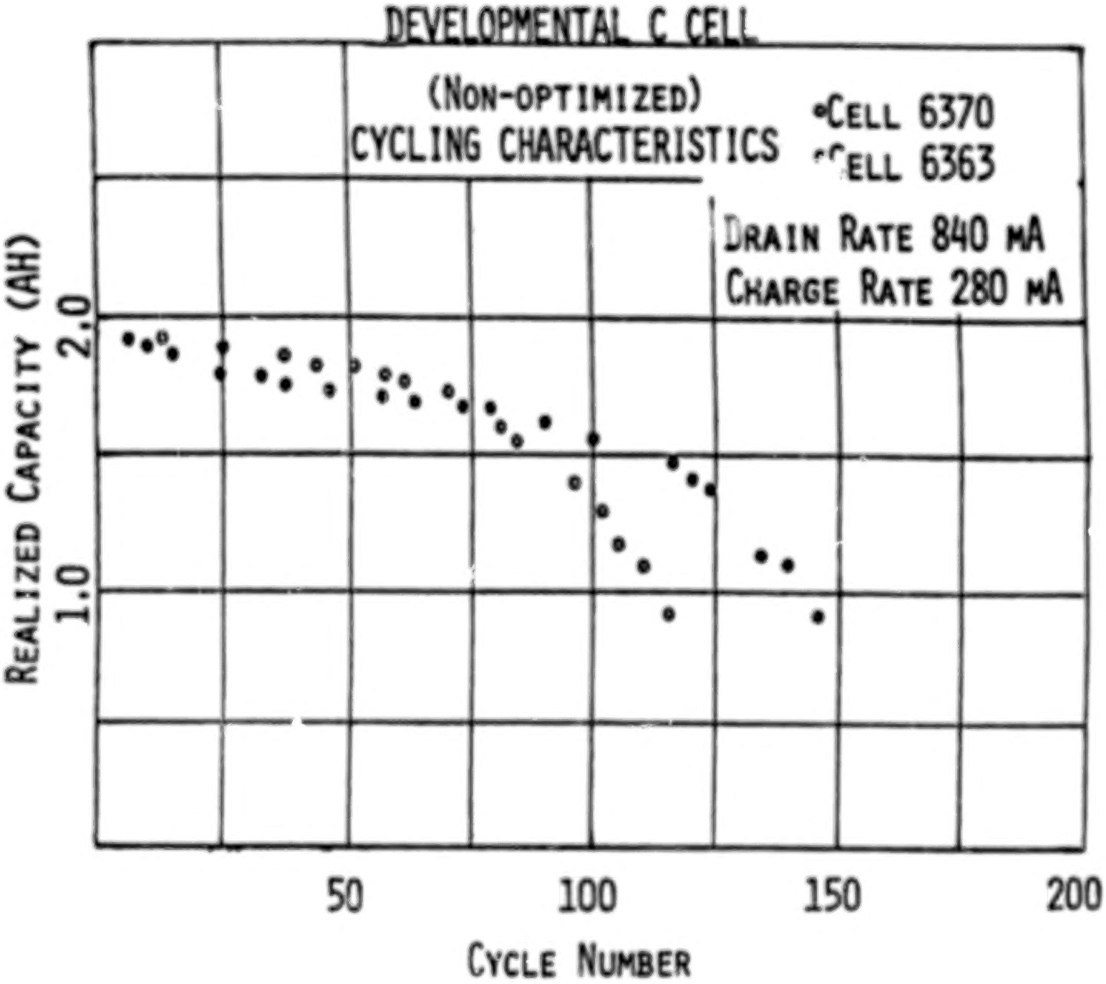
DEVELOPMENTAL C CELL
(NON-OPTIMIZED)
CYCLING CHARACTERISTICS
• CELL 6370
∘ CELL 6363
DRAIN RATE 840 mA
CHARGE RATE 280 mA
REALIZED CAPACITY (AH)
2.0
1.0
50
100
150
200
CYCLE NUMBER

Figure 10

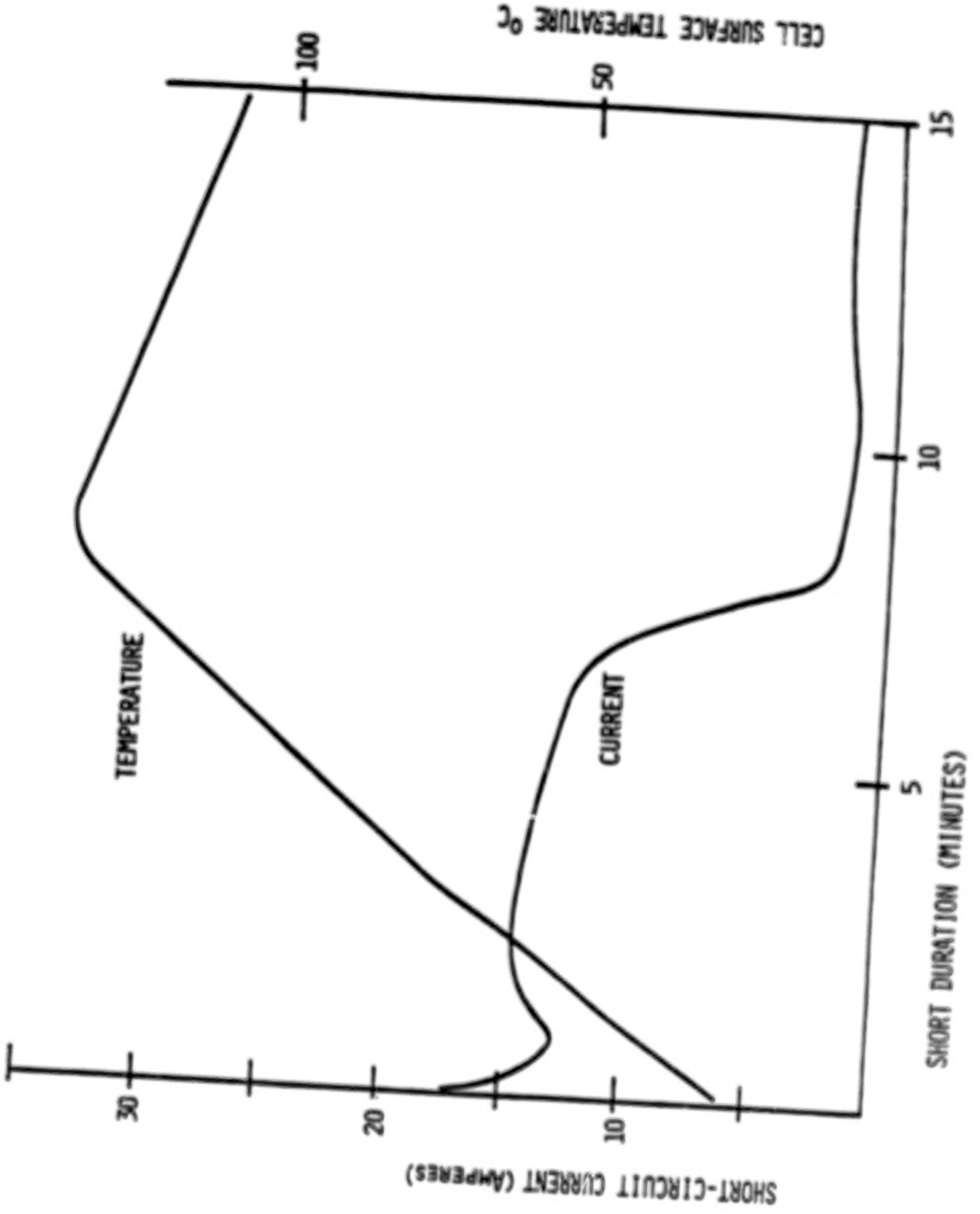
CELL SURFACE TEMPERATURE °C
100
50
TEMPERATURE
CURRENT
SHORT-CIRCUIT CURRENT (AMPERES)
30
20
10
SHORT DURATION (MINUTES)
5
10
15

Figure 11

Q. Somoano, JPL: I'd like to commend you on the progress you've made. That's some very encouraging data. Two questions: (1) Could you describe the nature of the electrolyte you used? (2) Tell us what the theoretical energy density is in terms of watt hours per kilogram and number of lithiums per many-sulfide.

A. Stiles, NPLI Energy, Ltd.: The first question I can't answer for you unfortunately. The second question - the energy density as quoted here is based on the intercolation of .6 electrons per molybdenum. It is possible to intercolate more molybdenum than that. That's rather an arbitrary figure. One could achieve a higher energy density by incorporating a larger fraction of lithium per molybdenum. However one does so at the sacrifice of cycle life and also with a wider voltage range during the discharge. One can, for example, charge all the way up to 2.7 volts and have it discharged down to 1.1 volts. If you did that you would enjoy approximately 25% increased energy density. But, as I say, you then have to accommodate the larger voltage variation and you have a penalty in cycle life.

Q. Sullivan, APL: There's two questions: (1) I'm wondering how you discharge a cell 400 percent. Is it with an external power supply? (2) You showed a slide where the short-circuit current of the battery dropped dramatically as the temperature went up and I'm wondering what the mechanism is that causes that to happen?

A. Stiles, NPLI Energy, Ltd.: The separator loses its porosity. The fusion of ions from the anode to the cathode is impeded at that temperature.

Q. Sullivan, APL: And that's designed to happen?

A. Stiles, NPLI Energy, Ltd.: Yes.

Q. Sullivan, APL: And the first one - how do you force discharge?

A. Stiles, NPLI Energy, Ltd.: With a power supply in series with the cell. With a very large voltage component so that, no matter what happens you maintain constant current.

Q. Sullivan, APL: What kind of a negative voltage do you get when you do that?

Q. Stiles, NPLI Energy, Ltd.: On the forced discharge?

A. Sullivan, APL: On the forced discharge.

A. Stiles, NPLI Energy, Ltd.: You can go up to about - 4 volts before you get a venting.

Q. Sullivan, APL: Per cell?

A. Stiles, NPLI Energy, Ltd.: The cell has a peculiar characteristic, actually. You don't actually get voltage reversal until you've discharged the cell to approximately 200-300% beyond the nominal end of discharge. So the property of the cathode prevents voltage reversals when you get out there.

Q. Yen, JPL: I have 3 questions. (1) Is your cell a lithium limited cell or cathode limited cell? (2) Do you add combative additive in your cathode? (3) I saw your cell configuration. What material is the mendral made of? Is that the cathode current collector? You know the C cell.

A. Stiles, NPLI Energy, Ltd.: I will answer the first question for now. As far as the lithium is concerned I'll just tell you that the mol ratio of lithium to molybdemum in the cell is 2½ to 1 - 2½ mols lithium to 1 molybdemum. I would rather not comment on the composition of the cathode at this stage. We do have a means of providing adequate connectivity but I'd rather not discuss how that's done. As far as the manderal materials are concerned - a wide variety of materials. It's not crucial to the operation of the cell.

Q. Yen, JPL: That is your current collector, I assume - the mandral?

A. Stiles, NPLI Energy, Ltd.: Yeah, the mandral is connected by a strip to the center terminal of the battery. The cathode is at the center terminal, potentially.

A. Yen, JPL: Well, I think even though you mentioned that there's a variety of material you can use probably some of the material may affect.

A. Stiles, NPLI Energy, Ltd.: Oh yes, you can't just use anything.

Q. Yen, JPL:: Yes, that's what I was asking. What type of current collector materials?

A. Stiles, NPLI Energy, Ltd.: I'd rather not comment right now.

Q. Kunigahalli, Bowie State College: In one of the viewgrafts I saw 3 discharge curves, depending on the number of cycles. Could you tell me whether the cells experienced the voltage degradation on the capacity degradation by virtue of increasing the number of cycles?

A. Stiles, NPLI Energy, Ltd.: When we cycled we charged at constant current and then terminated the charge when we reached 2.4 volts. Now the 2.4 volts was unchanged during the whole cycle life task.

A. Stiles, NPLI Energy, Ltd. (Con't): And we discharge the cell until the end voltage goes down to 1.3 volts. And, again, that 1.3 volts was unchanged during the entire cycle life task. So we're forcing just by the nature of the cycling regime. We're using, we're forcing the average voltage to remain constant during the test. So, in this test, there is no voltage degradation. One could cycle a cell in a different way. If you were to terminate the discharge on the basis of time, for example, rather than on voltage, one would see a lower average voltage as you increase the cycle number. But the second region we used just doesn't allow for a voltage droop.

N84
33673

UNCLAS

D5

N84 33673

CHARACTERIZATION OF OPEN CIRCUIT VOLTAGE AND CAPACITY AS A FUNCTION OF TIME

Paul W. Krehl and Russell C. Stinebring
Electrochem Industries
Div. of Wilson Greatbatch Ltd.

INTRODUCTION

Investigations were conducted to determine the effect of halogen/interhalogen addition on the performance characteristics of the $Li/SOCl_2$ inorganic system. As a result a high energy density battery system was developed: the Li/BrCl in $SOCl_2$ (Li/BCX) system.

The open circuit voltage (OCV) of the Li/BCX cell was found to be 3.90 ± .03V at 24 ± 3°C which is more than 0.2V higher than that of $Li/SOCl_2$ cells. One may speculate that the higher OCV is due to the presence of Cl_2 in solution resulting from a partial dissociation of BrCl. It was observed (ref. 1) that the addition of Br_2 in $SOCl_2$ also results in an increase in open circuit potential. The OCV of the Li/Br_2 in $SOCl_2$ cell was found to be 3.8V which is higher than either $Li/SOCl_2$ (3.6V) or Li/Br_2 (3.5V). It was speculated that the higher potential is due to the formation of a complex between Br_2 and $SOCl_2$. Similarly, a complex between BrCl and $SOCl_2$ should not be ruled out in the case of the Li/BCX cells.

Figure 1 shows a typical performance curve for fresh Li/BCX D cells discharged under a 10 ohm load. The cells exhibited a high voltage plateau during the initial stages of discharge and the load voltage decreased to a value of 3.5V after approximately 10% of the realized capacity of the cell was delivered.

During investigation into the discharge characteristics under pulsed load conditions it was observed that the open circuit potential of the cell changed as a function of delivered capacity. Figure 2 shows a comparison of the OCV and load voltage versus discharge time for cells subjected to a 0.25A constant current discharge at ambient temperature. The current was interrupted periodically so that the OCV could be determined. The initial OCV was 3.93V and decreased to approximately 3.67V after 12 hours of discharge. The load voltage profile is analogous to the OCV, i.e. the load voltage changes from 3.83 to 3.27V over the same period of time. The fall of the OCV closer to that of one expected for a $Li/SOCl_2$ cell suggests that in the initial few stages of discharge the concentrations of the more electroactive species are reduced.

Initial room temperature storage tests performed on twelve Li/BCX D cells showed that the OCV also varied with time. Figure 3 shows the relationship

C-2

PRECEDING PAGE BLANK NOT FILMED

between OCV and time over a test period of 12,000 hours. The initial OCV was 3.92 ± .02V and decreased to a value of 3.75 ± 0.03V after storage for 8,000 hours at 24 ± 3°C. This corresponds to a rate of decrease in OCV of 0.02 ± .01V per thousand hours. No additional significant change in OCV was observed after 8,000 hours. For example, the values for the OCV after 12,300 hours were still approximately 3.75 ± .03V

In a separate experiment the open circuit potential of BrCl versus Li was determined. Benzonitrile was used as supporting solvent for the $LiAsF_6$ electrolyte, and BrCl was dissolved in the solution. An open circuit potential of 3.77V was observed. This corresponds well with the observed OCV for Li/BCX cell after long-term storage.

The observed behavior of the open circuit potential of the Li/BCX cell with respect to both storage time and depth of discharge suggests that there may be a relationship between the OCV and cell performance. A test program was initiated in this laboratory to observe the effects of long-term room temperature storage on both the open circuit potential and cell capacity, and to determine if there was any correlation between the two parameters.

TEST PROCEDURE

Approximately 350 Li/BCX D cells were stored under room temperature conditions. An initial OCV measurement was taken two weeks after the date of manufacture and subsequent measurements were taken on a monthly basis. At each measurement period a group of 10-12 cells representing the full distribution of observed open circuit potentials was analyzed for capacity retention. The test cells were discharged under 10 ohm loads at room temperature. The load voltage measurements were taken through the use of a timed sequential electrometer coupled with a Hewlett-Packard (HP85) computer. The realized capacities were obtained to a 2V cutoff. The OCV was measured with a Keithley (Model 177) electrometer.

RESULTS AND DISCUSSION

A plot of the OCV versus time for approximately 350 Li/BCX D cells stored under ambient temperature conditions is presented in Figure 4. The average OCV for fresh cells (2 weeks old) was found to be 3.938. However, as the storage time increased the OCV gradually decreased until after approximately one year the average OCV was 3.783V. The results shown in Figure 4 also emphasize the variability in the open circuit potential at each specific measurement interval. Initially the open circuit voltages are grouped in a very narrow band ranging from 3.922 to 3.945 volts. However, the spread in the open circuit potential values continually increased to a range of 3.755 to 3.876 volts after one year of storage at room temperature. Comparing the data obtained from the original Li/BCX D cells stored for 12,300 hours to that obtained in this investigation, it may be speculated that the spread in the OCV values may begin to narrow as the actual open circuit potentials level at approximately 3.75 volts.

After each OCV measurement was taken, twelve samples were selected for rundown so that the original OCV distribution observed in the D cell population was not distorted. The cells were discharged under a 10 ohm load at room temperature. The results of the constant load discharge are presented in Figure 5. For fresh cells discharged under 10 ohm loads very little variability in realized capacity exists (14.45 ± 0.45 Ah). However, cells subjected to longer storage periods exhibit a lower realized capacity and a greater variability in cell performance. For example, the average realized capacity for cells stored 7 weeks was approximately 13.2 ± 1.5 Ah. The capacity for cells discharged after a storage period of 26 and 51 weeks showed a slight decrease in capacity (13.1 ± 1.4 and 12.4 ± 1.3 Ah respectively), but were not significantly different from the cells discharged after 7 weeks.

These test results show that both the cell open circuit voltage and cell capacity decrease with increasing storage duration. However, no correlation was immediately evident between the two parameters. The OCV and discharge data shown in Figures 4 and 5, respectively, were compared at individual time intervals to determine if the realized capacity was a function of the observed OCV. It was noted that cells that exhibited open circuit voltages at the extreme ends of the observed range could deliver nearly identical capacities. For example, cells stored for a period of 30 weeks showed a range in OCV of 3.914 to 3.790 volts. A particular cell that exhibited an OCV of 3.79V delivered 13.8 Ah to a 2.0V cutoff. Similarly, a cell with an OCV of 3.89V delivered 13.4 Ah.

Examination of a plot of OCV versus cell capacity (Figure 6) shows that in general cell capacity data is scattered over a wide range of open circuit potentials. It can be seen that cells with an OCV of 3.90V produced capacity values between 14.6 and 11.5 Ah. Similarly, cells with an OCV of 3.80V exhibited a range in realized capacity of 13.8 to 11.7 Ah.

SUMMARY AND CONCLUSIONS

It is noted from the data presented above that Li/BCX cells lose approximately 8% of their rated capacity in the first 2 months of storage. After this period of time, little difference is noted in the average realized capacity; however, a significant increase in the range is observed. Over the same period of time the OCV falls at a rate of 0.02V per 1,000 hours. After a period of 8,000 hours the OCV appears to stabilize at a value of approximately 3.75V. This may be related to changes in Cl_2 concentration due to self-discharge or other reactions. These data indicate that no correlation exists between the reduced open circuit voltage and the realized capacity.

REFERENCES

1. C. C. Liang, A New High Energy Density Lithium Battery System, Digest of the Combined 12th Int. Conf. on Medical and Biological Engineering and 5th Int. Conf. on Medical Physics, Part I (Aug. 1979) Paper 1.6.

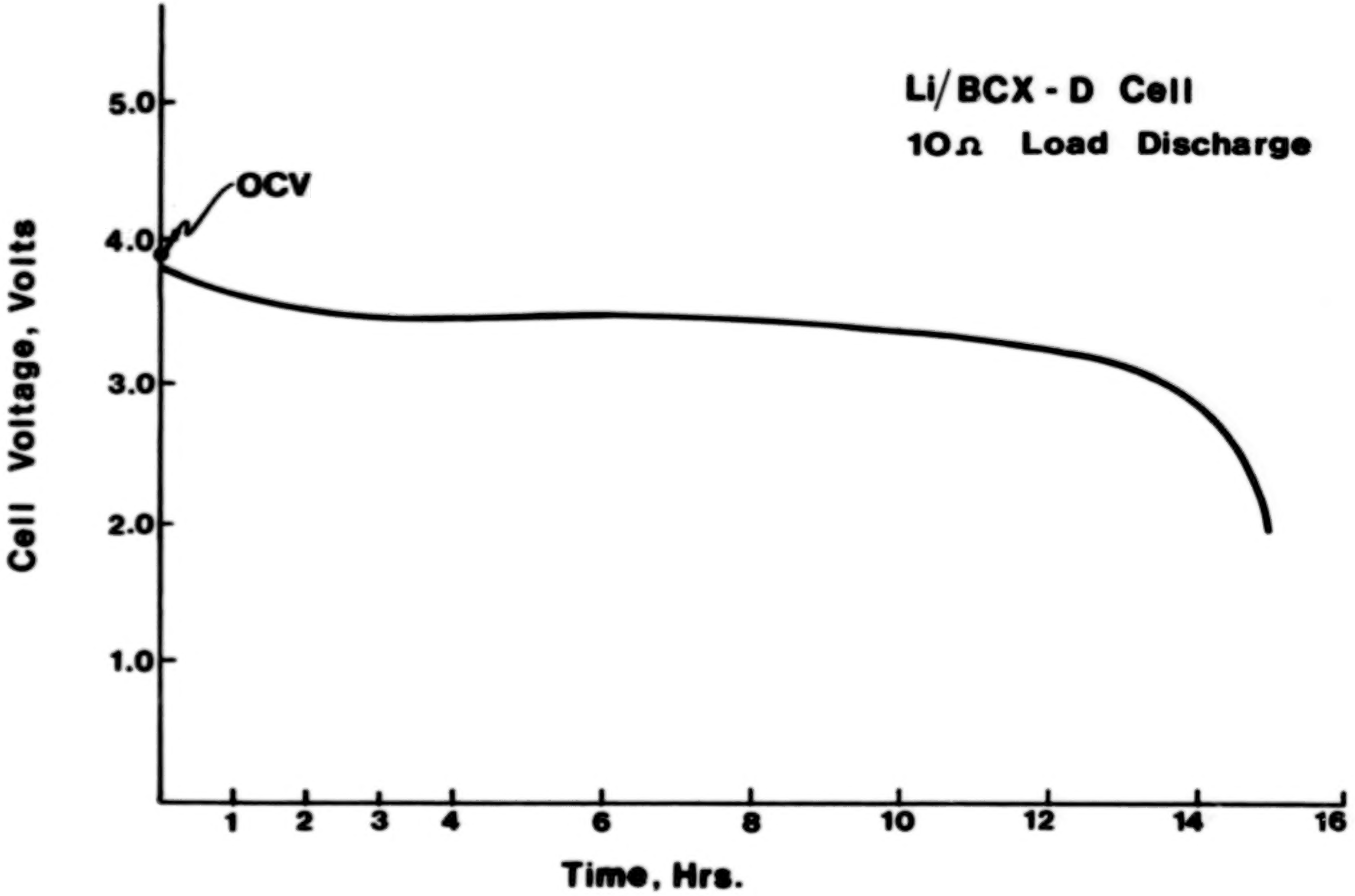

Figure 1. Typical constant load discharge characteristics for fresh Li/BCX D cells at room temperature.

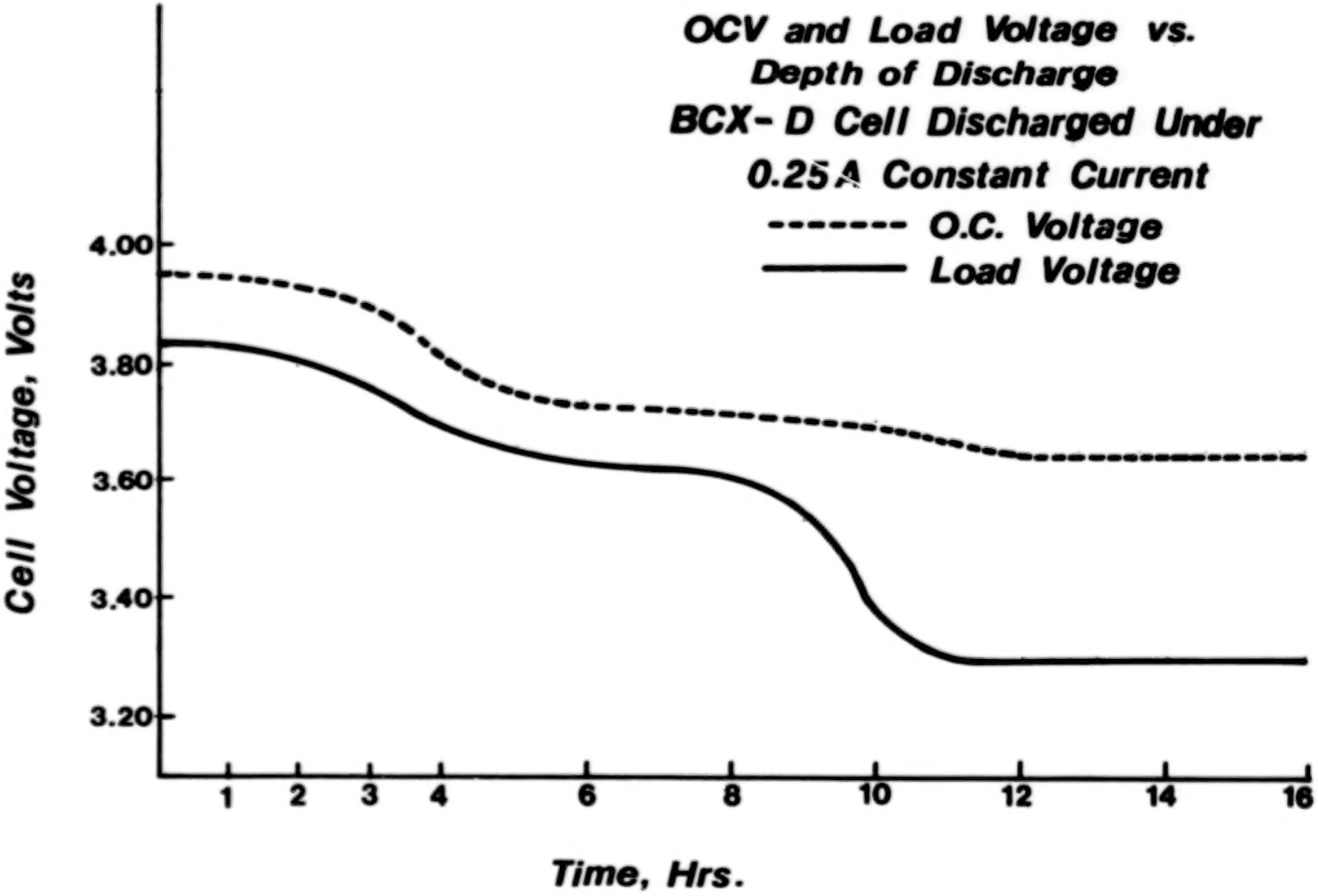

Figure 2. Comparison of the OCV and load voltage to discharge time under 0.25A constant current conditions.

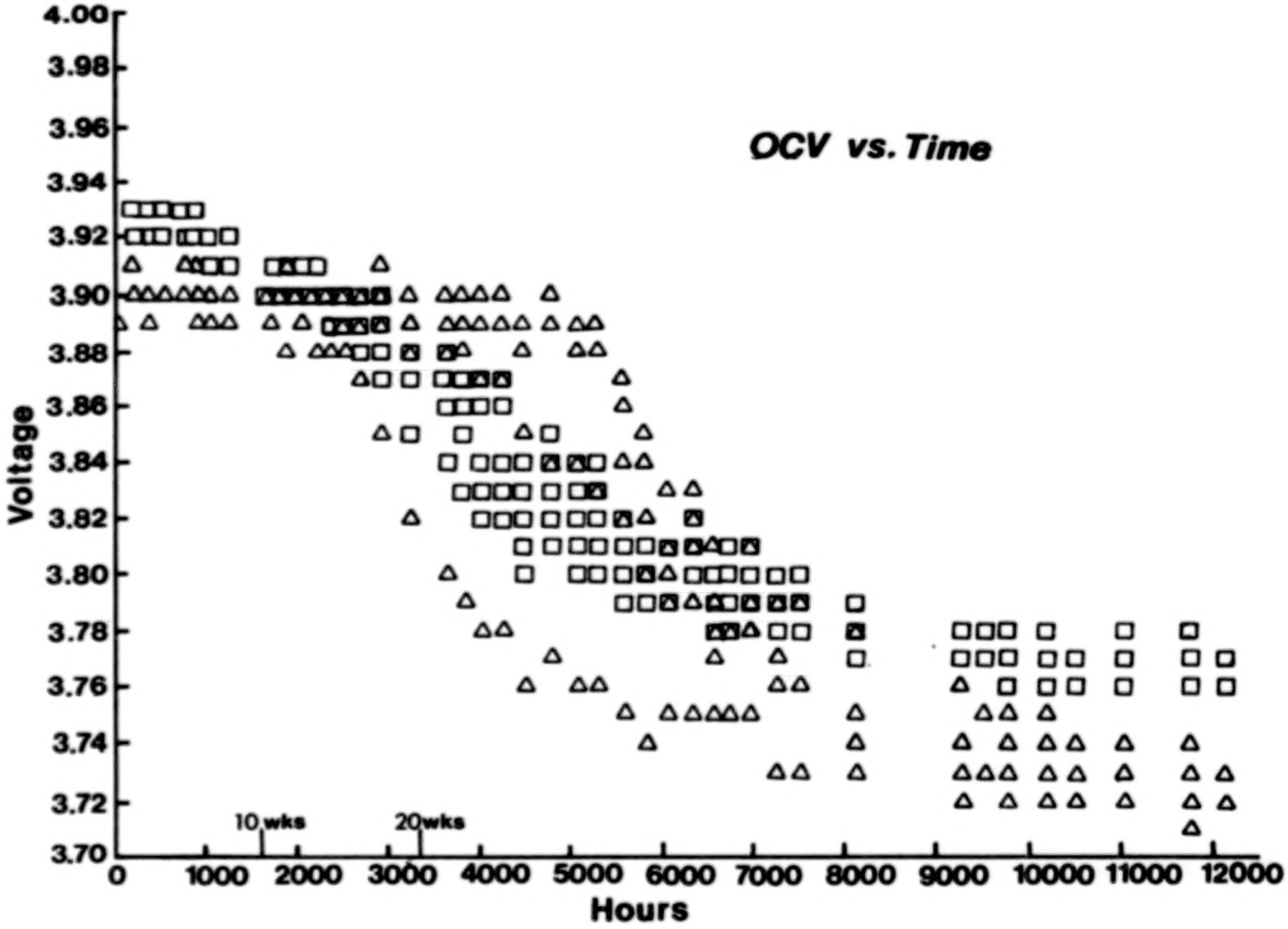

Figure 3. Comparison of the OCV to time under room temperature storage conditions.

ORIGINAL PAGE IS
OF POOR QUALITY

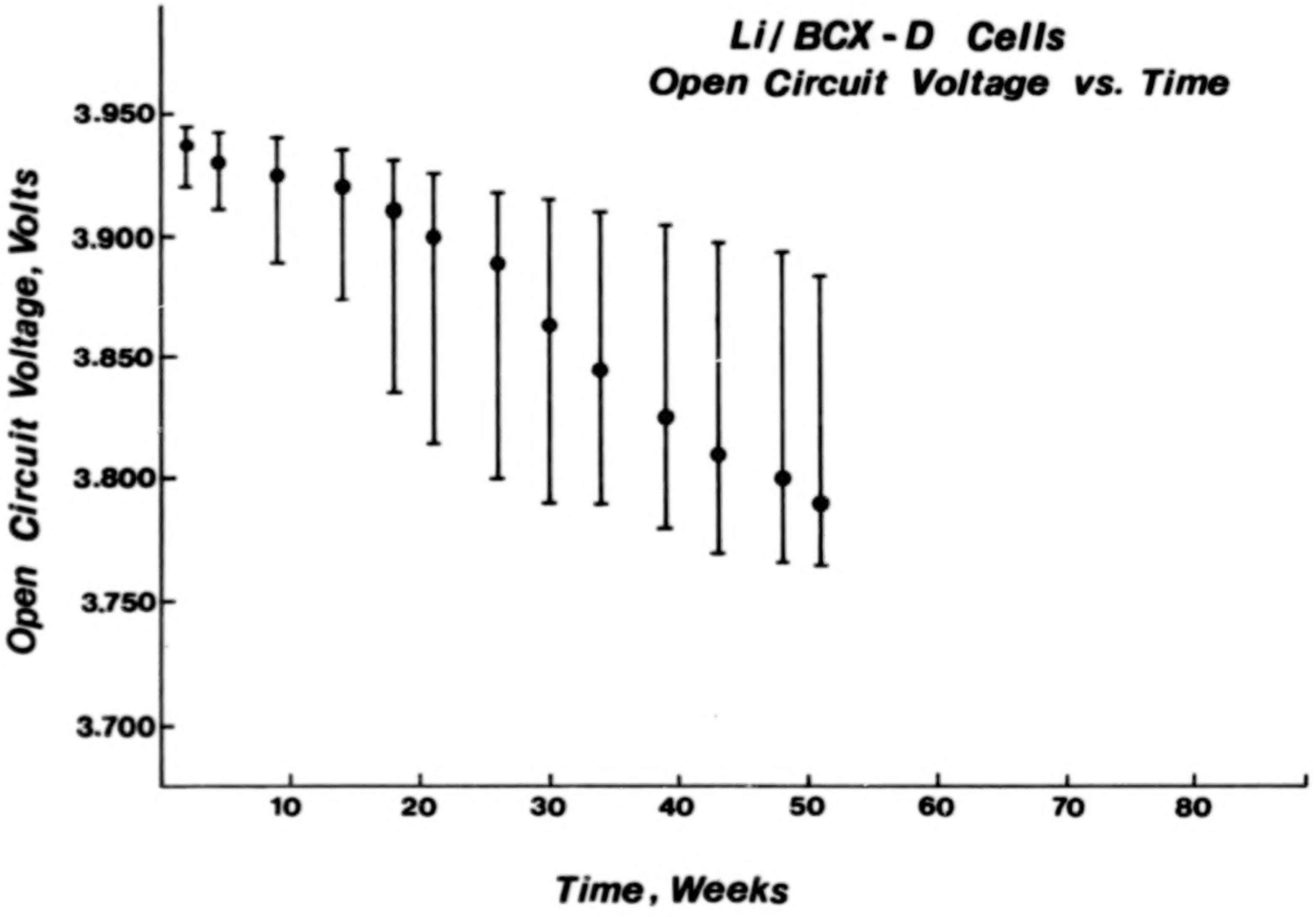

Figure 4. The average and range of measured open circuit potentials as a function of storage time.

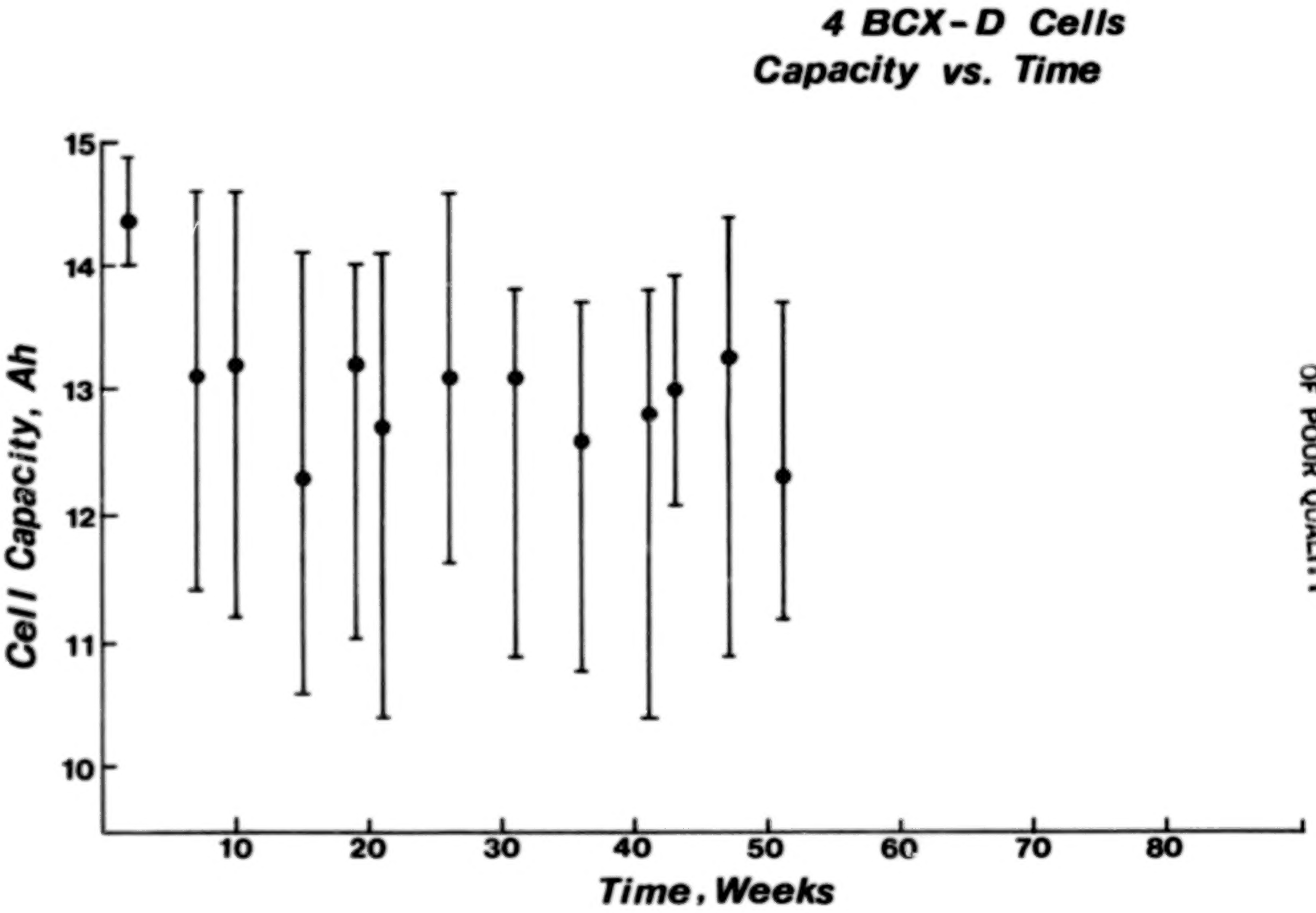

Figure 5. The average and range of realized capacities of cells discharged under 10 ohm loads as a function of storage time.

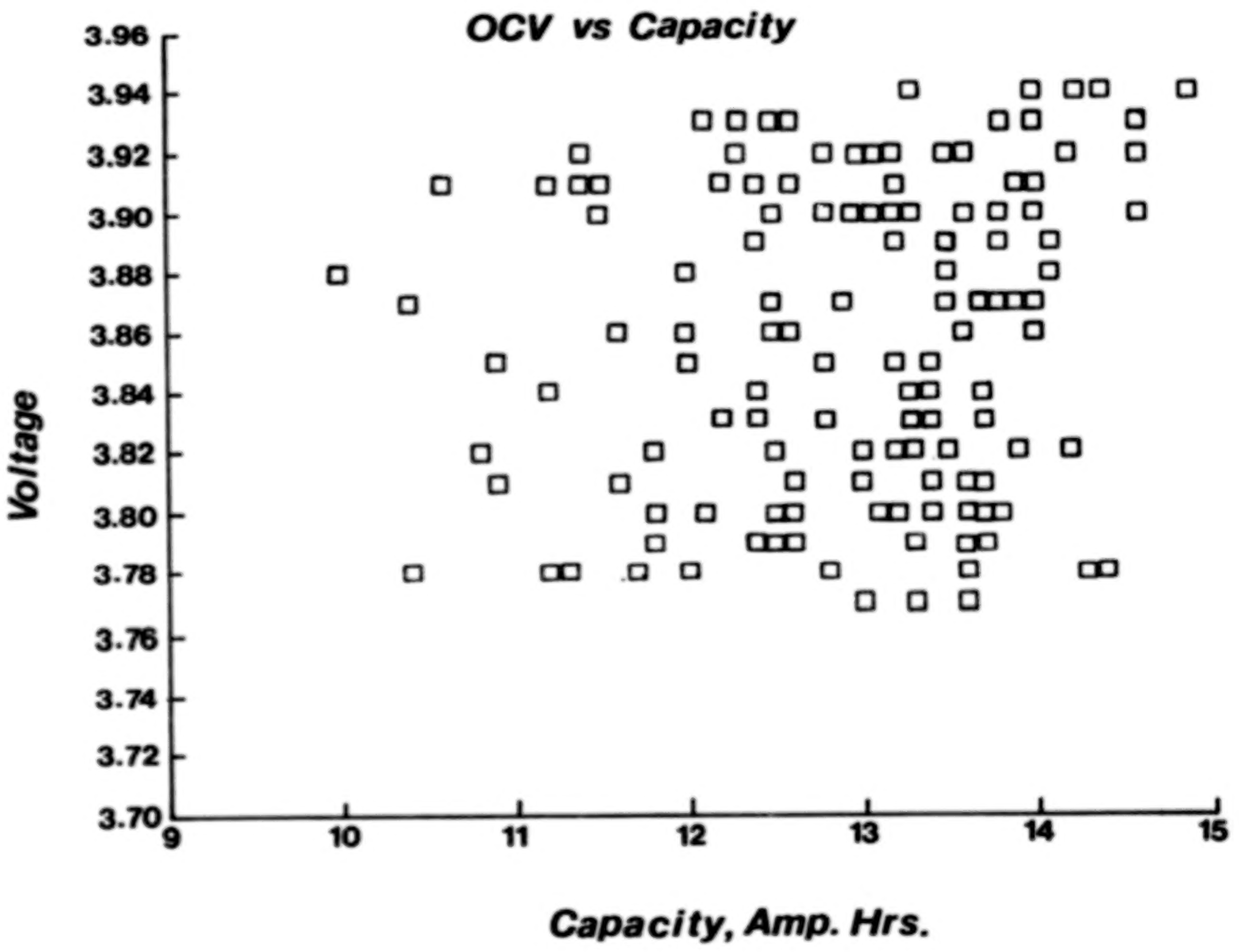

Figure 6. Comparison of OCV to realized capacity for cells stored for various periods of time under room temperature conditions.

Q. Kunigahalli, Bowie State College: Would you please tell me the mechanism that is causing the plateau? Is it the anode or the cathode or what may be the reaction?

A. Krehl, Wilson Greatbatch Ltd.: The high voltage plateau?

Q. Kunigahalli, Bowie State College: The low voltage plateau. I saw in one of the viewgrafts you showed the discharge curve showing the plateau - lower voltage plateau?

A. Krehl, Wilson Greatbatch Ltd.: Well, we think that's just the base solvent after any of the dissociation products are depleted and we get to the actual load voltage that the cell is going to see. The cell actually is cathode limited.

Q. Yen, JPL: You mentioned about the high open circuit voltage of over 3.9 volts due to the addition of PCX. Okay, over the standing and the cell voltage decline. Have you done any post-mortum analysis correlating the PCX content - the voltage decline and the capacity decline. Do you know anything about the chemistry?

A. Krehl, Wilson Greatbatch Ltd.: I'm sorry to say we really haven't done too many studies with respect to that. Some of our work was done with the cell. And the BRCL actually showed a peak I think it was actually 3.85 and as the cell discharged we could see that peak gradually decrease and we got a increase in a peak at about 4.15 which corresponded to bromine - free bromine. So it appeared that, if there was some dissociation there and giving free chlorine, we are depleting that and shifting things down to bromine, but we really haven't done too much in the way of studies there.

Q. Yen, JPL: Have you done any measurement about the dissociation constant of PCX and the correlation of the concentration of PCX use related to the voltage decline?

A. Krehl, Wilson Greatbatch Ltd.: We got a dissociation constant from now. It was in a non-polar solvent and it was .38. That, when we calculated out how much free chlorine and free bromine would be in a cell. We came up with the discharge curve showing about 70% of that capacity would be under those initial high voltage plateaus and then the rest would discharge under the lower plateau.

N84
33674

UNCLAS

N84 33674 D6

CHARACTERIZATION OF GLASS FIBER SEPARATOR MATERIAL FOR LITHIUM BATTERIES

S. Subbarao and H. Frank

Jet Propulsion Laboratory
Pasadena, California

ABSTRACT

Characterization studies were carried out on a glass fiber paper that is currently employed as a separator material for some $LiSOCl_2$ primary cells. The material is of the non-woven type made from microfilaments of E-type glass and contains an ethyl acrylate binder. Results from extraction studies and tensile testing revealed that the binder content and tensile strength of the paper were significantly less than values specified by the manufacturer. Scanning electron micrographs revealed the presence of clusters of impurities many of which were high in iron content. Results of emission spectroscopy revealed high overall levels of iron and leaching, followed by atomic absorption measurements, revealed that essentially all of this iron is soluble in $SOCl_2$.

INTRODUCTION

This work was carried out in collaboration with S. Subbarao (see Figure 1) who is a Resident Research Associate for NASA.

As indicated in Figure 2 the effort is part of NASA's Primary Lithium Battery Program wich is aimed at developing flight quality Li-$SOCl_2$ cells by FY86. One element of this program is being directed towards development and characterization of the components of as well as complete Li-$SOCl_2$ cells. The specific subject of this investigation is characterization of the separator material that is commonly employed in this type of cell. The separator is made by Mead Paper Company and is a non-woven paper made from micro filament glass fibers supplied by Johns Manville.

RESULTS AND DISCUSSION

Overall physical properties of the paper are given in Figure 3. The binder content was determined by extraction with dichloromethane and also verified by ignition described later. The tensile strengths were measured with an Instron Tensile Tester. Results shown therein reveal that the observed values for binder content and tensile strength are appreciably lower than those specified by the manufacturer.

Since the specific type of binder was not specified by the vendor, a sample of it was analyzed by Fourrier Transform Infrared Analysis. The resultant spectra is given in Figure 4. Comparison of this spectra with known spectra in the literature (1) revealed that the binder is an acrylic.

Samples of the material were examined by Scanning Electron Microscopy. Analyses revealed that the glass filaments are randomly oriented and their diameters range in size from approximately 0.2 to 2 microns. Further it was found that the material contains small clusters of impurities as shown in Figure 5. These particles are located throughout the roll of the paper. Energy Dispersive Analysis (EDAX) of these particles revealed that most of them contain appreciable amounts of iron as shown in Figure 6.

Emission Spectrographic Analysis of the material revealed that its overall iron content was 0.48%, as shown in Figure 7, and this value is somewhat higher than that claimed by the manufacturer. Although this amount of iron is low in terms of percentages, it is high from a contamination point of view in that very low levels of iron in the parts per million range can adversely affect performance of Li-$SOCl_2$ cells. Figure 7 also shows that the amount of material "lost on ignition" was 3.04% and this should correspond to the binder content. This value is in good agreement with the binder content determined by extraction as given in Figure 1.

Samples of the material were also leached in $SOCl_2$ solution for 24 hrs and the extract was analyzed for iron by Atomic Absorption. Results showed that essentially all the iron is soluble in $SOCl_2$.

Based on the above findings calculations were carried out to estimate the amount of iron that the separator would contribute to a typical "D" size Li-$SOCl_2$ cell. Results indicated that the amount of iron would correspond to about 150 ppm which is quite high in regard to tolerable levels of iron in these cells (2).

CONCLUDING REMARKS

As indicated in Figure 8, this separator material does not conform to the manufacturer's specifications, has low physical strength, and also contains impurities that are known to be deleterious to operation of Li-$SOCl_2$ cells. In its present form the separator would not be classified as of high enough quality for aerospace applications. Further, the manufacturer has not indicated a willingness to develop a high quality separator. On this basis it will be necessary to locate another manufacturer that can supply the desired high quality material. Investigations are currently underway to locate such a manufacturer.

ACKNOWLEDGEMENT

One of the authors, S. Subbarao, wishes to thank the National Research Council for support of his work for NASA.

REFERENCES

1. Haslam and Wills, Identification and Analysis of Plastics, Van Nostrand, p. 391, (1965).

2. Marincic, N., and Lombardi, A., "Sealed Lithium Inorganic Battery," Final Report from GTE laboratories, Waltham, Mass., for U.S. Army Electronics Command, Ft. Monnouth, N.J., ECOM Report No. 74-0108-F, p. 149-150, April 1977.

CHARACTERIZATION OF GLASS FIBRE SEPARATORS FOR LITHIUM BATTERIES

S. Subbarao
and
H. Frank

NASA GODDARD SPACE FLIGHT CENTER
BATTERY WORKSHOP

JPL

NOV. 15-17, 1983

Figure 1

JPL

CHARACTERIZATION OF GLASS FIBRE SEPARATOR MATERIAL

INTRODUCTION

- NASA SPONSORED PRIMARY LITHIUM BATTERY PROGRAM
- QUALIFY Li-$SOCl_2$ CELLS FOR FLIGHT BY FY-86
- PROGRAM ELEMENTS
  - RESEARCH ON CHEM RELATED SAFETY ISSUES
  - DEVELOPMENT OF PROTOTYPE CELLS/1st GENERATION CELLS FY-84
  - DEVELOPMENT OF FLIGHT CELLS
- COMPONENT CHARACTERIZATION PART OF PROTO CELL DEVELOPMENT
- UNCOVERED PROBLEM AREAS WITH EXISTING SEPARATORS

Figure 2

JPL CHARACTERIZATION OF GLASS FIBRE SEPARATOR MATERIAL
OVERALL PHYSICAL PROPERTIES

		VENDOR CLAIM
THICKNESS	3.5 mil	
WEIGHT / AREA	3.5 gms/ft^2	
DENSITY	0.43 gms/cc	
POROSITY	80%	
BINDER CONTENT	3%	8%
TENSILE STRENGTH ⊥	152 TO 174 psi	300 psi
TENSILE STRENGTH =	159 TO 170 psi	300 psi

Figure 3

JPL CHARACTERIZATION OF GLASS FIBRE SEPARATOR MATERIAL

ANALYSIS OF BINDER

- BINDER REPORTED TO BE SOME TYPE OF ACRYLIC BY VENDOR
- REMOVED BINDER BY EXTRACTION WITH DICHLOROMETHANE AND RAN FTIR ON EXTRACT
- RESULTS

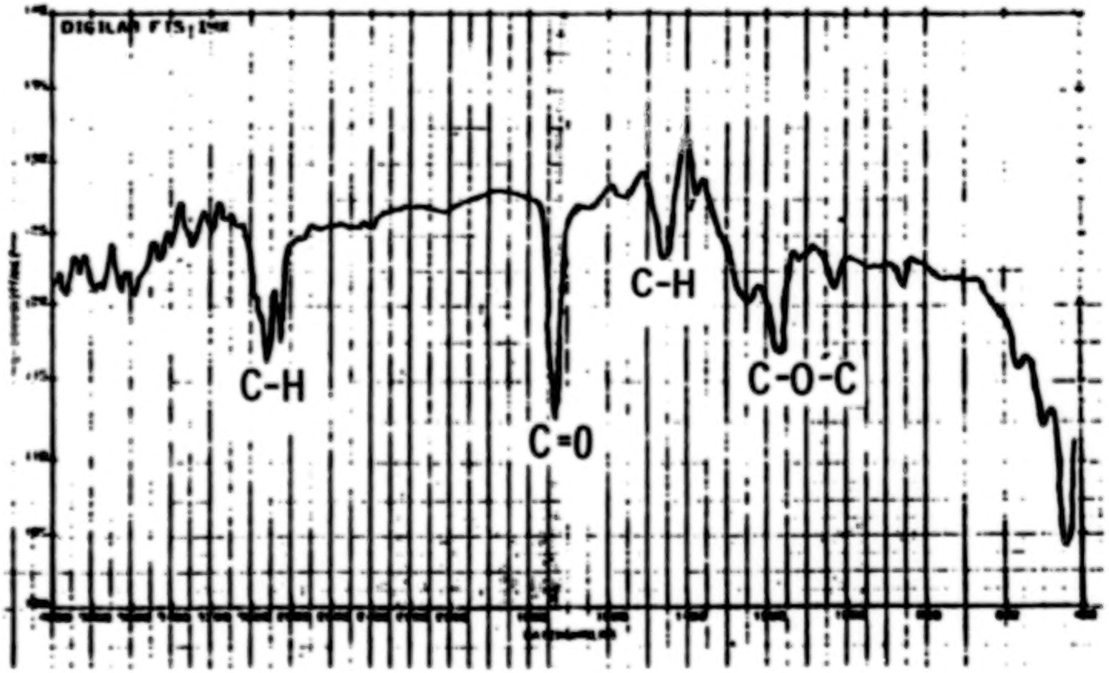

- CONCLUSION: BINDER IS ETHYL ACRYLATE -

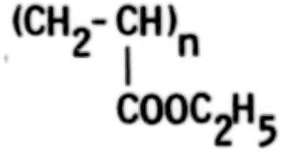

$$(CH_2\text{-}\underset{\displaystyle COOC_2H_5}{\underset{|}{CH}})_n$$

Figure 4

JPL CHARACTERIZATION OF GLASS FIBRE SEPARATOR MATERIAL

SEM ANALYSES

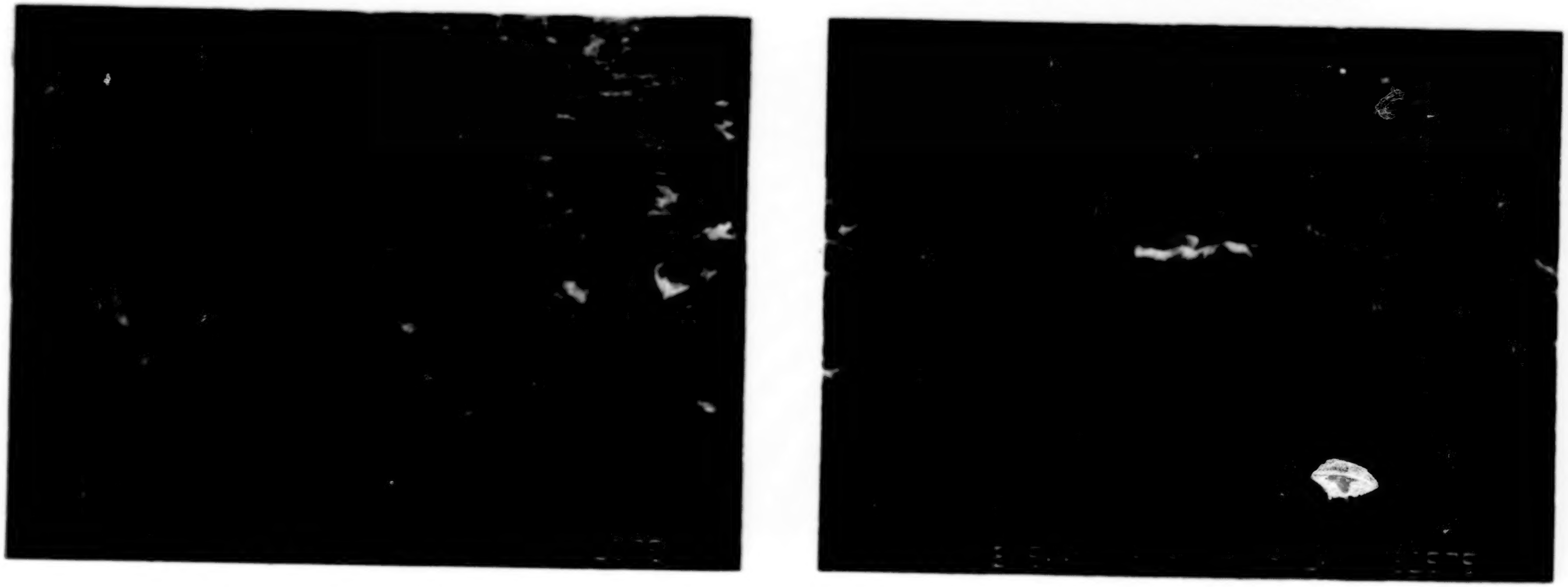

SEM PHOTO REVEALS CLUSTERS OF FOREIGN PARTICLES

MAGNIFIED SEM PHOTO OF A TYPICAL PARTICLE

Figure 5

JPL

CHARACTERIZATION OF GLASS FIBRE SEPARATOR MATERIAL

EDAX ANALYSIS OF TYPICAL FOREIGN PARTICLE

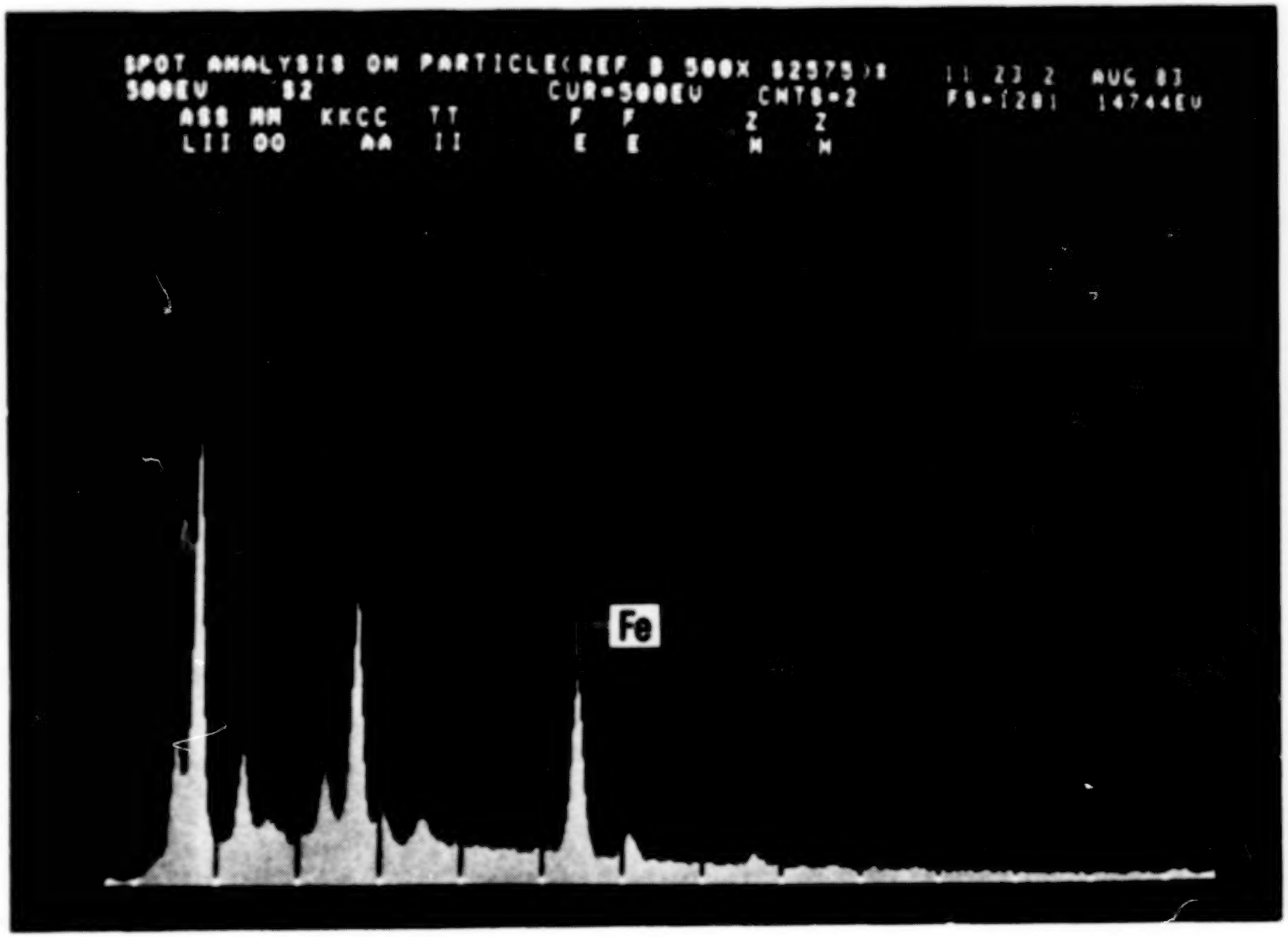

```
SPOT ANALYSIS ON PARTICLE(REF B 500X S2575)S    11 23 2  AUG 83
500EV     S2                CUR=500EV   CNTS=2    FS=(28)   14744EV
```

Figure 6

JPL

CHARACTERIZATION OF GLASS FIBRE SEPARATOR MATERIAL
SPECTROGRAPHIC ANALYSIS

SEMIQUANTITATIVE ANALYSIS

Si	21. %	
Al	13.	
Ca	14.	
Mg	1.3	
Sr	0.090	
B	0.72	
Mn	0.023	
Pb	0.018	
Ba	0.46	
Fe	0.48	← VERY HIGH (VENDOR CLAIMS
Ga	0.0099	$Fe_2O_3 < 0.3\%$)
Ni	0.014	
Na	0.87	
Cu	0.0014	
Zn	0.35	
Ni	0.0021	
Zr	0.029	
Co	0.0041	
K	TR < 0.10	
Cr	0.0024	
OTHER ELEMENT	nil	
LOSS ON IGNITION	3.04%	← BINDER

Figure 7

JPL

CHARACTERIZATION OF GLASS FIBRE SEPARATOR MATERIAL

SUMMARY AND CONCLUSIONS

- LOW BINDER CONTENT
- LOW TENSILE STRENGTH
- CLUSTERS OF IMPURITIES THROUGHOUT
- IMPURITIES HIGH IN IRON
- THE IRON READILY DISSOLVES IN $SOC\ell_2$ (YIELD 150 ppm IN CELL) AND WOULD CAUSE SEVERE VOLTAGE DELAY
- DUE TO INFERIOR CHEMICAL AND PHYSICAL PROPERTIES THIS MATERIAL DEEMED UNSUITABLE FOR AEROSPACE CELLS
- AVAILABILITY OF QUALITY MTL UNCERTAIN

Figure 8

Q. Roth, NASA HQ: I was wondering - this is more of a general question - not only to ask yourself but of the people here. What you said about the ability of NASA to get supplies to give them the type of materials they want is an across-the-board problem. And I'm just wondering - is it that significant a problem that it's going to cause trouble now and in the future - and I guess I'm asking everybody here the same question. We don't buy much of anything in high quantities.

A. Frank, JPL: I guess that's a good subject. I'm just running into it now at this level. Perhaps someone else wants to address it. Well I know that, from JPL's point of view, it's the same thing. Small quantities we are not interested in - one has to get the right source eventually if the problem is indeed one that would demand that it can be done one way or another and that's what we're in the process of doing here.

Q. Roth, NASA HQ: Did you ever get the feeling you might want to do it yourself?

A. Frank, JPL: Yes, we are doing it ourself. We tried for example to eliminate these impurities by dissolving them. But if we can devise a process and then go to some other company and have them use our procedures. We will do it - either that or by obtaining a better source. So we're looking at both avenues here on this particular problem.

Q. Osterhoudt, Eastman Kodak: What price are you paying for this per square foot?

A. Frank, JPL: Actually we pay for it by the pound. It's something like $10 a pound or in that range. But we're not interested in the cost.

Q. Osterhoudt, Eastman Kodak: What you be willing to pay for something that would work? No I'm serious - premium price for premium quality?

A. Frank, JPL: Yes, yes of course for manned space flight.

Q. Osterhoudt, Eastman Kodak: I didn't understand that part.

A. Frank, JPL: Yes, if it could not be obtained in a condition suitable for NASA, we would be considering a small developmental contract to obtain the necessary quality.

COMMENT

Unidentified: I would like to comment - if you go back 14 years, this battery workshop got started because nickel cadmium cells were framing during charge - for the OAO spacecraft - a very serious problem for NASA. There were some other problems as well, and the battery separator manufacturer was present. And we asked him about that problem and he had put in some wetting agent because somebody had asked him to do it. There were some other basis of the problem. But he also got up and made the same statement - "You tell us what you want and we'll give it to you." And we're still using the same separator today.

Q. Levy, Sandia National Lab: Have you noted any specific problems due to this separator or are you just conjecturing that this might cause some problems.

A. Frank, JPL: We're in the process of doing that right now, Sam. We are building the prototype cells and we are going to make the voltage measurements. From, well first of all the physical properties are quite evident. One could not use this in fabricating the cells. When you go to the rolling operations the strengths would be inadequate and that's most likely related to the binder. A direct answer to your question is no, but we are in the process of doing it. And in the literature there is evidence that these levels of iron cause severe voltage regulation problems. So we'll be verifying it shortly.

Q. Allvey, Saft America, Inc.: Your 150 ppm of iron seemed high so I assume that's a spiral round configuration.

A. Frank, JPL: Yes.

N84
33675

UNCLAS

N84 33675 D7

Kinetics of Open Circuit Processes in Undischarged Li/SOCl$_2$ Cells

by

Lee D. Hansen
Department of Chemistry and the Thermochemical Institute
(Contribution No. 336)
Brigham Young University
Provo, Utah 84602

and

Harvey Franks
Jet Propulsion Laboratory
California Institute of Technology
4800 Oak Grove Drive
Pasadena, California 91109

ABSTRACT

The kinetics of the heat producing processes in undischarged Li/SOCl$_2$ cells under open circuit conditions have been measured by heat-conduction microcalorimetry. The cells studied, Honeywell type G2666 reserve cells, were activated as needed and the rate of open circuit heat output determined as a function of time since activation and temperature. The results at each temperature can be described by an equation of the form $q = Bkt^x$ where q is the rate of heat output, B is the heat produced per unit of reaction, k and x are empirical constants, and t is the time since activation. Both x and k are found to be functions of temperature; therefore, accelerated testing at elevated temperatures is probably not valid for these cells until the processes involved are better understood.

INTRODUCTION

Shelf life testing of primary batteries is usually done at elevated temperatures in order to shorten the time required for the tests. The results at the elevated temperature are then extrapolated to room temperature. The results of such a procedure are valid provided that no change in the mechanisms of the parasitic processes occurs between room temperature and the temperature at which the tests were done. The work described in this report was designed to determine the kinetic constants necessary for the extrapolation of kinetic data on $Li/SOCl_2$ cells over the temperature range from 25 to 75°C.

A second objective of the work described in this report was to characterize as far as possible the parasitic processes which occur in $Li/SOCl_2$ cells since these processes may be important in understanding the potential hazards of these cells.

MATERIALS

The type G2666 $Li/SOCl_2$ reserve cells were purchased from Honeywell. These cells are 0.28 amp-hour cylindrical cells approximately 0.5" dia. by 0.8" long. The cell electrolyte, $LiAlCl_4$ dissolved in $SOCl_2$, is contained in a glass ampoule within the cell. The cell is activated when desired by breaking the glass ampoule by denting the stainless steel case in the center of the bottom of the cell.

EQUIPMENT

The calorimeter used to measure the heat output of the cells was a Tronac Model 351 RA. The constant temperature bath in this calorimeter has an upper limit of 45°C. Therefore, when measurements were made at temperatures above 45°C the calorimeter insert was moved to a Hart Scientific Model 5024 water bath. The electronics were thermostatted at 25°C in the Tronac air bath during these measurments.

RESULTS

The results on unactivated cells are given in Table 1. These data show that there was no significant heat production present in the cells prior to activation except at 65°C and above.

The results obtained on cells activated and kept at 25 or 65°C are shown in Figure 1 as a plot of ln q against ln t where q is the rate of heat production in microwatts and t is the time in seconds since activation. These results show that the cells follow a rate law of the form

$$q = Bkt^x \qquad (1)$$

where both k and x are functions of temperature. The constant B, the heat produced per unit of reaction, is probably not a function of temperature. The process producing heat under open circuit conditions is probably the direct reaction of Li with $SOCl_2$, the same reaction occurring when the cell is under load. The enthalpy change for the closed circuit cell reaction has been shown to be constant over the temperature range used in this study (1,2).

Figure 2 shows data taken on cells which have been cycled between 25°C and various temperatures up to 75°C. These data indicate that the rate of heat production is a function of the temperature and time since activation, but not of the temperature history of the battery.

DISCUSSION

At the time this work was begun, it was expected that the kinetics of heat production would follow the kinetics predicted from a parabolic film growth model. Data collected in a previous, but much abbreviated study, had suggested such a possibility (3). Also, much previous work has indicated that the growth of a LiCl passivation layer controls the kinetic properties of $Li/SOCl_2$ cells (4,5). However, three characteristics of the data in Figure 1 suggest that a parabolic film growth model is either incorrect or at least not sufficient. First, the slope of the ln p versus ln t curves are not -0.5; second, the slope changes with temperature; and third, cells which have been cycled to higher temperatures do not show a decreased heat production rate at lower temperatures when compared to cells which have been held at the lower temperature for the same period of time since activation.

The results of this study clearly show that either the mechanism of the heat producing reaction changes or the relative rates of the heat producing reactions change as a function of temperature. Thus, we are forced to conclude that accelerated testing of $Li/SOCl_2$ cells must be regarded with suspicion until the parasitic processes are more fully understood so that their kinetics may be modeled as a function of temperature.

REFERENCES

1. C.R. Schlaikjer, F. Goebel and N. Marincic, J. Electrochem. Soc. 126, 513 (1979).

2. H.F. Gibbard, Extended Abstracts, ESC Fall Meeting, 1979, Los Angeles, CA.

3. H. Frank, B. Carter and L. Hansen, Extended Abstracts, ESC Fall Meeting, 1982, Detroit, MI.

4. A.N. Dey, Thin Solid Films 43, 131 (1977).

5. E. Peled, J. Power Sources 9, 253 (1983).

ACKNOWLEDGEMENT

This work was supported by the National Aeronautics and Space Administration under contract No. NAS 7-100 to JPL.

Table 1
Heat Produced by Unactivated Cells

Cell	Temperature, °C	Heat Output, uW
2	25	0.0
3	25	0.0
4	25	0.0
2	55	0.0
3	55	0.0
4	55	0.0
2	65	2.6
3	65	0.9
4	65	1.7

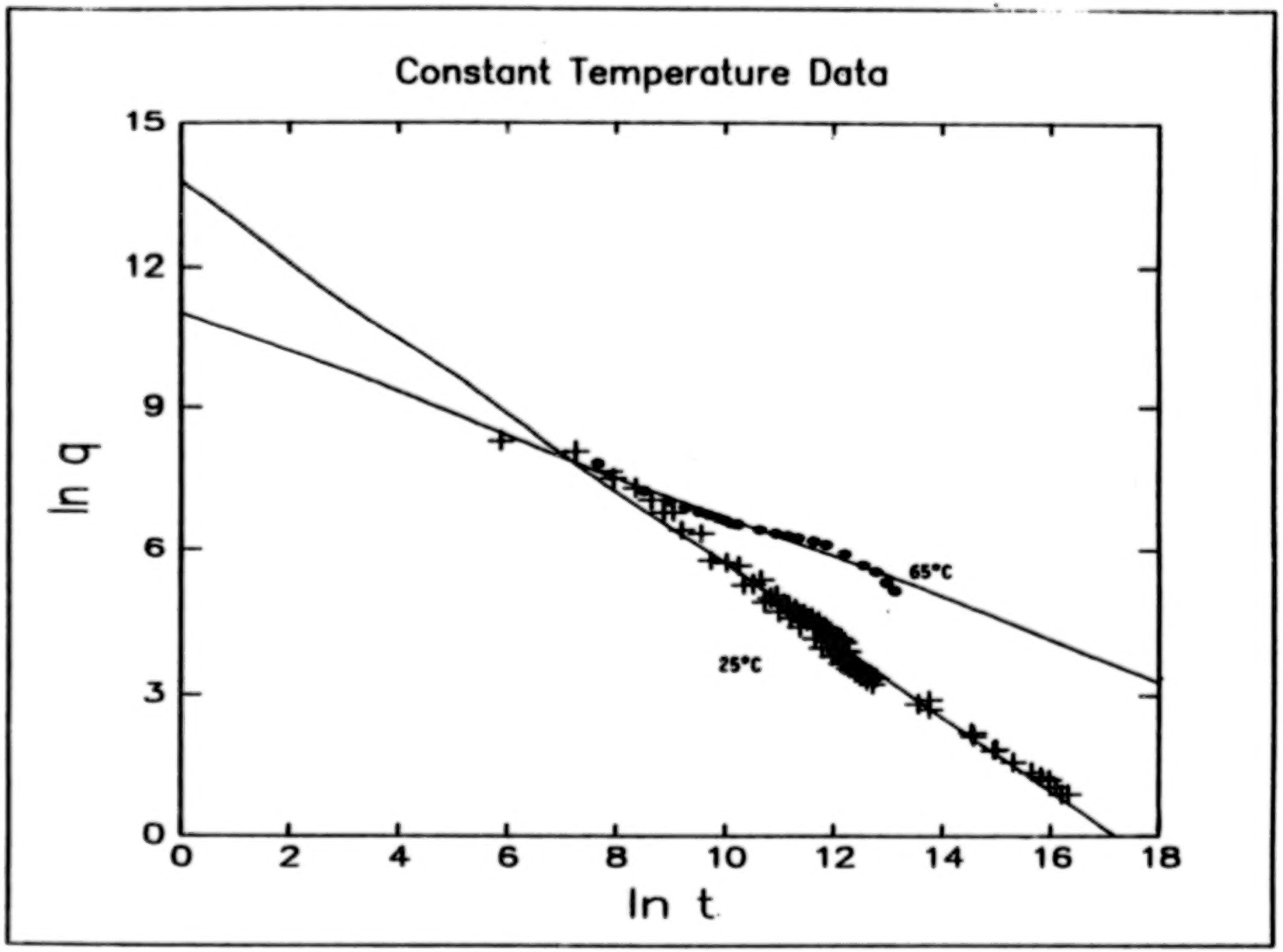

Figure 1. A plot of ln q, the rate of heat production in uW, versus ln t, the time since activation in seconds, for cells activated and maintained at constant temperature. The lines are linear least square fits to the data shown.

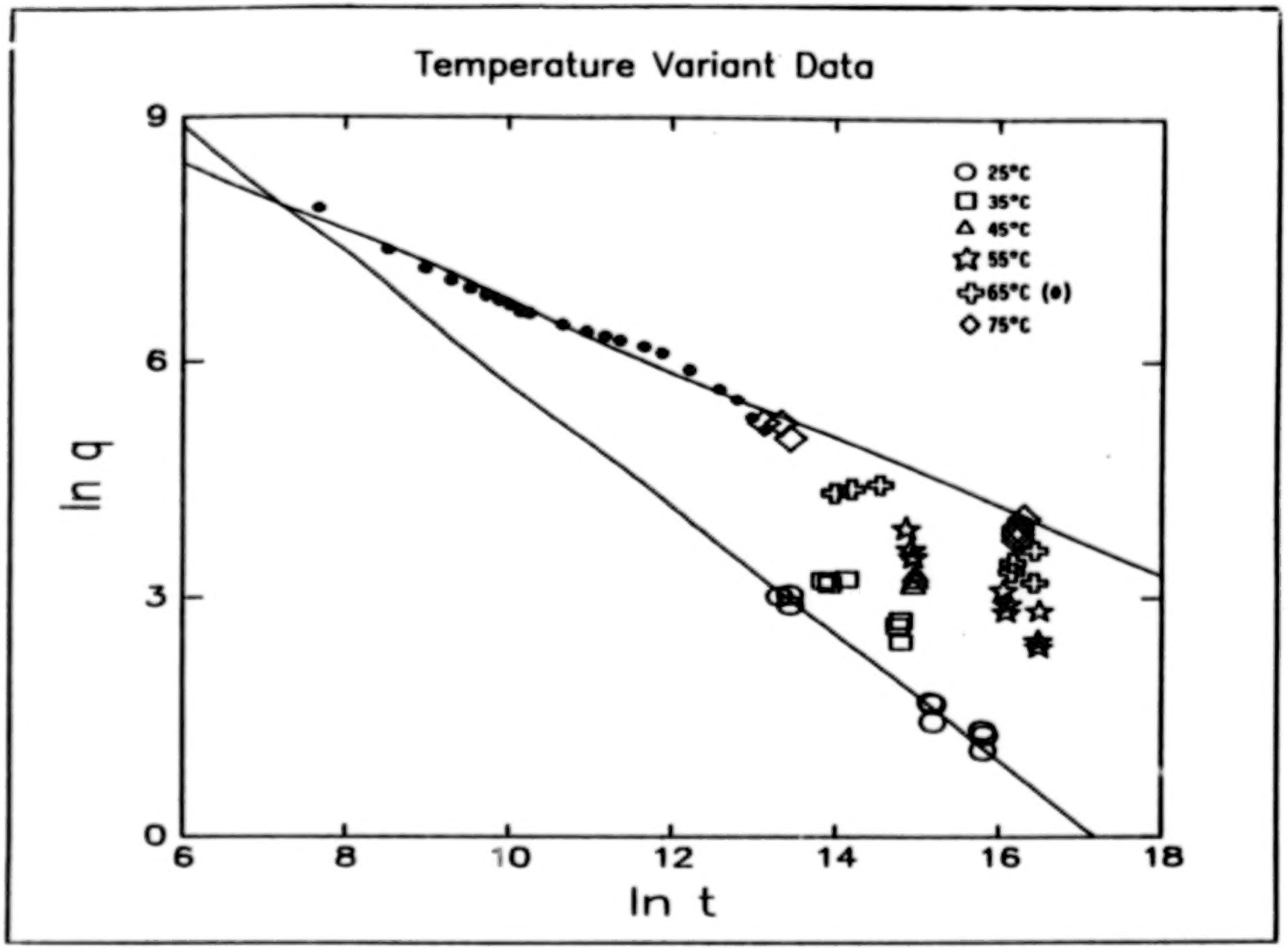

Figure 2. Data taken on cells held at 25^{o}C except during measurement at the indicated temperatures. Measurement at elevated temperature requred that the cells be held at the elevated temperature from 1 to 5 days. The lines represent the 25^{o}C and 65^{o}C constant temperature data as shown in figure 1.

N84
33676

UNCLAS

N84 33676 D8

RELATED STUDIES IN LONG TERM LITHIUM BATTERY STABILITY

R. J. Horning and D. L. Chua
Honeywell Power Sources Center
Horsham, PA 19044

INTRODUCTION

The continuing growth of the use of lithium electrochemical systems in a wide variety of both military and industrial applications is primarily a result of the significant benefits associated with the technology such as high energy density, wide temperature operation and long term stability. The stability or long term storage capability of a battery is a function of several factors, each important to the overall storage life and, therefore, each potentially a problem area if not addressed during the design, development and evaluation phases of the product cycle. Design (e.g., reserve vs active), inherent material thermal stability, material compatibility and self-discharge characteristics are examples of factors key to the storeability of a power source.

A significant amount of activity at Honeywell is directed toward characterizing and improving where necessary the storage affecting aspects of lithium batteries. This discussion reviews briefly, three segments of this work, the results of which are quite positive and as such, add to the confidence level associated with lithium units. These are:

- Long term storage evaluation of electrolytes and cell systems used in Army mines batteries.
- Material compatibility of thionyl chloride electrolyte with stainless steels used in reservoirs of reserve batteries.
- Terminal seal glass corrosion in Li/V_2O_5 cells and TA-23 glass as a corrective measure.

RELATED MATERIAL STUDIES

ELECTROLYTES (ORGANIC AND INORGANIC)

Honeywell currently has two 10-year accelerated storage programs to assess the material compatibility and stability of both organic and inorganic electrolytes in reserve cells and ampuls. A total of 2100 cells and 10,000 ampuls comprise these extensive storage plans. The organic electrolytes: $Li/2M\ LiAsF_6$, $0.4M\ LiBF_4$·Methyl Formate/V_2O_5, while the inorganic is $Li/1M\ LiAlCl_4$·Thionyl Chloride/$SOCl_2$. Both systems are stored at 64°C (147°F) to 84°C (183°F) environments and tested annually. Voltage monitoring for cells occurs monthly to determine if any reserve cells have prematurely activated. For ampuls, monitoring occurs more frequently to determine the number of fractures and the physical condition of the liquid. Fracturing is monitored because gas formation is a characteristic of electrolyte deterioration. Figure 1 shows the dimensions of cell and glass ampul.

The maximum adjusted storage times for the organic electrolyte ampuls is 6.4 years at a diurnal cyclic temperature, 32/71°C (90 to 160°F). Predictions for this cyclic environment, based on Arrhenius plots, show that these ampuls will store without fracturing for 15 to 20 years. The Army storage requirement is a minimum of 10 years at the same environment. Figure 2 demonstrates an Arrhenius plot for machine manufactured ampuls. The median time at which 50% of an ampul lot fractures is chosen as the relative point of comparison between lots. The inorganic thionyl chloride electrolyte shows excellent storage capability with no ampul fracture after 4.1 years at the maximum 84°C environment.

Figure 3 compares the yearly cell test results completed for the Li/V_2O_5 cells for two lots. The effect of reserve storage time on cell output is most pronounced at the -43°C (-45°F) test temperature with an apparent maximum capacity loss of 40% from the baseline value. However, the output at high temperature discharge is relatively unchanged for cells having identical storage exposure meaning a true capacity loss has not occurred. Cell impedance change as a result of anode filming with outgassing materials during high temperature storage is considered the cause of the change. This is finite and will stop once all outgassing materials have been consumed.

The reserve $Li/SOCl_2$ cell shows excellent performance at both the cold and hot test temperatures after 3-year storage. Figure 4 presents the cell life values for two lots across the storage environments and shows the small deviation from baseline performance.

MATERIALS OF CONSTRUCTION

Metal Reservoir (Thionyl Chloride)

Stainless steel reservoirs are used in reserve $Li/SOCl_2$ batteries. Specific types of stainless steel most commonly utilized are 321 S.S. and 316L S.S. Presented below are evidences for the corrosion resistance of these materials to neutral (1.5M $LiAlCl_4/SOCl_2$) electrolyte when subjected to long term storage at elevated temperature (71°C).

Electrolyte analysis for iron concentration by U.V. absorption techniques showed only a slight increase after 12-month storage at 71°C. SEM photomicrographs of the steel surfaces revealed the formation of a protective film which can either eliminate or reduce further material corrosion. The existence of this film is shown in Figure 5 for both 316L S.S. and 321 S.S. Additional SEM observations of the surfaces indicated film formation to be more rapid during their initial period of storage and with the 321 S.S. exhibiting higher degree of corrosion (based on Fe analysis) than 316L S.S. Metallographic analysis of the specimens showed no visible corrosion into the specimens, thus rendering additional support to the presence of a protective film on the 321 and 316L stainless steel's surfaces when exposed to $SOCl_2$.

Glass-To-Metal Seal (TA-23 Glass)

Glass corrosion has been clearly identified as a failure mode in Li/SO_2 system but also exists in other systems such as Li/V_2O_5 and $Li/SOCl_2$ in varying degrees. The corrosion mechanism was found to involve underpotential disposition of lithium metal onto the glass initiating at the glass/metal interface maintained at the lithium potential. The corrosion process causes the glass to become conductive so that once the glass is traversed, a conductive path will cause the cell to self-discharge and deplete the remaining capacity. The path presented in this section will focus only on the Li/V_2O_5 system.

The magnitude of corrosion in Li/V_2O_5 system with 9013 glass has been estimated using the radial corrosion distance outward from the pin across the glass surface. Corrosion rates, based on the measured corrosion distance and the age of the cell, were calculated and correlated to the integrated average temperature over the life of the cell using an Arrhenius-type relationship. This is shown in Figure 6. Fitted equation was obtained using the least squares method. This equation can be used for predicting time to failure for existing cells. Non-accelerated cells noted in Figure 6 were cells stored between 4°C and 57°C for varied periods of time. Radial corrosion distance has been shown to be a viable means of quantitizing the magnitude of glass corrosion in Li/V_2O_5 cells.

An approach to resolving the glass corrosion in Li/V_2O_5 cells is to change the glass from 9013 to TA-23 developed by Sandia National Laboratories. Hardware with TA-23 glass was submitted to an accelerated test plan (+71°C storage); with cells removed weekly for a 7-week period. Each cell, after storage, was discharged and postmortemed. Results of the postmortems showed no sign of corrosion (Figure 7).

SUMMARY

A key benefit of lithium based battery systems is the capability to store over a wide temperature range for very long periods of time. There are many factors important to this capability and a major portion of research and development resources have and continue to be dedicated to the characterization and improvement of the long term stability of lithium systems. The three examples discussed herein offer positive consideration to this area.

- Mine system cells and electrolytes in a 10-year scheduled program are providing good storage data after 4 and 3 years, respectively, so far.
- Thionyl chloride electrolytes have been shown to be compatible with the stainless steels most often used in reserve battery reservoirs.
- Glass corrosion can occur in Li/V_2O_5 systems with slightly less rapidit than in Li/SO_2 units. Sandia's TA-23 glass appears to be equally effective in solving the problem.

ACKNOWLEDGEMENTS

- U. S. Army, AMCCOM, Dover, N.J. for its support of the electrolyte and cell storage effort.

  Charles Vreeland, Army Contract Monitor

- U. S. Navy, NSWC, White Oak Laboratory for its support of the compatibility evaluation of stainless steels with electrolytes.

  Dr. G. Hoff and D. Warburton, Navy Contract Monitors

- Sandia National Laboratories, Albuquerque, NM for TA-23 Development Support.
- Honeywell's Project Engineers: M. J. Faust, Dr. N. Doddapaneni, R. A. Barnabei, and W. B. Ebner

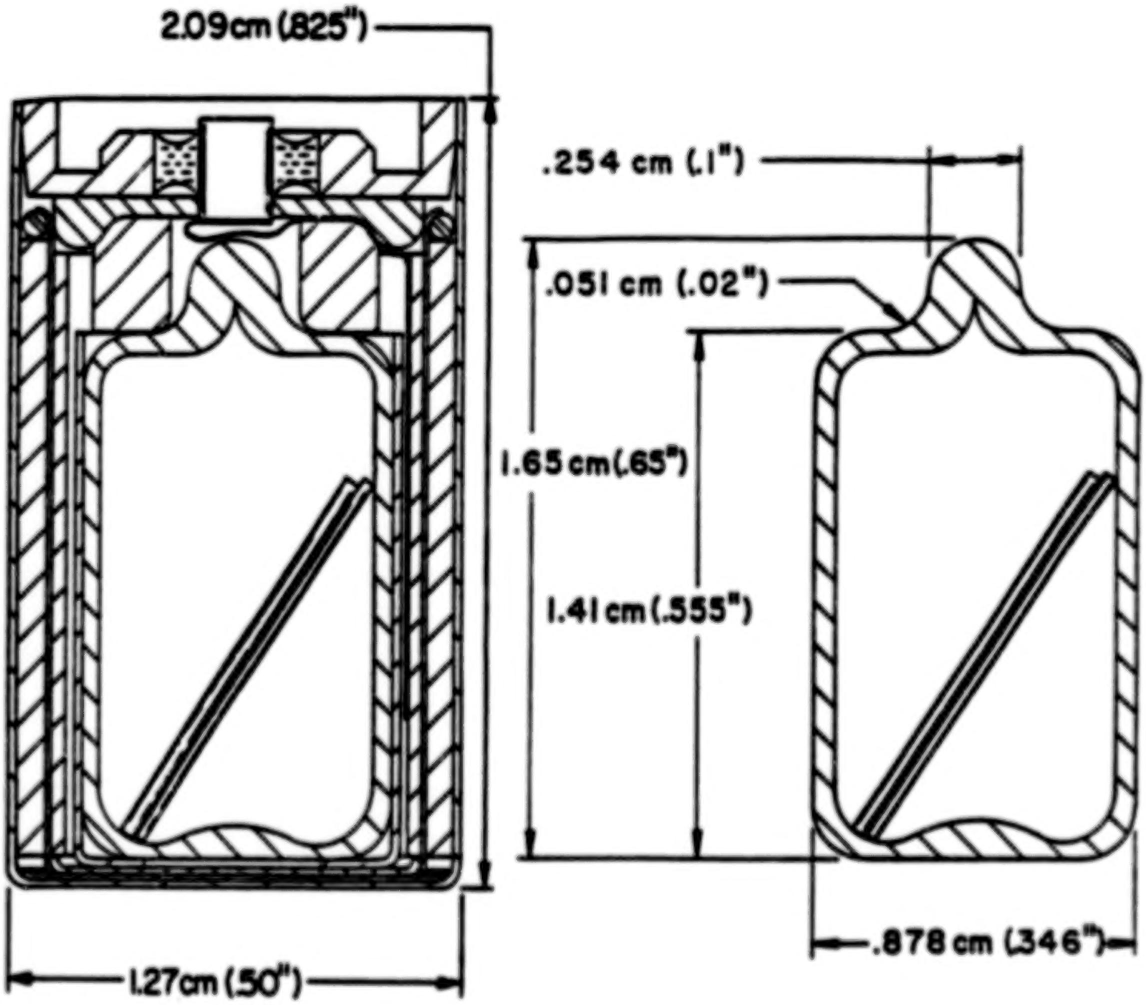
2.09cm (.825")
.254 cm (.1")
.051 cm (.02")
1.65 cm (.65")
1.41 cm (.555")
1.27cm (.50")
.878 cm (.346")

CELL

AMPUL

Figure 1. Cell and ampul used for long term storage evaluations.

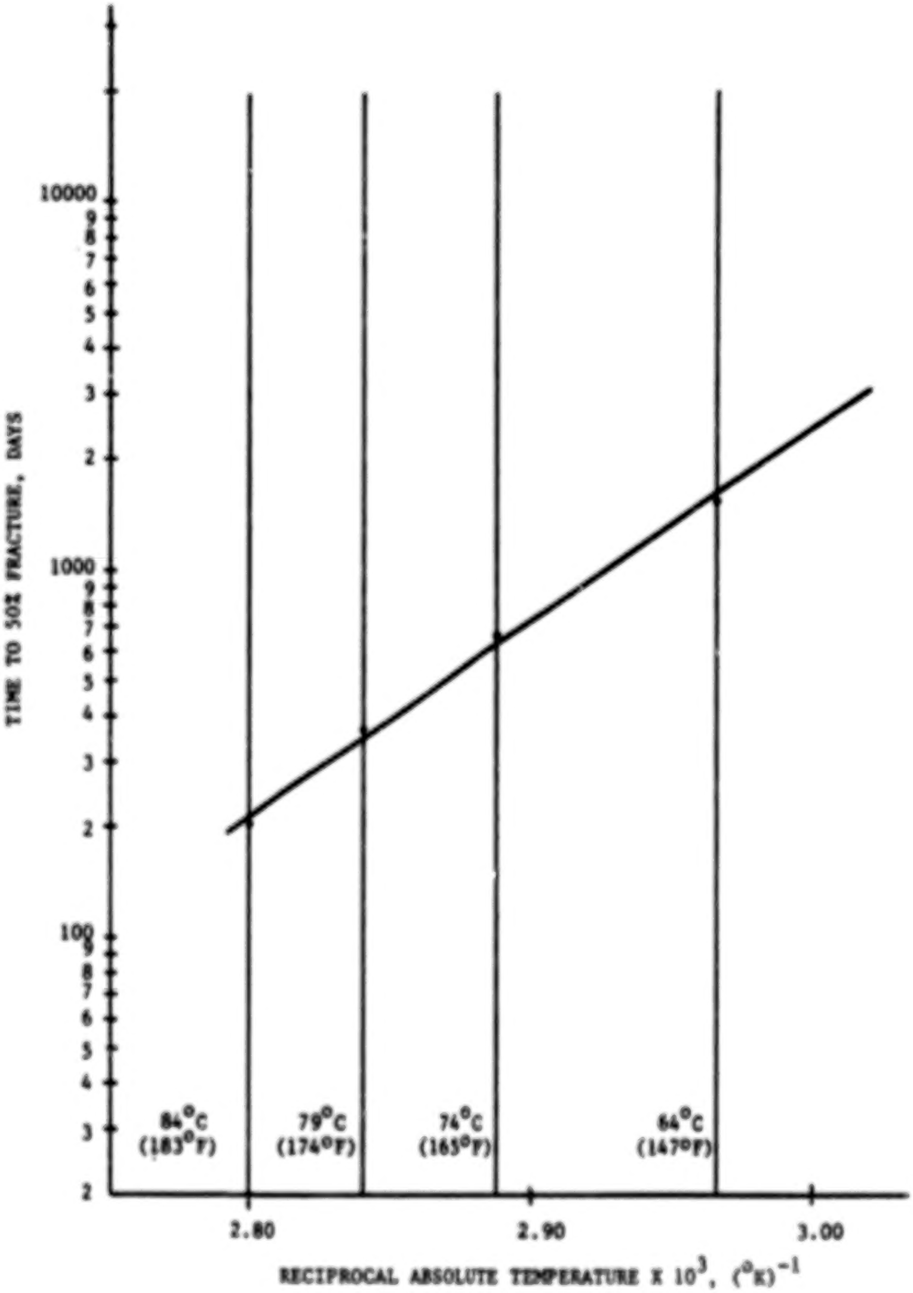

Figure 2. Arrhenius plot for machine manufactured ampuls.

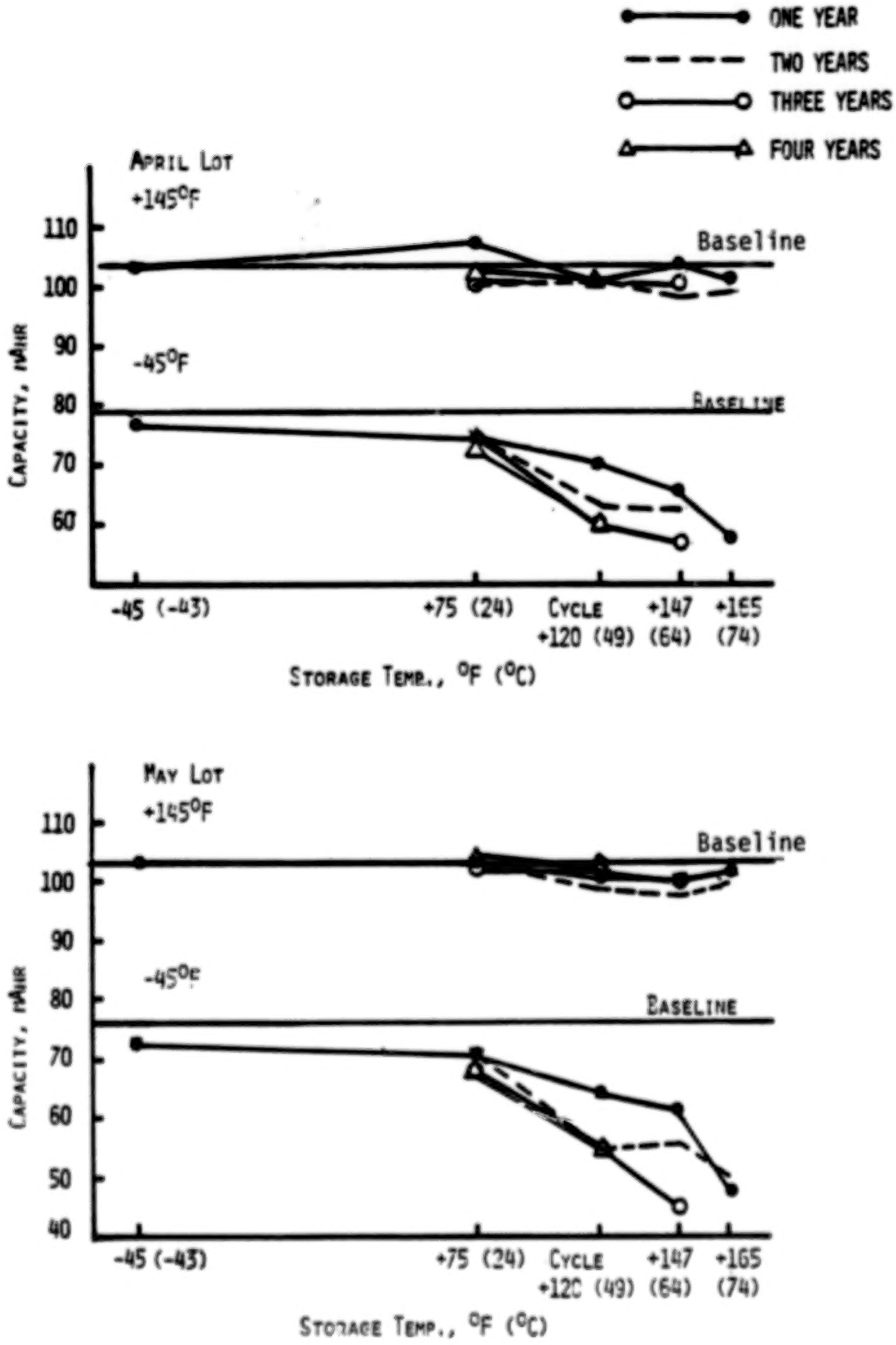

Figure 3. Capacity vs. storage temperature for Li/V_2O_5 cells.

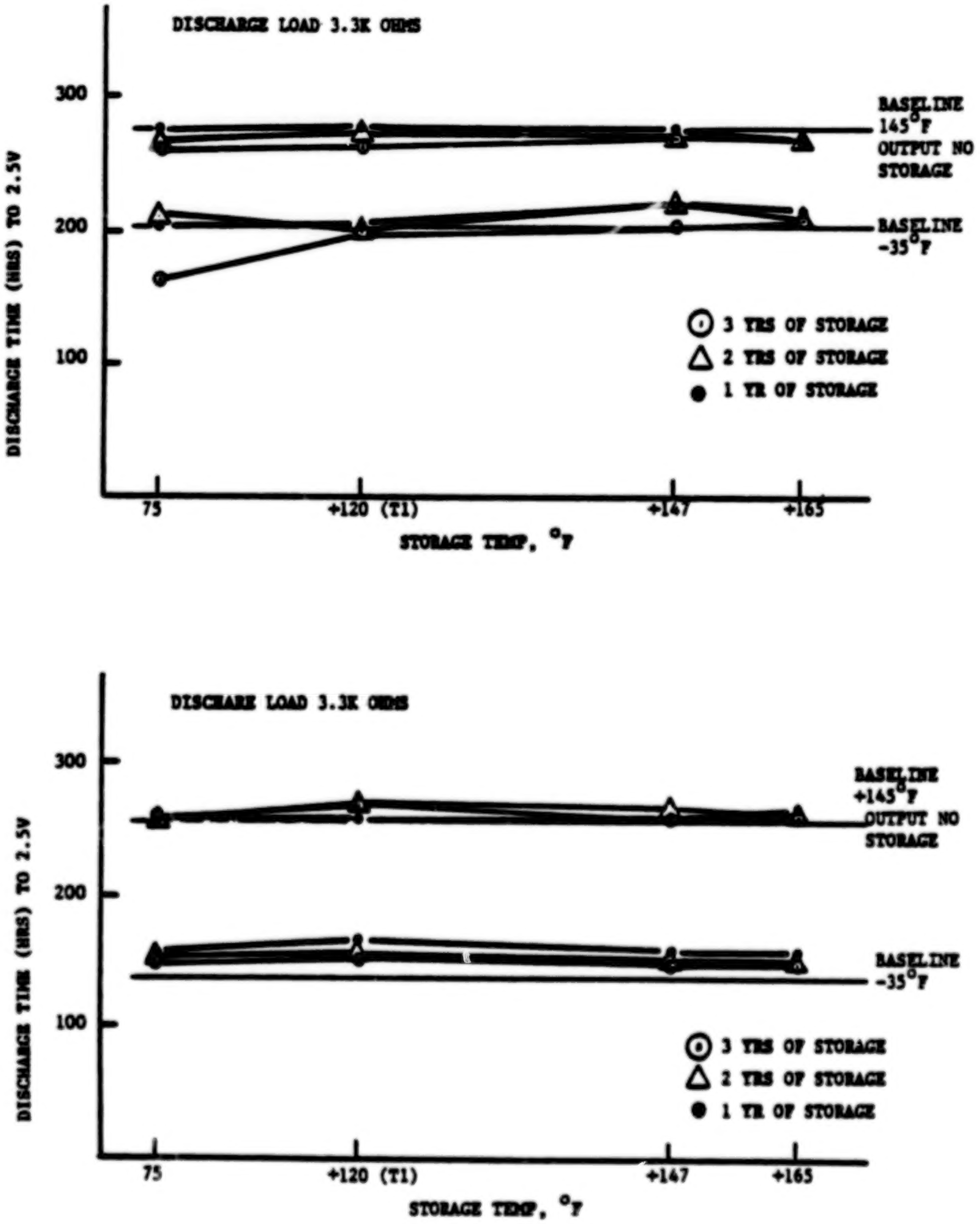

Figure 4. Reserve cell run time to 2.5 volts vs. storage time and temperature (Li/$SOCl_2$ system).

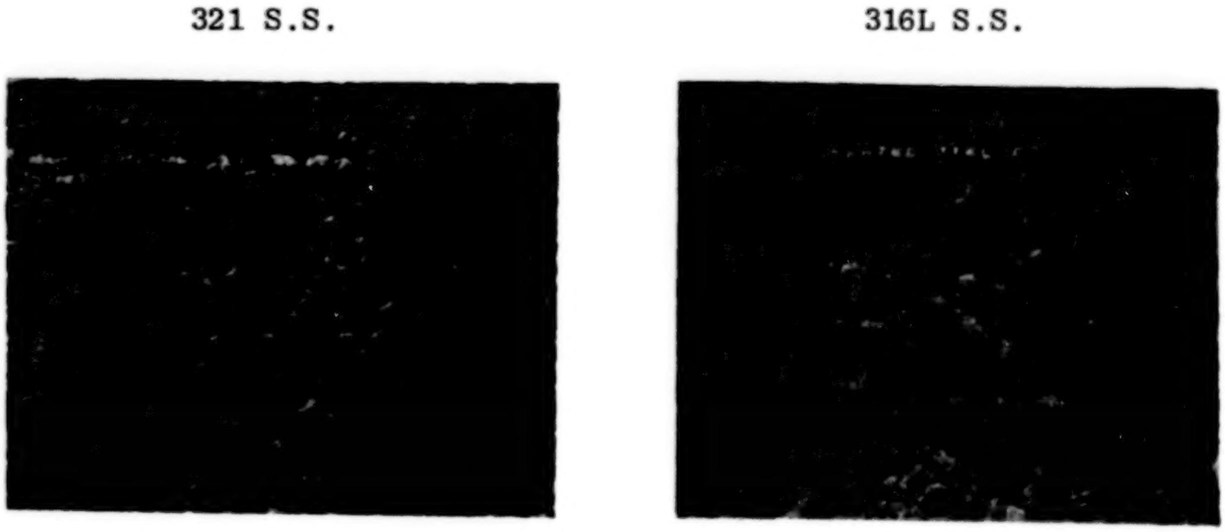

Before exposure to electrolyte

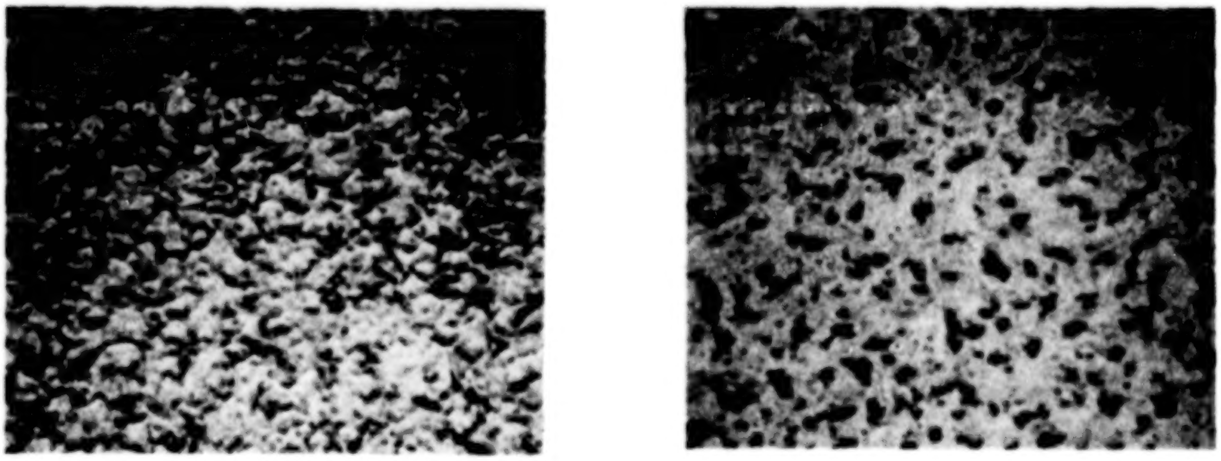

After exposure to electrolyte for 12 months at 71°C

Figure 5. SEM photomicrographs of the surfaces of 321 S.S. and 316L S.S. before and after exposure to the neutral electrolyte solution (1.5M $LiAlCl_4/SOCl_2$).

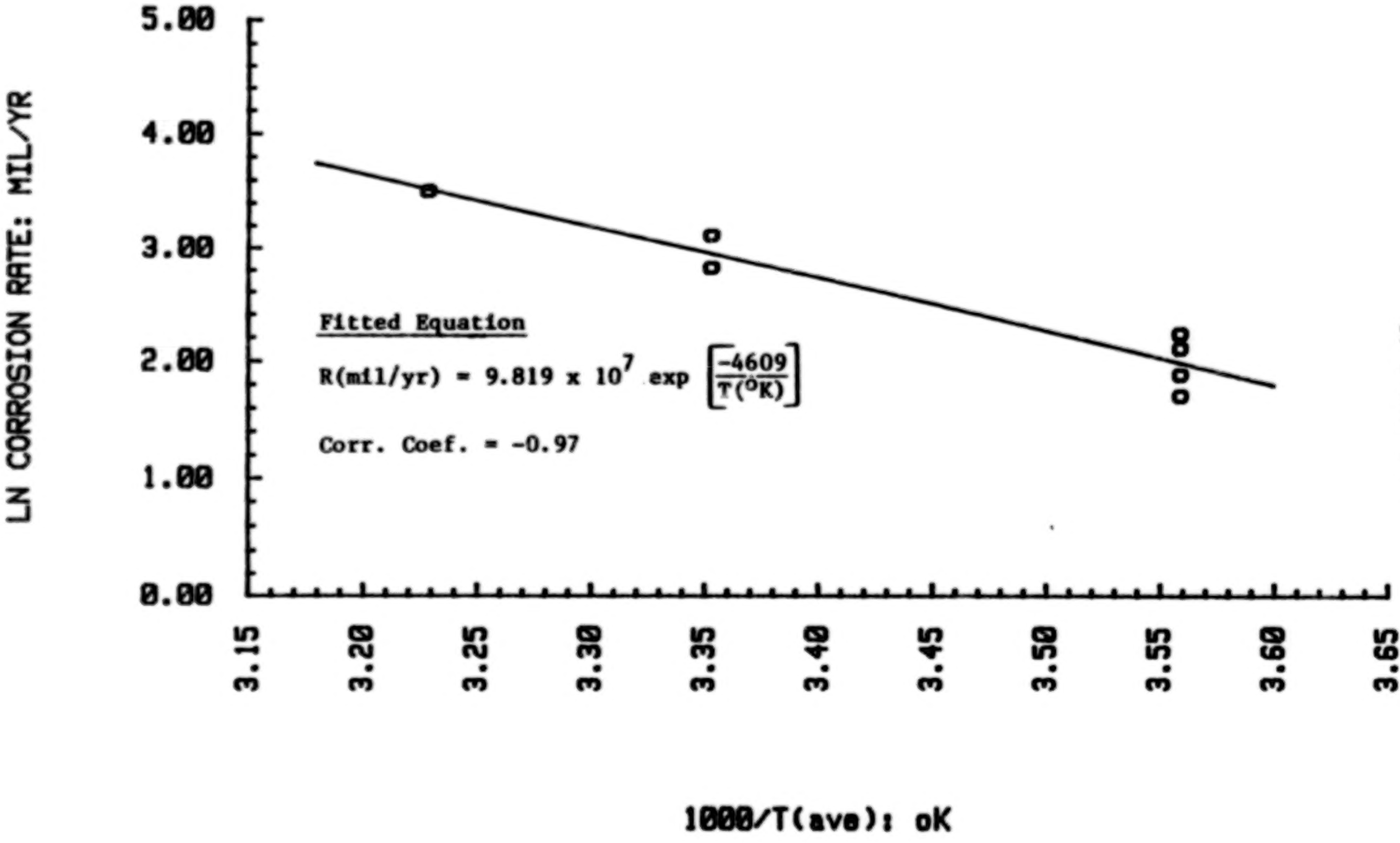

Figure 6. Arrhenius plot of corrosion data for nonaccelerated storage cells incorporating type 9013 glass seals.

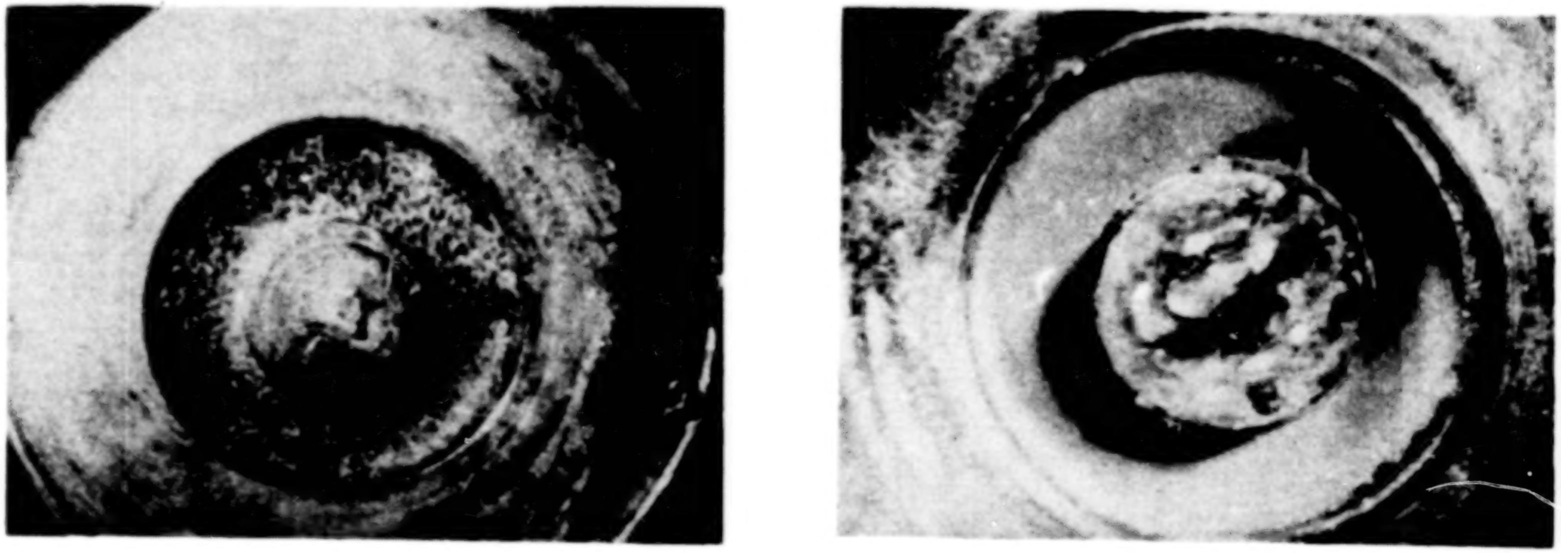

9013 Glass — Full Glass Corrosion

TA23 Glass — No Corrosion

Figure 7. Comparison of 9013 glass and TA-23 glass after accelerated test for seven weeks at 71^{O}C. Li/V_2O_5 system.

Q. Barnes, NSWC: In your work with the ampules, you talk about no breakage. Is that on passive storage or is that after a period of vibration?

A. Chua, Honeywell: That's on passive storage. I should, however, mention that, as part of the analysis of the storage we also, once a month, withdraw a sample for ACM analysis.

N84
33677

UNCLAS

N84 33677 D9

TESTING OF CANDIDATE BATTERIES FOR GLOBAL POSITIONING SYSTEM

James A. Barnes, F. C. DeBold,
R. Frank Bis, Susan Buchholz,
Patrick Davis, and L. A. Kowalchik

Naval Surface Weapons Center
Silver Spring, Maryland 20910

ABSTRACT

Three lithium batteries which have been proposed as candidates for use in the Global Positioning System have recently been studied by Code R33 of the Naval Surface Weapons Center (NSWC). The batteries were discharged at several rates and temperatures both before and after environmental testing. Batteries were heated inside a closed chamber until they vented. Samples of the vented gases were analyzed, especially for components which might be toxic. The test results reported in this paper raise concerns about each of the proposed batteries.

INTRODUCTION

We were tasked to review three lithium batteries which were proposed by prime contractors for use in the Global Positioning System. The batteries are to provide "back-up" power for computer memory circuits within the system. Our review included the discharge characteristics of the batteries under a variety of conditions including discharge after vibration at low and high temperatures. Because the batteries may be used in an environment closed to the atmosphere, we obtained analytical data on the gases which were released when the batteries were heated until they vented. This paper summarizes the results of our study; additional details of this program will be available elsewhere.[1]

The design characteristics of the three lithium batteries are listed in Table 1.

We purchased test lots of 100 of each of the candidate batteries directly from their manufacturers. The batteries were built to specifications developed by the manufacturers in conjunction with the prime contractors designing the Global Positioning System. As is clear from Table 1, the designs of the different contractors required batteries with different electrical characteristics.

EXPERIMENTAL PROGRAM AND RESULTS

The experimental program used for this project was very similar to our standard program which has been described previously.[2] After an initial inspection, we measured the open circuit voltage (OCV) and AC resistance (ACR) at 1000 hertz of each battery. Then the voltage under sequential loads of 1000, 100, and 10 ohms was measured. The ACR measurements were then repeated. The results of these non-destructive tests are summarized in Table 2.

DISCHARGE TESTS

Discharge tests were run on three to five batteries of each type at both the four month and 24 hour rates. Studies at the latter rates were conducted at several temperatures and before and after vibration testing.

Low Rate Discharge

Room temperature discharge at the four month rate produced predictable, acceptable behavior from all three battery types. Voltages during discharge were quite stable until end-of-life for the SO_2Cl_2/Cl_2 and $SOCl_2$ systems. The voltage of the $SOCl_2/BrCl$ batteries dropped slowly from 3.9 volts at the beginning of discharge to a plateau of about 3.6 volts after one month.

Higher Rate Discharge

Room temperature discharge at higher rates also gave acceptable results. The voltage of the $SOCl_2/BrCl$ batteries under a 50 ohm load dropped from an initial value of 3.7 volts to a plateau value of 3.5 volts after a few hours. About 28 hours into discharge, the battery voltages began to gradually drop; but they did not reach the tests' 2-volt cut-off until after more than 50 hours of discharge.

Under a similar 50 ohm load, the SO_2Cl_2/Cl_2 batteries delivered a steady 3.3 to 3.6 volts at room temperature until about 48 hours into the test. Then their loaded voltages rapidly dropped to below one volt within 1 to 3 hours.

At ambient temperature, the $SOCl_2$ batteries delivered a steady 6.9 volts under a 200 ohm load for 24 hours. Their voltages then began to drop until they reached the experiment's 3-volt limit at about 30 hours.

Discharge behavior at 71°C was very similar to that observed at room temperature. As might be expected, loaded voltages increased one or two tenths of a volt over room temperature. The decline of voltage at the end of discharge typically began 1 to 3 hours earlier than at ambient temperature.

A temperature of -50°C had a marked effect on the discharge behavior of the three batteries. Under a 50 ohm load, the voltage of the $SOCl_2/BrCl$ batteries dropped from about 3.4 volts at the beginning of discharge to a value of 2.8 volts after 3 hours. The voltage remained at this plateau until it dropped to the experiment's 2-volt cut-off at about 23 hours. Thus these batteries delivered only about 40% of the ampere hour capacity realized at room temperature. Under the same low temperature loads, the voltage of the SO_2Cl_2/Cl_2 batteries dropped to zero and did not recover during the 24 hour test; thus no capacity was recovered from these batteries at -50°C. The voltage of the $SOCl_2$ batteries at this temperature under a 200 ohm load never exceeded 3 volts and dropped to 2 volts after 24 hours. Since the minimum acceptable discharge voltage for this battery is greater than 3 volts, no usable capacity was available at low temperature even though there was some current flow.

Discharge Capacities

Discharge capacities were measured under several different conditions. Four or five batteries of each type were discharged at room temperature under loads of 50 or 200 ohms as described earlier. These discharges were completed within a month or two after we received the batteries. Twenty-four fresh batteries of each type were vibrated according to MIL-STD-810C at 71°C. Separate lots of 24 batteries were vibrated in the same manner at -50°C. After vibration, all of these batteries were discharged at room temperature using the same loads as in the previous tests. Because several months elapsed between the original discharges and the post-vibration discharges, five unvibrated batteries of each type were discharged as controls for the experiment.

The five, fresh $SOCl_2/BrCl$ batteries delivered an average of 3.48 ampere hours to a 2-volt limit. The capacities obtained ranged from 3.0 to 3.9 ampere hours. The capacities obtained from the 24 cells vibrated at 71°C ranged from 1.8 to 3.5 ampere hours with an average of 2.57. The cells vibrated at -50°C later delivered 2.0 to 3.6 ampere hours at room temperature; their average capacity was 2.82 ampere hours. The capacities of the five control batteries ranged from 2.5 to 3.6 with an average of 3.23 ampere hours.

The SO_2Cl_2/Cl_2 batteries gave similar results when discharged at room temperature through a load of 50 ohms to a 2-volt limit. The fresh cells' capacities ranged from 3.0 to 3.4 with an average of 3.14 ampere hours. After hot vibration, the range was 2.8 to 3.1 with an average of 3.01 ampere hours. The samples vibrated at low temperature yielded 2.7 to 3.2 ampere hours with an average of 2.95. The control samples varied from 2.7 to 3.0 with an average of 2.91.

The bobbin construction of the $SOCl_2$ cells in combination with an unwelded case gave rise to serious problems during discharge after low temperature vibration. Four fresh batteries discharged through a 200 ohm load at room temperature delivered 0.91 ampere hours capacity to a 4-volt limit with no significant variations. The capacities of the four control batteries discharged several months later ranged from 0.87 to 0.96 ampere hours with an average of 0.95. Of 24 batteries vibrated at 71°C, two delivered capacities of only 0.40 ampere hours while the capacities of the other 22 units ranged from 0.84 to 1.0 ampere hours with an average of 0.91. After low temperature vibration, only 6 of 24 batteries could deliver more than 0.8 ampere hours at room temperature. Five batteries had no usable capacity while the remaining samples delivered 0.1 to 0.7 ampere hours. Upon inspection, we found that the cells in many of these batteries had leaked and that corrosion of the cell cases and connectors had occurred.

The discharge capacities are summarized in Table 3. The SO_2Cl_2/Cl_2 batteries exhibited a rather wide range of capacities, but capacity was not affected by vibration at either of the temperature extremes. The fresh $SOCl_2/BrCl$ samples had the same wide range of capacities, and these capacities were adversely affected by vibration. The unvibrated $SOCl_2$ batteries showed little variation in capacities; unfortunately, some of these batteries failed under high temperature vibration and 75% of the sample failed after vibration at low temperature.

HEATING TESTS

Fresh samples of each of the batteries were heated inside a 2.8 liter pressure vessel until the cells vented. Heating at about 20°C per minute was accomplished by wrapping each battery with electrical heating tape. During each test the temperature of the outside of the battery, the ambient temperature inside the pressure vessel, the battery's open circuit voltage, and the pressure in the vessel were monitored. For most experiments, the chamber contained air; but in some experiments, the air was removed with a vacuum pump, and the chamber was refilled with either helium or oxygen.

Each of the $SOCl_2/BrCl$ batteries failed with a loud "BANG" when the temperature of the battery's wall was between 200 and 300 degrees Celsius. The force of the battery failure was often great enough to rock the stainless steel chamber on its supports. When the batteries failed, the pressure in the chamber spiked to over 100 pounds per square inch gage (psig) except in the experiment in which the chamber contained helium. In this latter case, the maximum pressure recorded was less than 50 psig. When we opened the chamber after each experiment, we found that the cell cases had been ruptured and that their contents were scattered about the chamber.

Fresh SO_2Cl_2/Cl_2 batteries behaved in a manner generally very similar to that described for the $SOCl_2/BrCl$ samples, except that the events associated with battery failure were less violent. It is difficult to quantify the loudness of a report or the degree of case rupture, but the pressure spikes associated with the venting of these batteries were only half that observed for the first system.

The $SOCl_2$ batteries failed in a much more benign manner. As the temperature increased from 200° to 300°C, the two cells would vent quietly. Often the moment of cell failure could be identified only from slight increases in chamber pressure. The existence of two distinct pressure increases leads us to surmize that the two cells in these batteries often vented independently. The maximum pressure observed rarely reached 20 psig. Upon examination at the end of each experiment, we normally found the cells still intact in their battery case; the cells had vented through the end closed with the crimp seal, but the ventings were mild enough so that most of the cells' contents remained inside the case.

GAS ANALYSIS

Gas samples were removed from the pressure chamber after each battery had vented during the heating tests just described. These samples were taken in stainless steel pressure bottles to another laboratory for qualitative and quantitative analysis using gas chromatography and mass spectrometry.[3] Several weeks often elapsed between battery venting and gas analysis, so the analysis would not be expected to identify any transient species.

The total amount of gas in the pressure vessel after a venting was calculated from the temperature and pressure data recorded during and after the event. We calculated the total quantity of toxic gases released by a battery venting by subtracting background gases (such as helium or nitrogen) and non-toxic products (such as carbon dioxide) from the total. We then assumed that these toxic gases would be evenly disbursed throughout a closed volume of 85 m^3 (3000 ft^3). We then calculated the concentration of these toxic gases in parts per million by volume. The results of these calculations for each battery tested are summarized in Table 4.

CONCLUSIONS

During this evaluation program, we identified several issues and concerns. We are very concerned about the safety of the SOCl$_2$/BrCl and SO$_2$Cl$_2$/Cl$_2$ batteries because their cell cases repeatedly fragmented during heating tests. The quantities of toxic gases released by some samples of the SOCl$_2$/BrCl battery under test conditions were also quite high relative to the other batteries. Concerns about capacity variability and performance at low temperatures of these two batteries have also been mentioned. The behavior of the SOCl$_2$ batteries is such that we are not overly concerned about their safe use in the Global Positioning System, but their performance after vibration and at low temperature causes serious concerns as to whether or not these batteries could meet all the requirements of the system.

REFERENCES

1. F. C. DeBold, James A. Barnes, R. Frank Bis, Susan Buchholz, Patrick Davis, and L. A. Kowalchik, Technical Report, Naval Surface Weapons Center, to be published (1984).

2. J. A. Barnes, R. F. Bis, F. C. DeBold, G. F. Hoff, J. D. Jensen, L. A. Kowalchik, and D. L. Warburton, 1983 Spring Meeting of the Electrochemical Society, San Francisco, Paper 2, (May 1983).

3. William Dorko, personal communication.

TABLE 1
BATTERY DESIGN CHARACTERISTICS

CELL CHEMISTRY*	CONSTRUCTION	CELL SIZE	CELLS IN BATTERY	VOLTAGE	CAPACITY
$SOCl_2/BrCl$	Spiral	AA	2 in Parallel	3.9 V	4 Ahr
SO_2Cl_2/Cl_2	Spiral	AA	2 in Parallel	3.9 V	4 Ahr
$SOCl_2$	Bobbin Crimp seal	2/3 AA	2 in Series	7.4 V	1 Ahr

*All cells contained lithium anode and carbon current collectors.

TABLE 2
NON-DESTRUCTIVE TEST RESULTS

CELL TYPE	OCV (Volts)	ACR (Ω)	LOADED VOLTAGE (Volts) 1000Ω	100Ω	10Ω	ACR AFTER LOADS
$SOCl_2/BrCl$	3.93	3.3	3.9	3.8	3.6	.55
SO_2Cl_2/Cl_2	3.94	3.7	3.8	3.6	3.3	1.0
$SOCl_2$	7.35	63.	7.0	6.5	5.3	2.4

Results represent the average value for measurements on 100 batteries of each type.

TABLE 3
AVERAGE CAPACITIES (AMPERE HOURS)

CELL TYPE	FRESH	AFTER VIBRATION HOT	AFTER VIBRATION COLD	CONTROL
$SOCl_2/BrCl$	3.48	2.57	2.82	3.23
SO_2Cl_2/Cl_2	3.14	3.01	2.95	2.91
$SOCl_2$	.91	.91	*	.95

*Average not meaningful, see text.

TABLE 4
TOXIC GAS CONCENTRATIONS (PPM) CALCULATED FOR A VOLUME OF 85 m^3

BATTERY CONDITION	CHAMBER GAS	H_2S	HCl	SO_2	CS_2
PART A: $SOCl_2/BrCl$ BATTERIES					
Fresh	Air	79	145	-	16
Fresh	Air	33	77	-	8
Fresh	Air	26	48	-	5
Fresh	Air	12	34	-	2
Fresh	Helium	7	15	.06	2
Fresh	Helium	7	25	.07	2
Fresh	Oxygen	8	24	.3	.4
Fresh	Oxygen	9	28	.3	.5
Discharged	Air	-	-	4	.2
Discharged	Air	-	-	6	.3
PART B: SO_2Cl_2/Cl_2 BATTERIES					
Fresh	Air	1.0	7	.6	.8
Fresh	Air	.9	1	-	.2
Fresh	Helium	11	27	-	2.
Fresh	Helium	-	12	13	1.
Fresh	Oxygen	1.4	5	1	.6
Fresh	Oxygen	6.4	19	-	.4
Discharged	Air	-	.8	5	-
Discharged	Air	-	1	9	-
PART C: $SOCl_2$ BATTERIES					
Fresh	Air	-	11	10	-
Fresh	Air	-	36	35	3
Fresh	Air	-	8	7	-
Fresh	Air	4	20	3	3
Fresh	Air	-	6	5	-
Fresh	Helium	-	8	6	-
Fresh	Helium	-	8	4	-
Fresh	Oxygen	-	2	3	-
Fresh	Oxygen	-	4	3	-
Discharged	Air	-	-	6	.1
Discharged	Air	.03	-	5	.05

Q. Felder, General Electric: Why was there a - 54 degree requirement? For a communications system in a submarine that seems kind of low.

A. Barnes, NSWC: The submarine people asked the same thing. In fact, the bigger and broader question is why do we need a backup with six month capability when, as we in the Navy recognize, a submarine loses power for six months, the memory is going to be a very small part of it. The current goal is to produce a common system for all services. And, therefore, there was a canvassing of all services to define the very worst possible use scenarios. And 54 degrees is a type of temperature that one might see in the Artic. The high in temperature is a desert or sitting on a runaway in California type temperature. So the temperature extremes and the lifetime extremes were non-Navy driven. But then when they looked for the worst place to put this, they decided the submarine was perhaps the most restrictive environment which is why we ended up during the testing.

A. Willis, Boeing: We have an application where we use a single AA BCX cell for memory retention. We have a six-month requirement and I notice your 24 hour rate. We use a 5,000 hour rate because that meets our application. In general we've had very good success with the test data on small sample lot and it looks like we're going ahead with that. It does not have the low temperature requirement. However, we have tested the PCX at intermittent periods of 93 degrees under that rate because of the desert application and found it still very satisfactory for that application.

A. Barnes, NSWC: We have, in our test program, included 4 month discharge. But Jerry told me to limit this to 20 minutes, so I didn't bring all of the viewgraphs. I tried to pick representative ones.

Q. Roth, NASA HQ: You used the term "remember these are only engineering items." Does that mean that these are better or worse than what you would get in production or what have you?

A. Barnes, NSWC: I know that the folks from Electrochem Industries are standing here. I don't know about Union Carbide. I think you better ask them. What I did want to say was that I know from what I said this morning they are making changes - improvements - so I don't know what would happen if we got samples from them today. This is what happened to the small sample we got 15 months ago. Does someone EI want to make any other comment?

Q. Cecil, Electrochemical Industries: The batteries that they used were production batteries. The assembly of the battery pack were engineering samples.

A. Hodosh, Power Conversion: You made the statement that, after the work was done, you made a recommendation and it was sort of turned down because the user said they wouldn't use it under any circumstances. It's kind of like catch-22. I think I read you correctly and I imagine the reason for continuing and doing additional work is that you hope to convince the user, I guess eventually, that perhaps he should use it. I'd like to hear an end to that.

A. Barnes, NSWC: As with all big systems - they're multiple level users. We are dealing with the electronics people who are developing the equipment. But they, in turn, must negotiate with the folks who are in charge of the various platforms. Because submarines are most restrictive, the people in charge of the submarine type desk were the people of most interest in these negotiations. At this point, the electronics people, that is, the people developing the GPS, are back talking, at the policy level, with the submarine people, weighing the relative merits of having anything that might release any toxic substance on the submarine as contrasted with the desire to produce a piece of equipment that will be common to all three services. And that's a policy-level issue. The submarine people's objection was categorical. They did not dispute our numbers. They did not question whether or not someone could survive if one of these batteries were to vent. They simply said, "you are talking about toxic materials. We don't think the need is great enough. Thank you very much." And or now it's a policy decision separate from our technical discussion.

Q. Osterhoudt, Eastman Kodak: You said they rejected lithium batteries. Is lithium the villain or is it the cathodes?

A. Barnes, NSWC: It was the toxic material.

A. Osterhoudt, Eastman Kodak: You mean the cathode.

A. Barnes, NSWC: The gases whicn were released when the battery vented, yes. I don't know how they would react if someone happened to propose a lithium battery that did not vent toxic materials.

Q. Halpert, JPL: Jim, do I understand from your discussion that the heat tape test is a standard test for lithium cells for all applications or only for certain applications?

A. Barnes, NSWC: The heat tape test is one of three tests called for in NAVSEA instruction 9310-1-A to be run on any lithium battery proposed, inside a piece of equipment, for a NAVY system. So, yes, the heat tape is a standard test. The other two standard tests are short-circuit and discharge in the voltage reversal and coming in the next revision of the instruction of the instruction will be a charging test as appropriate.

N84
33678

UNCLAS

D10

N84 33678

RESERVE Li/$SOCl_2$ BATTERY SAFETY TESTING[*]

C. T. Dils and K. F. Garoutte
Honeywell Power Sources Center

INTRODUCTION

Recent development and test effort at Sandia National Laboratories and Honeywell Power Sources Center has been directed at high rate Lithium-Thionyl Chloride batteries which address applications previously specifying thermal batteries. These applications typically demand reserve batteries having rapid rise times, high power capability, with operational life profiles extending from minutes up to 1 or 2 hours. This development work has resulted in the generation of battery parametric design information and concepts in a reserve mode for high rate applications.

Data obtained to date indicate that for some applications, the Li/$SOCl_2$ reserve systems being developed will have advantages over thermal batteries. These advantages occur primarily in terms of rate capability per unit volume, lower battery operating temperatures, longer life, and in some cases, improved rise time.

BATTERY DESIGN

A cross section of one such reserve 16-volt battery is presented in Figure 1. The battery contains five (5) torroidal shaped cells packaged in nested or stacked individual plastic cups.

Electrolyte is held in reserve within a stainless steel welded bellows assembly located on one end of the battery. Surrounding the outside of this bellows assembly is a pressure plenum containing Freon gas which provides the pressure required to collapse the bellows and thereby transfer electrolyte to the cells upon battery activation. This highly reliable approach has been used on key development programs at Honeywell where rapid omnipositional activation of a reserve battery is required. In particular, it has found application in underwater Navy mines/buoy programs.

Battery activation is accomplished when a piston actuator assembly protruding through the terminal plate of the battery assembly is electrically initiated. The actuator output shaft moves a sealed nickel diaphragm forcing an internal cutter within the battery through the seal holding electrolyte within the bellows assembly. Cutting of this seal activates the battery by allowing the Freon pressurized bellows system to function as described above.

---

[*] The battery development work presented in this paper was funded by Sandia National Laboratories.

PRECEDING PAGE BLANK NOT FILMED

The battery design contains a nickel burst diaphragm which functions as a safety vent under abusive extremes of temperature and pressure. The vent is designed to release internal pressure when the diaphragm deflects into a sharpened lance at a preset internal pressure. Overall battery dimensions are 2.2" high x 3.14" in diameter and the unoptimized battery weight is approximately 2.25 pounds. All structural components are 316L stainless steel and hermeticity is achieved through TIG welded construction. Glass-to-metal seals and a safety vent are provided within the terminal place housing.

Figure 2 is a photograph of an assembled battery after fabrication.

SAFETY TEST PARAMETERS

Prototype batteries have been assembled and successfully discharged to a specified load profile across the temperature range of interest (32°F to 111°F). In addition, a series of five (5) batteries have been subjected to abusive safety testing. Safety characteristics were evaluated under the following conditions:

A - Short circuit of a freshly activated battery at +70°

B - Short circuit of a partially discharged battery (discharged through one profile) at +70°C

C - Short circuit of a battery discharged through one profile at -40°C and then heated to +70°C prior to shorting

D - Reverse discharging of a battery previously discharged through one cycle of the profile at 22°C, then heated to +70°C and discharged into reversal under a 2 amp constant current

E - Charging of a fresh battery activated at +70°C and subsequently charged at 0.2A, 1.0A and 2.0A rates.

TEST FACILITY

The above described testing was conducted in the special test laboratory at Honeywell Power Sources Center. Test responsibilities include both acceptance and development testing. All testing is done to written requirements and with calibrated equipment traceable to the National Bureau of Standards.

Encompassing 5300 sq. ft., the lab is comprised of three major areas:

- Temperature and humidity testing, non-hazardous discharge and storage.

- Small cell hazard testing and postmortem <20 Ahr.

- Large cell hazard testing and discharge on units >20 Ahrs.

Testing conducted uses either hard wired permanent test stations designed and built by us or soft wire temporary test setups.

Test capabilities within these areas include:

- Temperature -70°C to +230°C, constant, cyclical and programmable
- Resistive and current testing to 250A, constant and pulse
- Load timing to 3 ms (computer controlled)
- Humidity and temperature, constant and cyclic
- Data acquisition via chart recorders, analog and digital osciloscopes, data loggers and computers (mainframe and desk top)
- Vibration - sinusoidal, small cells
- Drop testing - half sine and trapezoidal
- Computer control and monitoring of chamber temperature with shutoff control and off-site monitoring 24 hours a day.

FACILITY FOR ABUSE TESTING

All abuse testing is conducted in the Special Test Lab (STL). The STL has a floor space of 30' x 40' with about 24,000 ft^3 volume. The room is equipped with an air "scrubber" tank. The tank is charged with a sodium hydroxide and water solution. Room air is drawn through a spray of the solution at 2000 cfm to an outside exhaust. This minimizes airborne pollutants to the outside of the STL and building.

There are ten environmental temperature chambers designed to reduce the effects of explosions. These chambers (Figure 3) are capable of controlling the operating temperature between -60°C and 120°C. They have been tested successfully by heating to destruction of fresh $Li/SOCl_2$ cells as big as 500 Ah capacity and were designed to handle cells to 1000 Ah capacity.

The room is instrumented via ports through the walls. The area has restricted access during safety testing. Whenever there is a potential safety hazard, personnel entering the area must have Safety Committee approval, use respirators as needed, and must be assisted by at least one other person (buddy system) before entry. All test chambers are computer monitored with limit-sense for alarm. Alarm coverage is provided 24 hours per day. The alarm may be analyzed from a remote terminal which allows rapid assessment of the problem. Temperatures are scanned every 10 minutes and recorded and printed once every four hours.

TEST RESULTS

As would be expected, the battery vent functioned effectively during the short circuit test of a freshly activated battery and during the charging test of a freshly activated battery. The three remaining units from which a portion of the capacity had been removed prior to abusive testing did not vent during abuse but did exhibit heating and slight-to-noticeable deformation. None of the tests demonstrated "violent" reactions; i.e., exploding under any of the above abuse conditions.

Data associated with the charging of a fresh battery activated at +70°C and subsequently charged at 0.1A, 1.0A and 2.0A rates until battery venting was achieved is presented in Figure 4. This data is representative of the most severe conditions noted during the series of 5 abuse tests. The graph shows that a battery rise time of slightly under 70 ms was recorded to reach the 12.0 volt level. This is typical for reserve batteries employing this design concept.

During the 0.1A charge, the battery temperature stabilized at 75°C, while the battery voltage climbed steadily initially and then stabilized slightly over 20 volts.

The charging current was then increased to 1.0A with a resultant increase in battery temperature to 88°C prior to stabilization. The charging current was then increased to 2.0A level which resulted in a rapid rise in battery temperature from 88°C to 92°C within a five-minute interval. At this point, the battery safely vented. A peak temperature of 104°C was recorded two minutes after venting.

After the completion of the series of five (5) safety/abuse tests, the batteries were disposed of in the STL via puncturing each unit hydraulically under water. Figure 5 depicts the units after piercing and removal from the hydraulic fixture prior to disposal.

SUMMARY AND CONCLUSIONS

A reserve Lithium-Thionyl Chloride Battery concept has been developed and is currently undergoing feasibility testing in terms of performance, safety, and abusive conditions. The objective of this testing is to demonstrate the feasibility of employing a battery of this type to replace thermal batteries in certain applications.

In summary:

- Excellent performance of a $Li/SOCl_2$ reserve battery has been obtained across the temperature range of interest, 0°C to +44°C.
- Performance improvement over the thermal battery usage is greater by a factor of 3 when discharge time and energy density are compared.

- Performance over an expanded temperature range is also possible; for instance, at -40°C, satisfactory performance was demonstrated against typical thermal battery specifications.

- Safety and abusive testing was successfully accomplished on a series of five units. This series of tests did not reveal any abnormal condition due to the abusive nature of the tests performed. The battery vent functioned effectively during fresh short circuit and during battery charging. Three remaining tests did not vent during abuse, but did exhibit heating and slight deformation. None of the tests demonstrated "violent" reactions; i.e., exploding, under any condition of abuse.

- Further performance improvements can be achieved with additional development, particularly with regard to battery weight and volume reductions.

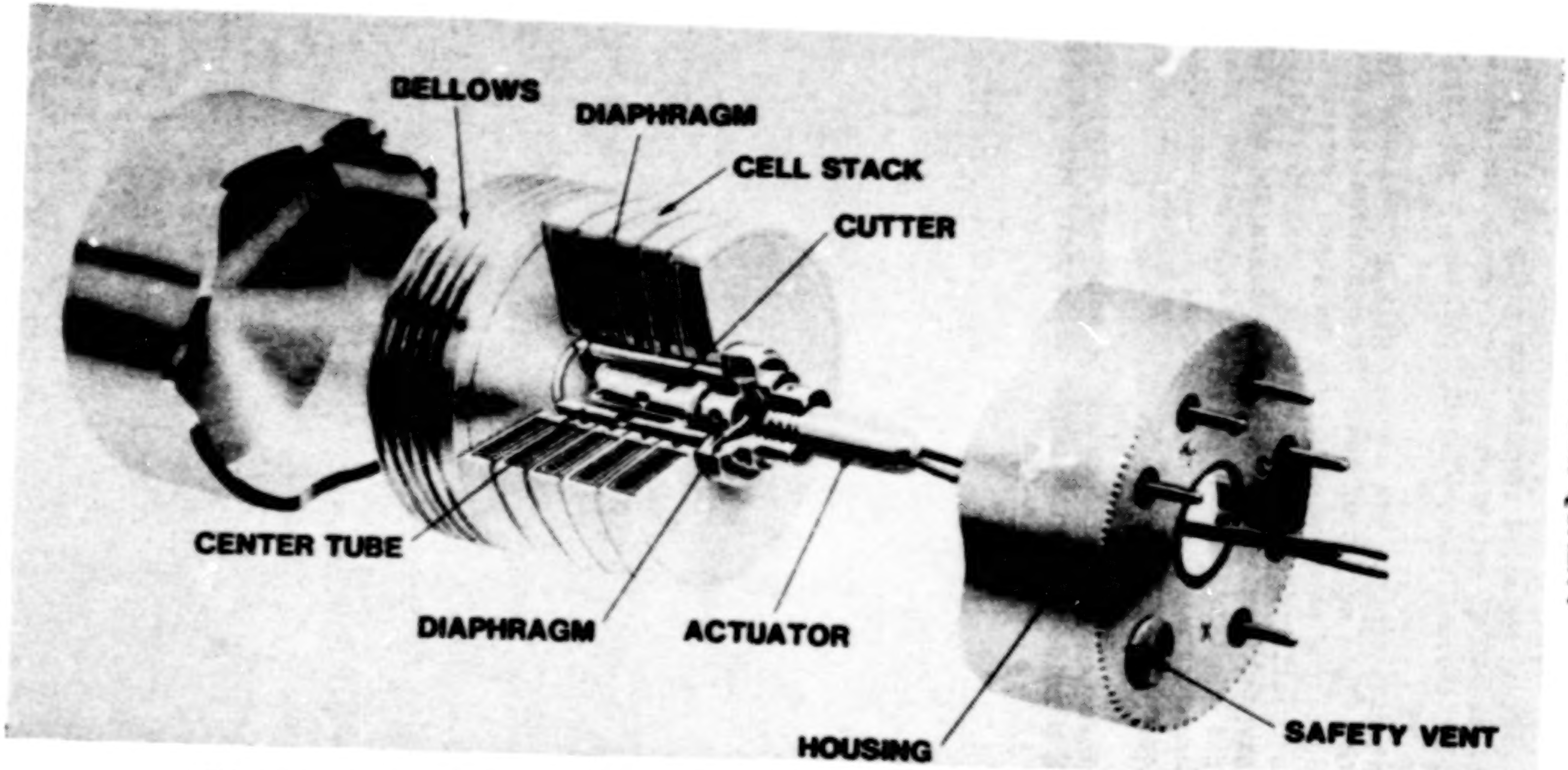
BELLOWS
DIAPHRAGM
CELL STACK
CUTTER
CENTER TUBE
DIAPHRAGM
ACTUATOR
HOUSING
SAFETY VENT

Figure 1. Reserve Lithium/Thionyl-Chloride (RLTC) Battery

ORIGINAL PAGE IS
OF POOR QUALITY

Figure 2. Assembled $Li/SoCl_2$ reserve battery.

Figure 3. Special test laboratory test setup.

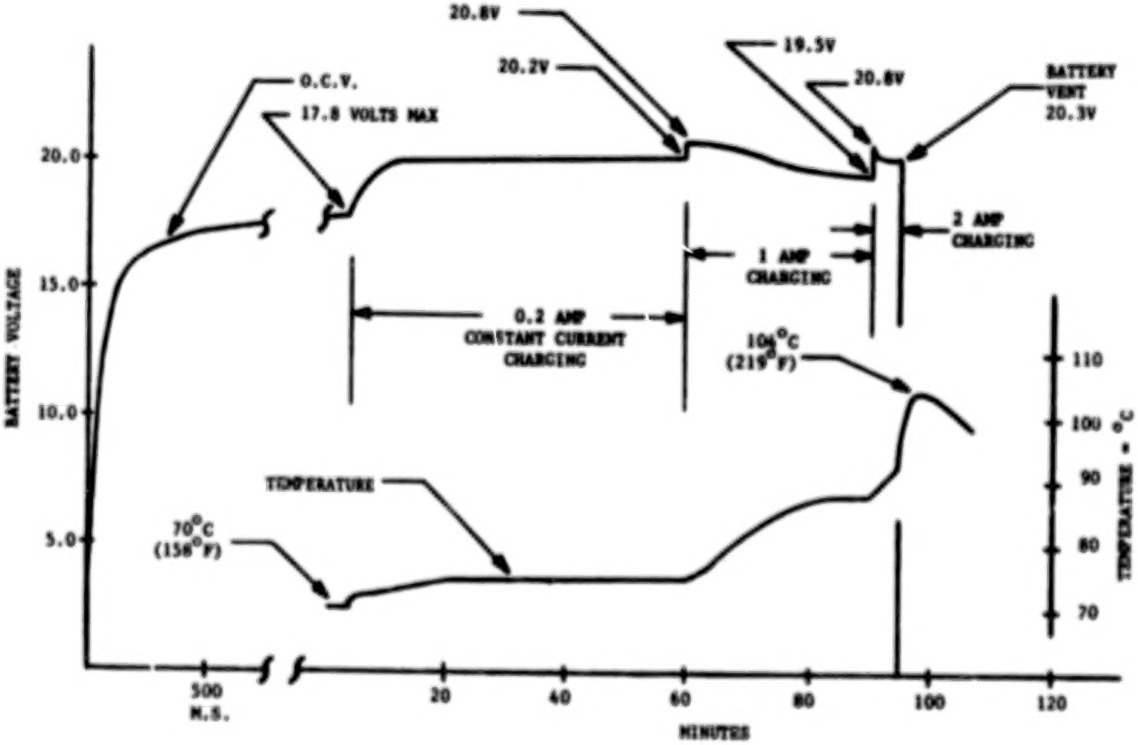

Figure 4. Constant current charging test at 70°C.

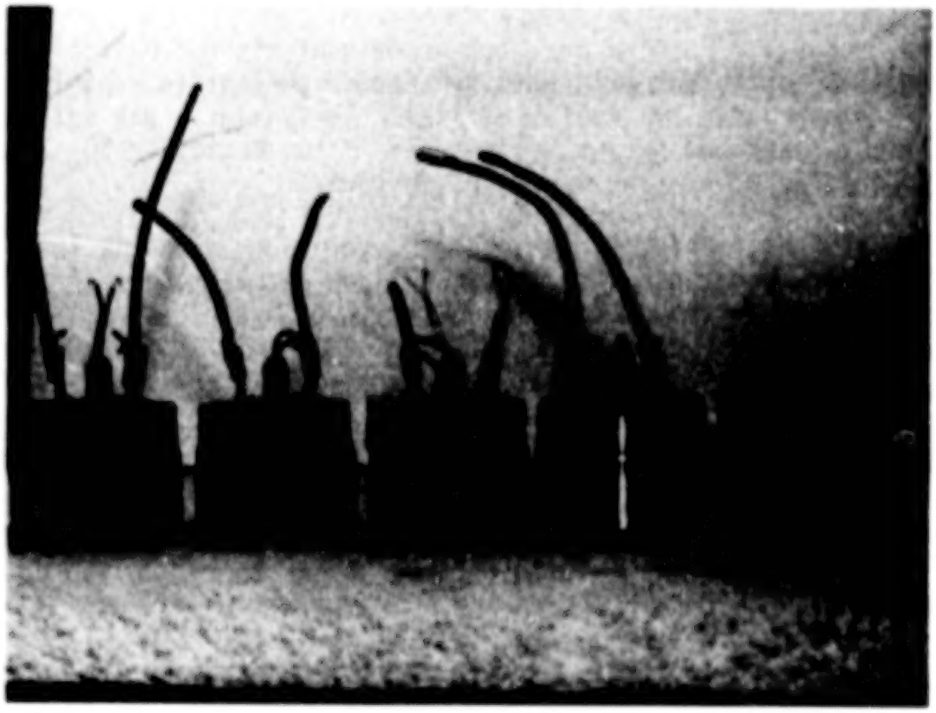

Figure 5. Safety/abuse test units prior to disposal.

Q. Roth, NASA HQ: I was wondering, in any of these tests, did you try to find out what the toxic constitutents are that came off? And the reason I asked that question is some people take certain measurements and not others and what I guess I don't see is any across the board systematic approach to all these where everybody is tending to try to get the same data so that they can pass it among each other.

A. Dils, Honeywell: We did not analyze any of the gasses off of these tests. There has been work done there. I can't discuss it. Maybe Dr. Chua would have some information.

A. Chua, Honeywell: There have been some analysis and basically the result is consistent with what Dr. Barnes percent is - basically hydrochloric acid and sulfur dioxide. The analysis was not on the particular set but on another program. It's basically SO_2 and hydrochloric acid - the major gas species.

Q. Roth, NASA HQ: Yeah, I guess the thought in my mind was looking at the other percentages - parts per million and that sort of thing - to see if it varies cell to cell or type to type.

A. Chua, Honeywell: That's hard to say.

A. Barnes, NSWC: In response to the question of safety - there certainly is a great deal of variability depending on how the cell is opened and whether or not the cell has been partially or fully discharged or whether it's a fresh cell. So that, yes, you do get a lot of variability depending on what regime you decide to run for your test program.

Q. Felder, General Electric: I think I must have missed it. What's the application of these batteries?

A. Dils, Honeywell: They were being evaluated against a thermal battery application.

Q. Felder, General Electric: For what? What application?

A. Dils, Honeywell: I can't answer that.

Q. Levy, Sandia National Lab: Since some of those cells vented in some way other than they're normally supposed to, is there anything in that battery design that could possibly have blocked off the safety vent?

A. Barnes, NSWC: Not that we could find. We took one battery pack apart and it was as typical of low production battery packs made from standard cells held together with glue and shrink wrap. It was not heavily potted or anything like that.

N84
33679

UNCLAS

N84 33679 D11

Performance and Safety to NAVSEA Instruction 9310.1A of Lithium-Thionyl Chloride Reserve Batteries

John C. Hall

Altus Corporation
1610 Crane Court
San Jose, CA 95116

1. Introduction

Reserve-bipolar Li/$SOCl_2$ batteries are preferred for military applications which require:

- Prolonged uncontrolled storage. In the reserve mode the storability of a Li/$SOCl_2$ battery is essentially indefinite.
- Safety prior to use. As the two active battery materials are stored in separate hermetic containers there is no possibility of a hazardous runaway reaction. It should be noted that this is not necessarily the case for reserve batteries employing solid anode and cathode materials.
- Very high specific power levels due to the bipolar design and the liquid catholyte.

This paper describes the design, performance and safety of a fully engineered, self-contained Li/$SOCl_2$ battery as the power source for an underwater Navy application. In addition to meeting the performance standards of the end user this battery has been successfully tested under the rigorous safety conditions of NAVSEA Instruction 9310.1A for use on land, aircraft and surface ships.

2. Battery Design and Performance

A schematic cross section of the battery is given in Figure 1. Prior to activation the catholyte and dry battery stack are separated by a burst disk in the central bulkhead. The stack itself consists of ten 25 cell series modules. During construction the dry stack is potted in epoxy with individual bus wires running down the outer surface of the epoxy shell.

The bus wires run to a terminal board at the base of the battery. The individual modules are connected in parallel to yield the required capacity and voltage upon activation. Per NAVSEA Instruction 9310.1A the modules are connected through protective diodes to prevent charging. In addition each module is protected from short circuit by fusing both the negative and positive bus wires.

Undersea activation of the battery occurs when water pressure bursts the disk above the piston and a bursting pressure is transmitted to the disk between the reservoir and the dry stack. As the device sinks increasing hydrostatic pressure fills the battery stack with electrolyte.

In its intended application the battery is required to provide hotel power and multi-kilowatt pulse power. A typical discharge curve for the battery is given in Figure 2. The total energy drained from the battery corresponds to 850 Wh.

The complete battery measures 29.5 cm in length, 12.7 cm in diameter and weighs 11.4 kg. This yields energy densities of 0230 Wh/l and 75 Wh/kg. The gravemetric energy density is strongly influenced by the heavy case (60% of the battery weight) required for deep undersea operation.

3. Safety

Operational Safety: The battery is intended for operation in unmanned devices and hence safety of activated batteries during discharge is not an issue. It is an issue during development and if device recovery is contemplated.

During preliminary development of the battery venting after discharge but prior to full energy depletion (approximately 24 hrs) was observed approximately 50% of time. The source of these vents was identified as the growth of lithium dendrites driven by the leakage currents in the common electrolyte bipolar filling manifold.

The solution to this problem was to clear the manifold of electrolyte after battery activation. This is accomplished by partially filling the reservoir with argon. Once the battery is filled the electrolyte bursts a rupture disk between the stack and an overflow reservoir. Upon rupture of this disk the piston forces electrolyte out and argon into the filling manifold. By clearing the manifold leakage currents are virtually eliminated and no dendritic ventings have been observed in six consecutive tests.

Short Circuit Safety: By design the battery is fused to assure complete safety during short circuit. This is combined with internal depletion resistors to fully deactivate the battery prior to retrieval.

Nonetheless, NAVSEA Instruction 9310.1A calls for short circuit tests with all fuses and diodes removed. This test was carried out at the systems level by heating the electrolyte reservoir of a shorted battery.

After 26 minutes of heating the reservoir temperature reached 230°C and the battery activated. The behavior of the battery after activation is depicted in Figure 3. To summarize, 54 seconds after activation there was a mild vent with no visible movement of the system. The maximum temperature reached was 506°C 10 minutes and 15 seconds after activation. Maximum short circuit current was 42 amps and a 10 psig pressure spike was observed above the battery vent. The battery presented no fire or explosive hazards.

Reserve Safety: The two areas of concern for an unactivated battery are:

- Maintenance of reserve integrity during shock and vibration
- Safety during a conflagration test

Batteries of an early design passed vibration testing but failed shock by rupture of the electrolyte burst disk when subjected to 330g for 1 msec. A failure analysis led to the conclusion that this resulted from mixing of the argon with the electrolyte and the development of stress concentrations at the disk.

The solution was to place the baffle shown in Figure 1 between the bulk of the reservoir and the burst disk. With the baffle design the batteries are capable of:

- Passing both shock and vibration
- Delivery of full capacity after both shock and vibration
- A 3.8 to 1 safety margin in the shock test

Conflagration tests in accordance with NAVSEA Instruction 9310.1A have been carried out at the systems level. Acceptance, while subjective is generally deemed as the absence of any fragmentation or flame.

An extensive testing, analysis and design program was implemented to meet this standard. Specific activities have included:

- Analytical calculation of reaction rates and battery internal pressure.

- Structural analysis of the battery casing and design as required to assure its integrity in a worst case situation.

- Introduction of a nonfragmentary burst disk.

Results of the reaction time-pressure analysis are summarized in Figure 4. The analysis showed reaction times of:

200 msec worst case
500 msec best estimate
1000 msec best case

Based on this analysis the bulkhead between the reservoir and the stack was designed to accomodate the worst case reaction time. In Figure 4 results of experimental verification of the case integrity are given.

The safety vent was changed to a nonfragmentary design with an increased rim thickness to assure weld integrity. This redesign was accompanied by modification of the vent hole pattern in the piston as shown in Figure 5. The new design eliminates excessive pressure at the center of the safety disk and reduces the blow torch phenomena typical of bipolar batteries venting up the fill hole.

The result of this through analysis and design to conflagration safety standards is graphically demonstrated in Figure 6. Although the system shows the effects of conflagration no fragmentation has occured and no flame was emitted during the test.

4. Conclusions

The $Li/SOCl_2$ system has potentially the highest energy and power density of any primary power source. Concerns with regard to battery safety increase with both energy and power density.

Development of the battery described in this report demonstrates that with careful engineering safe-reserve-bipolar $Li/SOCl_2$ are achievable.

To our knowledge this is the first reserve $Li/SOCl_2$ battery to have complied with the standards in NAVSEA Instruction 9310.1A. The lessons learned in this program are presently being applied at Altus to the development of larger, higher energy density batteries.

JH/5

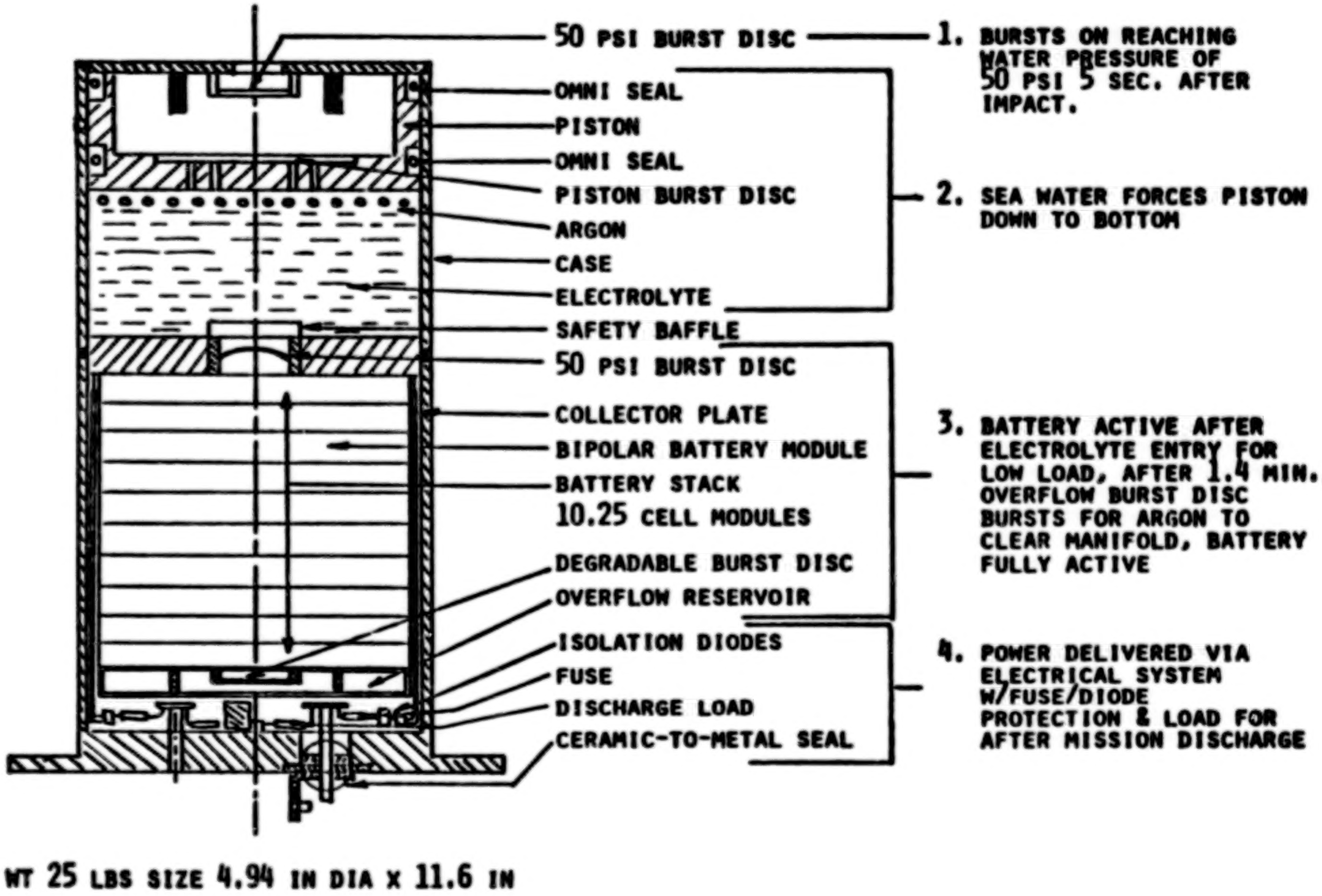
50 PSI BURST DISC
OMNI SEAL
PISTON
OMNI SEAL
PISTON BURST DISC
ARGON
CASE
ELECTROLYTE
SAFETY BAFFLE
50 PSI BURST DISC
COLLECTOR PLATE
BIPOLAR BATTERY MODULE
BATTERY STACK
10.25 CELL MODULES
DEGRADABLE BURST DISC
OVERFLOW RESERVOIR
ISOLATION DIODES
FUSE
DISCHARGE LOAD
CERAMIC-TO-METAL SEAL
1. BURSTS ON REACHING WATER PRESSURE OF 50 PSI 5 SEC. AFTER IMPACT.
2. SEA WATER FORCES PISTON DOWN TO BOTTOM
3. BATTERY ACTIVE AFTER ELECTROLYTE ENTRY FOR LOW LOAD, AFTER 1.4 MIN., OVERFLOW BURST DISC BURSTS FOR ARGON TO CLEAR MANIFOLD, BATTERY FULLY ACTIVE
4. POWER DELIVERED VIA ELECTRICAL SYSTEM W/FUSE/DIODE PROTECTION & LOAD FOR AFTER MISSION DISCHARGE
WT 25 LBS SIZE 4.94 IN DIA X 11.6 IN

Figure 1. $Li/SOCl_2$ reserve battery system.

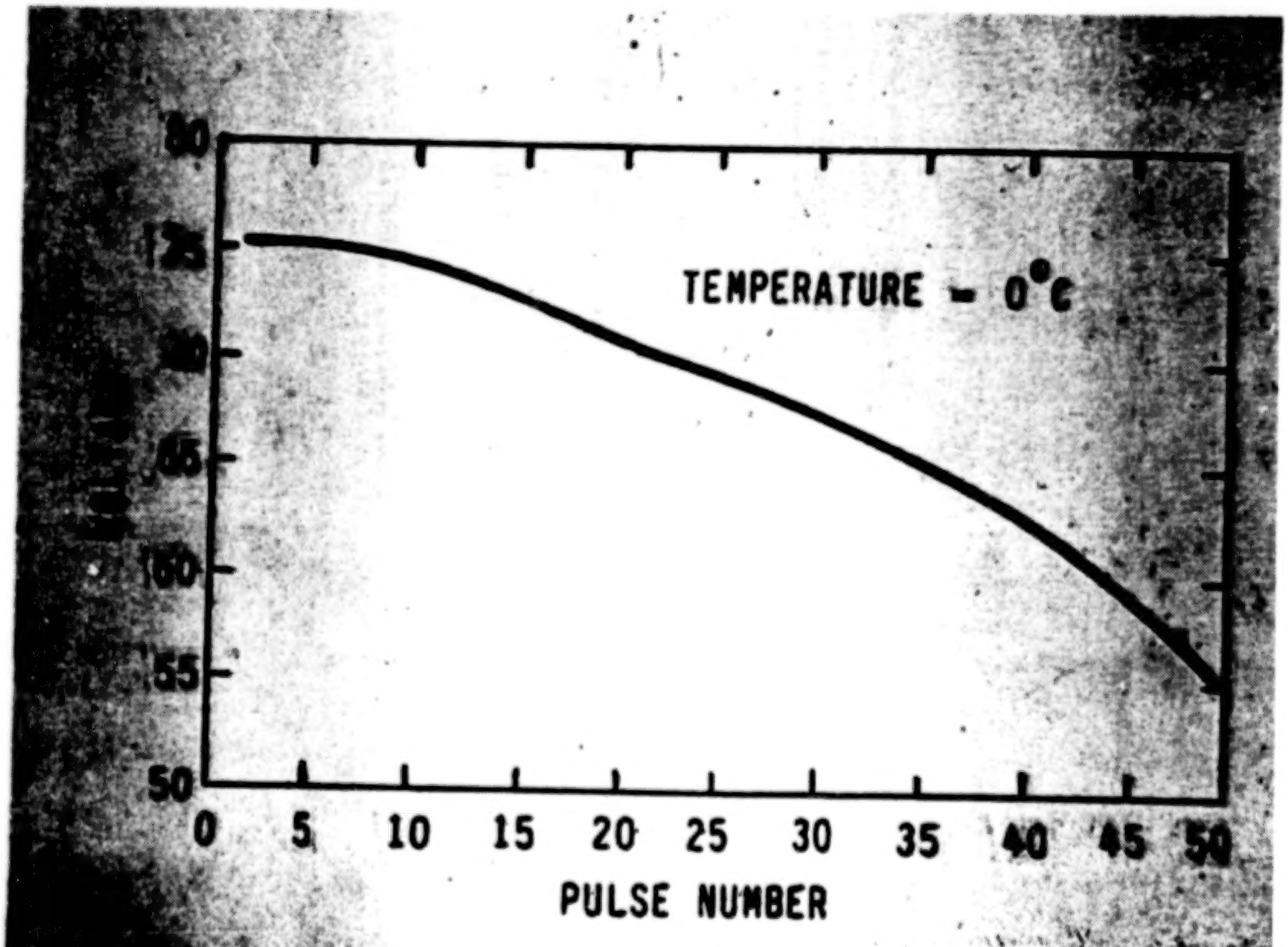

Figure 2. Discharge curve.

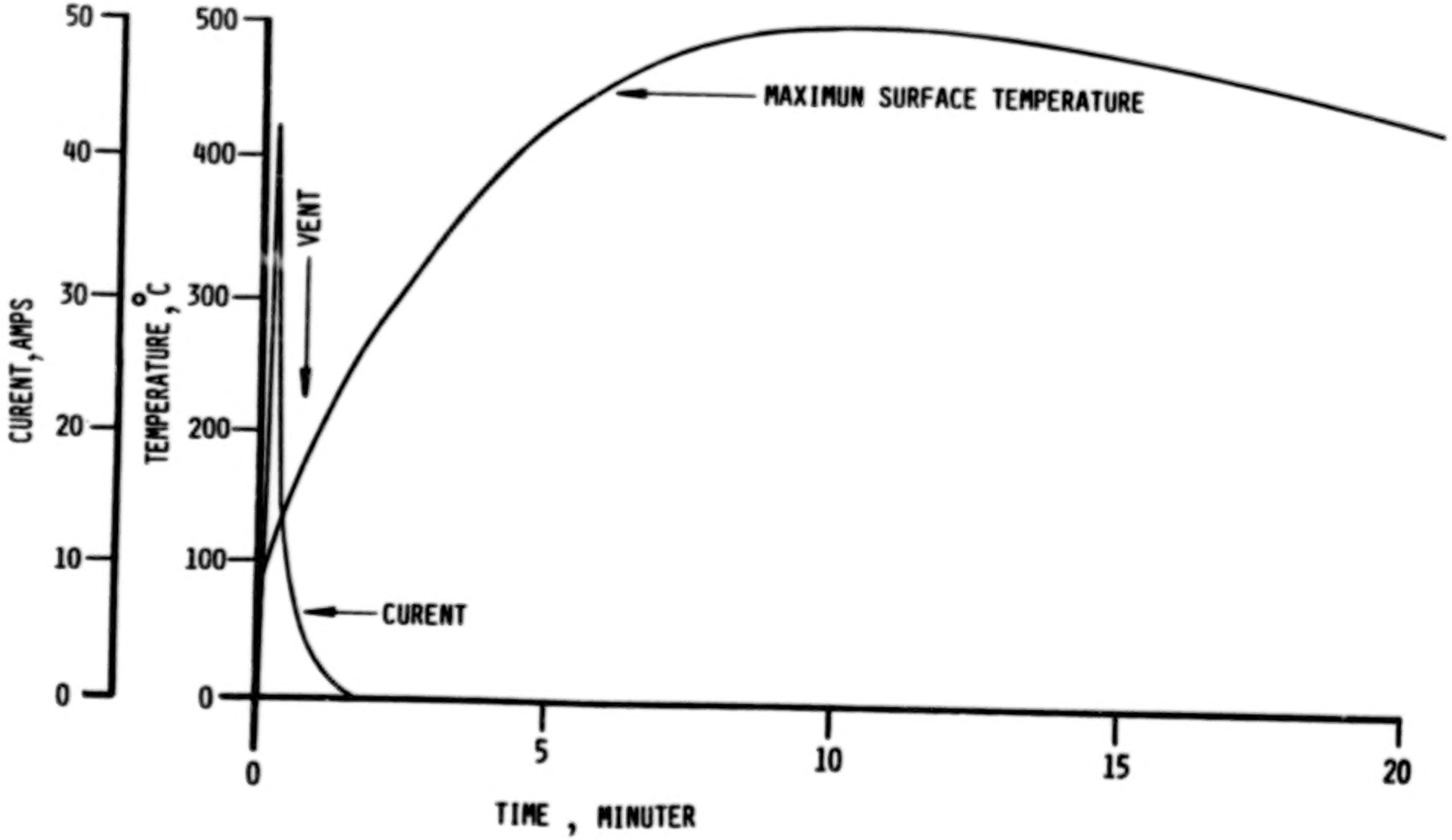

Figure 3. Short circuit test data.

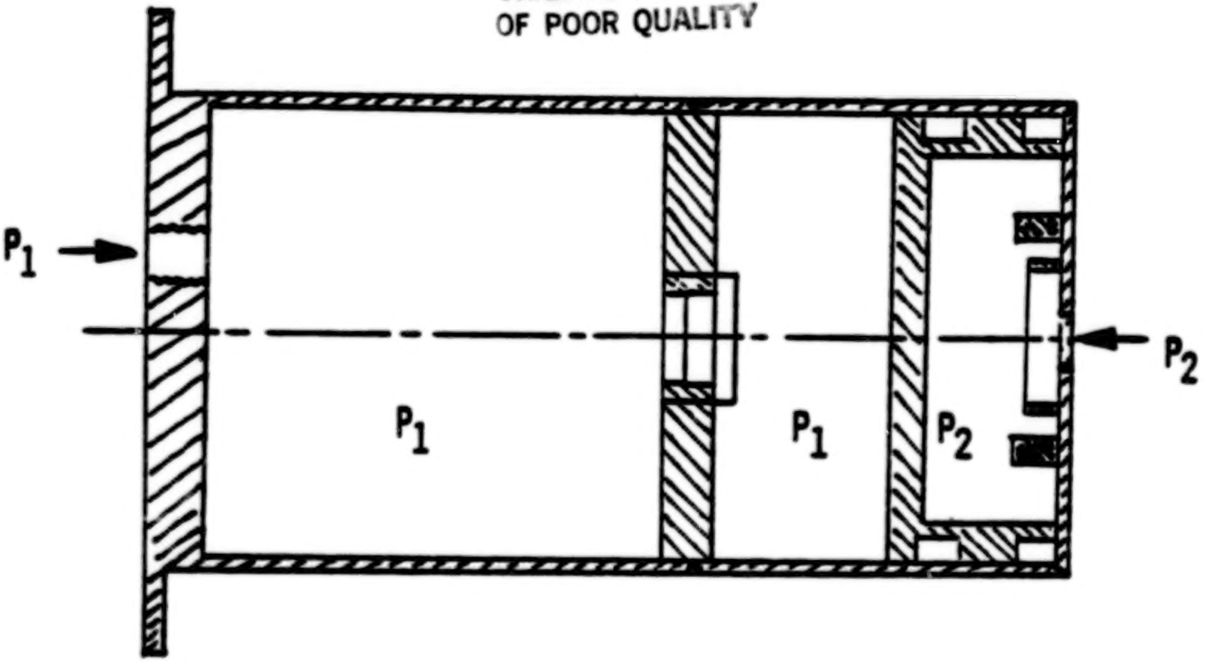

THEORETICAL PRESSURES

REACTION TIME (SECS)	P_1 (PSI)	P_2 (PSI)
0.500	1345	1088
0.200	2588	2058
0.080	3508	2720
0.000	4347	3579

TEST PRESSURES

	P_1 (PSI)	P_2 (PSI)
	1000	550
	1350	1000
*Lost pressure	2000	1500
**Battery top failed	2550	1950
	3000	2500
	3500	*2806
	**3750	0

Figure 4. Battery pressure test.

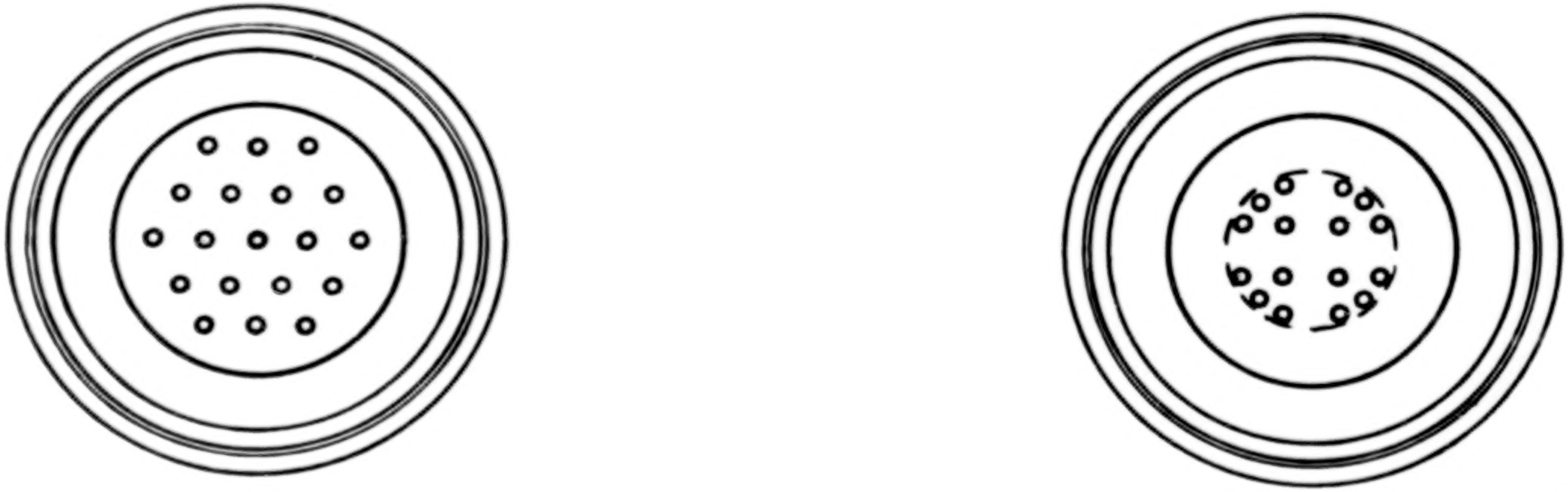

OLD DESIGN

NEW DESIGN

Figure 5. Change to piston safety disc hole pattern.

ORIGINAL PAGE IS
OF POOR QUALITY

AFTER

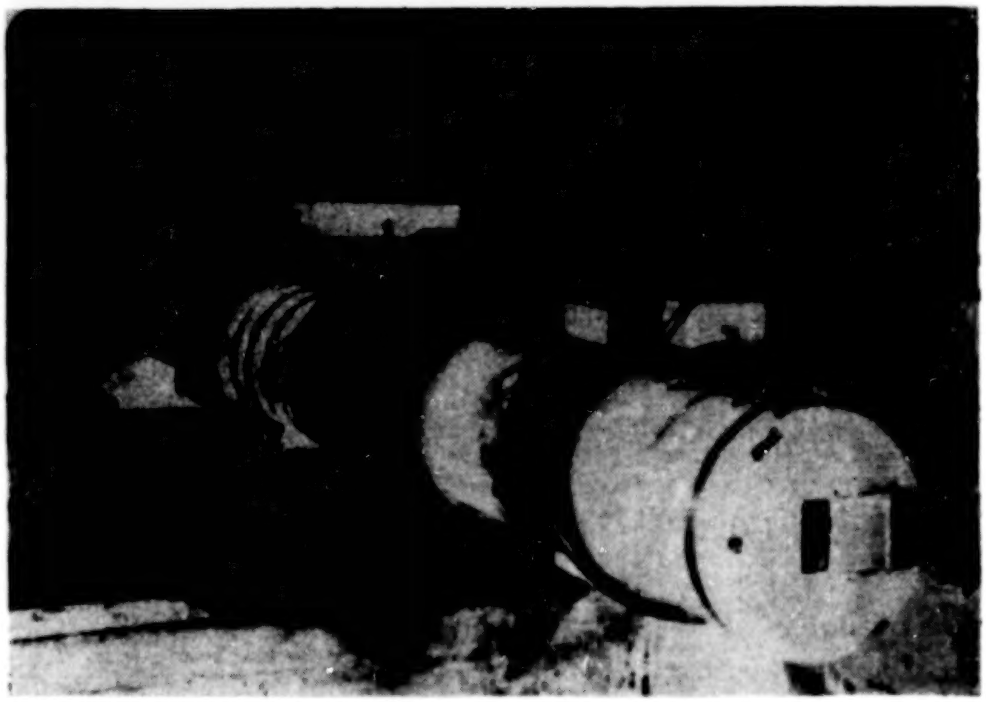

BEFORE

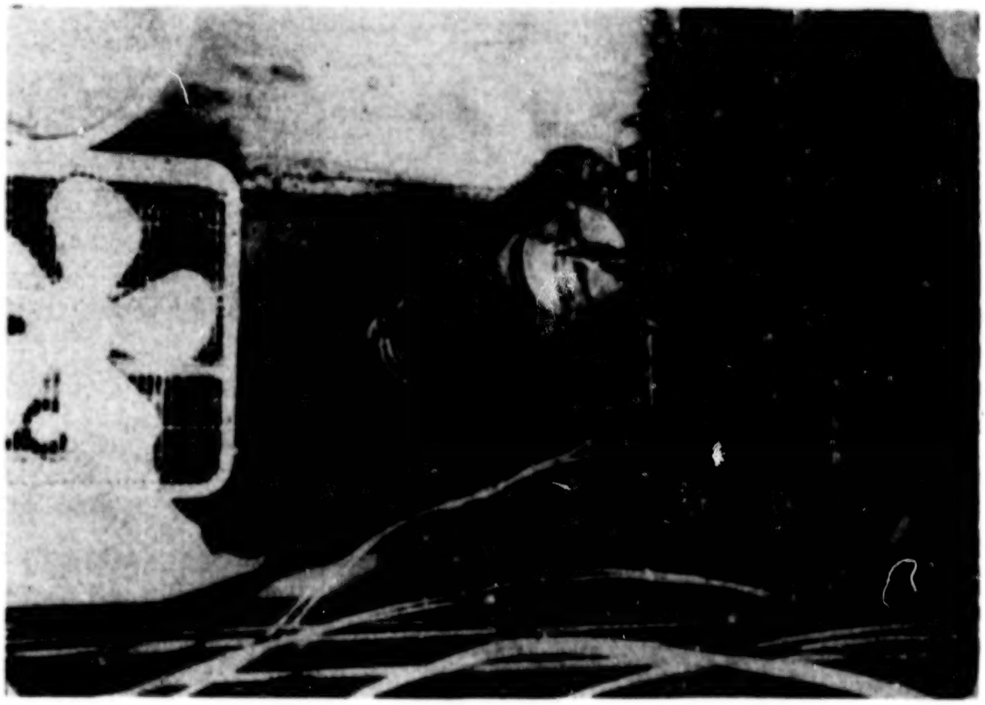

Figure 6. System level battery conflagration test.

N84
33680

UNCLAS

N84 33680 D12

HIGH RATE DISCHARGE STUDIES OF LI/SO$_2$ BATTERIES

James A. Barnes, Susan Buchholz,
R. Frank Bis, F. C. DeBold, and L. A. Kowalchik
Naval Surface Weapons Center, Silver Spring, Maryland 20910

ABSTRACT

A battery composed of twelve lithium/sulfur dioxide "D" size cells in series was forced discharged at 21 amperes. This current was established by the proposed use of the battery and represented a discharge condition which the battery manufacturer felt might produce venting. Discharge of the battery into voltage reversal resulted not only in cells venting but also in the violent rupture of at least one cell.

INTRODUCTION

The Lithium Systems Safety Group at the Naval Surface Weapons Center was recently asked to evaluate a battery under consideration for use in a piece of Navy equipment. The prospective user asked us to determine the battery's voltage response under forced discharge at 21 amperes and to characterize any safety hazards associated with this discharge. The Navy user provided us with several samples of a battery which had been proposed for the equipment by the equipment's manufacturer. This paper briefly describes our tests and some of the more dramatic results which we obtained. The experimental results and the data collected as a part of this evaluation offer several lessons to the community of lithium battery users.

EXPERIMENTAL DESIGN

The sample batteries were first characterized by physical inspection and the measurement of their open circuit voltage and AC impedance. Forced discharges were effected using a DC power supply limited to 21 amperes and 36 volts (the open circuit voltage of the batteries). Battery potential and battery temperature were measured at regular intervals throughout the experiment. The potential drop across a calibrated shunt was used to measure the current actually flowing in the circuit. All discharges were conducted in a facility designed for hazardous testing.

BATTERIES TESTED

All of the sample batteries contained 12 high-rate "D" size lithium/sulfur dioxide cells connected in series. Each battery was fused at 30 amperes with a "slow-blow" fuse. The batteries contained two hexagonal layers of six cells held together one on top of the other with elastic cement and enclosed in outer wrap of plastic film and cardboard.

The batteries were delivered to us by the Navy engineer who was considering them for use in a piece of equipment. He had obtained the batteries from the contractor who was developing the equipment. The contractor had in turn obtained the batteries from a manufacturer who had built the cells and assembled the battery. Upon inspection, it was clear to us that some of the batteries had been used and/or had developed internal problems during the course of this handling. The results reported in this paper represent data obtained on a battery which exhibited no physical or electrical indication of use or deterioration.

In order to obtain as much information as possible about the battery, we asked the manufacturer for information about the battery's history. The available records indicated that the batteries were probably assembled in mid-1979, a time consistant with the data code on the cells which showed that they had been built in April of 1979.

The manufacturer's representative was very helpful to us when we sought this information but was quite surprised to learn that we planned to evaluate batteries which were then four years old. We were told that our results would have only general applicability relative to the behavior of a battery built in 1983 because the construction and performance of the cells had been modified and improved several times since our batteries were built. Upon clarification, we learned that although the cells built in 1983 retained the same description and catalog number used in 1979, the cells actually were different enough that the manufacturer's representative doubted that our test results would apply to a new battery.

POINT 1

The information just summarized is a clear example of this paper's first point for lithium battery users: manufacturers often change cell designs, and these design changes are not always accompanied by a change in catalog number or description. This practice of incorporating changes into a cell without changing the catalog number seems to be the regular procedure of at least several of the major battery manufacturers, it is certainly not limited just to the cell we were testing. The community of users must view this practice with ambivalence. Manufacturers introduce changes into a cell to provide a product which they view as safer, more effective, and/or less expensive. Although users must find these goals to be generally admirable, we cannot help but be concerned that these "improvements" can reduce or destroy the value of performance data obtained on earlier versions of a cell. For data which required substantial time and effort to collect suddenly to become less useful because of a change in cell construction can be a very serious loss. The loss can be even harder to manage if the changed cell retains an unchanged catalog number.

BATTERY DISCHARGE RATE

The use for which this battery was suggested required that it deliver 21 amperes at 28 volts for several minutes over a wide temperature range. This current represents a very demanding, perhaps even abusive, discharge rate for any "D" size lithium/sulfur dioxide cell, even one of "high-rate" design. The battery's manufacturer was concerned enough about the consequences of a discharge at this rate to label each battery, "Caution: This battery when discharged at customer-required rates can be expected to vent SO_2 gas. Use extreme care to avoid breathing toxic fumes." The manufacturer's catalog also cautions against constant discharge of this cell at currents above 1.3 amperes.

POINT 2

The second point of this paper is now clear: users often ask more of a battery than it was designed to provide. The battery manufacturer's literature on this cell suggested that the battery would only marginally meet the discharge requirements of the equipment at room temperature; and at -40°C, the problem would have been even more severe. The contractor designing the equipment still proposed this battery in spite of clear indication that safety or performance problems would probably exist. The prudent user will make an effort to understand the limits of a battery as early as possible during the design process.

RESULTS OF FORCED DISCHARGE

Figure 1 shows the voltage and temperature data obtained during forced discharge of the battery. At a constant discharge current of 21.5 amperes, the battery voltage dropped from an open circuit value of 36 volts to 23 volts. The voltage recovered to about 26 volts before it began to drop as the battery was forced into reversal. About 20 seconds after voltage reversal occurred, one side of the battery was suddenly and noisely engulfed in flame. Subsequent failures (presumably at the cell level) spanned almost two minutes and bathed the battery in flame. Then a sharp, distinct BANG occurred. The battery fragmented, and cells were scattered over a radius of more than eight feet. (At the oral presentation of this paper at the Battery Workshop, a video tape recording of the battery failure was shown at this time.) The cells were collected and examined after the test. It was clear that most of the cell cases remained intact, and that these cells vented through the vents manufactured into them; but at least one case lost its end and another ruptured through its side.

POINT 3

Lithium/sulfur dioxide cells which have been discharged into voltage reversal at high rate can fail with significant violence. The failure described here is more severe than any we have previously observed for similar cells under conditions of abusive discharge or over discharge at room temperature.

SUMMARY

Our specific results are of particular value to the potential user of this specific battery, but we have identified three areas of concern for battery users in general.

- One must be aware that the characteristics of lithium cells may be changed as manufacturing processes are changed.

- One should avoid forcing a cell to perform beyond its safe design limits.

- One should be aware that even lithium/sulfur dioxide cells with vents can fail with a "BANG" when forced into voltage reversal at high rate.

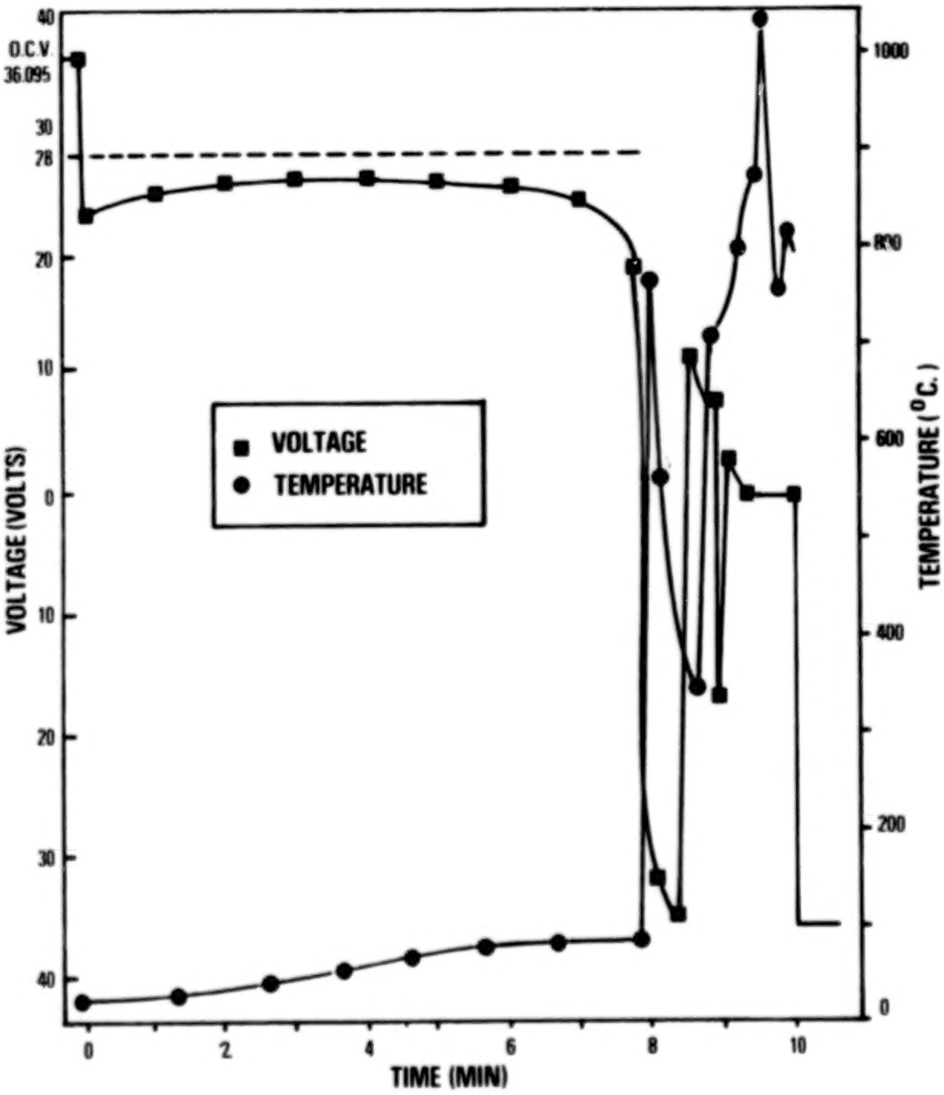

Figure 1. Voltage and temperature data for the forced discharge of a battery at 21 amperes.

Q. Halpert, JPL: This is a panel of experts and rather than having a panel of four or five members up here we have a panel of experts out here in the audience. The business of safety verus non-safety continues to go on. And depending on who is up here speaking and on what system they're speaking about, there's still a question about whether we can build a "safe cell". And it turns out that Gil Roth here from NASA headquarters has been asking this question for a long time - can we build a safe cell. I'm sure he'd like to see that one in NASA applications. But I thought I'd take an informal poll to see how we stand on the issue. Let's restrict it to Lithium SO_2, Lithium Thionylchloride or the BCX system. Is there any one of those systems that - let me phrase the question differently - do you feel we can build a safe cell for any application from those three electrochemical systems? How many of you feel as though they can build that? Is there a safe cell? Ah! There are some people that say I'm opening up the whole world. I want to know any application you could think of that you would select - SO_2, Thionychloride or BCX cell for use and feel - safer and that word has always got to be a defined word. I'm leaving that open now too. I saw some hands.

A. Allvey, Saft America, Inc.: I think you should phrase the question another way. It's basically my contention that there is no battery system - or very few - that I can't make hazardous, so the answer by definition is that you cannot build a safe battery system.

Q. Halpert, JPL: Well I was going to ask that as the second part of my question. I was going to ask you if you could build a safe and if I got no answer I was going to ask is everyone of them hazardous and then we'll go from there. But we do have some people who think that there is one of those three systems, in some applications, that can be safe. I saw four or five hands. Would anyone want to describe a system? Al Willis is using a cell and he raised his hand. Would you be willing to speak to the issue, Al?

A. Willis, Boeing: We have been experiencing the application of the lithium cell to the minuteman silos. GTE has built an assembly of cells or submodular three cells which, in any opinion, is built like the proverbial house and, as such, it has withstood all the abusive testing that we have been able to give to it or, that is, not necessarily me but the military. We have completed the discharge of one set of batteries in the silo satisfactorily and are now in the process installing some others in other silos. Last year I made an investigation concerning what happens when you operate several cells or several batteries in parallel. I speculated that potentially if you had one cell go bad in one battery, you would have a sharing of that current. In other words, would go down and then the other batteries would have to pick up the load. And so you would have a sharing of the load depending

A. Willis, Boeing (Con't): upon the voltage of each of the batteries. And as you got near the end where one cell would go bad in one battery, the other batteries would have to pick up that load until such time there was essentially one bad cell in each battery if you kept it going that length of time. This is a schematic of the installation where there is a power bus. There is a controller between the batteries and the bus. And when the bus got to a certain voltage the batteries were cut in. And the batteries were used until a certain voltage was reached and they were cut out of the circuit. There is nine cells in each battery. There is a diode and a fuse in each battery, as shown. Getting into the area of what happens when one cell goes bad, in this particular application - the OCU of 9 cells at 3.65 is 32.85 volts. The controller had a cut-off of 36.25 volts and so if all the cells went together that would mean an average voltage of 2.94 volts per cell. In the event that the current went to zero, then the - you'd have 29.2 which is still higher than that 26.5 which means eventually you're going to be reversing some cells. In the upper sketch there is the voltage times and the solid line shows the normal discharge. Now if one cell failed early - which is always the case - in parallel operation the other batteries could pick up the battery voltage in that particular stack would rise as the current went down. That shows the upper dotted line. The voltage on the other stacks or other batteries would go down because they are picking up more current. Eventually the voltage levels out and you have essentially one dead cell in each battery. That actually happened in our discharge test and there are at least two out of the four batteries that had cells that were driven so far in reverse that they would not recover the OCU. So that was our experience with batteries in parallel. It might be of interest to some of your applications. You will have a change in voltage as one cell goes dead and the other batteries will pick - up the load until you have essentially one dead cell in each battery.

Q. Halpert, JPL: Al were those thionylchloride cells?

A. Willis, Boeing: Yes.

Q. Halpert, JPL: And did you say what size they were incidently?

A. Willis, Boeing: 10,000 amphere hours - small ones.

Q. Halpert, JPL: Okay, so number one your comment is in your particular application if you have a very strong structure and if you have batteries in parallel you're safe. That's your contention at this moment and we won't push you any more on that. And there were some other people who said they had a safe design. Dave, you had your hand up. Would you be willing to talk for a moment on the issue?

A. Yalom, AT&R, Inc.: Everybody must recognize that a given battery must be designed for a given application. And if batteries are abused or misused, you're going to run into trouble. But I say that a battery can be made safe if it's designed for its end-item applications. That's what it boils down to.

Q. Halpert, JPL: I've got a lot of hands here. Anybody disagree with that. Well, I mean we have different kinds of tests. The Navy does heat tape tests. Are those cells safe if you blow them up like that? Are you satisfied with a cell if you see it blow up on a screen? Would you buy one of those? Well, where does safety begin and where does safety end? We're still in this bind and I'm trying to maybe separate out what it is we absolutely have to do to call it safe and what it is we're doing because we think we may have to do that to call it safe. There are a lot of people who felt that we have safe cells but you all didn't raise your hand. Does anybody else feel as though we can make a safe cell out of those systems?

Q. Levy, Sandia National Lab: If you make a cell for a specific application and the cell sees the conditions that it's supposed to see, that's one thing. But suppose this safe application gets involved in a fire or something. That's a whole other ball game. And how do you define safe? For instance, a $LiSO_2$ cell is designed to vent. If, in a certain application, it vents as it's designed to do is it considered safe? Or, does it have to not vent in the way its designed you know or just stay together? How do you define safe?

A. Halpert, JPL: Anybody want to answer that? Well, I think the comment about the application is certainly reasonable. It's got to be safe in the application. But, on the other hand, you have the two problems - one being the basic chemistry. Is the basic chemistry safe? And is the user handling it safe? That's where we have our problem and obviously why we don't want to use it in the consumer business. Because we know what people will do in the consumer business. But here we have military applications, we have aerospace applications and we have Burt Otzinger who wants to say something.

A. Otzinger, Rockwell International: I think one of the key items here is whether it is going to be used in close proximity to people or personnel versus using it in an application where personnel are not going to be imminently close to it. Because I think that, insofar as the lithium systems, what sets them apart from most other kinds of batteries is that the gasses that can come off when something goes wrong can be persinous or can cause real problems. If it weren't for that fact, I don't think it would be quite as big a problem. You can come up with your absolutely fail-safe system and so on and yet if you have a fire, a configuation or something - if it were to happen, say, in a spacecraft where they had no way

A. Otzinger, Rockwell International (Con't): to get out or do anything - as soon as the gasses evolved you've got a problem. It's a safety problem. So, how safe could you ever be in a situation like that. I don't think you ever can be. I think you're stuck. In some kinds of situations, a submarine - I think there are situations where because of the poisonous gas situation if you had some way to deal with that, then maybe you could finally say "Yeah, maybe we can handle that situation. But I think there are unmannered space probes - these kind of things where, sure, it could be made perfectly safe. I don't know about perfectly, but certainly safe.

Q. Halpert, JPL: Anybody else want to add to that? Feel free.

A. Taylor, Duracell International: Just to play the devil's advocate, I could argue that lithium managanese dioxide cells, lithium carbon monofluoride cells, lithium thinochloride cells are all safe - consumer safe. And the proof of that is that they are already available, all of them, in the consumer market place. I admit I've taken a bit of poetic license with thionylochloride, but I think that everybody is aware that union carbide, who talked about it last year, made these available in greater quantities. So, to make the statement deliberality, all three of those systems are available commercially already. You'll find managanese in your camera's shutter activating device. Though it's not a real time consumer application, you'll find carbon monofluoride in the Kodak disk camera. And I'm not quite sure where you'll going to find the thionylchloride, but it's coming. What does that mean? I think it means that lithium systems are going to have a commercial future and maybe it would be to some degree under definitions such as particular applications. Maybe that won't even be so in the future. I would hazard a guess that one or other, or more likely a range of them, are going to find commercial acceptance, never mind military acceptance. Because they can't do things other batteries cannot.

COMMENT

Gross, Boeing: I would like to, just for perspective, point out that the common lead-acid battery results in an order of two or three dozen explosions every year in this country, many of which cause a lot of personal injury and other kinds of damage. So, here is a battery that everybody considers safe, but yet, when it's misused or not used properly, it too can give us explosinos and unsafe conditions.

Frank, JPL: One understands the chemistry; one understands the thermal aspects of the system, followed up by quality control and handling, I think one can specify it safe for given applications.

Q. Otzinger, Rockwell International: One other issue - disposal. I tend to agree with the gentleman in that, yes, lithium cells are going to become more plentiful. I'm wondering how long it's going to be before disposal becomes a very serious problem?

A. Reiss, U.S. Army ERADCOM: We're buying considerable quantities of lithium sulfur dioxide batteries right now for the Army and for some of the other services. We have addressed the problem of disposal in significant efforts over the last three years. We have come up with certain conclusions to permit us to field the batteries are treated as a hazardous material. They are collected and centrally disposed of in secure land fills or hazardous waste land fills. It requires particular permitting for transportation to these sites. Within the military, we are going to be doing this through, routine contracts at each installation through the property disposal system. Each installation has one of these officers or works through a nearby installation. These people will be issuing contracts on a routine basis for the collection, not only of lithium batteries but of other hazardous wastes that are generated at the various installations, such as photographic wastes. It is a problem. We have come across particular scenarios that we are handicapped from a military point of view. When we got outside of the continental United States where batteries are airlifted in, totally in accordance with Department of Transportation rules and international rules. And yet when they are used they become a different item as far as the rules go and we can't put them back on an airplane to bring them out. We are addressing this problem right now. We do have certain controls within our system that will permit us to go on and perform our mission, but we think right now we're at a point where we can at least utilize the technology, utilize the various lithium densities. But there still has to be several issues resolved.

Q. Halpert, JPL: Okay, I would have to infer one thing from what you said to go back to your very first statement that you're buying large quantities lithium sulfur dioxide cells that you consider them safe. Am I supposing something that isn't safe for the application? What does your definition say?

A. Reiss, U.S. Army ERADCOM: As I implied, the Army has procured hundreds of thousands of batteries within the last three years alone in the lithium sulfur dioxide technology. We have used these batteries safely. We have used them in a variety of equipments. We have also had several problems. The statistics would show that we've had very few problems and I don't want to go into the numbers. We consider a dozen incidents too many out of 3 years. We are looking at military applications of these batteries. There has been some recent message traffic reporting, some of these incidents that are very disturbing to our commandus.

A. Reiss, U.S. Army ERADCOM (Con't): Words that we put into these teletypes say something like "the battery sounded like an incoming round when it ruptured." This is intolerable to an soldier. They cannot have batteries on their back or in their foxholes that are blowing up, or rupturing or venting or going "bang". Their purpose is to fight a war. They're not there to have their own equipment turn on them. And to that extent we feel yes the batteries have been used safely, but the safety record has to be improved.

Q. Halpert, JPL: I appreciate your making those comments off the cuff. Do any other people feel as though they have used or have applications where they really consider their SO_2, thionylchloride or BCX system safe or can be used in a safe application. Does that mean that every lithium SO_2, thianochloride or BCX cell is hazardous? Would you not use it? I think I beat it to death, huh. Well, we're frustrated - I'm frustrated, I shouldn't say we're frustrated. Maybe other people are frustrated too but I'm frustrated. I see a possibility of a real advance in the technology. We're talking about high energy density; we're talking about applications that would not be useful. I'll talk about the NASA mission, if you will where a man has a BCX cell in his helmet. And the only way he can get some decent hours out in the bay - out in the shuttle bay wondering around - is to have with him a cell of some kind so he can get enough amphere hours capacity so that he can see what he's doing. Otherwise he'd have to - he'd only have half an hour at the most by the time he got out and got back in.

N84
33681

UNCLAS

N84 33681 D 13

SHUNT DIODE DESIGNS IN Li/CF SHUTTLE BATTERIES

David Miller and Robert Higgins
Eagle-Picher Industries, Inc.

ABSTRACT

Although Li/CF cells and batteries have an excellent safety record, they have been included with other battery systems that require additional safety precautions. One precaution that has been suggested is the inclusion of shunt diodes into these batteries. This paper explores the benefits of this addition.

INTRODUCTION

The LCFS-20 is a popular double-"D" size lithium carbon-monofluoride cell currently used in several different batteries. One such battery is the MAP-9036-5, the Range Safety Battery used in the Space Shuttle Program. In an attempt to further increase the safety of the battery, a contract was proposed that included the incorporation of a shunt diode board into the battery. The resulting battery is designated MAP-9036-7. The vital statistics on the MAP-9036-7 are as follows:

Height:	5.3 inches	Nominal OCV:	38.0 volts
Width:	6.6 inches	Nominal Working Voltage:	29.0 volts
Length:	8.0 inches	Nominal Capacity:	20.0 a.h.
Weight:	9.0 pounds	Nominal Discharge Rate:	0.5 amperes
Cells:	13 LCFS-20	Operating Temperature Range:	+20°F to +140°F

The diode designated to be used was the IN5550 silicon rectifier diode. The vital statistics for the diode are as follows:

Working Peak Reverse Voltage Rating:	200 volts
Maximum Average Forward Current:	3 amperes
Surge Current Rating at +55°C:	150 peak amps maximum
D.C. Reverse Current at 100°C I 200V:	0.025 mA dc maximum
Forward Voltage Drop at +55°C at 3 amperes dc:	1.0 volts maximum

The diodes were included in the battery to act as a shunt in the event that any cell became overdischarged and began to reverse. The diode(s) would not allow the cell (or cells) to go into deep reversal and thereby would prevent any damage that this deep reversal might cause to the cell and the total battery voltage. A battery schematic is shown in Figure 1.

PRECEDING PAGE BLANK NOT FILMED

The battery was to be discharged at a constant rate of 0.50 amperes. This discharge was to be delivered anywhere within a temperature range of -25°F to +155°F.

The customer was especially concerned about cells that had been discharged, allowed to stand for a period of approximately three months, and then driven into reversal. This situation had caused problems in different battery systems and there was concern about how the Li/CF cells would react. As a result, cells approximating this condition were tested as were freshly discharged cells.

TESTING

The LCFS-20 cells were tested to the following outline:

1. Hot Test (165 + or - 5°F)

   A. Previously discharged cells
      1. Reversed with shunt diode
      2. Reversed without shunt diode

   B. Recently discharged cells
      1. Reversed with shunt diode
      2. Reversed without shunt diode

2. Room Temperature Test (outdoor ambient)

   A. Previously discharged cells
      1. Reversed with shunt diode
      2. Reversed without shunt diode

   B. Recently discharged cells
      1. Reversed with shunt diode
      2. Reversed without shunt diode

3. Cold Test (-25 + or - 5°F)

   A. Previously discharged cells
      1. Reversed with shunt diode
      2. Reversed without shunt diode

   B. Recently discharged cells
      1. Reversed with shunt diode
      2. Reversed without shunt diode

Cells used in these tests were standard production cells that were used as lot acceptance cells. They were discharged at a constant current of 0.50 amperes to an end voltage of 200 volts. To successfully complete lot acceptance, the cells must deliver a minimum of 19.8 ampere-hours of capacity. The history of the cells used is a follows:

Serial Number	Delivered Capacity (amp-hours)	Days from Capacity Test to Diode Test
1322	24.68	56
1327	24.35	57
1335	24.41	64
1354	23.96	65
1366	24.23	51
1377	24.65	50
1386	24.35	44
1395	24.26	42
1419	23.91	31
1460	24.34	10
1463	23.86	9
1471	23.74	4
1485	25.53	13
1500	24.92	14

The cells were allowed to equilibrate in their test environments for between 20 and 48 hours prior to discharge and reversal. Elapsed time, currents, voltage, and cell skin temperatures were monitored using standard calibrated timers, ammeters, DVM's and trendicators. The current was kept constant through the use of a power supply and a five-ohm resistor. A typical discharge/reversal set-up is shown in Figure 2.

Figures 3 through 8 show the results of the test discharges/reversals. Figure 3 shows the results of the previously discharged cells discharged at approximately 165°F. Cell Serial Number 1322 was discharged without a shunt diode. It reached a minimum voltage of -0.92 volts at approximately 2.5 hours. Shortly after this, the cell vented and the voltage began to rise. The test was discontinued at 2.75 hours. Cell Serial Number 1327 was discharged with a shunt diode and reached a minimum voltage of -0.12 volts at four hours. At this time, it also vented and the voltage began to rise. This test was terminated at 4.1 hours. The LCFS cells are vented by the placement of a downward-oriented sticker overlaying a thin diaphragm. As the pressure builds inside a cell, the diaphragm expands outward until it meets the sticker and is pierced. The above-mentioned cell vents were this type of very passive vent. The only indication that a vent had occurred was the distinct aroma of the cells' electrolyte. There was no evidence of anything other than vapor leaving the cell.

Figure 4 shows the test results of more recently discharged cells run at 165°F. Cell Serial Number 1485 was discharged without a diode for approximately 24 hours. At one hour, the cell had vented at a voltage of -0.40 volts. The reversal was continued and at the 2.5 hour mark (-0.83 volt), the diode began to carry current. The voltage stabilized at -1.52 volts with the diode carrying 0.483 amperes.

Figure 5 shows the test results for previously and freshly discharged cells reversed at outdoor ambient temperatures (57 + or - 10°F) without diodes. Both previously discharged cells (Serial Numbers 1354 and 1386) reversed quickly, and by thirty minutes into the reversal, had reached their minimum voltages of -4.68 and-1.46 volts, respectively. However, by the two-hour mark, both cell voltages had stabilized at -0.20 volts and remained there for the remainder of the test. The freshly discharged cells (Serial Numbers 1463 and 1471) both reversed only to approximately -0.10 volts by the five-hour mark and remained there for the remainder of the test.

Figure 6 shows the test results of both previously (Serial Number 1335) and recently (Serial Number 1395) discharged cells discharged at outdoor ambient temperatures with diodes. Within the first hour of reversal, both cells had reached their minimum voltages of -1.04 and -0.81, respectively. By the third hour, both cells' voltages had risen and stabilized around -0.15 volts, where they stayed for the remainder of the discharge. In both tests, the diodes began to function when the cell voltage reached -0.60 volts. The diodes gradually began to carry more and more of the current until they carried approximately 0.250 amperes at both cells' minimum voltages. As the voltages began to rise, the currents through the diodes began to gradually fall until they were no longer functioning, with neither functioning by the two-hour mark.

Figure 7 shows the test results of the cold (-25 + or -5°F) discharge of both the previously (Serial Number 1377) and recently (Serial Number 1500) discharged cells, each without diodes. Each cell reversed quickly with Serial Number 1377 reaching a minimum voltage of -29.4 volts at the ten-minute mark, and Serial Number 1500 reaching its minimum of -9.4 volts at 16 minutes. Each cell began to recover soon after, with Serial Number 1500 reaching -0.30 volts by the five-hour mark and -0.10 by the test conclusion. Serial Number 1377, the previously discharged cell took longer to recover, being -2.5 volts by the five-hour mark and -0.6 volts by test conclusion.

Figure 8 shows the test results of the previously discharged cell (Serial Number 1366) and the recently discharged cell (Serial Number 1460) both with diodes. Cell Serial Number 1366 reversed immediately upon discharge to approximately -1.10 volts where it remained until near the end of the discharge when it rose to -0.40 volts by the 24-hour mark. Its diode began to function immediately, carrying 0.425 amperes at the one-minute mark and slowly rising to 0.480 amperes by one hour. At the end of the discharge, when the cell voltage was -0.40 volts, the diode was not functioning. Cell Serial Number 1460 also reversed early in the discharge, having a voltage of -0.68 volts at the 19-minute mark where the diode began to function. By the two-hour mark, the voltage had reached its minimum of -1.28 volts and the diode was carrying its maximum load of 0.400 amperes. However, by the five-hour mark, the cell voltage had risen to -0.20 volts and the diode was no longer functioning.

EVALUATION AND RECOMMENDATIONS

All cells tested at the elevated temperatures vented regardless of length of time between being fully discharged and reversed or inclusion of the diode in the system. Cells discharged at ambient temperatures all show a relatively quick reversal, but by the two-hour mark, had stabilized at voltages that were high enough that the diodes were not functioning. Cells tested at depressed temperatures reversed the deepest of all cells tested, with the deepest reversal occurring very early in the test and voltages recovering to above -0.60 volts near the end of the tests.

These tests were conducted at only one rate of discharage. A higher rate of discharge may cause the diode to be used for longer periods of time instead of just the short transient periods observed. Conversely, at a lower rate of discharge, the diodes may not function at any time.

Historically, Li/CF cells have had no severe effects to reversal. Instead of any type of explosion or violent reaction, the passive vent is the worst observed response. This venting is generally attributed to the solvent reduction that occurs in this cathode-limited cell; however, preliminary testing has shown that anode-limited cells will eliminate the venting during hot reversal.

These observations are based on the testing of a small number of cells, and further cell testing as well as testing on the battery level is planned. Based on current information, the diodes would function as planned in a limited set of circumstances with limited benefit to the program.

We would like to acknowledge the support of the Marshall Space Flight Center in the conducting of this work.

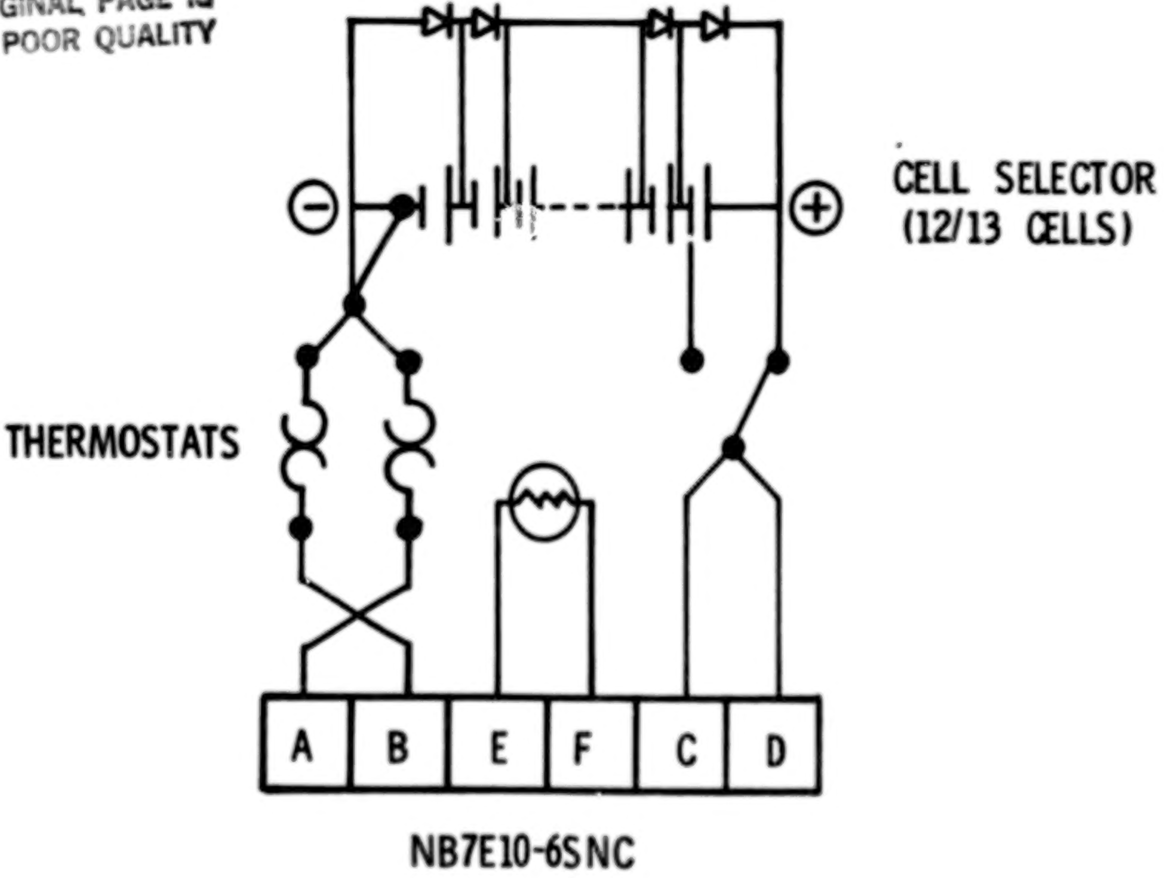
CELL SELECTOR
(12/13 CELLS)
THERMOSTATS
A
B
E
F
C
D
NB7E10-6SNC

Figure 1

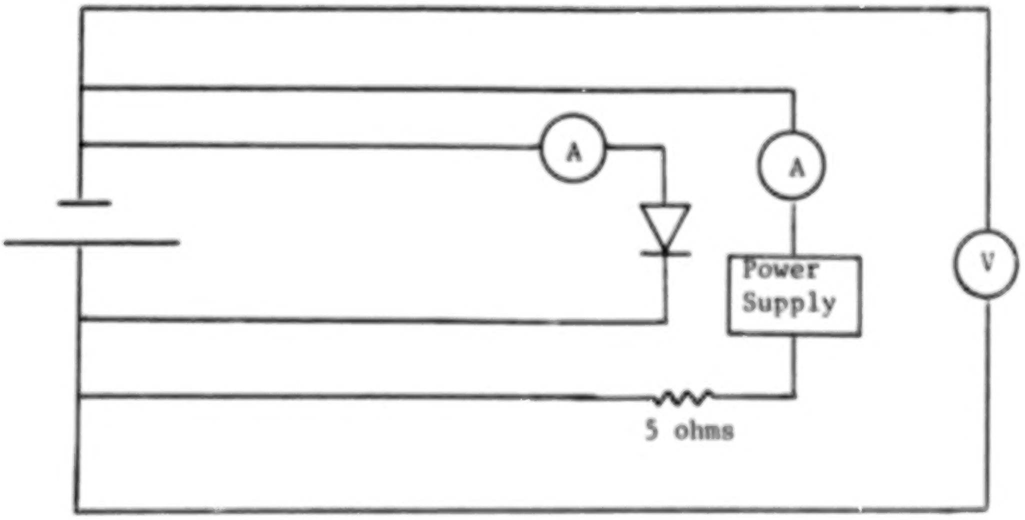
A
A
Power
Supply
V
5 ohms

Figure 2. Typical test set-up.

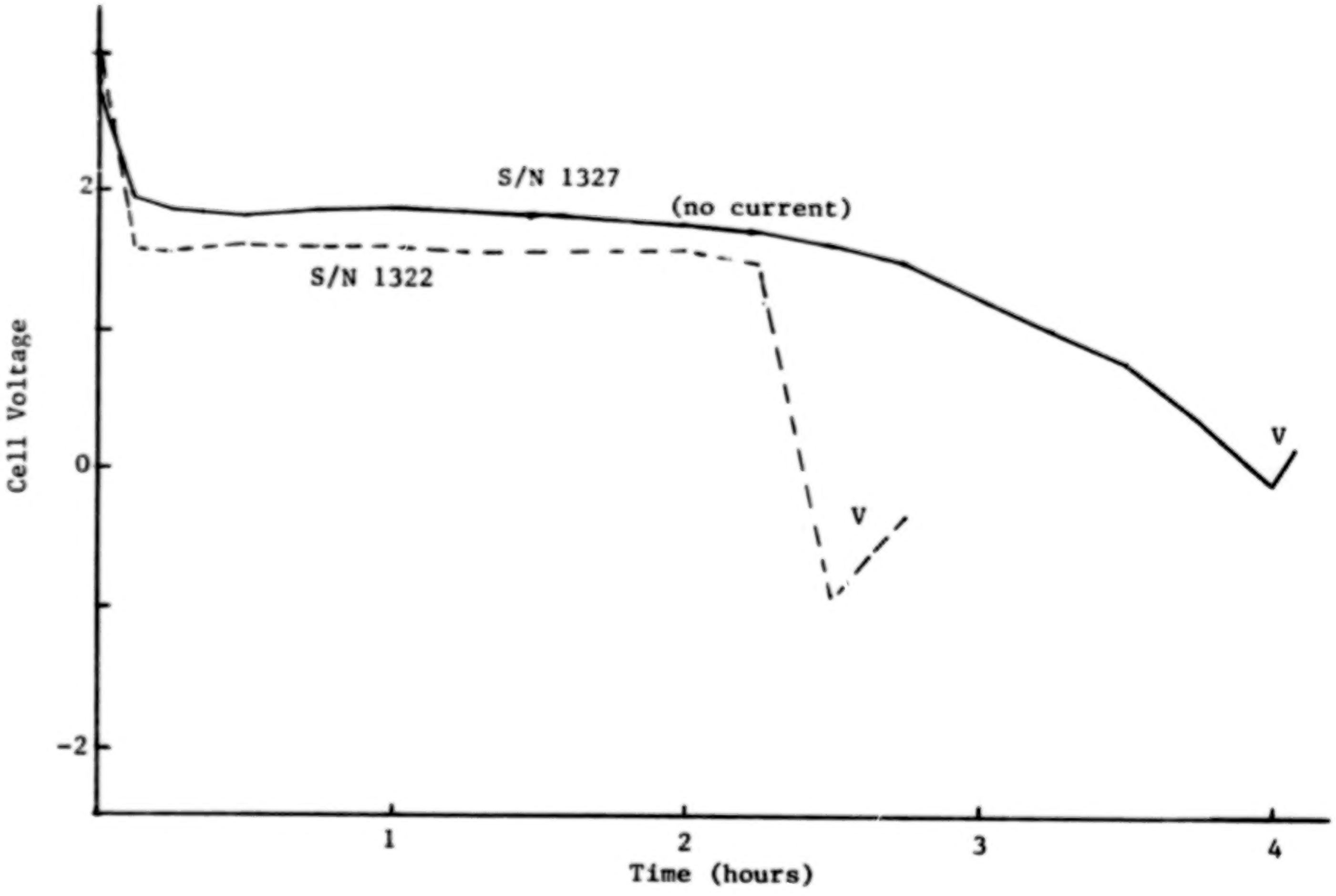

Figure 3. Hot test previous cells.

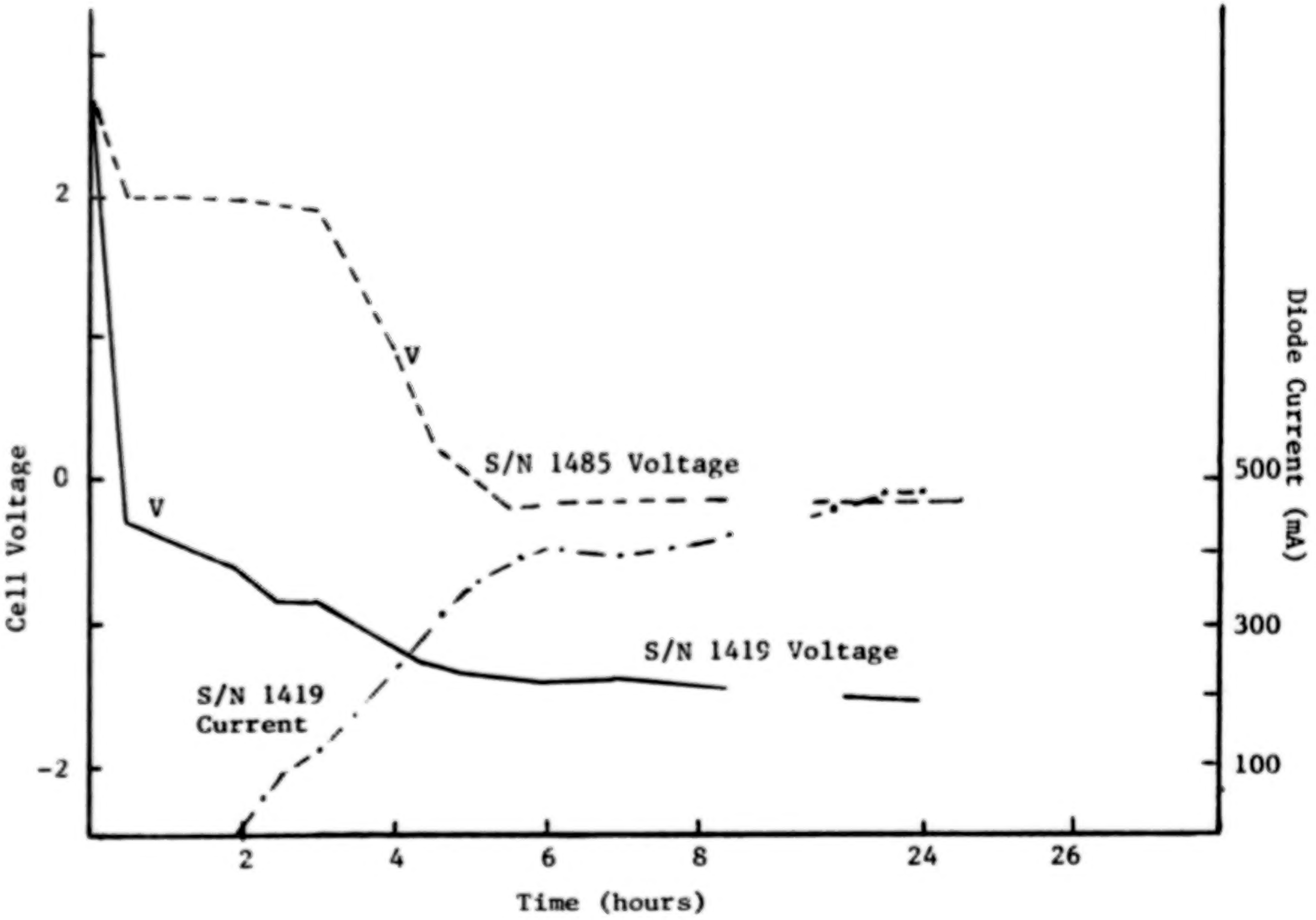

Figure 4. Hot test recent cells.

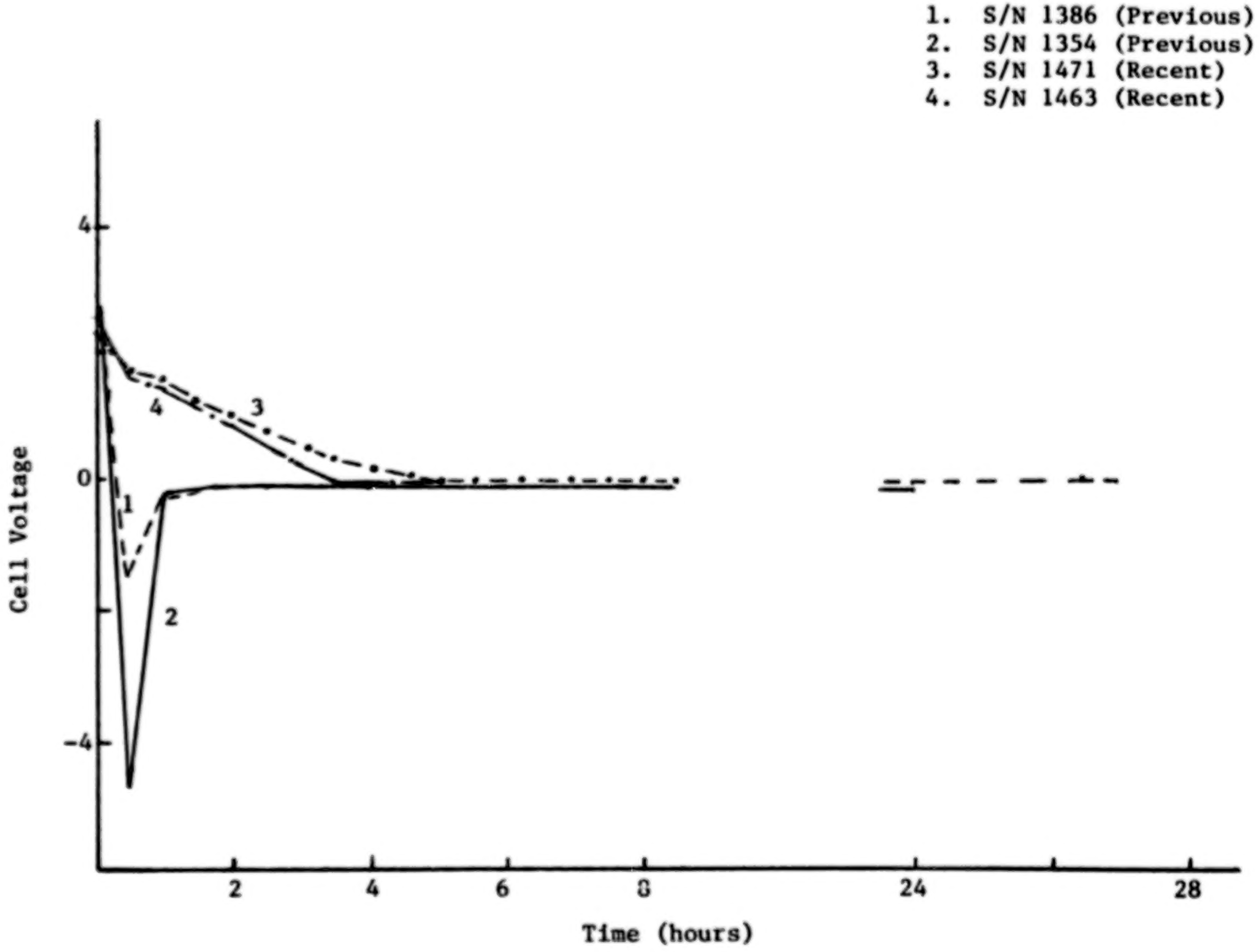

Figure 5. Ambient discharge without diodes.

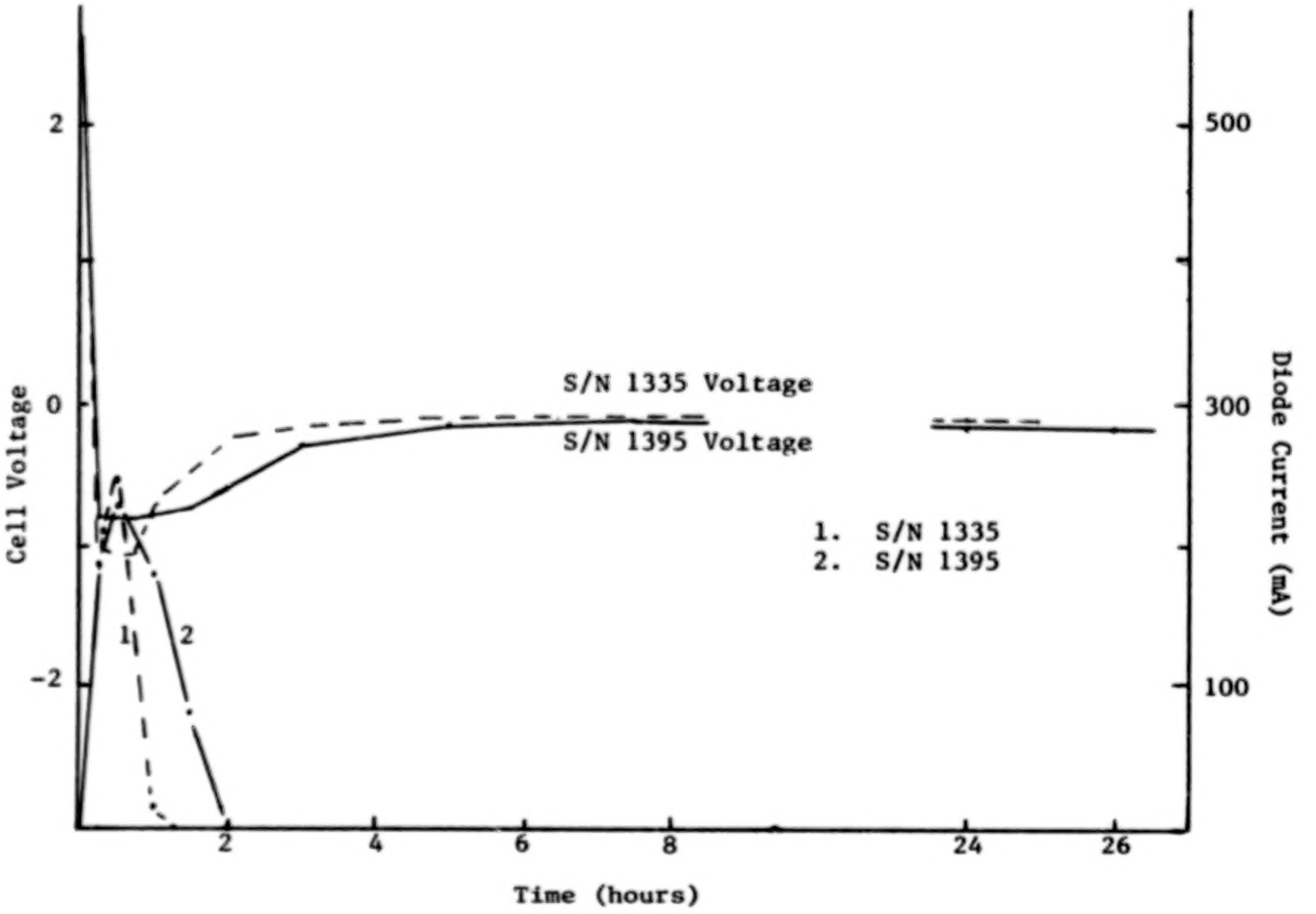

Figure 6. Ambient test with diodes (both previous).

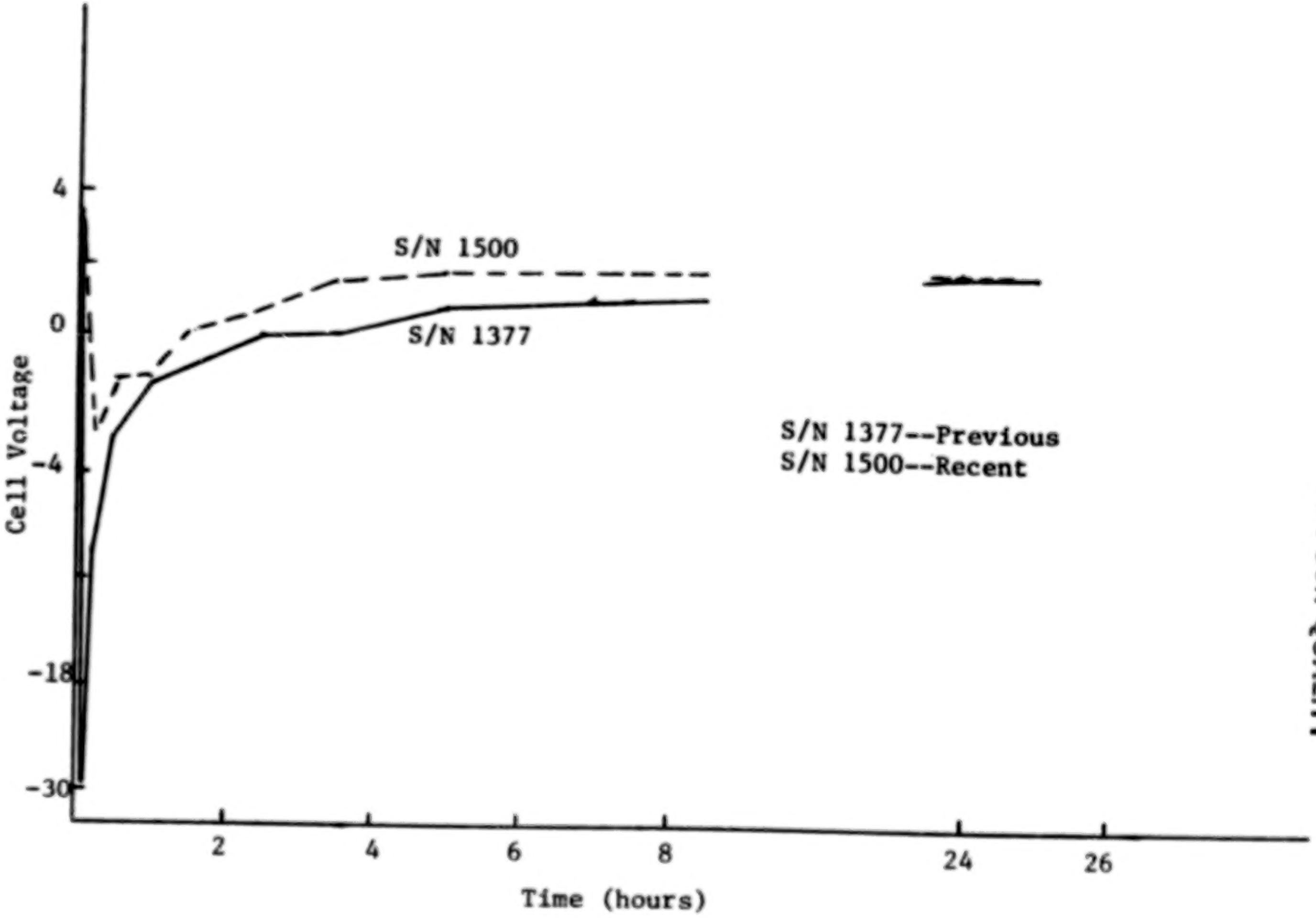

Figure 7. Cold test without diodes.

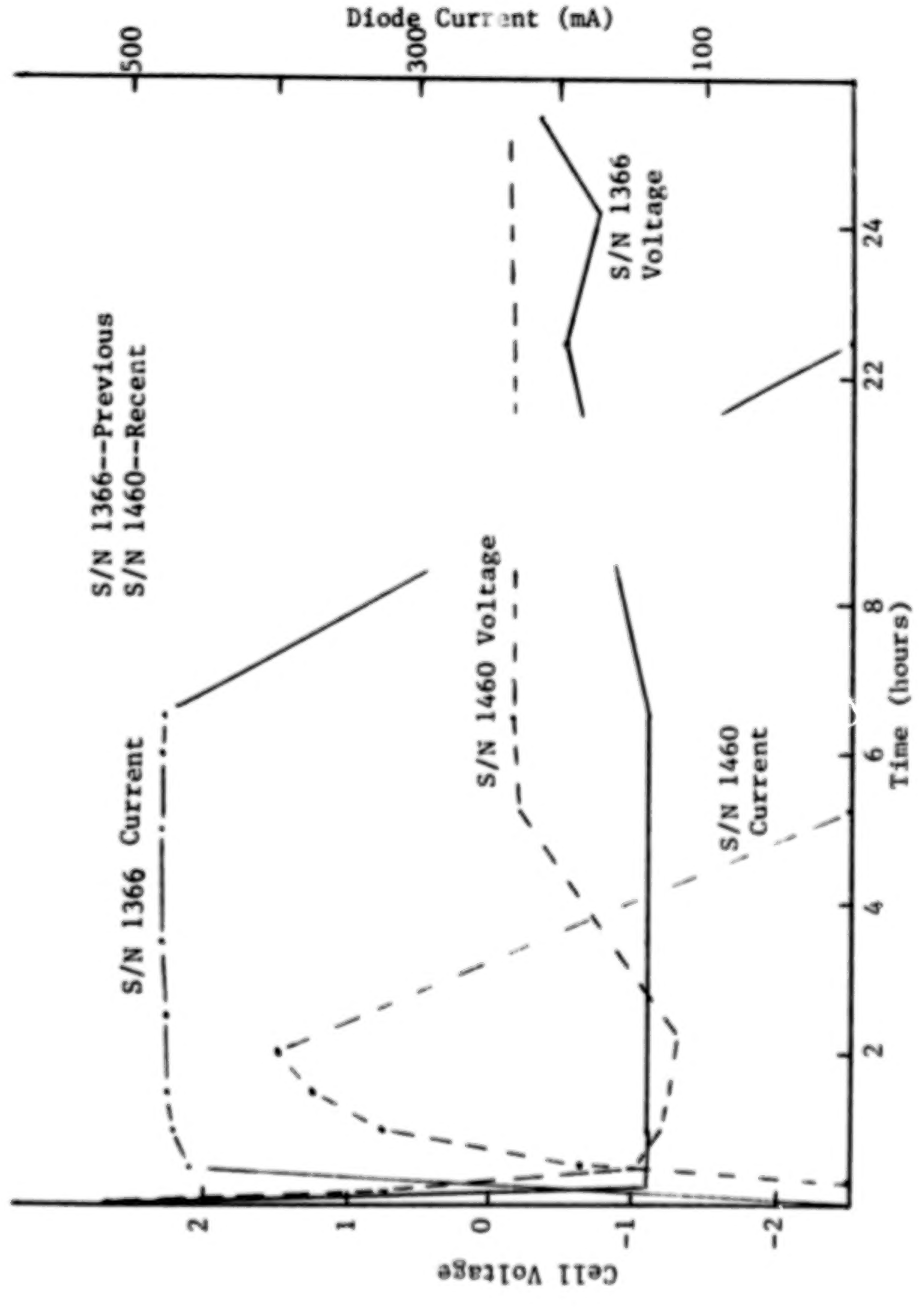

Figure 8. Cold test with diodes.

SESSION III

"NICKEL CADMIUM TECHNOLOGY"

Chairman: C. Badcock
Aerospace Corporation

N84
33682

UNCLAS

N84 33682 D14

SEPARATOR QUALIFICATION
for
AEROSPACE NICKEL-CADMIUM CELLS

For Presentation at:
1983 NASA/GSFC Battery Workshop

Martin J. Milden,
The Aerospace Corporation, El Segundo, Ca.

ABSTRACT

In late 1981 customers of General Electric Battery Business Department (GE/BBD) were notified that supplies of Pellon 2505ML separator would be exhausted in about 2 years. Efforts were made by Pellon Corporation to duplicate this material but were unsuccessful.

A joint Government program to qualify a new separator for nickel cadmium (NiCd) cells was proposed. The joint program would eliminate duplication of effort between Agencies and Contractors. Cell buys are being made by NASA/GSFC and Naval Weapons Support Center, Crane (NWSC). Cells will be acceptance tested and several cells will be operated in a charge/discharge characterization matrix. Cell packs will be life tested at NWSC in low earth orbit (LEO) and geosynchronous (GEO) orbit under real time and accelerated conditions.

It is anticipated that preliminary qualification data will be available in about 1 year with more complete data in about 3 years. A new Pellon Corporation separator will be evaluated by simulated testing in advance of actual space usage.

BACKGROUND

The separator material of choice for aerospace hermetically sealed NiCd cells has been Pellon Corporation product number 2505ML. This non-woven nylon fabric is used in virtually all aerospace NiCd cells today and is the only qualified material in most applications.

Manufacture of the 2505ML separator, which was part of a series of similar materials produced by Pellon Corporation, was discontinued in 1976 and the last available material at GE/BBD will be committed in 1984. All

PRECEDING PAGE BLANK NOT FILMED

future cell orders would require a new or replacement separator. In December, 1981 GE/BBD notified all users of the separator material of the coming problem.

At the instigation of GE/BBD and other users Pellon Corporation made several attempts to re-produce the 2505ML material. These attempts were made on equipment similar to the original production line which had been dismantled and utilized starting nylon fibers slightly different than previous material. The separator from several product runs was evaluated. Product characteristics were found to be variable.

At this point alternatives were examined. Since the manufacturing process utilized zinc chloride in a critical step and the process effluent could no longer be dumped without expensive treatment there was a serious cost impact. Further, a new non-polluting process, similar to one in use for about 10 years in Germany, was being installed to produce separator material claimed to be superior. Early evaluations of the new separator were positive. It was decided to wait for the new material produced by Pellon Corporation in their Lowell, Mass. facilities.

APPROACH

Informal discussions were held between NASA/GSFC, Naval Research Laboratory (NRL), Air Force Space Division (AF/SD), and Aerospace Corporation personnel active in NiCd usage. The benefits of a coordinated program in terms of cost and data base size were clear. The following program outline for a joint characterization/qualification test were formulated:

- NASA/GSFC purchase NASA standard cells
- AF/Navy purchase military program typical cells
- NWSC to conduct testing
- Generate a coordinated test/data base
- Coordinate with Contractors to assure test validity and acceptability
- Avoid duplicate qualification and life tests

AF/NAVY JOINT PROGRAM

Since the AF/Navy needs and cell requirements are close it was decided to have a common cell buy and center the program management function at NWSC. Technical support, component testing, and data analysis will be performed by Aerospace Corporation.

A single buy of 150 cells with the following general characteristics will be made:

- Cell Types
  - 26.5AH - 42B030AB10
  - 34 AH - 42B034AB02
  - 35 AH - 42B035AB02
  - 50 AH - 42B050AB24
- Electrode Types
  - All silver treated negatives except 26.5AH which is teflon treated
  - All positives are "standard" process
- Separator Types
  - Half Pellon 2505ML
  - Half Pellon Corporation new nylon material

Cells will be procured to a single procurement specification that is performance oriented. The unique features of this document are requirements for a listing of manufacturing documentation sufficient to define the methods, processes and procedures at a given point in time and mandatory customer inspection points at key manufacturing steps. The first requirement is intended to help clarify and identify any changes which may occur with time in the production of an aerospace cell. The second requirement is intended to provide close coordination and cooperation throughout the cell manufacturing cycle between customer and vendor.

After the cells receive an acceptance test at the vendor, GE/BBD, they will be acceptance tested at NWSC for comparison and pack matching. A sample quantity of cells from each subcategory will be vibrated to simulate launch environment then be placed in characterization testing. These characterization tests at various currents and temperatures will provide assurance there are no gross derivations between the "old" and "new" separator cells and the existing voltage-temperature charge curves are valid for the "new" separator cells.

Additionally, samples of each cell type will be set aside unactivated (dry) and activated (wet) to act as controls for possible use in future destructive physical analysis. Samples of separator material and electrodes will be provided to Aerospace Corporation for evaluation.

Following cell pack matching and assembly the packs will be placed on test according to the test matrix shown in Table I. In both LEO and GEO orbits two test levels were selected. The higher temperature and greater depth of discharge (LEO only) was chosen to simulate a worst case condition and offer an attempt at accelerating any degradation effects. The second set of test conditions was an attempt to simulate the actual use environments being experienced, except for acceleration of the GEO operation, for any possible long term or subtle differences well in advance of actual flight usage.

It should be pointed out the use of 10 cell packs is an attempt to get somewhat more significant statistical data. A constant source of irritation and consternation facing the test designer is that compromise between funding and the desire for more cells and test conditions. The partial use of 10 cells packs is an attempt to balance these needs.

Details of the testing conditions are shown below:

- LEO Orbit - Real Time
  - 33.6 minute eclipse
  - 67.2 minute sunlight
- GEO Orbit - Accelerated
  - 42 eclipses per season
  - 72 minutes maximum eclipse
  - 56 days per season
  - Recondition between seasons

The NASA/GSFC test matrix complements the AF/Navy test. Table II presents this test matrix which will proceed in parallel with the AF/Navy test and be conducted at NWSC. It can be seen that positive electrodes manufactured to earlier processes will also be compared to the latest GE/BBD electrode processes.

SCHEDULE

The joint program has been funded and is proceeding. A cell procurement specification has been reviewed and is in the final approval stages. A schedule of major activities is presented below:

o	Component Evaluation (start)	Nov 83
o	Cell Purchase Order	Jan 84
o	Detailed Test Plan	Sept 84
o	Cell Delivery	Nov 84
o	Cell Evaluation, NWSC	Nov 84 - Jan 85
o	Life Test Start	Jan 85
o	First Report	June 85

CONCLUSION

These separator qualification tests will provide a common and direct comparison of Pellon 2505ML and a replacement separator in advance of actual flight usage. When actual flight usage is imminent the confidence generated by an accumulated cell test data base will be appreciated. By performing this testing at a single location, NWSC, the quantity of directly comparable data can provide a more statistically valid data base at lower cost to each program.

To maximize test value a series of widely distributed, to typical NWSC distribution, is planned. There will be an acceptance test report including vibration and characterization data, annual NWSC life test reports, special reports on component evaluation, and trends analysis to the actual users.

Table I
AF/Navy Joint Program Test Matrix

				2505 ML SEPARATOR			NEW SEPARATOR		
ORBIT	DoD % ACTUAL	CHARGE CONTROL	TEST TEMP °C	50AH	34/35AH	26.5AH	50AH	34/35AH	26.5AH
LEO	25	V-T TAPER	5		5	5		5	5
LEO	40	V-T TAPER	20		10	10		10	10
GEO ACCEL	75	V-T TAPER	5	5	5		5	5	
GEO ACCEL	75	V-T TAPER	20	10	10		10	10	

Table II
NASA/GSFC Test Matrix

ORBIT	DOD RATED (%)	TEMP TEST (°C)	NASA STANDARD CELLS	OLD POS PLATE NEW SEPARATOR	NEW POS PLATE 2505 ML SEPARATOR	NEW POS PLATE NEW SEPARATOR
LEO	40	20	5	5	5	5
GEO (real time)	80	20		5		5
LEO	40	0				5

NOTE: ALL CELLS ARE 50 AH-NASA STANDARD MCD
MATRIX COURTESY D. BAER, NASA/GSFC

SESSION III

DISCUSSION

Q. Hendee, Telesat Canada: Quite interested in your program. I think it's a very valuable thing to be pursued. Several questions however. It might have been that I couldn't hear you. Incidently, next time don't use blue background. I can hardly see them back here.

A. Milden, Aerospace Corp.: It was for those who wanted to go to sleep.

Q. Hendee, Telesat Canada: Where you were saying the negatives were teflon and silver, is that one type of negative electrode that has both teflon and silver? Or is it two separate types of electrodes.

A. Milden, Aerospace Corp.: The 26½ ampere hour cell has teflonated negatives. All the others have silver.

COMMENT

Hendee, Telesat Canada: This is sort of a general comment which was made by some of the more subtle comments in the audience. I'd love to know what your standard positive is these days.

Milden, Aerospace Corp.: No comment. I don't think Guy is here.

Q. Hendee, Telesat Canada: Guy isn't here to defend himself. Okay, your cell spec that you're coming up with is this going to be generally available to other than the contributers to this program? Is the general industry going to be able to get copies of it?

A. Milden, Aerospace Corp.: I really don't think you'd want a copy of it, Ed. There's nothing unique in it. It's just a spec that defines the 4 cells we're trying to buy - nothing more. There's no secret proprietary or anything extra.

Q. Hendee, Telesat Canada: No, I know. We'd better not be after proprietary information, but - I'm getting to another one. You said the test information is only going to be available to the users. I'm getting - I'm terribly interested in this program. I think we all ought to be.

A. Milden, Aerospace Corp.: I'm sorry if there's any confusion on that, Ed. The reason we're having them do the testing is so that the information would be available to everybody. The comment that I made there is that on each of the individual programs that are actually paying for it, the program support people will be doing

A. Milden, Aerospace Corp. (Con't): analysis for that individual program, but that's over and above "the normal Crane reporting". We may want to get a computer dump of more accurate data or more detailed data than is normally available from Crane. But that's available to anybody at extra cost.

Q. Hendee, Telesat Canada: Okay, obviously I've got a great interest in this. Take that as a left-handed compliment. A couple of more things- your real time geosynchronous is basically what I'm interested in. Are you going to be doing periodical chemical analysis?

A. Baer, NASA/Goddard: As usual we didn't have much money. So we couldn't get really enough cells to do that much analysis ourselves So there probably won't be too much chemical analysis. There are a couple of extra cells and we probably will, at some point in time, pull a couple of them out and do some analysis. The other point I'd like to clarify is that in the NASA program they're all 50 ampere hour cells. They are all teflonated negatives and they're all going to be built to a NASA standard MCD, which is a little different than GE's standard MCD.

Q. Hendee, Telesat Canada: Now in your real-time geosynchronous life test, two things: Why did you pick 75% DOD and - which ties in - What kind of a lifetime are you expecting from these?

A. Milden, Aerospace Corp.: Well, the reason that was chosen is because there's a data base on it and it would be comparable to the existing data base. Dave and I have discussed that. Mike, I asked him the same question. You want to take the second part of it, Dave?

A. Baer, NASA/Goddard: As far as the real-time geo goes, I had thought about doing 60% - that's rated incidently. But, at 60% it's going to take a heck of a long time when you're running real time to know if they're any good or not. We do have somewhat of a data base at 80%. There have been tests run in the past and right now I'm thinking about doing 80% just to kind of accelerate a little bit. With a little bit of arm-twisting somebody might be able to change my mind if they know of a good reason to run 60 here. But it just seems like 80 is a nice compromise between getting some results in a reasonable amount of time and having something to compare to.

COMMENT

Milden, Aerospace Corp.: By the way, Ed. The actual life testing won't start for awhile. If anyone has any comments on the levels we've chosen or anything of that sort, I'd be very happy to listen. Because basically we're trying to have as universal a test as possible to avoid individual qualifications to your programs. So, if we can fit it in somewhere, we'd be more than happy to.

Hendee, Telesat Canada: There's one other comment. If you want some help or something maybe talk to me later.

Q. Roth, NASA HQ: This may be off base or maybe I just don't know much about these things but I wondered if it's as significant a problem as you say it is and the fact that you won't have this separator material and so on after next year. Do you have any contingency plans in case things don't work out the way you think they should?

A. Milden, Aerospace Corp.: The answer to that is we sort of have a contingency plan in that we've basically been waiting for the US manufactured material and Pellon-US has had some problems in starting up and they believe they're ready now - Lee is going to address those questions. And, in terms of contingency we always have the Freudenberg, that is Pellon's parent company, material which has been used successfully for a number of years in European satellite programs and in commercial cells in this country. I guess to a great extent we're saying that, pardon the expression, we're going to be a success oriented program. We don't foresee any differences because once the material has been looked at and gone through screening tests, it's not likely that there would be any major deviations. And, yes, it's a very important thing to examine - the Ni-Cd cell is a subtle thing and if you're looking at the cost you're talking about roughly \$1-1½ million to do the test and we launch how many billions of dollars worth of satellites a year? It's a drop in the bucket.

Q. Hafen, Lockheed: A number of years ago we had the 2503 separator and I was wondering about the availability of this and what your opinion is of the test results.

A. Milden, Aerospace Corp.: Well, the 2503 is manufactured using the same process as the 2505. It's just a different thickness and it will no longer be available either, because it uses the zinc-chloride step. Lee can comment on its equivalent and what will be available. Basically the industry is pretty much, except for 1 or 2 very limited applications, standardized on 2505 and I think I know what you're talking about. There is sufficient material available in 2503 to last a long time. I don't know how many years but we've checked that issue and the material is available and set aside.

Q. Rogers, Hughes Aircraft: When you use the zinc-chloride process you're certainly attacking the surface of the fibers.

Christensen, Pellon Corporation: No excuse me you're certainly attacking the fiber when you use zinc chloride process. Hot gas welding I should think would leave the surface in a very different condition.

Q. Rogers, Hughes Aircraft: How would you expect that this might affect the property and materials? It certainly wouldn't be the same or would it?

A. Christensen, Pellon Corporation: About the only way I can explain that if you, yes look at it microscopically you can recognize a difference in the two structures microscopically. From the standpoint of physical test and physical performance in the cells we don't really recognize any different in this respect. You're still attempting to set up a structure that holds electrolyte and still using the same fibers that cause the same degree of separation the pore size pore diameters of the structure are similar so that the filtration properties are the same, there would be no difference in temperature reactions, from this standpoint in all the testing we can do there doesn't seem to be any significant difference.

Q. Rogers, Hughes Aircraft: Okay. You emphasize the word physical twice. What about chemical differences?

A. Christensen, Pellon Corporation: Again the only difference I can find chemically speaking if I did not wash the new process then I would have the fiber finish on the fabric and that would be present in most of the commercial products we do. In terms of the product we are producing for this particular test we again wash the fabric so the fiber finishes are washed off and I find no chemical differences at this point or none that we can see.

Q. Unidentified, Hughes Aircraft: My question is in line with Howard's basically it looks like the cell matrix test is testing initial performance with the new material but I think at 5 or 10 degrees in two years when you are projecting perhaps to fly some of these cells you won't really have any results of the actual chemistry of that new material which we found in our own work.

A. Christensen, Pellon Corporation: Let me again address that you are using the same nylons - we are using the same blend of fibers, it's just a different bonding technique you're still using the same blend of fibers so to that extent you shouldn't expect any major difference.

Q. Gross, Boeing: When you say you are using the same blend of fibers do I take that to mean that we have a distribution of molecular weights? If so, do you know what that distribution is? I presume you're saying the distribution is the same.

A. Christensen, Pellon Corporation: I think that's what I'm saying but I'm afraid you've got me on that - I have a technical assistant here, Chester Petkiewicz from our R & D group. Chester can you answer that?

A. Petkiewicz, Pellon Corporation: What we are talking in terms of the zinc-chloride bonding process was a chemical attack on the nylon fiber - you actually had a hydrolysis of the nylon which was occurring and in order to have a consistent product you really needed to have a very consistent hydrolysis of the surface of the nylon fiber. It was at this time during the drying process that when you reached a certain level or a certain concentration of zinc-chloride the actual bonding of the fibers took place. This was a very critical process and we from a technical standpoint or from a manufacturer's standpoint really wanted to get out of this a long time ago because it was a very expensive process for us and the economics just weren't feasible to stay in the business. As Lee has indicated we tryed to stay in the business about the time that we tried to reproduce a product. One of the fiber suppliers told us they wanted to change a fiber, well which really threw us into a bit of a turmoil. But just going back to the zinc-chloride in order to do this the bonding took place because of the nylon fiber which meant that you are certainly going to have some low molecular weight components in that nylon fiber. You are actually physically, chemically, degrading a portion of that nylon in order to get the bonding to occur. Some of the low molecular weight nylon components could be washed out during the washing process - in order to get rid of the zinc-chloride we obviously had to wash the material after it had been bonded and dryed. In addition to washing out the zinc-chloride you could wash out some low molecular weight components of the nylon but at the same time you would have a change of the distribution of the molecular weight of the nylon. With the new process we feel it is a much more controllable process because all you are doing is thermally bonding in an indirect system. You're not physically degrading the nylon at all. There's no indication that the molecular weight distribution of the mylon fibers is changing at all contrary to what you might have in the zinc-chloride process. Some of the fiber finishes which are on the fibers are automatically driven off during the high temperature process that is used. We feel that you are going to have a much cleaner structure, a much more reproducible material, and a much more consistent product. We also feel that the pore size distribution will be better, more uniform, more consistent, from one production run to the next. Our equipment is in line. We spent a great deal of money putting up this new equipment. It is in line, the first production runs have been made. We have some minor changes that we are making to it at the moment but we feel very comfortable with this process - we feel very comfortable that the nylon you are going to be getting is going to be a cleaner more consistent product. We do have experience from around the world that this product has been used in nickel-cadmium cells for a good many years and the people in Europe and other parts of the world also had the same misgivings when they were asked to change from a zinc-chloride bonded product to this new product.

A. Petkiewicz, Pellon Corporation (Con't): The result was that they were quite surprised that the performance was consistently better. They found they had fewer problems in their cells, they had a more consistent product and we feel we will have the same thing here in the U.S. with our new process.

COMMENT

Christensen, Pellon Corporation: Just very quickly we plan to do the Hughes Malibu test when we have the separator materials available and try to finalize it by determining the loss of material. That's part of my characterization.

N84
33683

UNCLAS

D15

N84 33683

ELECTROCHEMICALLY DEPOSITED CADMIUM ELECTRODE FOR SEALED Ni-Cd CELLS

William H. Houston and Tim A. Edgar
Eagle-Picher Industries, Inc.
Colorado Springs, CO.

PRECEDING PAGE BLANK NOT FILMED

INTRODUCTION

Electrochemical impregnation processes for cadmium electrodes have undergone considerable development at Eagle-Picher under contract to the U.S.A.F. (ref 1). Previous work has focussed on thin high rate electrodes for vented, aircraft starting type batteries. A review of the history of cadmium electrochemical processes led to some feeling that an improved aerospace quality electrode might be manufactured using these processes. Electrochemically loaded cadmium electrodes are reported to have reduced cadmium migration over cycle life (ref. 2), more stable capacities than conventional electrodes (ref. 3) and possess an increased surface area that might provide good utilization and recombination ability.

Two similar processes for electrodeposition of cadmium in sintered plates have been known for some time and development has taken place at the USAF and Bell Laboratories. Production equipment for the USAF process has been installed at Eagle-Picher and could be utilized to produce high quality electrodes for sealed nickel cadmium cells. Our experience with electrochemical impregnation has indicated benefits in terms of lowered production costs and more importantly improved process control.

To evaluate the potential for improved flight quality cadmium electrodes, we instituted an investigation into the known work on electrochemical cadmium deposition processes. Subsequently, we set up a beaker impregnation system in the laboratory to investigate the practical limits of loading and the effect of various process parameters utilizing the USAF process (ref. 3). Reasonably high loadings of cadmium were obtained and the process appeared amenable to tight control and the production of uniform consistent electrodes. At this point, we constructed a pilot impregnation facility designed to further investigate either of the two known electrodeposition processes. Pilot system is a scaled down version of production USAF process equipment that we felt would allow real testing that would be applicable to full scale production. Both the inert anode (ref. 2) and consummable anode (ref. 3) processes were investigated. Results of this evaluation and an analysis of associated problems will be presented.

PROCESS DESCRIPTION

INERT ANODE

The inert anode process develped by Bell Laboratories (ref. 2) utilized platinum as the anode material and covered a broad range of parameters. Cadmium nitrate concentrations of 1.5

molar to saturation were investigated. Workable solution pH was identified as 1.4 to 4.3. Current densities of 0.25 to 1.0 amps/in^2 loaded electrodes to 2.25 g/cm^3 void in 30 to 60 minutes. Emphasis was placed on temperatures greater than 85°C and to prevent variation in pH an alkali nitrite buffer was used namely sodium nitrite. The respective electrode reactions are shown in figure 3.

CONSUMABLE ANODE

This process developed for the USAF (ref. 3) differs from the other process mainly in the use of an metallic cadmium anode that is consumed in the process. Work was done at temperatures near the boiling point of the solution and at pH of 3.0 to 5.0. Cadmium concentrations of 1.5 to 3.0 molar were utilized. Current densities of 1.2 to 1.6 amps/in^2 loaded electrodes to 2.33g/cm^3 void in times of 8 to 20 minutes. pH control was maintained by the addition of dilute nitric acid. Electrode reactions are presented in figure 4.

High Current Density With Current Reversal

Improvement in the USAF process was developed by Pickett and Puglisi (ref. 4), and consisted primarily of periodic current reversals during the impregnation. Forward to reverse time ratio was 8 to 1 and loadings of 2.50g/cm^3 void were obtained. It appeared that the current reversal technique was also beneficial to the problem of film buildup on the cadmium anodes.

Low Current Density With Current Reversal

Development of the consumable anode process by Fritz et al. (ref. 5) indicated that the process could be better controlled and loadings improved if operated at lower current densities (approximately 0.2 amps/in2) and utilizing current reversal techniques. Lower current densities required longer impregnation times, however, uniform loadings were reported and a forward to reverse time ratio of 8 to 1 at a frequency of 1 c.p.m. effectively inhibited film buildup on the cadmium anodes.

LABORATORY INVESTIGATIONS

The USAF process was evaluated at a beaker level in controlled laboratory environment. Two cadmium anodes 2 in. by 6 in. by 0.75 in. thick were spaced 1.5 in. apart.

Sintered plaque coupons were held in place by teflon forms, and the entire assembly was operated in a 2 liter beaker with heat and agitation supplied. Impregnation parameters are listed in figure 7. Sintered nickel plaques 1.75 in. by 4.5 in. by 0.30 were utilized and electrode potentials were monitored with a saturated calomel electrode. Temperatures of 75°C and boiling were employed to verify the importance of high temperature.

LABORATORY RESULTS

Low temperature testing at various current density levels yielded uniform but low loadings in the range of 1.5 to 2.0 g/cm^3 void. Increasing temperature to near boiling dramatically improved the results at all current densities. Plaque thickness increase was also lessened at high temperature. Monitoring of plaque potential through the impregnation indicated support for the work of Fritz et al. (ref. 6) in that excursions more negative than -0.650 volts vs. S.C.E. were accompanied by and significant electrode thickening and the formation of dark grey deposits on the electrode surface. Later runs in the laboratory set up employed variable current densities in an attempt to maintain plaque potential below -0.650 volts vs. S.C.E. for the maximum amount of time. Laboratory impregnation results listed in table 1 show the achievement of acceptable loadings at high temperature and a variety of low current densities. Improvement in loading is indicated with the variable current density technique.

PILOT FACILITY

DESCRIPTION

Pilot facility consists of a 40 liter impregnation tanks with 3 ft^2 working electrode capability. A batch tank holding 150 liters of bulk solution is maintained by intermittent addition of water and dilute nitric acid controlled by a process pH meter and level sensors. Impregnation and batch tanks as well as flow rate and counterelectrode spacing were designed to duplicate the parameters of the production equipment. Time, current density, and voltage are microprocessor controlled and adaptable to a wide range of impregnation regimes. Impregnation racks are fitted with balancing resistances for uniform current density. Plaque to anode spacing is maintained by teflon forms. A schematic of the pilot facility is shown in figure 9.

INERT ANODE: PILOT STUDIES

Impregnation Conditions

Cadmium nitrate concentration maintained at 2.0 molar. Sodium nitrite was used to maintain a pH range of 2.5 to 3.5. Temperature was held near the solution boiling point or approximately 98°C. Current densities of 0.07 to 0.20 amps/in^2 were investigated on a variety of plaque types. Anodes were 100 µ in. thick platinum plated on an expanded titanium grid.

Results

Inert anode impregnation results are presented in table 2. In general we verified the reported loadings for this process and extended that capability into lower current density regimes. Interesting results were obtained with oxidized plaque vs. unoxidized plaque that seem to verify the claims of Beauchamp et al. (ref 7).

CONSUMABLE ANODE: PILOT STUDIES

Impregnation Conditions

Pilot impregnations for this process utilized 1.0 in. thick cadmium anodes. Cadmium concentration was again held at 2.0 molar. Dilute nitric acid was used to maintain pH between 2.6 and 3.0. Current reversal techniques were used throughout in association with current densities of 0.10 to 0.20 amps/in^2. Laboratory results led us to perform all tests at the solution boiling point. Again, both oxidized and unoxidized plaque manufactured by both the dry sinter and slurry processes were tested.

Results

Results are tabulated in table 3. Loadings after plaque formation are comparible to the low current density, current reversal work of Fritz et al. (ref. 6). Later runs in the investigation where all parameters were held constant demonstrated very uniform plaque loadings.

DISCUSSION

Laboratory results proved to be reasonably accurate in the scale up to the pilot facility. Our results from pilot impregnations indicate that low current densities of 0.10 to 0.25 amps/in^2 are the most reliable regimes for impregnation on either of the two processes studied. Plaque potential monitoring vs. S.C.E. proved to be a reliable determination of effective loading limits under various regimes. Anode passivation with the consumable anode process is still a problem making multiple impregnations under the same conditions difficult. Work with forward/reverse current ratios and cycle frequency has demonstrated improvement on the anode film buildup, and planned future investigations show promise of solving the problem. The inert anode process may have a problem of eventual buildup of sodium in the solution affecting loading results. To date this problem has not surfaced, but investigations are continuing.

SUMMARY

This program has shown that acceptable cadmium loading levels are achieveable by either of the electrochemical processes tested. The added process controls incorporated in the pilot facility show promise of enabling production equipment to achieve higher loadings. Low current density regimes with reversal will be used to characterize production capabilities and anlyze the long term anode passivation problem. Inert anode investigations will continue on the pilot facility to identify the scope of the projected sodium buildup problem.

REFERENCES

1. Eagle-Picher Industries, Inc.: Manufacturing Methods to Establish Reliable Manufacturing Processes for Ni-Cd Batteries. Final Report, Contract No. F33615-76-C-5407, Oct. 1982.

2. Beauchamp, R. L.: Method for Producing a Cadmium Electrode for Nickel Cadmium Cells. U.S. Patent 3,573,101, 7 Jan. 1970.

3. Pickett, D.F.: Production of Cadmium Electrodes. U.S. Patent 3,873,368, 25 Mar. 1975.

4. Pickett, D. F.; Puglisi, V.: Electrochemical Impregnation of Sintered Nickel Structures with Cadmium Using Constant Current Step and Alternating Current Pulse Techniques. Interim Technical Report, USAF Contract No. F33615-75-C-2012, Jan 1971 - June 1974.

5. Fritts, D.; Leonard, J.F.; Palanisamy, T.: Method of Fabricating Cadmium Electrodes. U.S. Patent 4,242,179, Dec. 1980.

6. Palanisamy, T.; Fritts, D.; Kao, Y.K.; Maloy, J.T.: Electrochemical Aspects of the Cadmium Impregnation Process. Proceedings of the Electrochemical Society, Los Angeles, CA, Oct. 1979.

7. Beauchamp, R.L.; Maurer, D.; O'Sullivan, T.: Methods of Producing Electrodes for Alkaline Batteries. U.S. Patent 4,032,697, 28 June 1977.

ORIGINAL PAGE IS
OF POOR QUALITY

Table 1

Laboratory Impregnations

PLAQUE #	AMPS in^2	°C	IMPREG. TIME	AH INPUT	g/cm^3 VOID	THICKNESS CHANGE	
CD-5	.09	76°	145	1.17	1.69	0	
CD-6	.09	75°	135	.90	1.61	1	
CD-7	.10	76°	125	1.12	1.61	2	
CD-9	.10	75°	115	1.03	1.70	1	
CD-10	.11	76°	100	.98	1.58	5	
CD-11	.11	76°	77	.76	1.52	1	
CD-12	.12	75°	140	1.50	1.69	1	
CD-13	.12	75°	140	1.50	1.85	1	
CD-14	.2	76°	55	.98	1.47	1	
CD-15	.15	76°	155	2.08	2.10	1	
CD-16	.20	76°	67	1.20	1.58	3	
CD-17	.16	77°	148	2.15	2.22	3	
CD-18	.17	76°	106	1.66	2.04	1.5	
CD-20	.19	75°	75	1.26	1.66	1	
CD-22	.20	76°	42	.75	1.28	2	
CD-25	.16	77°	130	1.89	1.85	1	
CD-26	.155	76°	180	2.54	1.91	1½	
T-1	.16	97°	165	3.25	2.21	1	
T-3	.16	97°	190	3.77	2.18	0	
T-6	.16	97°	220	4.76	2.15	2	
T-12	.31	90°	125	5.2	2.40	1	
T-16	.25	95°	135	4.59	2.51	1	
T-18	.29	95°	110	4.22	2.50	1	
T-9	varied	97°	340	9.40	3.08	1	
T-11	varied	90°	180	6.07	3.34	4	
T-20	varied	95°	120	4.46	2.60	1	
T-22	varied	95°	130	4.75	2.55	1	
T-25	varied	96°	120	4.59	2.62	2	

ORIGINAL PAGE IS
OF POOR QUALITY

Table 2
Pilot System Impregnations-Inert Anode

PLAQUE #	PLAQUE DESCRIPTION	AH INPUT	ORIGINAL PLAQUE WEIGHT	g PICKUP $Co(OH)_2$	g/cm³ VOID	THICK. CHANGE	IMPREG. TIME	AVG. CURRENT DENSITY	FORM. g PICKUP	FORM. g/cm³ VOID	% Loss In g.
1-7242	oxidized dry sinter 34 mil 84% porosity 132 in²	137	127	126	2.13	-0.6	82 min.	.20	- - -	- - -	- - -
1-7243	"	137	128	121	2.03	-0.3	82 min.	.20	- - -	- - -	- - -
1-7244	"	137	127	124	2.08	-0.2	82 min.	.20	- - -	- - -	- - -
1-7245	"	137	126	112	1.89	0	82 min.	.20	- - -	- - -	- - -
2-7642	oxidized dry sinter 34 mil 84% porosity 160 in²	161	154	156	2.13	-0.1	120 min.	.19	- - -	- - -	- - -
2-8044	"	161	159	167	2.27	+0.2	120 min.	.19	- - -	- - -	- - -
3-4130	"	181	159	175	2.38	0.1	140 min.	.15	136	1.80	20
3-4131	"	186	157	185	2.51	0.2	140 min.	.15	145	2.02	19.6
4-4131	"	196	154	183	2.64	0.4	130 min.	.175	148	2.03	20.6
4-4132	"	196	156	186	2.56	0.8	135 min.	.175	153	2.14	19.0
5-4137	unoxidized dry sinter 34 mil 84% porosity 160 in²	207	161	212	3.01	1.0	190 min.	.16	173	2.46	22.5
5-4138	"	207	162	211	2.79	2.1	150 min.	.16	176	2.31	17.5
6-4146	"	232	161	234	2.97	3.9	192 min.	.15	203	2.58	13.2
6-4147	"	232	162	222	2.82	3.7	193 min.	.15	193	2.45	13.1
7-6029	unoxidized dry sinter 23 mil 84% porosity 160 in²	150	111	126	1.91	5.1	160 min.	.16	86	1.60	31.7
7-6030	"	150	112	112	1.85	2.5	160 min.	.16	90	1.61	19.6
8-041	"	150	112	120	2.15	1.0	160 min.	.11	97	1.81	19.2
8-042	"	150	113	111	1.91	1.8	160 min.	.11	90	1.68	18.9
9-042	oxidized dry sinter 25 mil 84% porosity 160 in²	188	113	146	2.49	0	240 min.	.09	118	2.01	19.2
9-043	"	188	114	134	2.72	0	240 min.	.09	108	2.20	19.4
10-3129	"	219	112	148	2.76	0.2	343 min.	.07	121	2.25	18.2
10-3130	"	219	112	143	2.66	0	343 min.	.07	117	2.18	18.2
11-4129	"	232	113	176	3.11	0.3	300 min.	.09	136	2.40	23.0
11-5130	"	232	113	153	2.85	-1.1	300 min.	.09	124	2.31	23.4

ORIGINAL PAGE IS
OF POOR QUALITY

Table 3

Pilot System Impregnation-Consumable Anode

RUN #	PLAQUE DESCRIPTION	NET AH INPUT	ORIGINAL PLAQUE WEIGHT	g PICKUP $Cd(OH)_2$	g/cm^3 VOID	THICK. CHANGE	IMPREG. TIME	AVG. CURRENT DENSITY	CYCLES PER MINUTE	-/+ TIME RATIO	FORM. g/cm^3 VOID	FORM. t	% LOSS
1-7129	unoxidized dry sinter-24 mil 85% porosity 160 in^2	165	113	158	2.94	- - -	180 min.	.16	2½	N/A	2.00	+0.2	31.6
2-8129	"	165	113	126	2.35	- - -	160 min.	.14	10	N/A	1.90	0.4	19.0
3-6133	"	162	114	117	2.17	- - -	210 min.	.09	3.5	N/A	1.82	-0.2	16.2
4-3129	"	187	113	140	2.62	- - -	225 min.	.13	3.75	3	2.14	0.4	17.1
5-4129	"	186	114	129	2.39	- - -	195 min.	.17	3.5	4	1.97	-0.1	17.8
6-129	unoxidized slurry-22 mil 163 in^2 -86% porous	157	100	96	1.89	- - -	210 min.	.12	3.75	6	1.62	- -	14.6
7-0136	"	149	100	103	2.04	- - -	195 min.	.12	3.75	6	1.71	- -	15.5
8-A	"	159	100	98	2.24	0.1	270 min.	.10	3.5	4	1.86	-0.1	14.3
9-5129	oxidized slurry-22 mil 163 in^2 -86% porosity	248	99	138	2.98	1.4	420 min.	.10	3.5	4	2.57	.25	15.9
10-7129	oxidized slurry-22 mil 163 in^2 -86% porosity	211	99	148	3.20	2.0	255 min.	.14	3.5	4	2.74	0.7	18.9
15-8130	"	215	99	165	2.88	5.7	180 min.	.20	3.5	4	2.69	2.0	21.2
17-4133	"	169	100	138	2.71	3.0	205 min.	.14	3.5	4	2.36	0.1	17.4
19-5175	"	165	99	142	2.60	4.2	200 min.	.14	3.5	4	2.51	1.2	18.3
22-5229	"	168	99	143	2.50	5.7	200 min.	.142	3.5	4	2.43	2.1	19.6
23-5227	"	162	100	136	2.49	4.7	205 min.	.134	3.5	4	2.33	1.7	19.1
24-5225	"	162	99	148	2.44	6.5	210 min.	.131	3.5	4	2.40	1.3	20.9
28-5217	"	163	99	136	2.54	3.3	210 min.	.131	3.5	4	2.33	0.9	18.4
29-0275	"	163	100	133	2.49	3.5	210 min.	.131	3.5	4	2.31	0.7	18.0
31-0269	"	163	99	121	2.55	1.7	210 min.	.131	3.5	4	2.25	0.4	16.5
32-0271	"	166	99	118	2.38	2.4	210 min.	.134	3.5	4	2.12	0.3	15.3
33-0267	"	166	98	116	2.45	2.1	210 min.	.134	3.5	4	2.18	0.1	15.5

- Potential Application of Improved Cadmium Electrodes in Aerospace Nickel-Cadmium Cells.
- Reduced Cadmium Migration.
- High Surface Area to Provide Good Utilization and Recombination Ability.
- Reduced Production Costs; Labor and Material.
- Basic Processes Established by U.S.A.F. and Bell Laboratories.
- Production Equipment and Vented Cell Technology in Place at E.P.I. - Colorado Springs under Air Force Contract No.
- Improved Process Control and Plate Uniformity vs. Traditional Electrode Processes.
- High Quality E.C. Cadmium Electrode to Match Proven E.C. Positive for Long Life, High D.O.D. Applications.

Figure 1. Electrochemically deposited cadmium electrodes.

- Baseline: E.P.I./U.S.A.F. Cadmium Electrochemical Impregnation Process for Vented Nickel-Cadmium Cells.
- Laboratory Investigation of Practical Limitations of Loading and Process Parameters.
- Pilot Facility Fabrication: Scaled Down Version of Production Equipment with Capability of Conversion to Either "EC" Process.
- Inert Anode Evaluation on Pilot Facility.
- Consumable Anode Evaluation on Pilot Facility.
- Comparison of Results/Analysis of Problems.
- Verification of Cadmium Electrode Producibility on Production Equipment.

Figure 2. Electrochemical impregnation: process evaluation.

- Platinum Sheet Counter Electrodes.
- Temperature Greater than 85°C.
- 0.25 to 1.0 Amps/In^2.
- pH 1.4 to 4.3.
- Cadmium Concentricity - 1.5 to 3.0 M.
- Impregnation Times 30-60 Minutes.
- Buffered with Alkali Nitrite ($NaNO_2$).
- 1.5 In^2 Nickel Sinter Electrodes.
- Reported Loading of 2.2-2.3 g/cm^3 Void.

ANODE REACTION

$$H_2O \longrightarrow \frac{1}{2}O_2 + 2H^+ + 2c^-$$

CATHODE REACTION

Reduction of NO_3^- with Subsequent Local pH Rise and Precipitation of $Cd(OH)_2$.

Figure 3. Inert anode: process description.

- Cadmium Sheet Counter Electrodes.
- Temperature - 95° to 110°C.
- 1.2 to 1.6 Amps/In^2.
- pH - 3 to 5.
- Cadmium Concentration - 1.5 to 3M.
- Impregnation Times - 8 to 20 Minutes.
- pH Control with 0.1 M HNO_3.
- 13 In^2 Nickel Electrode - 70 to 90% Porous.
- Reported 2.33 g/cm^3 Void Loading.

ANODE REACTIONS

$Cd \rightarrow Cd^{2+} + 2e^-$

CATHODE REACTION

Reduction of NO_3^- with Subsequent Local pH rise and precipitation of $Cd(OH)_2$.

Figure 4. Consumable anode: process description.

- Cadmium Sheet Counter Electrode.
- Temperature - 101°C.
- pH - 3.5.
- Cadmium Concentration - 2.0M.
- Impregnation Time - 12 Minutes.
- 1.6 Amps/IN^2.
- Reported Loading of 2.26 - 2.49 g/cm^3 Void.

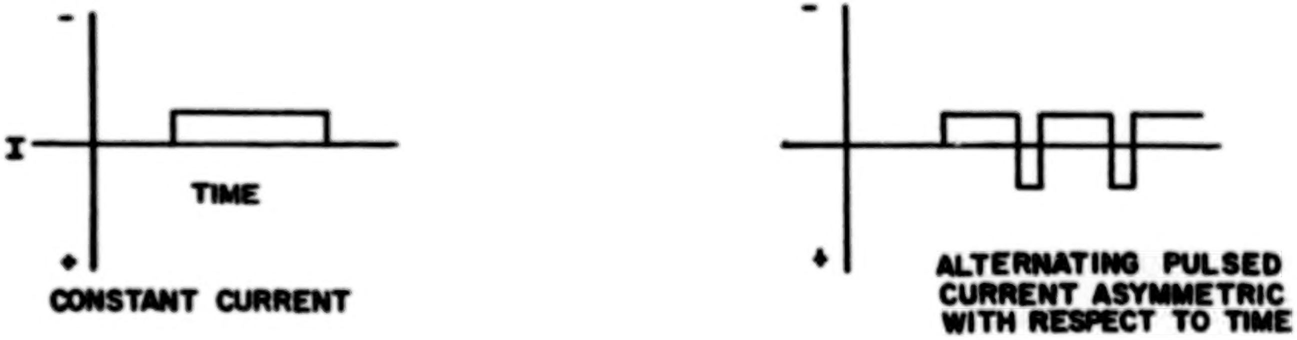
-
I
TIME
+
CONSTANT CURRENT
-
+
ALTERNATING PULSED CURRENT ASYMMETRIC WITH RESPECT TO TIME

Figure 5. High current density impregnation using current reversal.

- Consumable Cadmium Anodes.
- Temperature - 80 - 85°C.
- pH 3.5 ± 0.1.
- Cadmium Concentration - 2.0 M.
- Use of Current Reversal Techniques Where By Plaque is Made Anodic 10-20% of the Time.
- 0.2 Amps/In^2.
- Impregnation Times of 3 Hours or More.
- Reported Loadings of 0.9 g/IN^2 (~ 2.3 g/cm^3 Void).

Figure 6. Low current density impregnations using current reversal.

- Consumable Cadmium Anodes 3/4" Thick, 2" Wide x 6" High, 1½" Center to Center.
- Temperature - 75°C, Boiling (~ 95°C).
- pH - 2.5 to 3.5.
- Cadmium Concentration - 2.0 M.
- Calomel Reference Electrode Measuring Potential at Center of Plaque.
- Use of Current Reversal Techniques.
- 30 mil Thick Unoxidized Dry Sinter Nickel Electrodes 4½" x 1 3/4".
- Impregnations Carried Out in a 2 Liter Glass Beaker.

PURPOSE

Investigate Impregnation Parameters, Find Realistic Loading Expectancy, Determine Where to Begin Pilot Project Studies.

Figure 7. Laboratory investigations.

- Batch Tank, Flow Rate, Impregnation Tank Sized to Reproduce Production System Parameters.
- Automatic Continuous pH Control and Monitoring.
- Automatic Solution Level Control.
- Multiple Current, Voltage and Time Rase Capability Provided by Microprocessor.
- Impregnation Furnished with Balancing Resistance for Uniform Current Distribution.
- 3 Ft^2 Electrode Capacity.

Figure 8. Pilot system: description.

ORIGINAL PAGE IS
OF POOR QUALITY

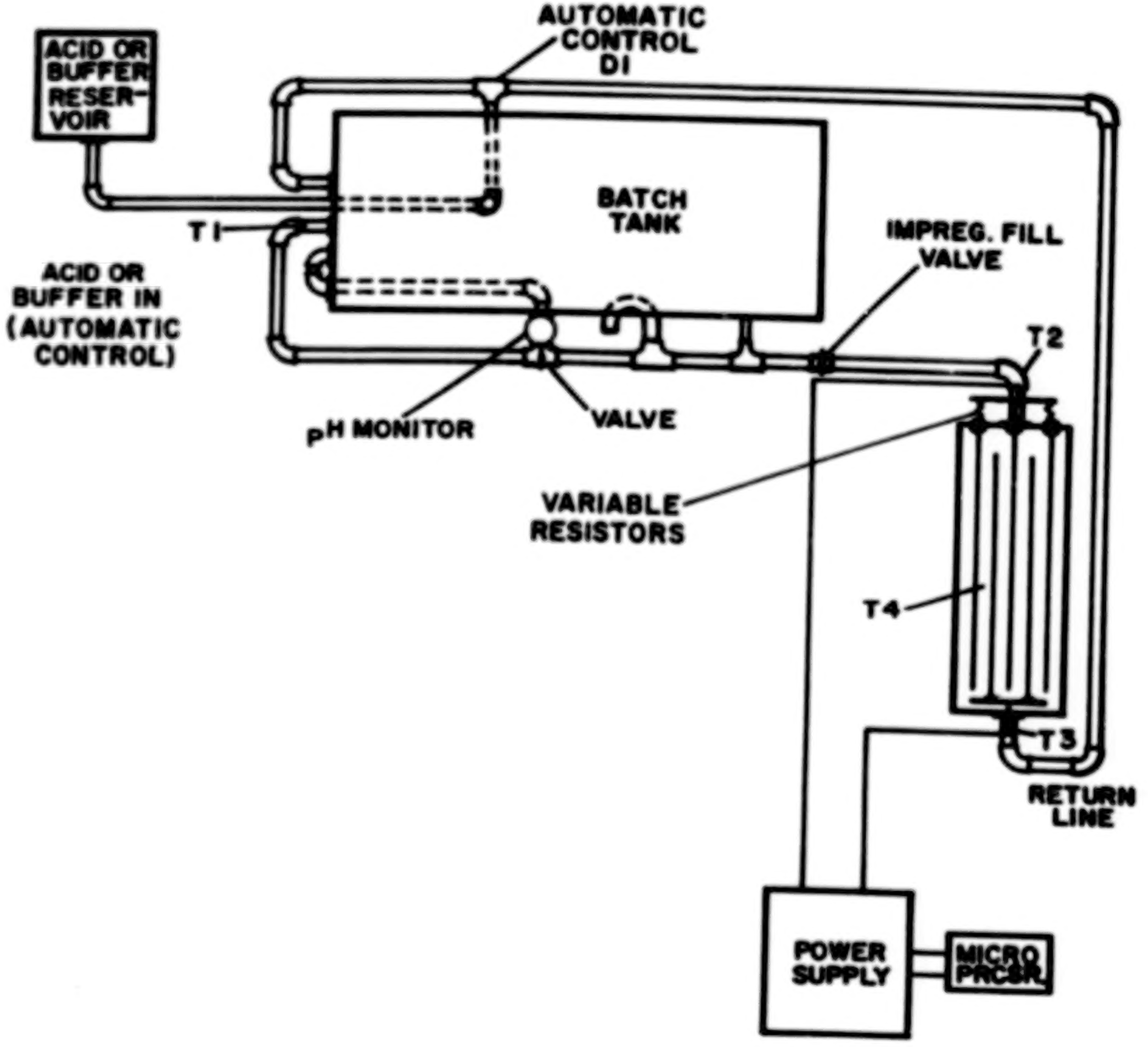
ACID OR BUFFER RESERVOIR
AUTOMATIC CONTROL DI
BATCH TANK
T1
ACID OR BUFFER IN (AUTOMATIC CONTROL)
IMPREG. FILL VALVE
T2
pH MONITOR
VALVE
VARIABLE RESISTORS
T4
T3
RETURN LINE
POWER SUPPLY
MICRO PRCSR.

Figure 9. Pilot facility schematic.

- Platinized Titanium Anode - 100 Microinches Thick platinum - 14" x 24".
- Cadmium Concentration - 2.0 M.
- pH - 2.5 to 3.5.
- Temperature - 95° to 98°C.
- Low Current Densities - 0.07 to 0.20 $Amps/In^2$.
- Dry Sinter Nickel Electrodes of Varying Thicknesses.
- Oxidized and Unoxidized Electrodes.
- $NaNO_2$ as a Buffer.
- Retained Loadings Greater than 2.40 g/cm^3 Void.

Figure 10. Pilot system impregnations-inert anode.

- Cadmium Sheet Anodes 14" x 24", 1" Thick
- Cadmium Concentration - 2.0 M.
- pH - 2.8 ± .02.
- Temperature - 95 - 98°C.
- Low Current Densities - 0.10 to 0.20 $Amps/In^2$.
- Current Reversal Techniques Used.
- Dry Sinter and Slurry Nickel Plaque - Varying Thicknesses.
- 10% HNO_3 Added to Control pH.
- Retained Loadings Greater than 2.70 g/cm^3 Void.

Figure 11. Pilot system impregnations-Consumable anode.

- Either Electrochemical Cadmium Impregnation Process Appears Capable of Leading Plaque to Acceptable Levels for Aerospace Applications.
- Additional Process Controls Incorporated in Pilot Facility Sould Enable Full Scale Production of Uniform Highly Loaded Electrodes.
- Low Current Density With Reversal on the Consumable Anode Process Demonstrates the Best Loading and Improves the Anode Passivation Problem.
- Evaluation of Anode Passivation and Sodium Buildup Problems Continuing.
- Full Scale Electrode Production Tests Planned.

Figure 12. Summary.

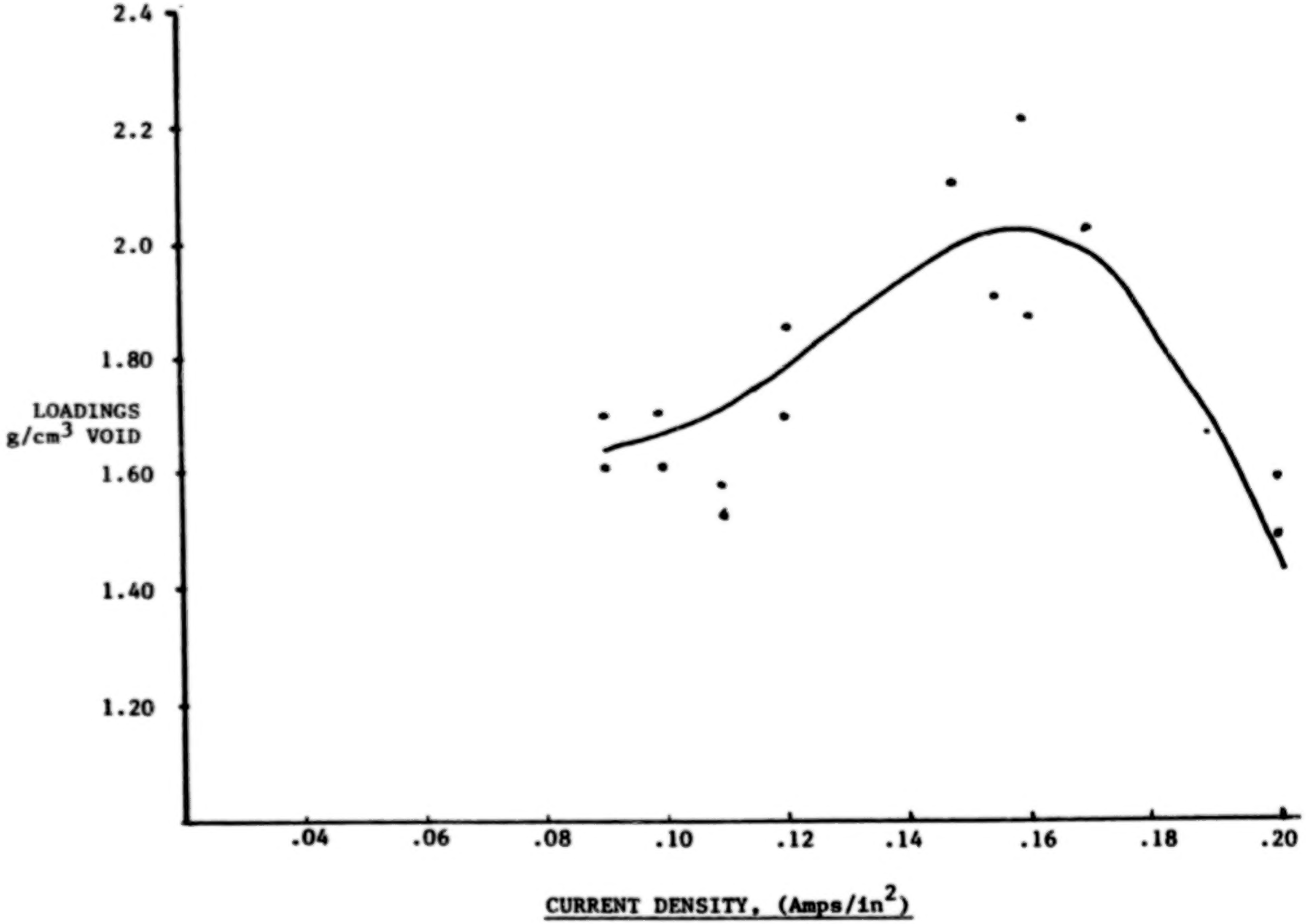

Figure 13. Plaque loading vs. current density, 75°C.

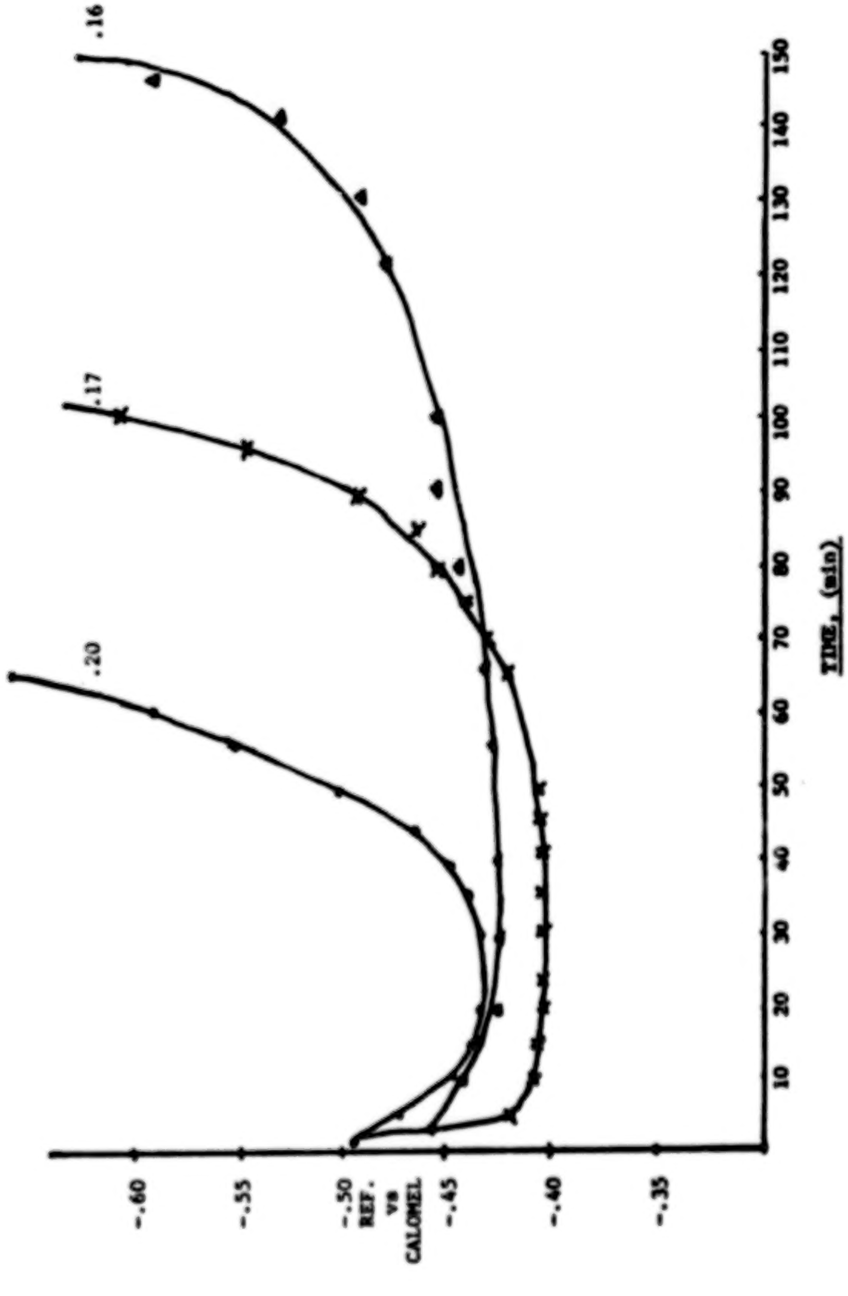

Figure 14. Reference V vs. time for varying current densities, 75°C.

Q. Unidentified: I've got one question. On this test it seems to me that all your impregnations are done by the alcohol process?

A. Edgar, Eagle Picher Company: That's true.

Q. Unidentified: I'm curious why you didn't include the Bell process as well. Since by the way one of these you don't have in the Bell process is the problem of the build up in capacity during formation.

A. Edgar, Eagle Picher Company: That's possibly true. The reason we ran the test on the Pickett process is we wanted to look at these electrodes essentially on a production type basis where we could involve a lot of them. And we are not set up at Colorado Springs to run the Bell process on this large of a scale.

COMMENT

Mallory, AT&T Bell Labs: I'll just take this opportunity to make a comment about the stress test and KOH concentration as it applies to the previous paper and this one. Burnhart and I reported some years ago that high KOH concentration has a substantial effect on growth rate. It increases the growth rate and it also increases the subceptibility to blister formation so during the stress test and lower KOH concentration is beneficial to the electrode if you want to put it that way. I also seem to recall that the cycle life of positives is reduced at higher concentrations. I'm not certain of that fact but I think it is.

Edgar, Eagle Picher Company: I guess maybe I didn't make it quite clear enough. The formation cycles were carried out 20% KOH but I believe the stress test cycles were carried out in 31%.

Ritterman, Comsat: You probably do form blister but at the higher concentration but primarily when the cell is reversed or when the positive electrode is reversed in this case.

A. Edgar, Eagle Picher Company: That's right it's 31%.

Q. Ritterman, Comsat: But you do avoid hydrogen gassing off of the positive electrode?

A. Edgar, Eagle Picher Company: Yeah we do avoid that significantly. It isn't absolutely clear to me that's when blister formation takes place but it's been reported that it may.

A. Ritterman, Comsat: It's not the only case but there is a higher tendency for blister formation when you do gas hydrogen.

Q. Gaston, RCA-Astro: Paul, could you please explain, you mentioned in your conclusion one of the benefits higher charge temperatures. I tested nickel hydrogen with higher temperatures. My capacity was considerably lower. I don't know. Give me some details.

A. Ritterman, Comsat: That's true. It will be lower as for the second viewgraph that I showed but now you can adjust long if you wanted to operate say 25 degrees instead of 20 or 10, or so you can adjust your concentration so that now you are allowed to operate at that temperature and the benefits of suppressing the oxygen getting the capacity you want with operating at the higher temperature.

N84
33684

UNCLAS

ORIGINAL PAGE IS
OF POOR QUALITY

N84 33684 D16

SECOND PLATEAU VOLTAGE IN NICKEL-CADMIUM CELLS*

Kunigahalli L. Vasanth
Bowie State College, Bowie

ABSTRACT

Sealed nickel-cadmium cells having large number of cycles on them were discharged using Hg/HgO reference electrode. It was found that the negative electrode exhibited the second plateau. SEM of negative plates of such cells show a number of large crystals of cadmium hydroxide. The large crystals on the negative plates disappear after continuous overcharging in flooded cells.

INTRODUCTION

Nickel-Cadmium cells are extensively used in satellite power systems. These cells undergo a large number of charge-discharge cycles. The changes in the battery voltage or capacity directly affect the power requirements and control unit function of the satellite power systems. It has been found more often that nickel-cadmium cells after a year's use show a voltage degradation during discharge. Such cells suffering with voltage degradation increases the load on the batteries and may sometimes result in loss of capacity. The voltage degradation during the discharge is commonly referred to as the second plateau or voltage plateau or stepped discharge curve.

Different views have been expressed as to which electrode is contributing and about the mechanisms causing such voltage degradation. One of the mechanisms (Reference 1) suggested is that the recrystallization of cadmium hydroxide at the surface of the cathode during cycling insulates the lower layers of active cadmium, as a result the discharge occurs at a very low rate. It has been reported (Reference 2) that an alloy Ni_5Cd_{21} formed in the negative electrode of nickel-cadmium cells subjected to continuous charging at elevated temperatures is the cause of voltage degradation. Russian workers (Reference 3) reported that under certain conditions, e.g., if the battery is stored in the charged state or cycled with

---

*Work performed under NASA Grant NSG-5009.

PRECEDING PAGE BLANK NOT FILMED

ORIGINAL PAGE IS
OF POOR QUALITY

incomplete discharge, some of the cadmium forms the intermetallic compound Ni_5Cd_{21} with nickel, and is discharged at a potential on the positive side of the usual potential by 0.1V. Recently, Barnard et al (Reference 4) have reported that the secondary discharge plateau is associated with the inefficient reduction of sintered plate NiOOH electrodes. They point out that the potential of the lower plateau is highly dependent on discharge rate and also to some extent on the charge regime applied to the electrode. Zimmerman and Janecki (Reference 5) also report that the voltage losses result from changes in the nickel electrode potential with cycling.

Gerald Halpert (Reference 6) presented the results of cycling 26.5 AH sealed nickel-cadmium cells. Sealed cells were cycled on a near earth orbit regime at 10°C and to a voltage limit. Cells showed voltage degradation after about 6400 cycles. Pack 26H that was discharged with 25% DOD showed a more significant voltage degradation than pack 26G cells with 20% DOD. In fact, this presentation prompted me to further examine the voltage degradation behaviour of sealed nickel-cadmium cells.

EXPERIMENTAL METHODS

1. Preparation of Hg/HgO Reference Electrode:

   a) Small amounts of mercury and mercuric oxide (red variety) were ground well with 2 to 3 drops of 31% KOH.

   b) The above mixture was put into a piece of teflon tubing of 50mm diameter which had a tiny hole at the bottom that is plugged with separator material.

   c) A few ml of pure mercury was put over the layer of Hg/HgO.

   d) A platinum or nickel wire was stuck in the mercury pool taking care to prevent the wire from touching the Hg/HgO interface.

   Such a Hg/HgO electrode served as a stable reference electrode and was used to monitor the potentials versus the negative and positive electrode of the nickel-cadmium cells.

2. Cells Used for the Study:

   History of the cells used is given in Table 1.

3. Identification of the Electrode causing the Second Plateau:

A 20 AH cell from pack 12 F was chosen for investigation. The cell had undergone 24958 cycles on a near earth orbit basis at Crane at 16 A of charge and discharge. The cell showed appreciable second plateau. The temperature was at 10°C and 40% DOD.

The following steps were carried out using the above mentioned sealed cell:

a) The fully charged cell was discharged to 50% and the Hg/HgO reference electrode was carefully introduced by drilling a hole on the top of the cell and sealing the hole all around with putty. Care was taken to prevent the cell from exposure to air by keeping it in a polyethylene bag filled with nitrogen.

b) The cell was recharged at the same charge regime to the specified voltage limit of 1.458 V and discharged at 10 A rate to 0.5 volt.

c) During the discharge, the reference versus negative and reference versus positive electrode potentials were monitored and recorded using a two-channel recorder. The cell voltage was also recorded separately. The results obtained from the discharge of the cell from pack 12 F is shown in Figure 1.

d) The discharged cell was once again cycled 10 times overnight and was discharged at 10 A while still monitoring the potentials of the negative and the positive versus the Hg/HgO reference. As expected, the cell now did not exhibit the second plateau due to earlier reconditioning effect.

I waited another year to confirm the findings by conducting similar experiments using 3 12 AH cells one each from pack 3H, 3J, and 3D and another 20AH cell from pack 1 K. These cells were discharged at Crane, Indiana using the reference electrode technique described earlier. In all the cases, the results show that it is the negative electrode versus reference which exhibit the second plateau.

I appreciate very much the help of Mr. Jim Harkness, Steve Hall, and S. Hammersely in carrying out the tests at NWSC, Crane, Indiana.

4. Experiments with Flooded Cells:

After discharging the cells using reference electrode these were brought from Crane to Goddard. Flooded cells were assembled in plexiglass cell cases using the negative and positive plates taken out from a cell that showed the second plateau. Each flooded cell consisted of two negatives and one positive separated by pellon. These flooded cells were charged to different voltage limits. Different charge rates as given in Table 2 were employed to charge the cells. The plateau reappeared in those cases marked with an asterisk and the voltage limit was 1.434 volt per cell.

RESULTS AND DISCUSSION

The results of the present investigation indicate that the negative electrode is responsible for the second plateau in nickel-cadmium cells. The negative and positive plates from such cells were used to assemble flooded cells in the laboratory. These were charged at different rates for different durations to a voltage limit and discharged. The second plateau could be induced again in some cases (see Table 2). The discharge profile of one such case is shown in Figure 2. In two cases, however, the reference versus positive potential showed a slight hump, a sample of which is shown in Figure 5. Comparing the positive versus reference electrode discharge profile to the negative versus reference electrode (Hg/HgO) profile in Figures 1 and 3, it can be seen that the magnitude of the second plateau on the negative electrode is larger (300 mv). In agreement with a number of workers, a shift in the second plateau with cycling is demonstrated in Figure 4.

The half-cell reaction at the cadmium electrode is well known:

$$Cd + 2\,OH^- \underset{\text{Charge}}{\overset{\text{Discharge}}{\rightleftharpoons}} Cd(OH)_2 + 2e^- \qquad (1)$$

The $Cd(OH)_2$ is also known to form through dissolution - precipitation mechanism: (Reference 7)

$$Cd + 3(OH)^- \rightleftharpoons Cd(OH)_3^- + 2e^-$$

$$Cd(OH)_3^- \rightleftharpoons Cd(OH)_2 + OH^- \qquad (2)$$

Reactions (1) and (2) precipitate cadmium hydroxide and migrate to the surface of the electrode, towards the separator and positive electrode. In the inital stages of cycling, the cadmium hydroxide is present as thin film masking some areas of active cadmium. As the cycling progresses, these films provide convenient sites for crystal growth and thus mask the active cadmium surface with large crystals of cadmium hydroxide. The SEMs of negative plates of cells that showed second plateau show very large crystals of cadmium hydroxide and the positives do not have any crystal growth (see Figures 6 and 7). Ford (Reference 8) demonstrated that the nickel-cadmium cells that had electrolyte starvation suffered both in voltage and capacity. The cells examined by him were Gulton 6 AH cells cycled at 20°C, 25% DOD with a voltage limit of 1.417 and C to D ratio of approximately 115. By simply increasing the electrolyte content the capacity degradation of such cells was overcome but the double plateau effect still existed. Increase of electrolyte seem to dissolve smaller crystals but there is still a bulk of large crystals masking the active surface of the electrode. The experiments in the present work have shown that continuous charging of negative electrodes with large crystal growth in flooded condition almost eliminates the crystals. SEMs of negative plates after gasing by overcharging in excess electrolyte show no trace of large crystals (Figure 8). This is in agreement with the results of Fritzwill and Hess (Reference 9) who pointed out that prolonged reduction leads to the dissolution of crystals of $Cd(OH)_2$.

The tear-down analysis of cycled cells have shown that the cadmium migration is quite heavy in the areas under compression and quite often the separator sticks strongly to the electrode surface. This may be explained by assuming that in sealed cells the electrolyte is squeezed out from areas where there is more compression and these electrolyte starved areas seem to be good nucleation sites for crystal growth. The crystal size grows as the cycling continues and finally result in loss of voltage and/or capacity. When no effort is made to restore the voltage and capacity by reconditioning, a situation may arise when the cadmium dendrites will pass through the weak separator and lead what is popularly called soft or hard shorts which will cause cell failure. It appears, if one can prevent cadmium migration and supress crystal growth the voltage degradation i.e., second plateau behaviour is taken care of.

From the Navigation Technology Satellite-2 (NTS-2) nickel-hydrogen battery performance, F.E. Betz, J.D. Dunlop and J.F. Stockel (Reference 10) have reported that the battery voltage level improves with continued cycling as the discharge duration increases. The increase in voltage was related to the positive electrode i.e., the nickel electrode. Stockel in an updated paper (Reference 11) reported that nickel-hydrogens have not shown any voltage or capacity degradation during 3.5 years in orbit and eight eclipse seasons.

CONCLUSIONS

1. The second plateau is exhibited mainly by the negative electrode.

2. Formation of large crystals of $Cd(OH)_2$ on the negative electrode during cycling is responsible for voltage degradation.

3. Continuous gasing of the negative electrode in flooded cells leads to the dissolution of large crystals of cadmium hydroxide.

FUTURE PLANS

It will be interesting to establish conditions that will minimize cadmium migration. It is planned to investigate the possibility of using some sort of coating, electroplating, or additives that may achieve this purpose. Also plans are underway to look into the effect of varying the compression on the plate stack.

REFERENCES

1. Carson, W.N., "A Study of Nickel-Cadmium Spacecraft Battery Charge Control Methods," NASA CR-82028, April 1966.

2. Barnard, R., Graham T. Crickmore, John A. Lee and Frank L. Tye, "A Cause of 'Stepped' Discharge Curves in Nickel-Cadmium Cells," Power Sources, Vol. 6, pp 161, 1977.

3. Pozin, Y.M., E.I. Garnaskin and M.Sh. Vogman, "Introduction of Ni^{2+} into Negative Sintered Metal Plates for Nickel-Cadmium Storage Cells," J. Appl. Chem. of USSR, pp 1490, 1970.

4. Barnard, R., G.T. Crickmore, J.A. Lee, and F.L. Tye, "The Cause of Residual Capacity in Nickel Oxyhydroxide Electrodes," J. Appl. Electrochem., Vol. 10, pp 61-70, 1980.

5. Zimmerman, A.H. and M.C. Janecki, "Voltage Losses and Reconditioning of NiCd Cells," Aerospace Corporation Report SD-TR-81-62, August 21, 1981.

6. Halpert, Gerald, "Appearance of Second Plateau Voltage," the 1980 GSFC Battery Workshop Proc., pp 305, 1980.

7. Meyer, S.W., J. Electrochem. Soc., Vol. 123, pp 159, 1976.

8. Ford, Floyd, "Effects of Reworking Cells," the 1975 GSFC Battery Workshop Proc., pp 70, 1975.

9. Will, F.G. and H.J. Hess, "Morphology and Capacity of a Cadmium Electrode," J. Electrochem. Soc., Vol. 120, No. 1, pp 1-11, 1973.

10. Betz, Frederick E., James D. Dunlop and Joseph F. Stockel, "The First Year in Orbit for the NTS-2 Nickel Hydrogen Battery," IECEC proceedings, Paper 789164, pp 67-71, 1978.

11. Stockel, J.F., "The NTS-2 $Ni\text{-}H_2$ Battery an Update," IECEC proceedings, Paper 819122, pp 212-215, 1981.

Table 1

Cell History and Operating Parameters

PACK #	12F	1K	3H	3J	3D
CELL #	3	1	3	3	2
NOMINAL CAP (AH)	20	20	12	12	12
VOL. OF KOH (ml)	85	85	41.5	39	40
POS. LOADING (g/dm^3)	1704	1704	2113	2130	2095
NEG. LOADING (g/dm^3)	1865	1865	2180	2542	2180
SPECIAL TREATMENT	NEG TEFLNTD	PELLON 2503	NO PQ TREAT	OLD PROC. NO PQ	CONTROL GROUP
ORBIT PERIOD (HR)	1.5	1.5	1.5	1.5	1.5
TEMP (°C)	10	20	20	20	20
CHARGE RATE (A)	16	16	9.6	9.6	9.6
NO. OF CYCLES	24,958	18,864	23,281	23,334	23,467
DOD (%)	40	40	40	40	40
VOLT. LIMIT (V)	1.457	1.434	1.453	1.453	1.453-1.473
AH-OUT TO 0.5 V (AH)	14.50	10.86	8.19	8.80	8.35
POS. THICKNESS (IN)	0.027	0.027	0.027	0.032	0.027
NEG. THICKNESS (IN)	0.0315	0.0315	0.031	0.026	0.031

Table 2

Conditions of Charge/Discharge for Flooded Cells

DISCHARGE RATE: C/2 ROOM TEMP

VOLT LIMIT	NASA LEVEL #	CHARGE RATE	# HRS CHARGED
1.475	V8	C/2	288
1.455	V7	C	288
1.434*	V6	C/2	480
1.434*	V6	C/2	672
1.434	V6	C	714
1.434*	V6	C	912
1.434*	V6	C	1248
1.414	V5	C/2	176
1.414	V5	C/2	288
1.414	V5	C/2	720

*SECOND PLATEAU APPEARED IN THESE CASES.

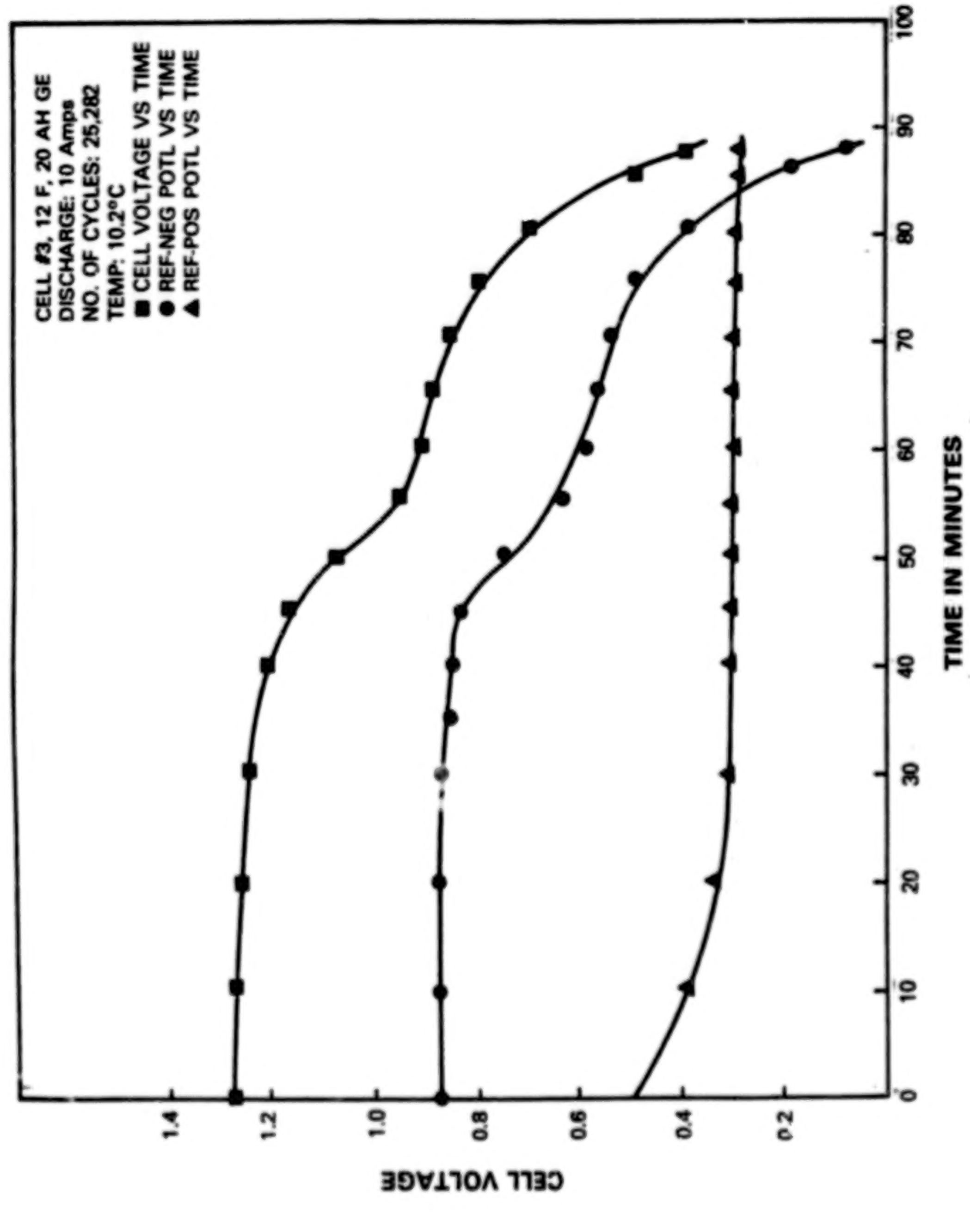
CELL #3, 12 F, 20 AH GE
DISCHARGE: 10 Amps
NO. OF CYCLES: 25,282
TEMP: 10.2°C
■ CELL VOLTAGE VS TIME
● REF-NEG POTL VS TIME
▲ REF-POS POTL VS TIME
CELL VOLTAGE
1.4
1.2
1.0
0.8
0.6
0.4
0.2
TIME IN MINUTES
0
10
20
30
40
50
60
70
80
90
100

Figure 1

ORIGINAL PAGE IS
OF POOR QUALITY

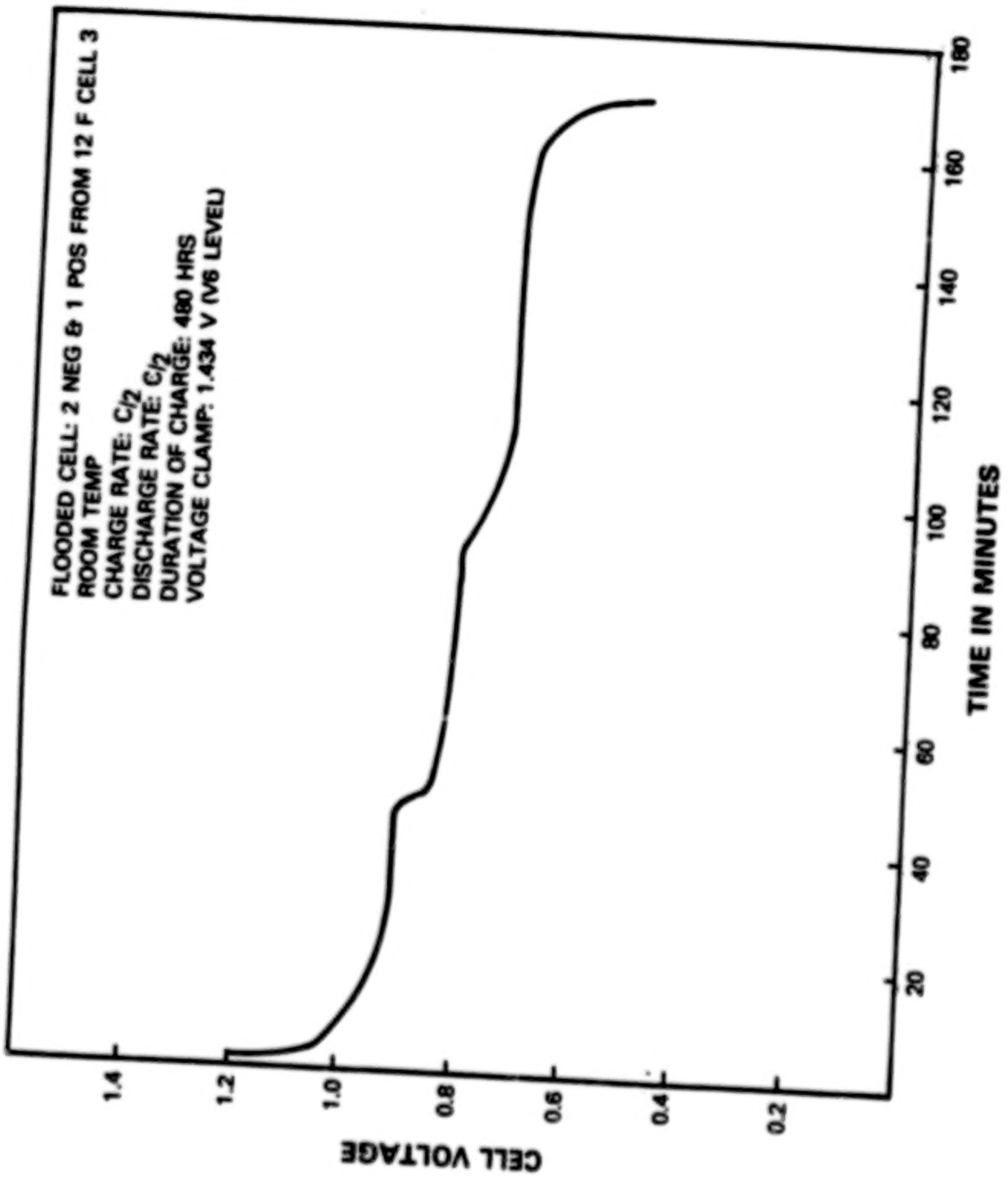

Figure 2

ORIGINAL PAGE IS
OF POOR QUALITY

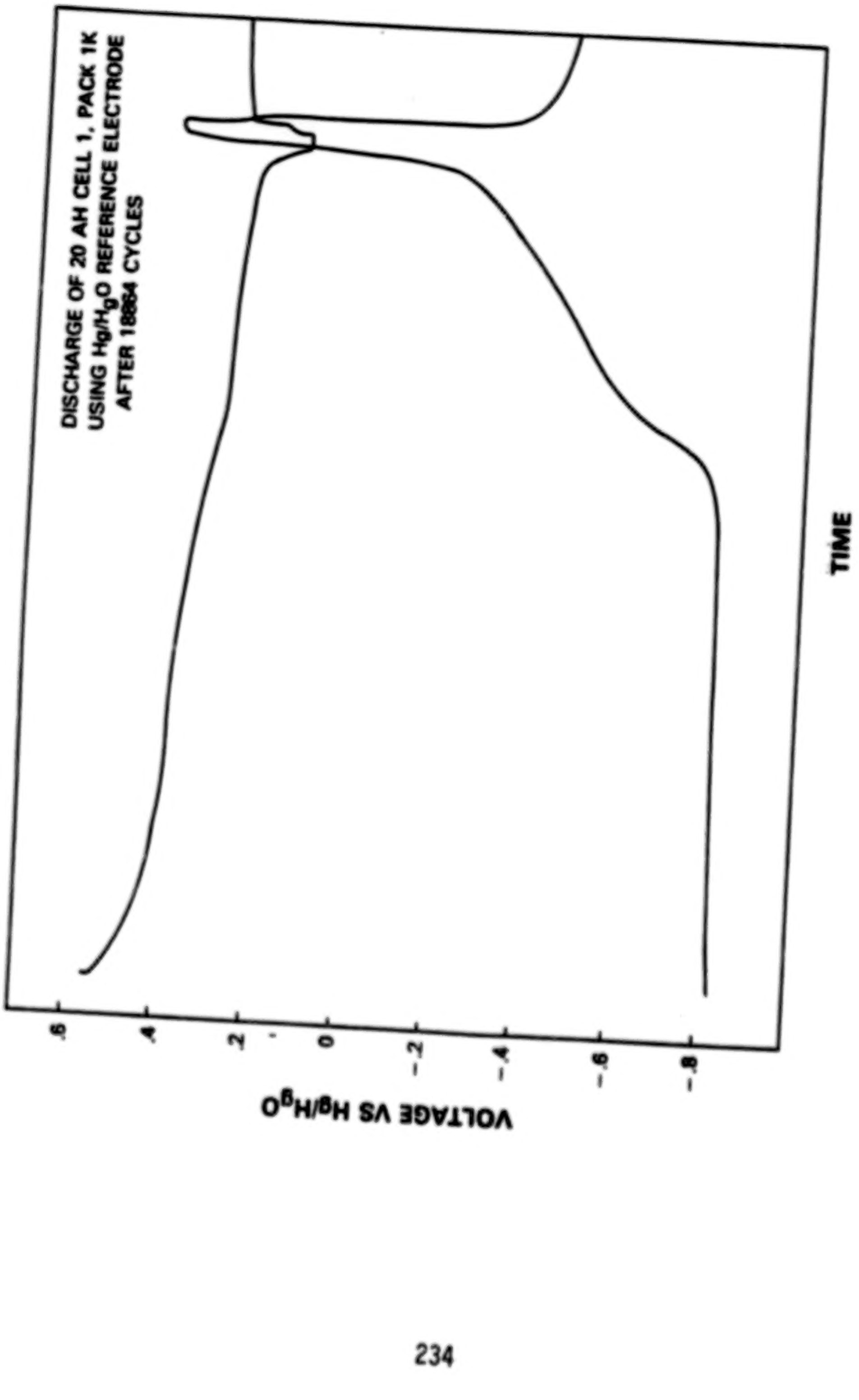

Figure 3

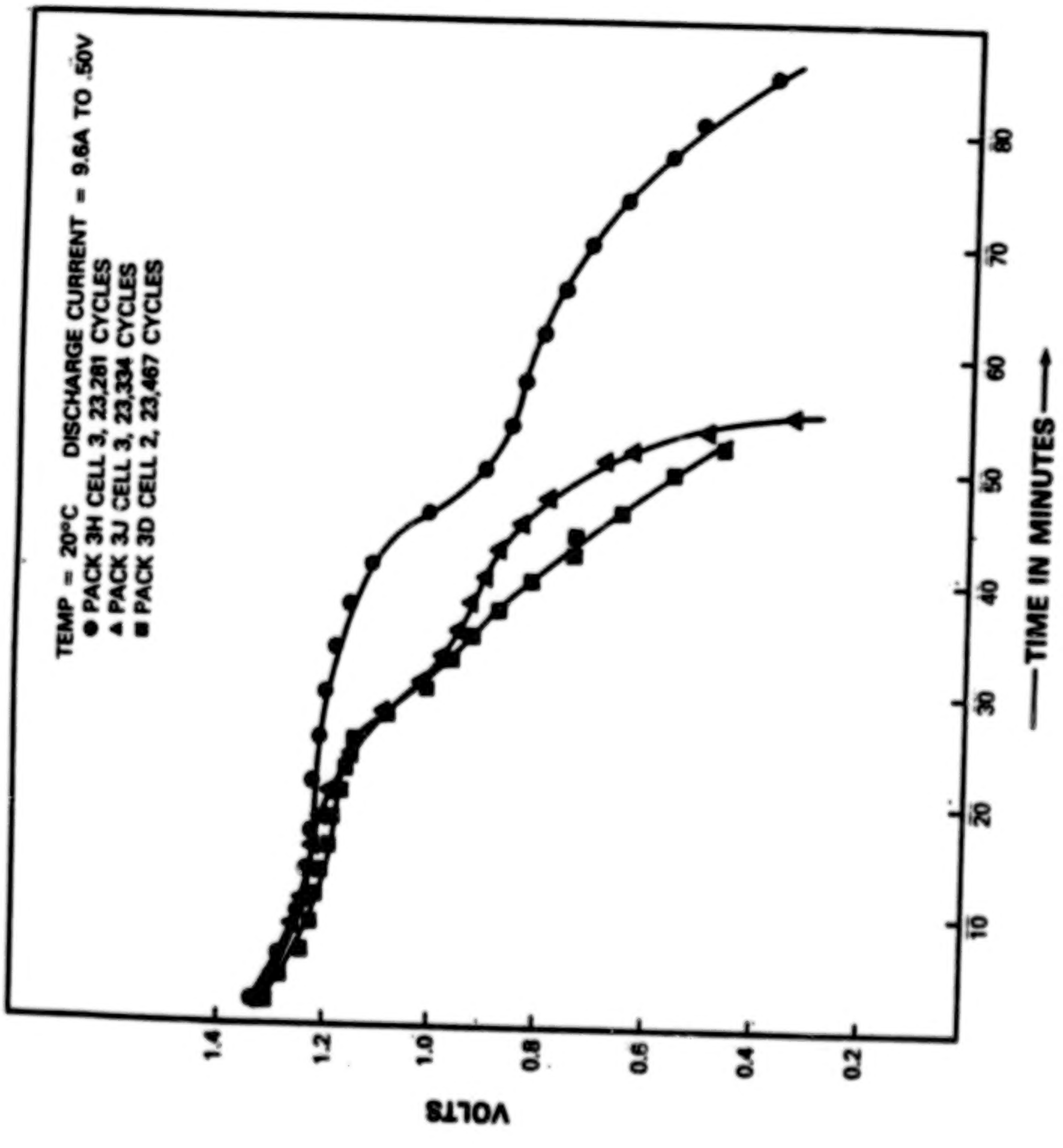
TEMP = 20°C DISCHARGE CURRENT = 9.6A TO .50V
● PACK 3H CELL 3, 23,281 CYCLES
▲ PACK 3J CELL 3, 23,334 CYCLES
■ PACK 3D CELL 2, 23,467 CYCLES
1.4
1.2
1.0
0.8
0.6
0.4
0.2
VOLTS
10
20
30
40
50
60
70
80
TIME IN MINUTES

Figure 4

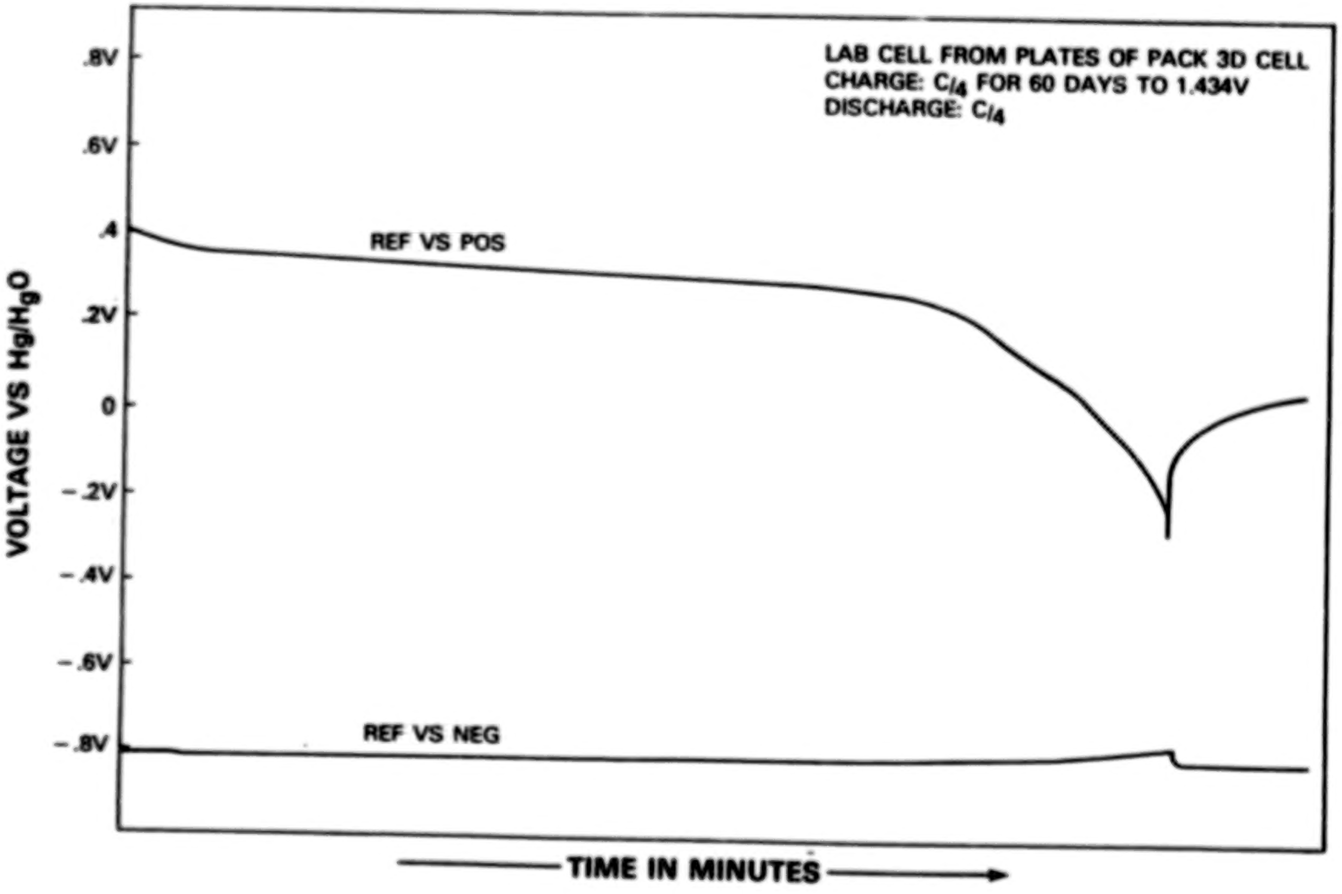

LAB CELL FROM PLATES OF PACK 3D CELL
CHARGE: C/4 FOR 60 DAYS TO 1.434V
DISCHARGE: C/4
VOLTAGE VS Hg/HgO
.8V
.6V
.4
.2V
0
-.2V
-.4V
-.6V
-.8V
REF VS POS
REF VS NEG
TIME IN MINUTES

Figure 5

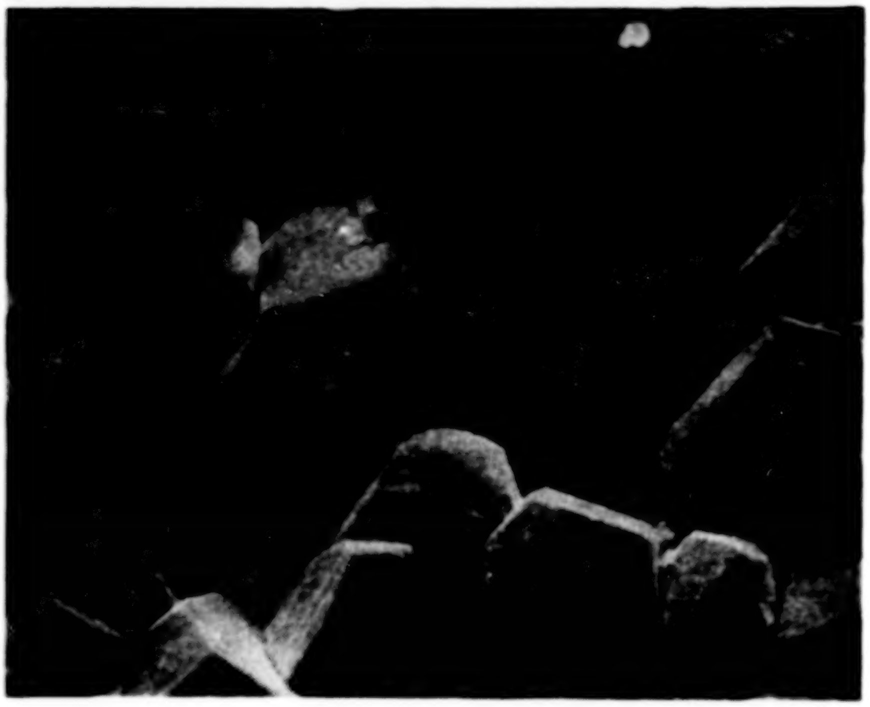

SEM of neg of cell 2, pack 3D at 640X show large crystals of β-Cd(OH)$_2$.

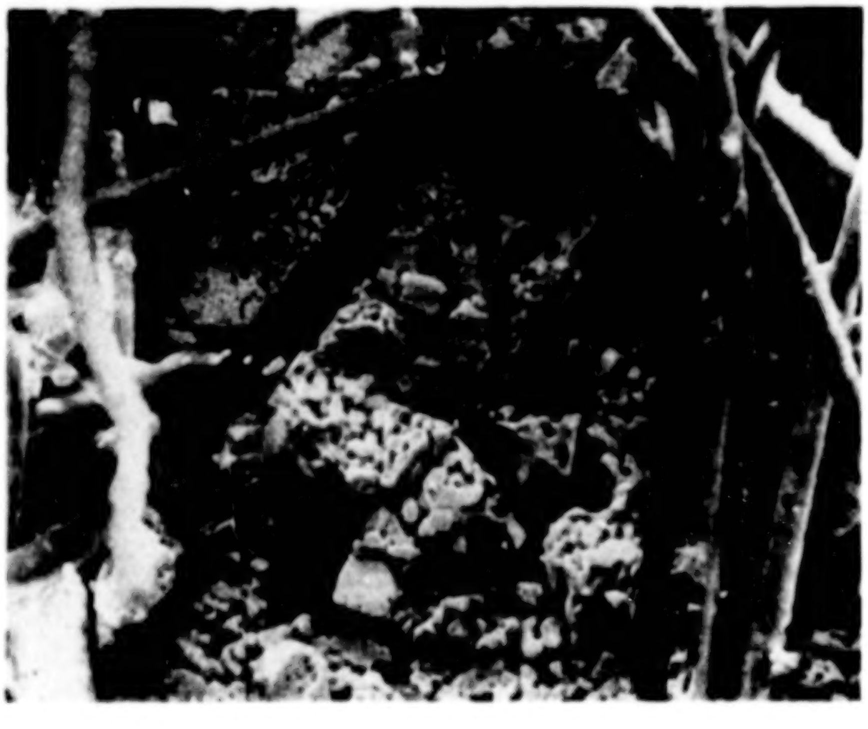

SEM of neg of cell 2, pack 3D at 340X show crystals of β-Cd(OH)$_2$ and fibers of separator.

Figure 6

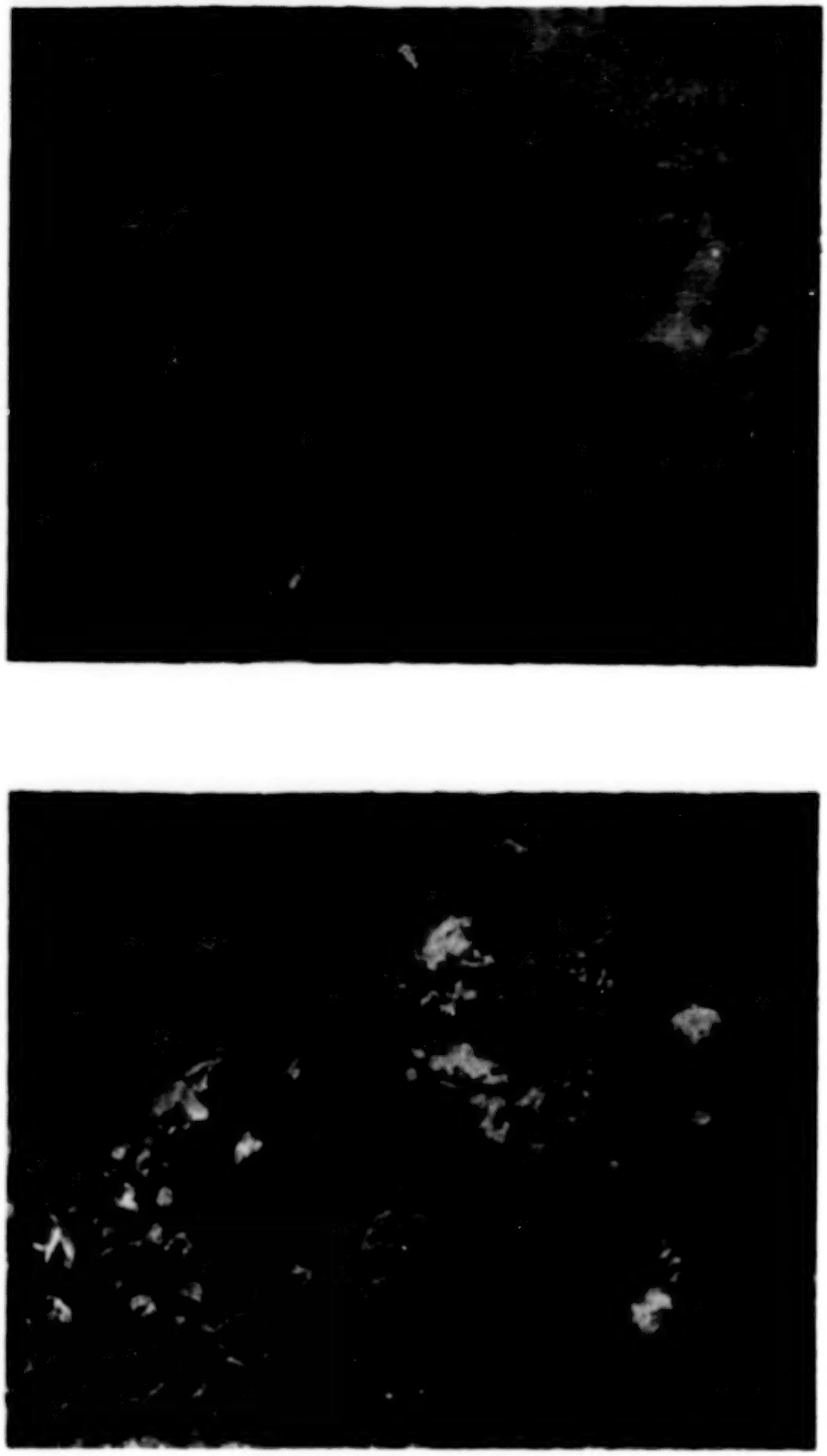

Figure 7. SEMs of POS of cell 2, pack 3D at 640X and 160X amorphous surface of POS with a lump of β-$Cd(OH)_2$ collected due to a short.

ORIGINAL PAGE IS
OF POOR QUALITY

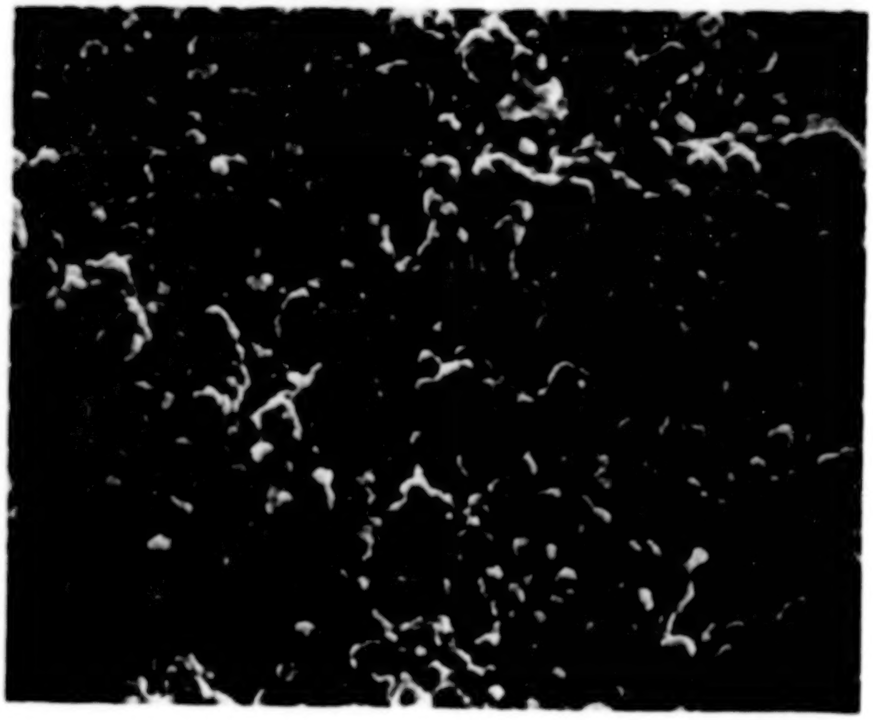

Figure 8. SEM of neg of cell 3, pack 12F at 320X after overcharging show absence of crystals.

Q. Unidentified: Do you observe a rate dependence or are those crystals different than the normal crystals that discharge or are they bigger?

A. Kunigahalli, Bowie State College: They are bigger.

Q. Unidentified: And then if you do it a very low rate you should not see a voltage plateau?

A. Kunigahalli, Bowie State College: If you do it.

Q. Unidentified: If you discharge at a very low rate you should not see a voltage plateau. Is that correct?

A. Kunigahlli, Bowie State College: Right. That's what I would expect. The higher rate suddenly drops to the plateau.

A. Unidentified: The reason why I asked that was reconditioning in space is where you see the voltage depression at very low rates, which suggests they are not just depending on the crystal size there has to be more to it than that because the current densities are dropped.

Q. Hendee, Telesat Canada: There were sealed cells you were working with?

A. Kunigahalli, Bowie State College: Right sir.

Q. Hendee, Telesat Canada: When you put the teflon tube in there with the mercury and you seal it how did you keep the balance of a cell? I noticed actually that you were negative limited on discharge which means that it's a considerably different cell. Am I correct on that?

A. Kunigahalli, Bowie State College: We took only aout 1 or 2 minutes to drill the hole and we introduced the teflon tubing which is the reference electrode. Okay?

COMMENT

Hendee, Telesat Canada: Something happened I think when you charged because you are a negative limited on discharge, definitely you were. The other comment I guess I would like to make: Why do we see this same plateau occasionally on different cells of nickel hydrogen which have no negative.

Kunigahalli, Bowie State College: I know I'm aware of that. Some people have indicated that second plateau has occurred in the work of Fred Burns and Dunlop Burns who reported earlier that reconditioning would actually improve the voltage cycling in nickel hydrogens.

Q. Hendee, Telesat Canada: Have you done any kind of continous impedance checks on discharge?

A. Kunigahalli, Bowie State College: No sir.

A. Hendee, Telesat Canada: I'm going to run right home and do that.

A. Kunigahalli, Bowie State College: Thank you.

Q. Sullivan, APL: Some of the recent satellites have been designed with discharge resistors so we can completely discharge a battery in orbit over a period of about a month and we've been wondering - the frequency with which we should do that. Would your studies indicate that we should be doing it frequently or infrequently? It sounds like to me it's something that should be done often.

A. Kunigahalli, Bowie State College: You mean the reconditioning?

Q. Sullivan, APL: The reconditioning cycle?

A. Kunigahalli, Bowie State College: I cannot suggest anything.

A. Sullivan, APL: Okay.

COMMENT

Maurer, AT&T Bell Labs: I guess I have a problem with the cadmium hydroxide crystal explanation. The plateau occurs on the discharge and on discharge you are going from the cadmium metal to the cadmium hydroxide and the cadmium hydroxide precipitating to the cadmium hydroxide crystal. So it's an end product of the reaction and not the electro-chemical step part of the reaction. So the size of the cadmium hydroxide crystals shouldn't have anything to do with the electro-chemical voltage. Also you haven't commented on the nickel cadmium intermetallic explanation for the same phenomena.

Kunigahalli, Bowie State College: Yes, I am aware of that. The mercury indicates that the intermetallic compounds are a large formation as Bernard puts it. That's the compound that they have examined formation. But I have a feeling this compound or crystal whatever is just insulating the active cadmium and that's maybe the reason then they will discharge the lower voltage.

Ford, NASA/GSFC: Ed, I'm surprised that you were surprised that these cells were negative limited on discharge. I've never seen cells cycle at this depth in LEO orbit that weren't negative limited on discharge after 20,000 cycles. Addressing Ralph's question, I don't think this gives you any insight into the effects of reconditioning per say. I recall though a few years

Ford, NASA/GSFC (Con't): back Dr. Will Scott had done some work at TRW. He showed I believe if you are going to recondition you have to start off early and continue it throughout the life and fairly frequent. That was my recollection.

Q. Jagielski, GSFC: I was wondering would you assume that this same mechanism would cause the third plateau that's been observed or would you assure that some other type of mechanism maybe precipitated by this growth of the large crystals?

A. Kunigahalli, Bowie State College: I can't answer unless I investigate what is the possible cause for the third plateau. I don't know but I have seen in many other cases the discharge curve showing more than two plateaus. So it needs some investigation.

Q. LaFrance, Aerospace Corporation: I thought I heard you say the prognosis for this problem to cure the large cadmium hydroxide crystals were overcharged and gassed. Did I hear you say that?

A. Kunigahalli, Bowie State College: Pardon me.

Q. LaFrance, Aerospace Corporation: You can eliminate these large crystals with gassing on overcharge?

A. Kunigahalli, Bowie State College: Yes in flooded cells but that's not in real sealed Ni-Cd cells.

A. LaFrance, Aerospace Corporation: Oh I see. Okay.

A. Kunigahalli, Bowie State College: In short what I found was gassing has eliminated those.

Q. Lim, Hughes Research Lab: Are any of your parameters a direct measure of the capacity?

A. McDermott, B&K Dynamics, Inc.: The reason I say it's what I would call apparent capacity is if you cut the rate of discharge down I think that would go off into another second plateau and you would get more capacity out of the cell. So it's not the absolute capacity of the cell. But what I think it's measuring is the quote memorized capacity of the cell that is after you've cycled the cell for a number of cycles you will find that tailoring off at the far region of the discharge due to changes or whatever in the cell. I'm not going to hazard a guess as to why that happens but it means at that depth of discharge and that rate that discharge rate you should expect that curvature of that nature and so you would call it the capacity of the cell at that rate of discharge and that age.

Q. Lim, Hughes Research Lab: Second question. Have you tried to determine whether that voltage you are analyzing is due to positive electrode voltage or negative electrode?

A. McDermott, B&K Dynamics, Inc.: No. It's just strictly, I'm looking at the cell as a black box. I'm just taking the voltage out but I'm saying that the equation itself is not totally a statistical analytical tool that I think the C parameter is related to capacity and I think Shepherd in his work around the 65 time frame actually was arguing for some physical chemistry behind some of these fit coefficients, he does some explaining with regard to electro-chemical reactions but I'm using it strictly as an analytical tool at this point.

Q. Hafen, Lockheed: Concerning the charge voltage you seem to be mostly concerned. On the charge voltage does that work as well and what is the meaning of x in that equation? Is it taken into account for the charge efficiency or?

A. McDermott, B&K Dynamics, Inc.: Yeah, that's the problem. X there is simply current passing through the cell and so as a tool we haven't actually used that in interpreting for life prediction. You could use it for interpreting or for predicting this voltage characteristic. I'd say it would be very good for that once you've established the slopes and the turning point when you go from phase 1 to phase 2 and phase 3. But as a life predicter when we haven't looked into that yet.

Q. Bell, Hughes Aircraft: Dr. McDermott the matrix you showed there has relative high depth of discharge high operating temperatures, does this model apply equally well to some of the Crane data in excess of 70 and 80,000 cycles at low temperatures and low depths of discharge?

Q. McDermott, B&K Dynamics, Inc.: Are you talking about the prediction equation?

A. Bell, Hughes Aircraft: The prediction equation, yes.

A. McDermott, B&K Dynamics, Inc.: Yes it does pretty well on that. I have given papers in the past here using that prediction equation for a broader set of conditions than this. I'm just I was using that equation relative to this data because we were doing this data analysis. But yes, the equation works. I can give you several references to other data that we have used it on.

A. Bell, Hughes Aircraft: Thank you.

N84
33685

UNCLAS

N84 33685 D17

PREDICTION OF BATTERY LIFE AND BEHAVIOR FROM ANALYSIS OF VOLTAGE DATA

Patrick P. McDermott, Ph.D.
B-K Dynamics, Inc.
Rockville, Maryland

Introduction

The object of this analysis is to develop a method for simulating charge and discharge characteristics of secondary batteries. The analysis utilizes a non-linear regression technique where empirical data is computer fitted with a five-coefficient non-linear equation. The equations for charge and discharge voltage are identical except for a change of sign before the second and third terms.

$$\text{Discharge Voltage} = A - \frac{B}{C - x} + De^{-Ex}$$

$$\text{Charge Voltage} = A + \frac{B}{C - x} - De^{-Ex}$$

Figures 1 and 2 show typical charge and discharge curves, with dots representing actual voltage data and the solid line representing the theoretical fit. The data is taken from a test of 12 amp-hr, NiCd cells cycling in a near-earth orbit regime at the Jet Propulsion Laboratory. The figures show that the theoretical fit is accurate to within 2-3 millivolts.

When coefficients A, B, C, D, and E are plotted versus cycles, certain trends are apparent. Figure 3 shows the five coefficients for cells cycling at a 50% depth of discharge and 20° C. A regression analysis was performed on voltage data at 100 cycle intervals up to 3000 cycles, with the exception of the first 100 cycles for which the interval was smaller.

For coefficients A, B, C, and E there is a sharp rise during the first 100 cycles, and for coefficient D, a sharp decline. After reaching the peak at 100 cycles, there is a gradual decline for approximately 1000 to 1500 cycles for coefficients A, B, C, and E; coefficient D shows a gradual increase over the same interval. By 1500 cycles, all coefficients have reached an equilibrium at which the value of the coefficient is stable.

The rates of change of the coefficients vary with temperature. Figure 4 shows coefficient A at 20, 30, and 40° C. The trends are similar at each temperature, except that the point of stability is reached at progressively earlier cycles, from 1500 cycles at 20° C to 500 cycles at 40° C.

PRECEDING PAGE BLANK NOT FILMED

We have found that coefficients A, B, and C are highly correlated. Figure 5 shows coefficient A plotted against coefficient C for the cells at 20° C.

Modeling the Voltage

For the remainder of this analysis, the different areas of the curves will be characterized as follows (see Figure 6):

- Phase I represents the initial sharp rise (or decline) from initial voltage I_0.
- Phase II represents the gradual decline (or rise) from the peak at II_0.
- Phase III represents the region of stability beginning at III_0.

In order to predict the charge or discharge characteristics at a given cycle, specific values for coefficients A, B, C, D, and E are substituted into the original non-linear equations where voltage is now the dependent variable. To establish specific values for the coefficients at a given cycle, the following calculations were made:

- The slopes for Phases I and II were calculated for all temperatures.
- A value for the coefficient in Phase III was calculated based on the mean over that phase.
- The values for I_0, II_0, and III_0 were estimated by intersection of the linear portions of each phase.

Figure 7 shows a generalized equation where slopes are symbolized by Δ and X represents the amp-hrs of charge removed from the cell in discharge or added to the cell in charge.

Once the slopes and initial values I_0, II_0, and III_0 are determined for a particular temperature and depth of discharge, it is a straightforward calculation to determine the charge and discharge curves for a particular cycle, whatever the range (Phase I, II or III).

Operational Significance

The spacecraft manager can be faced by a number of situations where the use of a voltage prediction model could be of use:

- Voltage prediction with sparse data
- Voltage prediction of a neighboring cycle
- Voltage prediction of a cycle later in life.

The first case prediction with sparse data is a practical necessity, due to the fact that there is often a limitation on the amount of data that can be telemetered to the ground during a spacecraft orbit. Furthermore, in managing the energy balance of a spacecraft's power system, it is often useful to track the battery's performance given specific loads and thus voltage prediction of neighboring cycles. Finally, in long-term missions, it could be very useful for the manager to be able to predict power system behavior several years later in the mission.

Candidates for Life Prediction

The purpose of life prediction is to find trends such as those established in Figures 3 and 4 which correlate well with life. It would be useful, moreover, if these trends could be established early in the life of a cell; during the first few hundred cycles, for example. In this analysis, a number of trend descriptors or signatures were investigated to see which best correlated with life. The candidates for correlation with life were as follows:

- Value of parameter during first cycles
- Value after initial rise or decline
- Slope during initial rise or decline (100 cycles)
- Slope after initial rise or decline (100-1500 cycles)
- Value of parameter after leveling off.

After considering each of these "candidates," it was determined that the most consistent results were found by correlating life with the fourth candidate, the slope after the initial rise or decline (100-1500 cycles).

Figure 8 shows the ln slope of three of the coefficients, A, B, and C, plotted against temperature for two depths of discharge, 35% and 50%. This figure suggests that as temperature increases there is a linear increase in the ln slope of these coefficients over the range under investigation. The difference between 35% and 50% depth of discharge is approximately 1.0 on the ln scale.

Correlation with Life

Figure 9 shows actual and predicted values of cycles-to-failure for three of the packs cycling at JPL, 50%/40° C, 50%/30° C, and 35%/40° C. The equation used to theoretically calculate mean cycles to failure was derived several years ago and is found in previous Proceedings of the Battery Workshop. The predicted cycles to failure are within 10% to 20% of the actual mean value cycle to value which are approximately 9,000 cycles for the 50%/30° C and 35%/40° C cells and approximately 3400 for the 50%/40° C cells.

In a very qualitative sense, increasing temperature and depth of discharge both lead to shorter battery life, and the rise in 10° C is roughly equivalent to a 15% increase in depth of discharge. In Figure 9, an increase in temperature from 30° C to 40° C for the 50% depth of discharge cells caused a drop in cycle life from approximately 9000 to 3400 cycles. The same sort of drop was seen in the two 40° C packs when the depth of discharge is increased from 35% to 50%.

These findings are consistent with those found in Figure 8, where the increase in ln slope over 10° C (approximately 1.0) is the same differential as was found between each of the 35% and 50% depth of discharge curves. This result demonstrates in a qualitative sense at least a 10° C increase in temperature is equivalent to a 15% increase in depth of discharge.

Summary

Figure 10 is an attempt to estimate the quality or reliability of a prediction based on the amount of data available. One star indicates a fair estimate; three stars indicates a good estimate. It is clear that accumulating data over early life (Phase I) is a less reliable basis for prediction than data accumulated in mid-life (Phase II). The best prediction for both voltage behavior and cycles to failure can be made after the test has passed point III_0 when the cell reaches its stability point after approximately 500-1500 cycles.

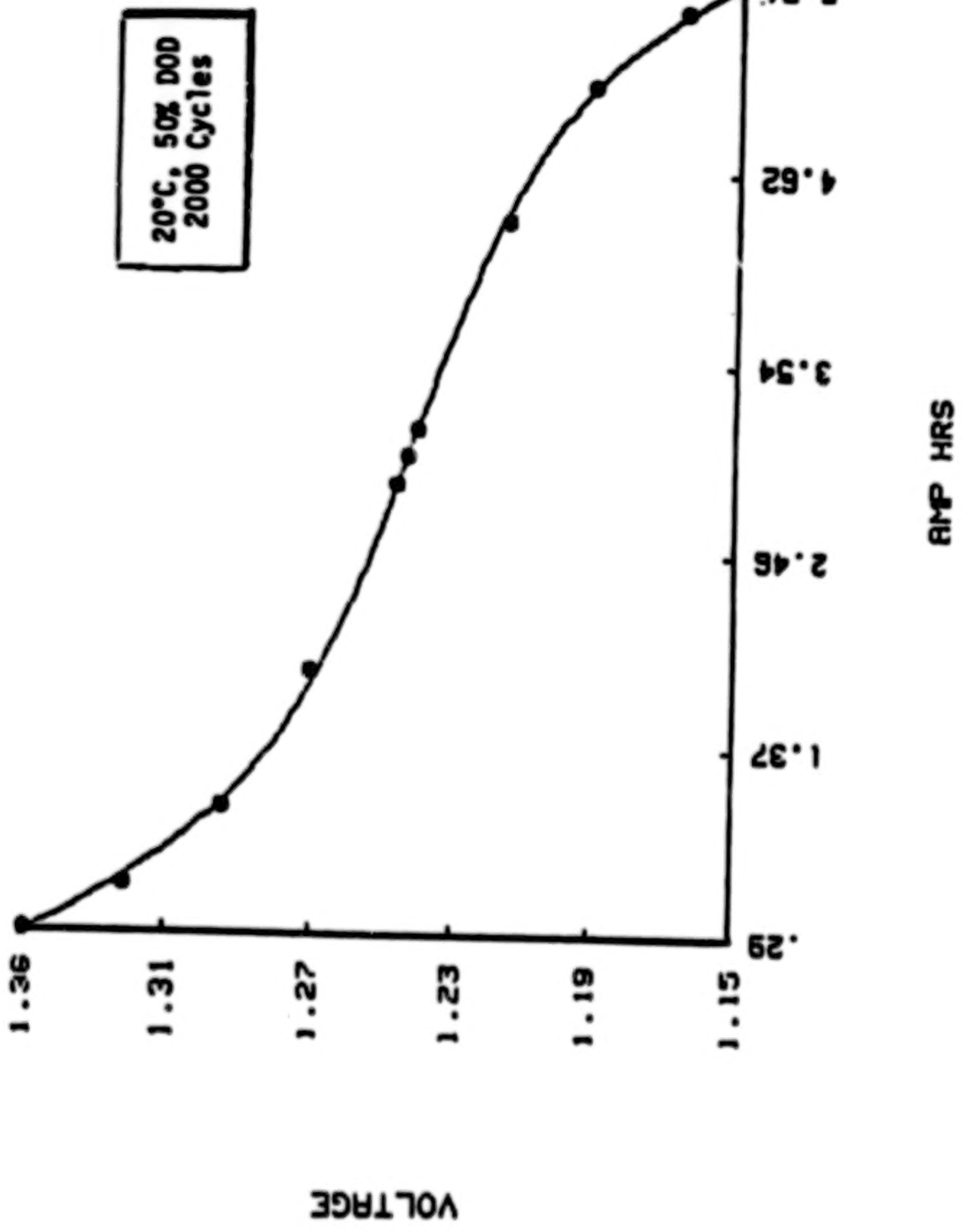

Figure 1. Five parameter discharge voltage fit.

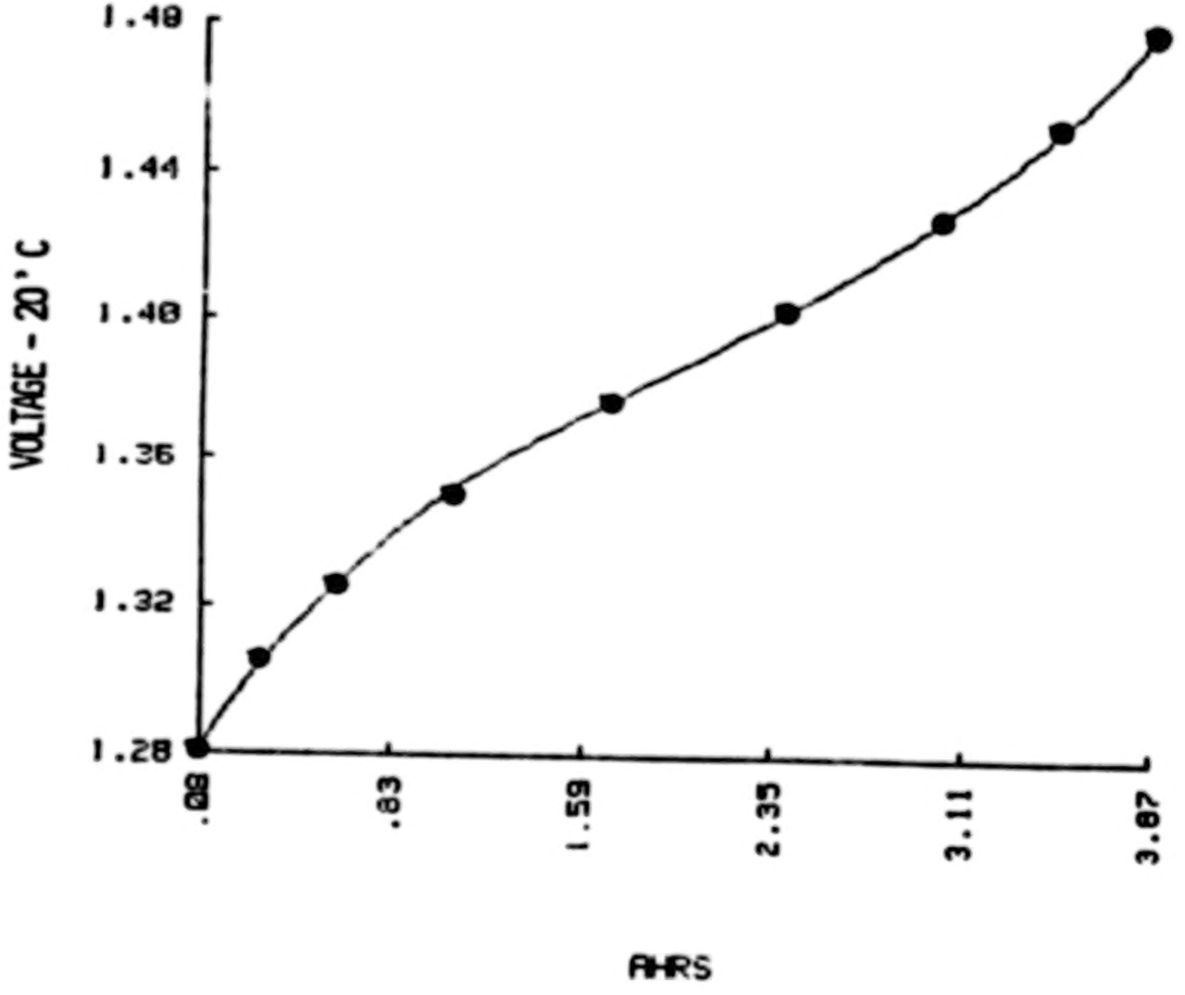

Figure 2. 5-fit charge 200 cycles 35% DOD.

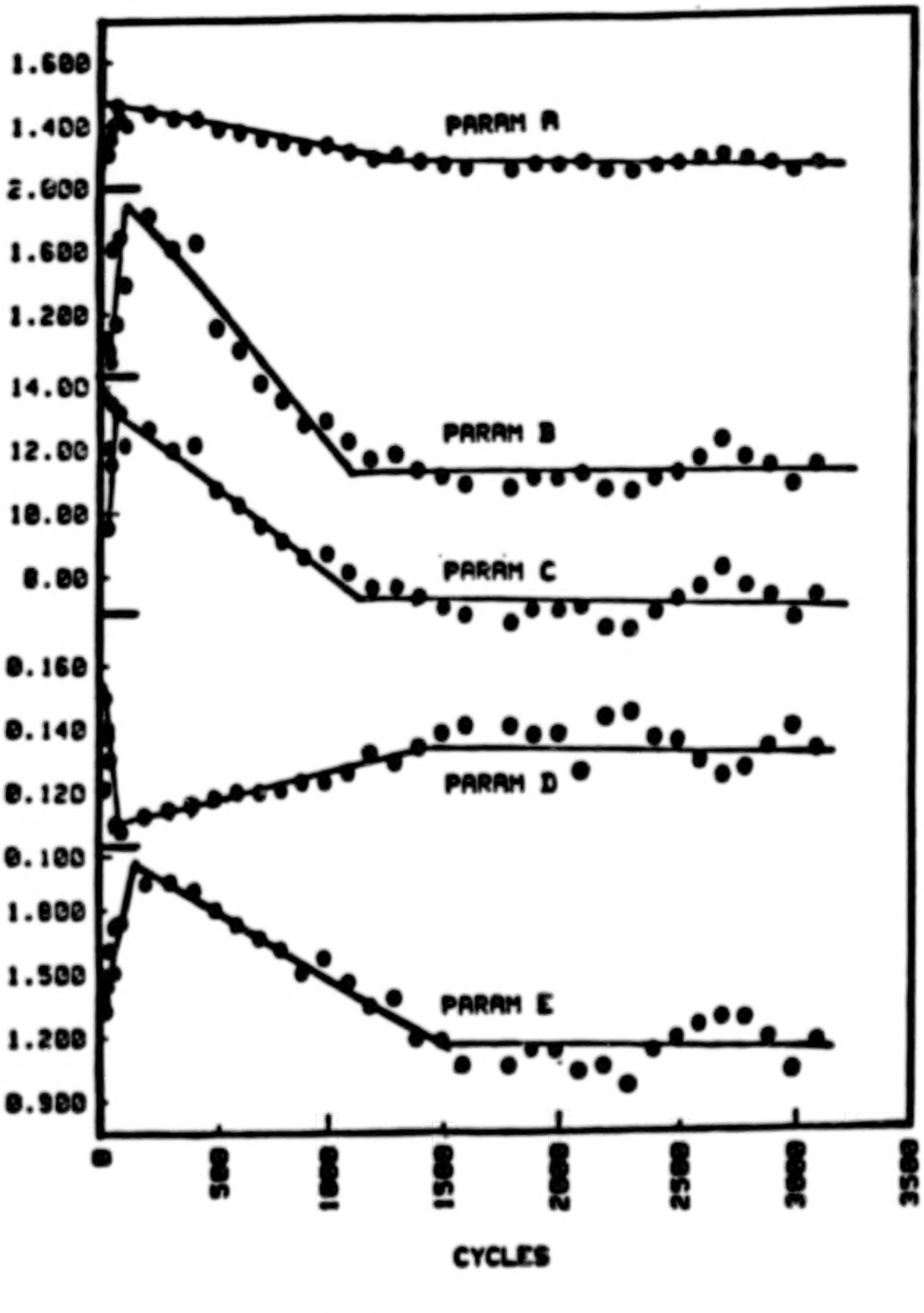

Figure 3. 5-fit discharge 50% DOD temp 20°C.

ORIGINAL PAGE IS
OF POOR QUALITY

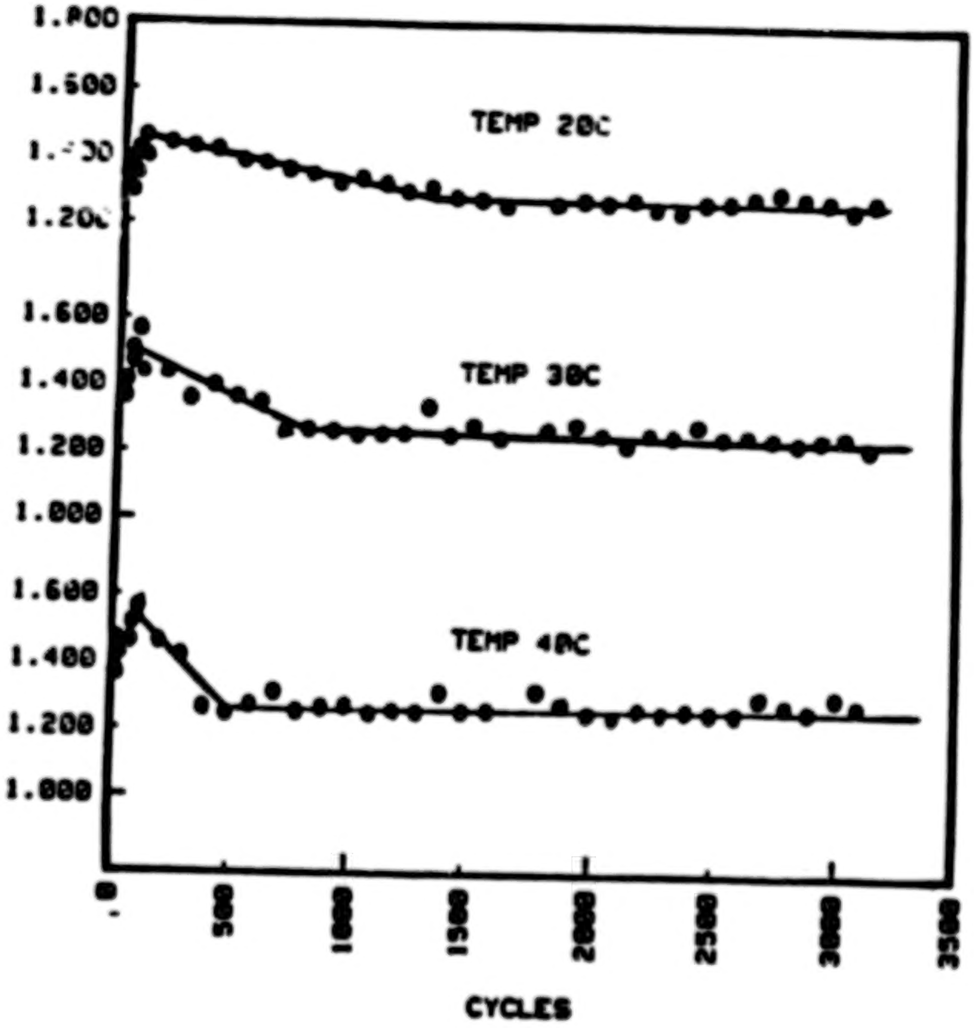

Figure 4. 5-fit discharge 50% DOD parameter A.

ORIGINAL PAGE IS
OF POOR QUALITY

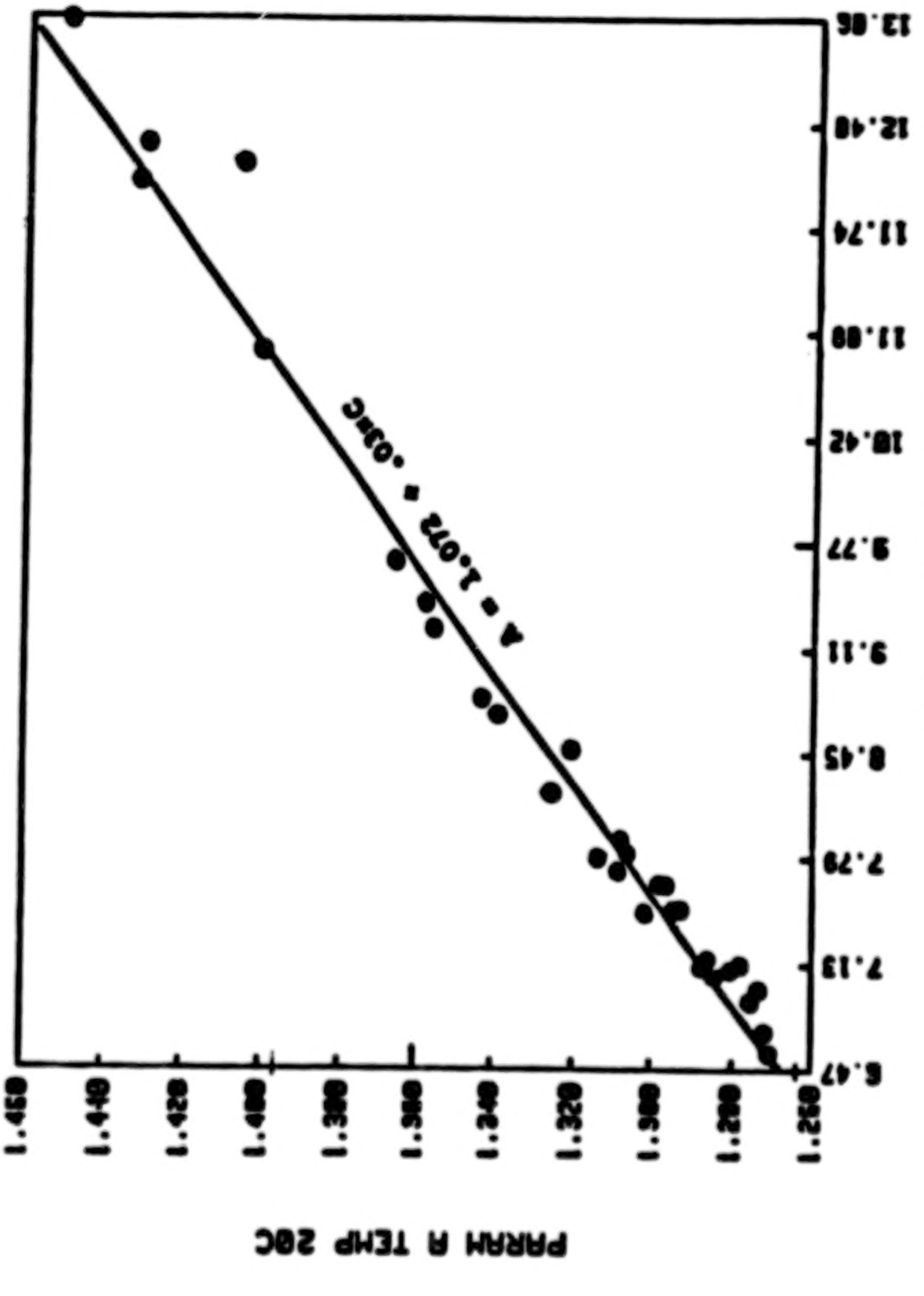

Figure 5. Correlation of coefficients A and C.

ORIGINAL PAGE IS
OF POOR QUALITY

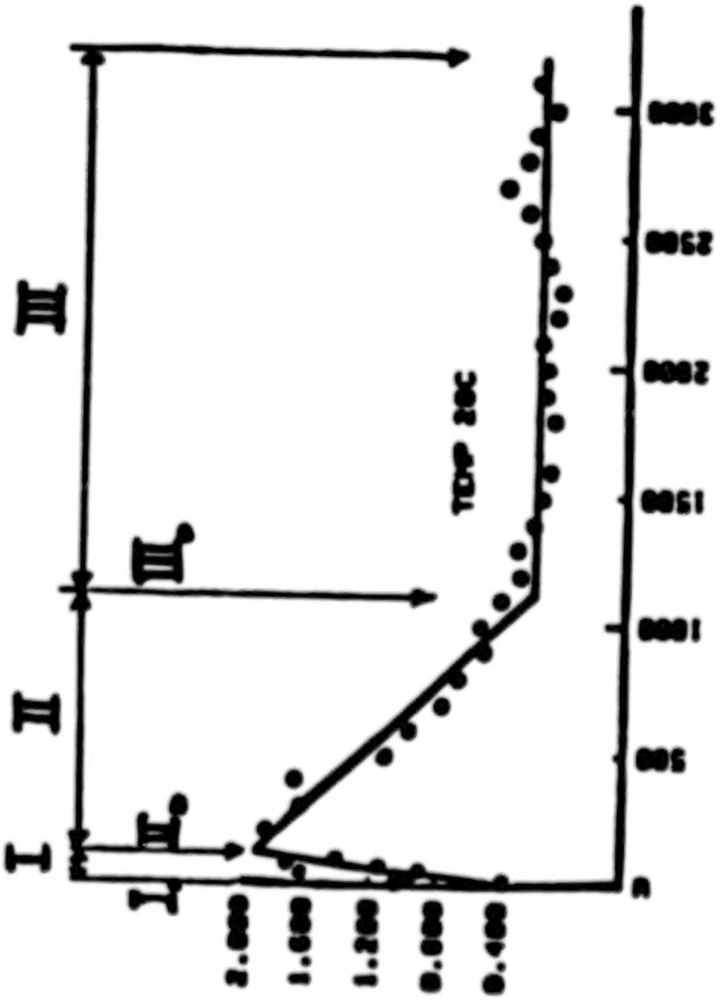

Figure 6. Discharge 50%DOD parameter B.

$$\boxed{\text{Voltage}} = A(I,II,III) \pm \frac{B(I,II,III)}{C(I,II,III) - X} \mp D(I,II,III) \exp^{-E(I,II,III)X}$$

$A(I) = A_{I\bullet} + \Delta A_I \times \text{Cycle No.}$ where ΔA_I = Slope of A during Phase I cycles

$A(II) = A_{II\bullet} + \Delta A_{II} \times \text{Cycle no.}$

$A(III)$ = Average Value of A over Phase III

$B(I) = B_{I\bullet} + \Delta B_I \times \text{Cycle No.}$

•   •   •   •

•   •   •   •

•

•

ETC.   ETC.   ETC.   ETC.

Figure 7. Voltage prediction.

ORIGINAL PAGE IS
OF POOR QUALITY

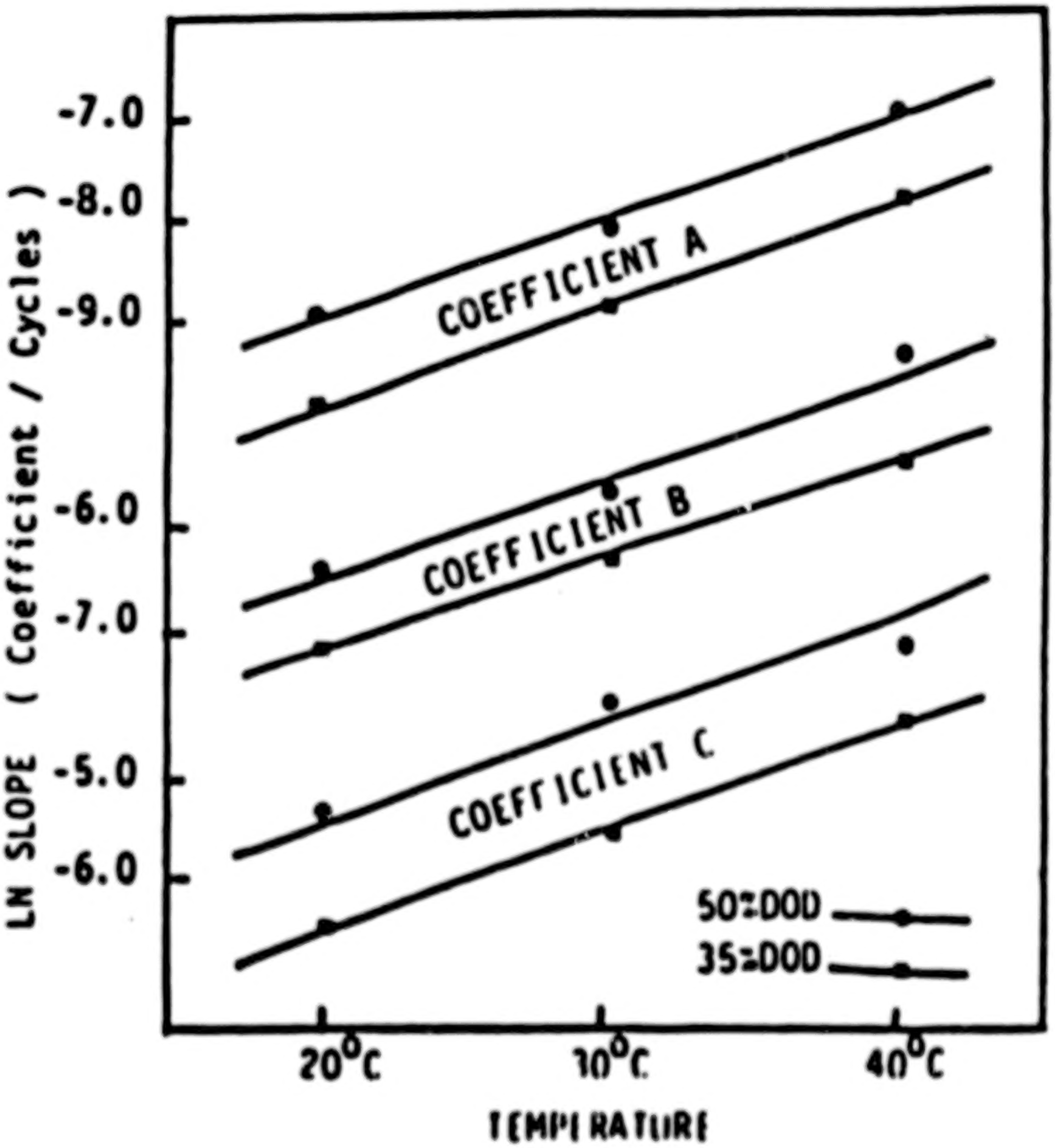

Figure 8. Ln slope vs temperature.

$$\text{MEAN CYCLES TO FAILURE} = 1500(67-\text{Temperature})e^{-0.038(\text{DOD})}$$

DOD/TEMP	50%/40°C	50%/30°C	35%/40°C
Cycles to Failure	3351 3441	10,367 8,600	9,042 9,042
Predicted	3800	8,300	10,700

Figure 9

ORIGINAL PAGE IS
OF POOR QUALITY

	Early Life	Mid Life	Later Life
Voltage Prediction with Sparse Data	**	**	**
Voltage Prediction of Neighboring Cycle	**	***	***
Voltage Prediction of Cycle Later in Life	*	**	***
Prediction of Failure Cycle	*	**	***

Figure 10. Estimate of quality of prediction.

Q. Ellason, Lockheed: The battery with the two shorted cells - would you care to comment on the age.

A. Pickett, Hughes Aircraft: Yeah, they were at least well the in orbit life time was about seven years and you can see that from the graph when the voltage dropped off significantly. The actual age of the cells themselves were about nine years.

Q. McDermott, B&K Dynamics, Inc.: I noticed that on several of the graphs your predicted value actually changed as you were changing the loads?

A. Pickett, Hughes Aircraft: That's right.

Q. McDermott, B&K Dynamics, Inc.: So you have current density terms in there that are sort of mapping those charges?

A. Pickett, Hughes Aircraft: That's in the depth of discharge.

Q. McDermott, B&K Dynamics, Inc: How come that the last one the predicted didn't seem to change very much when the low charged quite radically?

A. Pickett, Hughes Aircraft: The reason why is that there's several cells in a number of batteries which did not have shorts. That particular battery had shorts the other cells didn't and we would have to take an average or meaning of all the other cells on the consideration and the analysis and that's why the predicted didn't follow that particular curve.

Q. Weiner, Aerospace Corporation: Did you or do you intend to include the affect of any pre-use of the battery before launch such as times and activation temperature storage burn-in cycles or acceptance test cycles and so on.

A. Pickett, Hughes Aircraft: The answer to the acceptance test cycles and burn-in cycles that's kind of hard to do since everything we do is pretty much standard. It's hard to vary that. In answer to some of the other things we plan to look at possibly the wet life is something which we should look at as well as the time the batteries have to stay in open circuit. Although I will point out that in some of these batteries that we've used for systems test as well as spacecraft test you are aware that the batteries sometimes set open circuit at high temperatures maybe as long as two or three weeks something like that.

Q. Hafen, Lockheed: Does your model predict an operating temperature?

A. Pickett, Hughes Aircraft: You could probably get that out of it by doing some analysis with it. In other words, we were able to predict an optimum charge rate using it and I think we could probably do that with temperature as long as the temperatures are within the range of the data base.

Q. Hendee, Telesat Canada: Would the battery that developed the two shorts be one that I might possibly recognize?

A. Pickett, Hughes Aircraft: No it's not an ANIK satellite.

Q. Hendee, Telesat Canada: We've had some on that as well but okay.

A. Mallory, AT&T Bell Labs: I take it from the shape of the equation that the discharge in the early stages has no affect on the prediction that the later stages but it's each individual season that you have to worry about.

Q. Pickett, Hughes Aircraft: I'm not sure I understand your question Dean.

A. Mallory, AT&T Bell Labs: In some of your curves you showed a case where the load changed drastically from one season to the next.

A. Pickett, Hughes Aircraft: Yeah I would say that yeah the depth discharge is probably more - affects the battery more later. I think if you look at the model I believe there's some cross terms in there with respect to the depth discharge in time that takes care of that.

Q. Mallory, AT&T Bell Labs: Second question. Do you plan to include anything like the reconditioning depth of discharge?

A. Pickett, Hughes Aircraft: We haven't included it here or we didn't look at it here for two reasons. It probably should be done for completeness but to give you an isolated data point one satellite which had been reconditioned to one volt average per cell showed after eight years a minimum discharge voltage of about 1.18. One that had been discharged to 54% DOD showed an average of 1.16 there may be something significant there but just on the surface I would say that it's probably not that significant.

A. Maurer, AT&T Bell Labs: I was thinking of spacecrafts D1 & 2 where it was reconditioned to 115 volts/cell for the first 3 seasons the voltage dropped off then reconditioning to one volt the voltage jumped back up again.

A. Pickett, Hughes Aircraft: Yeah we've seen that and normally what we do is the beginning of life when we recondition or what we recommend to the customers is that during the first initial seasons they go to 1.15 v/c and then as the satellite ages we go down to lower than that but we never exceed an average of one volt per cell.

N84
33686

UNCLAS

N84 33686 ?18

PREDICTION MODEL FOR THE LIFE OF NICKEL-CADMIUM BATTERIES IN GEOSYNCHRONOUS ORBIT SATELLITES

J.H. Engleman, M.B. Zirkes-Falco,
R.S. Bogner, and D.F. Pickett, Jr.
Hughes Aircraft Company

ABSTRACT

Hughes has developed a mathematical model which predicts life of nickel-cadmium batteries designed for geosynchronous orbit satellites. A statistical analysis technique called regression was used to analyze orbital data on second-generation trickle-charged batteries.

The model gives average cell voltage as a function of design parameters, operating parameters, and time. The voltage model has the properties of providing a good fit to the data, good predictive capability, and agreement with known battery performance characteristics. Average cell voltage can almost always be predicted to within 0.02 volts for up to 8 years.

This modeling shows that these batteries will operate reliably for 10 years. Third-generation batteries, which are being used in the latest generation of Hughes satellites, are expected to operate even longer.

INTRODUCTION

Over the past 20 years there has accumulated considerable in-orbit data on batteries in geosynchronous orbit satellites designed and built by Hughes Aircraft Company. These satellites began in 1963 with Early Bird, the first geosynchronous communications satellite, and continue through the new HS 376 series. This series includes the SBS and Anik-C satellites recently launched by the Space Transportation System. Since launch of the Intelsat IV series of satellites in the early 1970's, one cell manufacturer, General Electric Company, has been used almost exclusively by Hughes for production of satellite batteries. Consequently, Hughes has an extensive data base of design and in-orbit data on General Electric battery cells.

These batteries, beginning with the Intelsat IV (ref. 1) and the Anik-A (Canada) (ref. 2) series of spacecraft, can be conveniently divided into three generations of designs. The first generation was the Intelsat IV (F2 through F7) and Anik A1 and A2 series of spacecraft batteries. The second generation was the Intelsat IV F1 and F8, Intelsat IV-A, COMSTAR, Anik-A3, WESTAR I, II, and III, Palapa-A (Indonesia) and MARISAT designs. The third generation is the

PRECEDING PAGE BLANK NOT FILMED

LEASAT and HS 376 design, which includes SBS (satellite business systems), Anik-C, WESTAR IV and V, Palapa-B, Telstar III (AT&T), Aussat (Australia), Brasilsat (Brazil), Galaxy (Hughes Communications), and Morelos (Mexico).

The first-generation batteries were stored open circuit and had temperatures close to 25°C, high active material loading in the positive electrode (12 to 13 g/dm^2), low levels of electrolyte (2.5 cm^3/A-hr), and low plate areas, resulting in high current densities (5.5 to 5.9 mA/cm^2). These batteries did not reach their design life of seven years at 50 to 60 percent depth of discharge (DOD). Low battery voltage dictated removal of some of the spacecraft loads after 5-1/2 years.

In order to reduce early degradation, second-generation battries were stored trickle-charged in orbit at 15° to 23°C. More electrolyte was added to the cells (3.0 cm^3/A-hr), and other improvements were made. These changes resulted in batteries which have now exceeded 7 years of in-orbit operation without load reduction at DOD levels greater than 50 percent.

Prior to design of the HS 376 batteries, several significant relationships were established and quantified, such as separator degradation as a function of time and temperature, the effect of electrolyte quantity, and the effect of positive plate swelling (ref. 3, 4). These discoveries, along with improvements in the spacecraft power electronics, have resulted in a third-generation design life of over 10 years. The complete power system designs for the HS 376 series of spacecraft have been described earlier (ref. 5, 6).

DATA BASE AND PARAMETERS

The data base used in the analysis consisted of telemetered data from batteries in operational satellites. It included data on forty batteries on twenty satellites comprising ten different programs. The longest operating time was 16 eclipse seasons, or 8 years. All batteries were trickle charged. The battery cell sizes ranged from 6 to 24 A-hr, and were all procured from General Electric. All cells were of the second-generation type.

The measure of battery performance used was average cell voltage at end of discharge during the longest eclipse each season. The end of battery life is taken to be the time when this voltage drops below some specified value.

The design and operational parameters that appear in the final model are: depth of discharge, eclipse temperature, trickle-charge rate, electrolyte loading, and time in eclipse seasons. The minimum, maximum, mean, and standard deviation for these parameters are listed in table I. In addition, we also studied the effects of solstice (non-eclipse) temperature, discharge current, density, percent recharge, high charge rate, percent electrolyte, and cumulative depth of discharge.

METHODOLOGY

We selected, evaluated, and then modified a statistical model that employs multiple regression for use in predicting the life of nickel-cadmium in geosynchronous orbit satellites. Our goal was to obtain a model which provides good fit and predictive capability, for both the group of batteries and individual batteries.

A set of parameters thought to influence battery life was identified. Relationships between these parameters were examined by looking at correlations. This information was used in later stages to help select potential variables for use in the model.

All possible regression models with the selected parameters were examined (ref. 7), and several models were selected for further investigation. This selection was based on statistics that measure the models' ability to fit and predict observed phenomena well. The meaningfulness of physical relationships implied in the model was also considered. A reduced set of potential variables of interest was identified, and the process of model evaluation and selection was repeated.

Our initial set of variables was ten battery parameters, time, time^2, and time^3. Based on the results obtained by an iteration using these variables, a set of eight main effects and all first-order iterations of these eight main effects were selected for further investigation. This process was repeated several times. Two models were selected as final candidates. These two were than compared by investigating the following relationships: voltage versus number of eclipse seasons, battery life versus depth of discharge, and R(t) (probability of surviving at least t eclipse seasons). Judging from the standpoints of overall fit, fit to individual battery performance, prediction, and agreement with known battery characteristics, we selected a model. Variables not listed did not significantly reduce the amount of unexplained variation and therefore were not included in the model. Although those variables may have a significant influence on voltage, their effect in modeling is minimal, owing to their correlation with other variables used in the model. Addition of a variable correlated with another variable already in the model does not produce a significant reduction in unexplained variability.

RESULTS AND DISCUSSION

The selected battery voltage model is as follows.

$$\text{Voltage} = 1.12 - k_1 (D) + k_2 (D)E + k_3 (TCR) - k_4 (ET)\, TCR^2$$

$$- k_5 (D)T + k_6 (T^2) - k_7 (ET)(T^3),$$

where:

Voltage = Minimum end of discharge voltage, averaged for all cells in a battery

D = Depth of discharge in percent

E = Electrolyte in CC/A-hr

TCR = Trickle charge rate in A/A-hr

ET = Eclipse temperature in °F

T = Time in eclipse seasons

$k_1 - k_7$ = Statistically determined coefficients (constants)

The value of the coefficients were, of course, derived in the analysis but are omitted here because of other considerations.

Figure 1 shows voltage as a function of time for all other variables set to their means. Symmetric prediction intervals are presented at the 99, 95, and 75 percent levels for a response (voltage) at a specified set of conditions. With a given confidence, we can say that a future observation will be within the specified interval.

It is important to note the large effect that depth of discharge has on voltage and consequently on battery life. The lower the depth of discharge, the longer the battery will last. (See figure 2.) This relationship follows our expectations. Similar results have been obtained for batteries on life test. The model also indicates that we could operate our batteries at a higher depth of discharge than is currently being done. An interaction of $D^{2.3}$ with time (from results obtained by previous Hughes battery research) was considered for inclusion in the model (ref 8). However, this relationship did not provide results as good as those obtained by using the interaction of D with time.

Temperature seems to affect the batteries late in life, as might be expected. We feel it is appropriate that eclipse temperature rather than solstice temperature appears in the model, since eclipse temperature was the temperature at the time the voltage measurements were taken. Also, this is a case where two variables closely correlate and therefore only one of them needs to be in the model.

These relationships can be used, within the ranges of the parameters, to design and operate nickel-cadmium batteries that will have increased longevity. Extrapolation beyond these ranges should be avoided for several reasons. 1) Prediction error increases with distance from the mean of the data. 2) This model may be not a true representation of the underlying relationships but rather a good approximation within the range of our data. By creating a model that is sound from an engineering standpoint, we have minimized this effect.

3) Regression assumptions may no longer be valid outside the range of the data. An example of this fact is the occurrence of shorts late in life, which affects prediction error and could violate the assumption of constant variance over time. 4) Main effects and interactions omitted from the current model may be more influential outside the range of data used.

Figure 1 shows prediction intervals about the regression line. The individual prediction lines can be used to estimate reliability versus time in the following way. First, note that the lowest prediction line is such that, for any given time, the voltage will exceed that value with 0.995 probability. Thus for a given voltage and given probability, we can find the time which corresponds to the voltage and probability. For a fixed voltage, we can then construct a plot of probability versus time. The probability of exceeding a given voltage at a given time can be used as an approximation of reliability at that time.

Reliability versus time was investigated for voltage values of 0.90 to 1.10, because required voltage may vary, depending on specific satellite requirements. The probability that voltage, as defined in the model, is above the minimum requirement of 1.00 is 1 for the number of eclipse seasons less than or equal to 23. This probability value was obtained from a relationship relating reliability to prediction intervals, as described above, when all variables except time are set to their means. At voltage = 1.05, the reliability is 1 for 20 eclipse seasons, and then drops quickly. This is illustrated in figure 3a. When voltage = 1.10, this drop in reliability occurs sooner, after 17 eclipse seasons. (See figure 3b.) These results correspond quite well to currently accepted estimates of mean battery life as being on the order of 12 years. In addition, these results agree favorably with mission duration and design lives of 7 to 10 years.

The R^2 value for this model is 0.68. Although not as high as we would have liked, it is a good value, given that the model uses actual orbital data and is not a controlled laboratory study. A designed, controlled study has certain advantages. It can highlight situations that occur late in life, by increasing the duration of the test; it can make predictions over a wider range by controlling the levels that parameters of interest take on; and it can study specific interactions. However, results obtained from controlled laboratory environments are sometimes criticized for being unrealistic or inappropriate. A model based on orbital data has the advantage that the batteries have been operated in a real environment.

One use of the model is to predict the performance of the new third-generation cell designs now with limited (up to five seasons) orbital experience. The new HS 376 design improvements include increased electrolyte quantity, lower operating current density, and lower operating temperatures. This work is still in progress.

The most prudent conclusion that can be drawn thus far from these results is that the HS 376 batteries can easily meet their design goal of 10 years at 50 percent DOD, since they are an improvement over those analyzed here.

For a prediction at the 65 percent DOD extreme of the data base, a different statistical approach should probably be used.

The data base includes data on two batteries on two different satellites, having two shorted cells each. All four shorts occurred late in life and caused complete loss of voltage in the four cells. The remaining cells are functioning as expected, in view of the additional loads being imposed on them. The fact that the data base included shorts which occurred late in life had a strong effect on the model, making the time^3 term more significant. (Note, however, that in our earlier paper (ref. 9), the time^3 term was also present, and there were no shorted cells in the data base at that time.)

Because the effect of shorts is included in the voltage model, it is included in the reliability plots as well. This has important implications for reliability analysis as practiced in reliability engineering. The cell short failure mode has been treated as having a constant failure rate. However, this treatment may now be inappropriate in view of the fact that the shorts occurred late in life. Future reliability analysis should address this matter.

The model is derived from aggregate data on a large number of batteries. In such cases, the resulting model often fails to accurately predict the performance of an individual member. However, as shown in figures 4 and 5, our model does accurately predict the voltage versus time of individual batteries. (Fluctuations in voltage, both for actual and predicted values, are explained by adjustments to depth of discharge.) These plots of actual versus predicted voltage are typical of the fits which were obtained. Figure 5 shows the model's fitting of the performance of a battery experiencing two shorts at the sixteenth eclipse season. Since some batteries at this time had shorts and others did not, the model tends to overpredict voltage in the presence of shorts. When shorts occur, depth of discharge is reduced at the ground station to increase remaining life. This fact explains the increase in predicted voltage at the sixteenth eclipse season.

CONCLUSIONS

The model described in this paper has many important features. First, it fits the orbital data and provides accurate predictions. (Although the fit to the data is not as good as one typically sees with laboratory data, we feel the model is more realistic, being based on orbital data.) It is a useful tool in designing and operating batteries for longer lives. The effect of shorts has been included, making this model more complete than its predecessors. Finally, the model predicts that a typical second-generation battery will last well beyond ten years. We believe that a typical third-generation battery could last even longer. This is true even at depth of discharge levels higher than those presently used.

Hughes intends to update this analysis periodically.

REFERENCES

1. Dunlop, J.D. and Earl, M.: Evaluation of Intelsat IV Nickel Cadmium Cells. Proceedings of the 25th Annual Power Sources Symposium, May 1972, pp. 40-42.

2. Wick, H.M.: Design and Performance of the Telesat Power Subsystem. Proceedings of the 9th IECEC, August 1974, p. 53.

3. Lim, H.S. et al: Studies on the Stability of Nylon Separator Material. Proceedings of the 27th Annual Power Source Symposium, May 1975, p. 83.

4. Lim, H.S. and Verzwyvelt, S.A.: Expansion Mechanism of the Nickel Electrode in an Alkaline Storage Cell I Electrode Bending Experiments. Proceedings of the 15th IECEC, August 1980, p. 1619.

5. Kettler, Jack, R.: Leasat Power System. Proceedings of the 15th IECEC, August 1980, p. 1047.

6. Miller, Michael W.: Electrical Power System for the SBS Communications Satellite. Proceedings of the 15th IECEC, August 1980, p. 1064.

7. Draper, N.R. and Smith, H.: Applied Regression Analysis (second edition), John Wiley and Sons, 1981, p. 296.

8. Levy, E.: Life Test Data and Flight Predictions for Nickel Hydrogen ($Ni-H_2$) Batteries. Proceedings of the 17th IECEC, August 1982, p. 774.

9. Engleman, J.H. et al: Battery Life Model for Synchronous Orbit. Proceedings of the 16th IECEC, August 1981, pp. 205-208.

Table I
Summary of the Data Base

Variable	Unit	Minimum value	Maximum value	Mean value	Standard deviation value
Average cell voltage	volts	1.08	1.23	1.18	0.018
Time	eclipse seasons	1	16	6.6	3.8
Depth of discharge	%	24	62	43	8.0
Electrolyte	cc/A-hr	2.9	4.2	3.2	0.31
Eclipse temperature	°F	50	66	55	3.1
Trickle-charge rate	A/A-hr	C/62	C/36	C/50	-

ORIGINAL PAGE IS
OF POOR QUALITY

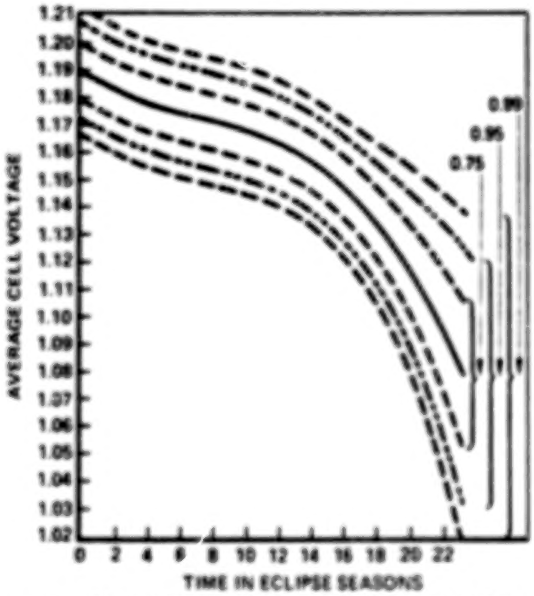

NOTE: ALL OTHER VARIABLES SET TO THEIR MEANS

Figure 1. Voltage versus time.

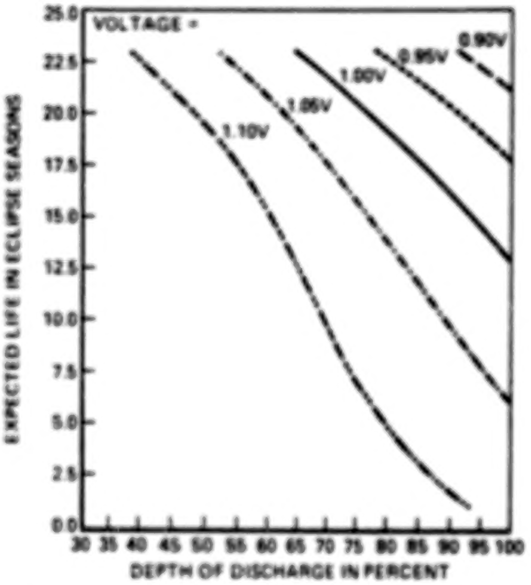

NOTE: ALL OTHER VARIABLES SET TO THEIR MEANS

Figure 2. Expected life versus depth of discharge.

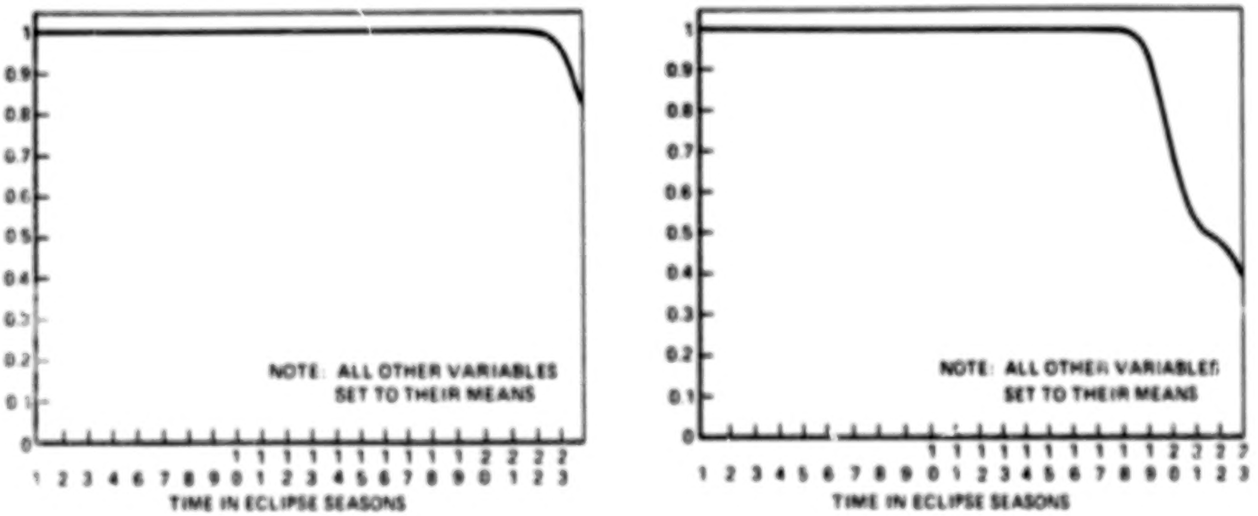

a) VOLTAGE = 1.05 VOLTS

b) VOLTAGE = 1.10 VOLTS

Figure 3. Reliability versus time.

ORIGINAL PAGE IS
OF POOR QUALITY

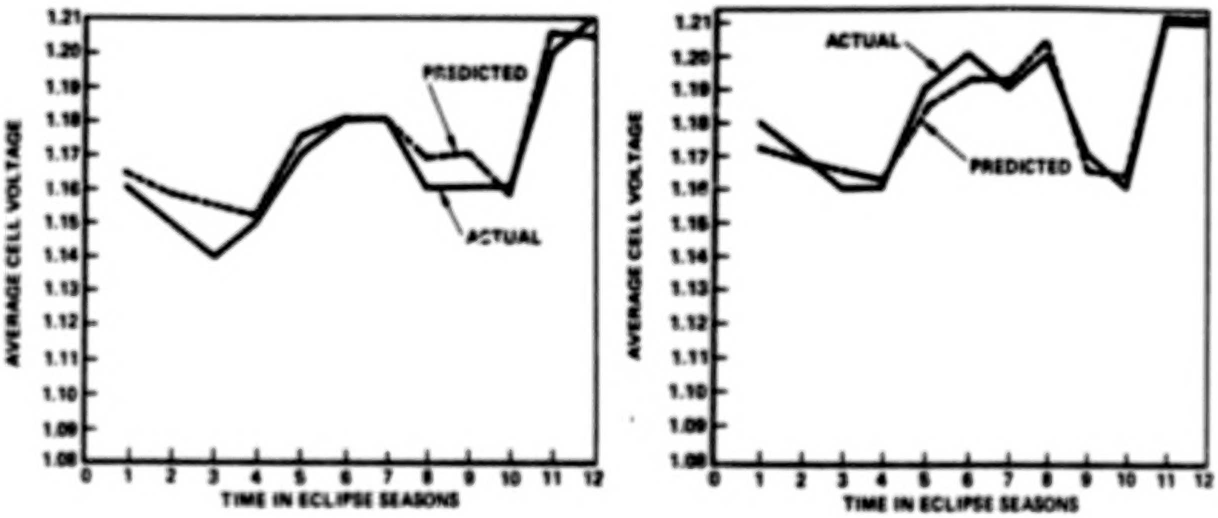

a) BATTERY A

b) BATTERY B

Figure 4. Voltage versus time for typical batteries.

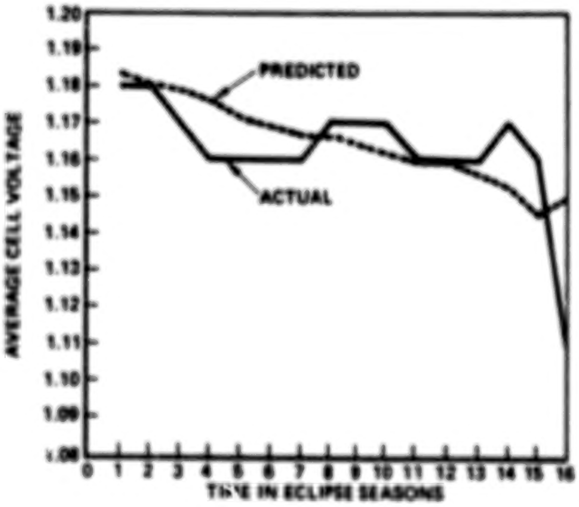

Figure 5. Voltage versus time for a battery containing two shorted cells.

Q. Unidentified: Did your survey include the launch handling of batteries at all or is this after launch life?

A. Broderick, GTE Satellite Corporation: No this was just data. I would assume that many of these test points that in orbit performance would include integration and test.

Q. Unidentified: Some of them like you mentioned TRW do not use flight batteries for integration testing?

A. Broderick, GTE Satellite Corporation: Okay, it never has been. Ford I think has presented information before that he thinks that in orbit or integration in test will age at about twice the rate of in orbit performance. So if you assume 3 months of integration and test double that then you might lose 6 months of performance on the ground.

Q. Unidentified: Did you include anything like the differences of the depth of discharge during reconditioning in orbit?

A. Broderick, GTE Satellite Corporation: What I've assumed is that all of these will be deep discharge reconditioning and that is one of the reasons why we've been able to make such improvements on life.

Q. Rogers, Hughes Aircraft: You emphasized that the newer MOS devices used have lower internal resistance have lower voltage drive than the older ones.

A. Sullivan, APL: Yes, that's right.

A. Rogers, Hughes Aircraft: That may be the particular devices but that's contrary to normal devices.

A. Sullivan, APL: Contrary to normal devices?

A. Rogers, Hughes Aircraft: In other words, for the same area or same weight device chip you'll get considerably lower resistance in a newer device and that is not what you want.

A. Sullivan, APL: Well all I was referring to is the older transistor which they had like 6/10 of a volt drop silicon devices as compared to the newer devices that we look at. I was looking at like 2/10th's of an ohm resistance in their on-stage.

N84
33687

UNCLAS

N84 33687 D19

Ni-Cd BATTERY LIFE EXPECTANCY IN GEOSYNCHRONOUS ORBIT

Richard J. Broderick
GTE Satellite Corporation

ABSTRACT

Nickel Cadmium battery life expectancy data is required as one key element of a power system design. However, at present there are no widely accepted analytical models for predicting NiCd life expectancy for a geosynchronous orbit. This paper is an attempt to review the literature, life test data, and in orbit performance data to develop an up to date estimate of life expectancy for NiCd batteries in a geosynchronous orbit.

INTRODUCTION

GTE Satellite Corporation (GSAT) is a subsidiary of General Telephone and Electronics Corporation, one of the nation's leading communication and electronics enterprises. In December 1980, GSAT was granted authority by the Federal Communications Commission to construct and operate an advanced domestic communications satellite system providing customized digital transmission networks to a variety of users. GSAT's new satellite system is scheduled for operation in mid 1984. The space segment consists of two satellites operating in the 12/14 GHz frequency band, with two satellites to be held in reserve. The first satellite, GSTAR 1, is scheduled for launch in the second quarter of 1984.

The GSTAR baseline design uses three 30 Ampere-hour Nickel Hydrogen batteries. However, a parallel alternative is being developed in which three 27 Ampere-hour Nickel Cadmium batteries will be used if flight qualified NiH_2 batteries are not available. A study was initiated to examine the feasibility of this alternative. Initially a literature search was conducted with respect to the life expectancy of NiCd cells in a geosynchronous orbit. Life test data, prepared by the Naval Weapons Support Center (NWSC) at Crane, IN, manufacturing data and in orbit flight experience was reviewed and compiled. A curve was deduced, from the compilation of the various sources, for a prudent design criterium for batteries built in 1983 with respect to life versus depth of discharge (DOD). The data was not scrutinized to remove "bad apples" but was plotted as objectively as possible. The study assumes that deep discharge reconditioning (DDR) circuitry is available on the Spacecraft and that average battery temperatures over the year will be less than 15°C. No attempt was made to study only certain manufacturers or certain specific cell designs. The paper will be organized into a discussion of the literature search, life test data, in orbit performance data, life expectancy, and conclusions.

C-4

PRECEDING PAGE BLANK NOT FILMED

LITERATURE SEARCH

Figure 1 presents life expectancy for a NiCd battery operating at less than a 15°C average temperature in geosynchronous orbit. The curve is actually presented as allowable depth of discharge versus expected life time in years. The first user, GSFC, adopted this convention so I will continue using this format, whereas my personal application will be given a DOD as to what life time I can expect. This figure originally appeared in Reference 1, but recently appeared in Reference 2. The figure was originally plotted in terms of actual DOD. I have scaled it up to rated DOD assuming actual capacity to be 110% of rated. Since this curve appeared in 1976 I will use it as my 1976 baseline performance for NiCd life expectancy in a geosynchronous orbit. 60% DOD for this case would indicate a 3.4 year life.

Figure 2 presents another estimate of where life expectancy was and also where it was capable of going (Ref. 3). Sparks emphasized the importance of temperature control and DDR in extending life performance. This absicissa and ordinate will be used repeatedly for baseline comparison. As an example we will take 60% DOD and follow it through the paper. Sparks indicates that in 1973 one could expect a 5 year life and a capability of 15 years life at 60% DOD.

LIFE TEST DATA

Figure 3 presents real time life test data from the Crane Life Test program (Ref. 4). This figure only considers test packs with operating temperatures below 15°C. Three distinctions are made for the plotted data: failed cells, discontinued packs and ongoing tests. If we draw a curve between the earliest cell failures, we get a curve which correlates well with the earlier cell performance curves. A second curve drawn through the later cell failures would be indicative of what good cells can do. As you can see there are packs which have gone beyond this point before being discontinued, or are still continuing to date. The packs that were discontinued had cell failure(s) earlier in the test but continued cycling the remaining cells. Table 1 summarizes this data and shows what packs are associated with the points plotted. I think the dotted line would be a compromise curve, if one could be drawn, for this data. 60% DOD would indicate a 7.2 year life.

Figure 4 also shows Crane real time life test data for 20-25°C. The dotted line represents a compromise curve for this scattering of data. This line is not much different than the less than 15°C curve. However, it does go in the logical direction of increased temperature and decreased life expectancy. Table 2 summarizes this data. 60% DOD would indicate a 7 year life.

Figure 5 is a plot of accelerated life test data which was available, and this data is summarized in Table 3. The FLTSATCOM accelerated life test program claims 44 simulated eclipse seasons of life (Ref. 5). This data point could be indicative of great things to come. However, at this time I don't think one can skew a curve out to 22 years at 75% DOD. My estimate of a reasonable representation of the data is shown. 60% DOD would indicate an 8.4 year life for this curve.

IN ORBIT PERFORMANCE

Figure 6 indicates in orbit performance to date for available S/C. Some of the points shown are design requirements as opposed to actual flight performance. The curve shown tends to show the leading performances to date. Since most S/C operate over a range of DOD, the ranges are shown. 60% DOD would indicate a 7 year life for this curve. Table 4 summarizes this data.

Figure 7 is a composite of the curves previously shown. Real time life (RTL), accelerated life test (ACL), and in orbit performance (IOP), tend to be reasonably close. All three indicate the improvement from 1976. Since IOP and RTL do correlate well with ACL, I will use ACL as being representative of 1983 state of the art. This would again represent an 8.4 year life for 60% DOD.

Figure 8 now shows just the 1976 and 1983 curves for life expectancy. For 60% DOD we see an improvement from 5 years to 8.4 years, or 3.4 years. If we assume that improvement over the next 7 years was to continue at half this rate, we may expect a 1.7 year improvement. The curve marked desired indicates cells built today using 1983 NiCd technology could possibly last 10.2 years at 60% DOD.

CONCLUSION

A study was done to examine where NiCd technology was in terms of DOD versus life time for batteries in geosynchronous orbit. The assumption was made that cells would be operated in an average temperature environment below 15°C and subjected routinely to deep discharge reconditioning. Real time life test data, accelerated life test data, and in orbit performance data were examined as to expected life as a function of depth of discharge. The results would indicate that a prudent battery design for 1983 for a 60% DOD would be an 8.4 year life expectancy. A desired lifetime for this DOD could rationally be 10.2 years.

SYMBOLS

ACL	Accelerated life test
C	Continuing
D	Discontinued
DDR	Deep Discharge Reconditioning
DOD	Depth of Discharge
F	Failed Cell
GSAT	GTE Satellite
IOP	In Orbit Performance
NWSC	Naval Weapons Support Center
RTL	real time life test

ORIGINAL PAGE IS
OF POOR QUALITY

Table 1

Crane Life Test -- Real Time

PACK #	DOD(%)	TEMP(°C)	COMPLETED ECLIPSE SEASONS	STATUS
222A	60	10	9	F
			14	D
223A	60	0	14	D
232A	50	0	6	C
232B	50	15	3	C
203A	40	0	27	C
205A	60	0	27	C
206A	80	0	4	F
			11	F
			22	D
227D	52	15	4	C
207A	60	0	11	F
			19	F
			20	F
			23	D

Table 2

Crane Life Test -- Real Time

PACK #	DOD(%)	TEMP(^{o}C)	COMPLETED ECLIPSE SEASONS	STATUS
221A	60	20	11	F
			14	D
228A	80	20	11	C
226A	50	20	17	D
226B	50	20	13	D
229C	60	20	6	C
229A	60	20	9	C
229B	60	20	6	C
229D	60	20	5	F
			6	C
202A	40	25	16	F
			22	D
209A	60	20	22	F
			24	C
208A	80	20	17	F
			19	F
			23	D
210A	80	20	11	F
			18	F
			20	F
			23	D
227B	60	20	6	F
			10	D
227C	60	20	11	D
201A	40	25	16	F
			22	C

Table 3

Accelerated Life Test Data
Geosynchronous

DESCRIPTION	DOD(%)	TEMP(°C)	COMPLETED ECLIPSE SEASONS
NWSC 231A	80	10	9
NWSC 227E	52	15	12
NWSC 227F	52	15	12
FACC INTELSAT V (Ref. 6)	55	10	6
FACC INSAT (Ref. 6)	55	10	6
RCA (1)	66		11
RCA (2)	66		14
TRW FLTSATCOM (Ref. 5)	75	9	44

Table 4

In Orbit Performance Data

PROGRAM		DOD(%)	TEMP(°C)	PERFORMANCE (YEAR)		
				ACTUAL	EXPECTED	DESIRED
TDRSS		50	5		10	
GOES		50	15		7	
		60	15			7
IUE		57-60	15	6		
FLTSATCOM	1	65-70	<15	5		
	2	65-70	<15	4		
	3	65-68	<15	3		
	4	65-68	<15	2		
SATCOM	1	55-58		7-1/2		

ORIGINAL PAGE IS
OF POOR QUALITY

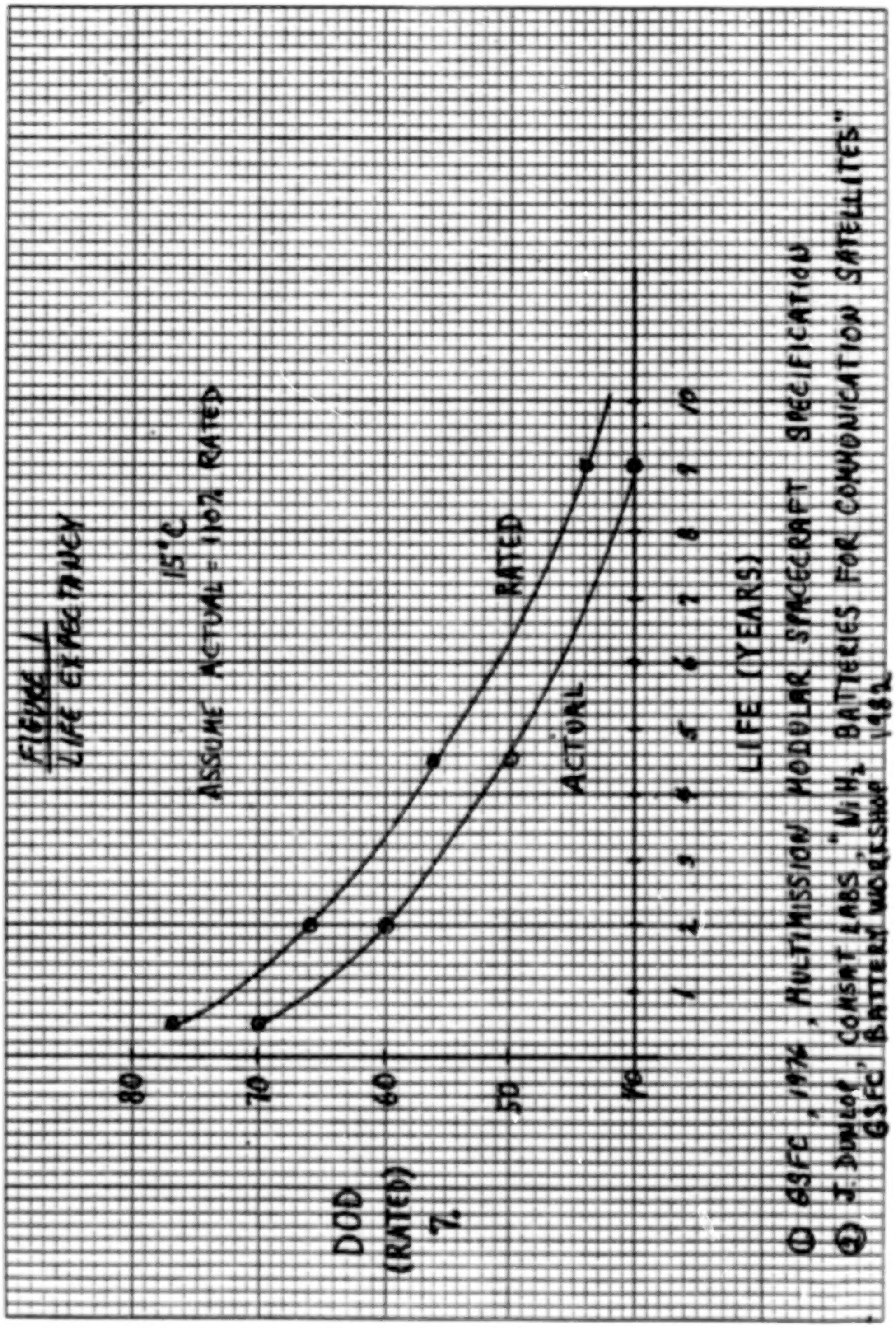

Figure 1. Life expectancy.

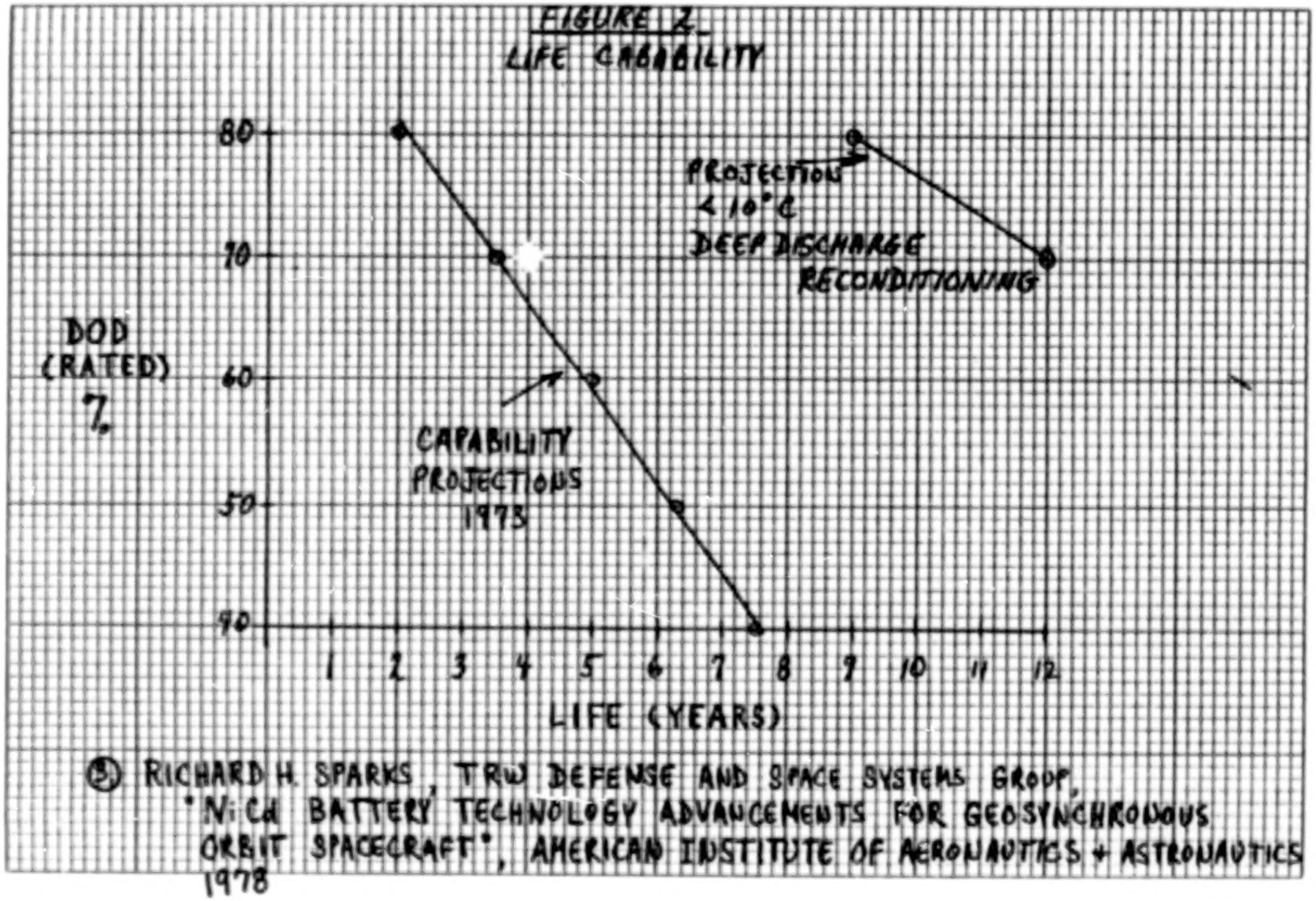

⑤ RICHARD H. SPARKS, TRW DEFENSE AND SPACE SYSTEMS GROUP,
"NiCd BATTERY TECHNOLOGY ADVANCEMENTS FOR GEOSYNCHRONOUS
ORBIT SPACECRAFT", AMERICAN INSTITUTE OF AERONAUTICS + ASTRONAUTICS
1978

Figure 2. Life capability.

ORIGINAL PAGE IS
OF POOR QUALITY

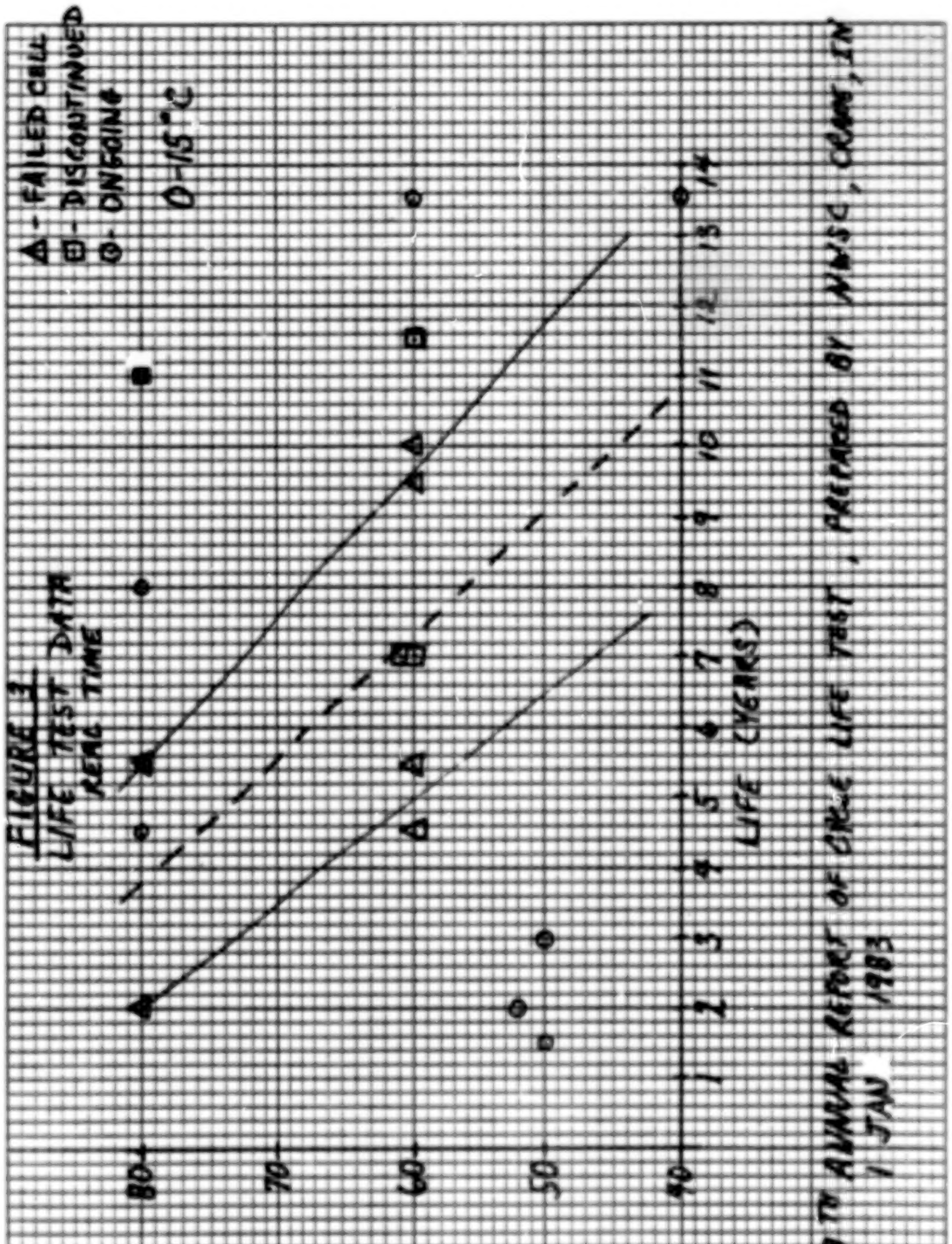

Figure 3. Life test data real time.

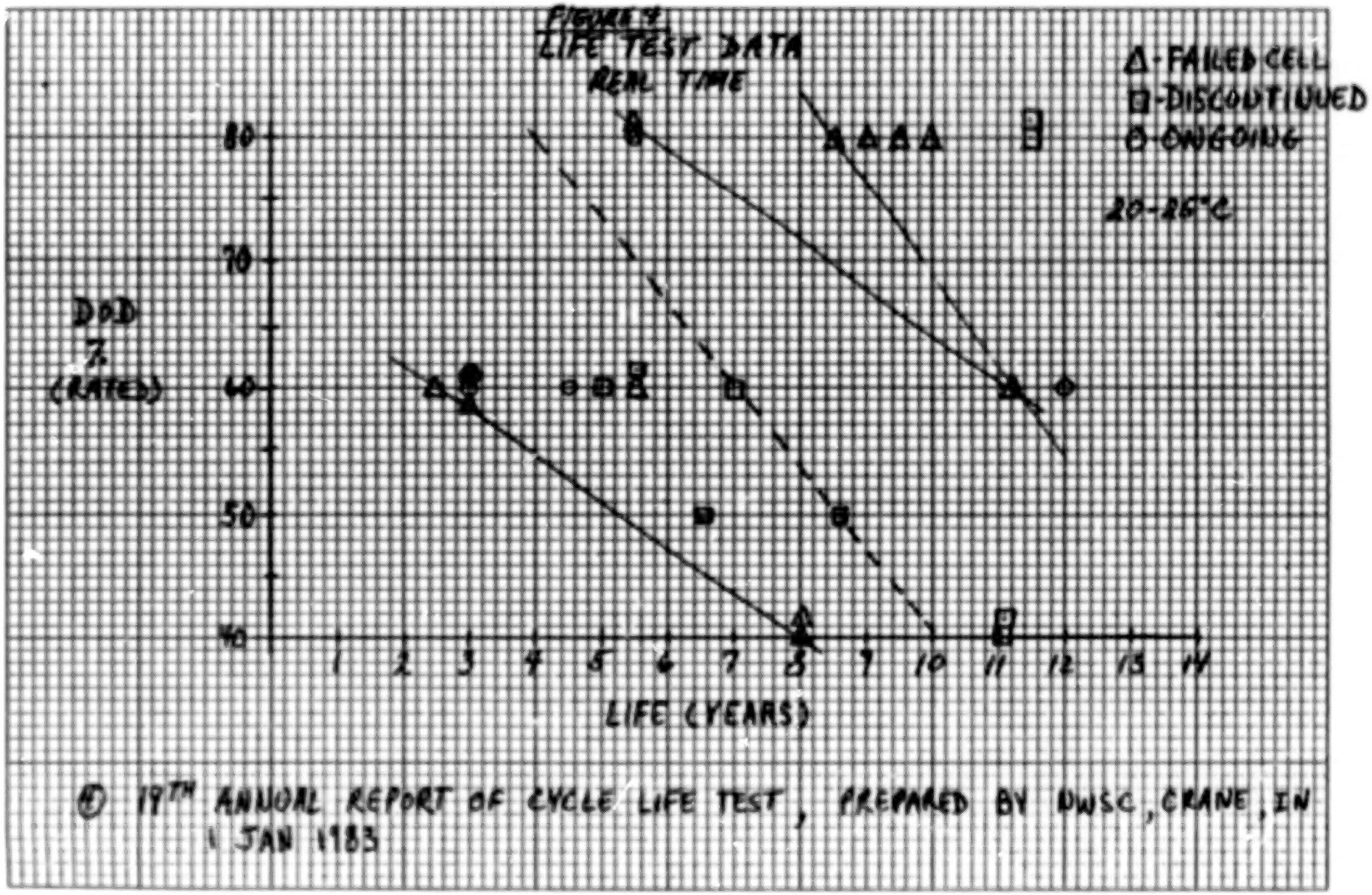

Figure 4. Life test data real time.

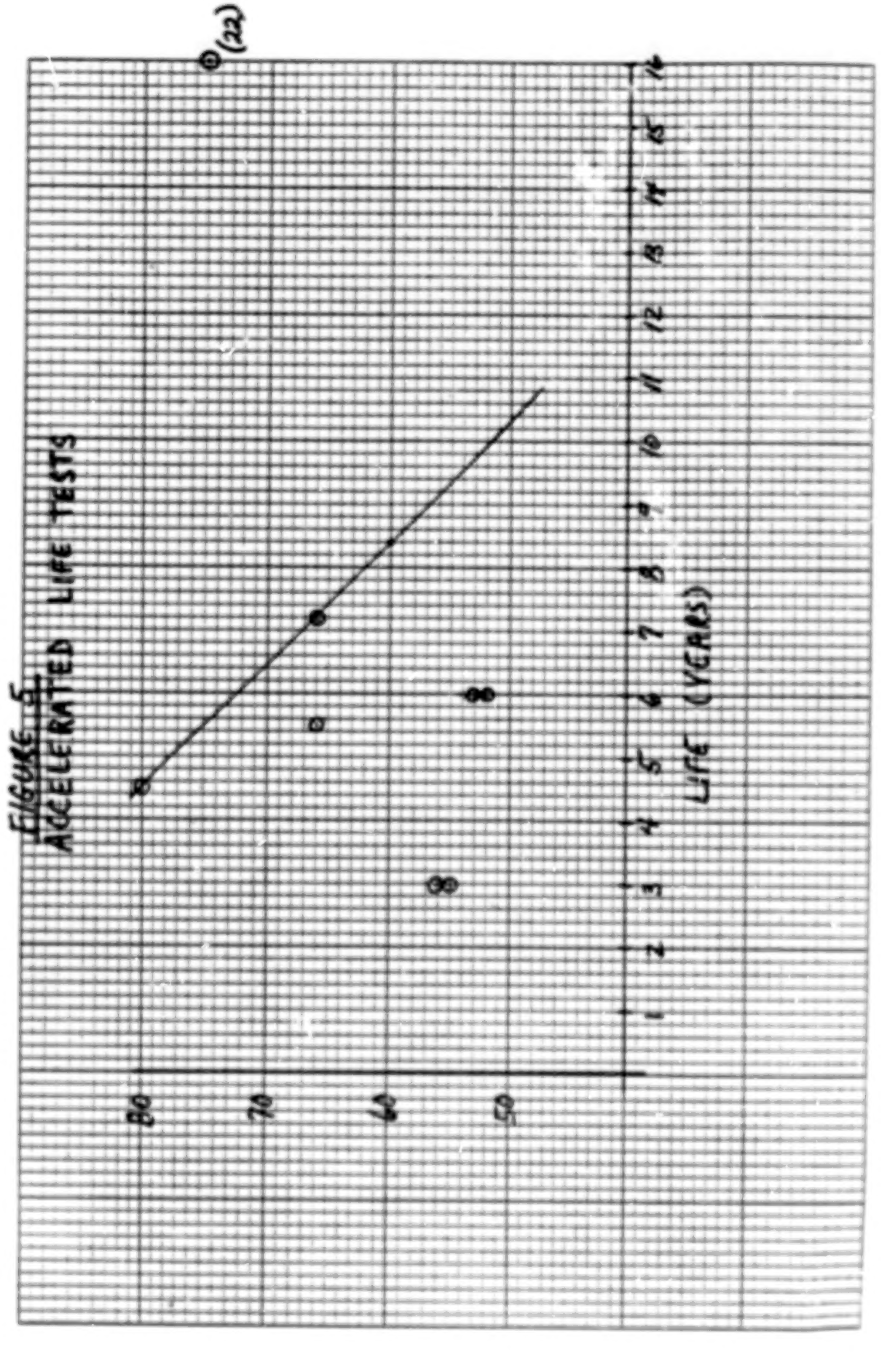

Figure 5. Accelerated life tests.

ORIGINAL PAGE IS
OF POOR QUALITY

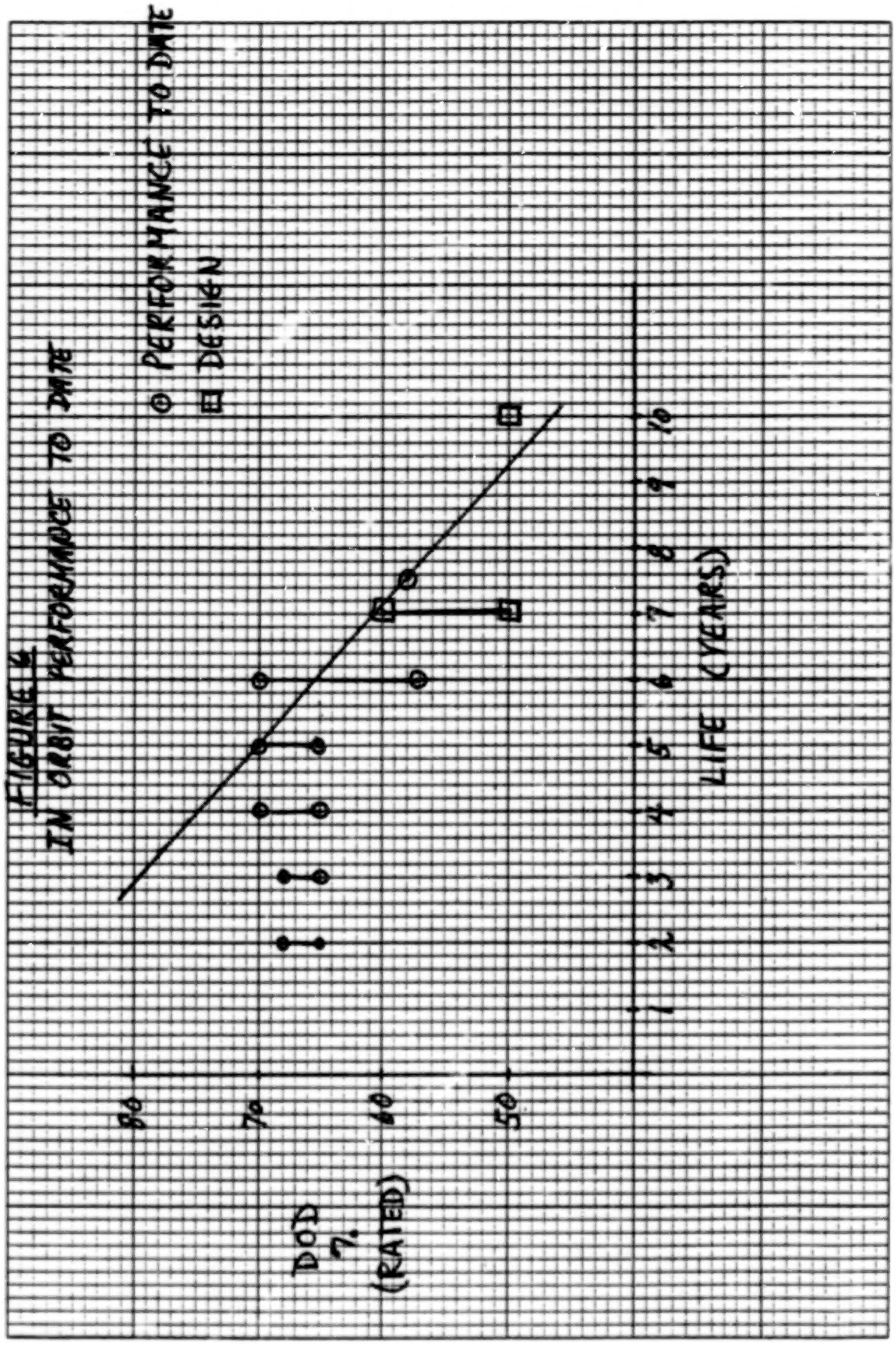

Figure 6. In orbit performance to date.

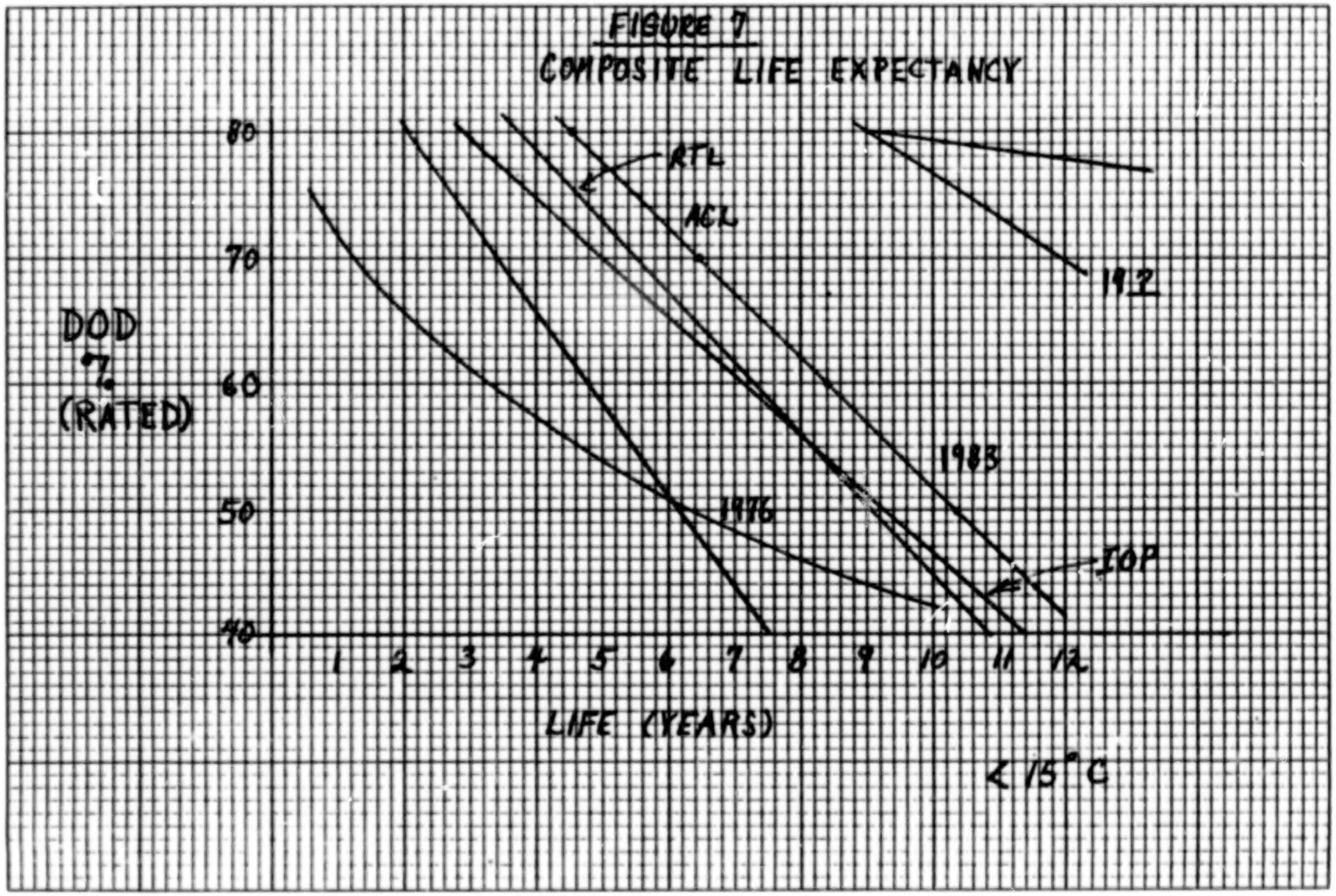

Figure 7. Composite life expectancy.

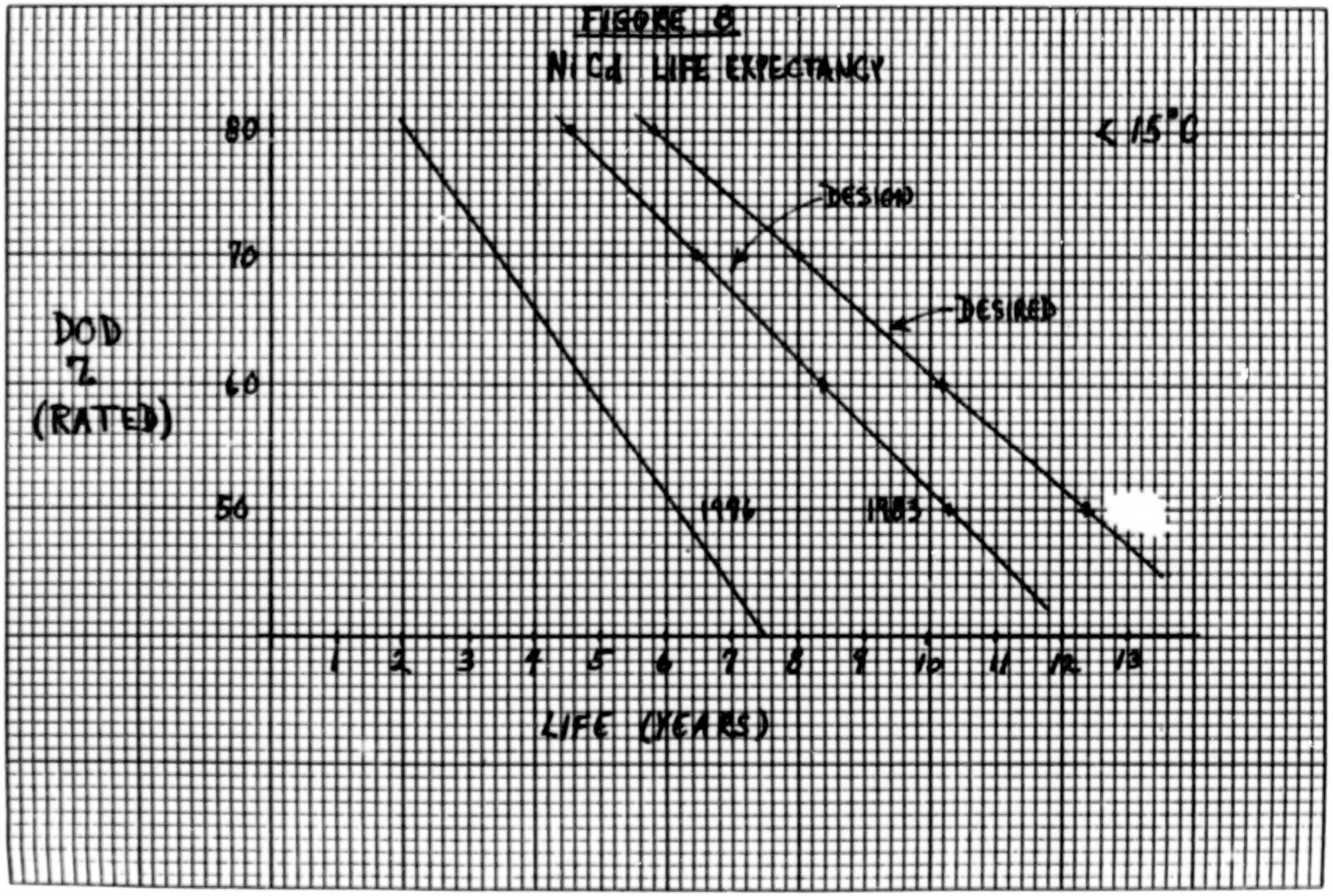

Figure 8. NiCd life expectancy.

N84
33688

UNCLAS

N84 33688 D20

NICKEL CADMIUM CHARGE CONTROL CONCEPTS

Ralph M. Sullivan

Johns Hopkins University Applied Physics Laboratory

ABSTRACT

APL has used several different types of charge control systems on their spacecraft. Some have used dissipative shunts to get rid of the excess solar array power; some have used non-dissipative shunts and some have used a hybrid system. Although they have all worked reasonably well, there are tradeoffs to be made between the impact on the thermal design caused by the dissipative devices and the generation of conducted emissions caused by the switching of non-dissipative devices.

INTRODUCTION

The primary function of a spacecraft battery charge control system is to provide sensible limits of battery discharge, recharge and overcharge to prevent undue stresses within the battery. In most cases this means that the charging current from the solar array must be reduced after the battery has reached 'full charge'. This leads to some interesting thermal problems, not just for the battery, but for the entire spacecraft.

SAS A/B

Figure 1 shows one of the early attempts to solve this problem at APL on the Small Astronomy Satellites (SAS) A and B. These satellites were small, using a single battery of eight 6 ampere hour cells to sustain a 30 watt load through a 36 minute eclipse which recurred every 96 minutes (a 300 nmi equatorial orbit). The Low Voltage Sensing Switch was set at 1.1 volts per battery cell (8.8 volts) to preclude excessive discharge which could result in the reversal of a low capacity cell.

For such a small battery the instantaneous variation in the array power was large (40 to 100 watts). This led to the need for correspondingly large shunts driven by a sophisticated Charge Regulator and Monitor (CRAM) system. CRAM monitored the bus voltage, the battery current and the battery temperature. It had a voltage limiter that limited the bus voltage in accordance with a voltage - temperature curve whether the battery was on the line or not. It also had an electronic coulometer that both monitored and controlled the

PRECEDING PAGE BLANK NOT FILMED

battery recharge in parallel with the voltage limiter. There were four commandable percent returns: 105%, 110%, 125%, and 'monitor only' or infinite return.

Figure 2 shows a typical charge, discharge profile. The electronic coulometer counted down to a value indicative of the ampere - minutes discharged. During recharge it counted back at a slightly different rate depending on the percent return that was selected. After about 90 to 95% of the charge was returned, the voltage limiter would start to reduce the battery charge rate in order to limit the bus voltage to the value required by the V-T curve. When the coulometer was satisfied (110% return for the case of figure 2), then the battery trickle charge rate was reduced to a preset trickle charge rate of C/20 (300 ma). This resulted in a corresponding drop in the bus voltage.

Aside from these gradual changes in the bus voltage, the bus was relatively quiet, with little or no noise or conducted emissions being generated by the charge control system. This was true even without the battery on the line (Solar Only Mode) and was primarily due to the use of linear shunts.

Returning to figure 1, we see two groups of linear shunts; one internal and four external. The reason for an internal linear shunt was to provide internal heat if requested by a properly located thermistor. This was done over the protests of the thermal designer since the heat was provided during a short period at the end of sunlight after the battery was charged. For this reason and because the shunt driver can be relatively heavy, this concept is not recommended and has not been used on subsequent APL spacecraft.

The external shunt was divided into four parallel units, one mounted on each of the four solar panels and was designed with a total capacity of 120 watts (30 watts each) so that the system could function even if one shunt were lost. Referring to figure 3, we can see that the shunt resistor(s) must be designed to accept all the available power of 30 watts each. This was accomplished by placing a distributed resistor under the solar cells on each of the four solar panels covering an area of 1.4 ft^2. The shunt drive transistors, however, could not be distributed. We see from figure 3 that they experienced a peak power dissipation of Pmax/4 when shunting about one-half their maximum current. This is about 7-1/2 watts, an acceptable power level, but not ideal for long life. Indeed on SAS-A, we did experience failures of the shunt drive transistors within a year. This was found to be due to a defect in the transistor which was corrected on SAS-B by replacing the transistor with one of a different manufacture.

SAS-C

Due to a near doubling of the power on SAS-C, the charge control system was expanded to include digital shunts (see figure 4). The solar array was divided into 24 equal, parallel segments; each with a shorting transistor controlled by CRAM. The linear shunt could then be sized to have slightly more capacity than one of the digital shunts. Although the shunt drive transistor still had to be designed for 9 watts power dissipation, it was placed in a benign environment inside the spacecraft since there was only one of them.

Any abrupt change in the power balance was accommodated by the linear shunt. If it became saturated (or empty), then the digital shunts were shorted (or opened) sequentially until the power imbalance could be accepted by the linear shunt. SAS-C was also designed to operate without a battery (Solar Only). Since the battery was one of the few non-redundant items on the spacecraft, it was thought that we should at least be able to operate during the sunlit portion of the orbit in the event that the battery failed. An Active Ripple Filter (not shown) was employed to reduce bus transients when switching digital shunts without a battery on the line.

AMPTE/CCE

The charge control concept of a recent APL satellite, AMPTE/CCE (The Active Magnetospheric Particle Tracer Explorers/Charge Composition Explorer), is shown in figure 5. This is the first charge control system at APL to use a microprocessor, an RCA 1802. The figure shows one side of a two battery system for simplicity. The actual array power, shunt power and load are double those shown. The coulometer has no control function in this system, but is simply a monitor. Also, there is no linear shunt, but only a shorting transistor for each solar array segment. The transistors used in this case are MOSFETS IRF130 with a very low saturation resistance, which further reduce the power dissipation.

This system is simpler and of lower power dissipation than its predecessors, but it does result in some additional bus noise as shown in figure 6. Also, this system does not have any 'Solar Only' capability.

OPEN PROGRAM

Figure 7 shows still another charge control concept. One that is being proposed for three satellites for the OPEN (Origin of Plasmas in the Earth's Neighborhood) program and which will make extensive use of a microprocessor. At first glance, the much higher power levels of 470 to 800 watts from the solar array would seem to dictate another digital (non-dissipative) system. However, there is a strong desire to have very low conducted emissions on these satellites, a requirement that has forced us to re-think the linear shunt.

Sixteen linear shunts with a capacity of 25 watts each will accept the entire 800 watts from the array. The distributed resistors can once again be placed on the solar panels under the solar cells. To reduce the power in the shunt driver package, each of the shunts will be driven sequentially in tandem. That is, only one drive transistor will be allowed to operate at the maximum power dissipation point. All other energized shunts will have been driven to saturation. With this type of design, aided by the use of MOSFETs, the maximum power in the driver package can be contained to approximately 10 watts. This design should provide us with a quiet bus and allow us to once again consider the use of the 'Solar Only' mode.

V-T CURVES

Although the electronic coulometer has proven to be a very good charge control method, the simple voltage limiter has also proven to be very effective. Using an empirically developed transfer function, the voltage versus temperature (V-T) curve, the voltage limiter causes actuation of the shunts to keep the battery voltage below the level defined by this curve. Figures 8 through 10 show the V-T curves that were used for the SAS and AMPTE satellites. The more recent satellites have used more than one V-T level which can be selected by ground command. The reason for this is to provide flexibility. If the power dissipation is too high for a given thermal condition, it is possible to switch to a lower curve which will result in a lower battery overcharge rate. Also, when the battery charge voltage increases with age, it is possible to switch to a higher V-T curve in order to charge the battery.

ACKNOWLEDGEMENTS

The Author wishes to acknowledge that a large number of people were involved in the design and test of these power systems. However, the contributions of the following three people were major:

Mr. Arthur F. Hogrefe--Design of the CRAM II and III charge control systems for the SAS satellites.
Mr. Stanley Mantel--Design of the battery charge regulator (BCR) for the AMPTE satellite.
Mr. Walter E. Allen --Power system design for the AMPTE satellite.

REFERENCE

Sullivan, Ralph M.: Design and Test of the SAS-A Power System. Applied Physics Laboratory TG 1106, 1970.

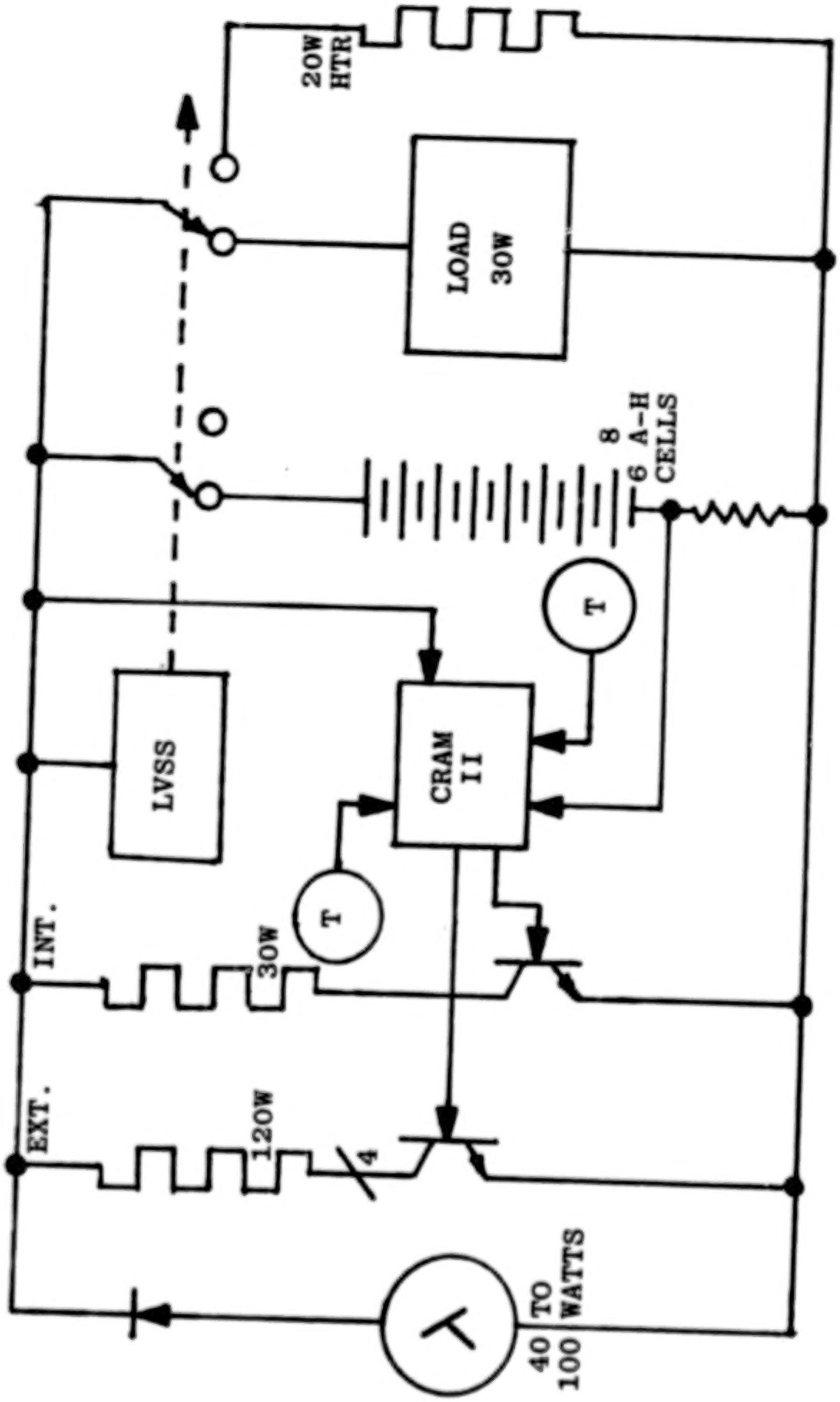
20W
HTR
LOAD
30W
8
6 A-H
CELLS
T
LVSS
CRAM
II
T
INT.
30W
EXT.
120W
4
40
100
TO
WATTS

Fig. 1 SAS A/B POWER SYSTEM (1969)

ORIGINAL PAGE IS
OF POOR QUALITY

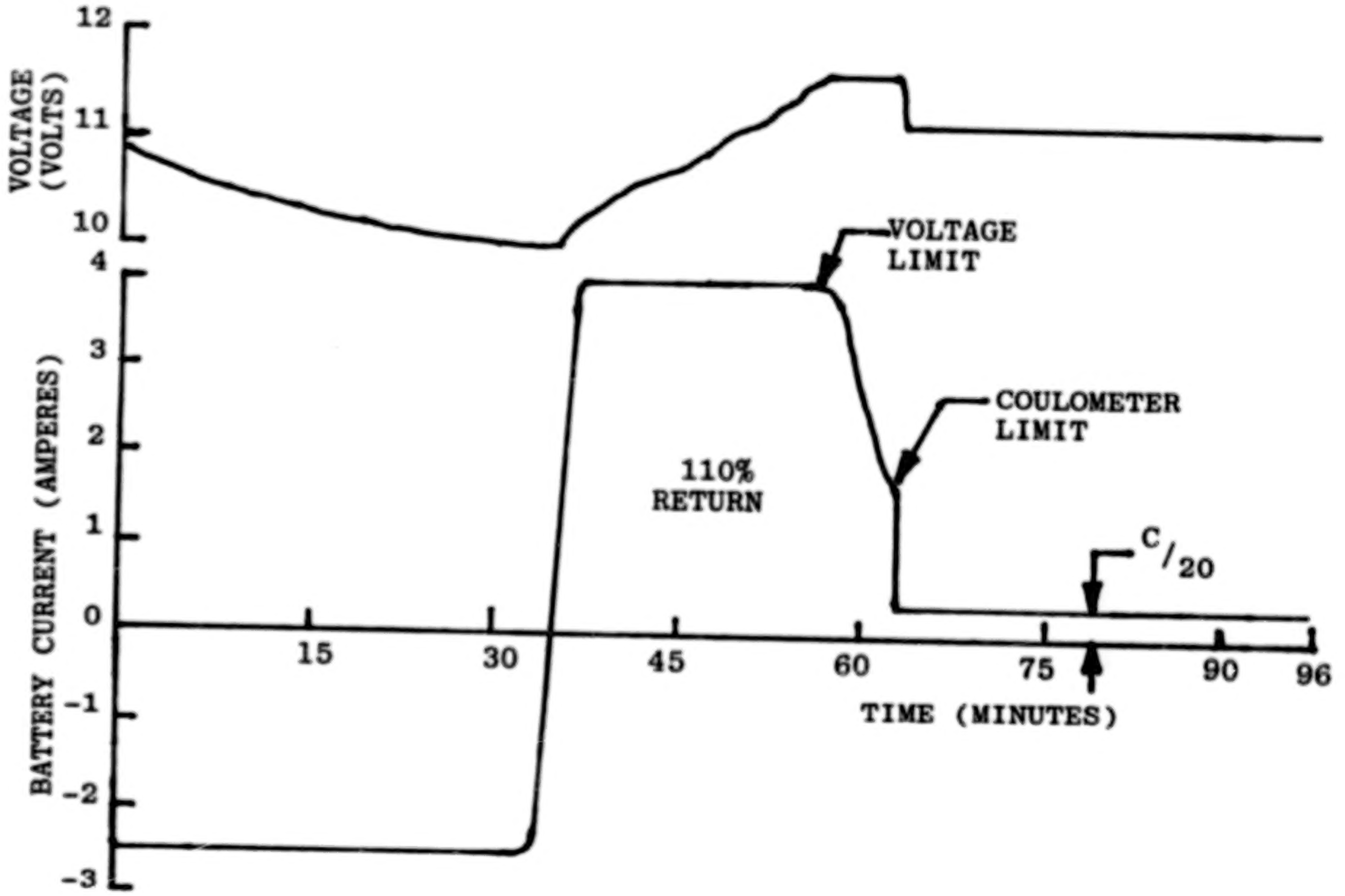

Fig. 2 SAS A/B CHARGE/DISCHARGE PROFILE

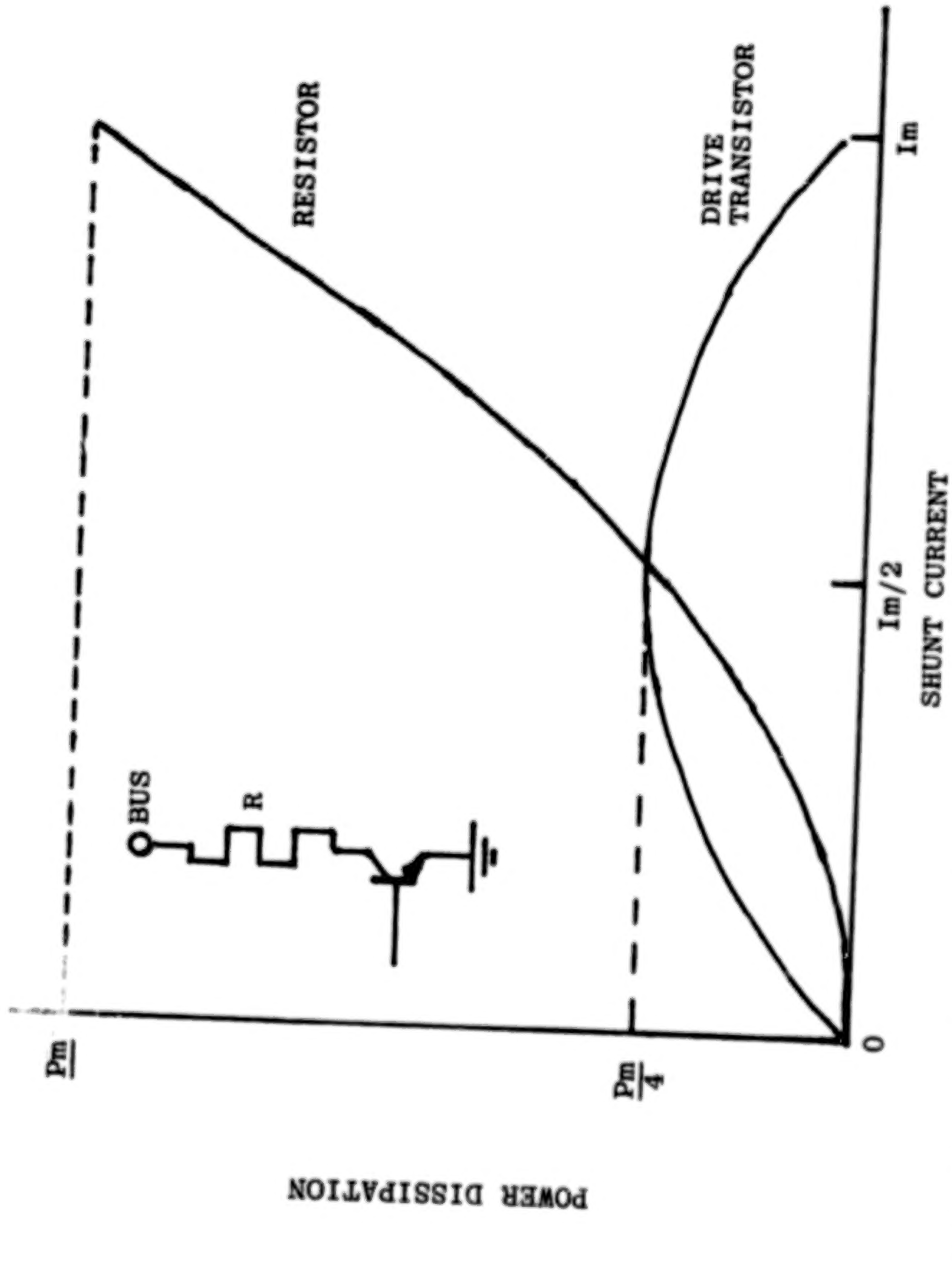

Fig. 3 POWER DISSIPATION IN EACH SHUNT ELEMENT

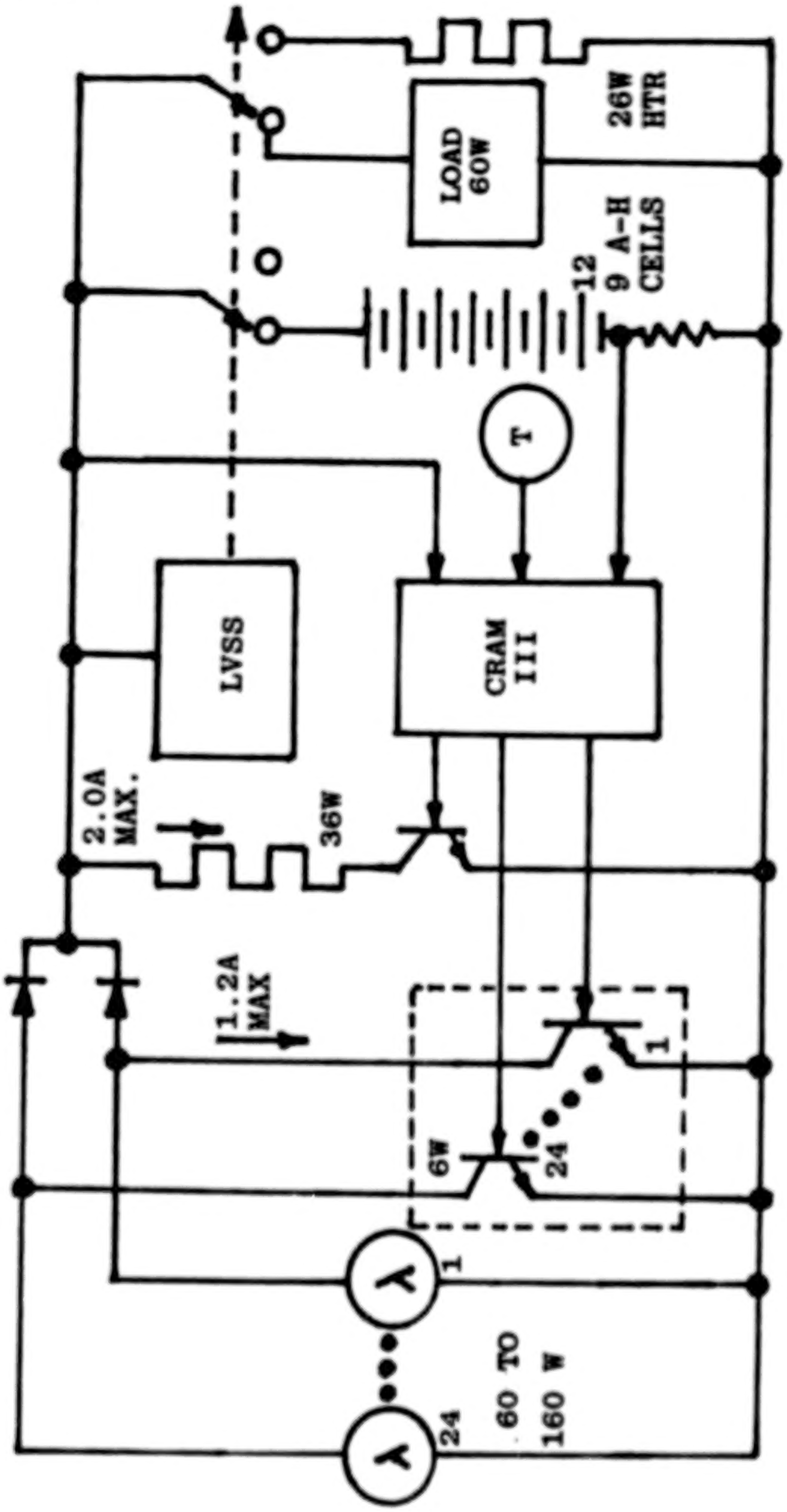
LOAD
60W
26W
HTR
12
9 A-H
CELLS
T
LVSS
CRAM
III
2.0A
MAX.
36W
1.2A
MAX
6W
24
1
Y
1
Y
24
60 TO
160 W

Fig. 4 SAS-C POWER SYSTEM (1975)

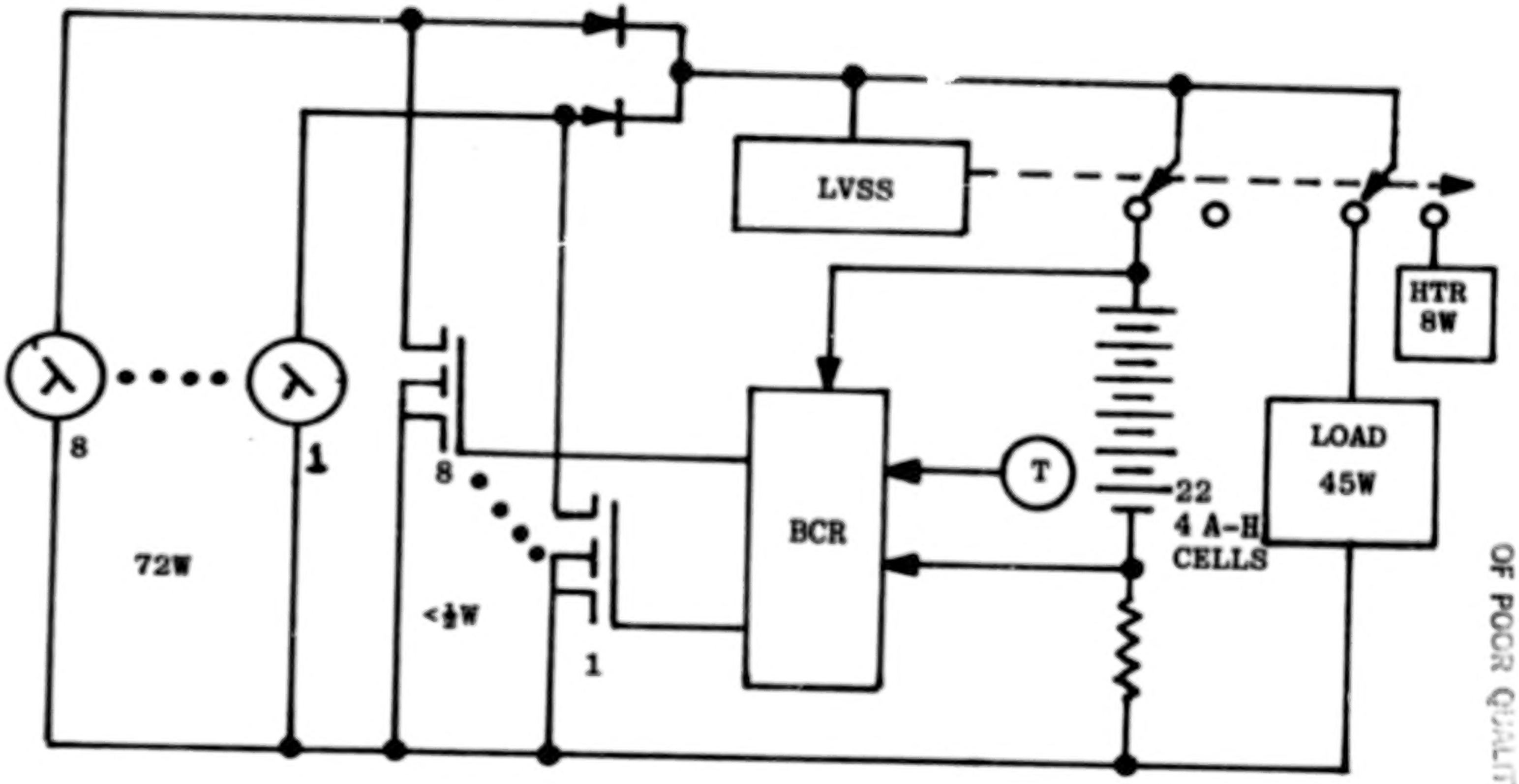
LVSS
HTR
8W
LOAD
45W
BCR
T
22
4 A-H
CELLS
8
1
8
1
72W
<½W

Fig. 5 CHARGE CONTROL CONCEPT AMPTE/CCE (1983)
(ONE SIDE OF TWO BATTERY SYSTEM)

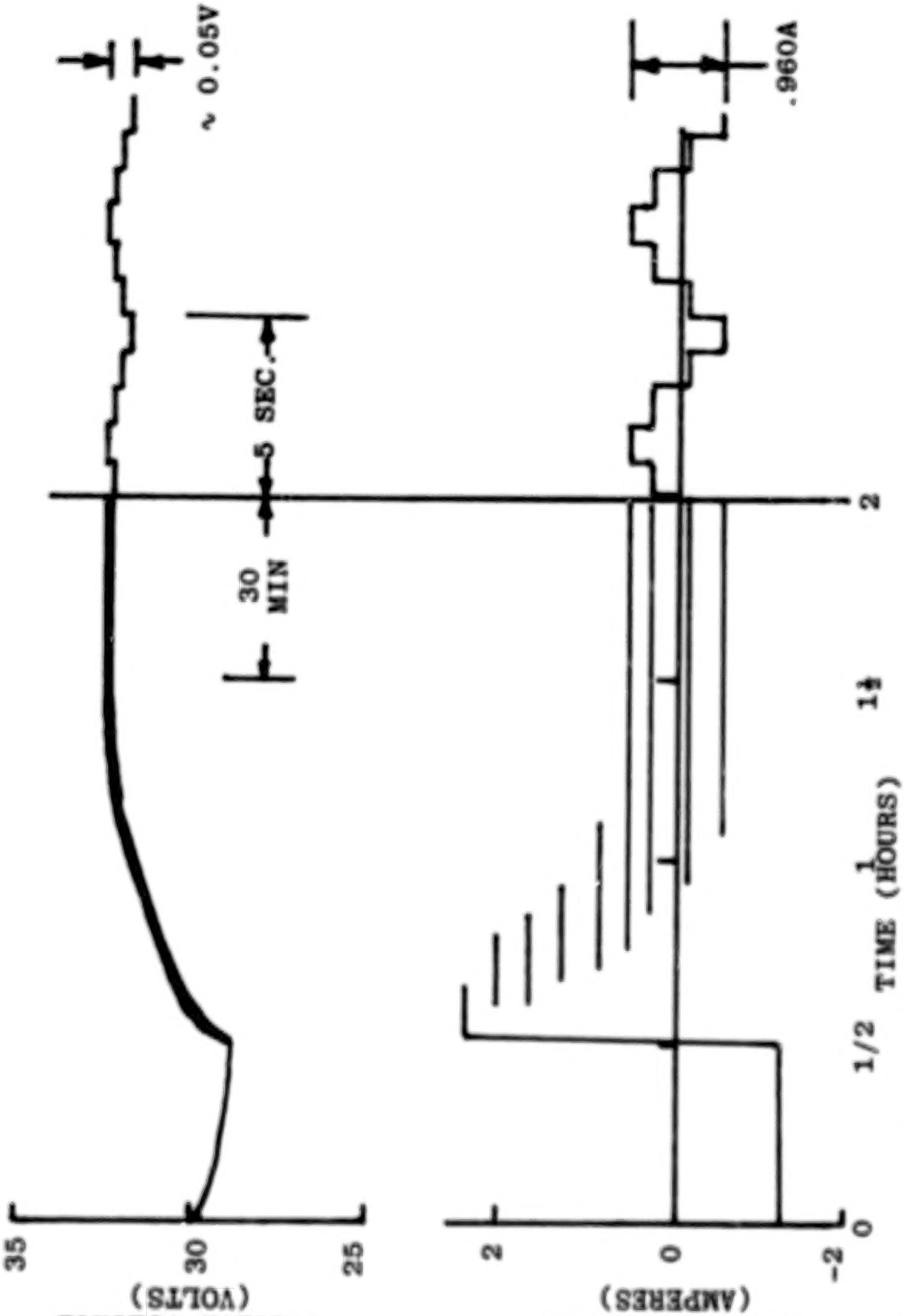

Fig. 6 AMPTE/CCE CHARGE/DISCHARGE PROFILE

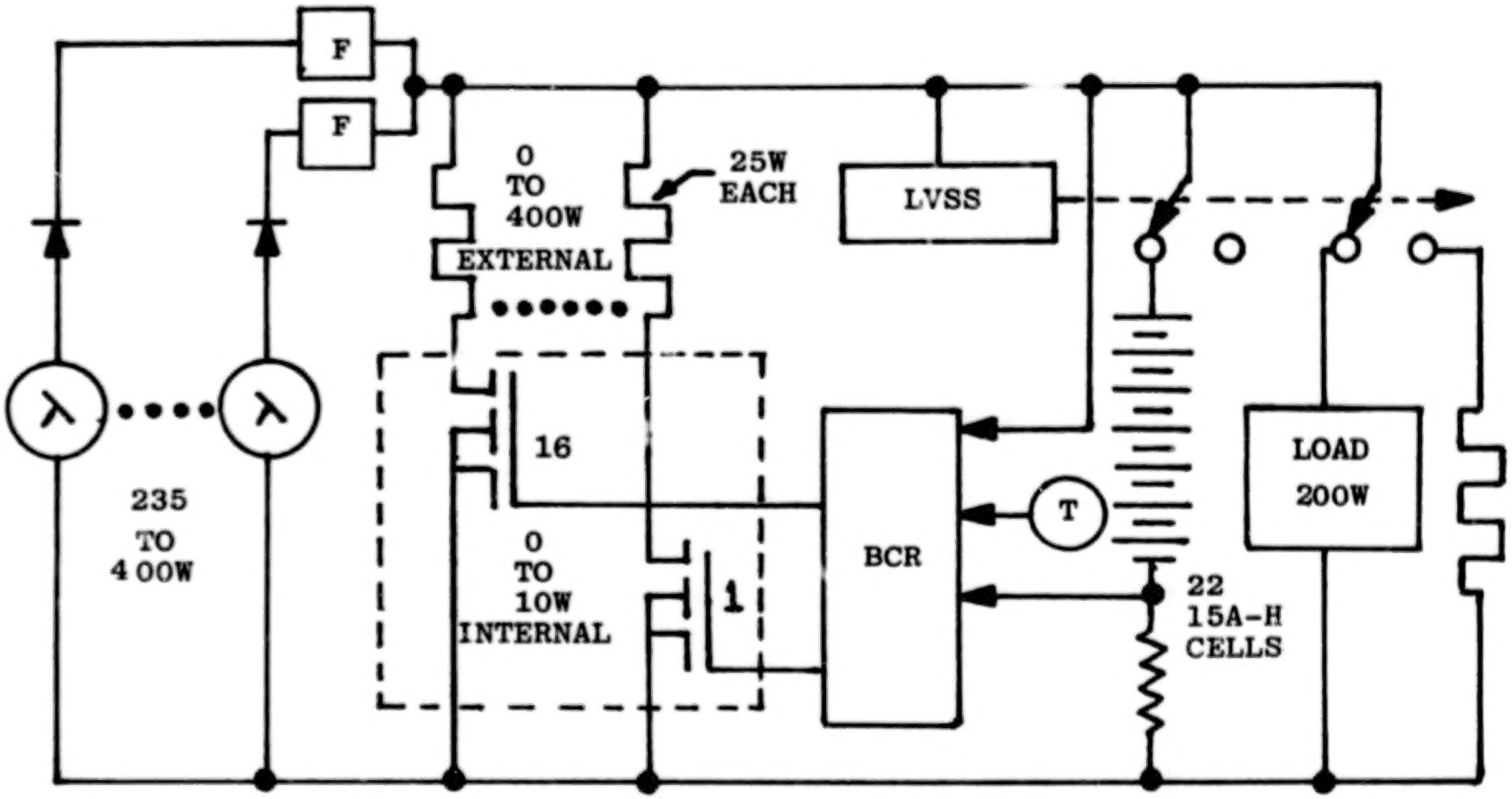
F
F
0
TO
400W
EXTERNAL
25W
EACH
LVSS
LOAD
200W
16
0
TO
10W
INTERNAL
1
BCR
T
22
15A-H
CELLS
235
TO
4 00W

Fig. 7 PROPOSED CHARGE CONTROL CONCEPT, OPEN PROGRAM (ONE SIDE OF TWO BATTERY SYSTEM)

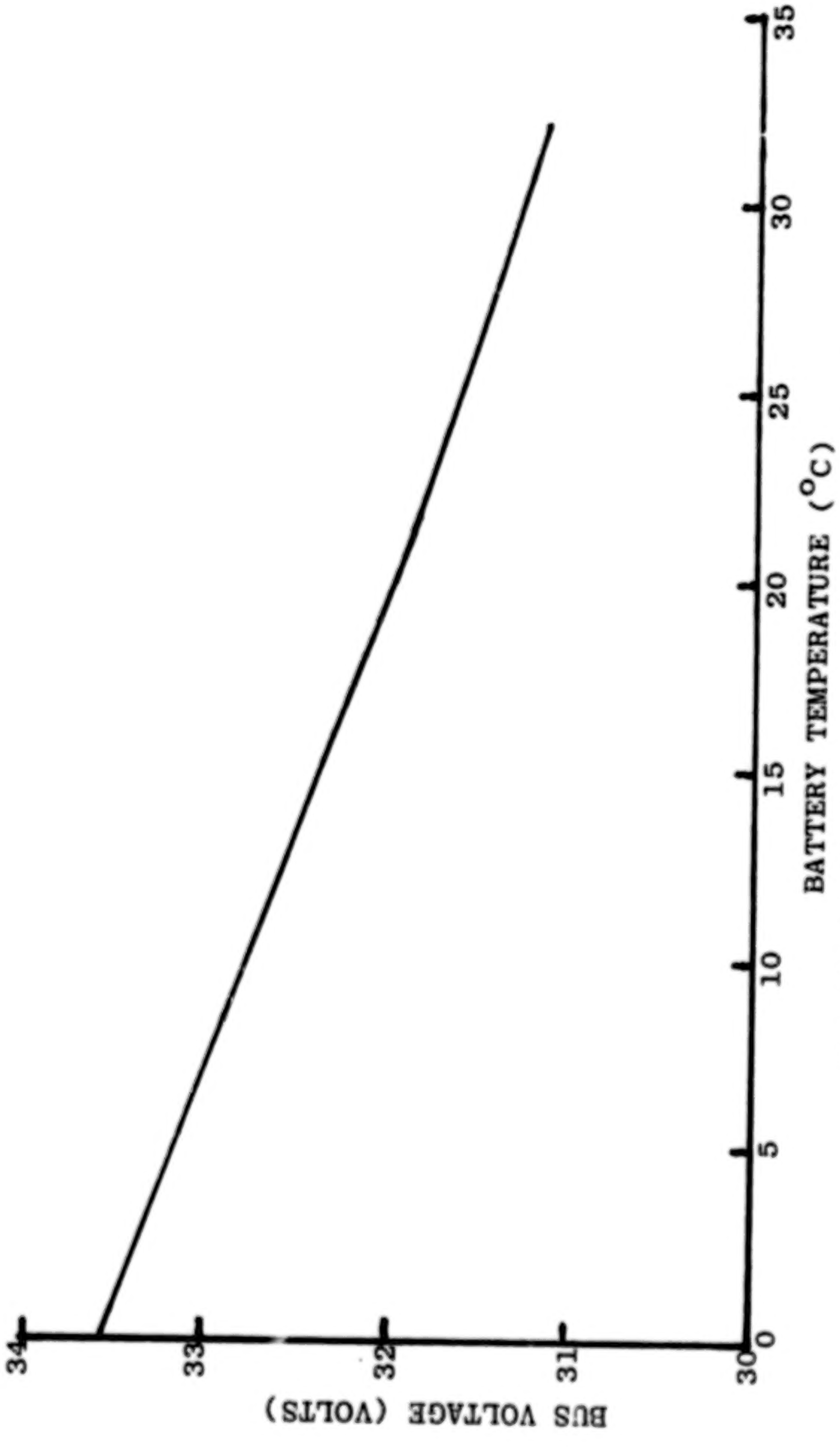

FIGURE 8 SAS-A/B BATTERY VOLTAGE LIMIT

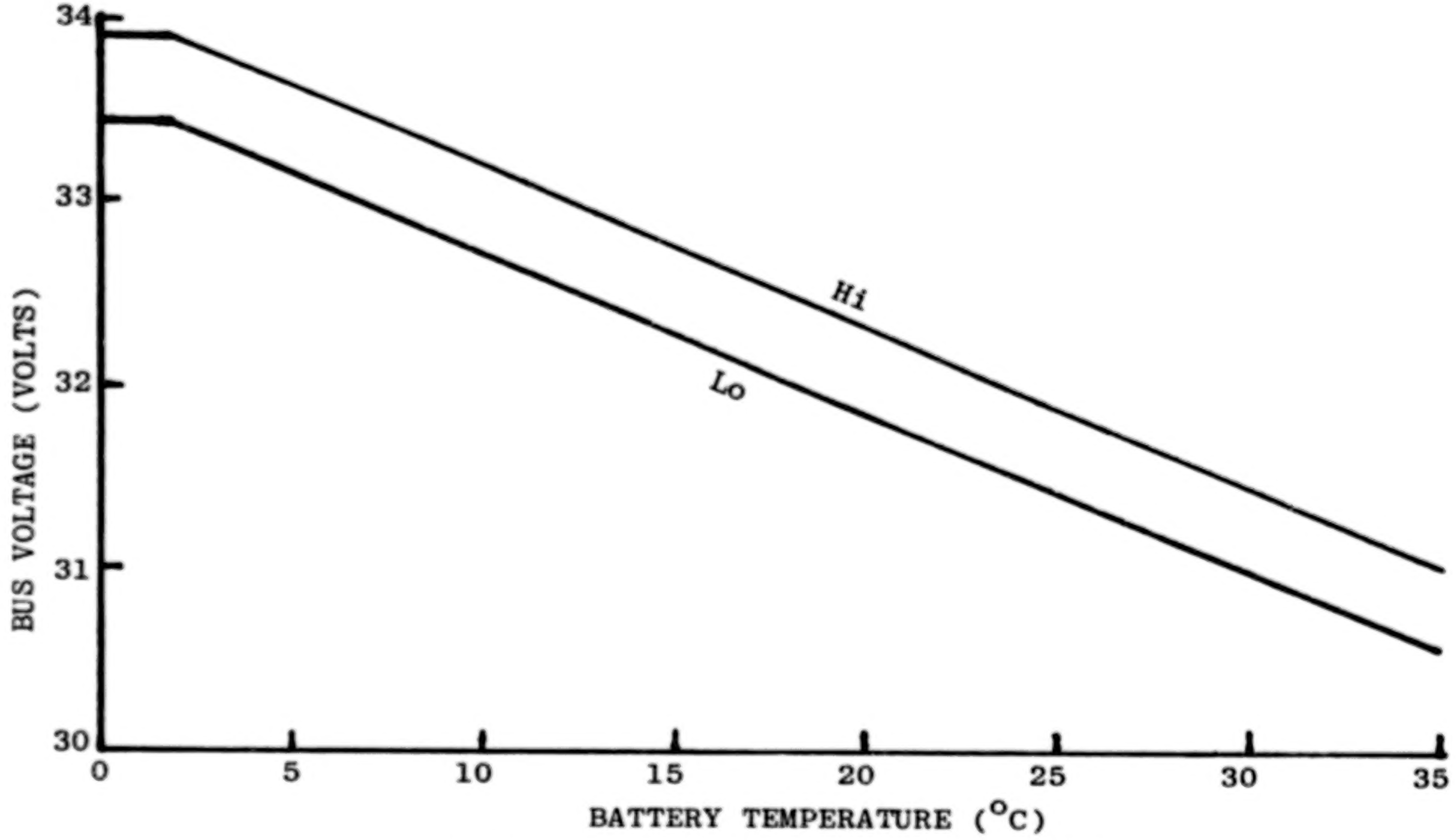

FIGURE 9 SAS-C BATTERY VOLTAGE LIMITS

ORIGINAL PAGE IS
OF POOR QUALITY

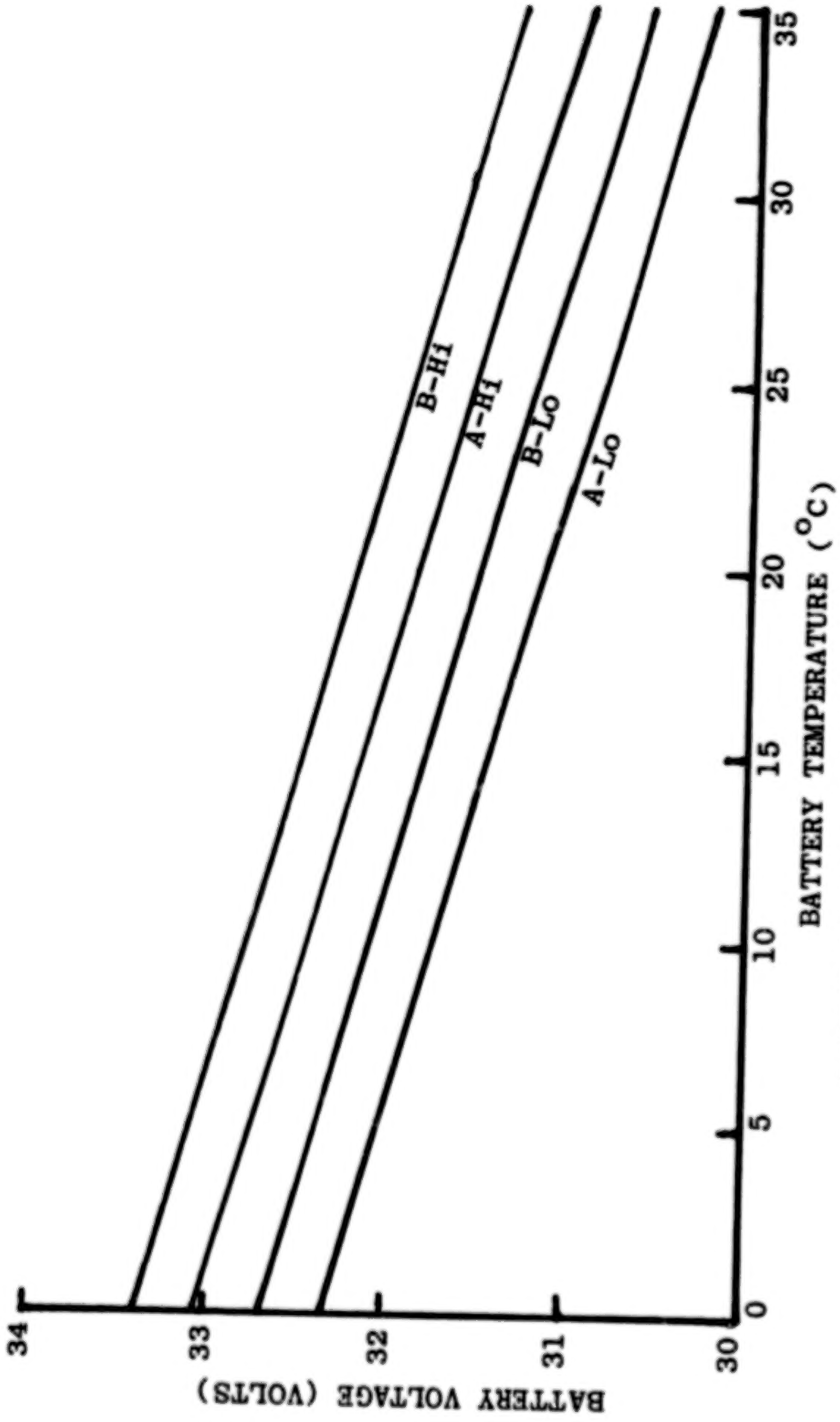

FIGURE 10 AMPTE/CCE BATTERY VOLTAGE LIMITS

A. Rogers, Hughes Aircraft: The newer silicon transistors would probably be a quarter of that in the same current device.

A. Sullivan, APL: Oh you are saying that there's another transistor I should be looking at. Okay thank you.

SESSION IV

TESTING AND FLIGHT EXPERIENCE

Chairman: J. Harkness
National Surface Weapons Center

PRECEDING PAGE BLANK NOT FILMED

N84
33689

UNCLAS

N84 33689 D21

DEEP RECONDITIONING TESTING FOR NEAR EARTH ORBITS

F.E. Betz and W.L. Barnes
Naval Research Laboratory
Washington, D.C. 20375

INTRODUCTION

During ground testing of nickel cadmium cells, deep reconditioning is accomplished by resistively loading the individual cells until the cell voltage approaches 0.0 volts. This type of reconditioning has been shown to improve discharge voltage performance and the capacity of the cells. RCA has implemented this technique in a synchronous satellite application (Ref. 1) with encouraging results.

Others have adopted a battery reconditioning technique in orbiting spacecraft using a single resistor across the entire battery. The level of discharge is limited to 1.1 or 1.0 volt per cell average to prevent cell reversal and hydrogen evolution within the cell. This method has not met with great success in improving voltage, capacity or life.

TRW has shown data for a deep reconditioning procedure in a synchronous orbit test regime (Ref. 2) that shows substantial improvement in life cycling capability and voltage performance. Their technique is to discharge the entire battery to nearly 0.0 volts at low rates and permit the cells to reverse. Their data shows reduced hydrogen evolution, hydrogen recombination, and no damage to the cells or battery. A possible advantage of the TRW method over the RCA method lies in its simplicity and reduced weight.

No data, however, exists to show the problems or benefit of deep reconditioning to near earth orbit missions with the high cycle life and shallower discharge depth requirements.

OBJECTIVE

A simple, battery level approach to deep reconditioning of nickel cadmium batteries in near earth orbit would be useful to spacecraft designers. Successful reconditioning would lead to increased reliability, higher utilization, and therefore reduced costs and subsystem mass. All worthy goals. To evaluate the concept of deep reconditioning for near earth orbit missions, a direct comparison with an alternative to reconditioning should be constructed.

APPROACH

A test plan was developed to perform deep reconditioning in direct comparison with an alternative trickle charge approach. Assuming a near earth orbit with a precession rate that produces periods of 100% sun; battery reconditioning opportunities appear. The option of trickle charge or reconditioning the batteries

PRECEDING PAGE BLANK NOT FILMED

occurs when the satellite solar array can support the loads in 100% sun with little or no battery support, (depending on battery redundancy).

Since battery life testing takes so long, in this test some acceleration was applied. For near earth, long term missions (i.e. 5 years) discharge utilization of less than 15% - 20% is appropriate. Acceleration to 40% discharge depth appeared reasonable and not excessively stressful. The orbital analysis for the sample showed 100% sun intervals varying between 50, 100, and 150 days. As discharge depth was accelerated by roughly a factor of two, reconditioning interval was divided by two. Table 1 shows the orbital 100% sun interval, accelerated test interval, and cycle number for the planned test reconditioning intervals. The next column shows the actual cycle numbers of reconditioning. Such deviations do not affect the value of the data. The durations of each reconditioning period are also shown.

Table 2 provides information on the test articles and other specifics of the selected cycling regime. The cells were delivered from December 1975 through February 1976, had been tested for acceptance and selection, and were designated as flight spare cells. They had been stored at room ambient until the start of this test. Reacceptance evaluation began in December, 1979, and life cycling in February 1980. In both voltage and capacity performance, the cells to be used for the reconditioning and trickle charge comparison were virtually identical. The actual charge - discharge cycling was performed with both groups of cells in the same circuit, experiencing the same current, and in the same temperature controlled bath. At the designated time for reconditioning, the circuit was broken, and one group of cells subjected to trickle charge while the other group was reconditioned. The reconditioned group was then charged at 0.60 ampere for 24 hours prior to return to cycling.

RESULTS AND DISCUSSION

Both the cycling and reconditioning appeared nominal through the sixth reconditioning after 3666 cycles. Both the first and sixth reconditioning (See Figures 1 and 2) show uniform capacity and voltage performance. Maximum reversal voltages approached -0.20 volts and maximum reversal currents fall from initial rates of C/200 (0.030 amps) to C/3000 when the reconditioning was terminated. End of discharge voltage, identical for both groups until the first reconditioning, followed expected patterns. (See Figures 3 and 4) The non-reconditioned, trickle charged cells end of discharge voltage decreased substantially with cycling. Reconditioning provided immediately improved voltage performance at end of discharge, although the effectiveness appears to be decreasing. Immediately following each reconditioning, end of charge voltages tended to increase, and continued to increase with each reconditioning. As cycling continued, the end of charge voltages would decrease and stabilize between reconditioning periods. Also observed in the end of charge voltages was an increasing divergance in only the reconditioned cells.

In the next reconditioning period, a greater divergence in capacity appeared; and the eighth period gave cause for concern. (See Figure 5) We cannot explain the strange behavior of cell number 9's voltage. Cycling and reconditioning continued, with the reconditioned group of cells showing divergence in both cycling voltage and reconditioning capacity and voltage.

Suddenly, within two cycles after 8321 cycles and the twelfth reconditioning and recharge, cell number eight failed by shorting and was removed. Within 50 cycles after the thirteenth reconditioning at 8921 cycles, cell number six end of discharge voltage was falling below 1.0 volts. Its voltage barely held on between 0.6 and 1.10 volts at end of discharge until the fourteenth reconditioning at cycle 9323. It showed only 3.6 ampere hours of capacity in that reconditioning. (See Figure 6). It operated normally following reconditioning and cycled normally for about 700 cycles before again falling below 1.0 volts at end of discharge. Figures 7 and 8 depict the results of a 4.0 ampere capacity discharge at cycle 10,142. Note the relative uniformity of capacity of the trickle charged cell group compared to the four remaining reconditioned cells. All cells were then reconditioned with 1Ω resistors prior to return to cycling. Cell six failed completely within 20 cycles. Cell number seven also had an end of discharge voltage below 1.0 volt, but continued to perform and degrade until complete failure 150 cycles later at 10,303. By cycle 11,100, cell number ten fell below 1.0 volt at end of discharge, but continued cycling; degrading slowly until ultimate failure on cycle 12,743. After 2000 additional cycles, the test was terminated without additional failures. The cells in the trickle charge group had been showing increasing end of charge voltages since shortly after cycle 9000, but no end of discharge voltage in the trickle group ever fell below 1.0 volt.

CONCLUSIONS

The results of these tests clearly demonstrate that the deep reconditioning procedure described and reported here for near earth orbit application is inferior to the alternative of trickle charging. Cell failures, seemingly related to the reconditioning itself, begin to occur at almost half the cycle life of the trickle charge group. Certainly end of discharge voltage, at least for most of the cycling duration, was higher for the reconditioned cells; but the trade off in lost reliability does not appear warranted.

Some might reason that the test is not applicable because of the age of the cells, separator material, recharge method, or other reason. We have no argument. Our hope was to demonstrate improved reliability due to the deep reconditioning procedure. Our evidence is opposite. We welcome further explanation and contrary data and encourage those considering deep reconditioning at the battery level for near earth orbit missions to develop their own data and share their results.

REFERENCES

1. Napoli, J.: "Reconditioning of RCA SATCOM Batteries in Orbit", The 1976 Goddard Space Flight Center Battery Workshop, X-711-77-28, Nov. 1976, pp. 185.

2. Scott, W.R.: "Life Tests and Reconditioning", IBID, pp. 199.

Table 1
Reconditioning Schedule

TYPICAL ORBITAL 100% SUN INTERVAL -DAYS-	ACCELERATED RECONDITIONING INTERVAL -DAYS-	PLANNED RECONDITIONING -CYCLE-	ACTUAL RECONDITIONING -CYCLE-	RECONDITIONING DURATION -HOURS-
100	50	650	668	264
50	25	998	1025	241
100	50	1663	1681	232
50	25	1995	2012	237
100	50	2660	2747	219
150	75	3658	3666	310
150	75	4655	4677	364
100	50	5320	5331	360
50	25	5653	5667	362
100	50	6318	6318	340
150	75	7315	7331	405
150	75	8313	8321	337
100	50	8978	8959	288
50	25	9310	9323	382

Table 2

Battery Cell And Cycling Information

Test Articles: Ten GE 6 Ah nickel cadmium cells, P/N 42B006AB34, polypropylene separator, Ag Treated Negative.

Temperature : 20°C ±1°C, immersed in controlled bath.

Simulated Orbit Period : 108 minutes

Discharge Parameters : 35 + 1, -0 minutes

4.00 ±.04 ampere

40% nominal depth of discharge

Charge Parameters : 73 + 0, -1 minutes

2.10 ±0.10 amperes adjustable (actual 2.04 ampere)

Trickle rate, Group A : 100ma, C/60

Reconditioning rate, Group B : Resistive, 112 ohms (100 ohms plus line resistance)

C/100 nominal discharge

C/130 at 1.0 volt avg.

ORIGINAL PAGE IS
OF POOR QUALITY

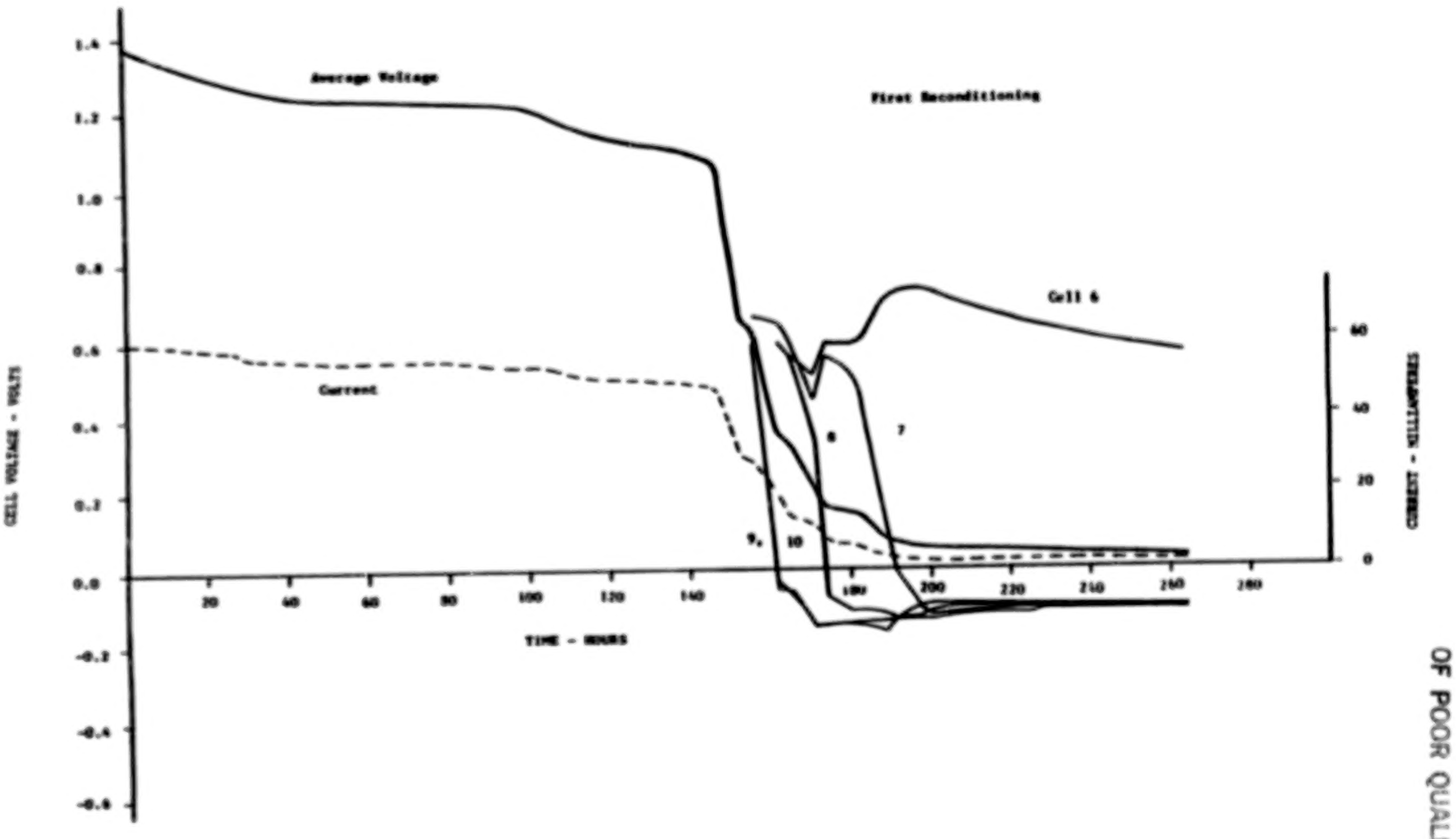

Figure 1. Voltage and current vs. time, 5 cell battery during reconditioning with 100 ohm resistor, after 667 cycles at 40% depth of discharge.

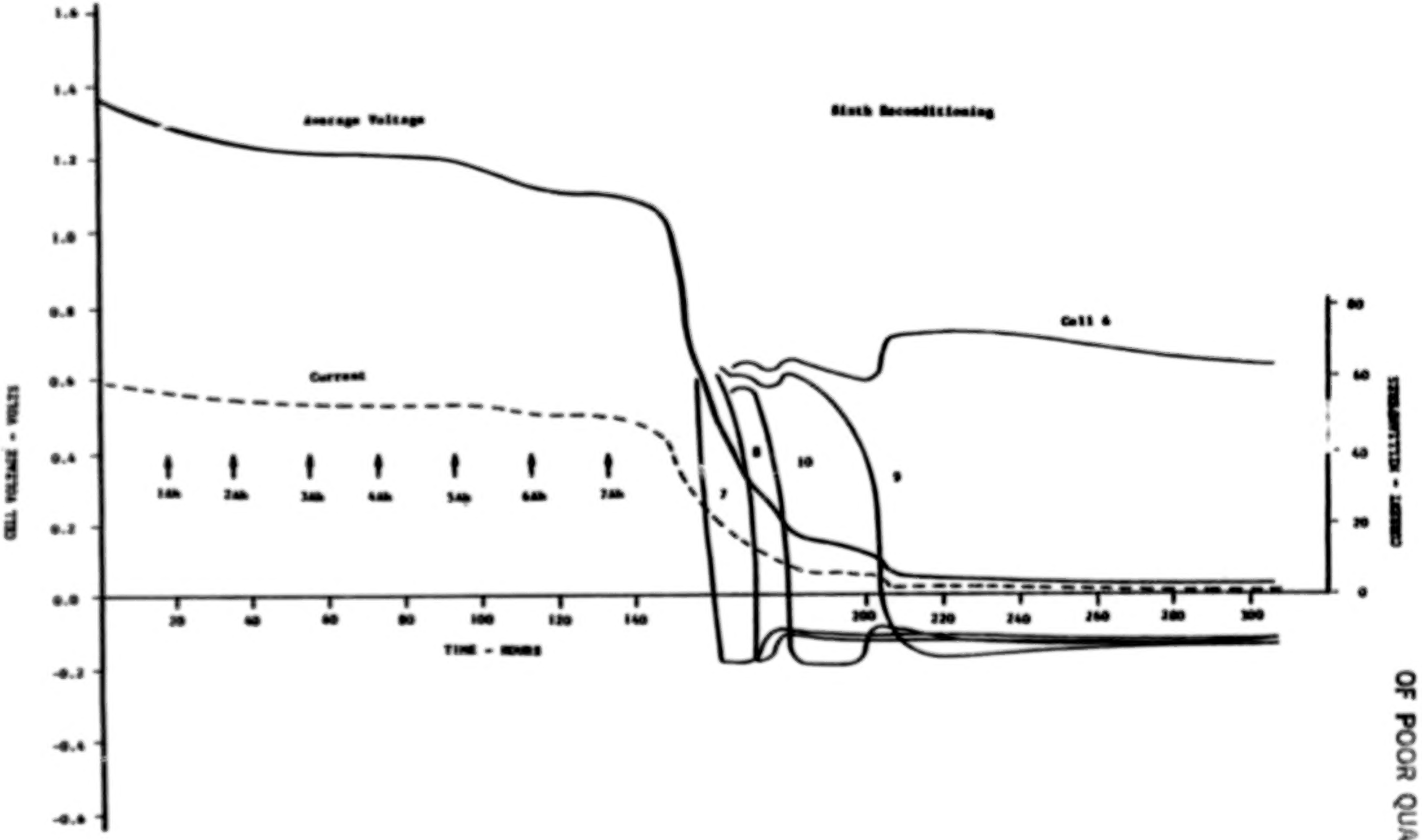

Figure 2. Voltage and current vs. time, 5 cell battery during reconditioning with 100 ohm resistor, after 3666 cycles at 40% depth of discharge.

ORIGINAL PAGE IS
OF POOR QUALITY

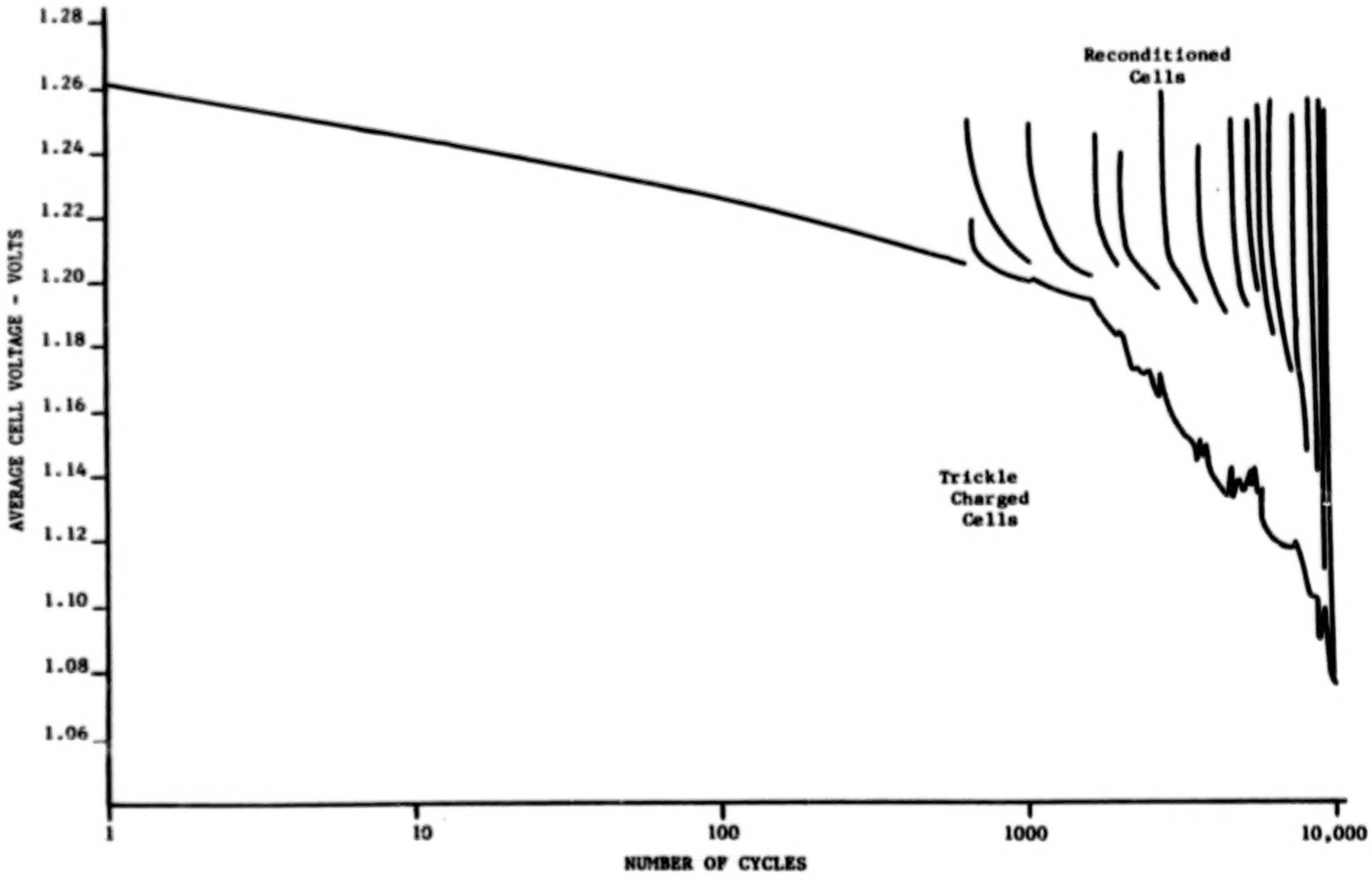

Figure 3. End of discharge voltage vs. number of cycles, reconditioned and trickle charged cells, cycled in 108 minute period, 20°C, 40% depth.

ORIGINAL PAGE IS
OF POOR QUALITY

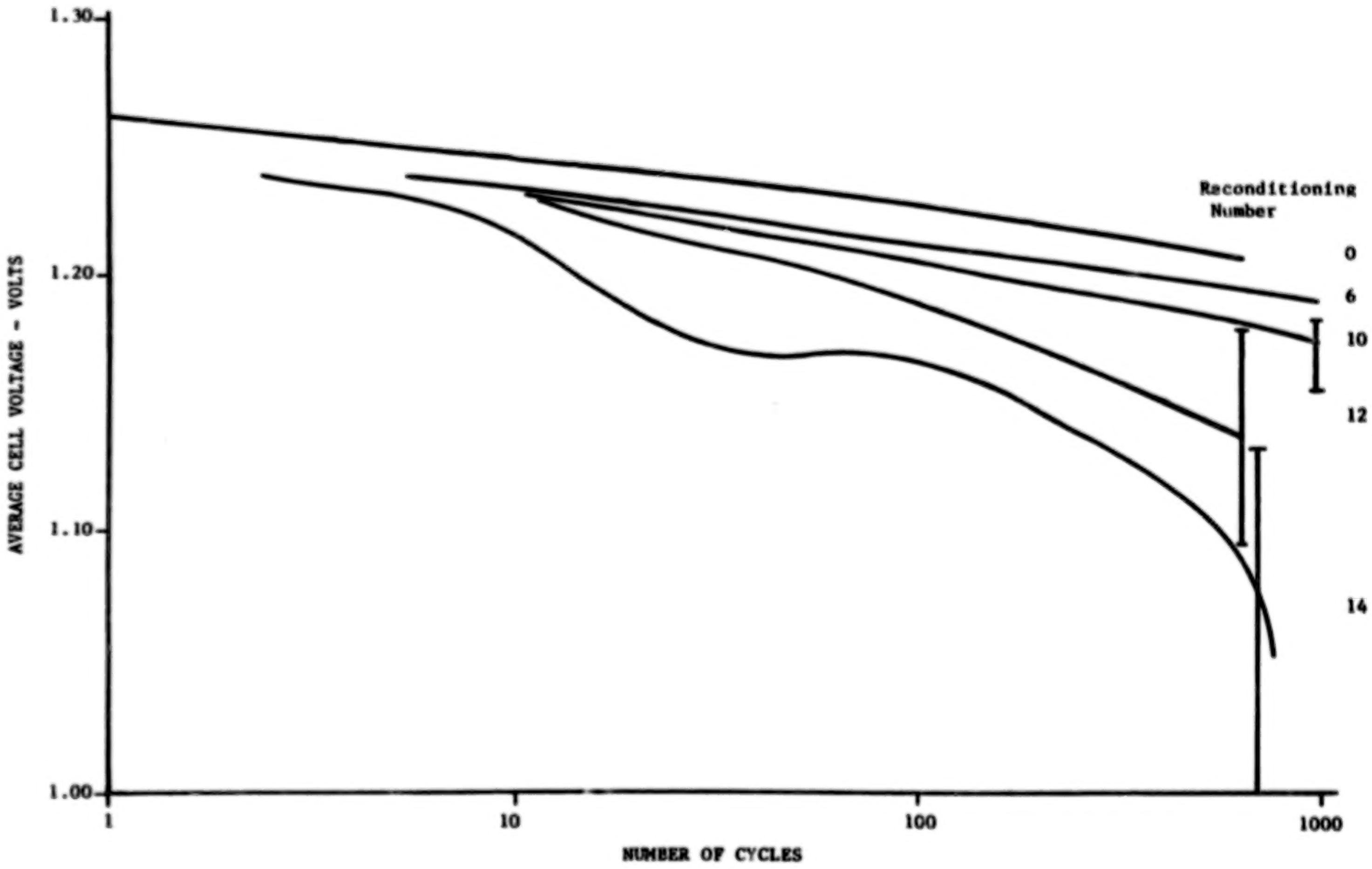

Figure 4. End of discharge voltage vs. number of cycles since reconditioning, data from before reconditioning and after selected reconditionings.

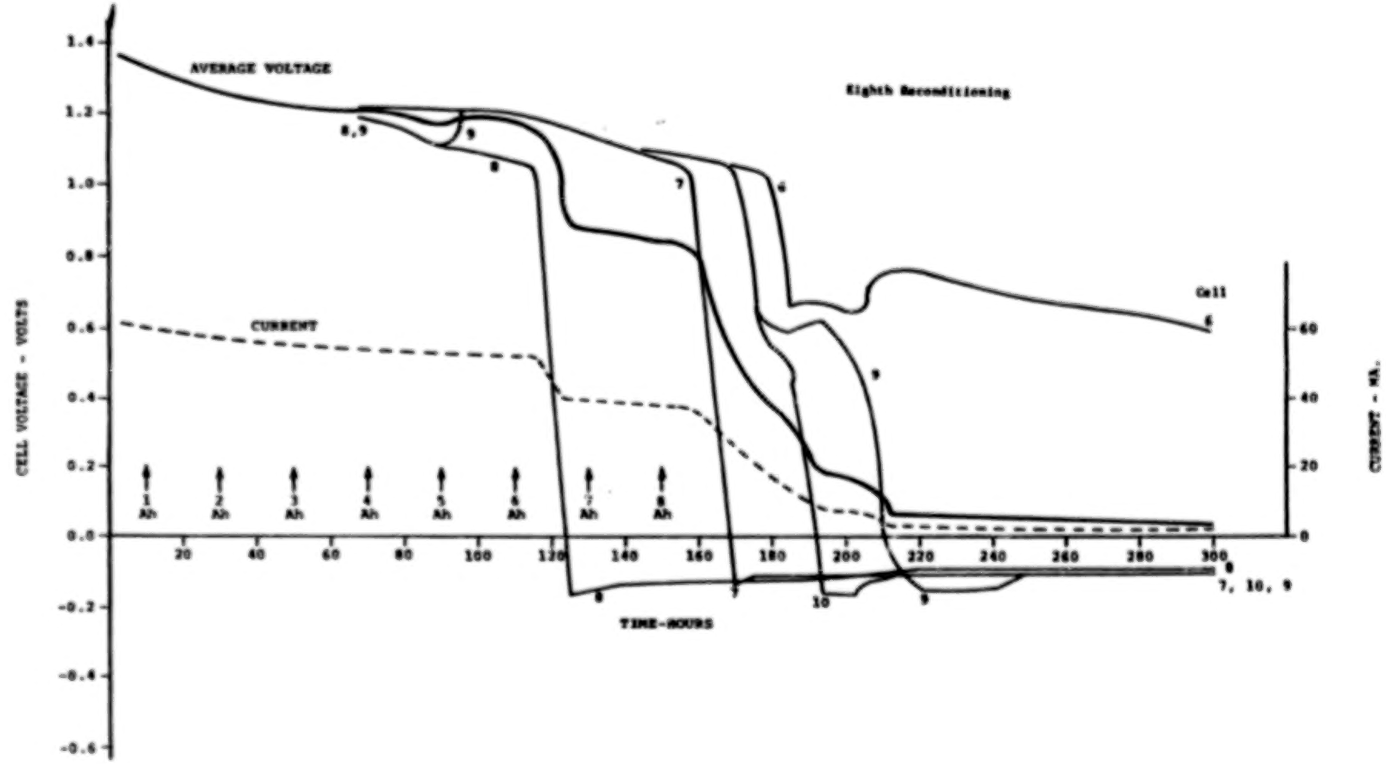

Figure 5. Voltage and current vs. time, 4 cell battery during reconditioning with 100 ohm resistor, after 5331 cycles at 40% depth of discharge.

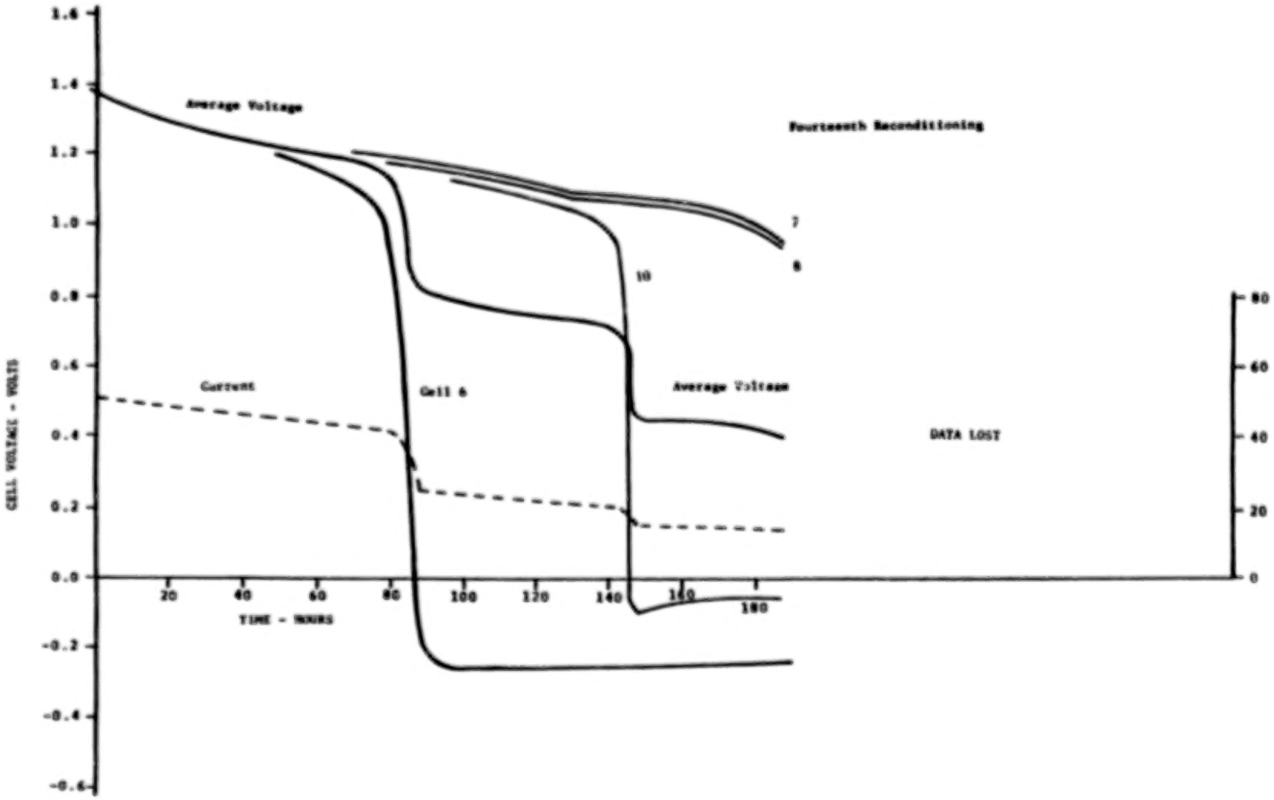

Figure 6. Voltage and current vs. time, 5 cell battery during reconditioning with 100 ohm resistor, after 9323 cycles at 40% depth of discharge.

ORIGINAL PAGE IS
OF POOR QUALITY

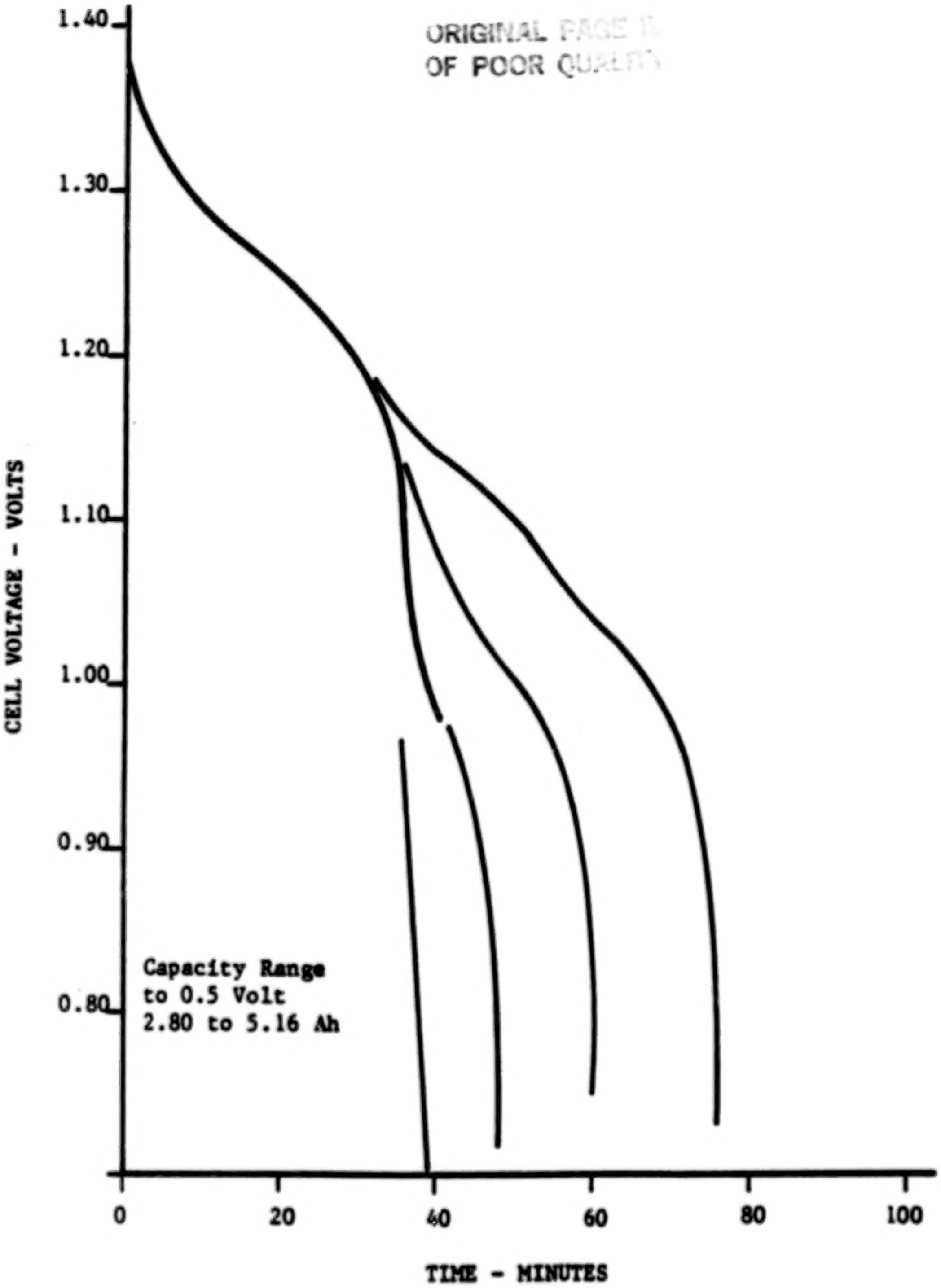

Figure 7. Discharge voltage vs. time, four reconditioned cells, after cycle 10142, 4 ampere rate.

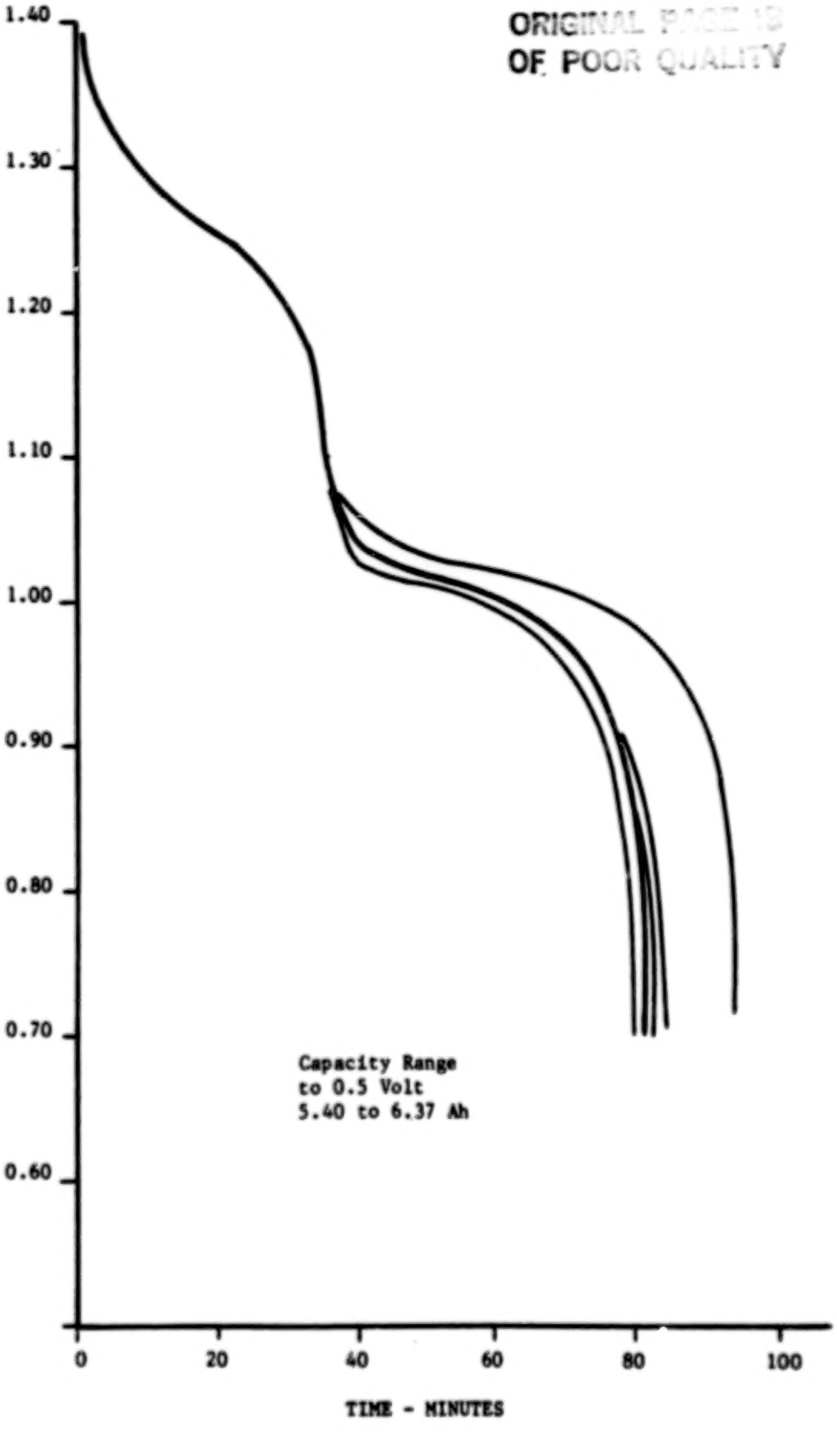

Capacity Range
to 0.5 Volt
5.40 to 6.37 Ah

Figure 8. Discharge voltage vs. time, five trickle charged cells, after cycle 10142, 4 ampere rate.

SESSION IV

DISCUSSION

Q. Badcock, Aerospace Corporation: Fred, could it be that you reconditioned it to death. I mean you reconditioned them an awful lot? Was it necessary to do it that often I guess is what I'm really asking?

A. Betz, Naval Research Lab: The idea I guess was to take the opportunities when they were available which were 100%. It's a valid question. I don't know. Someone had said this morning maybe we ought to recondition more often. I guess it does better but my evidence says not so. It was rather frequent but we did accelerate the depth in discharge also. The variability was 25,50 and 75 days.

COMMENT

Ritterman, Comsat: You anticipated my comment. With all my experience in reconditioning which was in test as well as orbit application indicated that deep reconditioning does help the capacity. I think you might be creating a wrong impression about reconditioning even though you stated that you used it. If you had run the same kind of test with cells and gotten the same results I would say you are reconditioning it to death or it's inappropriate to use it in this application. But I think not necessarily overwhelming but considerable data on reconditioning indicates that it shouldn't be used in every instance but for chosen ones it is very good.

Betz, Naval Research Lab: I agree with you Paul. My problem I guess is that I have many cells working in the exact circuit side by side and the only difference was trickle charge. I certainly should have expected some of those guys to act up somewhere along the way.

Q. Sullivan, APL: Fred, did you do anything special to limit the cell reversal voltage to 2/10th's of a volt?

A. Betz, Naval Research Lab: No, that was the natural reverse potential.

Q. Sullivan, APL: Do you think that had anything to do with the degradation that is if you had not allowed them to reverse would have been better results.

A. Betz, Naval Research Lab: If I had prevented them from reversing then I would have not been reconditioning by the method that we had kind of agreed upon before the test. So the test assumed that I was going to permit cells to reverse. I don't know if there would have been better results.

Q. Question inaudible.

A. McDermott, Martin Marietta: Okay I guess my first question, are you talking about the flight battery or the one where we are doing life cycle test on.

A. Mani, Energy Conversion Devices, Inc.: The life cycle testing one.

A. McDermott, Martin Marietta: We haven't done anything other than doing the life cycle test. We haven't pulled a battery out to do any kind of cell evaluation because it is still on life cycle test. We've achieved over 16,000 cycles right now at a 20% depth discharge. I would say when the battery would fail or we would have a cell failure or something like you know we probably would do a failure analysis on it but we haven't done anything to date.

Q. Mani, Energy Conversion Devices, Inc.: My second question is when you used the L-shaped kind of device inside the battery how that is going to reduce the heat affect which elevates the temperature from 20 degrees to 32 or something like that?

A. McDermott, Martin Marietta: Oh it wasn't just that. We also improved thermal spacecraft design if you want to call it on the spacecraft. But how the L-bracket basically helped is it allowed a direct heat transfer down to the plate we mounted on. See the cells when they are mounted there's an aerospace on the bottom and that aerospace serves as a hard thermal gap for the heat to get out. So by putting the L-bracket on the side and underneath actually up touching the bottom also we provided a direct heat transfer to the plate.

A. Mani, Energy Conversion Devices, Inc.: Thank you.

N84
33690

UNCLAS

D22

N84 33690

IN FLIGHT PERFORMANCE OF A SIX AMPERE-HOUR NICKEL-CADMIUM BATTERY IN LOW EARTH ORBIT

Joseph K. McDermott
Martin Marietta Denver Aerospace
Denver, Colorado

ABSTRACT

A low earth orbit (LEO) spacecraft has successfully completed over 17,000 orbital cycles. The energy storage system for this spacecraft supplies eclipse power and power for peak loads, and is a 28 volt, 6 ampere-hour Nickel-Cadmium battery system. There are two batteries per spacecraft, and each battery consists of 21 series connected, hermetically sealed Nickel-Cadmium cells. The cells utilize a pellon separator, a standard positive plate and a silver-treated negative plate.

This paper reviews and summarizes flight data for 17,000 orbital cycles. Discussion focuses on battery trend analysis used in determining the feasibility of extending mission life.

SYSTEM DESCRIPTION

The battery function on this spacecraft is power production during eclipse periods and power provision for power conditions in which the required load exceeds the solar array power. The average bus load for the completed 17,000 orbital cycles was 40 watts. The batteries equally share the bus load, although the system was designed so that either battery could support the load during eclipse periods. A simplified electrical power system (EPS) block diagram, Figure 1, shows that each battery has its own battery charger comprised of a primary (A) and backup (B) charger. The primary charger utilizes the Voltage/Temperature (V/T) charge curves shown in Figure 2. The lower V/T curve (A) is approximately equivalent to level 4 of the NASA Modular Power System V/T curves. The backup charger operates at a constant C/10 charge rate or a commandable C/60 trickle charge rate. Only the primary charger has been employed for the completed 17,000 cycles with all operations at level A.

PRECEDING PAGE BLANK NOT FILMED

The spacecraft solar array system comprises three body-mounted solar panels and four deployable solar paddles. There are a total of 53 solar cell strings. Thirty-five strings are permanently wired to the power bus while 18 strings can be ground commanded IN or OUT. The power control and distribution unit routes and controls power to the battery chargers and from the solar arrays or batteries. Excess power is controlled with the 18 switchable solar cell strings. When the bus voltage rises above 32 volts, a shunt control unit switches shunt resistor banks ON to dispense excess power.

CELL/BATTERY DESCRIPTION

Nickel-Cadmium cell design parameters are summarized in Figure 3. Plate loading and the negative-to-positive capacity ratio are standard for sealed spacecraft cells (ref. 1). The material for the positive and negative terminals is Nickel 200, the separator is Pellon 2505 and the cell case is 304L stainless steel. The cell height, including terminals, is 3.63 inches. Width is 2.13 inches and thickness 0.82 inches. The cell weight averages 285 grams.

The six ampere-hour, 28 volt Nickel-Cadmium battery, depicted in Figure 4, consists of 21 series connected cells. Battery dimensions are provided in Figure 4, and the battery weight is 16.3 pounds. Three thermistor temperature sensors are strategically placed on each battery. Data from the two thermistors mounted to the top surfaces of cells number six and eleven are included in telemetry data. A third thermistor is mounted between cells number 16 and 17, and is used for the V/T charge control. The battery is mounted to an aluminum honeycombed deck in the spacecraft with an RTV-60 compound for improved heat transfer.

FLIGHT DATA

The battery data base for this spacecraft includes battery temperature, recharge fraction (charge/discharge ratio), average daily depth-of-discharge (DOD), minimum battery voltage and the bus load. Battery performance is directly related to solar array performance, which is influenced by percent illumination, alpha angle (complement of beta) and solar flux. The solar flux is normalized to a standard 135.3 milli-watts per square centimeter. These parameters are provided in Figure 5 as a function of orbit number.

The average battery temperature for the 17,000 cycles was approximately 20°C. Battery temperature versus revolution (orbit) is plotted in Figure 6. Comparison of Figures 5 and 6 illustrates battery temperature is largely a function of the alpha angle, although percent illumination and solar flux also influence battery temperature. The temperature plot, Figure 6, indicates spacecraft battery temperature is high compared to other aerospace LEO vehicles (ref. 2). High battery temperatures occurred only on this spacecraft, the first of a series. Several subsequent spacecraft have maintained battery temperatures to less than 10°C.

The average daily DOD for both batteries has been consistently below 10 percent. The low average DOD results from the conservative design approach; i.e., sizing the power system for operation with one battery failure. The DOD largely depends on the eclipse period, with larger DOD during an eclipse greater than 22 percent of the orbit period. This condition is illustrated, Figure 7, for DOD and recharge fraction, which are closely related. The recharge fraction for eclipse periods greater than 22 percent of the orbit is from 110% to 120%. This recharge fraction is considered normal for a temperature of 20°C and for the V/T charging leve' used for this spacecraft.

The minimum battery voltage is the most easily observed cell degradation characteristic (ref. 3 and 4). Figure 8 shows minimum battery voltage as a function of orbit number. As seen in the figure, minimal cell voltage degradation has occurred during the 17,000 orbits. Minimum battery voltage for seven percent DOD as a function of revolution is shown in Figure 9. Data for the first 7000 cycles was for an Alpha 90° condition, thus was not plotted due to its particularity. The end-of-discharge voltage has remained reasonably stable during the past 10,000 orbits, ranging from 26.1 to 26.3 volts. This corresponds to cell voltages of 1.24 to 1.25 volts. This is substantially above the minimum acceptable bus voltage of 23.8 volts. Barring any sudden changes in performance, the batteries will almost certainly meet and exceed the mission requirement.

LIFE TEST DATA

Life testing on a flight type battery has been conducted in parallel with the mission. Over 16,000 LEO cycles at 20 percent DOD and 25°C have been completed to date. The minimum battery voltage degradation for 20 percent DOD is shown in Figure 9. The end-of-discharge battery voltage was stabilized around 25.7 volts up to orbit 11,500. An appreciable battery voltage degradation of 0.5 volts has occurred during the last 4,000 cycles. The same V/T charge level as the flight battery is utilized. The discharge regime consists of a 2.0 amperes constant current discharge. A capacity check prior to the start of the life test yielded 7.80 ampere-hours. The capacity check was performed at a C/2 discharge rate to a battery voltage of 23.8 volts.

Similar capacity checks at cycles 308 and 1264 yielded 7.35 ampere-hours and 5.55 ampere-hours respectively. The charge and discharge regimes for cycles 2200 and 15465 are compared in Figures 10 and 11. The end-of-charge voltage curves for cycles 2200 and 15465 are basically identical, thus only one charge voltage curve is present in Figure 10. The charge current increase from cycles 2200 to 15465 is considered normal and has been previously reported (ref. 5 and 6). The end-of-discharge battery voltage degradation, depicted in Figure 11, from cycles 2200 to 15465 is analogous to the life test minimum battery voltage degradation depicted in Figure 9. This voltage degradation is inherent to Nickel-Cadmium and is considered acceptable.

SUMMARY

The Nickel-Cadmium battery system on this spacecraft has successfully completed 17,000 low earth orbit cycles without a failure or an abnormality. The in-house life test data for 20 percent depth-of-discharge, Figure 9, indicate design life requirements would be reached, even at a deeper depth-of-discharge. The relatively simple, predictable and repetitive load profiles for this spacecraft, in conjuntion with the conservative power system design approach, will result in the capability to extend mission life.

REFERENCES

1. Scott, W. R., and D. W. Rusta. Sealed Nickel-Cadmium Battery Applications Manual, NASA Reference Publication 1052, December 1979.

2. DOD-STD-1578 (USAF). "Nickel-Cadmium Battery Usage Practices for Space Vehicles," 27 July 1981.

3. Kent, J., "Analysis and Evaluation of Spacecraft Battery Life Test Data, Phase 2, Summary Report," NASA CR-107119, October 1969.

4. "Evaluation Program for Secondary Spacecraft Cells," Annual Reports of Cycle Life Test, Contracts W11,252B, W12,397, S23404G, and S53742A6, Weapons Quality Engineering Center, Naval Weapons Support Center, Crane, Indiana, 1965-1976.

5. Thierfelder, H., "ITOS Battery Life Cycling Test, Final Report," Report TM-SP-PO-100, RCA, Hightstown, New Jersey, March 1968.

6. Johnson, C.R., "HEAD Battery Cell Life Test (Mod. 100), Final Report," Engineering Report 77-8725.6-108, TRW Systems Group, Redondo Beach, California, February 22, 1977.

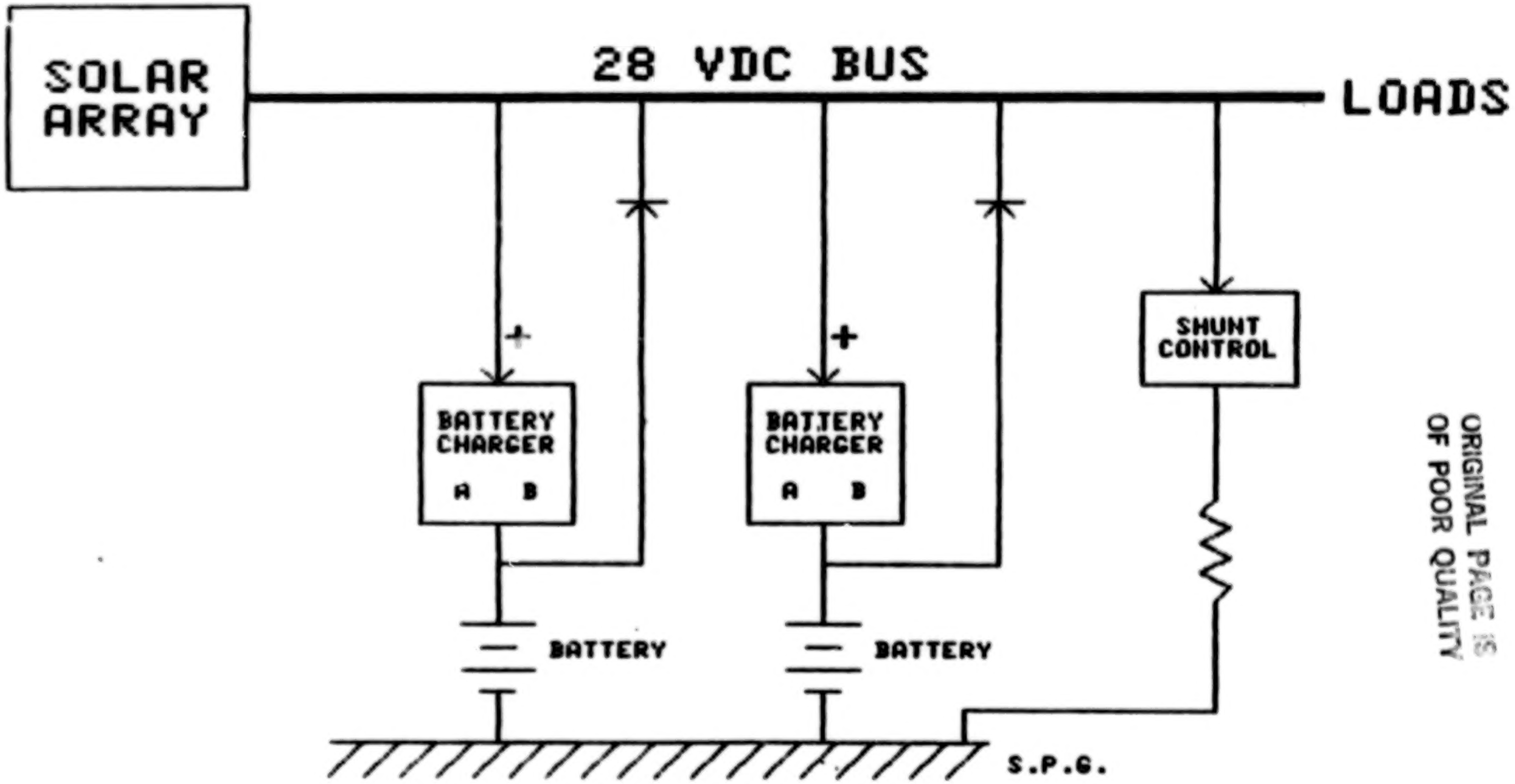
SOLAR ARRAY
28 VDC BUS
LOADS
+
+
BATTERY CHARGER
A
B
BATTERY CHARGER
A
B
SHUNT CONTROL
BATTERY
BATTERY
S.P.G.

Figure 1. Electrical power system block diagram.

ORIGINAL PAGE IS
OF POOR QUALITY

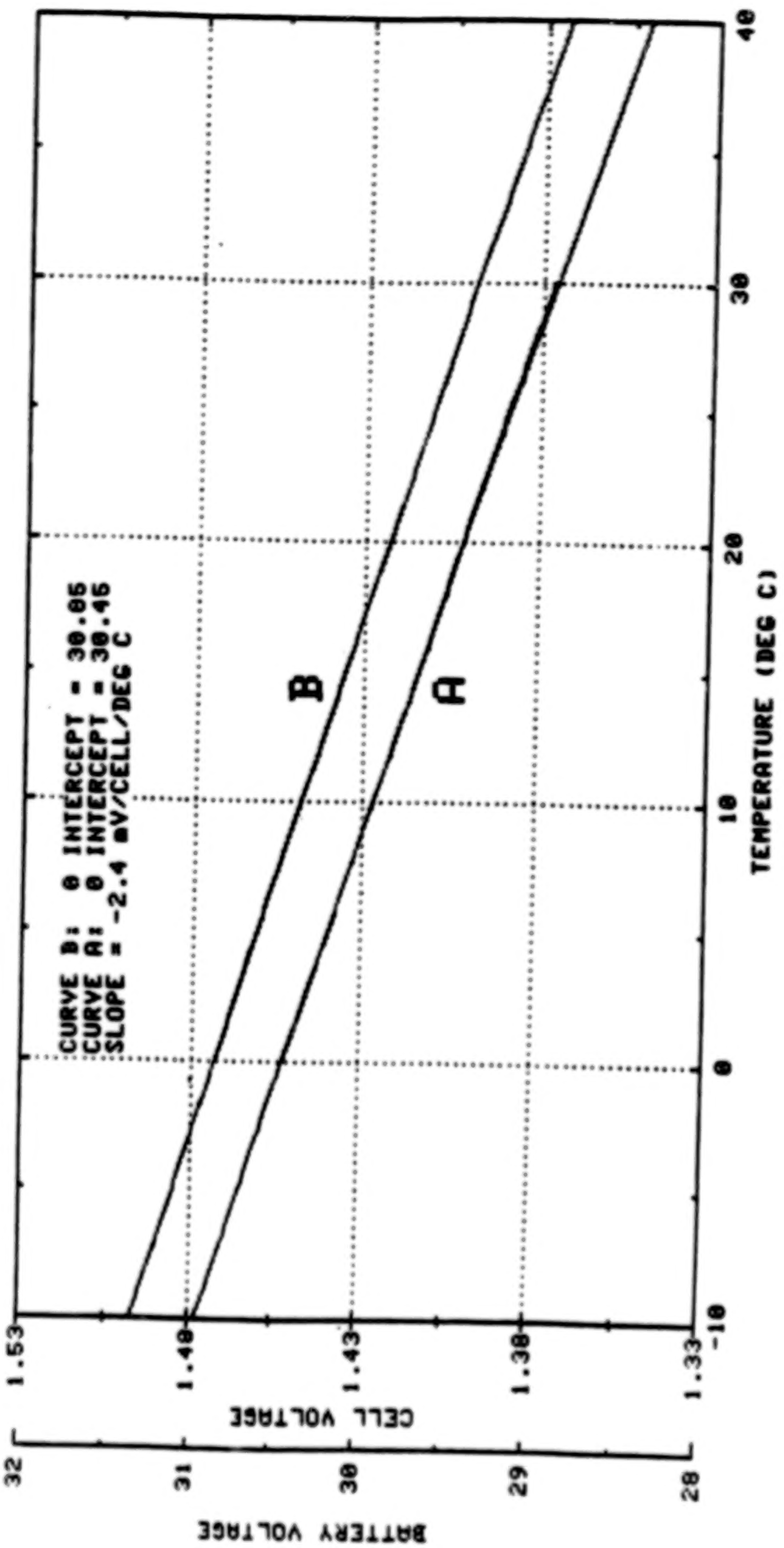

Figure 2. Cell/battery voltage limit versus temperature.

PART NUMBER	6AB67
NAMEPLATE CAPACITY (AH)	6.0
SHIPPING WEIGHT (GRAMS)	285
NO. OF PLATES (+/-)	10/11
POSITIVE LOADING (G/DM^2)	12.51
POSITIVE AREA (CM^2)	275.5
NEGATIVE LOADING (G/DM^2)	15.50
NEGATIVE AREA (CM^2)	303.1
NEGATIVE TREATMENT	SILVER
NEGATIVE/POSITIVE RATIO	1.73
OVERCHARGE PROTECTION (AH)	3.3
KOH LOADING (CC)	21.0

Figure 3. Cell design parameters.

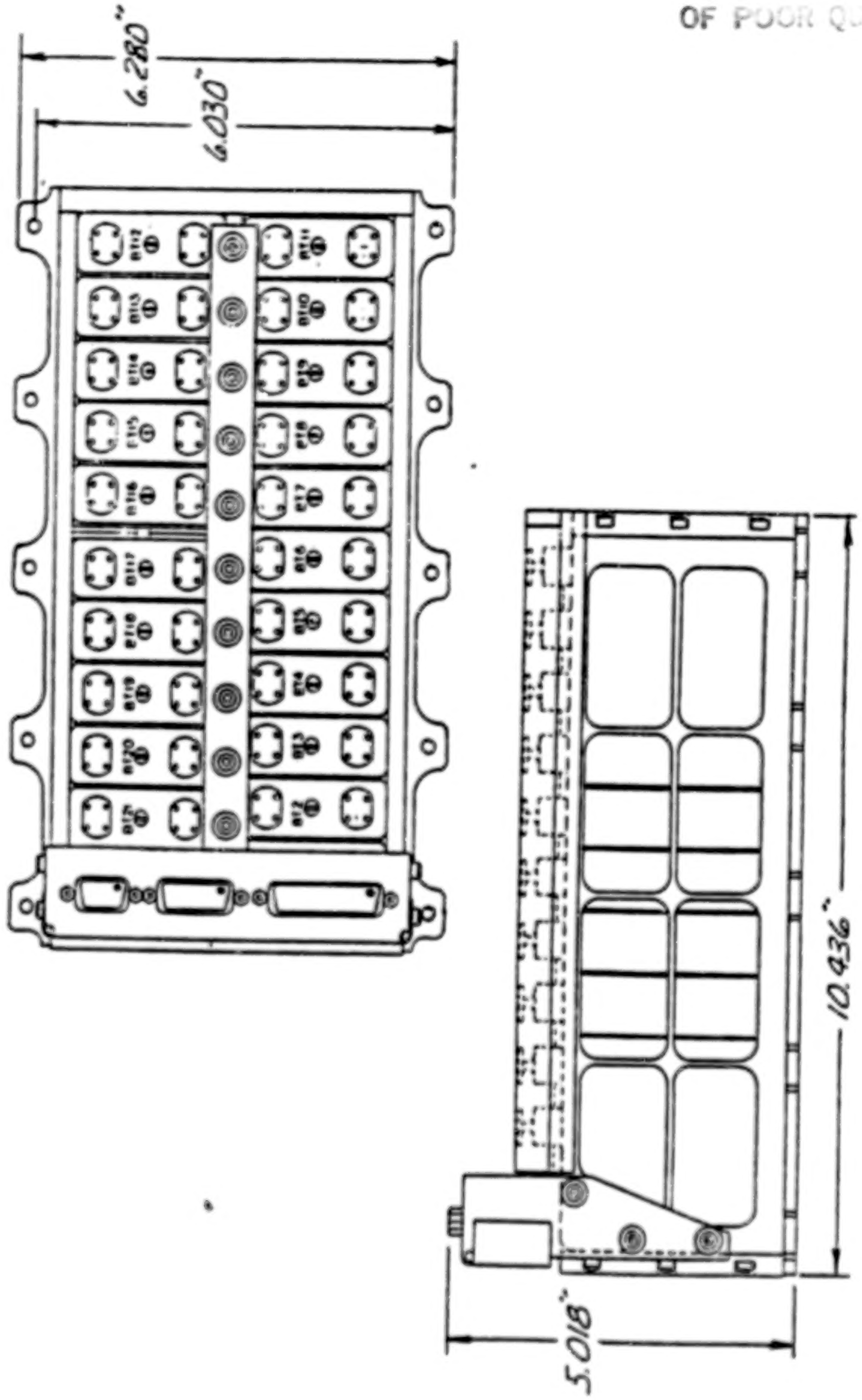
6.280"
6.030"
10.436"
5.018"

Figure 4. 28 volt, 6 AH battery configuration.

ORIGINAL PAGE IS
OF POOR QUALITY

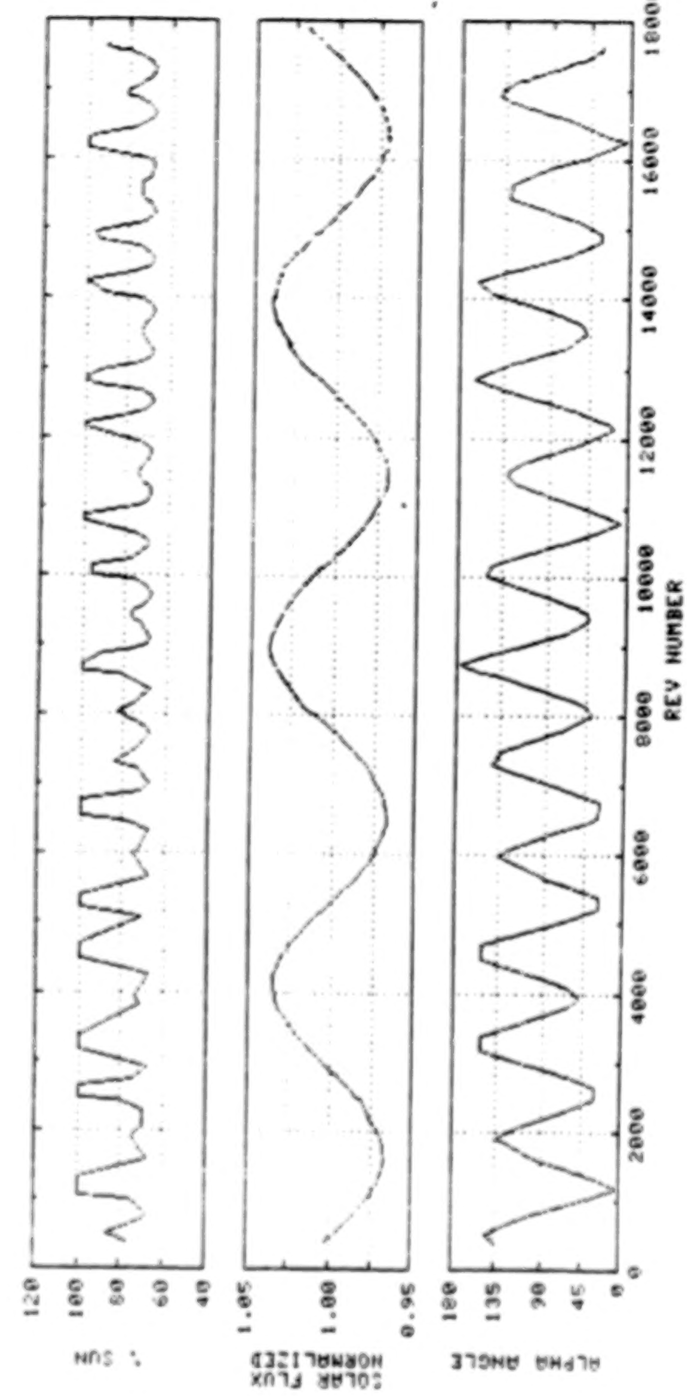

Figure 5. Spacecraft profile.

ORIGINAL PAGE IS
OF POOR QUALITY

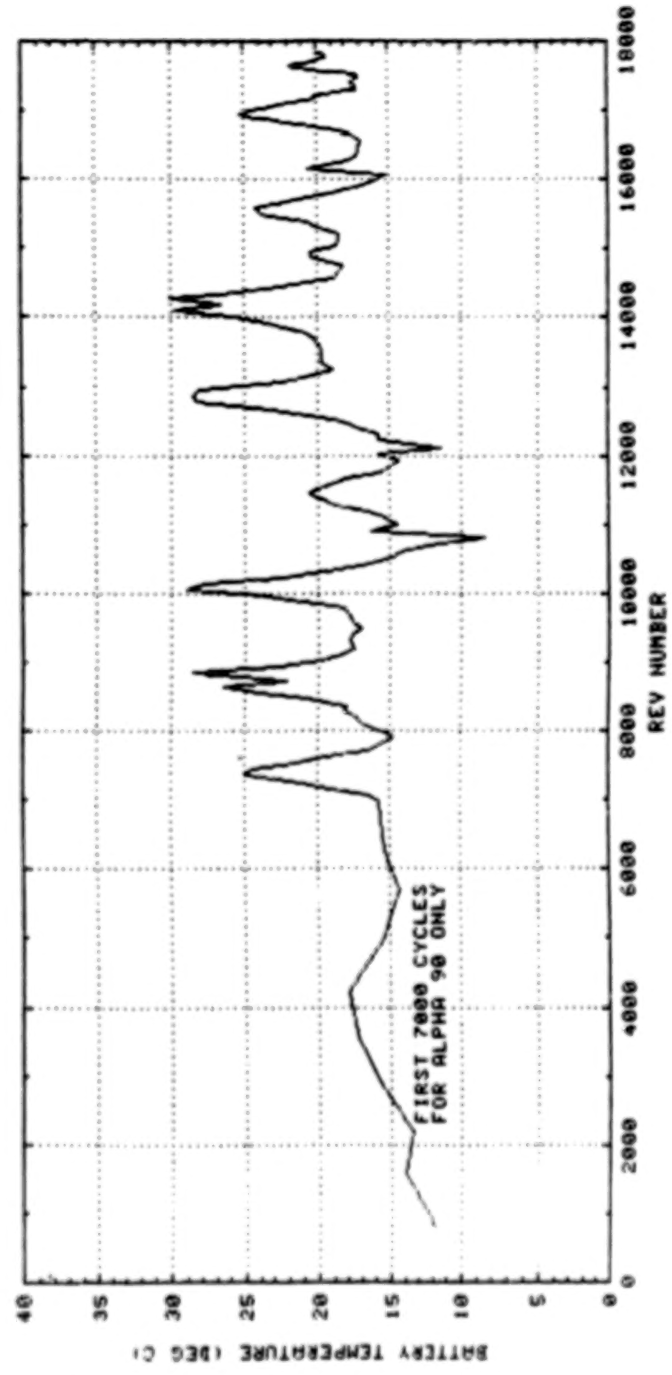

Figure 6. Battery temperature profile.

ORIGINAL PAGE IS
OF POOR QUALITY

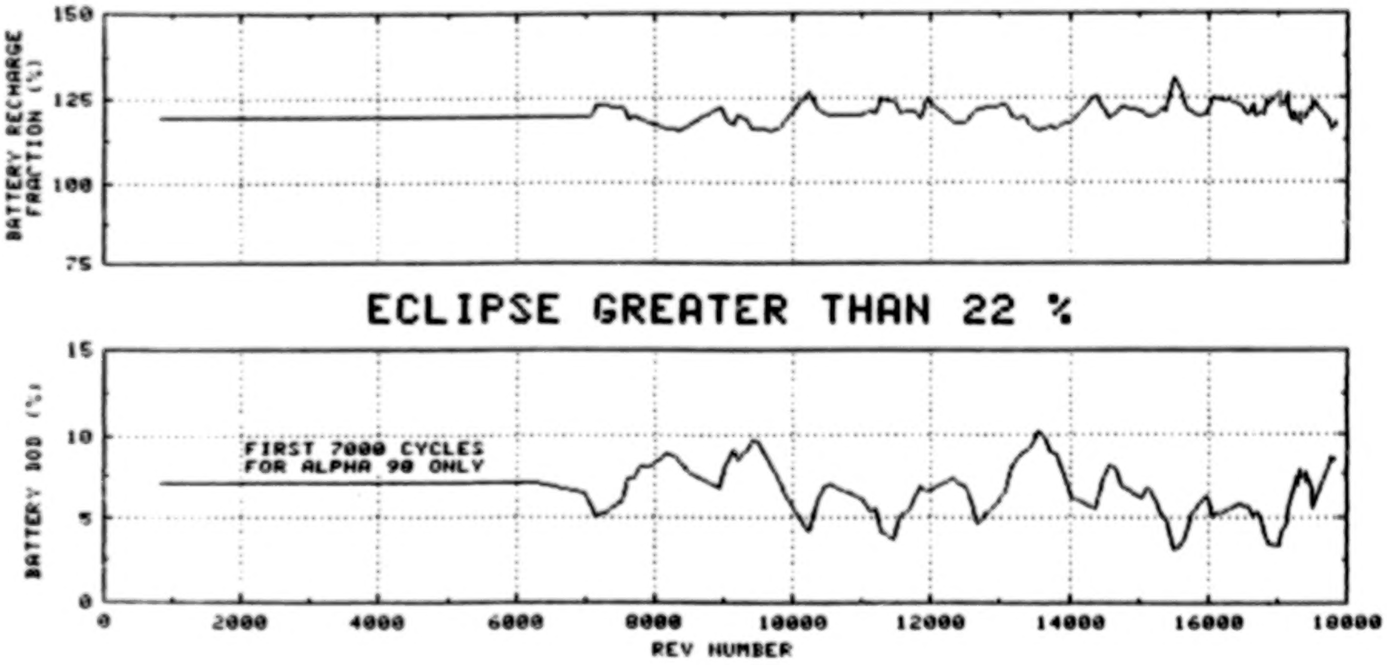

Figure 7. Daily average recharge fraction and depth-of-discharge.

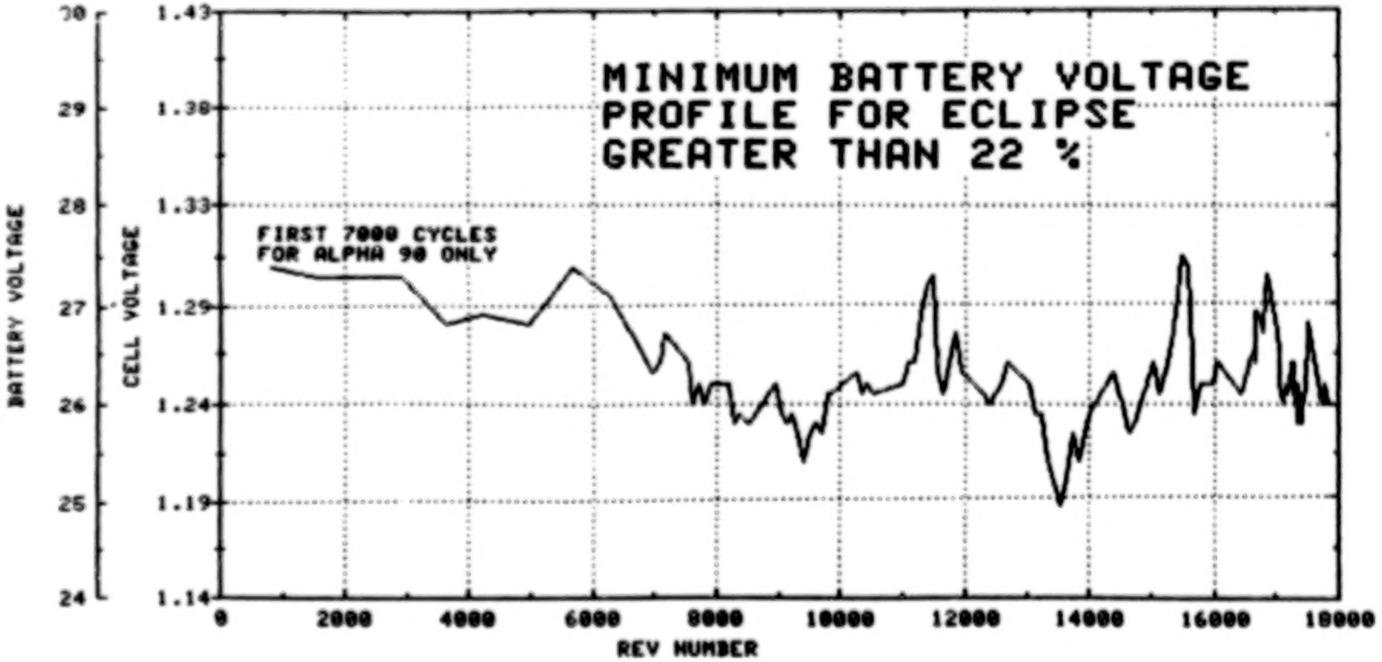

Figure 8. Minimum battery voltage profile.

ORIGINAL PAGE IS
OF POOR QUALITY

ORIGINAL PAGE IS
OF POOR QUALITY

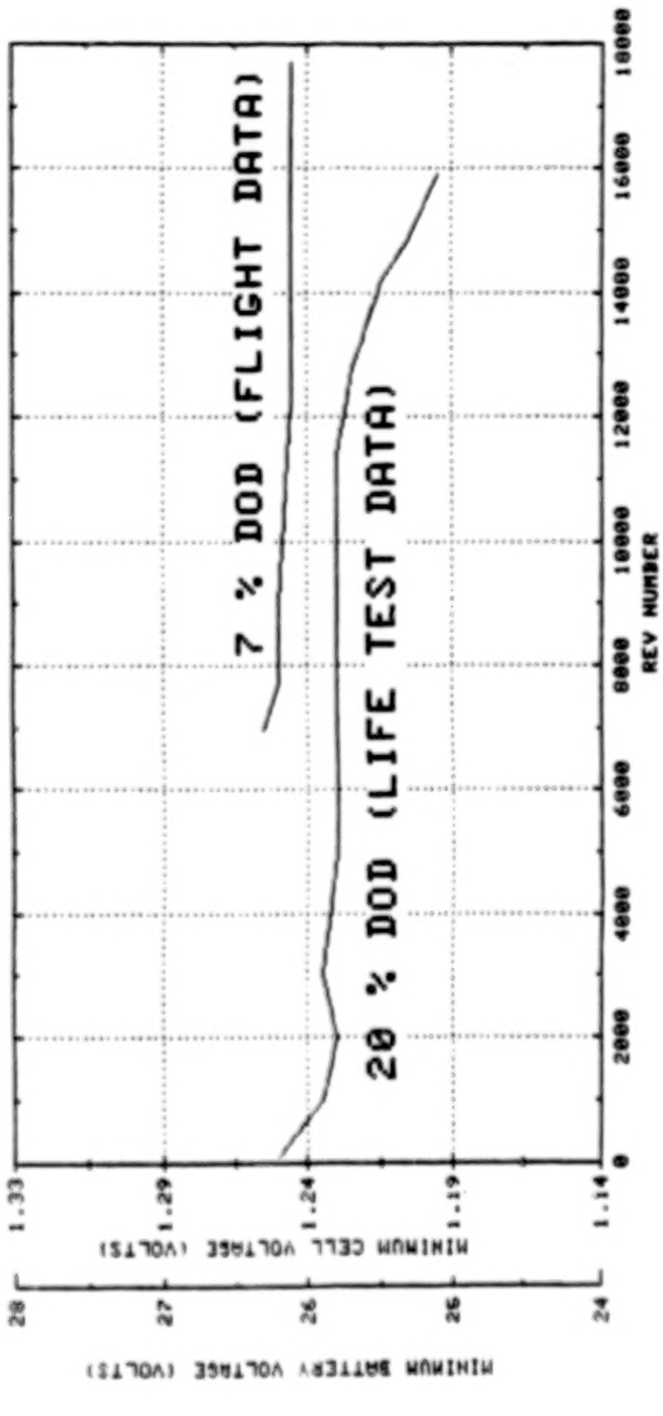

Figure 9. Flight battery versus life test depth-of-discharge comparison.

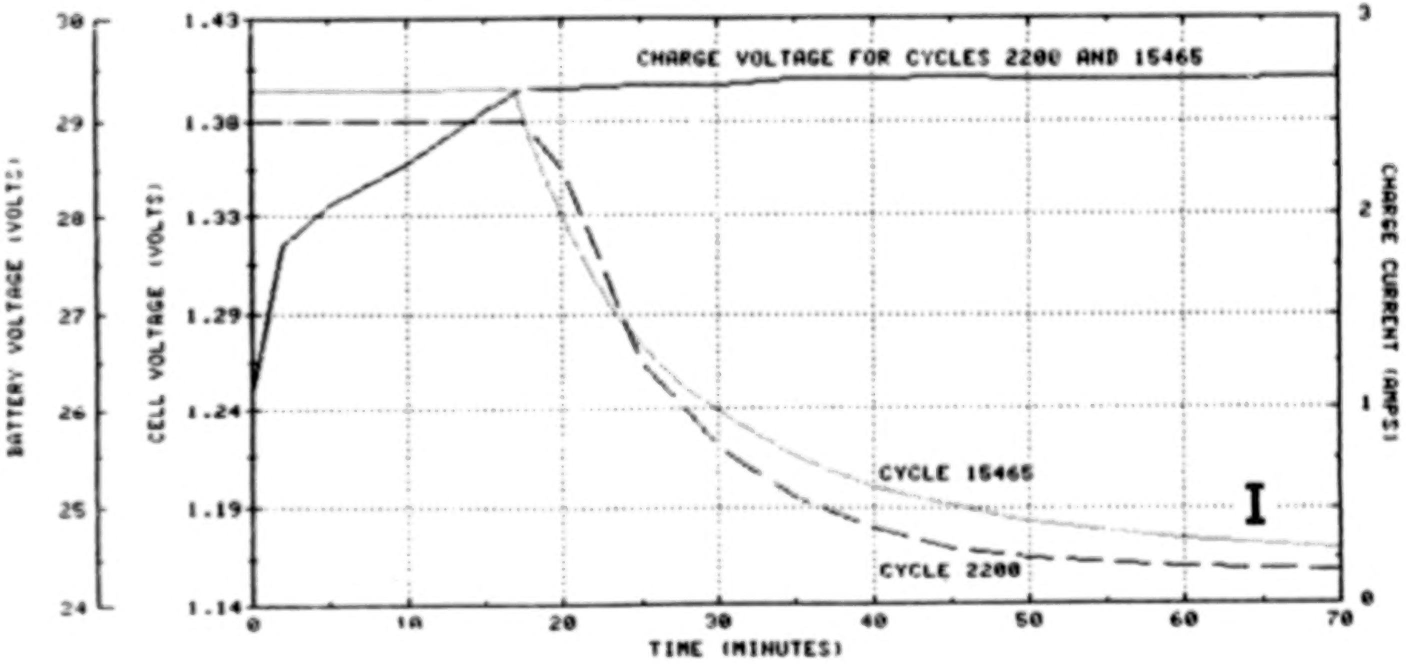

Figure 10. Life cycle test charge curves.

ORIGINAL PAGE IS
OF POOR QUALITY

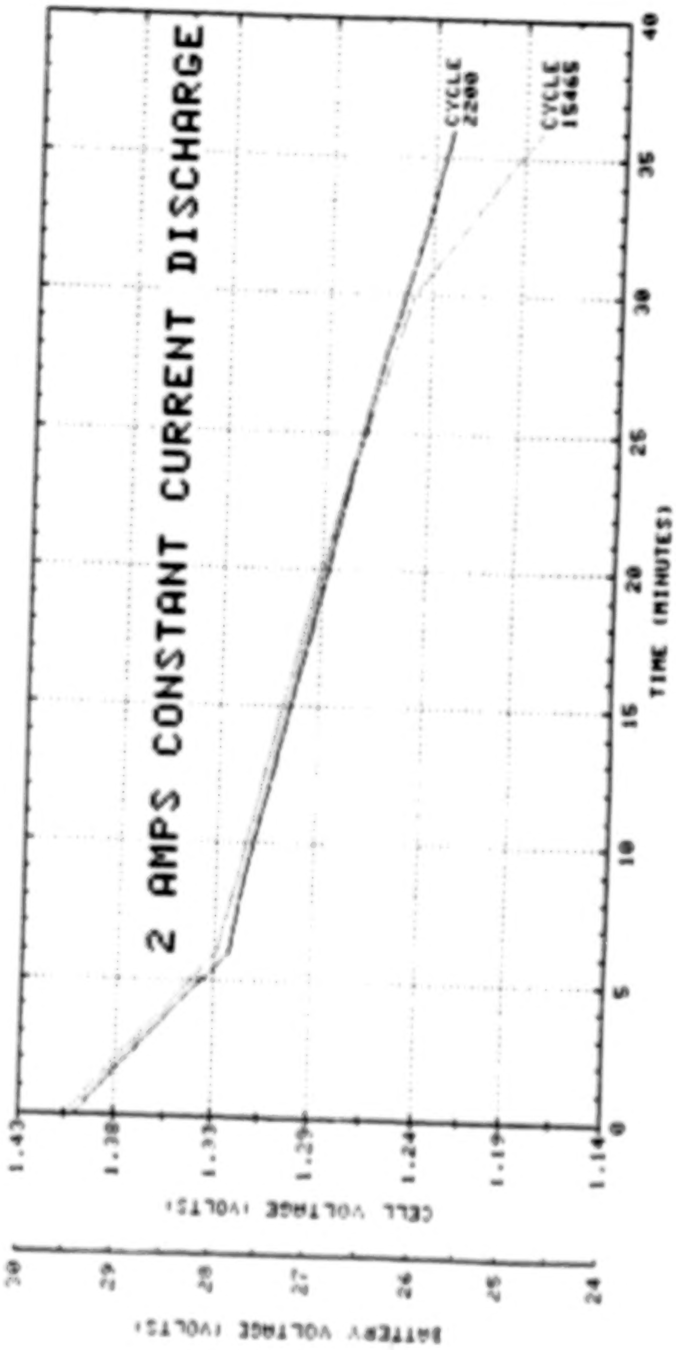

Figure 11. Life cycle test discharge curves.

N84
33691

UNCLAS

N84 33691 D23

RCA SATCOM BATTERY IN-ORBIT PERFORMANCE UPDATE AND ACCELERATED LIFE TEST RESULTS

Stephen J. Gaston
Stephen F. Schiffer

RCA - Astro-Electronics
Princeton, N.J.

ABSTRACT

The oldest operating RCA Astro geostationary spacecraft, SATCOM F1 and F2, have now completed almost 8 and 7-3/4 years in orbit, respectively, with no significant degradation of their nickel-cadmium battery performance. Battery minimum discharge voltage data are presented for these spacecraft.

In addition, 2 groups of nickel-cadmium cells which are representative of those in orbit are undergoing real time eclipse-reduced suntime cycling in the laboratory. These groups of cells, which are being cycled at a maximum of 53% and 62% depth of discharge (based on actual capacity), have completed 14 and 15 eclipse seasons, respectively. Data for these groups of cells are presented and are compared with the in-orbit battery data.

INTRODUCTION

Eight (8) geostationary spacecraft, manufactured by RCA Astro, are presently operating in orbit. As described previously, in References (1) and (2), the nickel-cadmium batteries in all of these spacecraft contain unique battery reconditioning circuitry which permits individual cell reconditioning to practically zero volts without the danger of cell reversal.

The oldest and longest operating of these spacecraft, SATCOM F1 and F2, have now completed almost 8 and 7-3/4 years, respectively, in orbit without any noticeable degradation in battery performance. Battery data for both of these spacecraft are summarized herein.

In addition, data from the real time eclipse-reduced suntime life cycling of groups of representative cells in the laboratory at two depths of discharge have been overlayed over the in-orbit data. The results show a remarkable similarity in "Minimum Discharge Voltage vs. Eclipse Season" results between the laboratory life-cycling cells and actual in-orbit battery performance over the 15 eclipse seasons presently achieved.

BATTERY PERFORMANCE IN ORBIT

RCA Astro has manufactured 8 geostationary spacecraft which are presently operating in orbit using nickel-cadmium batteries. Their nomenclature and launch dates are listed in Table 1. All batteries are performing well.

The battery performance of SATCOM F1 and F2 is of prime interest since they have been operating the longest in orbit, almost 8 and 7-3/4 years, respectively. Their design and earlier mission performance were reported in 1980 (Reference 1) and at the 1976 through 1982 Goddard Space Flight Center Battery Workshops.

Figure 1 shows the maximum average depth-of-discharge (DOD) for the SATCOM F1 and F2 batteries as a function of eclipse season. For both F1 and F2 it ranges from 57% to 52% based on the nominal capacity for their first 14 and 12 eclipse seasons, respectively. For F2 on eclipse season 13 the DOD was reduced to 42% since traffic was transferred to the SATCOM 3 and 4 satellites. The loads on both spacecraft were further reduced this year when SATCOMS 6 and 7 were launched.

Figure 2 shows the minimum average battery voltage for SATCOM F1 and F2 as a function of the number of eclipse seasons in orbit. SATCOM F2 had received a forced daily eclipse of approximately 27% depth-of-discharge during the continuous suntime duration until eclipse season number 6. This daily eclipse, in conjunction with a less than full recharge achieved between these eclipses, had resulted in some voltage degradation. This voltage however, recovered when the daily eclipse sequence was discontinued following eclipse season number 6. The batteries of both spacecraft in general show very small, if any, voltage degradations, excluding eclipse season number 1 on F1 and correcting for the different regime applied to F2 during the first 6 seasons as described above.

Figure 3 shows the same data as for Figure 1, except it presents the minimum average cell voltage using an expanded scale and shows the predicted voltage degradation established earlier using Crane data of packs 207A and 209A (Reference 3). It can be noted that the voltage degradation was considerably less than was predicted and cell voltage is substantially above the minimum required for a full payload operation.

CELL PERFORMANCE IN ACCELERATED LIFE CYCLE TESTING

In early 1981, RCA began a real time eclipse-reduced suntime life test of two groups of 17Ah (nameplate) nickel-cadmium cells as used on the ANIK B and SATCOM 3 and 4 spacecraft. The cells were manufactured by G.E. in 1979 and are of the same generic design as used in the other RCA spacecraft batteries (Ref. GE P/N 42B017AB01).

The cells are being cycled in a typical 44-day geosynchronous eclipse-cycling regime. Maximum depth of discharge is based on an initial average capacity of 19.8 Ah at 5°C. Group A (control) is being discharged at 8.9 amperes; its maximum DOD is 8.9 A x 1.183 hours/19.8 AH = 53.2% based on actual and 62% based on nameplate capacity. Group B (higher DOD) is being discharged at 10.4 amperes; its maximum DOD is 62% based on actual and 72% based on nameplate capacity. These data have been added to Figure 1 as shown in Figure 4. In this test, the "suntime" duration has been reduced from 138 days to 4 days for reconditioning.

The depth of discharge for the test cell groups, relative to the batteries in orbit, and minimum average battery voltages (7 cell data scaled to 22 cell battery voltages) have been added to Figures 1 and 2 as shown in Figures 4 and 5. Although the absolute voltage values are lower than the in-orbit results, as would be expected due to the higher depths of discharge applied, the trends over 15 eclipse seasons of simulated orbit testing are remarkably similar to those in the spacecraft. Testing of these cells will continue until failure, to provide an input for predicting the life of nickel-cadmium batteries at these higher depths of discharge in orbit.

CONCLUSIONS

1) On RCA Geostationary Battery In-Orbit Performance

Both SATCOM F1 and F2 batteries reported herein have been operating successfully in orbit for about 8 and 7-3/4 years, respectively. Their end-of-discharge voltage degradation with increase in eclipse seasons has been minimal for approximately equal depth-of-discharges. This degradation is considerably lower than originally predicted. This can be attributed to a large extent to the unique RCA Astro reconditioning procedure applied prior to each eclipse season.

2) On Real Time Eclipse-Reduced Suntime Life Cycling in the Laboratory

The extended depth-of discharge group of cells (62% based on actual capacity) and the control group (53% DOD based on actual capacity) have shown only minimal voltage degradation over the equivalent of 15 eclipse seasons. Comparing these data to the in-orbit data shows good concurrence to date.

REFERENCES

1. Gaston, S. J.: RCA SATCOM F1 and F2 Ni-Cd Battery Orbital Performance, Proceedings of the 15th Intersociety Energy Conversion Engineering Conference, 1980, Reference 809320.

2. Gaston, S. J.: Unique Battery Reconditioning Cycle for RCA's Geostationary Satellites and Its Applicability for Low Earth Spacecraft, 1982 Goddard Space Flight Center Battery Workshop Proceedings, Page 311.

3. Harkness, J. D.: Evaluation Program for Secondary Spacecraft Cells, Synchronous Orbit Testing of Nickel-Cadmium Cells, WQEC/C 81-120A, 1 June 1981, Page 212.

ACKNOWLEDGEMENTS

The authors gratefully acknowledge Mr. Dave Stewart of RCA Americom for the valuable SATCOM spacecraft battery flight performance data.

Table 1
RCA Astro Geostationary Spacecraft Operating in Orbit

SPACECRAFT	LAUNCH DATE	CUSTOMER	CELL CAPACITY * (AMP-HOURS) (NAME-PLATE)
o SATCOM F1	DECEMBER 1975	RCA AMERICOM	12
o SATCOM F2	MARCH 26, 1976	RCA AMERICOM	12
O ANIK B	NOVEMBER 1978	TELESAT OF CANADA	17
o SATCOM 3	NOVEMBER 1981	RCA AMERICOM	17
o SATCOM 4	JANUARY 1982	RCA AMERICOM	17
o SATCOM 5	OCTOBER 27, 1982	ALASCOM INC	24
o SATCOM 6(IR)	APRIL 11, 1983	RCA AMERICOM	24
o SATCOM 7(IIR)	SEPTEMBER 8, 1983	RCA AMERICOM	24

* 22 CELLS PER BATTERY, 3 BATTERIES PER SPACECRAFT

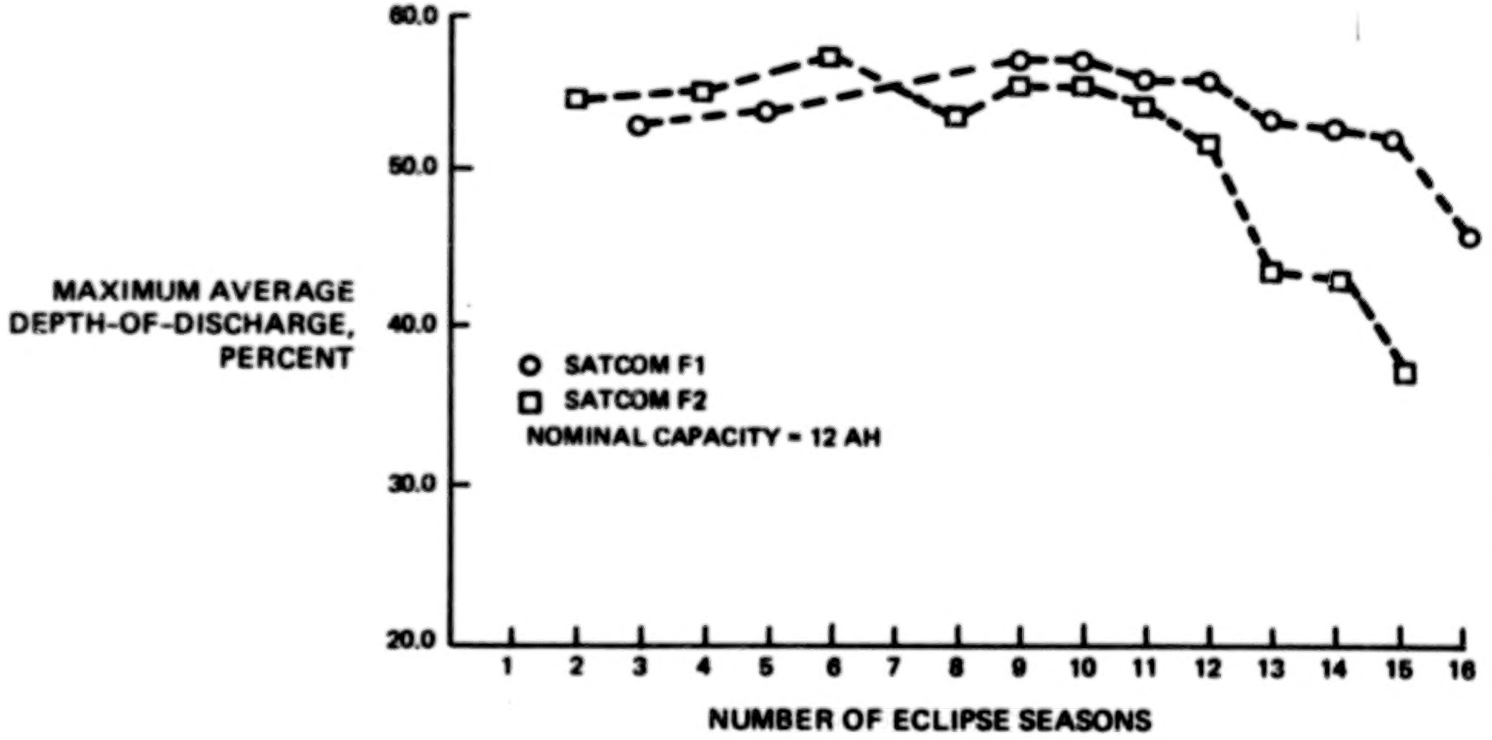

Figure 1. Maximum average depth-of-discharge during eclipse vs. number of eclipse seasons.

ORIGINAL PAGE IS
OF POOR QUALITY

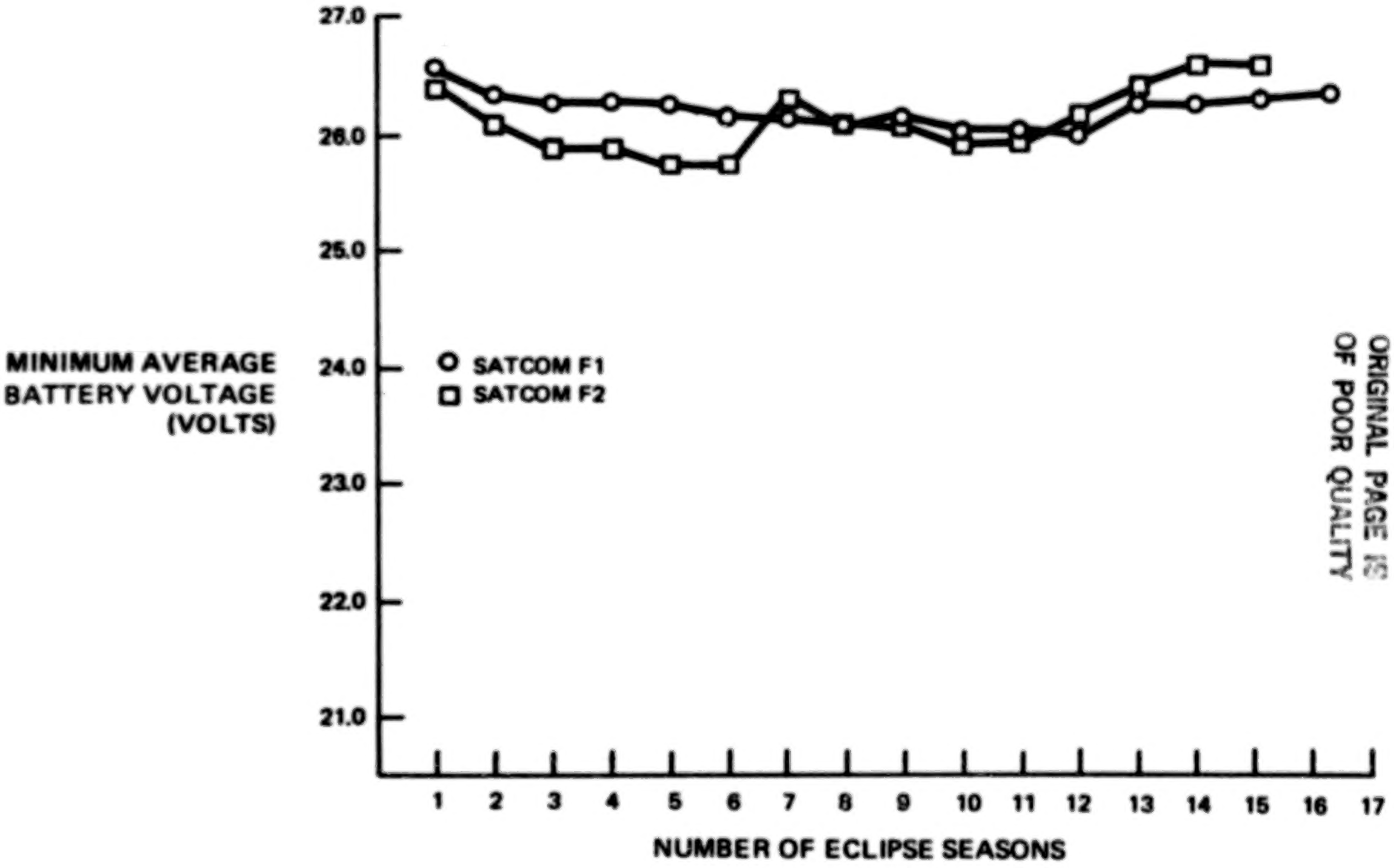

Figure 2. Minimum average battery voltage vs. number of eclipse seasons.

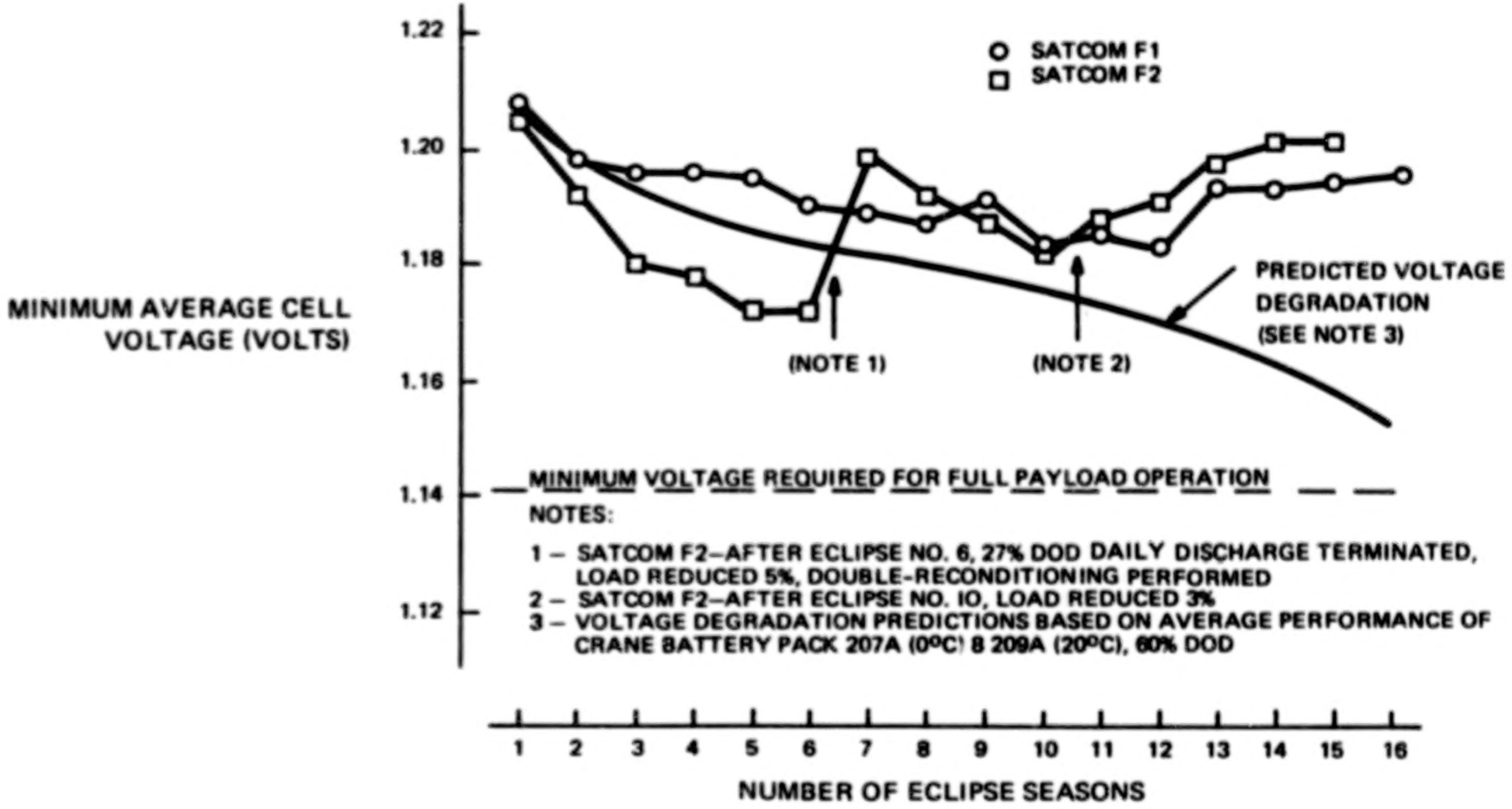

Figure 3. Minimum average cell voltage during eclipse vs. number of eclipse seasons.

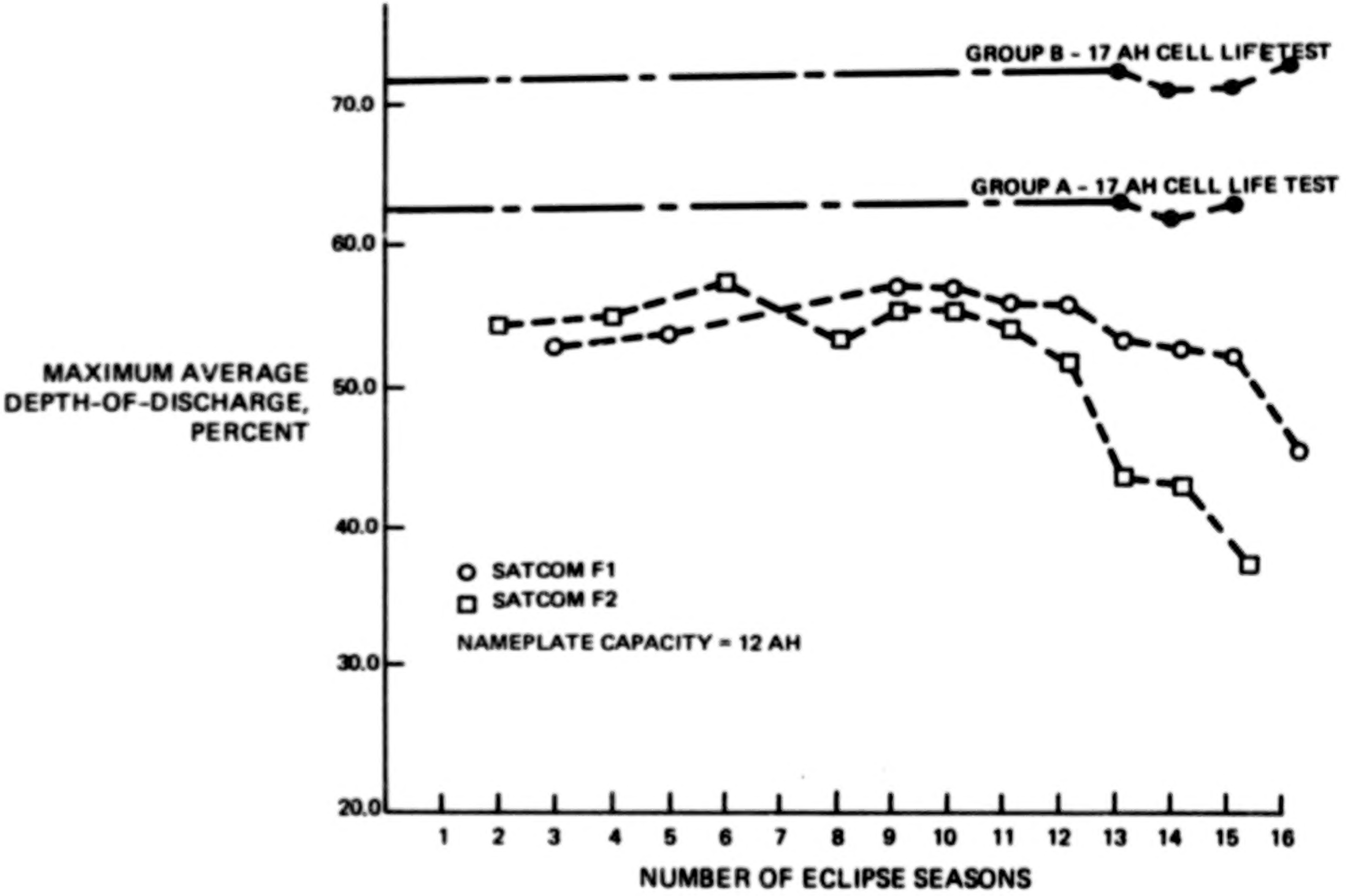

Figure 4. Maximum average depth-of-discharge during eclipse vs. number of eclipse seasons.

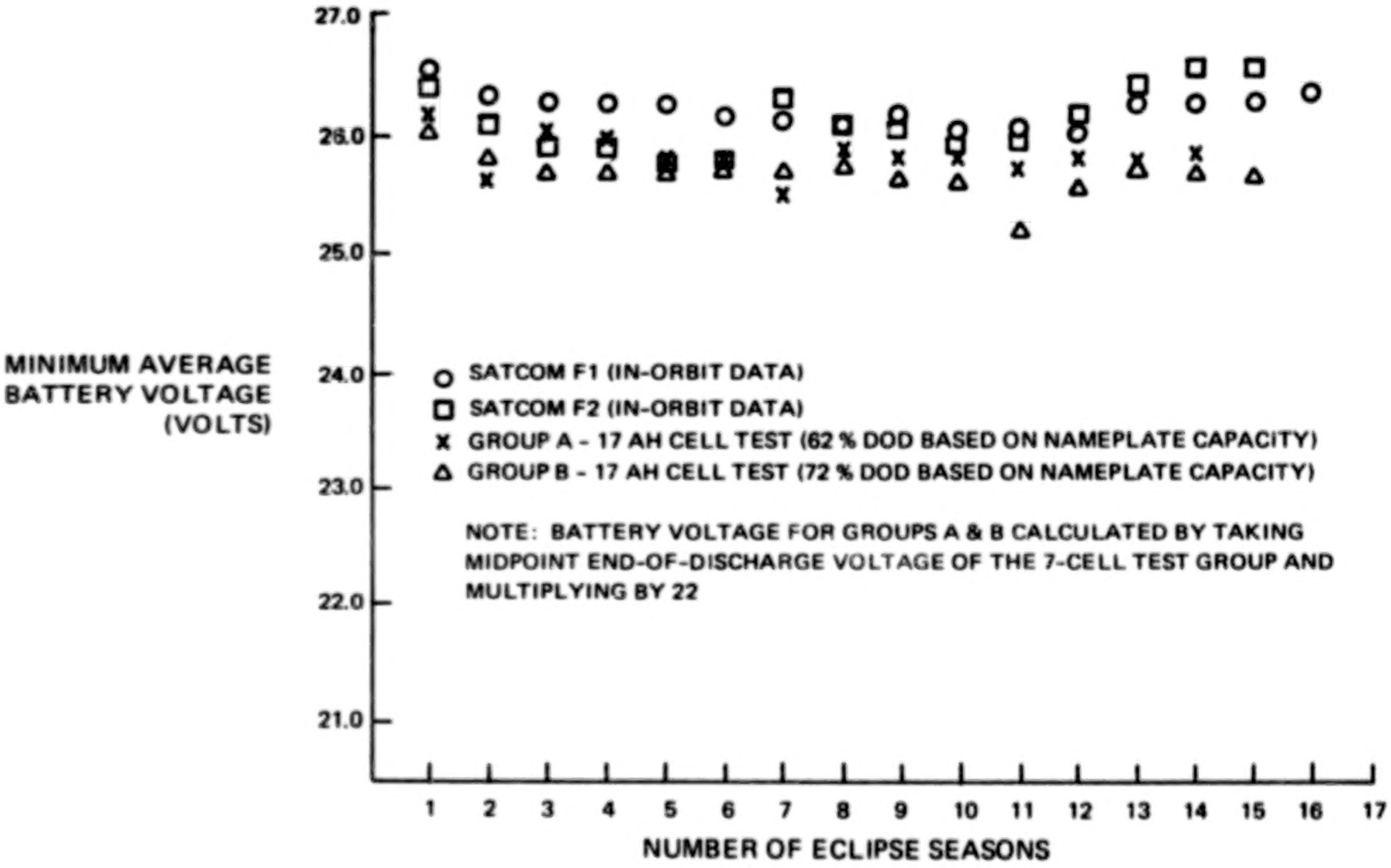

Figure 5. Minimum average battery voltage vs. number of eclipse seasons.

ORIGINAL PAGE IS
OF POOR QUALITY

Q. Kunigahalli, Bowie State College: Could you tell me what is the unique procedure that is different from other procedures?

A. Gaston, RCA-Astro: We have a series of wheel outs in each battery and each relay leads to a reconditioning which actually needs two relay contacts to get the resistor on, ground command all the relays click on and all the relays close to have these crystals draining all in the same time so all are separate. Each cell has its own resistor. So it is different from the others. So you can drain it and not worry about any reversal.

Q. George, NASA/Marshall Space Flight Center: You said that you applied this unique reconditioning method prior to each eclipse season?

A. Gaston, RCA-Astro: Yes.

Q. George, NASA/Marshall Space Flight Center: How long prior to each, immediately prior?

A. Gaston, RCA-Astro: There are always some operation problems. The operation problems as follows you got three batteries and you have a fixed time you want to be sure you cannot you don't want to recondition all three at the same time you always want to have some batteries on. So it's about two to three weeks prior. Is that the correct date Stewart? We start about 2 to 3 weeks prior to start the eclipse so we can recondition the first battery - battery 1, battery 2 or battery 3 or whichever way you like to.

Q. George, NASA/Marshall Space Flight Center: So it takes approximately a week to recondition the battery - run it down and recharge it.

A. Gaston, RCA-Astro: Well giving yourself, it shouldn't take quite that long but just give yourself a little time extra - time in case you want to try it longer or in case you just want to make sure you are ready in time.

A. George, NASA/Marshall Space Flight Center: Thank you.

Q. Armantrout, Lockheed: Steve would you comment on what the plateau looks like when you do this reconditioning and is it changing with time?

A. Gaston, RCA-Astro: Well I don't have it here to show, you're talking about the discharge voltage profile. Right? Is that what you are referring to? Right?

A. Armantrout, Lockheed: Yes.

A. Gaston, RCA-Astro: I don't have it here but when I get chance some day we will discuss it over the phone. I think there are some slight differences but not very significant. I haven't seen them yet.

COMMENT

Hendee, Telesat Canada: Really there is negligible being of course now this is a resistive discharge not a constant current or anything it's a resistive discharge and we see a negligible plateau perhaps barely perceptible plateau if you were to go ahead and correct that back to say some kind of a constant current discharge. Like to say one other thing. We abuse those cells tremendously and we have been mistreating them on the Anik B discharging several times everyday and quite a few things have been running out quite well. The original cells which were allocated to Anik B were retrofitted just prior to launch. I can see at this point where all our abuse we're just starting to see a slight spread in the cell of voltages at the end of discharge whereas the flight simulation, they are locked in tight as can be.

Gaston, RCA-Astro: Interesting.

Hendee, Telesat Canada: One other thing you didn't mention is your charge sequence Steve, and that is a major difference to other people as well and I've been getting a lot of questions at Telesat. Well what do you think about the sequential charge and as far as I can tell actually the sequential charge which we do five minutes fast charge and ten minutes off. Actually, it seems to be beneficial or I won't say it's beneficial let me say that I see certainly no degrading affects due to that.

Gaston, RCA-Astro: Let me just add, Anik B was launched I mentioned before that's the table I was missing was launched November 1978 so it's five years, ten eclipse seasons.

Q. Bell, Hughes Aircraft: Steve, do you have individual cell voltage data on the battery?

A. Gaston, RCA-Astro: No we do not. We felt at that time we don't need it. It's usually when you have a common charging system you are concerned about reversing some cells so you like to go to some threshold value then you would need cell voltages, individual ones. No we don't.

Q. Bell, Hughes Aircraft: Just one other question, because in some laboratory testing that we've done depending on the length of the lead wire on the resistor with a series string of batteries sometimes the individual cell resistors act like a 22 resistor string across a 22 cell battery. That was the reason why I asked about the individual cell voltages.

A. Gaston, RCA-Astro: We don't have it on this spacecraft and in the whole series.

A. Bell, Hughes Aircraft: Thank you.

N84
33692

UNCLAS

N84 33692 D24

PERFORMANCE OF THE IUE SPACECRAFT BATTERIES AFTER 70 MONTHS

Smith E. Tiller
Goddard Space Flight Center

ABSTRACT

The IUE spacecraft was launched on January 26, 1978 into an eccentric synchronous orbit with inclinations of 28.94° to the equator. The IUE power system contains two 6 ampere hour nickel-cadmium batteries designed to provide a beginning life of 145 watts during the eclipse seasons. In addition, battery power is required when the main buss exceeds the solar array output. The spacecraft design life was for three years with a design goal for 5 years. As of November 1983 the batteries have supported the spacecraft requirements for 70 months with excellent performance.

Papers presented at the 1978 and 1979 battery workshops describe the properties of the IUE power system including battery and cell characteristics. The objective of this paper is to update the battery performance since 1979.

CONFIGURATION

The battery in figure 1 is typical of the two flight batteries aboard the IUE spacecraft. Each battery contains 16 regular 6 ampere hour nickel-cadmium cells and 1 signal electrode cell. The batteries are diode coupled to the main buss via a boost regulator that provides 28 volts of regulated power to the spacecraft. Battery telemetry data includes battery voltage, current, signal electrode voltage and battery temperature.

INTRODUCTION

The eccentric synchronous orbit requires the spacecraft to experience 2 eclipse seasons each year, in coincidence with the solar equinox. Shadow period range from 14 to 77 minutes with each eclipse season lasting from 23 to 25 days. During periods when the solar array (spacecraft beta angles less than 0° or greater than 130°) is sufficient to supply the spacecraft power requirements, the batteries are required to augment the spacecraft needs.

FLIGHT PERFORMANCE

Each battery charger was designed to provide charge control as illustrated in figure 2a. This was accomplished by a C/10 (0.6 amp) charge current limit followed by a taper charge to be controlled by the signal electrode. Details of this charging scheme was presented during the 1978 battery workshop. During the early part of the eclipse season 1 it became apparent that the signal electrodes were not performing in accordance with design. Figure 2b represents a typical charge profile as observed in orbit. Because of the operational anomaly, procedures were modified for manual switching of the battery chargers to a trickle charge mode once the signal electrode had exceeded 0.1 volts for 3 hours. The trickle charge rate is 0.1 amps. The IUE cells on life test at the Naval Weapons Support Center (NSWC) at Crane, Indiana did not initially show the anomalous behavior. However after several eclipses there was a progressive loss of signal electrode sensitivity that resulted in the test cells experiencing an increase in overcharge. As a result, the test at Crane was modified to be indicative of the spacecraft recharge scheme for the flight batteries.

During the solstice seasons the spacecraft batteries are maintained in the low rate trickle charge mode except during periods when science activities require battery power to augment spacecraft operations. As a result of normal solar array degradation, the beta angles at which the power system buss remains power positive has decreased. Consequently additional demands have been placed on the batteries to support an increase in the demand for scientific data. These activities have required the batteries to be discharged at low rates while augmenting solar array power. Because of the additional demands being placed on the batteries operational constraints were developed to minimize battery degradation and/or damage. The constraints included a lower limit of battery voltage of 20.9 volts for average spacecraft loads, and 20.5 volts for peak loads. When either of these conditions occur the spacecraft is maneuvered to a more favorable sun angle for battery recharge.

Since the exact relationship between the above stated battery voltage, and battery state of charge was not clear, the life test at Crane was interrupted to evaluate these new conditions. Following an 8 week trickle charge (0.1 amp), the Crane cells were discharged at .05 amps to a 20.5 volt limit. Following the discharge, the cells were recharged and placed on a trickle charge for 7 days prior to repeating the test at a .1 amp discharge rate. Figure 3 depicts the discharge profile for both of these conditions and compares the data with the voltage limits selected for spacecraft operations. Typically the amount of ampere hours experienced from the spacecraft batteries at the normal discharge rates (3 to 4 amps) is 2.3 to 3.8. This is contrasted with the 4.5 to 6 ampere hours obtained at the 0.5 amp and .1 amp discharge rates.

Figure 4 is a summary of the composite of the summer solstice periods using data of 100 day intervals. A deviation from the normal trend is illustrated at approximately day 1150 (Eclipse season 7) when the signal electrode of battery SN 05 increased to an output level observed prior to launch. The reason for this peculiar behavior of the signal electrodes are not known at this time. The low point observed at around 1300 days is attributed to the mode of operations of the spacecraft. This figure also shows the battery temperature history and illustrates the approximate 8 degree battery temperature delta that has been prevalent throughout the mission.

During the early stages of eclipse season 12, the first indication of battery current divergence on discharge is apparent (Figure 5). By day 5 of the season the battery current divergence reached a maximum of .8 amps near end of discharge. By day 16 load sharing between the two batteries was back to near normal. The exact cause of this divergence is not known. However, it is thought to be associated with variation in the plateau voltage between the 2 batteries. Battery current divergence will be further analyzed during the future eclipse seasons.

Figure 6 illustrates a summary of GSFC cell test, spacecraft battery performance, and results of cell life test conducted at Crane as compared to pre-launch predictions. The battery voltage degradation prediction curve shown in this figure, was obtained from data acquired during synchronous orbit testing of older cells of similar design. The available power degradation prediction curve was calculated using the above battery voltage prediction data, solar array degradation and the efficiency factor of the power system boost regulator.

The GSFC test results shown in figure 6 was acquired from inhouse test on flight cells to an 80% peak depth of discharge and using the signal electrode for charge control. The test was accelerated by reducing the solstice periods from 5 months to 1 month. This test result was used as a baseline for prior to launch predictions.

The spacecraft battery voltage shows the trend for the end of eclipse voltage since launch. The first 6 eclipses typically required the battery to experience 60 to 75% depth of discharges. In addition the spacecraft loads required each battery to be discharged in excess of 4 amps during the eclipse operations. In the interest of obtaining maximum battery life (new goal of 10 years life) power conservation measures were implemented to limit the maximum battery discharge to 4 amps per battery. The selection of the 4 amp rate was predicated on life test experience.

The Crane data depicted in figure 6 illustrates the results of real time data from synchronous orbit testing at Crane with cells from the flight lot. The Crane data also follows the voltage prediction curve for eclipse seasons 1 through 7 but at a slightly higher voltage level than the predicted curve. During the early eclipse seasons the signal electrode degraded to a point where the current taper was being controlled by the battery voltage control alone. During eclipse 7 the control was switched to another signal electrode cell in the test pack. During eclipse seasons 8 and 9 no improvement was evident in controlling the battery overcharge. Prior to eclipse season 10 the charge control was modified to duplicate that being used by the spacecraft, as depicted in 2b.

The Crane test also provided for capacity discharge during the peak of the eclipse seasons. Cells were selectively discharged beyond the 80% depth of discharge level to 1.0 volt. For eclipse season 1, cells 9 and 10 were discharged, eclipse season 2, cells 8 and 9 were discharged. For each eclipse season an additional cell was added to each discharge group, until all cells had been capacity discharged. Analysis of the data from these type capacity checks indicated that it was creating a voltage divergence between the cells during discharge. Consequentially, prior to eclipse season 11 the capacity discharges were modified to incorporate all cells being discharged simultaneously. The data as illustrated in figure 6 for eclipse seasons 11 through 14 indicate a progressive increase in the test pack voltage at the 80% depth of discharge level.

Figure 7 illustrates the lowest voltage level that the spacecraft batteries reached at the end of discharge of each eclipse period of seasons 1, 6, and 12. The data give an indication of the rate of battery voltage degradation over the life of the spacecraft. The constraints (limiting the battery discharge rates to 4 amps) were effective in minimizing battery degradation.

Figure 8 illustrates the discharge profile for a day in eclipse season 2 and 12 where shadow period were of equal time. The discharge for day 6 of eclipse season 12 was constrained by the maximum discharge rate of 4 amps.

CONCLUSION

It can be concluded that the changes made in the battery operational procedures have enhanced the operations. The loss of battery signal electrode sensitivity in flight was accommodated by changes in the battery operational procedures. It was anticipated that the battery would start to show some aging effects after several eclipse seasons and that the effects would be somewhat amplified by the 8°C temperature delta that the batteries have experienced during their lifetime. The overall objective has been to adjust battery operations without unduly constraining science activities. Based on the performance of the flight batteries over the first 6 years, it is believed that these batteries will meet the new 10 year design goal.

ORIGINAL PAGE IS
OF POOR QUALITY

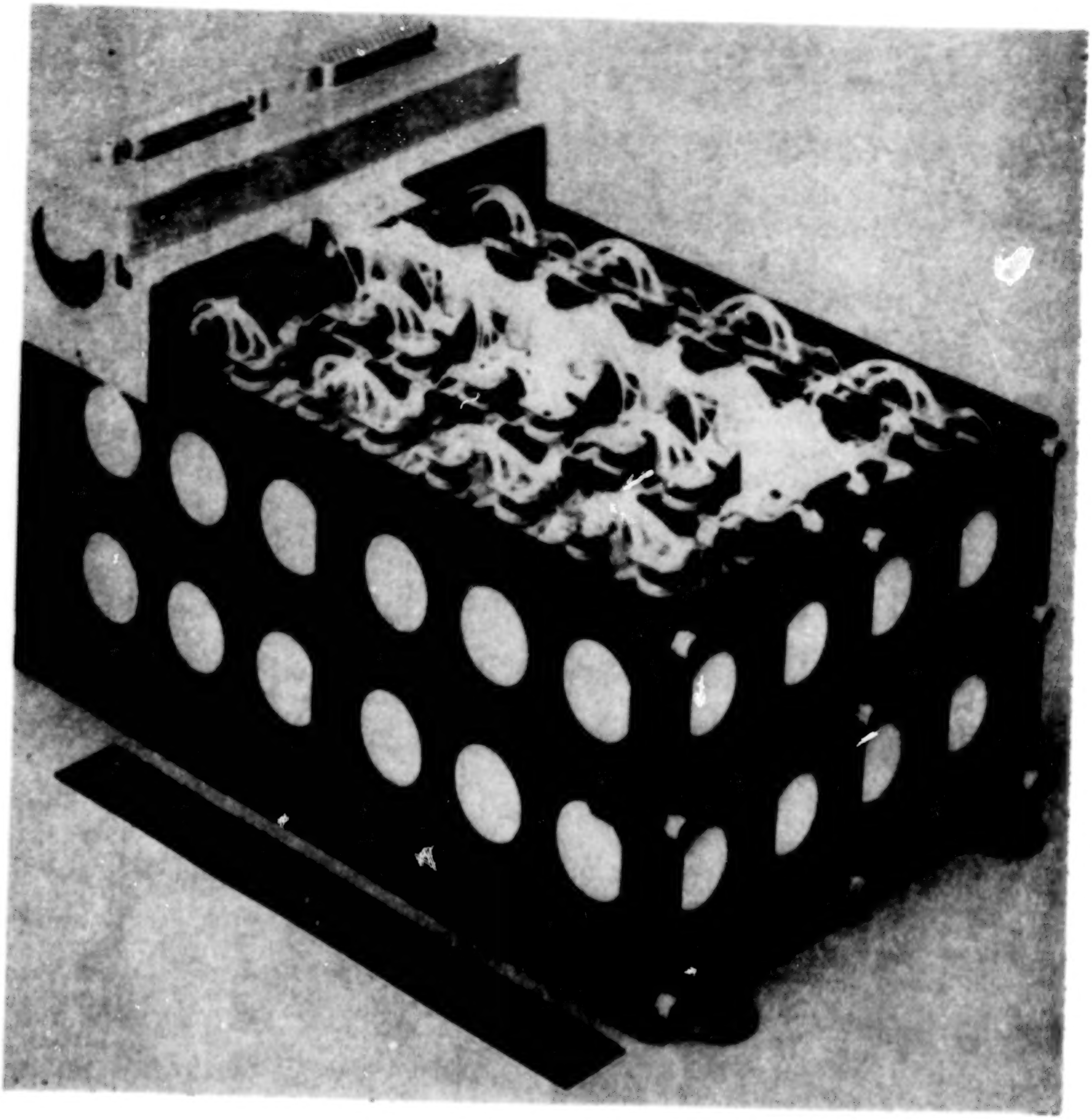

Figure 1.

IUE Spacecraft
Battery Recharge Characteristics
Eclipse Season 12
Day 13

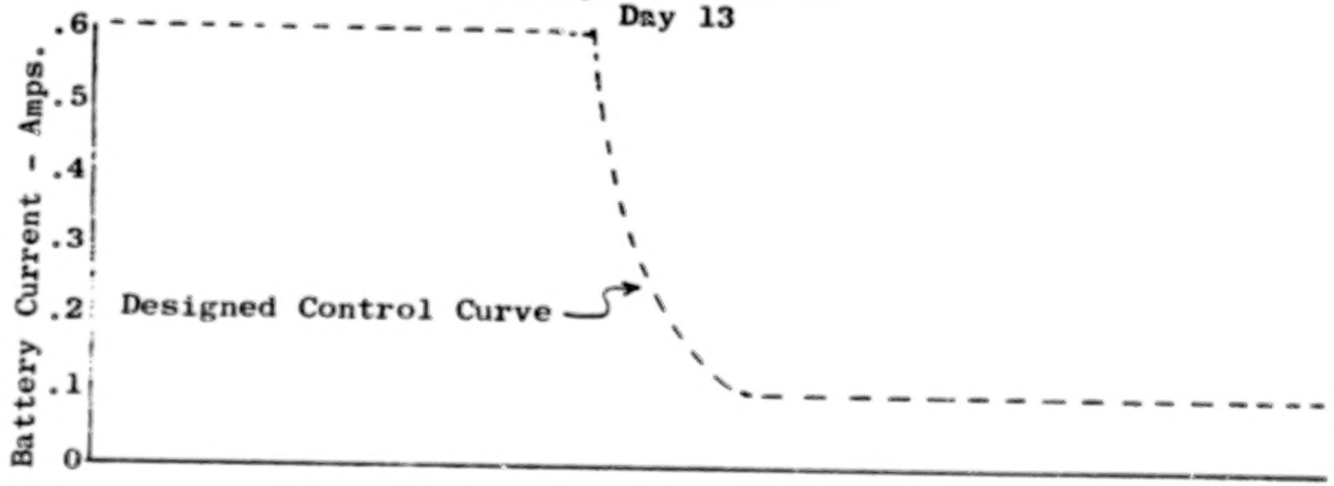

Figure 2a

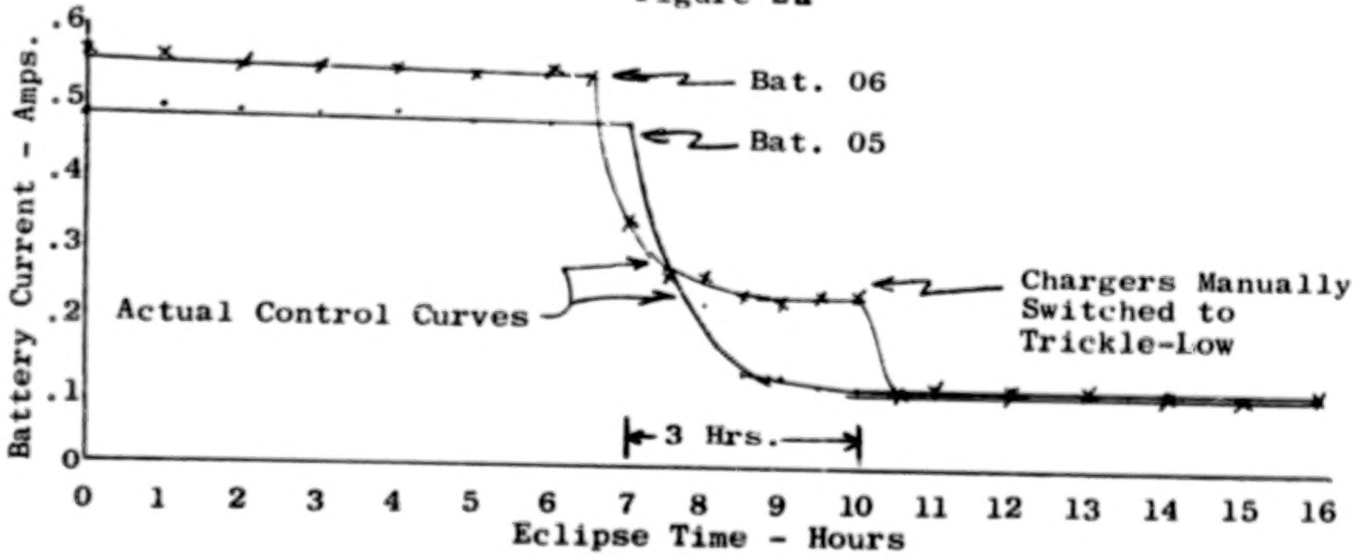

Figure 2b

IUE Test Cells Capacity Vs
Normalized Battery Voltage At
Low Rate Discharge
10°C

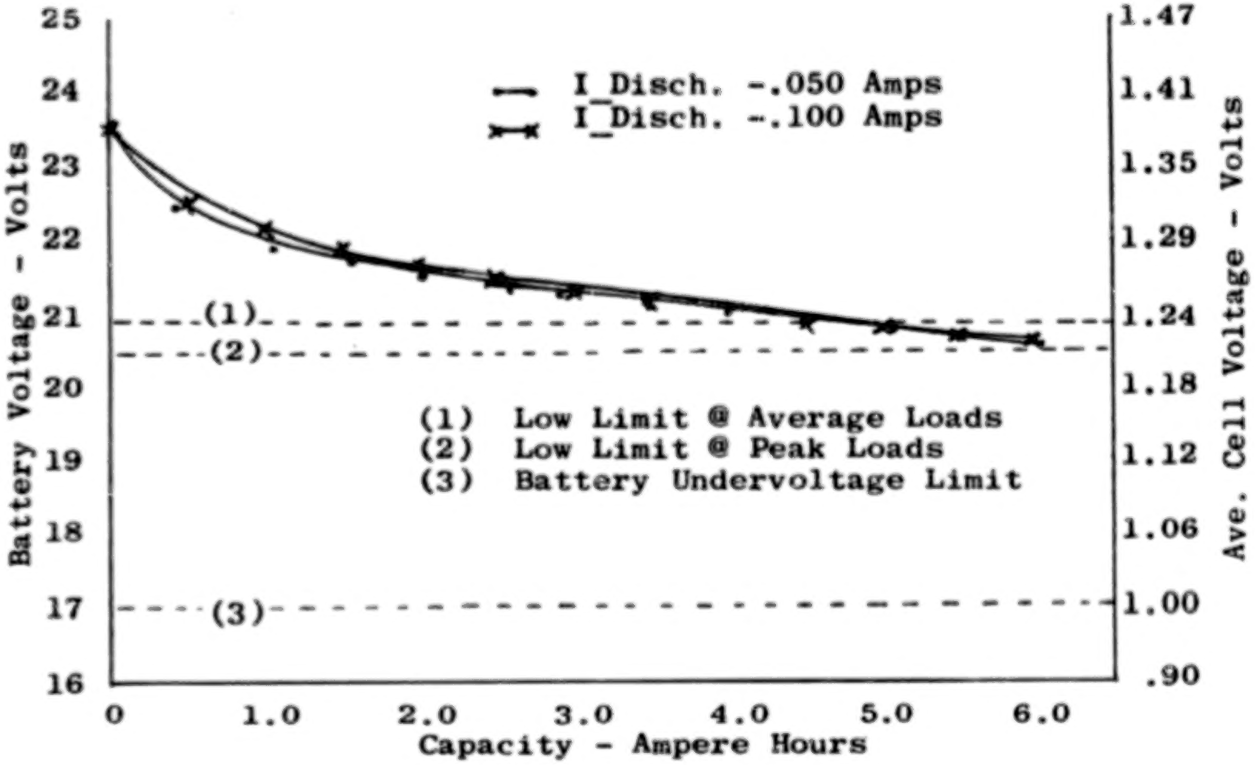

Figure 3

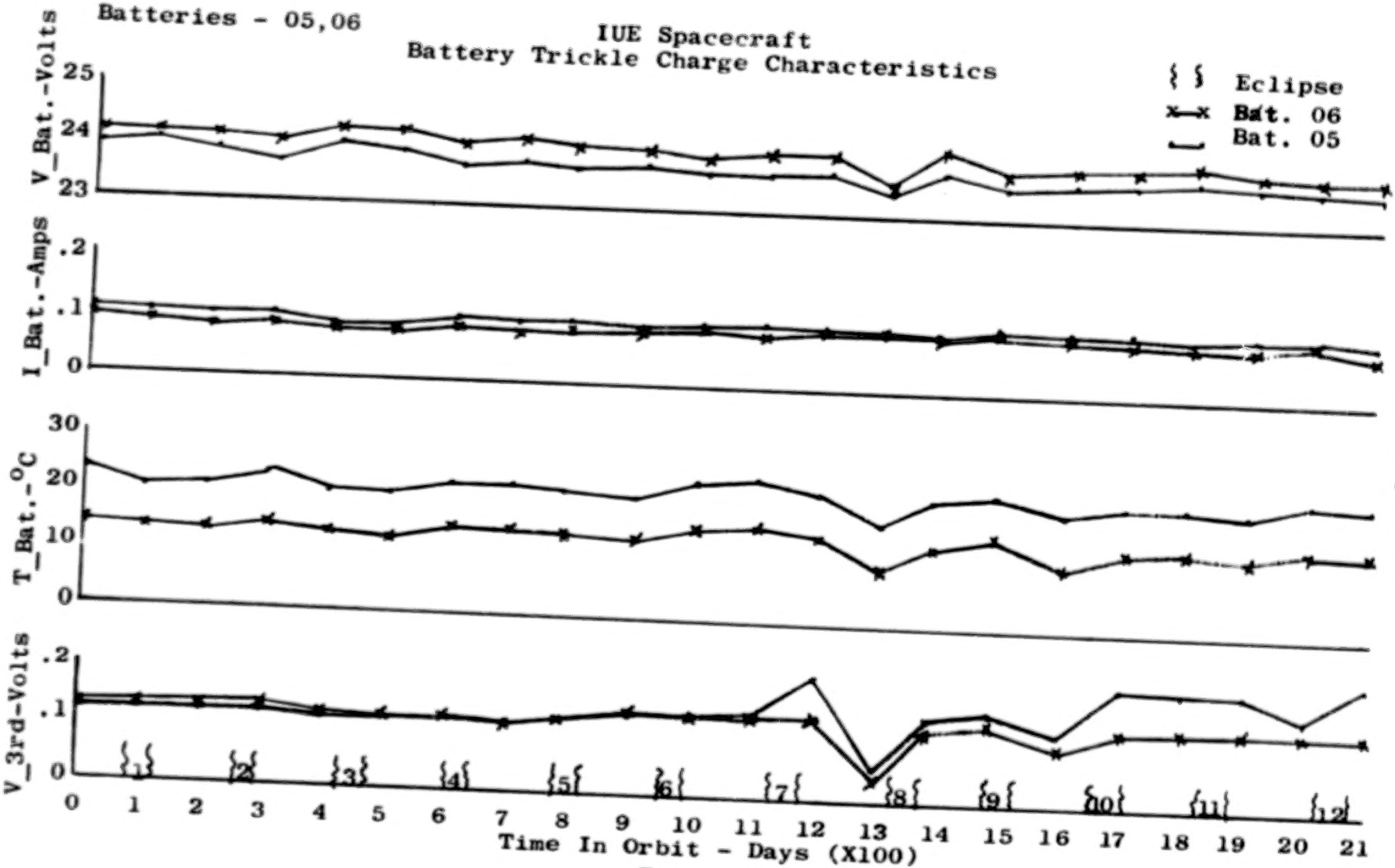

Batteries - 05,06

IUE Spacecraft
Battery Trickle Charge Characteristics

Figure 4

Batteries - 05,06

IUE Spacecraft Battery
(Reconditioning Effects)
Battery Current VS
Eclipse Period Time
Eclipse Season #12

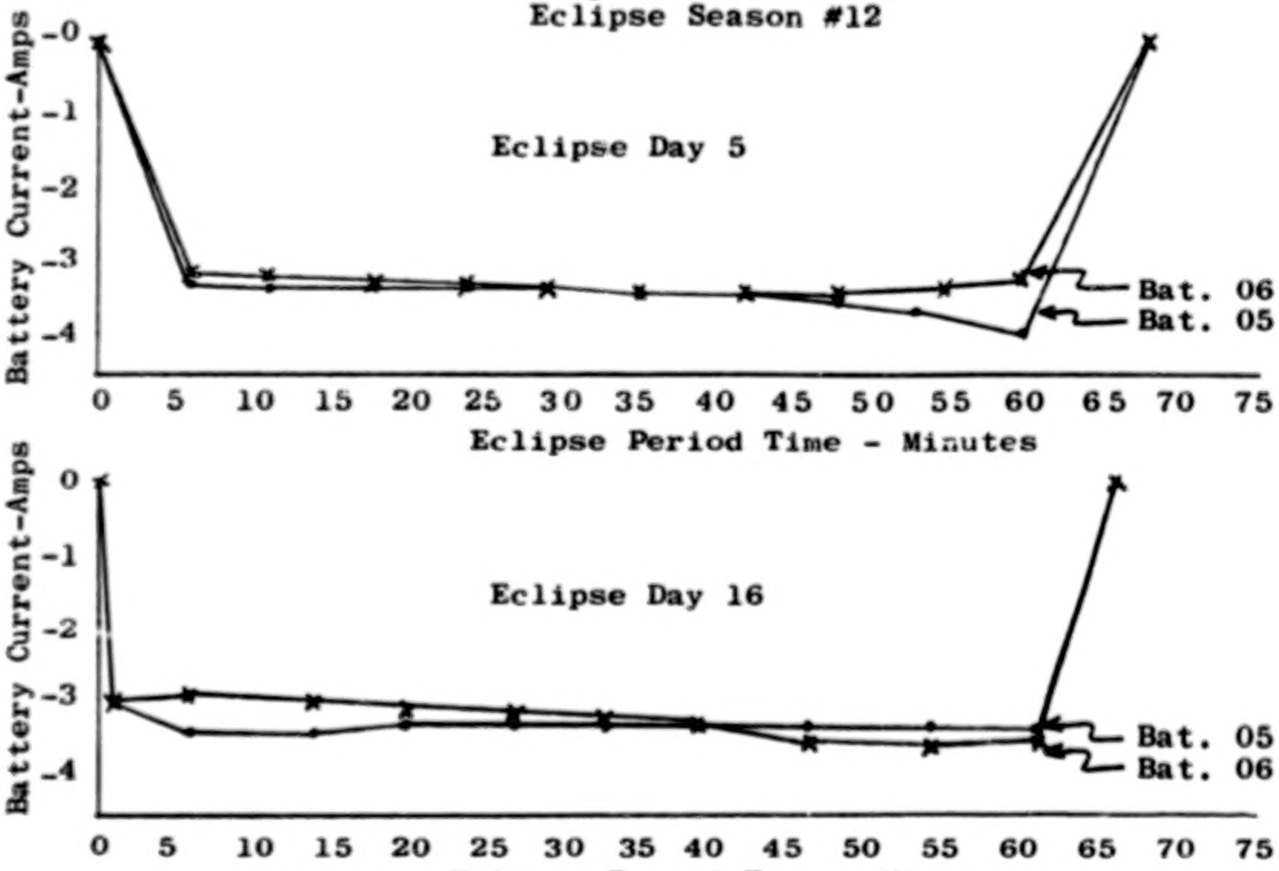

Figure 5

IUE Spacecraft Battery
Available Power And Voltage Vs
Eclipse Seasons
Predicted Performance
At 80% D.O.D.

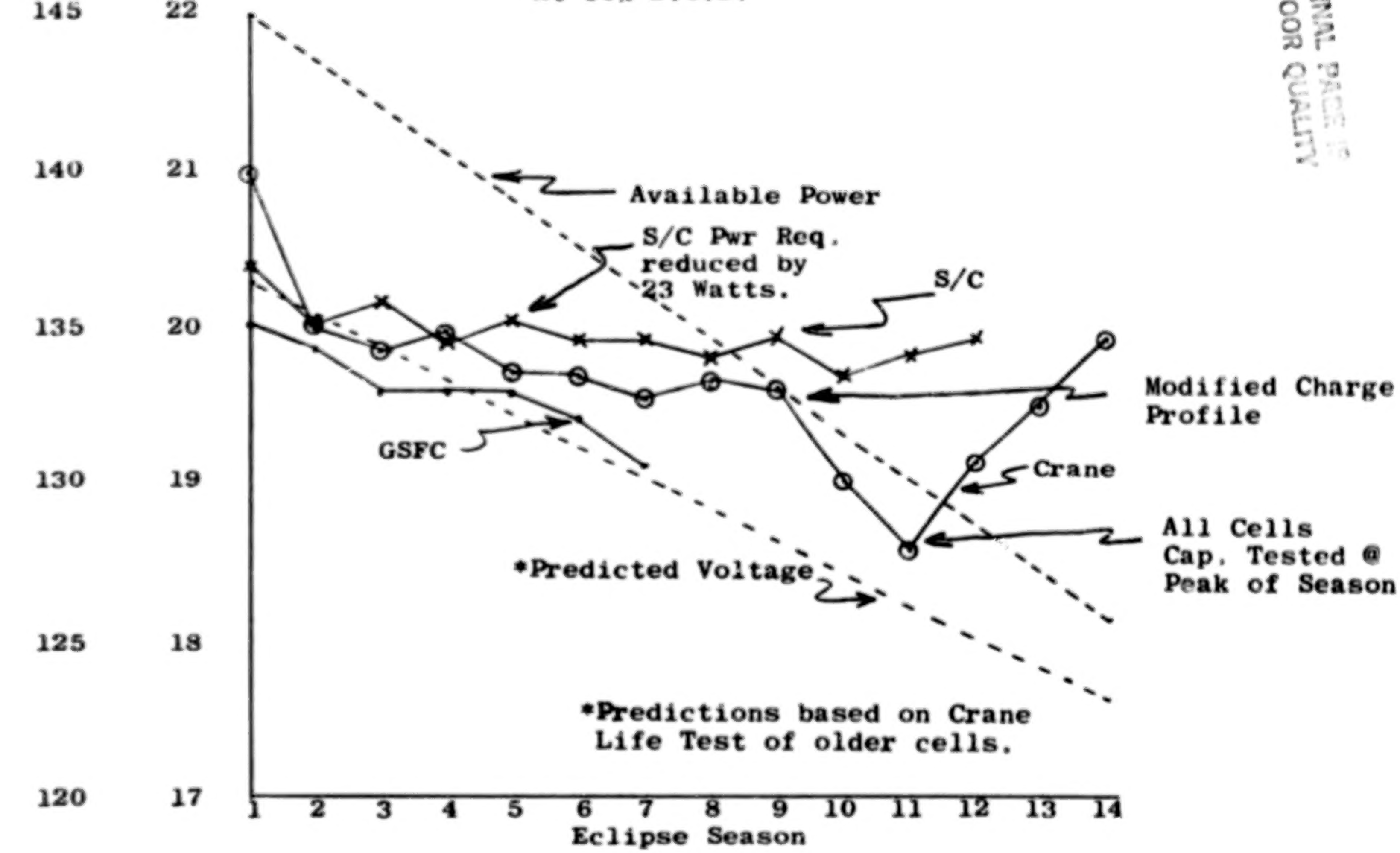

Figure 6

IUE Spacecraft
Peak Battery Discharge Voltage Vs
Day In Eclipse

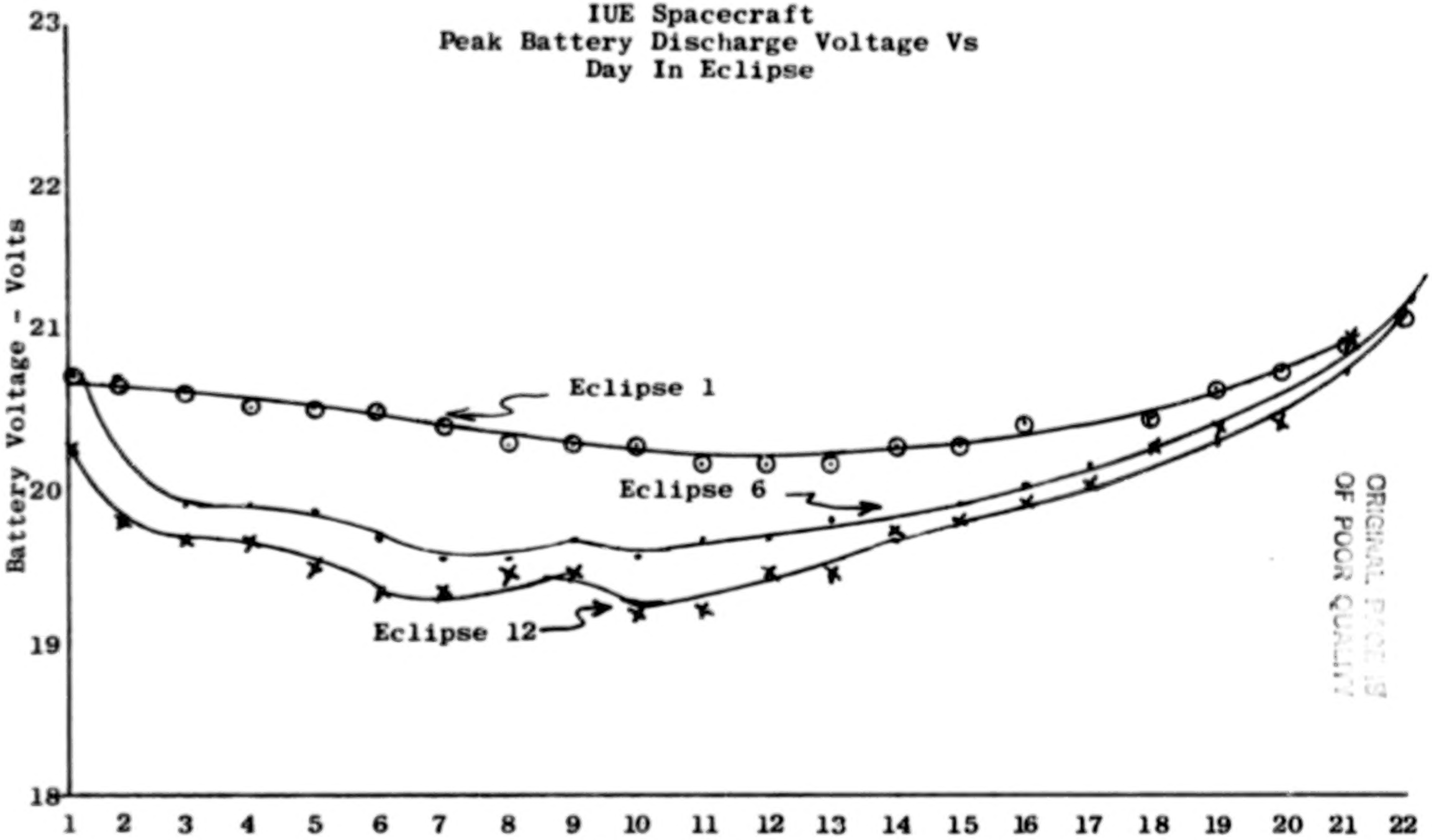

Figure 7

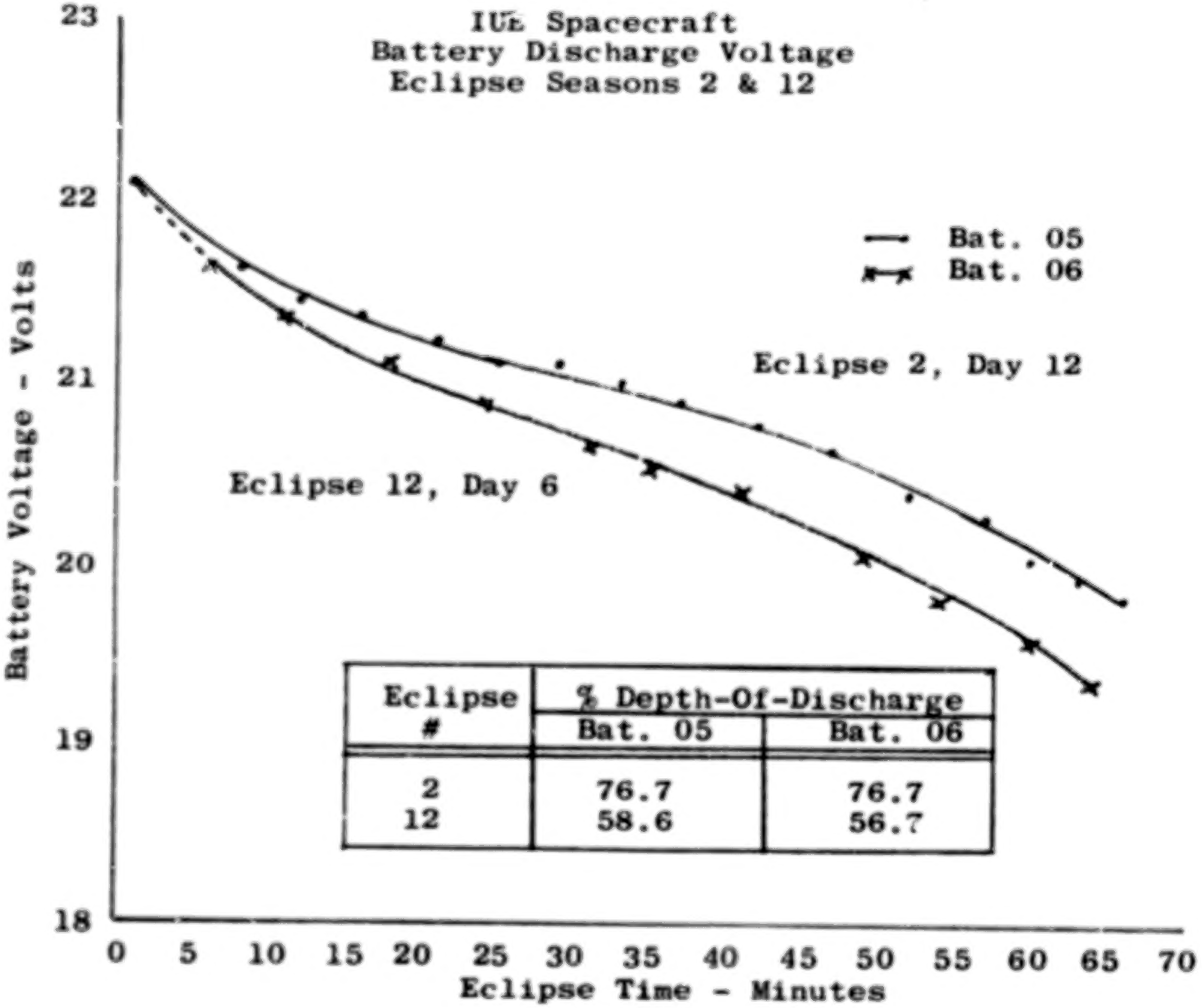

Eclipse #	% Depth-Of-Discharge	
	Bat. 05	Bat. 06
2	76.7	76.7
12	58.6	56.7

Figure 8

Q. Russell, Space Communications Company: When your batteries are used to supply the spacecraft power do you have to command them into service or does it happen automatically?

A. Tiller, GSFC: It happens automatically. The batteries are on line all the time so it just automatically picks it up if they should slue the spacecraft to an angle that we lose data acquisition the batteries automatically since they are connected to the main bus automatically that go into operation.

N84
33693

UNCLAS

N84 33693 D25

MANAGEMENT AND PERFORMANCE OF APPLE BATTERY IN HIGH TEMPERATURE ENVIRONMENT

M. S. Suresh
A. Subrahmanyam
B. L. Agrawal
ISRO Satellite Centre
Bangalore, India

ABSTRACT

India's first experimental communication satellite, APPLE, carried a 12 AH Ni-Cd battery for supplying power during eclipse. Failure to deploy one of the two solar panels resulted in the battery operating in a high temperature environment—around 40 C. This also resulted in the battery being used in diurnal cycles rather than just half yearly eclipse seasons. This paper describes the management and performance of the battery during its life of two years. An attempt to identify the probable degradation mechanisms is also made.

INTRODUCTION

APPLE (Ariane Passenger Payload Experiment) spacecraft was launched by Ariane LO3 on June 19, 1981. This was a 380 Kg (in orbit mass) three-axis stabilized satellite parked at 102 E longitude and designed for a two-year life to conduct communication experiments. The power system was comprised of two deployable, sun-tracking solar panels supplying 250 watts of power to a regulated 28 volt bus. A 12 AH, 16 cell Ni-Cd battery was employed to supply eclipse, transfer orbit, and peak loads. Figure 1 shows the block schematic of the power system.

The battery charge path had two chargers—one for the transfer orbit phase and the other for the on orbit phase. The on-orbit charger was a fixed 2 ampere charger with the 8-level voltage-limited auto and manual control for the changeover to a 350 mA trickle charge. The transfer orbit charger was a variable current charger which maintained the bus voltage at 23 volts or 28 volts as selected by ground command, and thereby pumping all the extra current into the battery. Control of the transfer orbit charger was also possible by the 8-level voltage limit or by ground command. However, the transfer orbit charger opened the charge path once the battery was completely charged.

BATTERY DESIGN

The battery was a single, 16 cell, 12 AH battery supplied by SAFT, France. The cell case was, in fact, identical to that of the 10 AH cell, and cells with a slightly higher loading were selected to achieve the capacity of 12 AH. The design parameters and constructional details of the battery are given in Tables 1 and 2. The cell details are provided in Table 3. The battery was designed for an operational life of two years at 72% maximum depth of discharge, thereby undergoing four

PRECEDING PAGE BLANK NOT FILMED

eclipse seasons. Complete reconditioning was not envisaged in view of its short life, and limited reconditioning to about 17.6 volts was possible by proper choice of charger and control combinations.

Table 1

Battery Design Parameters

Capacity	12 AH
Number of cells in series	16
Operating voltage range	19-24 volts
Temperature range of operation	0 C-25 C (Average 20 C)
Peak depth of discharge	72%
Operating life	2 years - 180 cycles (4 eclipse seasons)
Charge current onorbit	1.8 0.2 Amps
Transfer orbit	0 to 5 Amps
Trickle charge current onorbit	120 10 mA
Transfer orbit	0 (No trickle-battery open)
Discharge current	6 Amps
Expected EOL capacity	9.5 AH
Expected EOL discharge Voltage	18.6 volts at the end of 70% discharge
Thermal control	Passive

Table 2

Battery Details

Battery type	Nickel Cadmium
Capacity	12 AH (Nominal)
Dimensions	225 x 135 x 225 mm
Mass	9.3 Kg
Thermal cutout	35 2 C
Temperature sensor	4K thermistors (two)
Cell type	VO 10 S2
Vendor	SAFT, France
Cell bypass diodes	Provided
Heaters	5 Watts (two)
Mounting	Under the ABM strut on the bottom deck

Table 3

Cell Details

Cell type	VO 12 S2
Capacity	12 AH
Mass	490 gms
Dimensions	85 x 29.2 x 76.2 mm
Positive Electrode Number	12
Thickness	0.76 mm
Loading	13.2 gm/dm^2
Negative Electrode Number	13
Thickness	0.89 mm
Loading	17.5 gm/dm^2
Negative to Positive Ratio	1.8
Case Thickness	0.4 mm
Negative Treatment	None
Inter-electrode Distance	0.26 mm
Separator	Villidon 2119
Electrolyte	KOH
Specific Gravity	1.306

Figure 2 shows the life predictions by SAFT for their cells and it is seen that the design was adequate to meet the two-year life goal at 20 C with 0.99 reliability. The thermal control of the battery was passive control backed up by two heaters.

ORBIT OPERATION

The spacecraft was put into synchronous orbit on the sixth transfer orbit, but the north solar panel could not be deployed resulting in covering a large area provided for thermal control. The battery temperature thus attained very high values. Another problem also arose as a consequence. As can be seen from the power system schematic, certain heater loads were directly connected onto the battery apart from the emergency and power control loads. It was envisaged in the design that the charger current in the trickle charge mode be set to 500 mA which 370 mA was assigned to the loads and 130 mA for charging the battery. However, due to the thermal problems, these heaters were not switched ON regularly and about 350 mA was flowing into the battery. In trickle charge mode, this would be wasted as heat resulting in the battery attaining a higher temperature. It was thus decided to change over to the transfer orbit charger in trickle mode, subsequent to the charging by the on-orbit charger. Since the transfer orbit charger in trickle mode opens the charge path, a small amount of discharge (120 mA) was experienced by the battery. During the non-eclipse seasons, thus, the battery was discharged daily to about 19.8 volts at 120 mA and was charged subsequently at a time when the temperature was low, ie., around 5 UT.

The battery was thus subjected to diurnal cycles apart from the eclipse cycles. The operating temperatures were too high from any standards for a battery. Reduced generated power due to the nondeployment of one solar panel did not cause much problem as the margin available was large but the thermal problems were acute. The eclipse loads were reduced to a minimum to enhance the life of the battery. The maximum discharge was about 3 AH during the peak eclipse at 2.5 A rate and during the non-eclipse season it was about 2 AH at 0.12 A rate.

In Figure 3, battery voltage, current, and temperature are plotted for one complete day, September 20, 1981, a day on which the eclipse duration was 64 mins. It is obvious that the battery spends most of the time with low discharge in the transfer orbit trickle charge mode. Prior to and soon after eclipse, the battery was charged.

Table 4 lists the major events in the life of the battery in chronological order. The battery was not reconditioned prior to the first and second eclipses. Before the third eclipse, limited conditioning was done. Perhaps, it is more appropriate to call them just deep discharges as the battery was discharged only up to 19.5 volts at 300 mA. The problem about reconditioning was that manual control of charge/discharge was possible only with the redundant charger system and when all the main systems were working satisfactorily, changeover to the redundant system was not advisable. Only prior to the fourth eclipse season a meaningful reconditioning was possible and even then the discharge was not complete as the battery was required to supply peak power to the momentum wheel assembly.

Table 4

Major Events In The Life Of The Battery

Launch	June 19, 1981
Orbit acquisition	June 22, 1981
First eclipse season	August, September 1981
Second eclipse season	February, March 1982
Limited reconditioning	August 11, 1982
Third eclipse	August, September 1982
Reconditioning after change-over to redundant systems	February 17, 1983
Fourth eclipse season	February, March 1983
Reconditioning cycle	August 16, 1983
Fifth eclipse season	August 24, 1983
End of mission	Spetember 12, 1983

In the reconditioning performed on February 17, 1983, discharge was up to 18.7 volts in the first cycle and up to 18.5 volts in the second cycle. Discharge beyond 18.5 volts was not attempted as the eleventh cell voltage reached 0.7 volts, whereas the other cell voltages were still above 1.15 volts. The charge/discharge characteristics of these two cycles are shown in Figure 4. The improvement in the characteristic is evident.

Before the fifth eclipse season, three reconditioning cycles were completed but this time reconditioning was done, rather inadvertantly, down to 17.1 volts. The fifteenth cell reversed to -0.16 volts for a few minutes. Figure 5 shows the charge/discharge cycles. The improvement in capacity from 5 AH to 6.5 AH and improvement in the voltage performance are clearly evident.

C-5

On September 12, 1983, during the fifth eclipse season, soon after an eclipse, the solar panel failed to track the sun resulting in a total discharge of the battery down to zero volts. This was the first opportunity when the battery capacity was measured at normal discharge rate of 2.5 amps. During this discharge, the battery delivered 6.25 AH down to zero volts. The 12 AH battery had degraded by 50%! Considering the extremes of strain to which the battery was subjected, this was a remarkably good performance.

BATTERY PERFORMANCE

Figures 6 and 7 show the variation of the battery temperature. Figure 6 shows the diurnal variation for days which are approximately six months apart and Figure 7 shows the variation of the maximum and minimum temperatures over its life. The days selected in Figure 6 correspond to the minimum temperature encountered by the battery during the equinoxes and the maximum temperature during the winter solstice. It is observed that for most of the time, the battery temepratures were above 30 C and for a considerable time, above 40 C, reaching a maximum of 55 C on certain days (not shown in the figure). Increase in the battery temperature over its life was also due to the degradation of the passive thermal control elements - OSR. Consequent to this, a crucial problem regarding battery management was the setting of the voltage at which the battery should change over from charge to trickle charge. Improper setting would result in the battery getting either grossly undercharged or overcharged. No data is available regarding battery performance at temperatures above 30 C making predictions almost impossible.

Table 5 summarizes the details of the performance of the battery during the four eclipse seasons. The battery temperature during charge was maintained within a degree. The post-eclipse end-of-charge voltage varied from 22.83 volts to 23.13 volts. These values are the forced values rather than the values that would have been attained had the battery been allowed to charge completely under normal circumstances. In fact, it is evident that during the third and fourth eclipse seasons the battery was not charged completely. However, the battery was charged sufficiently before every eclipse to supply the required 3 AH of discharge.

A comparison of the change in the charge voltage can be made by examining the battery charge characteristics during reconditioning before the fourth and fifth eclipse seasons—refer Figures 4 and 5. During reconditioning the charging was done in the manual mode and the battery was charged until it definitely showed signs of overcharge. During the first reconditioning, the battery charge voltage was 23.25 volts and during the second reconditioning, 24.75 volts. These two values correspond to temperatures of about 31 C. End-of-charge voltages on average cell basis correspond to 1.55 volts during the second reconditioning. This was rather unexpected and clearly shows a significant increase in the over potentials—increase in the internal resistance. The charge characteristic also is very much different from what one would normally expect at this temperature—not flat and sharply rising while nearing end-of-charge. The over charge factors calculated from these cycles are around 1.2.

If one looks at the discharge characteristics—refer to Figure 8—one cannot figure out much, as there is hardly any change in them from the first eclipse season to the fourth eclipse cycle. Our first opportunity to measure the capacity was during the first reconditioning cycle before the fourth eclipse season. For a discharge rate of 0.3 amps, the capacity down to 18.4 volts (1.15 volts/cell) was 6 AH. In the second reconditioning cycle, the battery delivered 6.25 AH at the same rate. The actual details of the discharge cycle are shown in Figure 9.

Figure 10 compares the discharge characteristics with those of the fresh battery, as determined by ground tests prior to launch. Superposed over its characteristics are the discharge characteristics during the first eclipse and the last discharge cycle. It is observed that up to 2.5 AH discharge, there is absolutely no voltage degradation.

CONCLUSIONS

In conclusion, one can observe the following degradation modes:

(a) Very high end-of-charge voltage—1.55 volts—an abnormal value for this high operating temperature.

(b) Reduction in the battery capacity by about 50%.

(c) No appreciable discharge voltage degradation up to 2.5 AH, but a sudden fall subsequently.

Abnormal end-of-charge voltages indicate very high internal impedance due to the hydrolysis of the separator resulting from operation at high temperatures. This could also partly be due to electrolyte redistribution. The charge characteristics also indicate a significant loss of negative electrode capacity, approaching negative capacity limitation. The loss in capacity is due to the combined effects of separator hydrolysis and electrode degradation.

The surprising fact is the non-appearance of voltage degradation. Considering the fact that the battery has undergone 730 diurnal cycles in addition to the eclipse cycles and without proper reconditioning, this is remarkable.

ACKNOWLEDGEMENTS

The authors are grateful to Mr. S. Kini for the assistance provided during all the tests conducted on the battery.

The authors are also grateful to Mr. R. Ashiya, Head Electronics Division and Director, ISAC, for their constant encouragement and permission to publish this paper.

Table 5

Battery Performance During Eclipse Seasons

Eclipse Season	Date	Eclipse duration minutes	Eclipse discharge AH	End of discharge voltage	Post eclipse charging: End of charge voltage	Post eclipse charging: End of charge temperature	Post eclipse charging: Charge input AH	Remarks
1	Sept.20, '81	64	2.7	19.43 1.214/ cell	22.83 1.427/ cell	20°C	3.1	
2	Mar. 20, '82	69	2.9	19.53 1.22V/ cell	23.13 1.45V/ cell	28.3°C	2.9	
3	Sept.18, '82	70	2.92	19.04 1.19V/ cell	23.13 1.45V/ cell	28.7°C	2.75	
4	Mar. 8, '83	66	2.75	19.14 1.196V/ cell	23.13 1.45V/ cell	31.5°C	2.7	Battery conditioned before eclipse

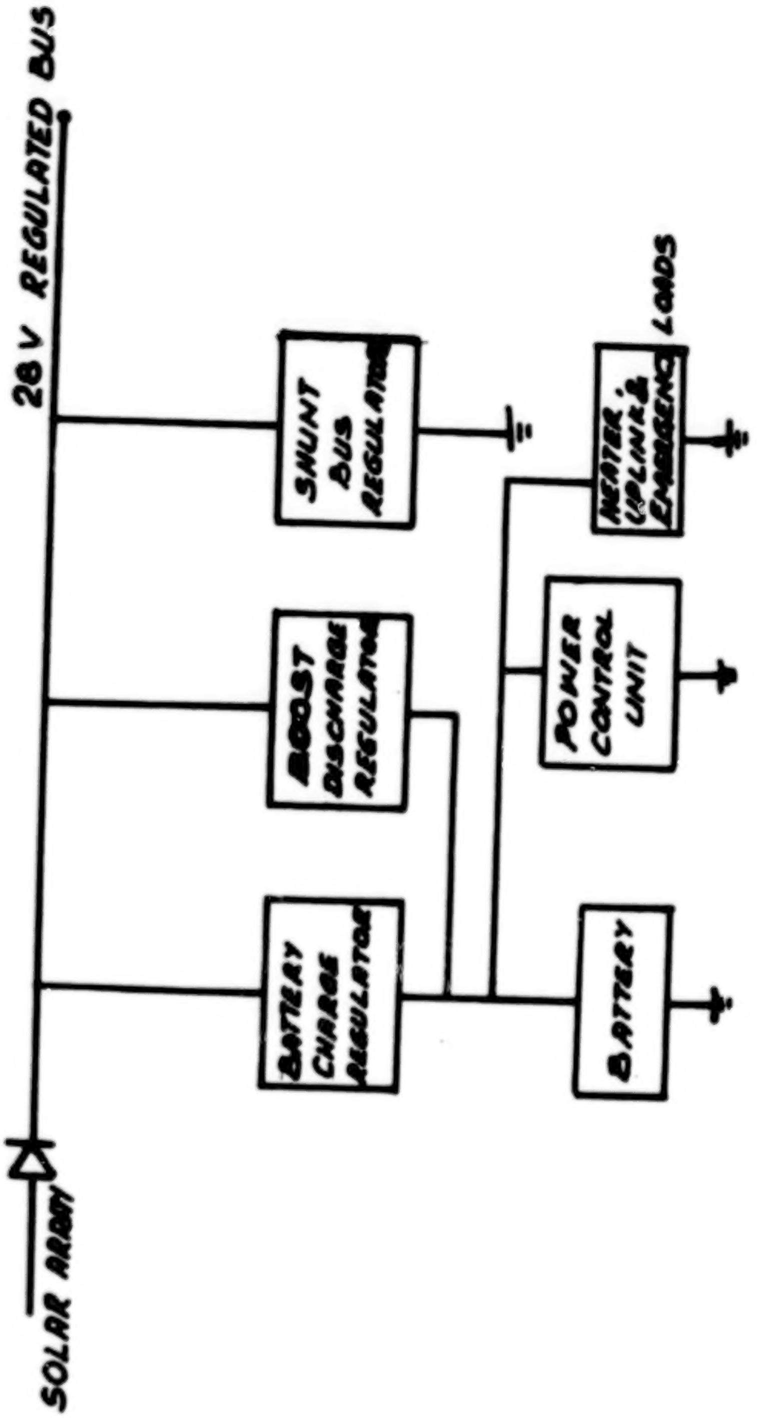
28 V REGULATED BUS
SOLAR ARRAY
BATTERY CHARGE REGULATOR
BOOST DISCHARGE REGULATOR
SHUNT BUS REGULATOR
BATTERY
POWER CONTROL UNIT
HEATER, UPLINK & EMERGENCY
LOADS

Figure 1. Apple power system schematic.

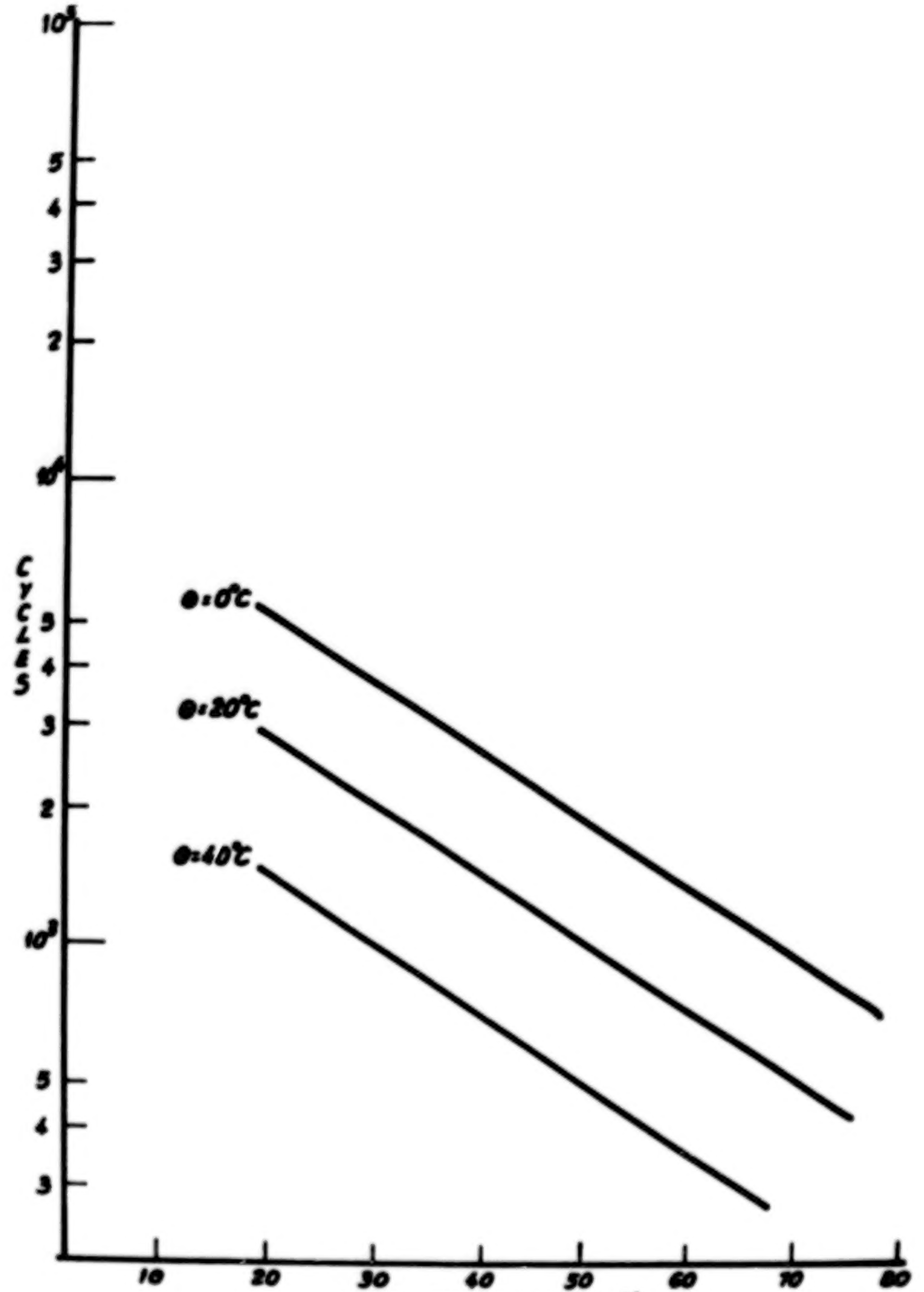

Figure 2. Life expectancy of Ni-Cd cells 24h orbit.

ORIGINAL PAGE IS
OF POOR QUALITY

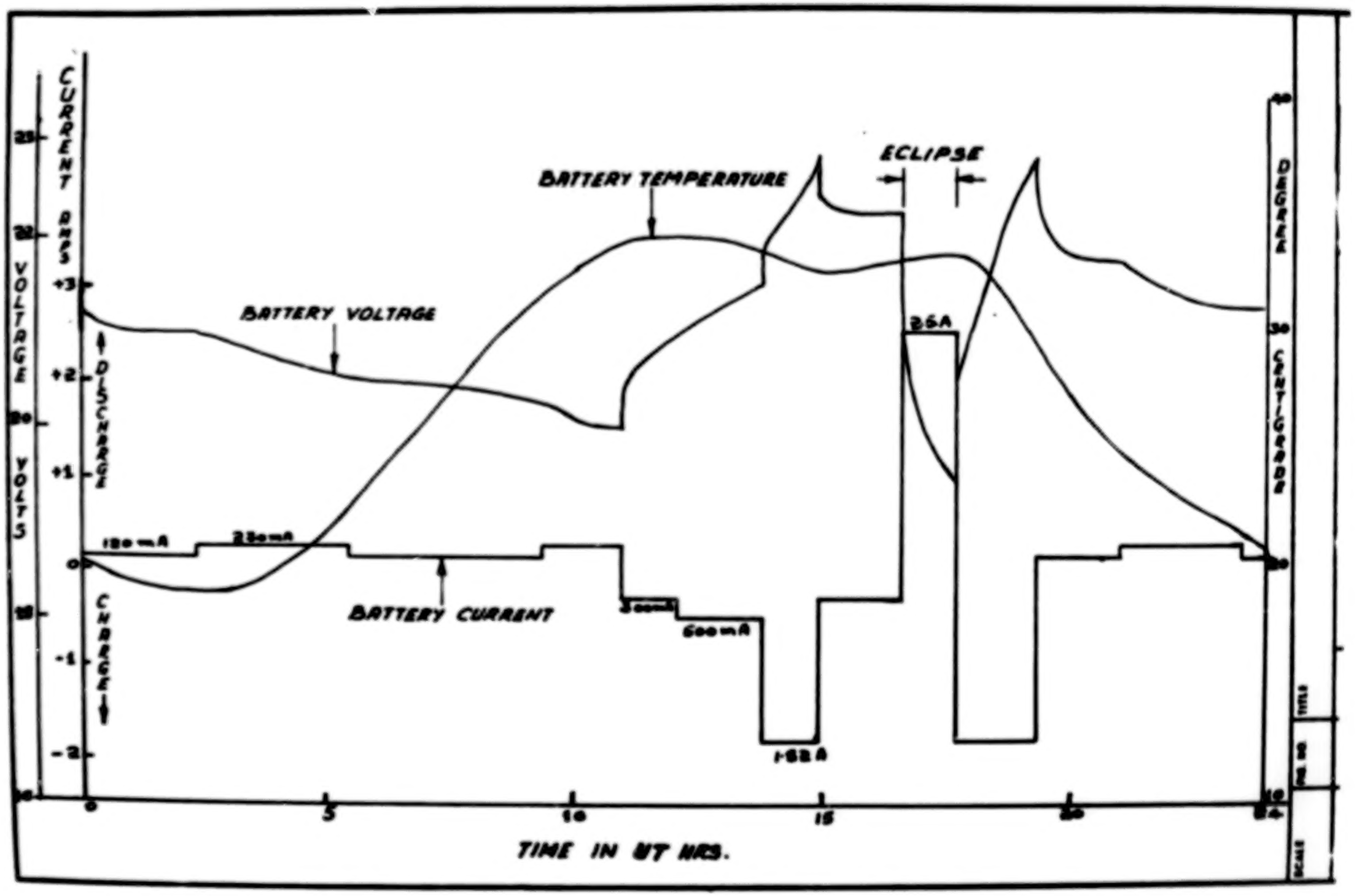

Figure 3. Battery Diurnal cycle (Sept.20, 1981).

ORIGINAL PAGE IS
OF POOR QUALITY

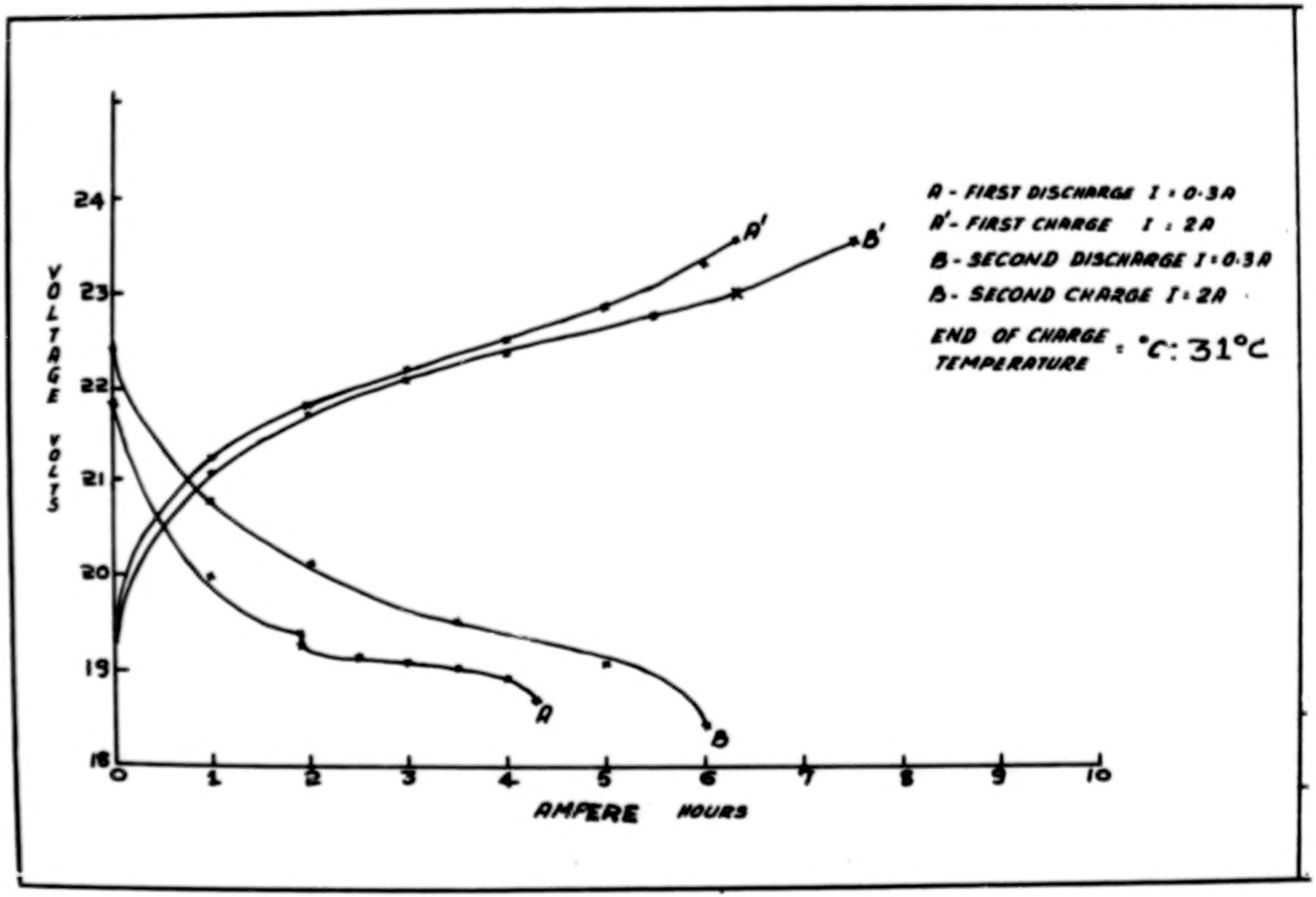

Figure 4. First reconditioning (before 4th eclipse).

ORIGINAL PAGE IS
OF POOR QUALITY

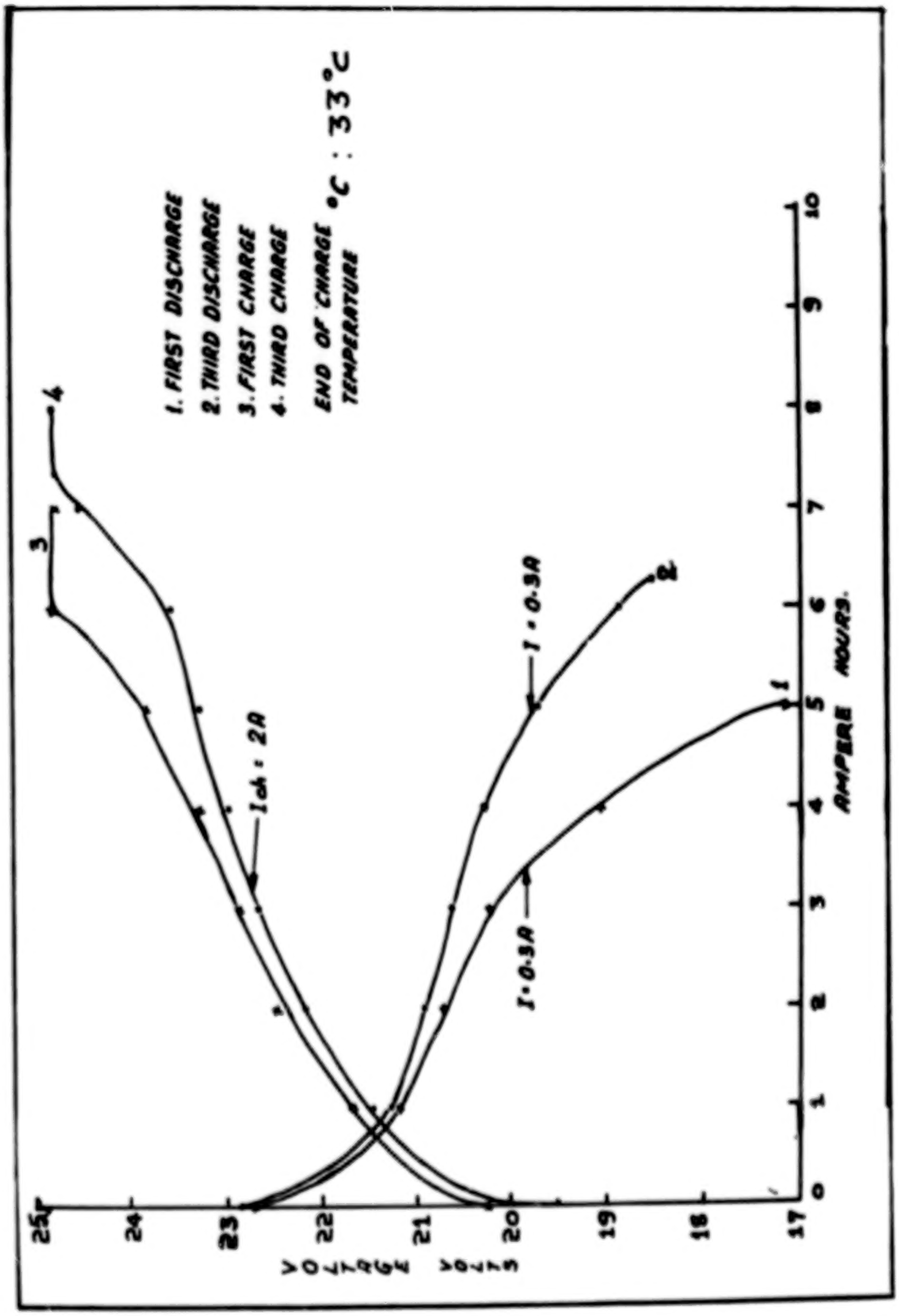

Figure 5. Second reconditioning (before 5th eclipse).

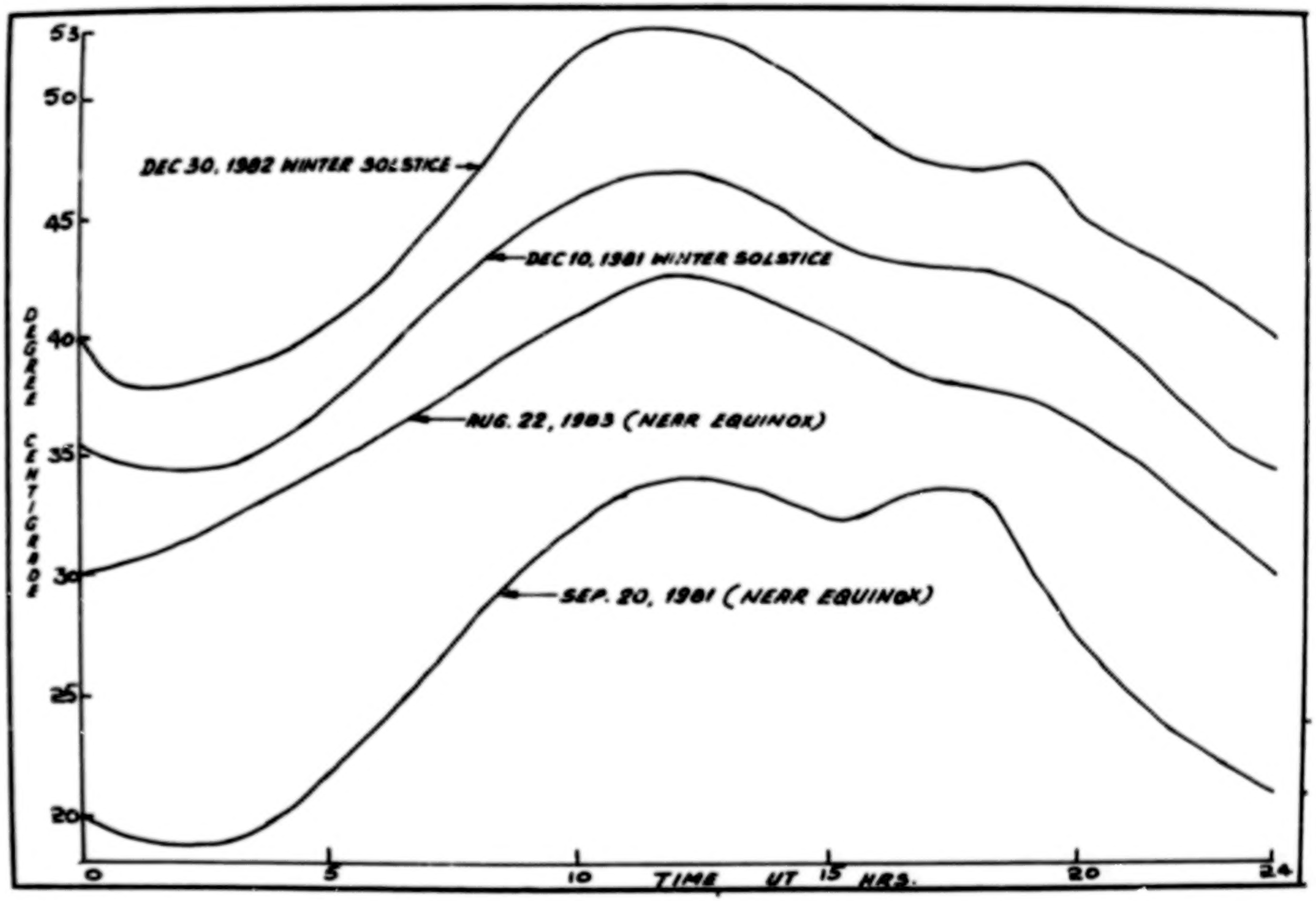

Figure 6. Diurnal variation of battery temperature.

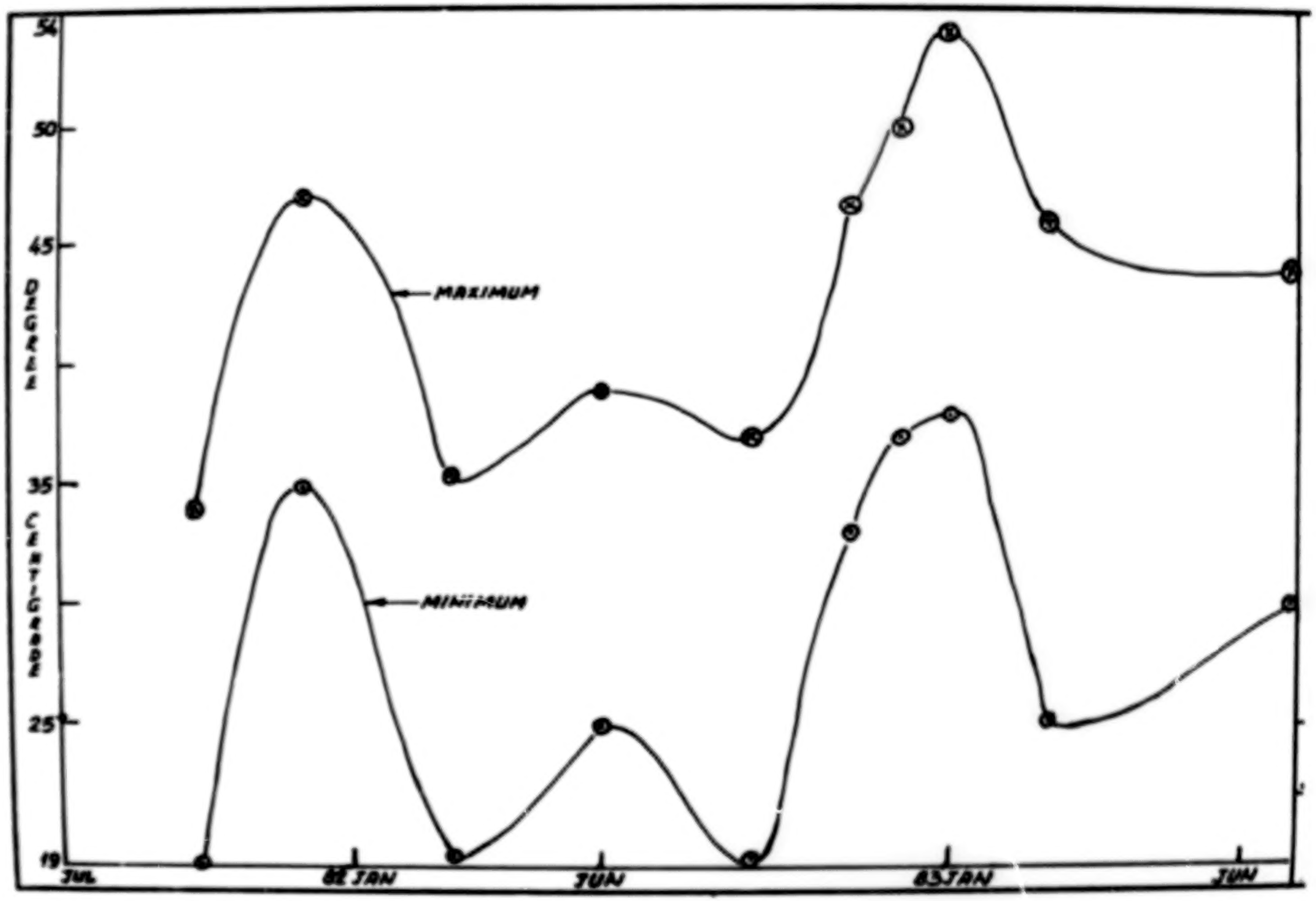

Figure 7. Variation of maximum & minimum temperature over life.

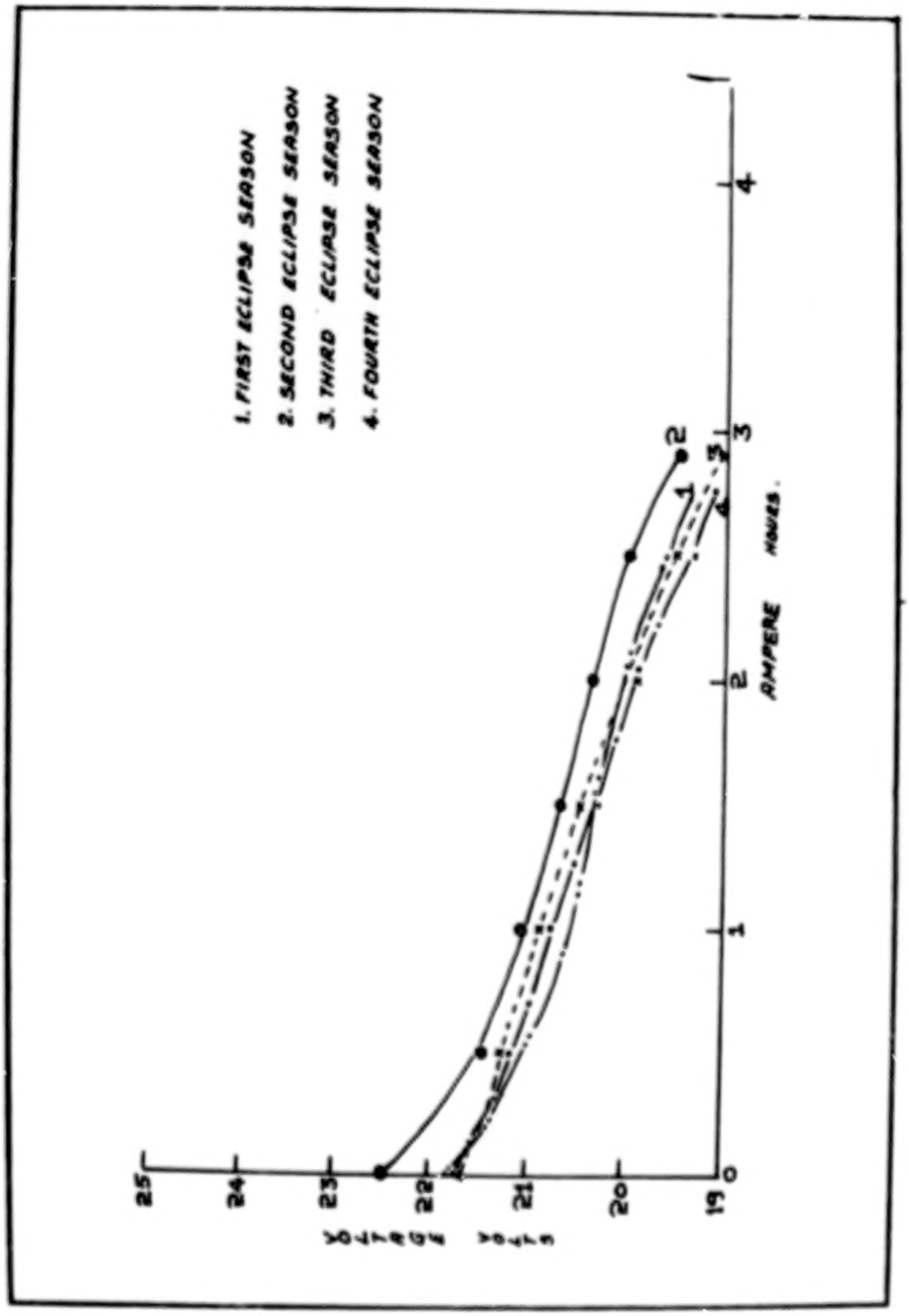

Figure 8. Eclipse discharge characteristics.

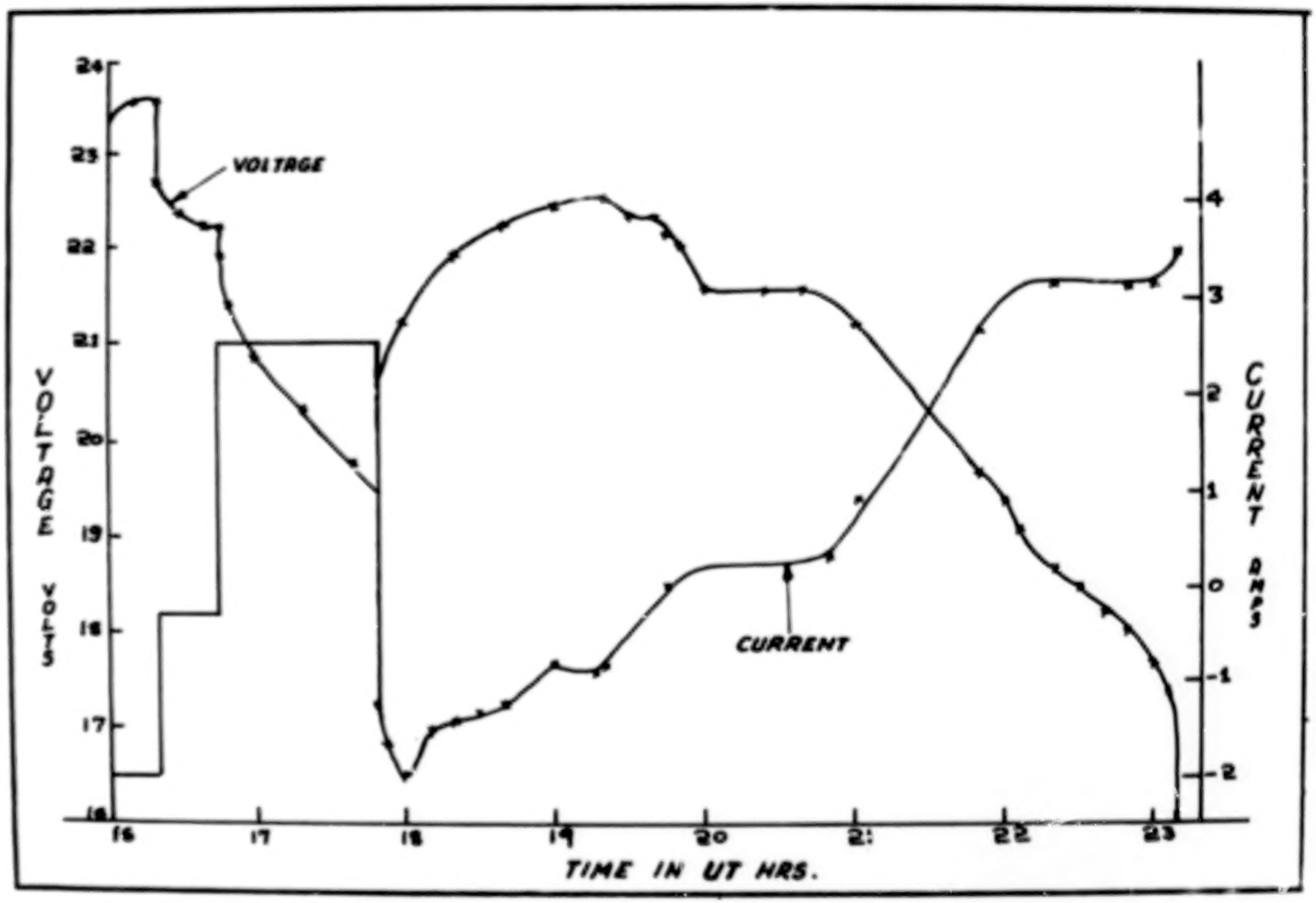

Figure 9. Final battery discharge (Sept.12, 1983).

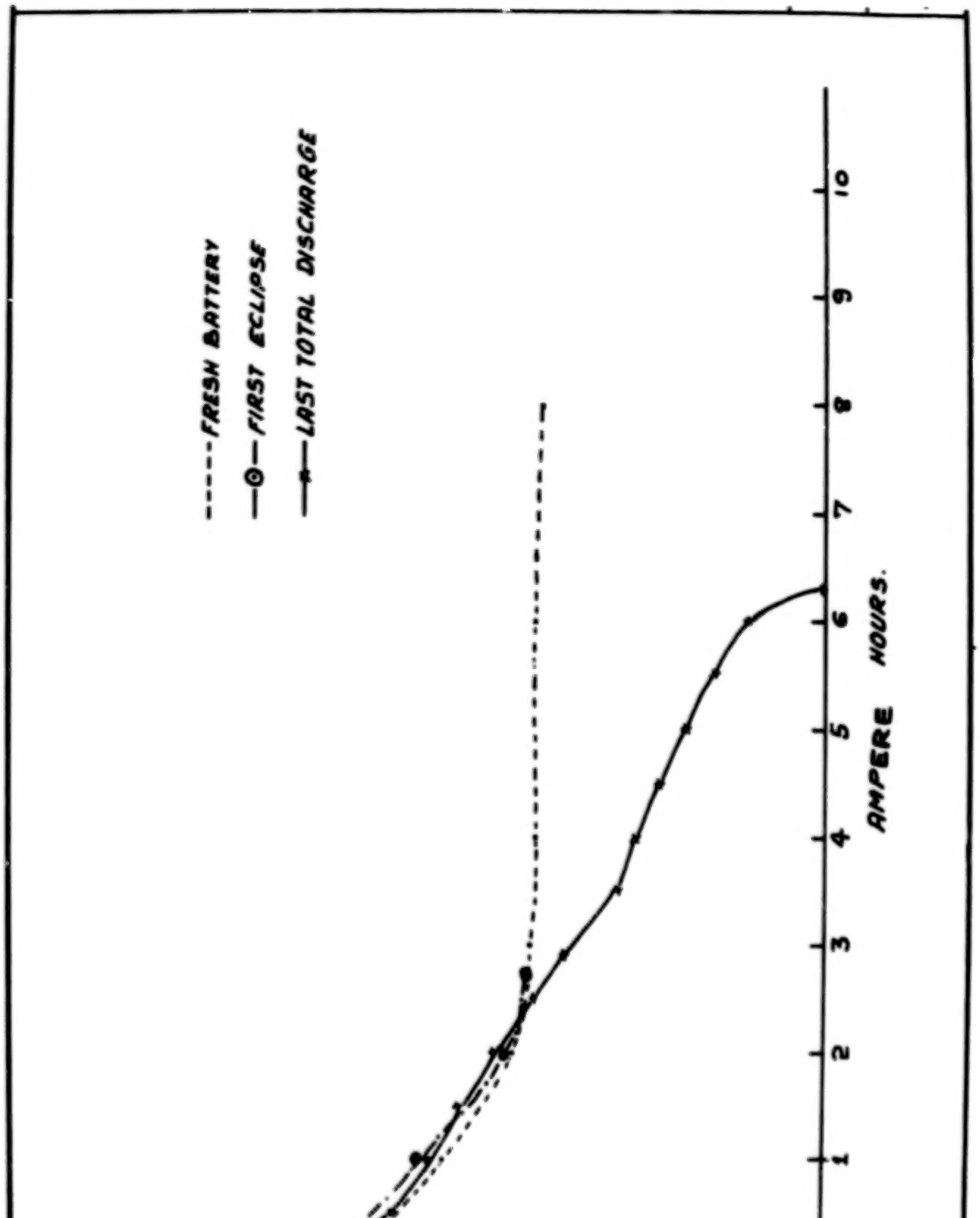

Figure 10. Comparison of discharge characteristics.

N84
33694

UNCLAS

N84 33694

D26

COMPARISON OF STANDARD AND HEART-PACER TYPE 3RD ELECTRODES IN DESIGN VARIABLE CELLS

George W. Morrow
NASA/GODDARD SPACE FLIGHT CENTER

ABSTRACT

Nine packs of General Electric (G.E.) sealed aerospace nickel-cadmium cells were put on life test at the Naval Weapons Support Center in Crane, Indiana in February 1979 under the Design Variable Program. Each 5 cell pack contained one cell with a standard sensor signal electrode and one cell with a new heart-pacer sensor signal electrode. Testing was discontinued in May 1983 and the signal electrode performance data was studied. It was found that the heart-pacer electrode generally provided a greater voltage swing over a cycle; that both types of electrodes lost significant sensitivity during life, and that both types of electrodes show great signal variation from cell to cell.

INTRODUCTION

In 1977, the G.E. Battery Business Department patented a new sensor signal electrode (heart-pacer electrode) for use in sealed aerospace nickel-cadmium cells and announced that this new type would replace the standard signal electrode when existing supplies were depleted. The differences in construction of these electrodes are shown in Table I. Since any change in the manufacture of aerospace Ni-Cd cells requires qualification, a program to test the new electrode was proposed and implemented by David Baer as a part of a larger test program, Design Variables. The cells used in this program were G.E. 12 a-h sealed aerospace Ni-Cd cells. One pack was a control pack with the standard cell construction. The other 8 packs contained cells with various design changes. Testing began at the Naval Weapons Support Center in Crane, Indiana in February 1979 and was discontinued in May 1983. The Design Variable Program Test Regime is shown in Table II. A formal report on the Design Variable Program was given at the 1978 Goddard Battery Workshop.

SIGNAL ELECTRODE TEST RESULTS

In reviewing the data on the signal electrodes it was discovered that both signal electrodes performed consistently in only 3 out of the 9 packs on test, packs 3D, 3G, and 3H. In all other packs, the signal generated by the electrode varied from pack to pack and cycle to cycle in a particular pack. Because of a pressure transducer malfunction in pack 3H, packs 3D and 3G were used for this comparison of performance.

Figure I shows a comparison of the standard and heart-pacer electrode performance in pack 3D near the beginning of life. From the plot it can be seen that the heart-pacer electrode produced approximately a 350 mV signal swing over a cycle while the standard electrode swing was only 100 mV. There was a 113% recharge for that cycle and a pressure delta of 9 psia.

Figure II is a comparison of the signal performance of the 2 electrodes near the end of life. It appears that the standard electrode is now out performing the heart-pacer type, but this performance

PRECEDING PAGE BLANK NOT FILMED

reverse is not as clear cut as it appears and is not indicative of the trend that is shown in the Standard Electrode Life Performance Comparison shown in Figure III. As can be seen, the trend with age was for the electrode signal to slowly degrade through cycle 17200. Then, near the end of life, the electrode suddenly produced a better signal and swing than ever before. This is partly explained by looking at the percent return for that last cycle. From cycle 17200 to cycle 23257 it increased from 108% to 119% and also caused the cell pressure delta to increase dramatically from 4 psia to 20 psia as Figure IV shows. This pressure increase was probably responsible for the performance improvement during that last cycle.

While the increase in percent return produced a greater pressure delta in the standard electrode cell, it procuded no effect in the heart-pacer cell. There the pressure delta slowly decreased over the entire life ending at 2 psia on cycle 23257 as Figure VI shows. In Figure V, the signal degradation is shown for the heart-pacer electrode. It was a slow degradation from about cycle 200 to cycle 17200 with the signal swing remaining good throughout. It was not until cycle 23257 that the electrode showed a dramatic loss of signal. Hence, the great reversal in performance shown in Figure II also had as a contributing factor the rapid signal loss of the heart-pacer electrode between cycles 17200 and 23257.

The data from Pack 3G was studied next. The life degradation of the heart-pacer electrode in pack 3G is shown in Figure VII. It was the same type of degradation as was shown for the heart-pacer electrode of pack 3D, the only difference being a more rapid occurrence of signal fall-off. Here, a noticeable amount of degradation was seen by cycle 5200, whereas before significant sensitivity loss was not evident until cycle 17200. Figure VIII shows that cell pressure was consistent over life with no great changes appearing.

The standard electrode life plot, Figure IX, shows a more consistent degradation in pack 3G than that shown in pack 3D. In 3G there was no great signal increase at the end of life, even though the percent recharge and cell pressure again made a dramatic increase in the last few cycles as is shown in Figure X. The signal magnitude and swing was not good in the standard electrode of Pack 3G (80 mV to 90 mV), but was consistent with Pack 3D.

CONCLUSIONS

The heart-pacer signal electrode generally produced a signal of higher magnitude and greater voltage swing than the standard signal electrode, although both types of signal electrodes lost considerable sensitivity with life. This loss of sensitivity with life and the great signal variation from signal electrode to signal electrode of the same type would make the implementation of a reliable signal electrode charge control system very difficult, if not impossible.

Some contributing causes of poor performance in the electrodes could be: the large volume of KOH present in cells of this design, and the lack of significant pressure variation over a cycle especially in the cells with the heart-pacer signal electrode.

REFERENCES

1. Baer, D.; Cell Design and Manufacturing Changes During the Past Decade; p. 49, NASA Conf. Pub. 2088, The 1978 Goddard Space Flight Center Battery Workshop; Nov. 14-16, 1978.

TABLE I

SIGNAL ELECTRODE CONSTRUCTION

Heart Pacer Electrode	Standard Electrode
● Nickel Plated Steel Substrate Coated with Sintered Nickel Powder.	● Nickel Plated Steel Substrate Coated with Sintered Nickel Powder.
● Impregnated with Cadmium, Silver Treated, and Coated with a Hydrophobic Fluorocarbon Polymer.	● Coated with a Hydrophobic Fluorocarbon Polymer.
● External Resistor: 10 OHM	● External Resistor: 300 OHM

TABLE II

DESIGN VARIABLE PROGRAM TEST REGIME

- Temperature: 20°C
- Depth of Discharge: 40 Percent
- Orbit Period: 90 Minutes
- Charge Current: 9.6 Amps ($\frac{C}{1.25}$)
  To a Voltage Limit
- Discharge Current: 9.6 Amps ($\frac{C}{1.25}$)

ORIGINAL PAGE IS
OF POOR QUALITY

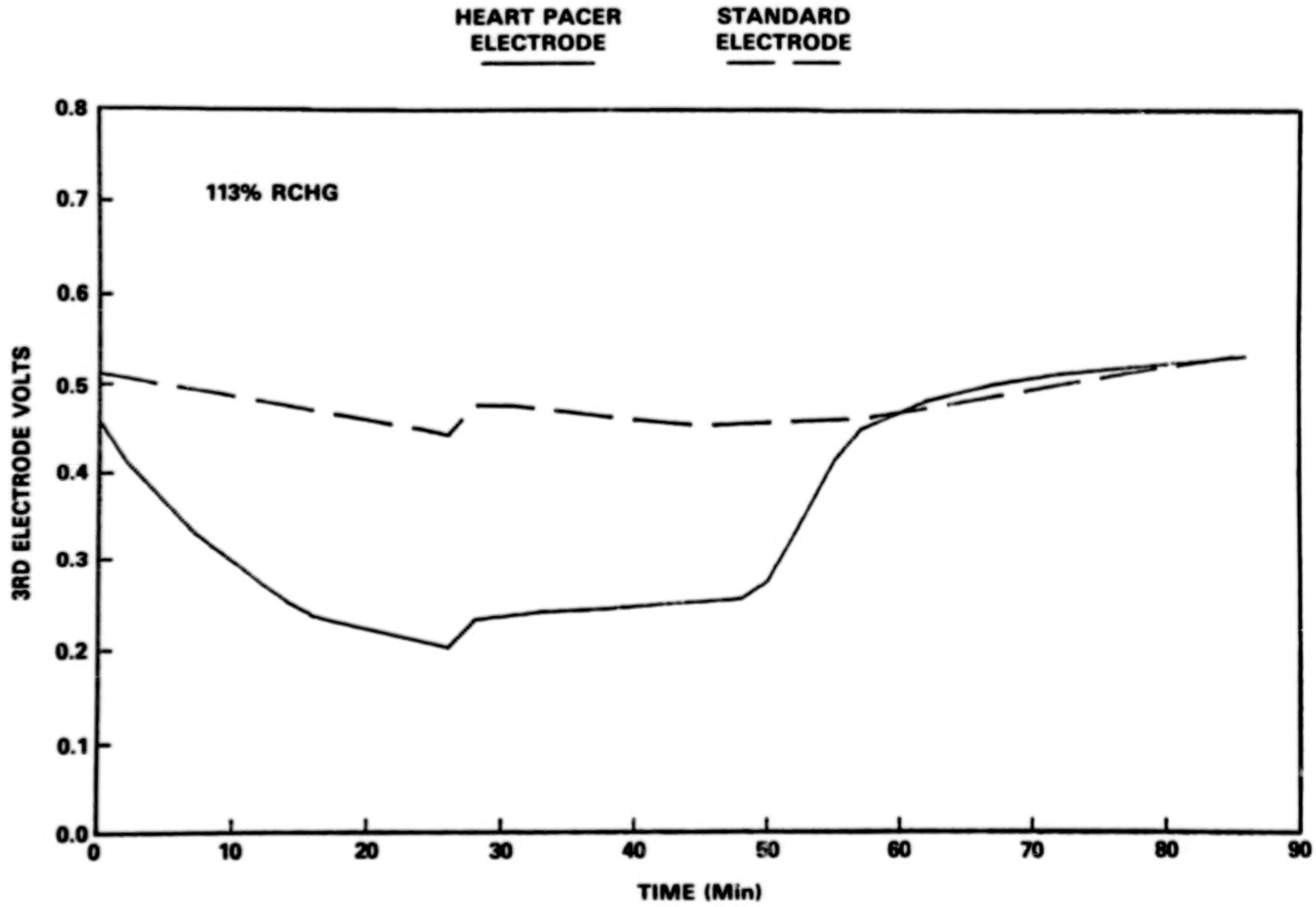

FIGURE I DESIGN VARIABLE 3RD ELECTRODE STUDY TYPICAL CYCLE DATA, PACK 3D, CYCLE 222

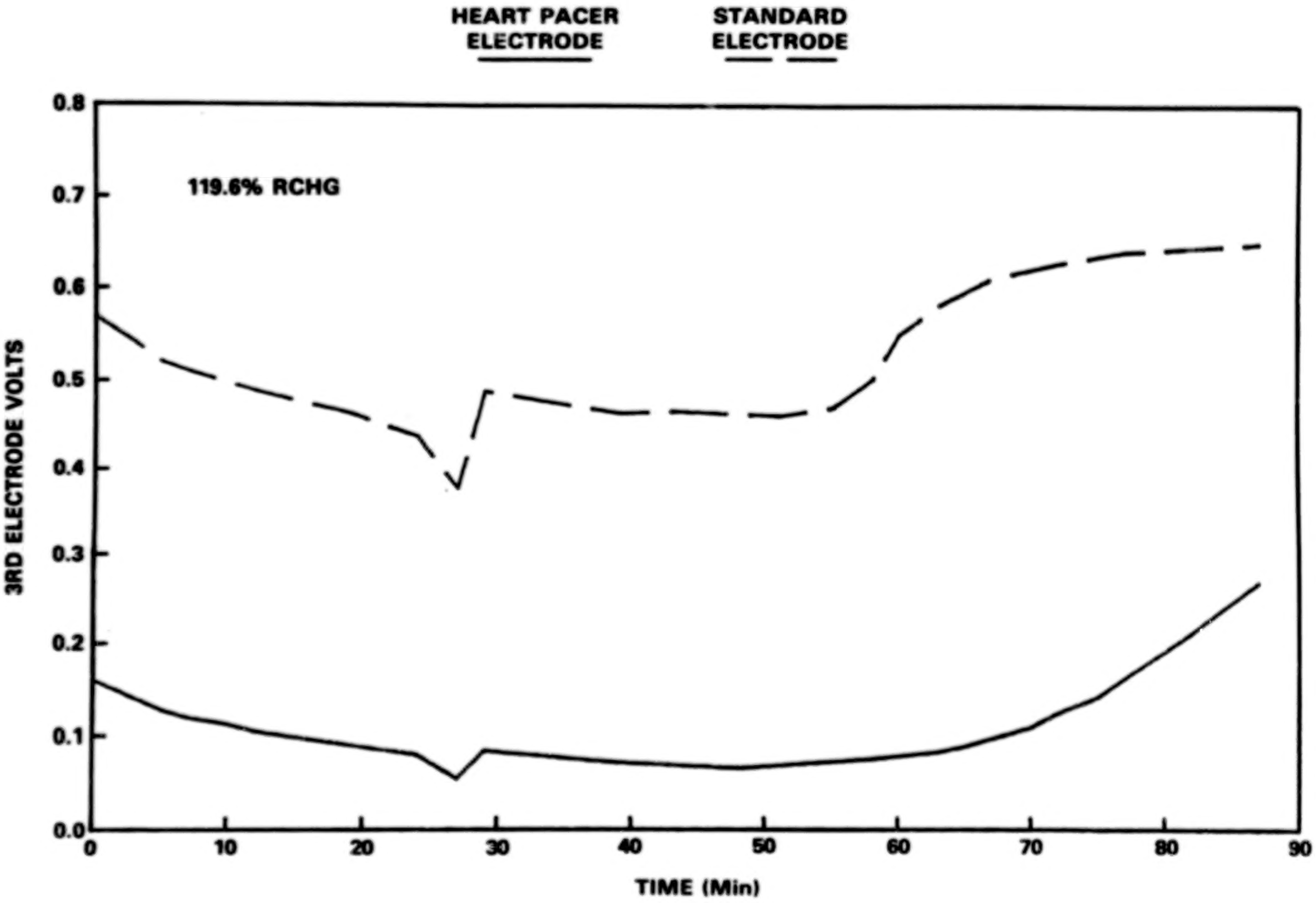

FIGURE II DESIGN VARIABLE 3RD ELECTRODE STUDY TYPICAL CYCLE DATA, PACK 3D, CYCLE 23257

ORIGINAL PAGE IS
OF POOR QUALITY

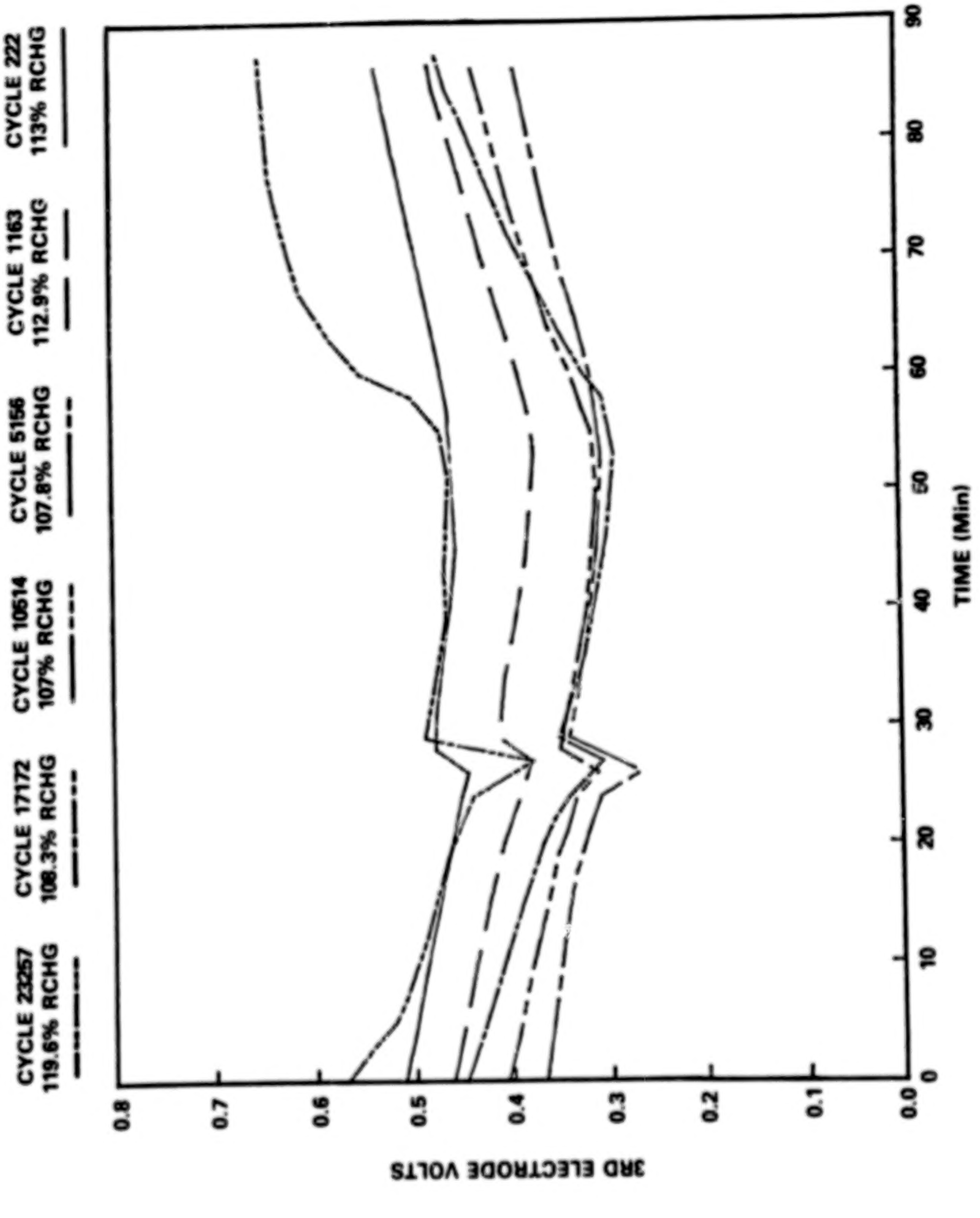

FIGURE III DESIGN VARIABLE 3RD ELECTRODE STUDY STANDARD 3RD LIFE BY TYPICAL CYCLE, PACK 3D

ORIGINAL PAGE IS
OF POOR QUALITY

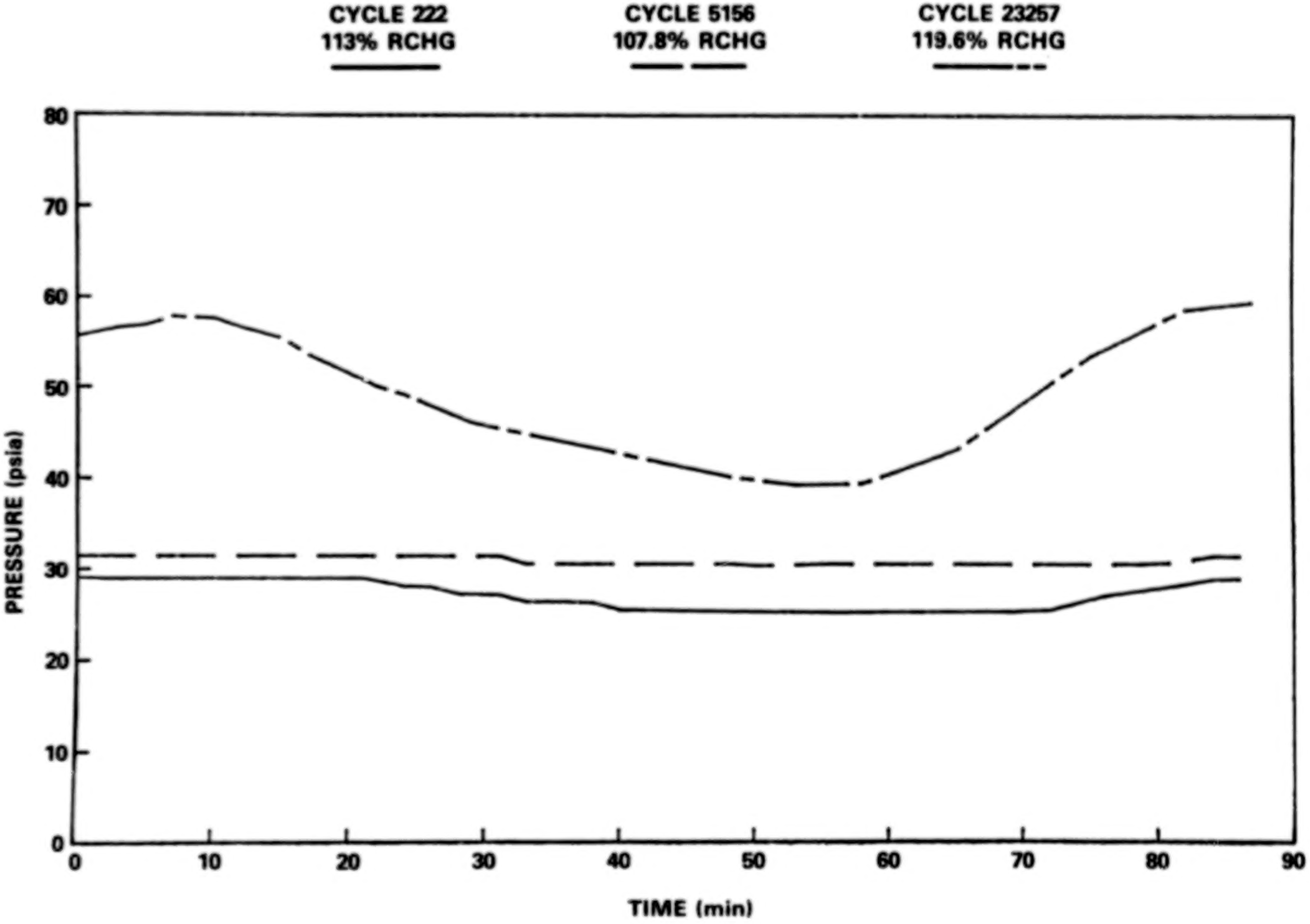

FIGURE IV DESIGN VARIABLE 3RD ELECTRODE STUDY STANDARD CELL TYPICAL CYCLE PRESSURE, 3D

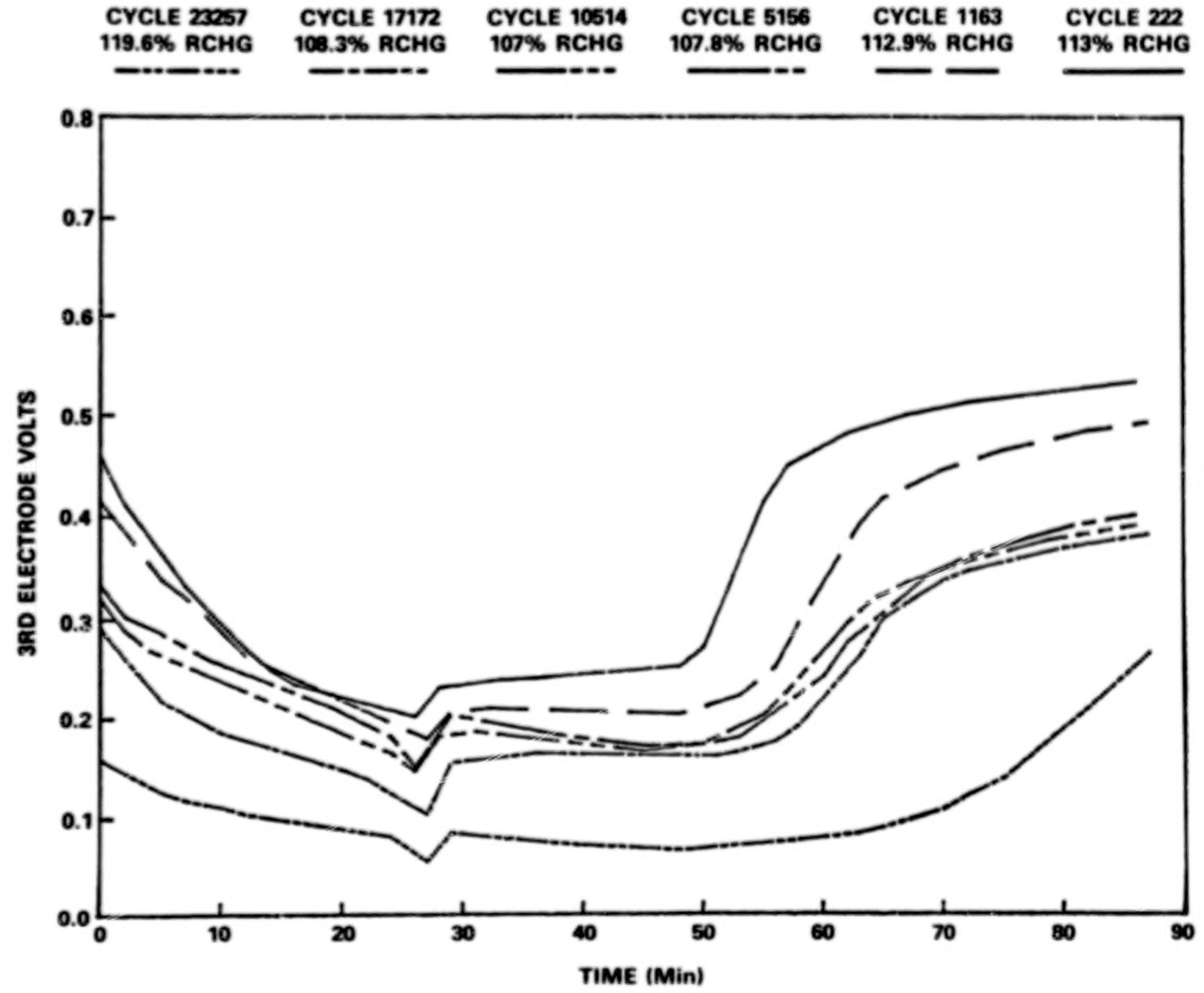

FIGURE V DESIGN VARIABLE 3RD ELECTRODE STUDY HEART PACER LIFE BY TYPICAL CYCLE, PACK 3D

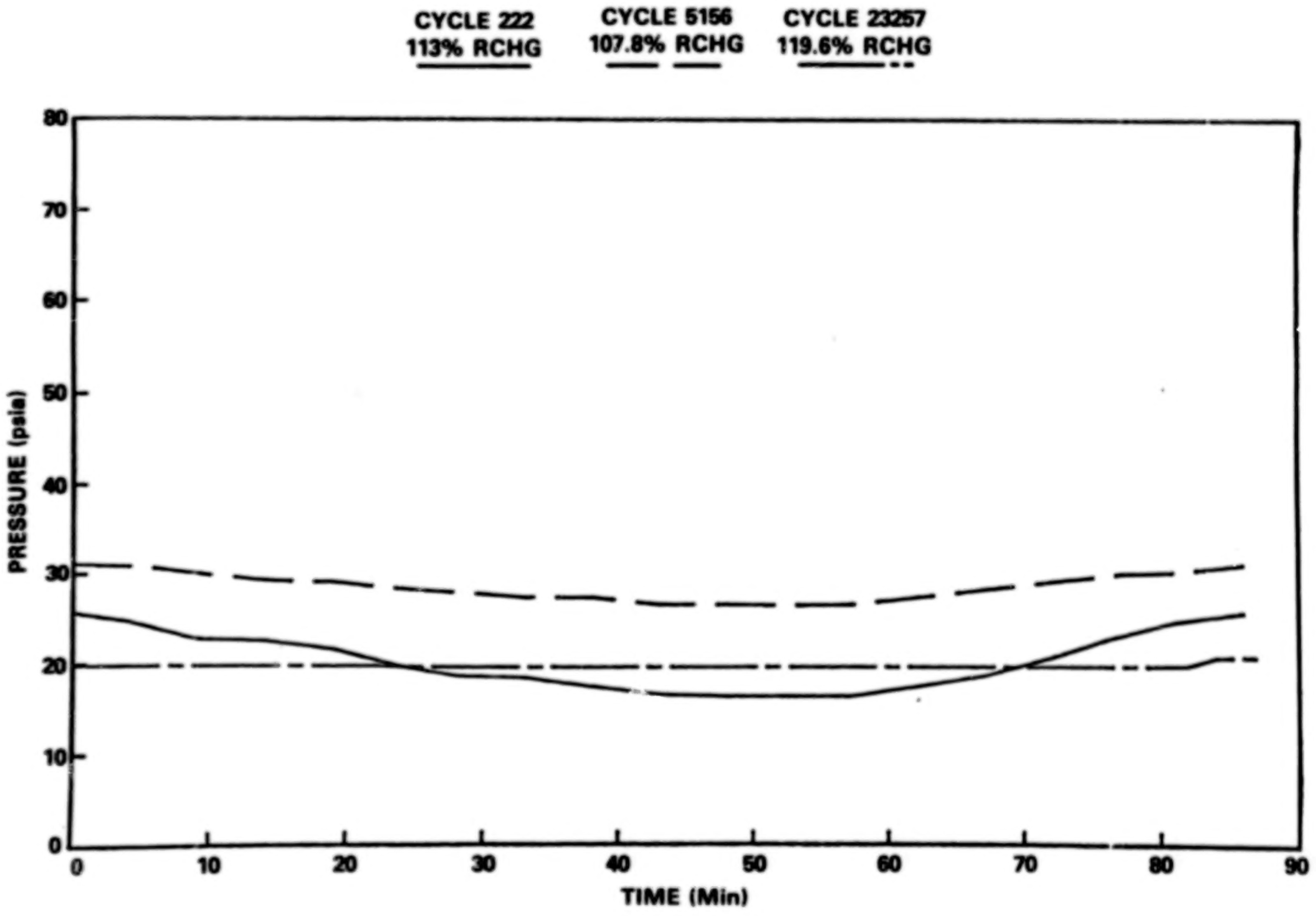

FIGURE VI DESIGN VARIABLE 3RD ELECTRODE STUDY HEART PACER CELL TYPICAL CYCLE PRESSURE, 3D

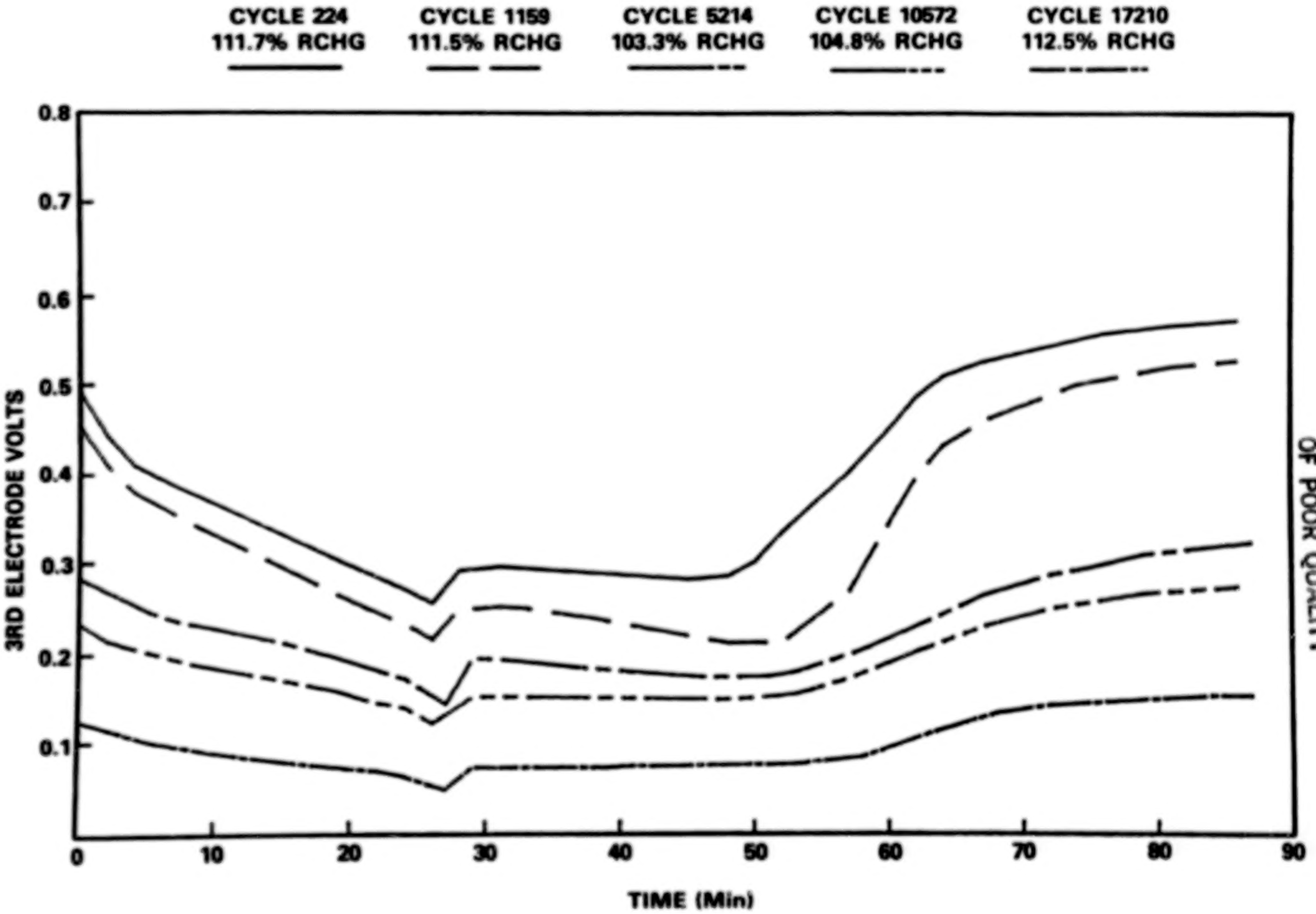

FIGURE VII DESIGN VARIABLE 3RD ELECTRODE STUDY HEART PACER LIFE BY TYPICAL CYCLE, PACK 3G

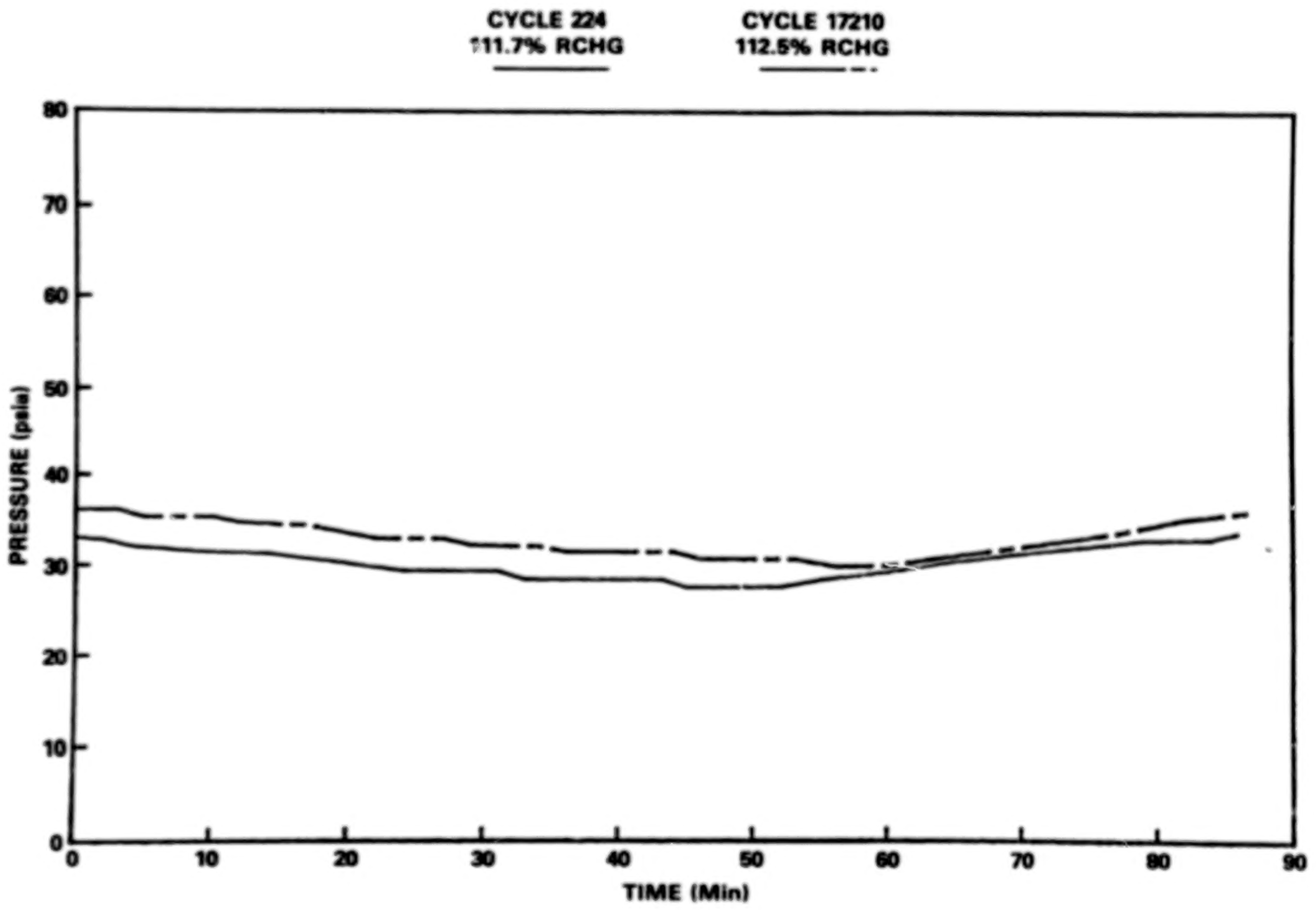

FIGURE VIII DESIGN VARIABLE 3RD ELECTRODE STUDY HEART PACER CELL TYPICAL CYCLE PRESSURE, 3G

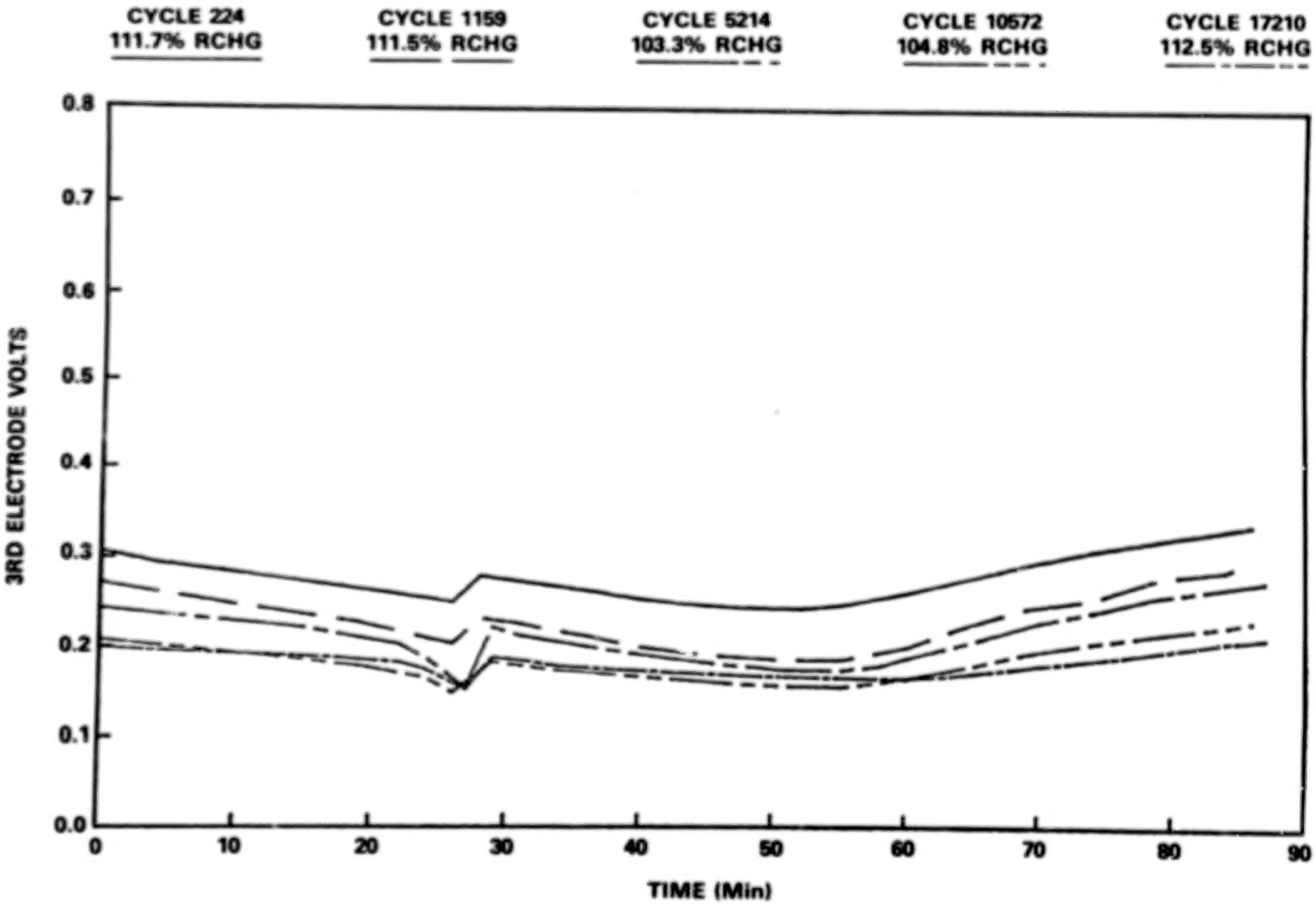

FIGURE IX DESIGN VARIABLE 3RD ELECTRODE STUDY STANDARD 3RD LIFE BY TYPICAL CYCLE, PACK 3G

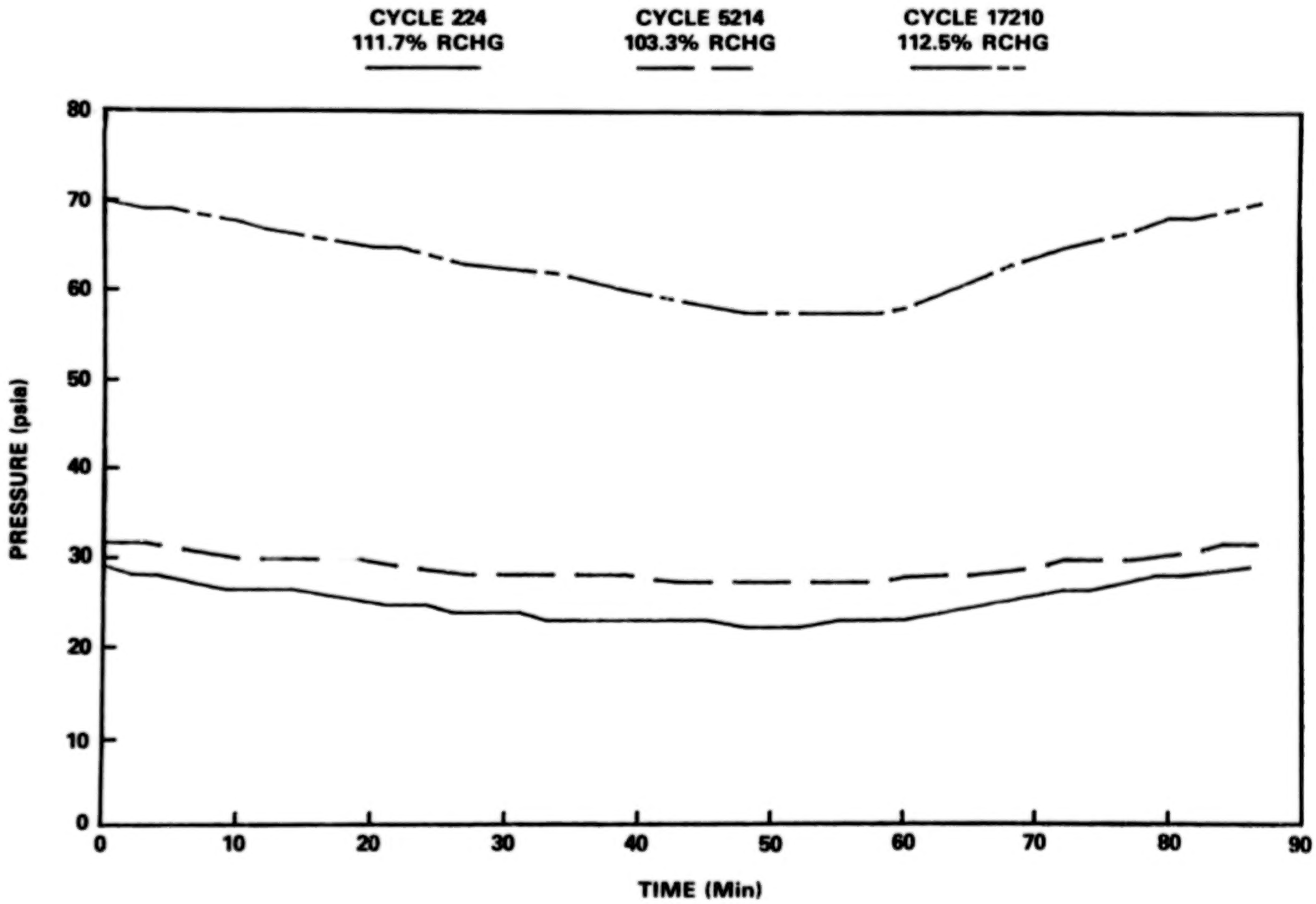

FIGURE X DESIGN VARIABLE 3RD ELECTRODE STUDY STANDARD CELL TYPICAL CYCLE PRESSURE, 3G

Q. Ritterman, Comsat: I guess you are talking about a nickel cadmium cell or a bunch of nickel cadmium cells with two different types of charge control electrodes?

A. Morrow, GSFC: Signal electrodes.

Q. Ritterman, Comsat: Oh signal electrodes. And you didn't get any variation in pressure. I mean that's what I essentially saw. What does each electrode respond to? I mean normally the signal electrode responds to some sort of oxygen pressurized, the hydro directs the proportion of pressure. The old GE signaling electrode is just the minute you start getting any amount of oxygen you start getting a rise. I guess your auxilliary electrode is your signaling electrode is attached to be resistant to the negative electrode. A whole bunch of things I didn't understand. What the cycle was, how wet the cells were in respect to CC's of KOH per amp hour? Could you identify the cells?

A. Morrow, GSFC: Dave is a little more up on the design variable cells than I am.

A. Baer, GSFC: For the most part they had around 4CC's per amp hour.

A. Ritterman, Comsat: Yeah that should still be enough to give you a little better recombination than you've got.

A. Baer, GSFC: I think the thing that puzzled us was at the beginning of life some of them weren't too bad and at the end of life when you expect the cells to start drying out you weren't getting the expected pressure rise.

Q. Ritterman, Comsat: Are you charging it at about the same rate that you were discharging?

A. Baer, GSFC: Yes. I think there was about 9.6 amps for a 12 amp per hour cell.

Q. Rogers, Hughes Aircraft: The electrode that you have I assume, it is suppose to react with oxygen?

A. Morrow, GSFC: Right.

Q. Rogers, Hughes Aircraft: You've got cadmium on it. Now I guess I see two competing reactions. How does the electrode know what to do?

A. Morrow, GSFC: The new electrode was designed for heart pacer applications and in that they really have to watch what the oxygen pressure does since it will be inside the body. So what they did was they tried, they wanted to put silver on the electrode which would, silver is a little more catalytically active with oxygen so it would produce a higher voltage and the cadmium is placed in contact with the silver so that it holds it more to the electrode not letting silver oxide form and therefore migrate to the cells.

A. Baer, GSFC: Howard, let me say this is GE's reference electrode and all we are doing is comparing the two. It's what they want to switch to and we want to compare the two to see if they are compatible. The electrode wasn't our idea, I guess is what I'm saying.

A. Rogers, Hughes Aircraft: The reason for my question is that you were talking about a cadmium electrode which normally is not used as an oxygen recombination electrode.

A. Morrow, GSFC: Right.

A. Rogers, Hughes Aircraft: That's what the question came from.

N84
33695

UNCLAS

N84 33695 D27

SPECIAL TEST METHODS FOR BATTERIES

Sidney Gross
Boeing Aerospace Company
Seattle, Washington 98124

A variety of methods has been used for determining heat generation in primary and secondary batteries (References 1 - 3). One method useful for sealed primary batteries it to insulate the battery with multilayer vacuum insulation, discharge it in a vacuum, and observe it's temperature change with time (Figure 1). Six layers of aluminized mylar separated by low outgassing bridal-veil type material has proved to be effective, resulting in nearly negligible heat loss. Heat transfer through supports is made insignificant by suspending the battery with nylon string. Heat transport through supports, leads and insulation is small, but calibration is advisable nevertheless. The heat generation rate is then:

$$dQ/dt = W\, C_p\, (dT/dt) + A \qquad \text{EQN (1))}$$

where Q is heat generated, W is battery mass, C_p is specific heat, T is temperature, t is time, and A is the calibration factor. This method was applied to a sealed silver-zinc battery.

Where a thermal vacuum chamber is not available or is impracticable, alternative methods can be used for measuring heat generation. One method is to insulate the battery and make a correction for the heat transport through the insulation. A convenient way to make the correction is to test with different thicknesses of insulation, and extrapolate results to the condition of zero heat loss. A preferred way to make the correction is the analytical method described in Reference 1. Typical results using that method are shown in Figure 2, with heat generation correlated on the basis of enthalpy voltage. With this method, the heat generation rate is equal to cell current times the difference of enthalpy voltage and cell voltage.

Heat generation measurement of large batteries presents special problems. A method used successfully was to attach an insulated battery to a water-cooled coldplate suitably instrumented to function as a calorimeter. The battery heat generated is the sum of the heat transported to the fluid plus the heat stored within the battery, plus or minus heat transported through the insulation (Figure 3). High flow rates through the cold plate are preferred to minimize temperature gradients, but this results in a small temperature rise of the fluid through the cold plate. To obtain accuracy in spite of having only a small temperature rise, a sensitive instrumentation system is used which measures temperature difference directly (Figure 4). Calibration curves of this sensor are shown in Figure 5. Insulation of the battery should be done in a way that is repeatable and permits calibration. A conformally shaped insulation box with fiberglass surfaces inside and outside served these needs. Calibration with a battery and heat exchanger installed and electrical cables attached resulted in overall conductance in ambient air of 0.2 W/°F at a battery temperature of 50°F, increasing linearly to 0.4 W/°F at a battery temperature of 180°F.

Specific heat of batteries (Figure 6) can be determined in a way similar to heat generation, provided a heater is attached to the battery (Figure 7); in the case of a sealed secondary battery, steady state overcharge can be used in lieu of a heater. Thermal vacuum testing gives the least error; an alternative is to encapsulae the battery with a heater in waterproof insulation and immerse it in a water bath for the test. A method used satisfactorily is to precool the battery below the water

PRECEDING PAGE BLANK NOT FILMED

temperature, and allow the experiment to continue until the battery is hotter than the water bath (Figure 7). Specific heat is determined using equation 1, with minimum heat correction at the isothermal point.

A common method for cooling spacecraft cells is by sandwiching the cells between cooling plates, thus removing heat from the broad faces of the cells. This raises the need for determining cell thermal conductance in that direction. One method that has been used is to sandwich a cell between two thick plates whose thermal conductivity is known and is also close to that of the cell; heat is then forced through the assembly by means of two heat exchangers (Figure 8), with insulation around the assembly to minimize error. Plexiglas Type 2 has suitable properties for this test and has been used satisfactorily. Cell thermal conductance can be determined by comparison of the temperature gradient across the cell with the gradient across the plexiglas of known thickness; the use of two layers of plexiglas permits an assessment of the error.

Thermal vacuum tests have been found to be very useful in determining thermal conductance within batteries. The batteries are insulated around all sides except the bottom, which radiates to an adjacent temperature-controlled plate. Steady state overcharge at high rates will exaggerate the temperature gradient and provde data needed to determine conductance. A test that is especially useful is to lower the temperature of the plate heat sink with time in a programmed manner so the battery temperature will reduce linearly with time. This induces temperature gradients between the cells and the battery case which are constant with time (Figure 9). This test has been used to identify poor thermal bonding between cells and the case of a battery package.

Measurements have been taken of the temperature gradient in nickel cadmium cells during cycling for possible use in charge control. This is based on the principle that charge efficiency decreases as a nickel cadmium cell approaches a full state of charge, resulting in a sudden increase in the heat generation rate within the cell. Since spacecraft batteries are generally mounted so there is a good thermal path between the cell bottom and the heat sink, this heating results in temperature gradients across the cell. The temperature difference may be taken between the cell top and cell bottom, between the cell top and the heat sink, or between the cell bottom and the heat sink. Heat flux transducers are an alternative approach. For a simulated 24-hour orbit, the temperature difference signal starts to rise at a recharge fraction of approximately 0.95 (Figure 10). The tests showed that temperature gradient sensing can provide an effective means of charge control for 24-hour orbit satellites. However, the method is not suitable for low-earth orbits since the heat generated during discharge has insufficient time to dissipate before charging commences.

Auxilliary electrodes can be useful for conducting tests on battery charge control. For the Ni-Cd system, an oxygen-sensitive electrode coupled to the negative electrode through a resistor provides a signal which gives a measure, though nonlinear, of oxygen partial pressure. This has been applied to compare pulse charging and constant current charging.

A variety of battery-level tests has been used to characterize nickel cadmium cells. Such tests can be conducted on cells at the beginning of a cyling test, then repeated at intervals to quantize the degradation. A discharge sweep with current increasing linearly with time has been used; similar tests have also been done with two-second discharge pulses with current increasing at each pulse. This quickly distinguishes the resistance-limited regime from the diffusion-limited regime. Current-sweep tests have also been done for charge, with current increasing linearly with time.

Another battery test which has proved useful is a linear sweep of current from charge to discharge. The crossing point where current is zero is identified as the zero-current voltage. It is related to the open circuit voltage, except that it eliminates the problem of a continuously varying open circuit voltage that is associated with batteries having nickel electrodes. The other advantage is that it is a measurement that sometimes can be obtained from telemetry of flight spacecraft. This has proven useful in identifying incipient shorting during flight operation of Ni-Cd batteries.

Definition of fast transient behavior of batteries in the microsecond range has been of interest for some applications. Silver zinc batteries, for example, exhibit a brief discharge voltage dip following open circuit with Ag_2O_2 present (Figure 11). Visicorders are not fast enough to define some of these transients. A transient voltage monitor system is used which takes data every 200 nanoseconds. The signal is processed by an analogue-to-digital converter and stored in memory. Following the test, the memory is fed repetitively to an oscillosope through a digital to analogue unit for immediate viewing, and also transferred to magnetic tape for computer processing and point-by-point data printout.

A number of tests have been conducted on cell components. One unique test is the determination of the electrical conductance of nickel sinters in the thickness direction. This is considered important because corrosion and mechanical stress from cyling will reduce conductance significantly. A die was used to cut 15/16 inch diameter discs of electrodes or electrode sinters, indium foil, and copper. These are assembled into a stack: copper, indium, sinter, indium, copper (Figure 12). Sometimes multiple indium-sinter sandwiches are used in series. The stack is compressed to obtain good contact of the indium foil and the sinter, yet not crush them. The electrical conductance of the stack is measured, and an adjustment is made for the calibration of the stack without the sinter.

Mechanical problems have been experienced in the vibration of nickel-cadmium batteries (Reference 4). Tests to simulate the cycling fatigue of the steel tabs connecting the plates to the comb showed that a wide variation could be expected in the fatigue life of these tables. Nickel cadmium cells must be under some compression when packaged for spacecraft use, but surprisingly little is known about the visco-elastic behavior of cells under such conditions. An analytical model of a cell under compression is shown in Figure 13. One series of tests defined the distribution of forces when cells are compressed during battery packaging. These tests showed that there was a significant relaxation of compressive forces on the plates with time.

References

1. S. Gross, "Heat Generation in Sealed Batteries", Energy Conversion, Vol. 9, pp. 55-62, 1969.

2. S. Gross and J. Malcolm, "Thermal Considerations in Sealed Nickel Cadmium Cells", in Power Sources 4, Proceedings of 8th International Symposium, September 1972, D. H. Collins, Ed., pp. 257-275, Oriel Press (1973).

3. S. Gross, Development and Fabrication of Advanced Battery Energy Storage System, Contract NAS9-6470, Final Report, Oct. 1967.

4. S. Gross, "Designing for Vibration with Sealed Nickel Cadmium Cells", The 1976 Goddard Space Flight Center Battery Workshop, Nov. 1976, Report X-711-77-28.

ORIGINAL PAGE IS
OF POOR QUALITY

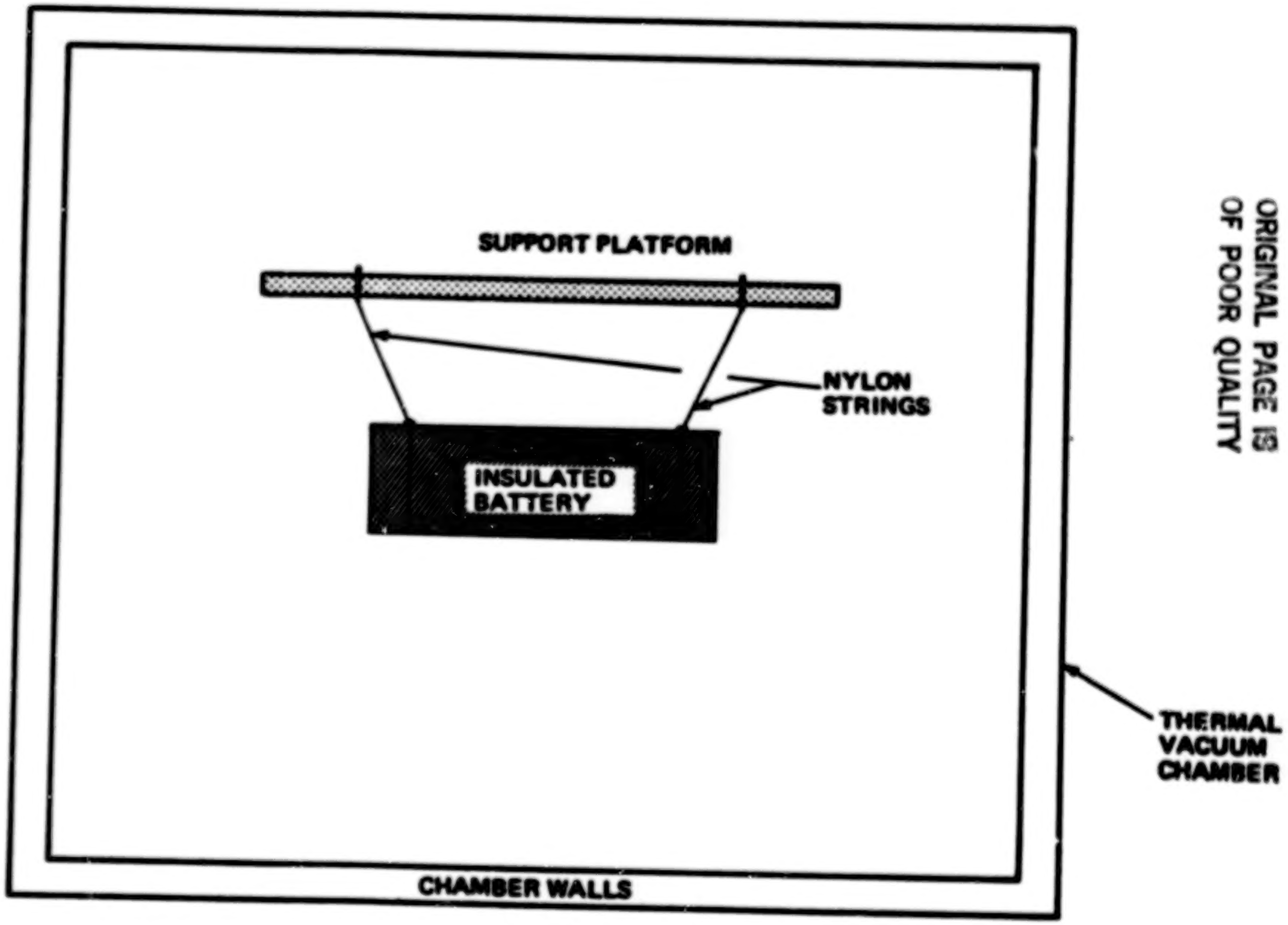
SUPPORT PLATFORM
NYLON
STRINGS
INSULATED
BATTERY
THERMAL
VACUUM
CHAMBER
CHAMBER WALLS

Figure 1. Thermal Vacuum Chamber Installation for Measurement of Battery Heat Generation

ORIGINAL PAGE IS
OF POOR QUALITY

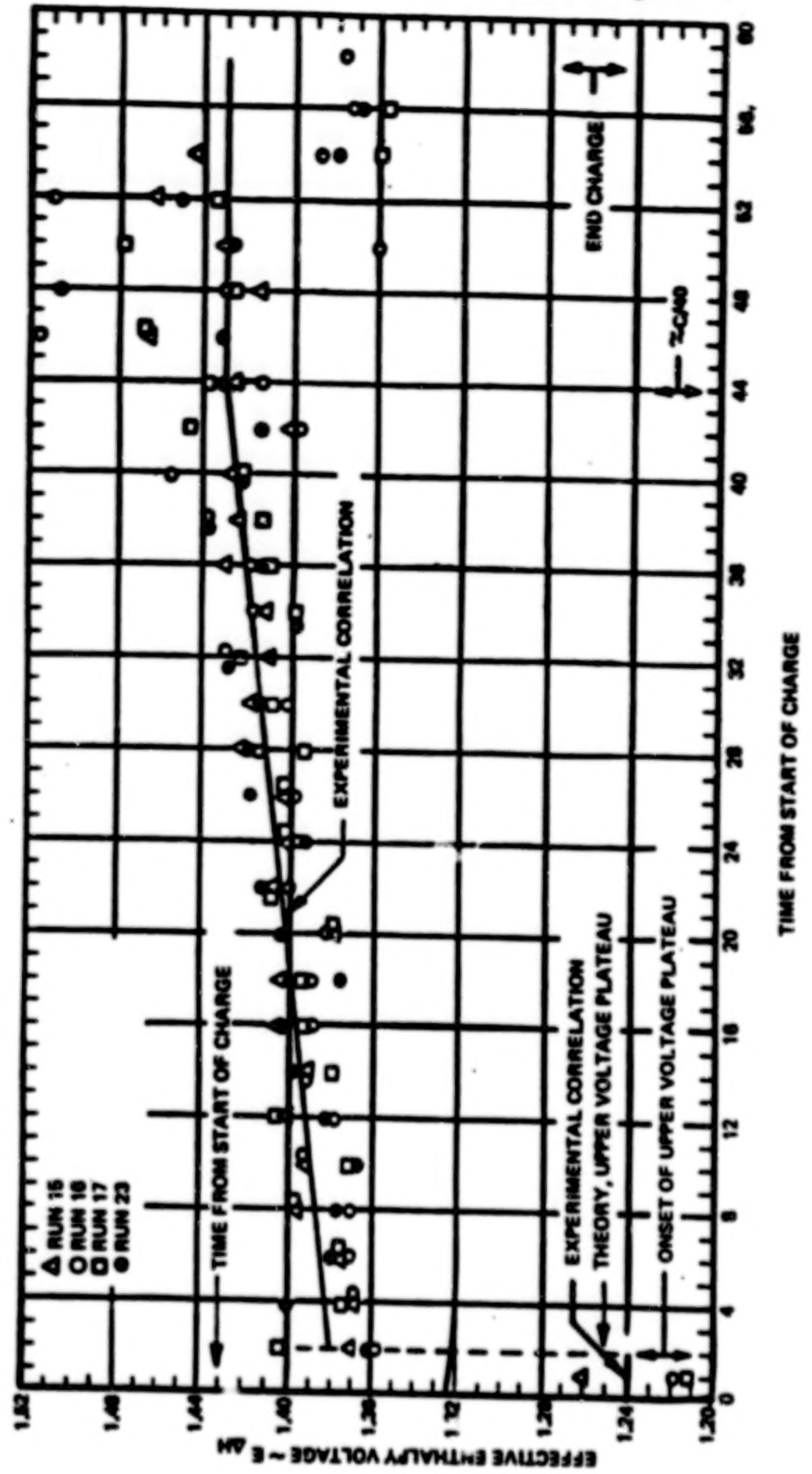

Figure 2. Correlation of Heat Generation Enthalpy Voltage During Charge of Silver-Cadmium Cells

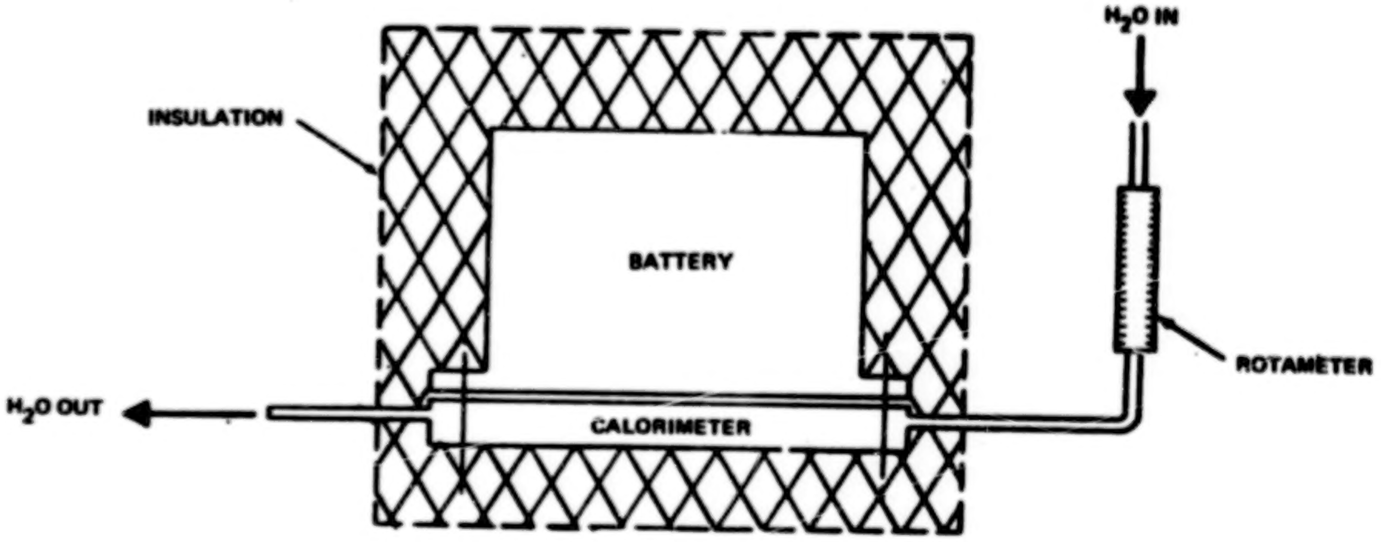
H_2O IN
INSULATION
BATTERY
ROTAMETER
H_2O OUT
CALORIMETER

HEAT GENERATED = HEAT TO FLUID + HEAT STORED + HEAT LOST

MEASUREMENTS
1. BATTERY TEMP ——— THERMOCOUPLES
2. FLOW RATE ——— ROTAMETER
3. FLOW ΔT ——— THERMOPILE OR THERMISTORS

Figure 3. Battery Calorimeter Concept

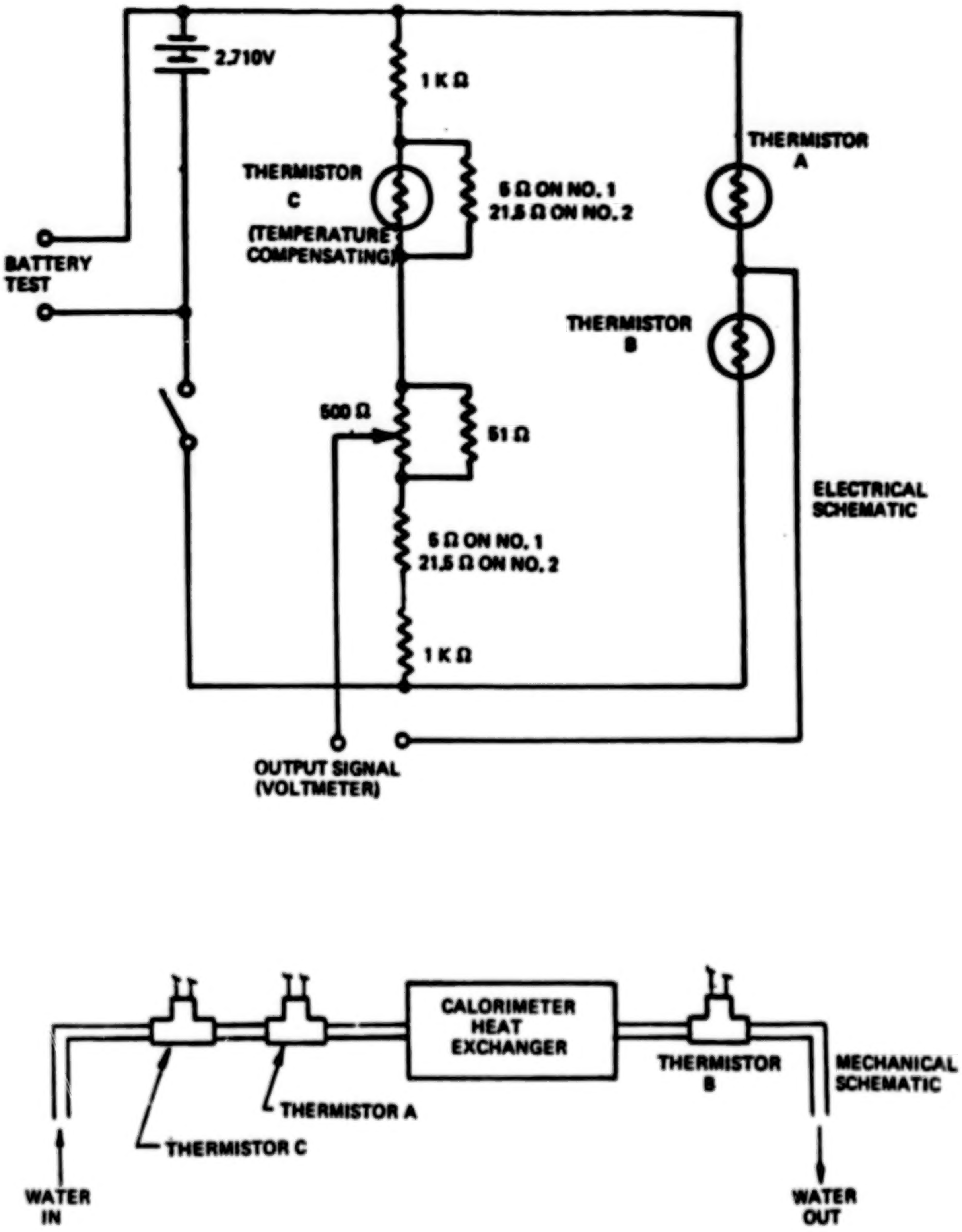
2.710V
1 K Ω
THERMISTOR C
(TEMPERATURE COMPENSATING)
5 Ω ON NO. 1
21.5 Ω ON NO. 2
THERMISTOR A
BATTERY TEST
THERMISTOR B
500 Ω
51 Ω
ELECTRICAL SCHEMATIC
5 Ω ON NO. 1
21.5 Ω ON NO. 2
1 K Ω
OUTPUT SIGNAL (VOLTMETER)
CALORIMETER HEAT EXCHANGER
THERMISTOR B
MECHANICAL SCHEMATIC
THERMISTOR A
THERMISTOR C
WATER IN
WATER OUT

Figure 4. Schematic of Calorimeter Temperature Difference Sensor

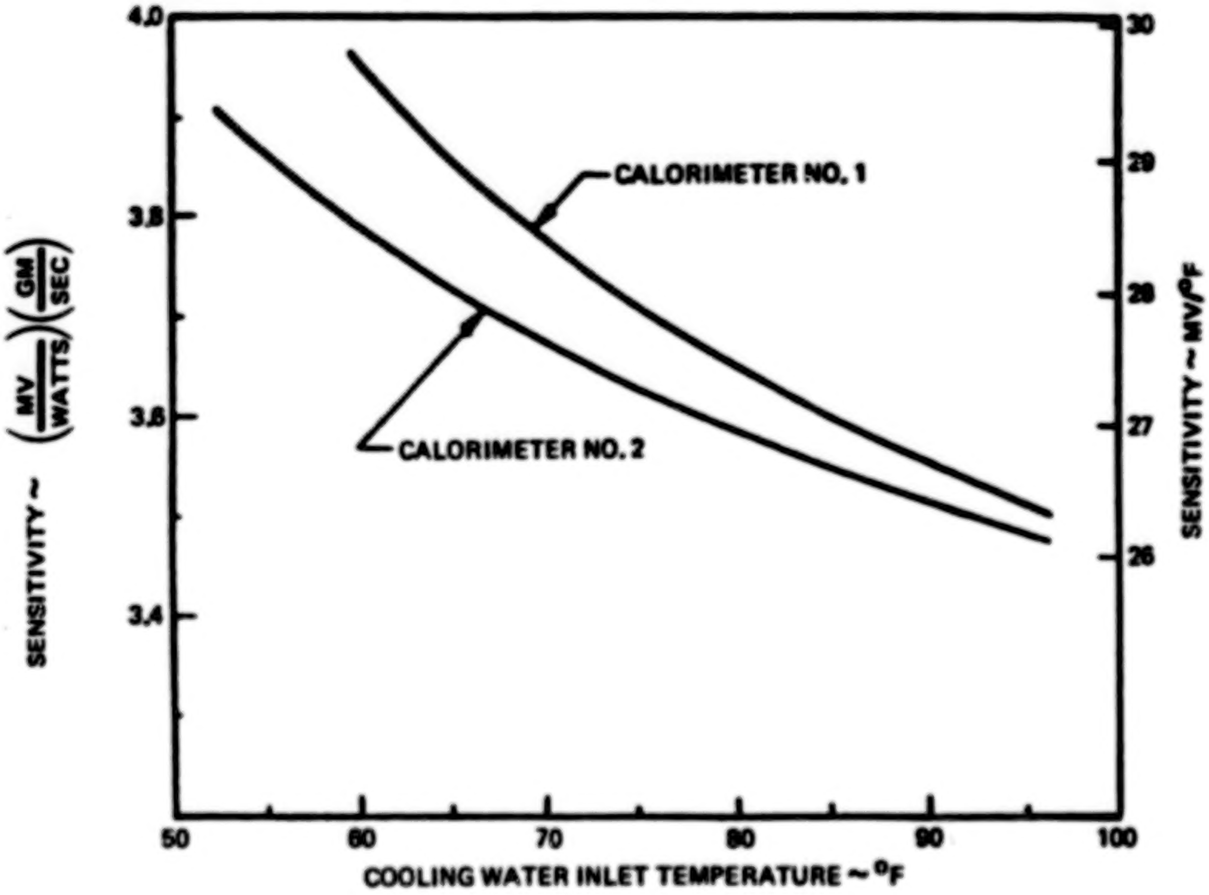

Figure 5. Sensitivity Curve—Calorimeter Temperature Difference Sensor

ORIGINAL PAGE IS
OF POOR QUALITY

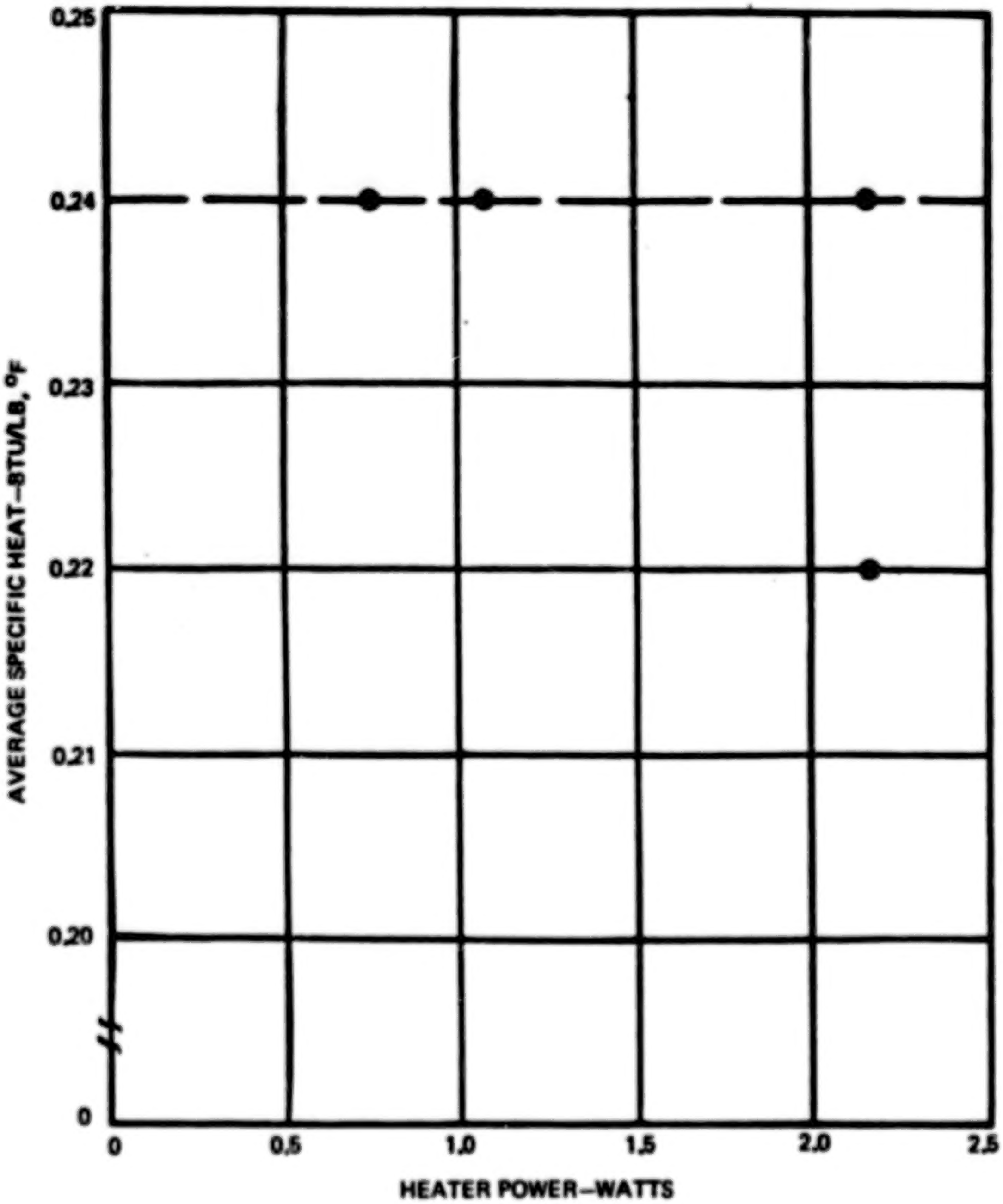

Figure 6. Specific Heat Test of 70 AH Silver Cadmium Cell

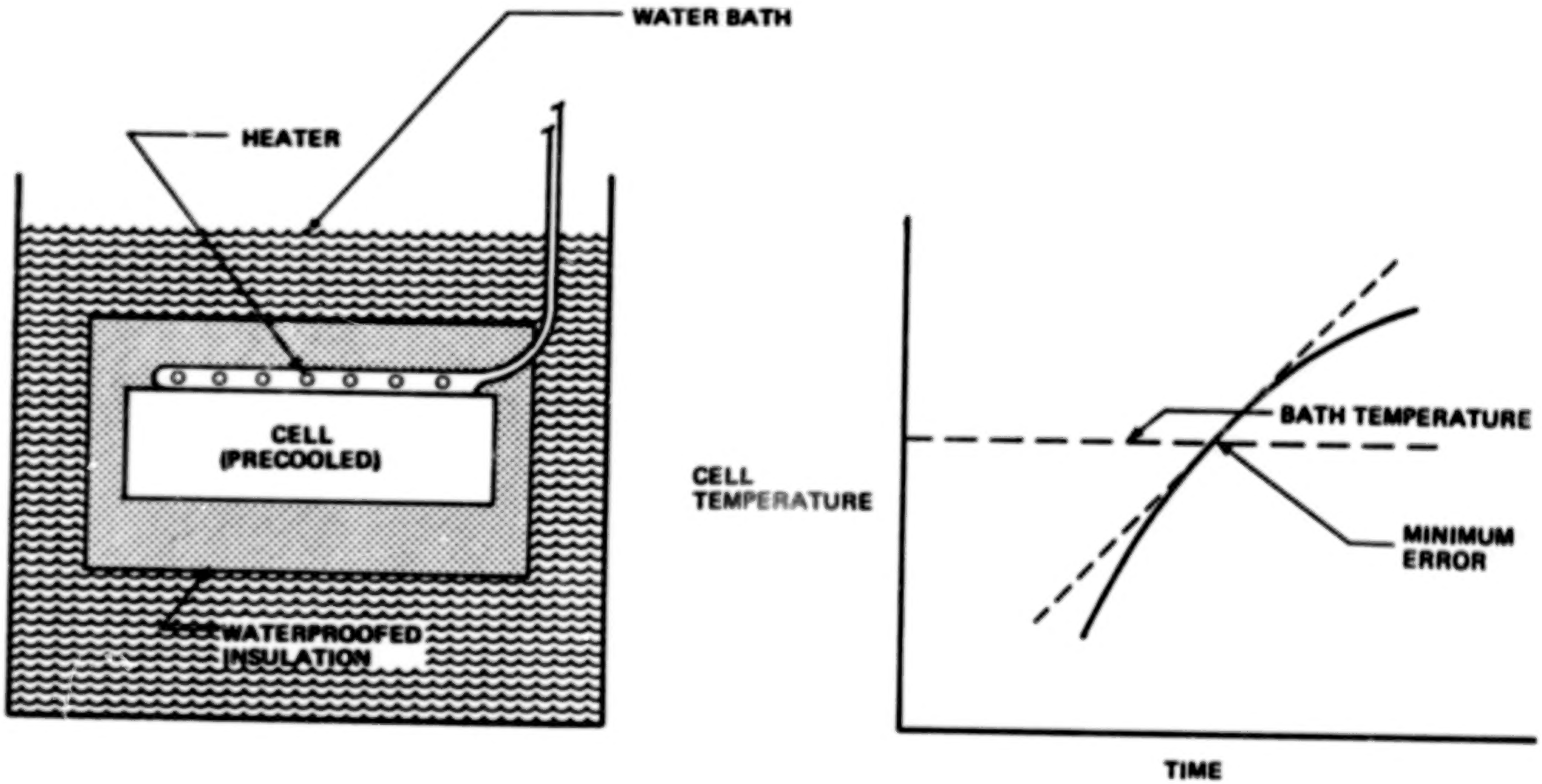
WATER BATH
HEATER
CELL
(PRECOOLED)
WATERPROOFED
INSULATION
CELL
TEMPERATURE
BATH TEMPERATURE
MINIMUM
ERROR
TIME

$$\frac{dQ}{dt} = W C_p \frac{dT}{dt}$$

CALCULATE FROM DATA

Figure 7. Cell Specific Heat Test

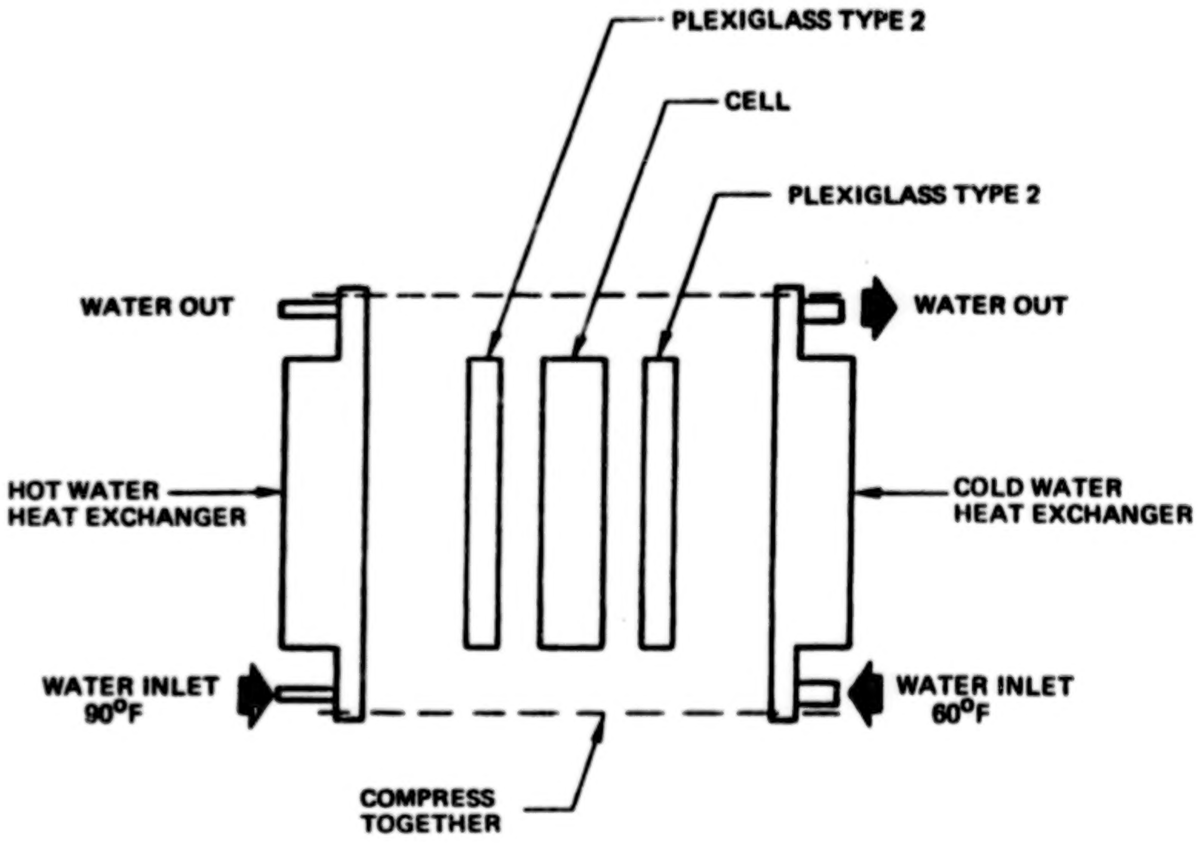
PLEXIGLASS TYPE 2
CELL
PLEXIGLASS TYPE 2
WATER OUT
WATER OUT
HOT WATER HEAT EXCHANGER
COLD WATER HEAT EXCHANGER
WATER INLET 90°F
WATER INLET 60°F
COMPRESS TOGETHER

Figure 8. Cell Thermal Conductivity Test

ORIGINAL PAGE IS
OF POOR QUALITY

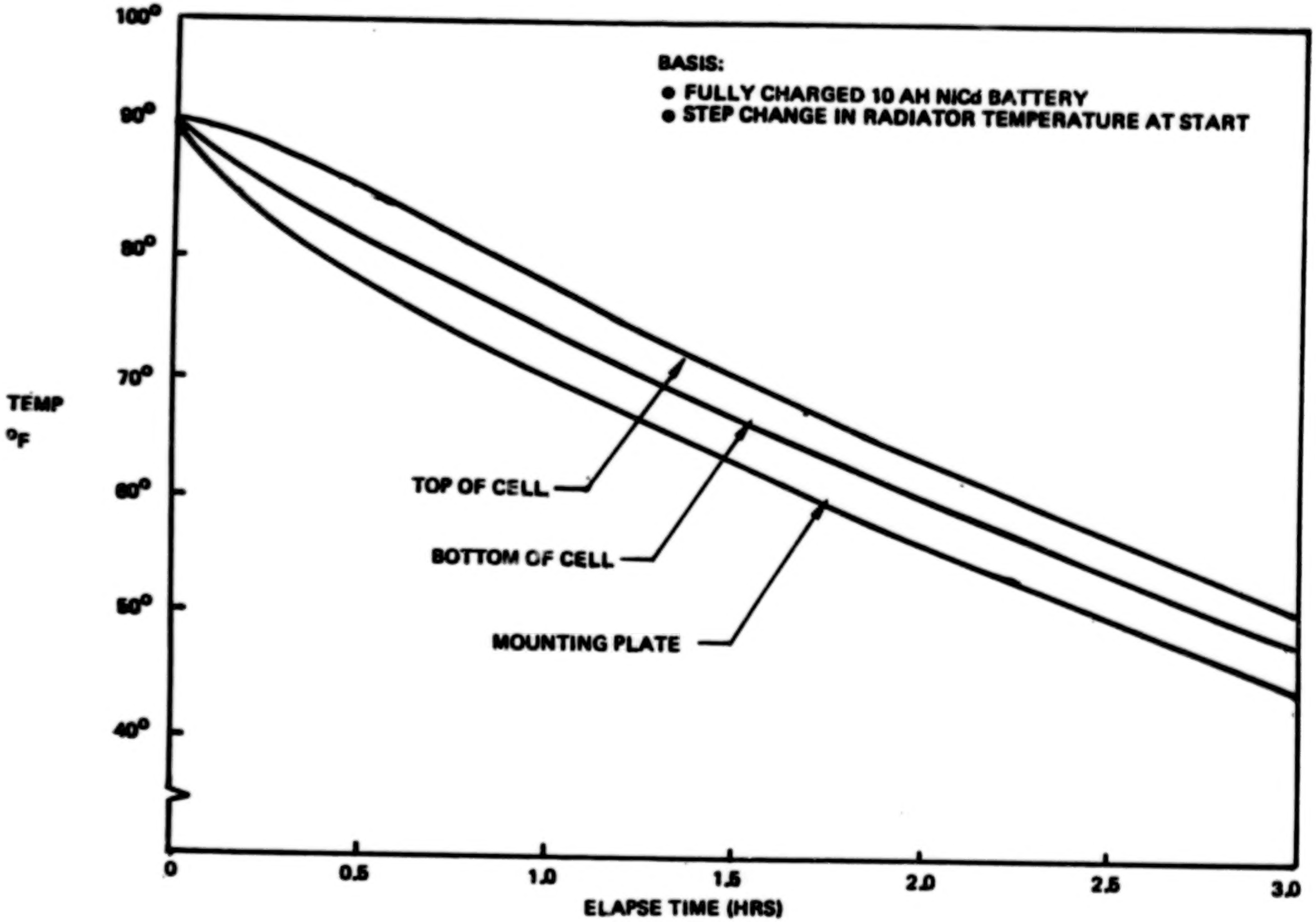

Figure 9. Radiant Cooling Vacuum Test of 10 AH Ni-Cd Battery

- SIMULATED 24-HR ORBIT
- 12 AH SEALED Ni-Cd CELL
- DISCHARGE 1.0 HR AT 8.0 A (67% DoD)
- CHARGE AT 3.0 A (C/4)
- TEMPERATURE DIFFERENCE MEASURED AT CELL MOUNTING
- COMMENCE CHARGE WHEN ΔT < 0.5°F

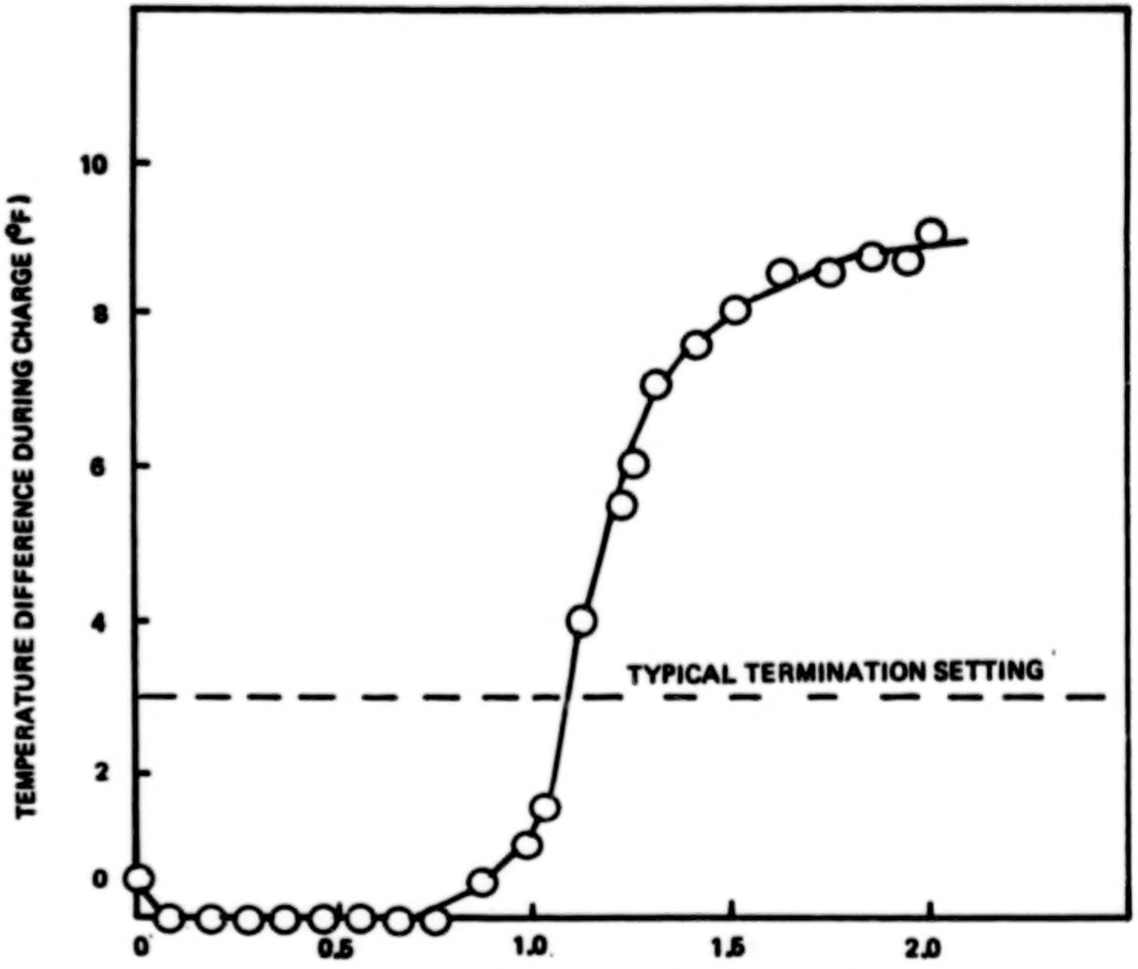

Figure 10. Sensitivity of Temperature Difference Sensing for Charge Termination

ORIGINAL PAGE IS
OF POOR QUALITY

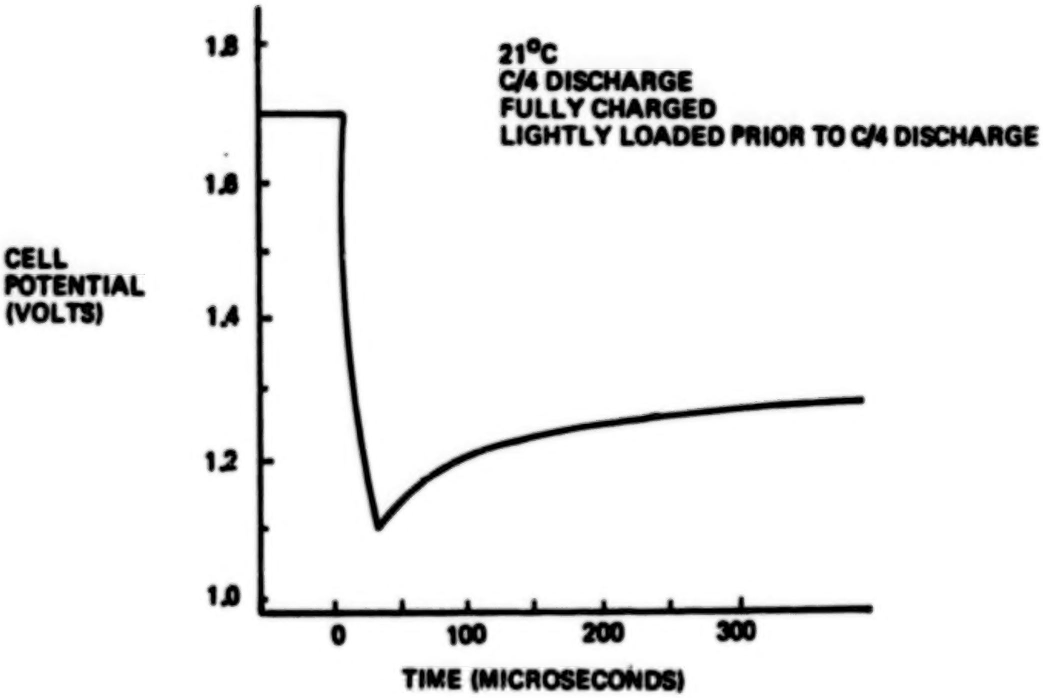

Figure 11. Typical Voltage Delay Behavior of Silver-Zinc Cells

ORIGINAL PAGE IS
OF POOR QUALITY

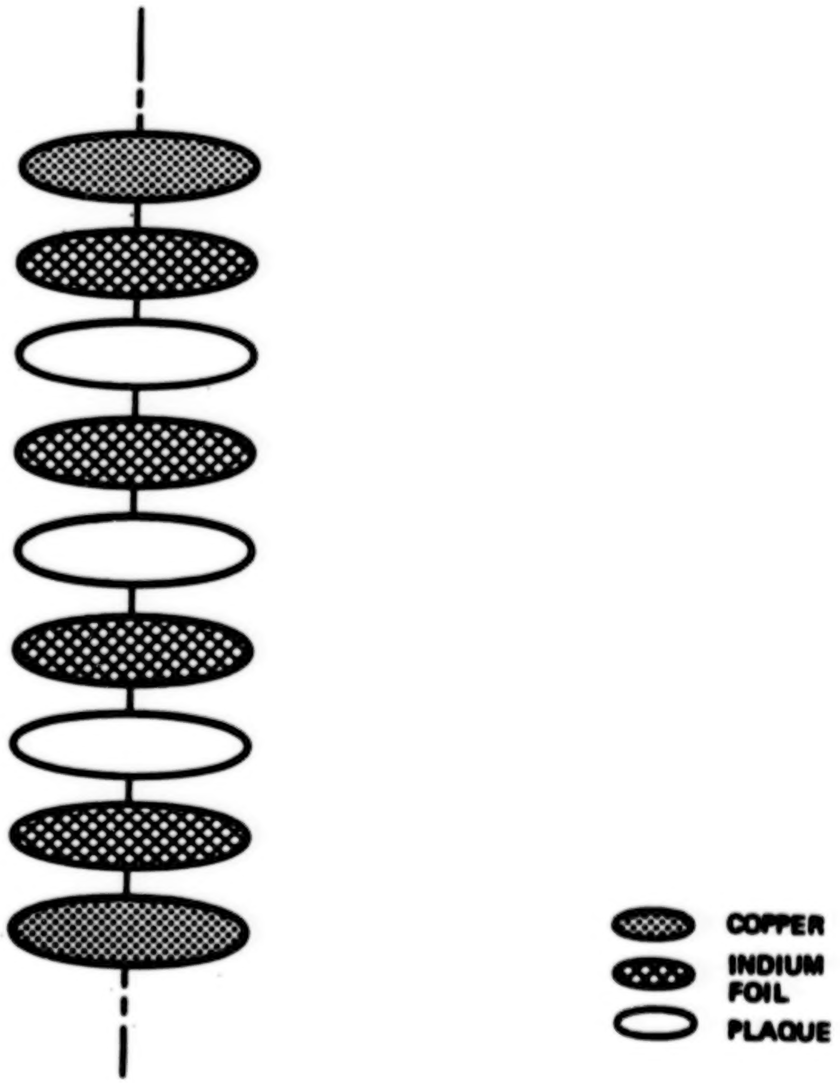
COPPER
INDIUM FOIL
PLAQUE

- DISCS 15/16 INCH DIAMETER
- MEASURE STACK RESISTANCE UNDER COMPRESSION

Figure 12. Test for Electrical Resistance of Plaque in Thickness Direction

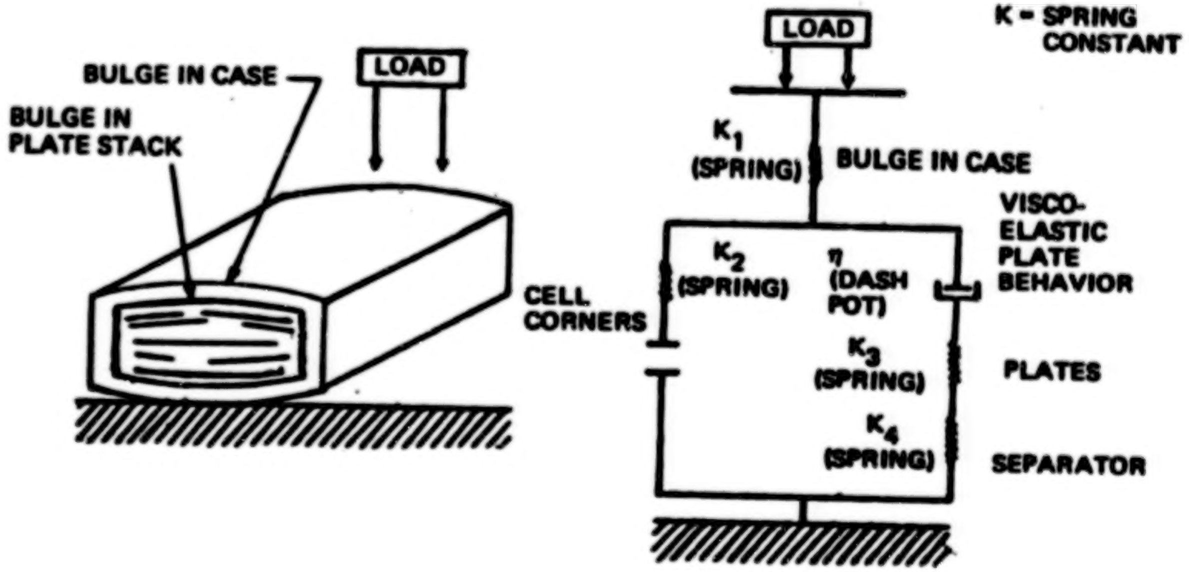
BULGE IN CASE
BULGE IN PLATE STACK
LOAD
CELL CORNERS
LOAD
K - SPRING CONSTANT
K_1 (SPRING)
BULGE IN CASE
K_2 (SPRING)
η (DASH POT)
VISCO-ELASTIC PLATE BEHAVIOR
K_3 (SPRING)
PLATES
K_4 (SPRING)
SEPARATOR

Figure 13. Analytical Model of Cell in Compression

ORIGINAL PAGE IS
OF POOR QUALITY

Q. Mani, Energy Conversion Devices, Inc.: What kind of equipment did you use for this heat capacity measurement? What type of heat capacity you measure by this method?

A. Gross, Boeing: What kind of heat capacity does one measure by?

Q. Mani, Energy Conversion Devices, Inc.: This kind of heat capacity. The one where you are , I mean showed in the figure?

A. Gross, Boeing: Okay, well the data shown for the example was heat capacity of 0.2 and which is the same in let's see that the same in engineering units that BTU's per pound per degree fahrenheit.

Q. Mani, Energy Conversion Devices, Inc.: You said the heat capacity you measure is. Don't you think it is distributed more in the alkaline. And how you can differentiate you are going to measure one as a total but the cell capacity mostly differs upon the electrode and the alkaline interface. How are you going to differentiate this one?

A. Gross, Boeing: Well, this is a net heat capacitance cell and if you know exactly what the percentage is of each material that goes into the cell and the specific heat of those materials you can calculate the average heat capacitance but we didn't have, we weren't competent that we had good data and that was the reason we wanted to run the test.

A. Mani, Energy Conversion Devices, Inc.: Thank you.

Q. Unidentified, Eastman Kodak: Your plaque resistance test. Was that a DC or a AC test?

A. Gross, Boeing: That was a DC test.

Q. Unidentified, Eastman Kodak: Was it pressure sensitive or was it temperature sensitive?

A. Gross, Boeing: We tested the affects of pressure and we found that very low pressure gave us unreproducible results and very high pressure also gave us results where we would squeeze down too much and would give us we felt, we were compressing the materials too much and we found in between was an exceptable range where we got reproducible results and yet we didn't feel as if we were injuring any of the parts.

Q. LaFrance, Aerospace Corp.: I found the techniques are interesting. I would like to ask you more of a question about the results however. For example, essentially the charging you mentioned was in endothermic region you reached about 80% charge, then it becomes essentially exothermic. Now is this true at a charge rate of C over 10 or C over two or something like that during the endothermic region.

A. Gross, Boeing: Well that data was for nickel cadmium cell and nickel cadmium cell is endothermic during charge except that in for large cells or even small cells that height charge rates the endothermic amount is frequently offset by our eye drop due to the charge current so frequently when you actually measure a cell you will get very close to zero. It's been our experiences it's very close to zero as a result of the two cancelling out and then of course the point at which the heat generation starts is dependent upon the temperature and the charge rate. So you really can't generalize to say exactly what the shape of the heat as a function at the end of charge.

Q. Unidentified, Aerospace Corp.: Sid, what is the purpose of the foil and the thickness resistance measurement.

A. Gross, Boeing: The purpose of the foil is to get electrical contact to the plaque material otherwise you can't easily make an electrical contact over its entire surface.

N84
33696

UNCLAS

N84 33696 D28

EMU BATTERY/MODULE SERVICE

TOOL CHARACTERIZATION STUDY

Charles F. Palandati
Goddard Space Flight Center

ABSTRACT

The power tool which will be used to replace the attitude control system in the SMM spacecraft is being modified to operate from a self contained battery. The extravehicular mobility unit (EMU) battery was tested for the power tool application.

The results obtained during this study show the EMU battery is capable of operating the power tool within the pulse current range of 2.0 to 15.0 amperes and battery temperature range of -10 to 40 degrees Celsius.

INTRODUCTION

The Solar Maximum Mission (SMM) spacecraft was launched February 14, 1980. The attitude control system (ACS) has developed problems which have effected the normal spacecraft operation. During the shuttle mission (STS 13) scheduled April, 1984 the ACS will be replaced while the spacecraft is attached to the "flight support system" located in the cargo bay of the shuttle.

A power tool (Figure 1) has been designed and developed to operate from the alternating current (AC) power bus in the shuttle and therefore the area in which the tool can operate is limited. A direct current (DC) motor is being designed to operate from a battery contained in the tool, thereby allowing the power tool to operate independent of the shuttle's power bus.

Figure 2 shows the Extravehicular Mobility Unit (EMU) battery which is used by the astronauts during EVA maneuvers. The size, weight (4.35 Kg) and nominal capacity (25 Ah) of this silver-zinc battery is compatible with the power tool application. The battery is presently required to support one 15 amp pulse for 5 seconds and seven hours of continuous operation at 3.5 amperes (Reference 1) at the minimum battery temperature of 4.4 degrees Celsius (Reference 2), whereas the gearmotor of the power tool will introduce numerous high pulse current loads to the battery during initiation of removing the bolts from the ACS, which requires a high torque capability from the power tool.

There were no data available to define the EMU batteries' minimum operating temperature required to support the high current for the power tool application in the thermal environment of outerspace, and therefore it was necessary to perform this characterization study of the EMU battery as shown in Figure 3.

TEST PHILOSOPHY

In order to determine the temperature range in which the battery could operate for the power tool application, it was necessary to establish discharge voltage profiles at various pulse current loads and temperature levels to a 100 percent depth of discharge (DOD). The 3.5 ampere constant current drain for the EMU regime was used to simulate the power tool "full speed" current drain and the battery's maximum pulse current capability of 15 amperes for a 5 second duration was used to simulate the gear motors "stall time" current load. Figure 4 is a plot of the typical discharge profile used throughout this study. The battery was discharged at 3.5 amperes and pulsed at 15 amperes every other minute. At minute 59 of each hour the battery was sequentially pulsed at seven different current levels (2.0 to 14.0 amperes). Battery current, voltage and temperature data was monitored every minute, three times during each pulse current level, and one second after the completion of each pulse regime. In order to prevent cell reversal, each discharge was terminated (voltage cutout) when the voltage decreased to 12.0 volts.

Although the power tool application will not require "battery recharging" during the shuttle mission, this battery was recharged many times during the study. Battery charging was performed according to the EMU specifications (Reference 1), 1.5 amperes and 21.8 volt cutout at 20°C or at 1.0 amperes. Two different charge currents were used to allow sufficient time for the battery temperature to stabilize at the next successive discharge regime (approximately one hour per Δt of 10°C). The data were monitored every ten minutes.

EMU DISCHARGE CHARACTERIZATION TESTS

The first discharge (cycle 1) was performed at 20°C ambient temperature in order to establish the baseline voltage characteristics and battery capacity after the 7 month stand period, since the 3 previous cycles and recharge were accomplished at room temperature ambient. The capacity output was substantially greater than the pre-shipping recharge capacity because the battery had not been discharged to 100% DOD during the initial 3 cycles. Figure 5 is a plot of the entire discharge and Figure 6 shows the first sequential pulse regime during this discharge.

There was a significant decrease in battery voltage during the 0°C discharge and a severe decrease of -10°C (Figure 7). There was also a decrease in discharge capacity at the lower temperatures due to the inefficiency of the electro-chemical reactions within the battery cells. The battery voltage was slightly above 15 volts at the end of the first sequential pulse (Figure 8).

There was very little change in the battery voltage between the steady state load and pulse current load during the 40°C discharge shown in (Figure 9) which occurred during the seventh discharge of this test regime. The higher battery voltage which was evidenced at the beginning of this discharge is attributed to Ag_2O_2 which gradually increased during the extensive cycling regime rather, than the higher test temperature.

CONCLUSIONS

The battery is capable of operating the power tool within the pulse current range of 2.0 amperes to 15.0 amperes and battery temperature range of -10°C to 40°C.

The "plateau" voltage which occurs when the silver electrodes are at the monovalent voltage level substantially decreases at the lower temperatures and higher pulse currents during the sequential pulse regime presented in Figure 10. The battery impedance ranged from 73 milliohms when battery temperature was 42°C and increased to 162 milliohms when battery temperature was -6.7°C. Figure 11 is a graph of the calculated battery impedance derived from the change in battery voltage (ΔV) which occurred at the various current levels during the sequential pulse regimes after the battery voltage stabilized at the monovalent potential.

Although the battery was capable of supporting numerous simulated "stall time/full speed" power tool operations at all temperature levels, the number of power tool operations will be reduced at sub zero temperatures if the power tool requires a higher operating voltage than the 12.0 volt cutout used to terminate all discharges throughout this study.

REFERENCES

1. "Space Shuttle Activation And Recharging Procedures For The Shuttle EMU & MMU Battery," Document JSC 11617 (Rev. A) February 11, 1982.

2. "Battery Manufacturing Control Document 04236," Martin Marietta Corporation.

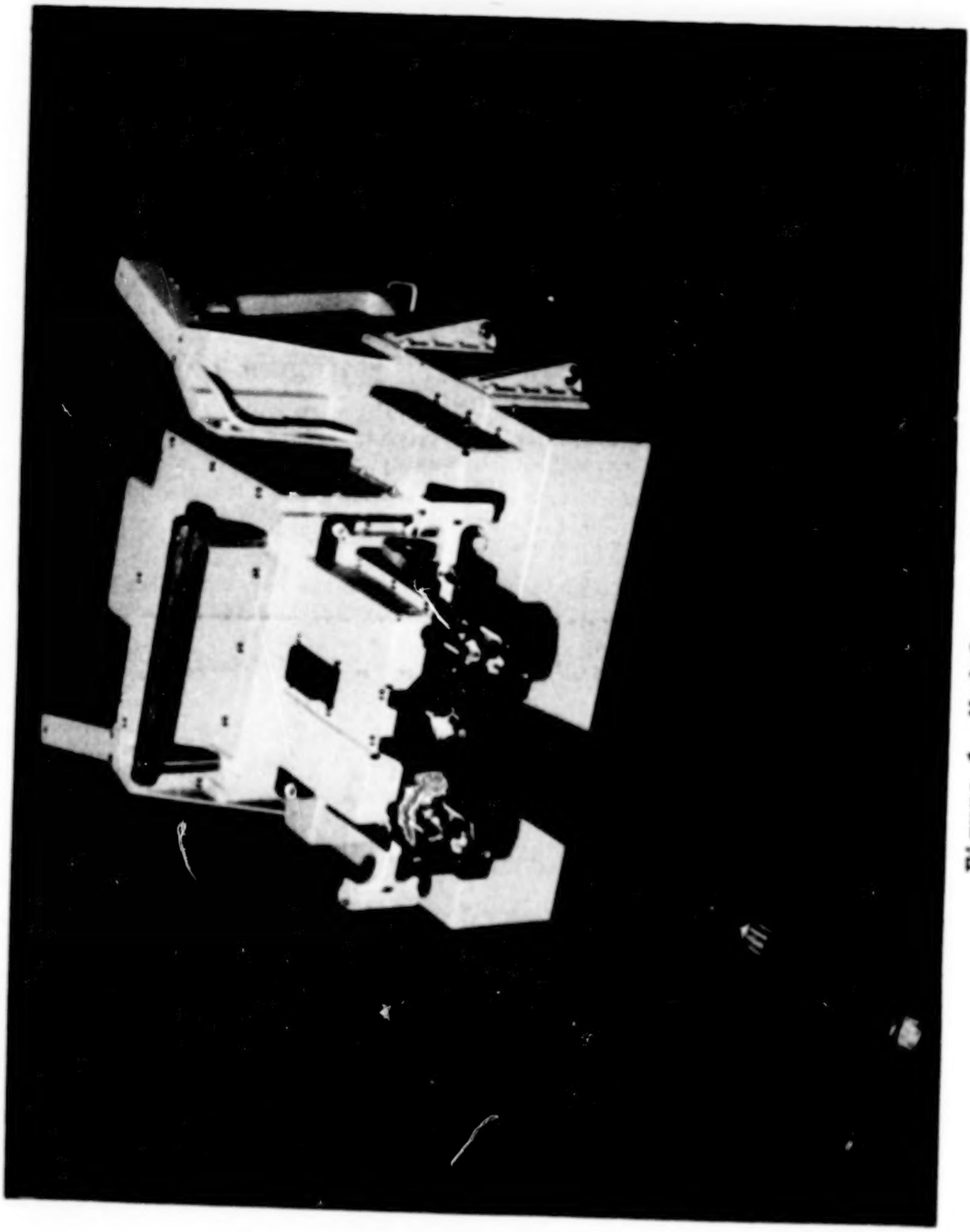

Figure 1. Module service tool.

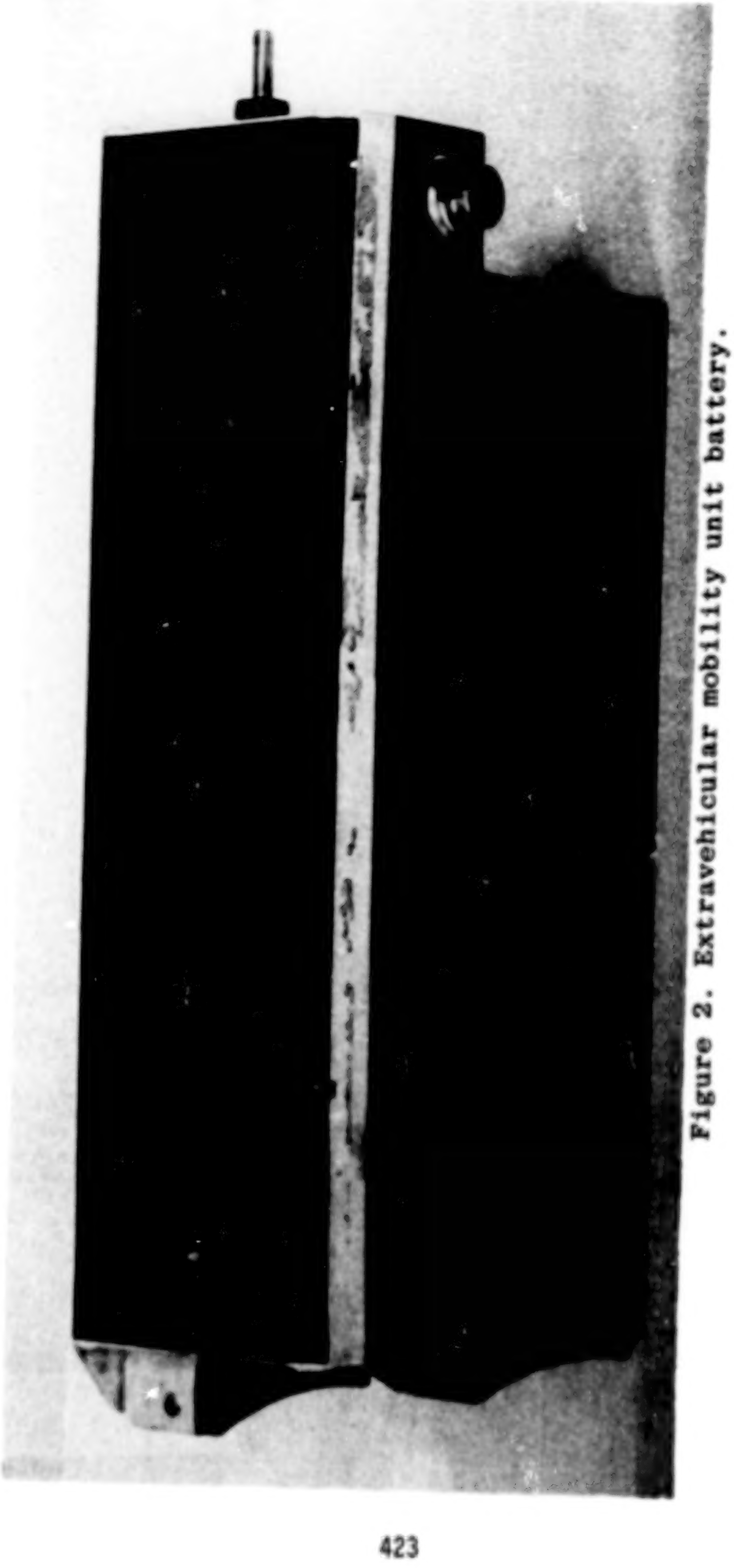

Figure 2. Extravehicular mobility unit battery.

EMU BATTERY/SMM POWER TOOL CHARACTERIZATION STUDY

PURPOSE

- DETERMINE TEMPERATURE RANGE FOR BATTERY OPERATION WITHOUT HEATERS
- ESTABLISH VOLTAGE PROFILES AT VARIOUS PULSE CURRENT LOADS AND TEMPERATURE LEVELS
- CHARACTERIZATION OF BATTERY IMPEDANCE FOR EACH TEMPERATURE LEVEL
- DETERMINE BATTERY DISCHARGE CAPACITY AND EFFICIENCY AS A FUNCTION OF TEMPERATURE

TEST PARAMETERS

- BATTERY CHARGING AT 20°C AND 1.0 OR 1.5 AMPS
- 3.5 AMP CONSTANT CURRENT LOAD (POWER TOOL FULL SPEED LOAD)
- 15.0 AMP, 5 SECOND PULSE LOAD (POWER TOOL STALL LOAD)
- SEQUENTIAL PULSE REGIME (2.0 TO 14.0 AMPS, 5 SECOND DURATIONS)
- 100% DOD AT -10°C TO 40°C (10 DEGREE INCREMENTS)

Figure 3. Characterization study profile.

EMU BATTERY / SMM POWER TOOL CHARACTERIZATION TEST

DISCHARGE PROFILE

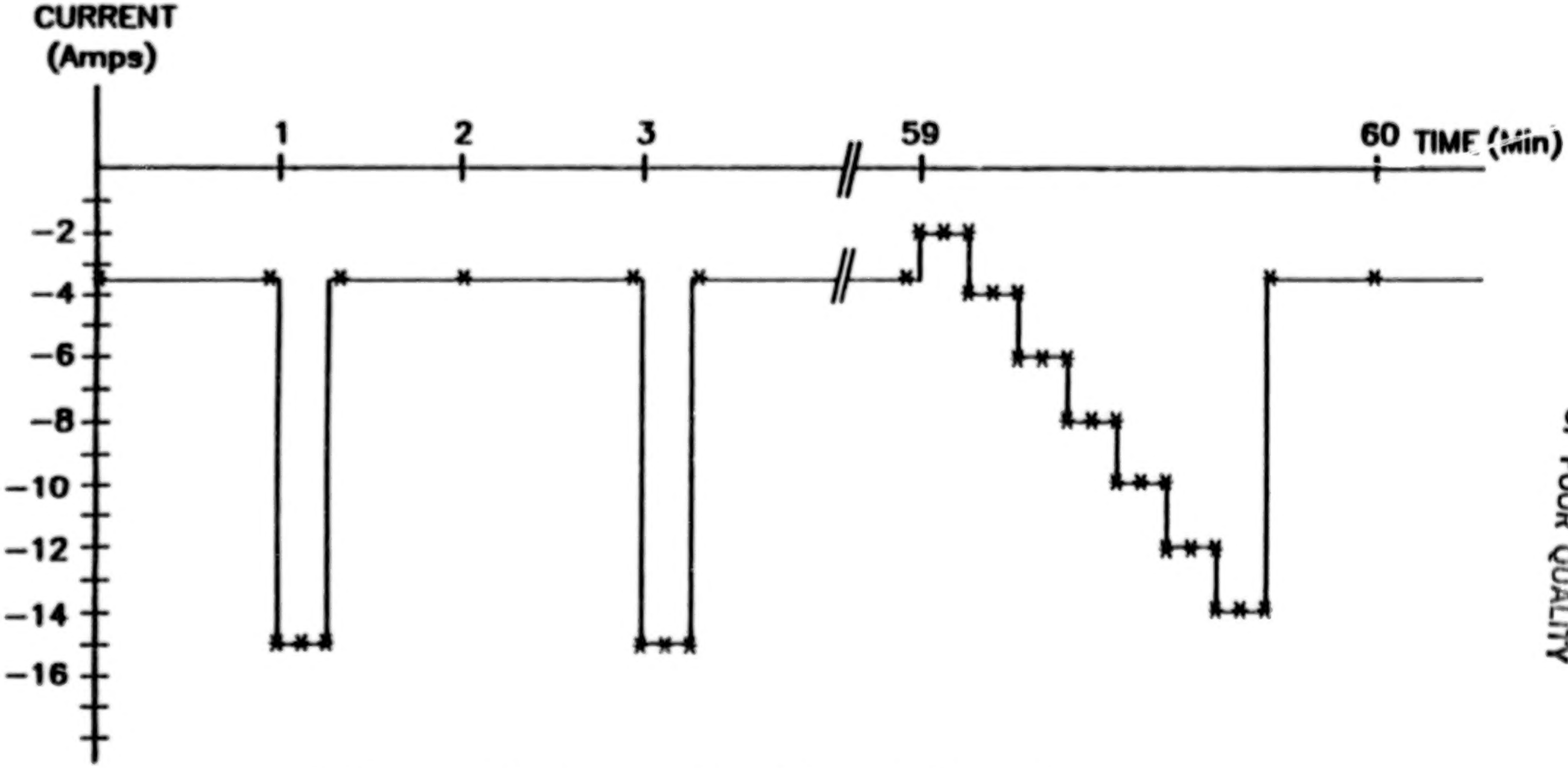

NOTE: * indicates readings taken at this point

Figure 4. Typical discharge profile.

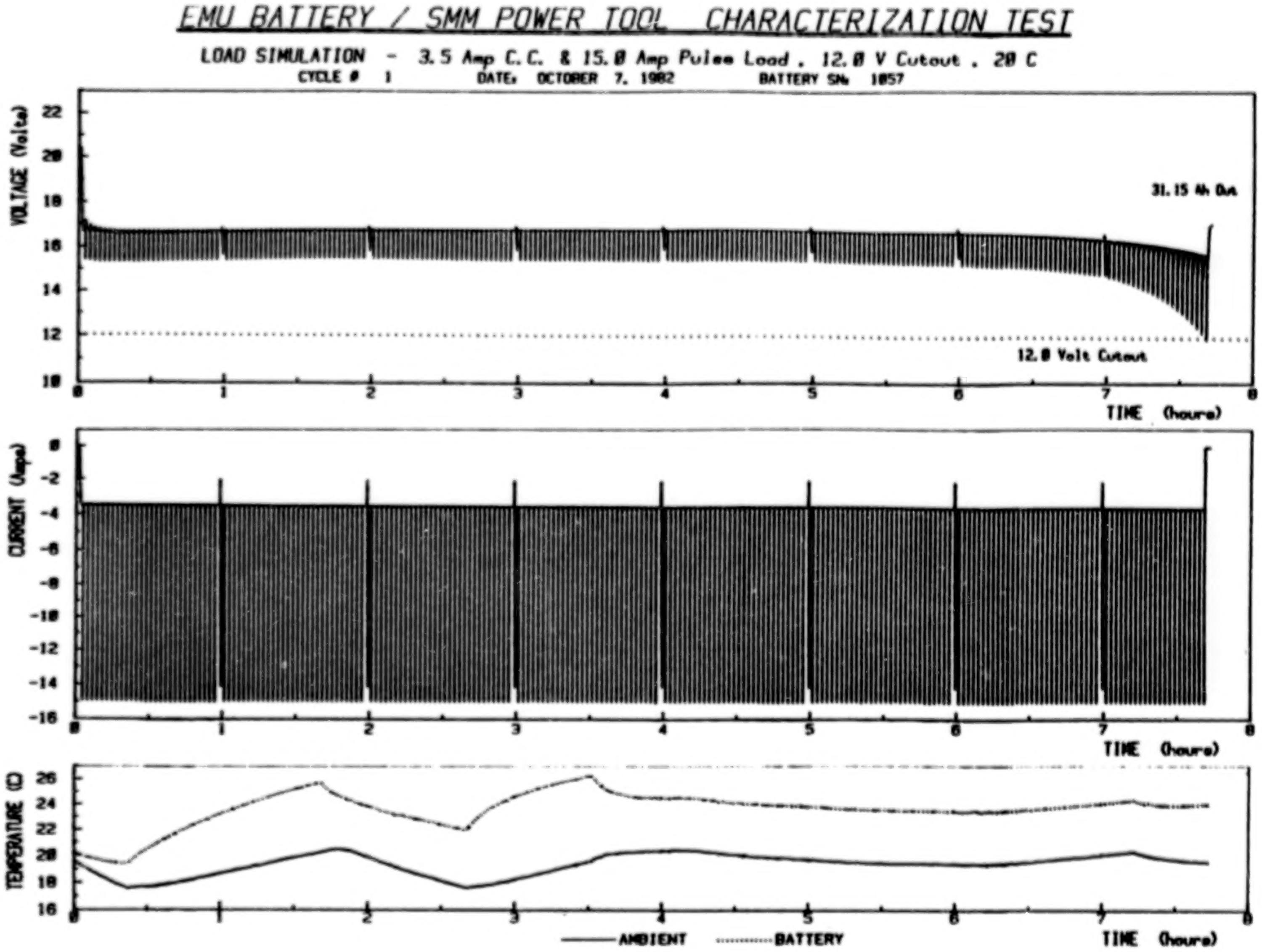

Figure 5. 20°C discharge characterization test.

ORIGINAL PAGE IS
OF POOR QUALITY

ORIGINAL PAGE IS
OF POOR QUALITY

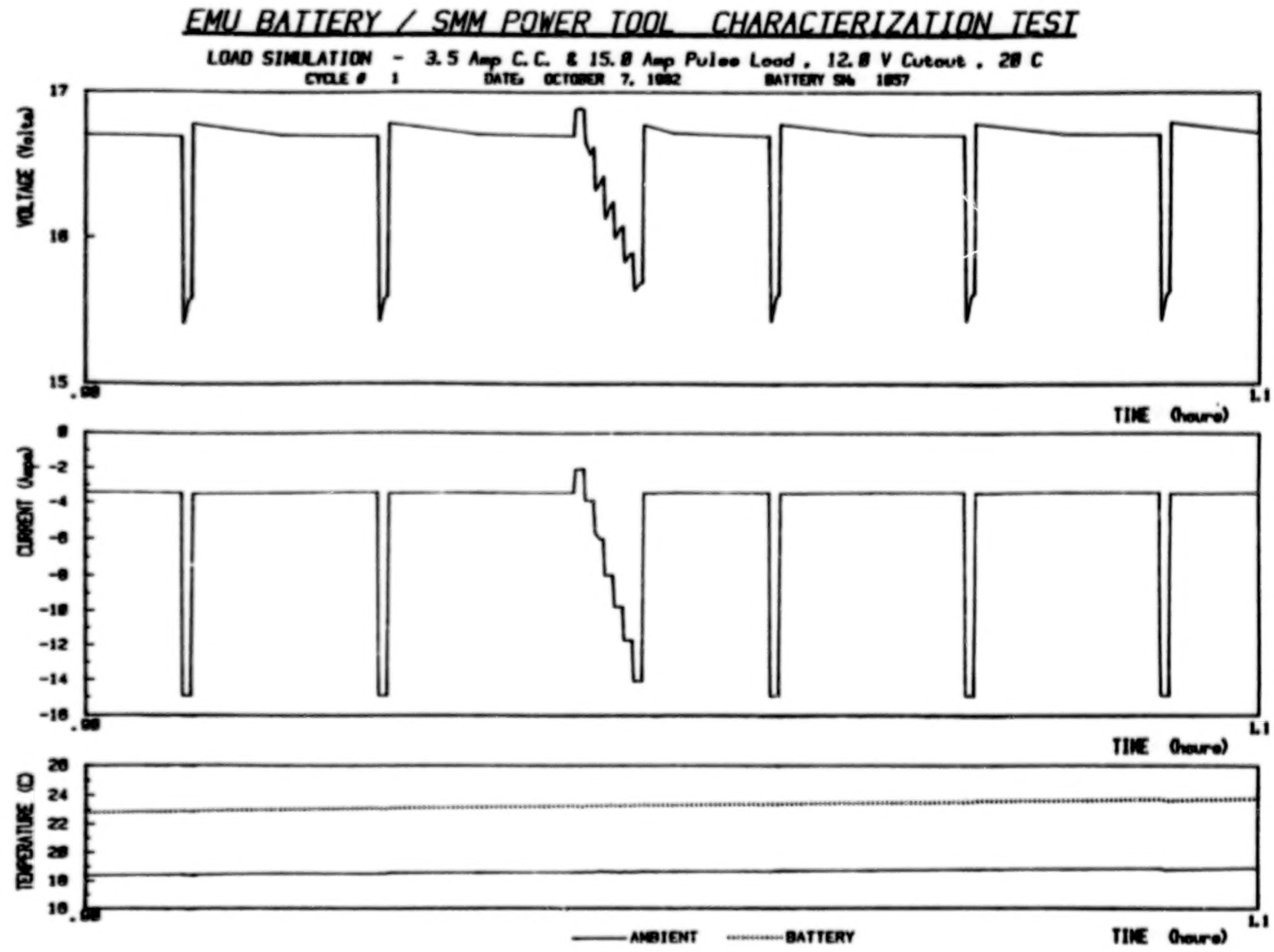

Figure 6. First sequential pulse regime at 20°C.

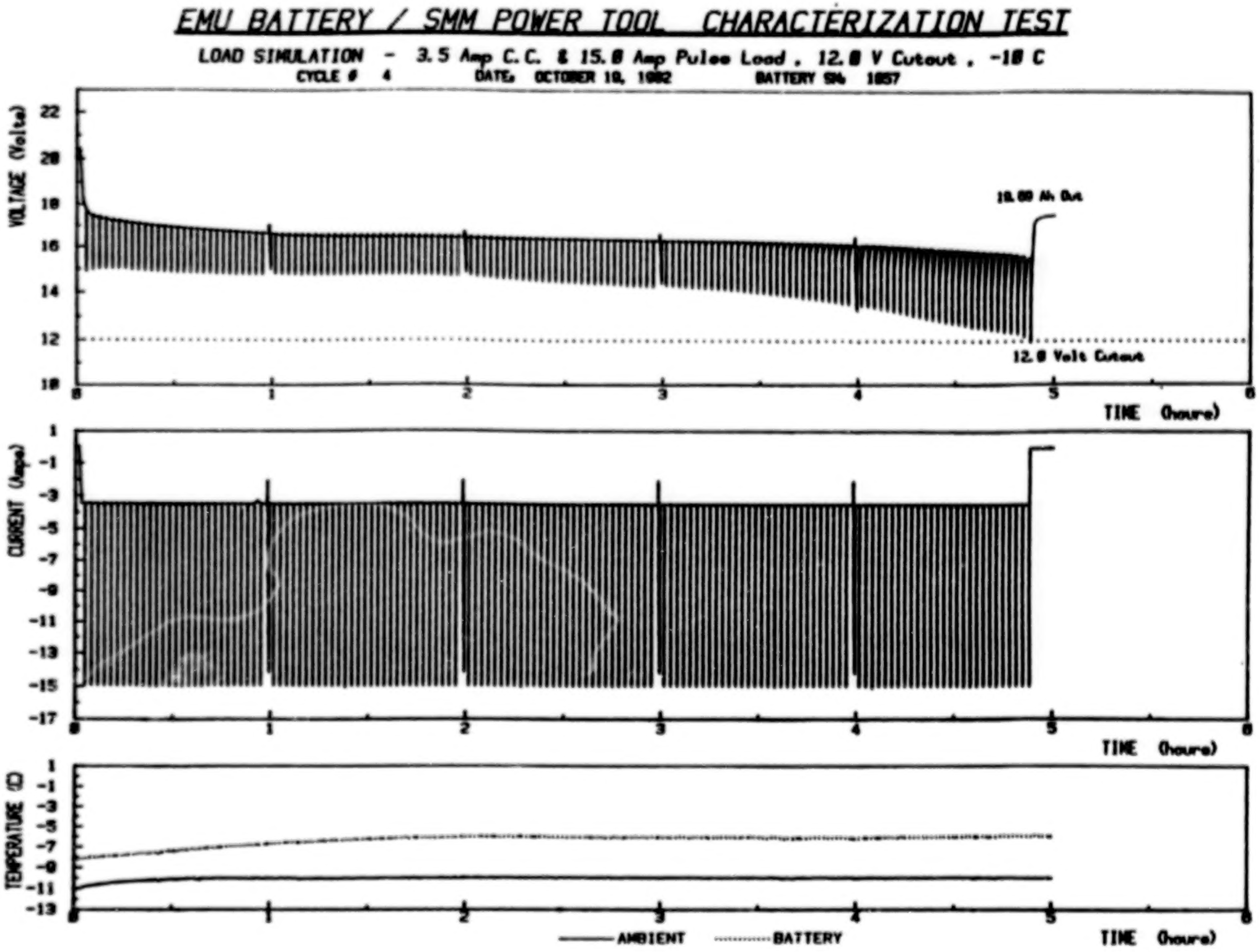

Figure 7. -10°C discharge characterization test.

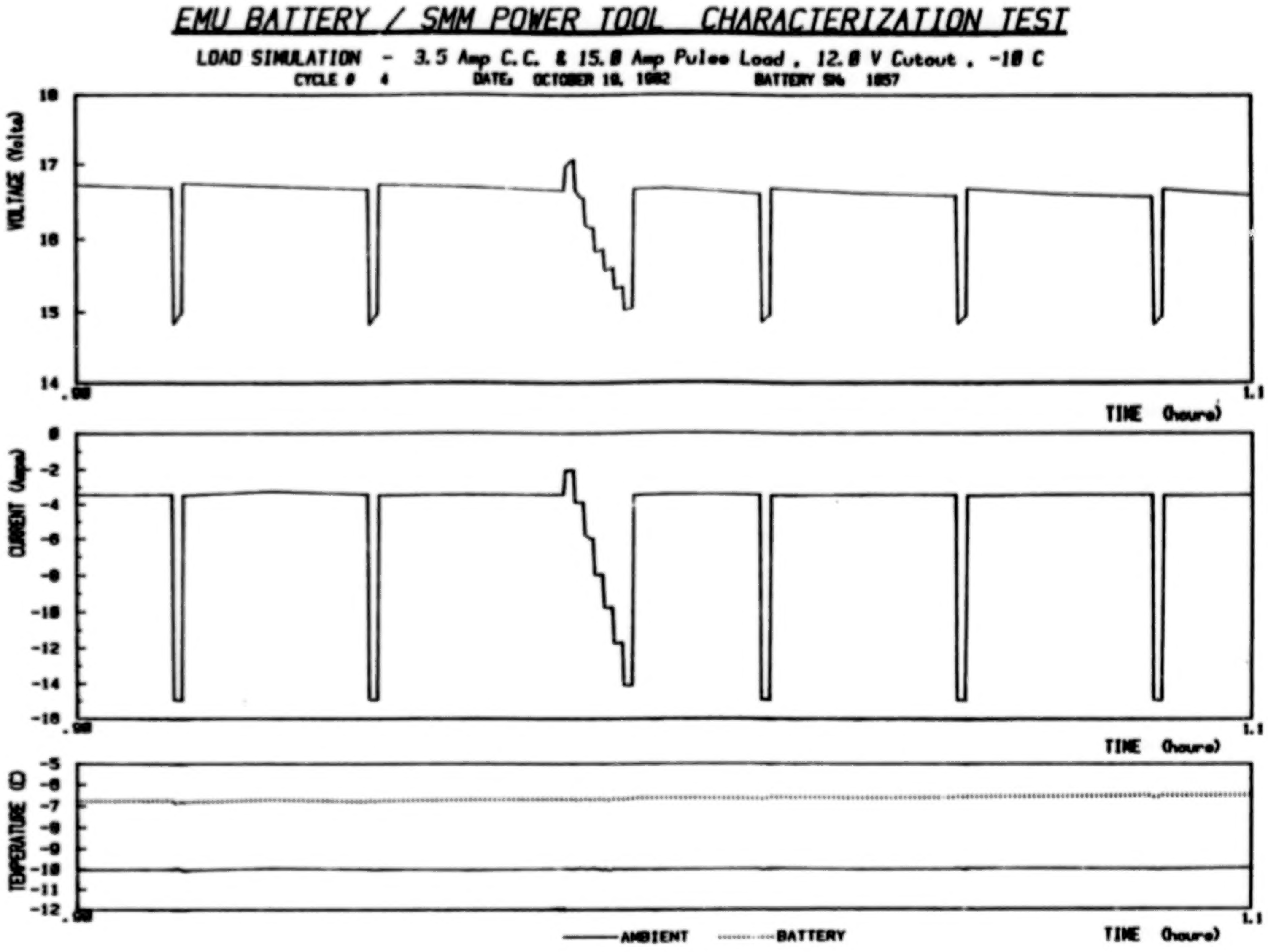

Figure 8. First sequential pulse regime at -10°C.

ORIGINAL PAGE IS
OF POOR QUALITY

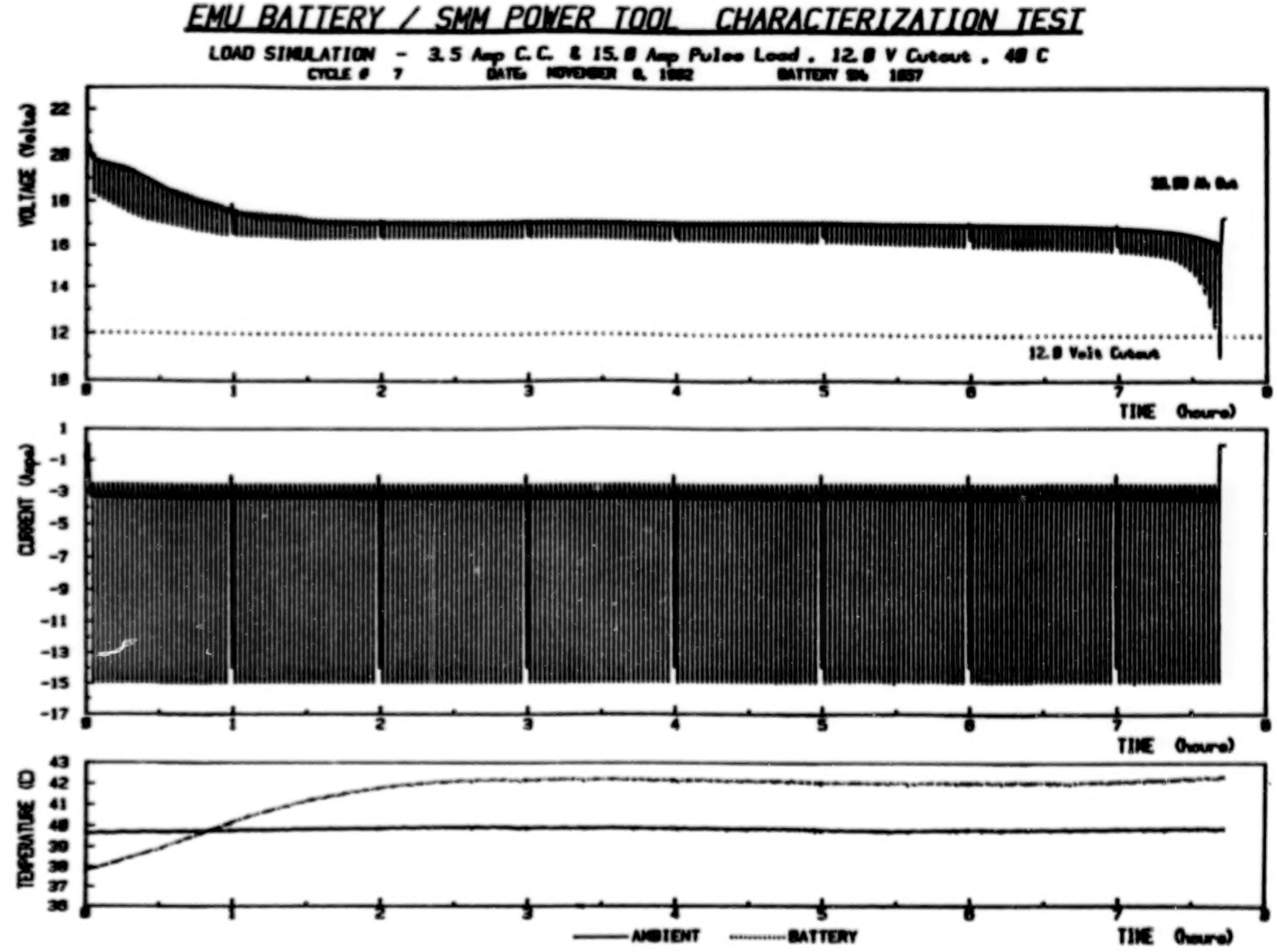

Figure 9. 40°C discharge characterization test.

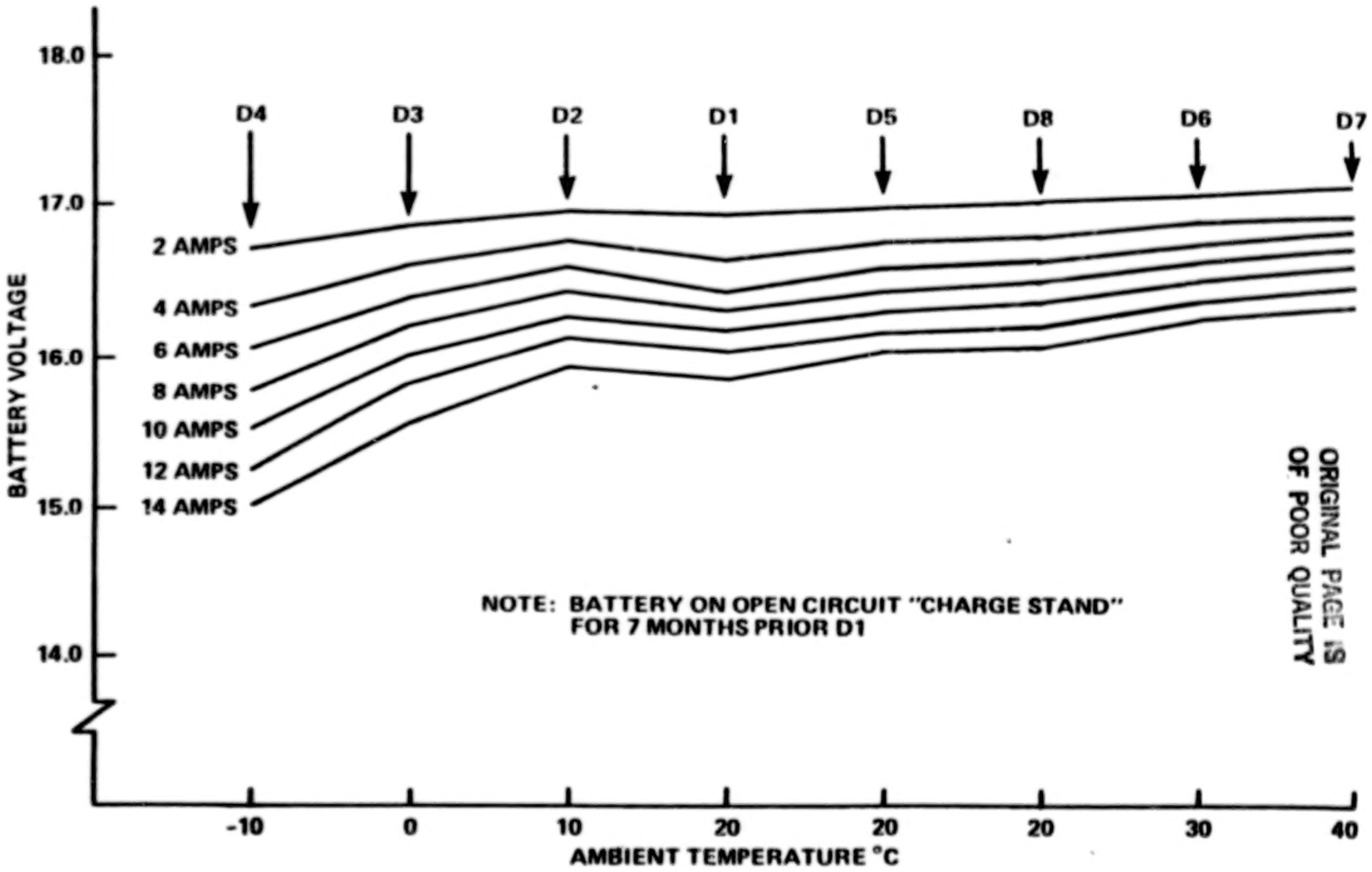

Figure 10. Plateau voltage vs. temperature during sequential pulsing.

ORIGINAL PAGE IS
OF POOR QUALITY

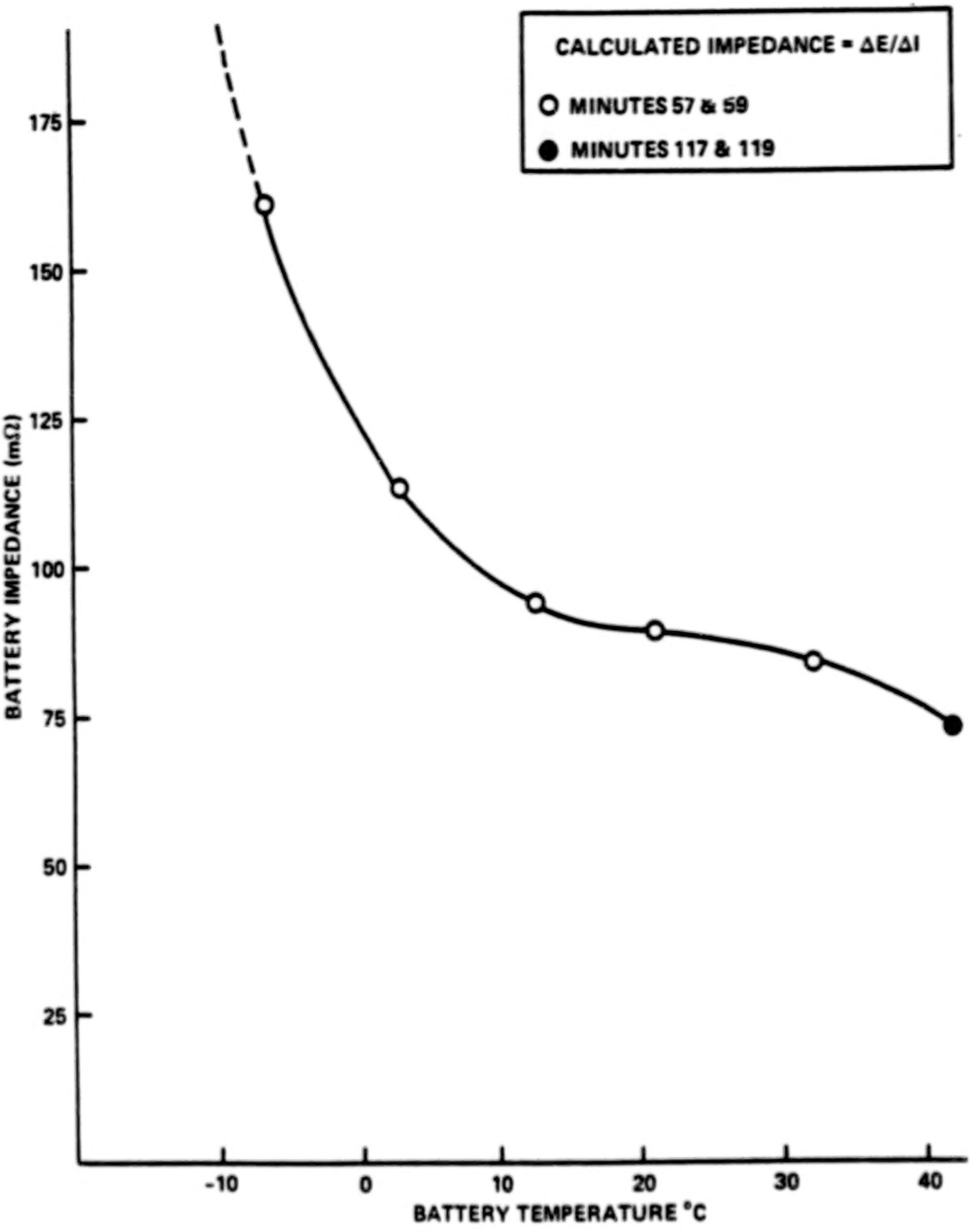

Figure 11. Battery impedance vs. temperature.

SESSION V: METAL HYDROGEN

Chairman: L. Thaller,
NASA/Lewis Research Center

N84
33697

UNCLAS

N84 33697 D29

PRELIMINARY SILVER-HYDROGEN CELL TEST RESULTS

Charles Lurie
TRW Space and Technology Group

ABSTRACT

Silver-hydrogen cells have been on test at TRW since July, 1982. The objective of the test is to estimate useful life by operation at accelerated, simulated geosynchronous orbit conditions. Ten simulated seasons have been run and are summarized. The results to-date reflect stable, trouble-free performance and indicate that the silver-hydrogen couple shows promise as a lightweight alternative to the nickel systems.

INTRODUCTION

The silver-hydrogen couple is attractive because of its high specific energy and energy density. At the last Battery Workshop SAFT presented test results obtained with silver-hydrogen cells designed and built in their aerospace facility in Romainville, France.(1) The results reported were encouraging and projected a specific energy in the range 65 to 80 Wh/kg and an energy density in the range 50 to 60 kWh/m^3. TRW purchased four of these cells in 1981 and started testing in 1982. This paper presents a summary of the testing to-date including the objectives, the test articles, the test plan and setup, and preliminary test results.

The primary objective of the test is to estimate the useful life of the SAFT silver-hydrogen cells by operating them at accelerated, simulated geosynchronous orbit conditions. Testing is restricted to the geosynchronous orbit application because the limited number of test articles dictate a single set of operating conditions, and it appears that booster limitations will continue to make battery specific energy a more important parameter for high-altitude missions than for low-altitude missions.

A secondary objective is to identify spacecraft integration issues peculiar to the silver-hydrogen couple. These will include discharge voltage characteristics, thermal characteristics, and charge management issues.

TEST ARTICLES

The test articles are type HRA 46S silver-hydrogen cells manufactured by SAFT in Romainville, France. SAFT rates the cell at 46 ampere-hours and indicates that beginning-of-life capacity, for an 11.2-ampere discharge at

PRECEDING PAGE BLANK NOT FILMED

23 ±2°C, is 58 ampere-hours following 22 hours of charge at 2.8 amperes. This discharge is terminated at 0.8 volts and the charge voltage limited at 1.65 volts. Testing at TRW, using the same charge-discharge cycle, yielded average capacities of 54.8 ampere-hours at 10 ±2°C and 56.0 ampere-hours at 15 ±2°C. Analysis of these data results in a capacity temperature coefficient of 0.25 Ah/°C.

Maximum cell operating pressure is specified at 40 atmospheres for the HRA 46S cells using Inconel 625 containers. New containers made from Inconel 718 are available and will be rated at 70 atmospheres maximum pressure. Rated specific energy is 75 Wh/kg at 23 ±2°C. During characterization testing at TRW the average specific energy observed was 69 Wh/kg at 15 ±2°C. Following eight charge-discharge cycles, each consisting of 22 hours of charge at 2.8 amperes followed by an 11.2-ampere discharge to 0.8 volts, the observed specific energy was 66 Wh/kg. The cells weigh 880 grams and are filled with 193 ml of 10.3 N potassium hydroxide electrolyte.

With the exception of the silver electrode and the separator the components of the silver-hydrogen cells under test are similar to those of a nickel-hydrogen cell. The chemistry, as indicated in figure 1, is simply that of the silver and hydrogen electrodes. The silver electrode, made by the SAFT continuous rolling process, is 0.57 millimeter thick with a porosity of 60 percent and utilizes an expanded silver grid. The separator consists of multiple layers of nonwoven nylon Pellon material adjacent to the silver electrode and multiple layers of Yardney C19 cellophane.

TEST PLAN

The four silver-hydrogen cells were placed on test in July 1982 and have been operating continuously since. The life test simulates geosynchronous orbit cycling and is preceeded by a series of characterization cycles which will be repeated after completion of the life test. Eclipse seasons during the life test consist of 45 12-hour days with the "stepped" eclipse duration profile shown below. Solstice seasons are shortened to one week during which the cells are discharged at 29.2 amperes to 0.8 volt and recharged.

Day	Eclipse Duration (Minutes)
1-5, 41-45	32
6-10, 36-40	50
11-15, 31-35	62
16-20, 26-30	68
21-25	72

During the course of the test it is anticipated that conditions will be varied to simulate various loads and charge management approaches.

The test cells are mounted in aluminum jackets heat sinked to a thermostatically controlled thermal plate maintained at 5 ±2°C.

Charge management consists of charging the cells at 3.8 amperes until the capacity recharged equals the capacity discharged during the cycle or the cell voltage exceeds 1.67 volts. The cells are then trickle charged until the next eclipse entry. The objective of this approach is to maintain a recharge ratio very close to 1:1. The silver-hydrogen couple's high charge efficiency and low self discharge rate make this feasible. Maximum end-of-charge cell pressures are maintained below 600 psi.

Thus far all eclipse discharges have been at the 29.2-ampere rate. For the maximum duration (72 minutes) eclipse discharges this is equivalent to depths-of-discharge of 76 percent of rated capacity or 63 percent of measured capacity.

RESULTS

Typical voltage, current, temperature, and pressure characteristics observed during low-rate charging are shown in figure 2. The two-plateau voltage curve and the linear pressure rise are characteristic of the system.

Similar characteristics are depicted in figure 3 for a typical C/2 rate discharge performed prior to the life test. The small contribution of the peroxide plateau is typical of results obtained with this type of cycling. The pressure curve is linear.

Inspection of the plot of minimum end-of-discharge voltages versus eclipse season day for Seasons 3, 5, 7, and 10 shown in figure 4 reveals two interesting points:

- The range of end-of-discharge voltages observed during a season is less than observed with a nickel system.
- No season-to-season trend is apparent indicating the absence of degradation through the 10 simulated seasons depicted.

The voltage levels may appear to be a little low but are attributed to an average end-of-discharge temperature of about 8°C.

The cell internal pressure versus eclipse season day relationship shown in figure 5 is typical. Data are presented for both end-of-charge and end-of-discharge pressures. The end-of-charge pressure data plotted represents end-of-trickle charge pressure as this is a more accurate indication of state-of-charge, going into eclipse, then the pressure recorded at switch down from full to trickle charge. The relationships are smooth and suggest a stable configuration.

Despite the smooth and stable end-of-charge and end-of-discharge pressure relationships, analysis of the evolving data base revealed that the minimum end-of-discharge voltage was tracking the previous end-of-charge pressure as can be seen in Figure 6. Although this observation has not yet been investigated, it appears to be related to the fact that it is difficult to return to the same state-of-charge each day when the charge management approach is based on a recharge ratio of 1:1.

It seems probable, as a general observation, that charge management approaches for the silver-hydrogen cell will need to be more sophisticated than for either the nickel-cadmium or nickel-hydrogen system.

CONCLUSION

Results to date indicate that the silver-hydrogen cell shows promise as a lightweight alternative to the nickel systems. Testing at TRW has been restricted to geosynchronous orbit simulation, and this conclusion should be considered in that context. However, the stable, trouble-free performance observed thus far suggests that the system should also be evaluated at low earth orbit conditions.

REFERENCE

1. B. J. Goualard, P. Fougere.: Status of SAFT Silver Hydrogen Cell Development. 1982 Goddard Space Flight Center Battery Workshop, 16-18 November 1982, NASA CP 2263, p. 347.

- Silver Electrode

$$2\,Ag + 2\,OH^- \rightleftharpoons Ag_2O + H_2O + 2e$$

$$Ag_2O + 2\,OH^- \rightleftharpoons 2\,AgO + H_2O + 2e$$

- Hydrogen Electrode

$$4\,H_2O + 4e \rightleftharpoons 2\,H_2 + 4\,OH^-$$

- Overall Reaction

$$Ag + H_2O \rightleftharpoons H_2 + AgO$$

- During Overcharge

$$4\,OH^- \longrightarrow 2\,H_2O + O_2 + 4e \qquad \text{(Silver Electrode)}$$

$$2\,H_2 + O_2 \longrightarrow 2\,H_2O \qquad \text{(Hydrogen Electrode)}$$

Figure 1. The Silver-Hydrogen Couple.

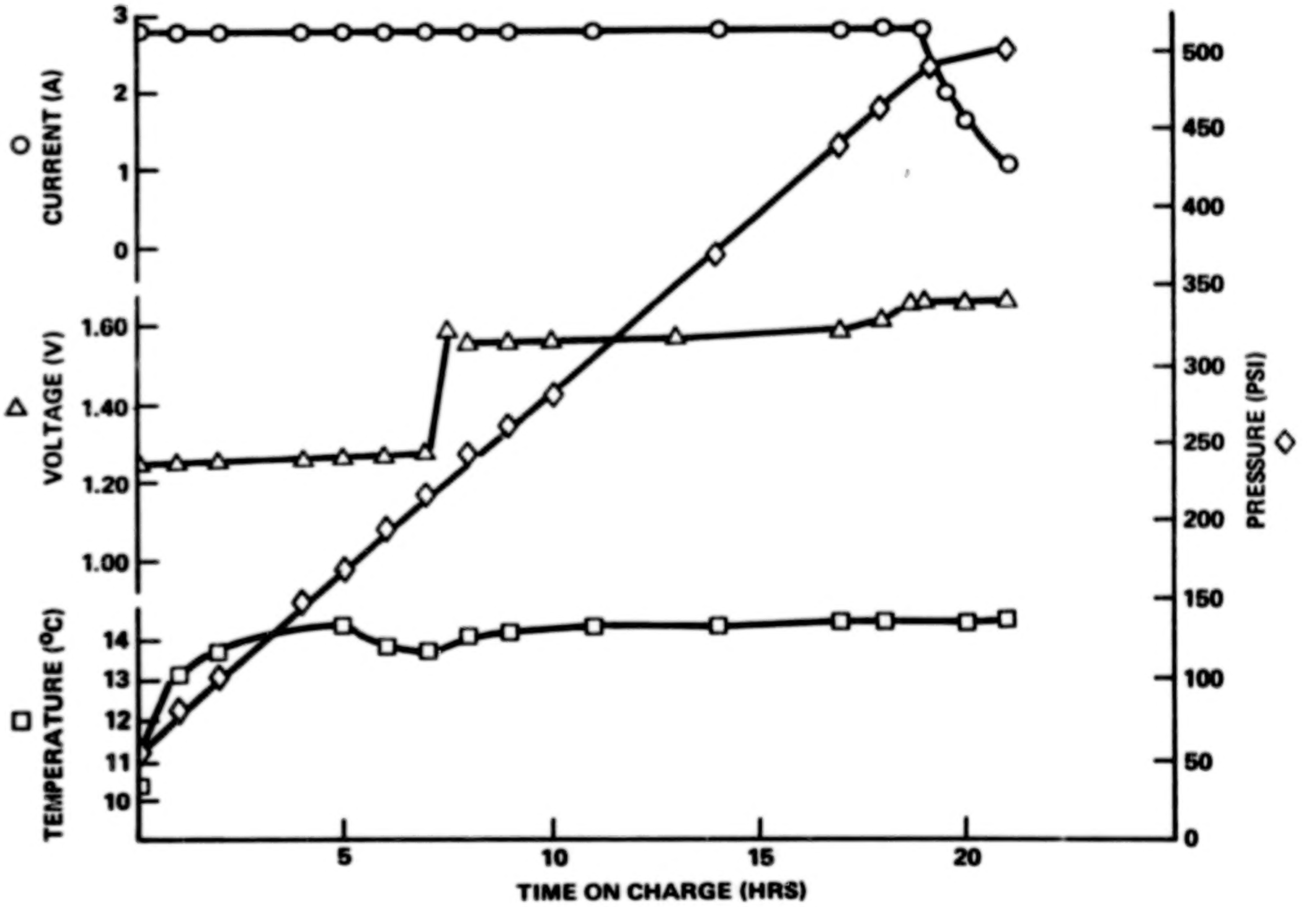

Figure 2. Typical Low-Rate (C/16) Charge Characteristics Prior to Life Test.

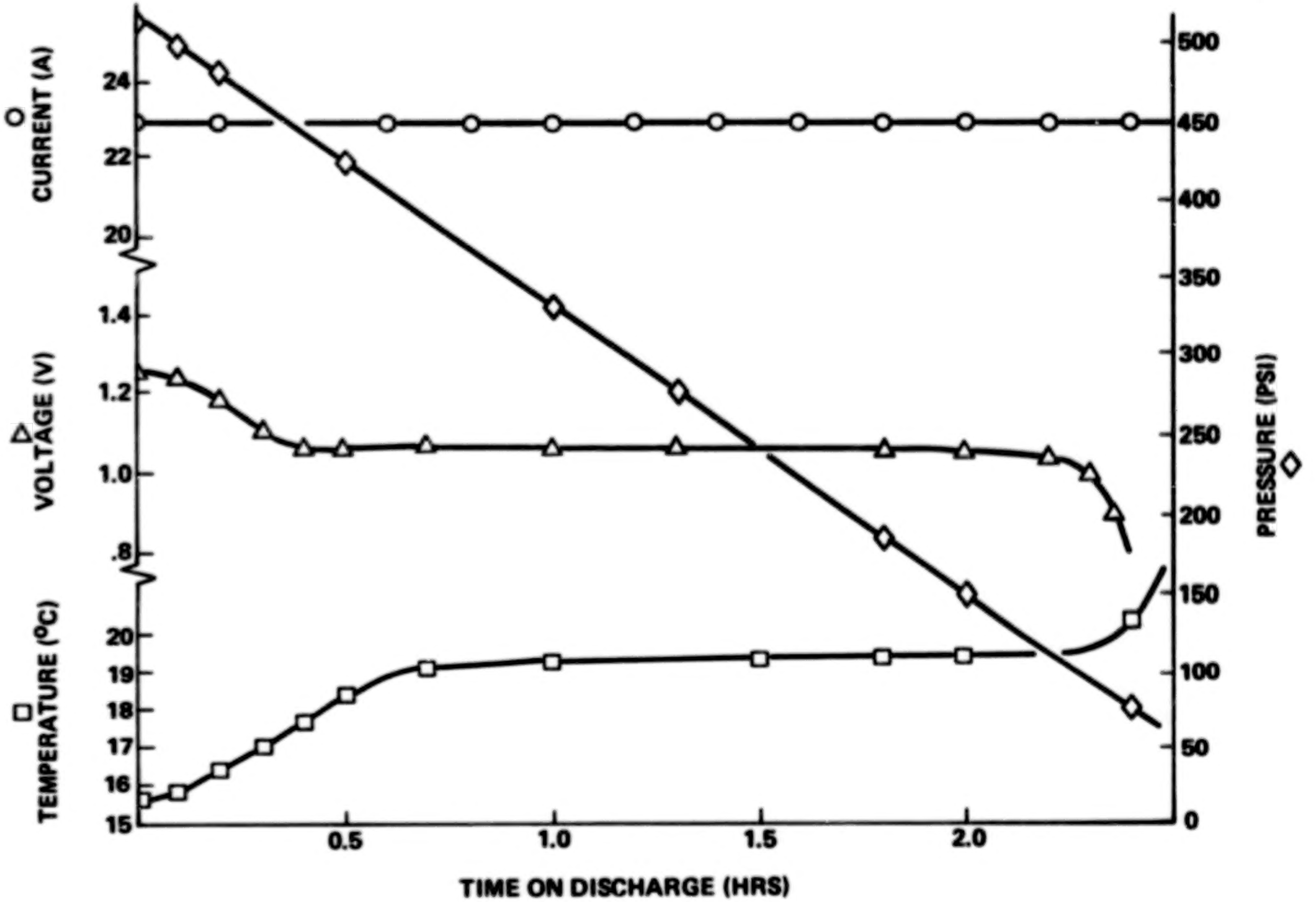

Figure 3. Typical C/2 Discharge Characteristics Prior to Life Test.

ORIGINAL PAGE IS
OF POOR QUALITY

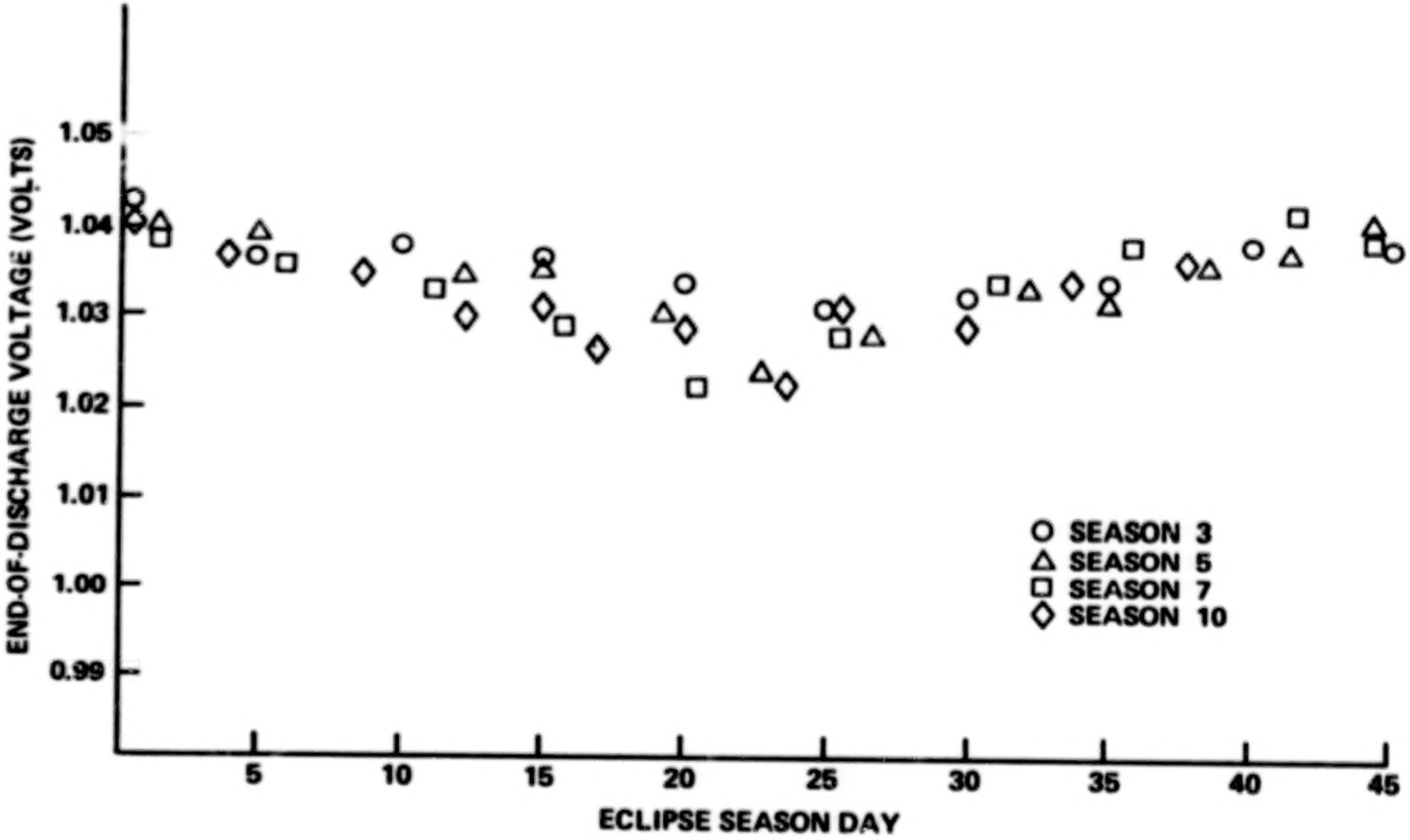

Figure 4. End-of-Discharge Voltage Versus Eclipse Season Day for Seasons 3, 5, 7, 10.

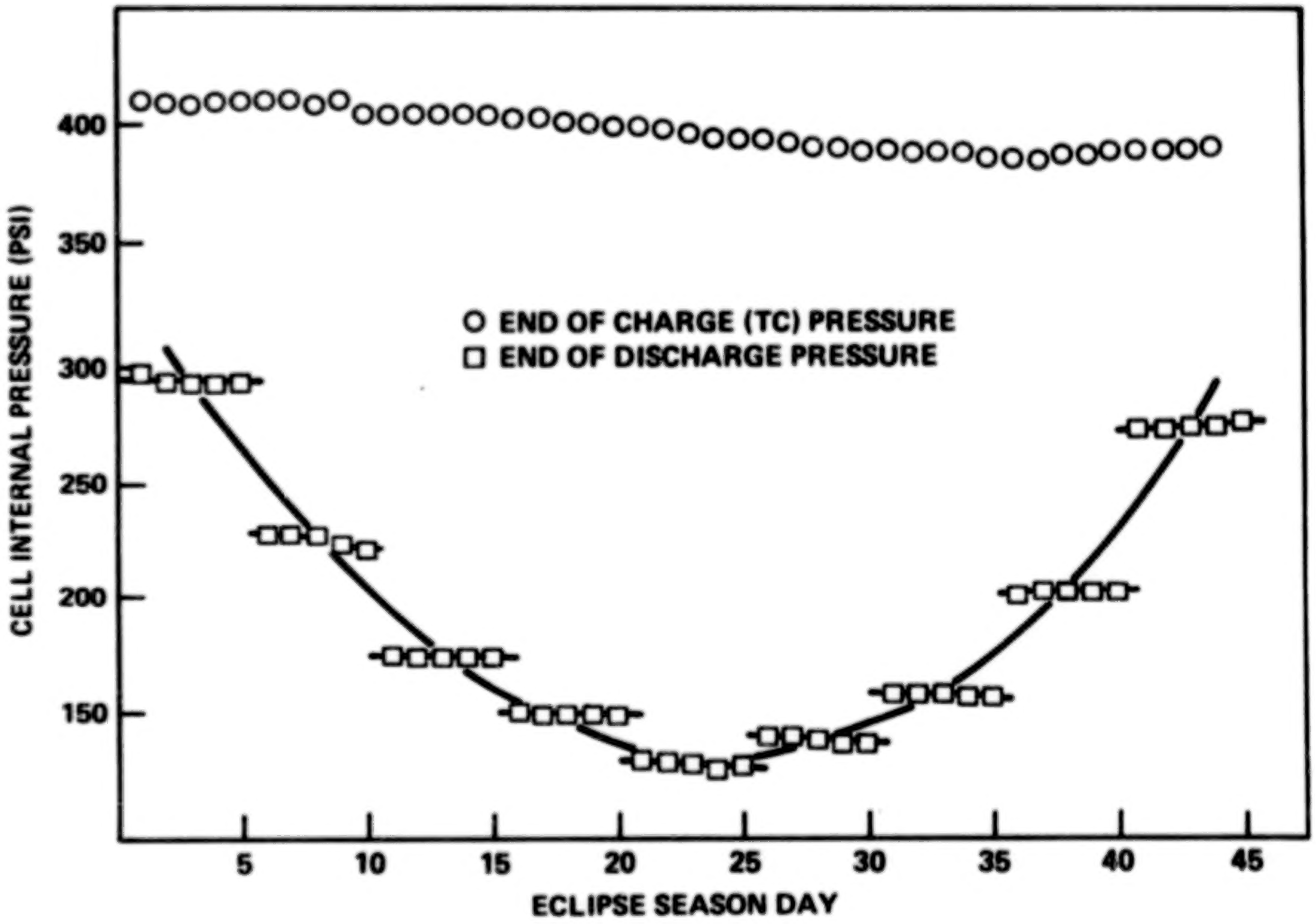

Figure 5. Cell Internal Pressure Versus Eclipse Season Day - Season No. 7.

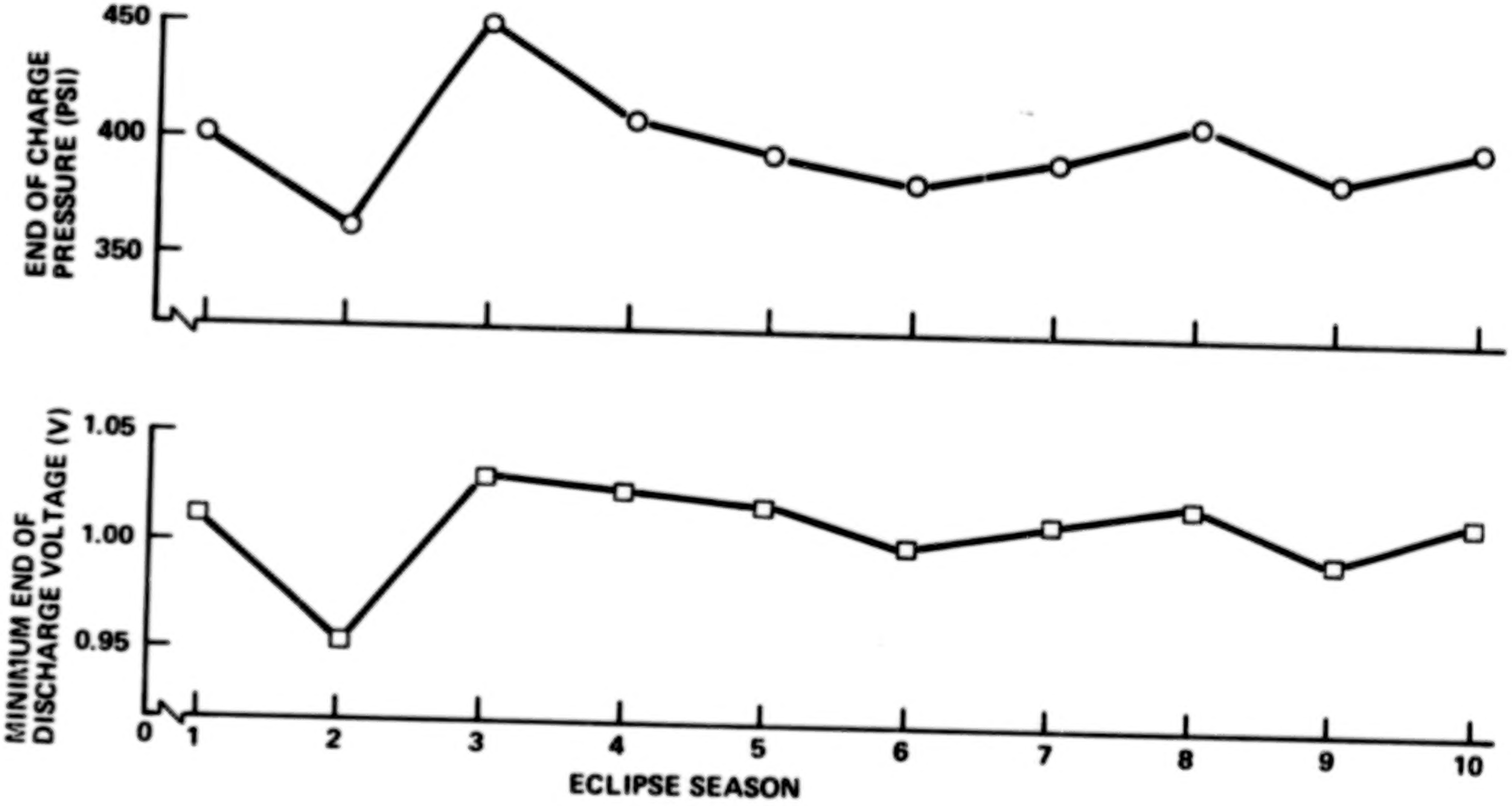

Figure 6. Relationship Between End-of-Charge Pressure and Subsequent End-of-Discharge Voltage.

SESSION V

DISCUSSION

Q. Unidentified, Aerospace Corp.: Have you taken any cells apart yet?

A. Lurie, TRW: No we are going to wait for one to fail.

Q. Dunlop, Comsat: One question when you are estimating 25% energy density or weight savings the only thing I don't understand is you've got about 10% improvement in energy density. Your measured 66 watt hours per pound or one hour per kilogram rather is about the same as the 60 watt hours per kilogram now so you got about a 10% advantage right now.

A. Lurie, TRW: That's .66 we ought to compare apples and apples that 66 was an actually achieved number at a given temperature. If we take the maximum specific energy that we could measure if we were looking for the maximum number I think we would be up near 80. This was a 66 under specific set of conditions at a temperature which gave us less than the max and after eight deep cycles.

Q. Unidentified: What would be the maximum conditions?

A. Lurie, TRW: A higher temperature for one thing.

Q. Unidentified: What temperature you gave a number of 2.5 amp-hours per degree or something. I don't know what the number was.

A. Lurie, TRW: If you look in the region of about 5 degrees Centigrade to 25 degrees. Centigrade and it looked as if the coefficient was minus .25 amp hours per degree centigrade.

Q. Unidentified: Was there a peak, is there some peak?

A. Lurie, TRW: We don't have enough data, it's based on three points. I might say that to clarify that a bit. The actual specific energy that we achieved in the cycling in the GO cycling was around 43 or 44. The useable specific energy at 75% up to discharge.

A. Lurie, TRW: When I say that 25% I'm talking about on a battery basis. Useable specific energy.

Q. Gordon: You indicated that you thermostatically controlled the base plate or heat sink mounting. Did you do any work in monitoring envelope temperature to determine the delta?

ORIGINAL PAGE IS
OF POOR QUALITY

A. Lurie, TRW: That was shown on the one of the curves was temperature. Yeah, the battery temperature did go up above that certainly.

Q. Jagielski, GSFC: On one of the features you showed a very very linear relationship between pressure and I was wondering if that is typical of the silver hydrogen cells or is that just typical of your charge control scheme?

A. Lurie, TRW: It's typical of the silver hydrogen cells that we've just tested.

Q. Jagielski, GSFC: Do you foresee maybe pressure sensing as a viable control method then?

A. Lurie, TRW: I don't see why not if someone can figure out how to measure temperature reliability over a ten-year period.

A. Jagiewski, GSFC: I said pressure sensing.

A. Lurie, TRW: Measure pressure reliably over a long period of time. I think the sensor is possible more of a problem than the pressure characteristics of a cell.

Q. Rogers, Hughes Aircraft: You give accelerated orbit and I'm wondering whether there's any data relating the results you get to the accelerated orbit with those you might get in a real orbit. How do we relate this to what one would really expect?

A. Lurie, TRW: You mean because this is silver and not nickel.

A. Rogers, Hughes Aircraft: No.

A. Lurie, TRW: Just in general. That's a question that's always a fair question to ask in fact we don't know.

Q. Ritterman, Comsat: You mentioned that you had a charge/discharge ratio of 1 to 1. You mentioned it again and that you did have some trickle charges now silver hydrogen as you showed by the two slopes on the charge/discharge curves has very low self discharge so when you trickle you are actually putting in some capacity?

A. Lurie, TRW: Yeah. The trickle charge rate was 50 milliamps. It was so low that it amounted to a very very small fraction of an amp-hour. Oh less than that much less than that.

Q. Betz, Naval Research Lab: Chuck, why do you go to such lengths to avoid overcharge at what really doesn't seem to be such a high rate if you look at nickel hydrogen 3.8 amps on a 46 amp hour cell.

A. Lurie, TRW: Okay the 3.8 was dictated by the 12 hour day. That is not a desirable current density for this system. We don't want to overcharge it just based on what we know of the silver electrode. If we are looking for really long life we don't want to overcharge it and because of the efficiency of the system it's not necessary.

Q. Betz, Naval Research Lab: It's not a separator problem it's the positive electrode problem?

A. Lurie, TRW: Yes, that's my understanding. Nothing has failed yet but we are assuming that the silver electrode is the potential problem for long life.

N84
33698

UNCLAS

N84 33698 D30

LONG LIFE NICKEL ELECTRODES FOR A NICKEL-HYDROGEN CELL: CYCLE LIFE TESTS

H. S. Lim and S. A. Verzwyvelt
Hughes Research Laboratories

ABSTRACT

In order to develop a long life nickel electrode for a Ni/H_2 cell, cycle life tests of nickel electrodes were carried out in Ni/H_2 boiler plate cells. A 19 test cell matrix was made of various nickel electrode designs including three levels each of plaque mechanical strength, median pore size of the plaque, and active material loading. Test cells were cycled to the end of their life (0.5v) in a 45-minute low earth orbit (LEO) cycle regime at 80% depth-of-discharge (DOD). This is an interim report of this cycle life test. The results to date show that the active material loading level affects the cycle life the most with the optimum loading at 1.6 g/cc void. Mechanical strength did not affect the cycle life noticeably in the bend strenth range of 400 to 700 psi. The best plaque type appears to be one which is made of INCO nickel powder type 287 and has a median pore size of 13 μm.

INTRODUCTION

Nickel electrodes have been recognized as the life limiting components of nickel-hydrogen cells. In order to develop a long life nickel electrode for a nickel-hydrogen cell, we are engaged in a study program under a contract for NASA-Lewis Research Center. In this study we investigated the effects of various electrode parameters on the cycle life of the electrodes. These parameters include plaque pore size, plaque mechanical strength, and active material loading level which were varied in three levels for each parameter. The overall program effort is outlined in Fig. 1. Various fabrication parameters of nickel plaques including nickel powder type, powder density, and sintering time were studied in order to fabricate plaques with desired parametric variations.[1] Selected plaques (7 types) were impregnated in three levels of active material loading using the standard Air Force/Hughes electrochemical deposition process in an alcoholic bath. Subsequently these electrodes were tested by a Hughes standard stress test procedure (200 cycles) as a part of their evaluation. For a cycle life evaluation of these electrodes, 19 different nickel-hydrogen boiler plate test cells were fabricated and tested for initial cell performance. These results have been published earlier[1]. The present report describes interim results of the cycle life tests which are still in progress.

PRECEDING PAGE BLANK NOT FILMED

TEST CELL MATRIX AND DESIGNATION OF ELECTRODES

The nickel-hydrogen boiler plate test cells matrix includes 19 out of 21 various designs of electrodes as shown in Table 1. Each electrode was designated as follows for convenience of later discussions: The first two digits represent the nickel powder type and the median pore size, i.e. 55 for INCO nickel powder type 255 and 10 μm pore size, 25 for 255 powder type and 16 μm pore size, and 87 for 287 powder type and 13 μm pore size, respectively. The last two digits represent mechanical strength (bend strength): 40 for 400 psi, 55 for 550 psi, and 70 for 700 psi. For example, an 8755 plaque is made of 287 type powder with the bend strength of 550 psi and the median pore size of 13 μm.

TEST CELLS AND CYCLE LIFE TEST

All test cells contained three standard flight type nickel electrodes in a recirculation stack design[2] and 31% KOH electrolyte. The capacity of the cells were rated into three groups, i.e., 2.7, 3.0 and 3.3 AH, based on capacities measured by charging the cells for 80 minutes at C rate and then discharge to 1.00V at 2.74 C rate. The measured capacities ranged from 2.8 to 3.1 AH, from 3.1 to 3.5 AH, and 3.5 to 3.9 AH for 2.7, 3.0, and 3.3 AH ratings, respectively.

The cycle life test of all the 19 boiler plate test cells were carried out at 23°C by a continuous cycling to 80% depth-of-discharge (DOD) of their rated capacities using a 45-minute cycle regimes except for interruptions for periodic capacity measurements after approximately every 1500 cycles. The cycling regime included a 2.74C rate discharge for 17.5 minutes and a 27.5 minute charge at 1.92C rate for 110% recharge. End-of-charge voltages (EOCV), end-of-discharge voltages (EODV), end-of-charge pressures (DOCP), and end-of-discharge pressures (EODP) of the cells were monitored daily (every 32 cycles).

CYCLE LIFE TEST RESULTS

Plots of EODV and EODP of various cells vs. number of the life cycles are shown in Fig. 2A and 2B. The group of electrodes made of 2540 plaques showed the lowest cycle life, as shown by the EODV curves, regardless of the active material loading level. The next lowest cycle life group included all electrodes with the lowest active material loadings (L-series; 1.4 g/cc void), regardless of the plaque type. The comparison of the cycle life of the remaining electrodes was not as clear cut as the other electrodes. However, the general trend showed that the medium loading level (M-series; 1.55 g/cc void) gave better cycle life than the high loading level

(H-series; 1.7 g/cc void). No noticeable trend was observed with the variation of plaque mechanical strength. In regard to the effects of pore size, the best plaque appears to be the 87XX series which are made of 287 type nickel powder with 13 µm median pore size. These series of plaques with M or H level loading showed slightly higher cycle life on the average than the 55XX series with comparable loadings. The 55XX are made of 255 type nickel powder with 10 µm median pores. The 2540 plaques with 16 µm pores were the worst plaques as discussed above.

The EOCV's of the cells showed neither any appreciable variations with various electrode types nor any appreciable change during the cycle life test.

The EOCP's and EODP's of a given cell changed parallel to each other as expected by the fixed quantity of charge and discharge. The cells with short cycle life showed overall lower pressure than the other cells. These short life cells, which include the 2540 types and all L-series, also showed a pressure peak. The pressure of these cells were initially increased with cycling along with other cells up to about 1000 cycles and then started to decrease while the pressure of the other cells on the average either remains constant or increases with cycling.

The cycle life of various cells to 0.5 and 0.9 v of EODV are plotted against active material loading level in Figs. 3 and 4, respectively. Both curves show that the loading level for the optimum cycle life is about 1.6 g/cc void. These figures also show the effects of plaque type on the cycle life. The 87XX plaques on the average give better cycle life than the other types with comparable active material loading as discussed above.

CELL PRESSURE AND ACTIVE MATERIAL UTILIZATION

A normalized cell pressure after full charge and discharge, $(P-P_o)/C_o$, where P is cell pressure, P_o is precharge pressure, and C_o is theoretical capacity of nickel electrode, is plotted against active material utilization of the cells after 1700 life cycles in Fig. 5. The term $(P-P_o)/C_o$ is a measure of the average oxidation state of nickel active material. The plots after full charge and full discharge of the cell gave straight lines, respectively. The values of $(P-P_o)/C_o$ at charged state were increased while the values at discharged state were decreased as the utilization increased. The values at charged state increased more rapidly than those at discharged state decreased when the utilization increased. This result appears to indicate that an increased active material utilization is more dependent on reaching a high average oxidation state than on discharge to a low average oxidation state. This observation after 1700 cycles is quite contrary to an earlier observation at the beginning of life on the relationship between $(P-P_o)/C_o$ and the active material utilization[1] as shown in Fig. 6. The earlier observation showed that the average oxidation state in the charge state was independent of the utilization. The utilization was entirely dependent on the oxidation state in the discharged state. This change of the relationship between the utilization and $(P-P_o)/C_o$ with cycling may indicate the change of the mechanism of the active material utilization.

The plots of $(P-P_o)/C_o$ vs. the utilization at various life cycles are shown in Fig. 6. An additional trend observed in this figure is that the overall value of $(P-P_o)/C_o$ is increased with increased number of cycles. This increase appears to be due to either an increase in the average oxidation state of active material or a gradual corrosion of the nickel sinter to be converted to nickel oxides or hydroxides, or both.

CONCLUDING REMARKS

This report is an interim report of our studies on various parametric effects on the cycle life of a long life nickel electrode for nickel-hydrogen cells. The following remarks are based on the combination of the results of present cycle life test and the initial performance reported earlier[1].

- Among all parameters studied presently, the active material loading level affected cycle life of the nickel electrodes the most. The optimum loading level was about 1.6 g/cc void.
- No noticeable effect of the plaque mechanical strength on the cycle life was found in the bend strength range of 400 to 700 psi.
- Type 87XX plaques with 13 μm median pore size showed the longest cycle life on the average and slightly were better than type 55XX plaques which have 10 μm pore size. However, the active material utilization at the beginning of life was slightly higher with 55XX than 87XX. Type 2540 plaques with 16 μm median pore size showed the poorest life performance of all types.
- Values of $(P-P_o)/C_o$ gradually increased with the cycling.

- The relationship between active material utilization and $(P-P_o)/C_o$ indicated that the mechanism of maximum utilization of the active material may be changing with cycling.

REFERENCES

1. H. S. Lim, S. A. Verzwyvelt, C. Bleser, and K. M. Keener, "Long Life Nickel Electrodes for a Nickel-Hydrogen Cell: I. Initial Performance", Proc. 18th IECEC, Orlando, Florida 1983. P. 1543.

2. G. Holleck, "Failure Mechanisms in Nickel-Hydrogen Cells", the 1976 Goddard Space Flight Center Battery Workshop Proceedings, NASA Publication X-711-77-28, P. 297.

**ORIGINAL PAGE IS
OF POOR QUALITY**

Table 1

Boiler Plate Test Cell Matrix and Designation of Cell Types

BEND STRENGTH	400 psi			550 psi		700 psi	
PORE SIZE, μm / ACTIVE MATERIAL LOADING LEVEL	10	13	16	10	13	10	13
1.4 g/cc VOID	• 5540L	• 8740L	• 2540L	• 5555L	• 8755L	5570L	• 8770L
1.55 g/cc VOID	• 5440M	• 8740M	• 2540M	• 5555M	• 8755M	• 5570M	• 8770M
1.7 g/cc VOID	• 5540H	• 8740H	• 2540H	• 5555H	• 8755H	5570H	• 8770H

*INCLUDED IN 19 TEST CELLS

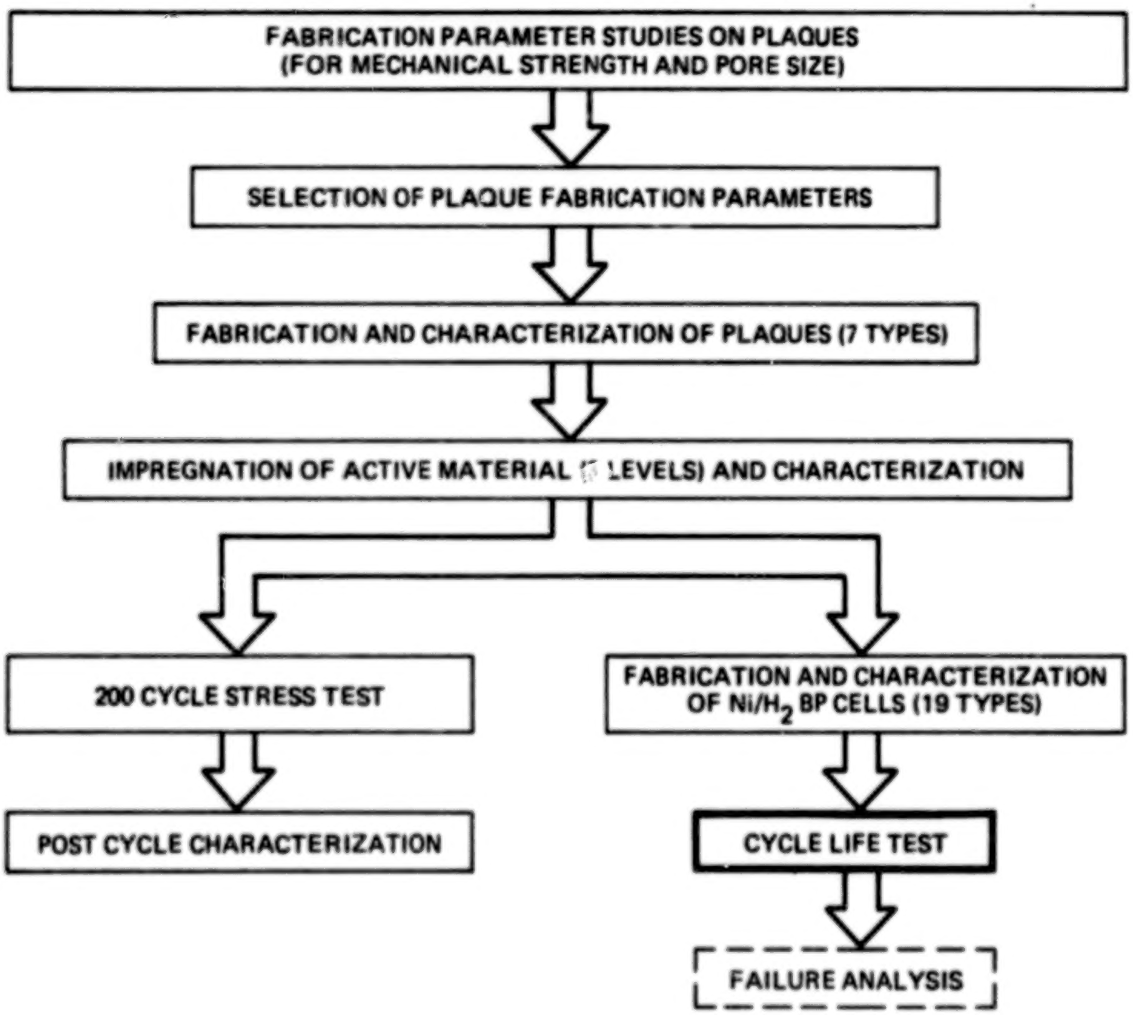
FABRICATION PARAMETER STUDIES ON PLAQUES
(FOR MECHANICAL STRENGTH AND PORE SIZE)
SELECTION OF PLAQUE FABRICATION PARAMETERS
FABRICATION AND CHARACTERIZATION OF PLAQUES (7 TYPES)
IMPREGNATION OF ACTIVE MATERIAL ([illegible] LEVELS) AND CHARACTERIZATION
200 CYCLE STRESS TEST
FABRICATION AND CHARACTERIZATION OF Ni/H_2 BP CELLS (19 TYPES)
POST CYCLE CHARACTERIZATION
CYCLE LIFE TEST
FAILURE ANALYSIS

Figure 1. Outline of program.

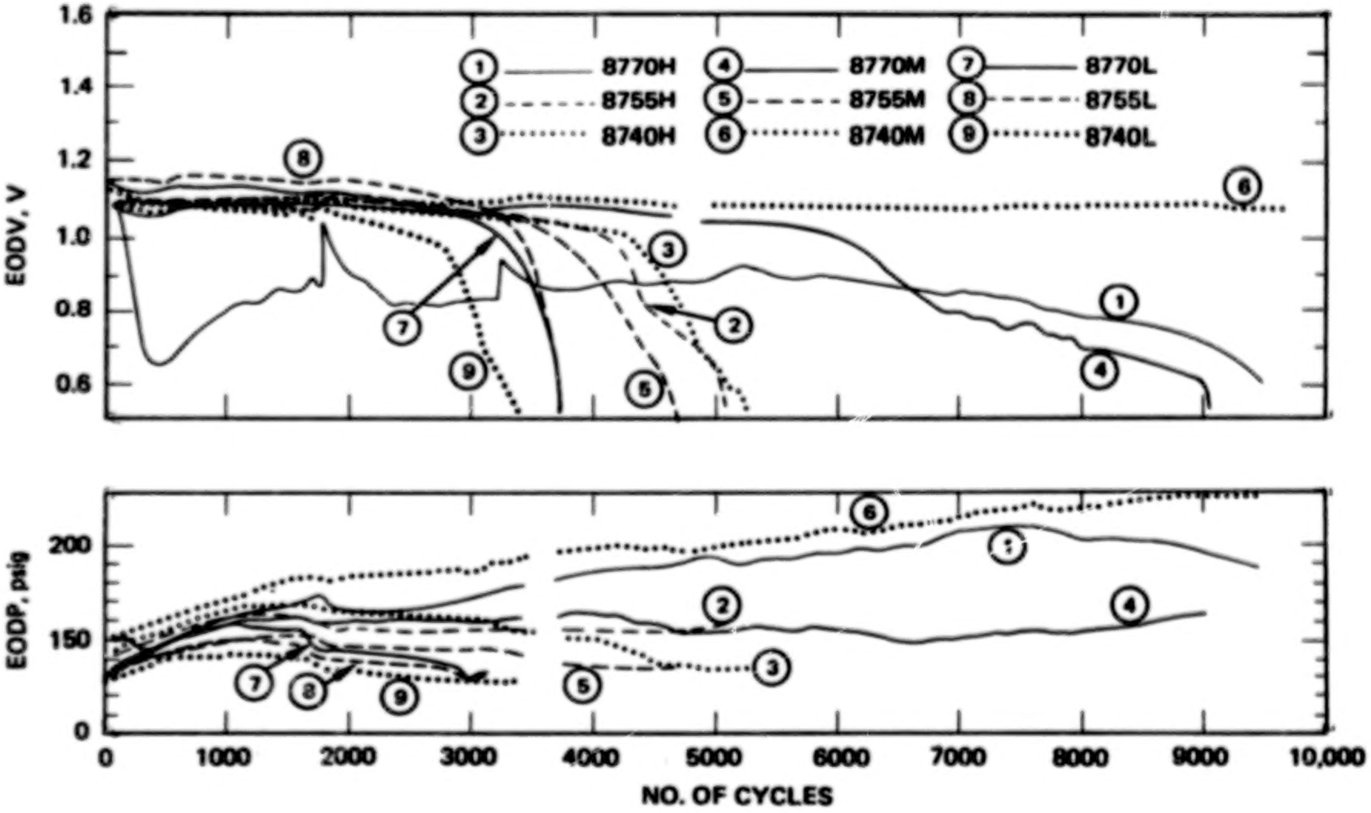

Figure 2A. Plots of EODV and EODP vs. number of cycles for 87XX electrodes.

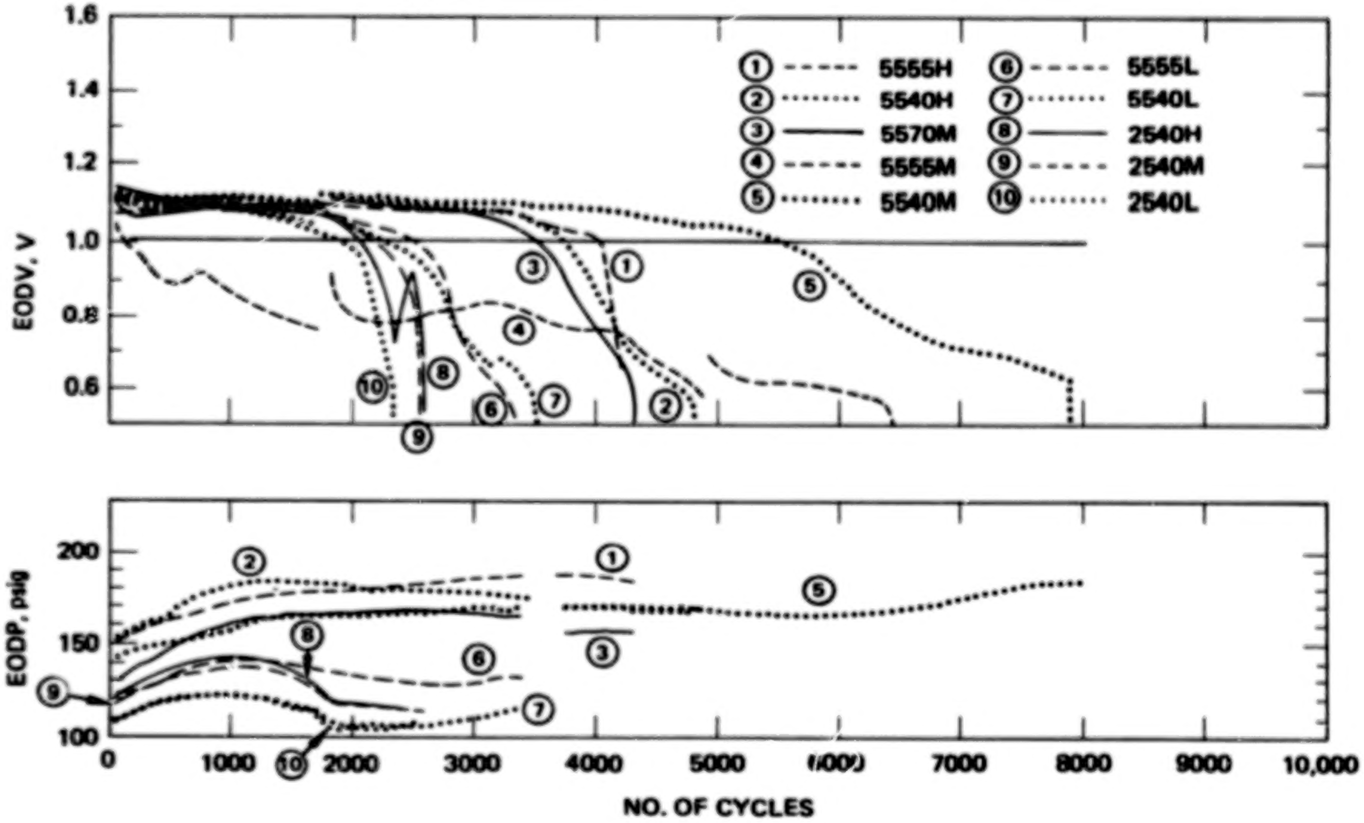

Figure 2B. Plots of EODV and EODP vs. number of cycles for 55XX and 2540 electrodes.

ORIGINAL PAGE IS
OF POOR QUALITY

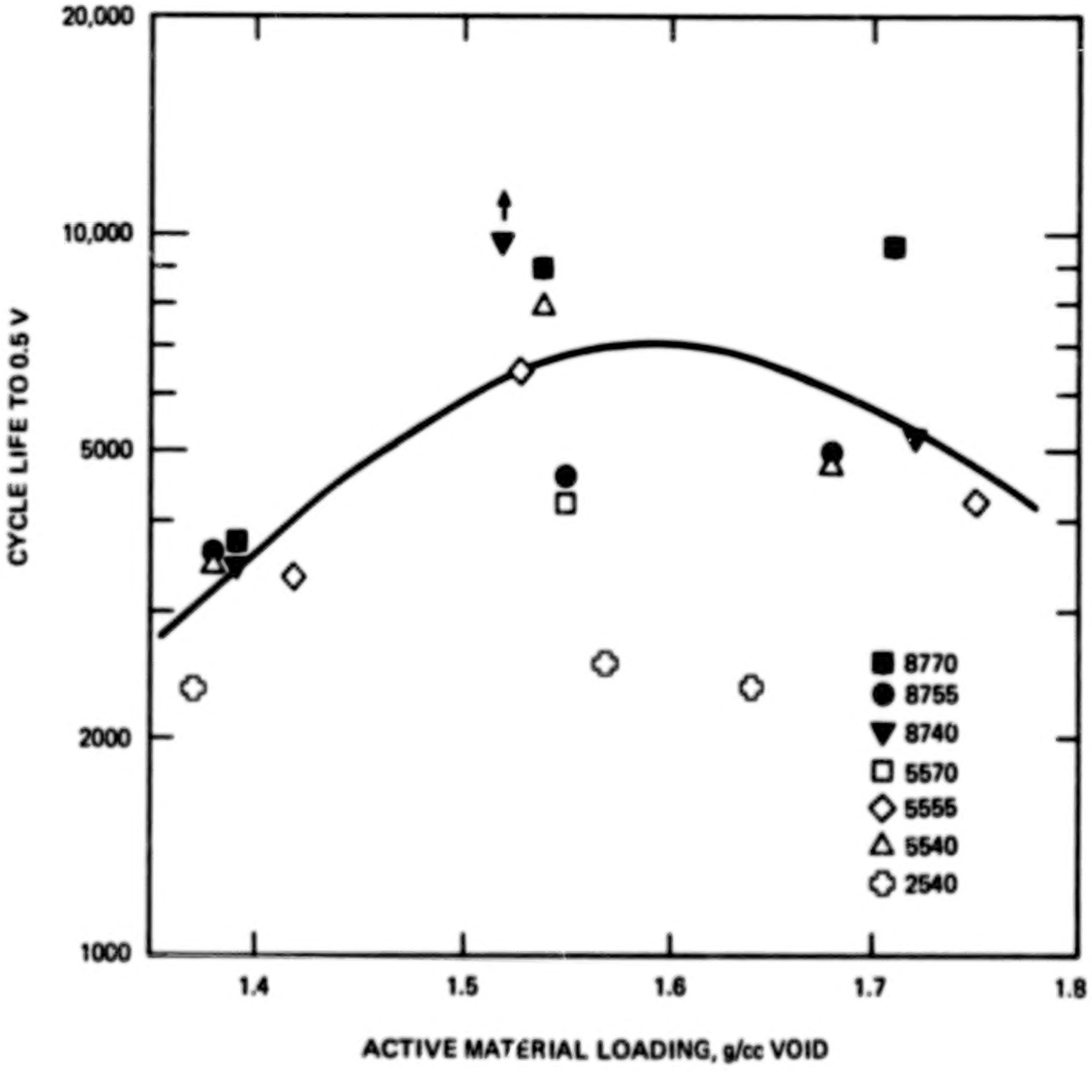

Figure 3. A plot of cycle life to 0.5V of EODV vs. active material loading level.

ORIGINAL PAGE IS
OF POOR QUALITY

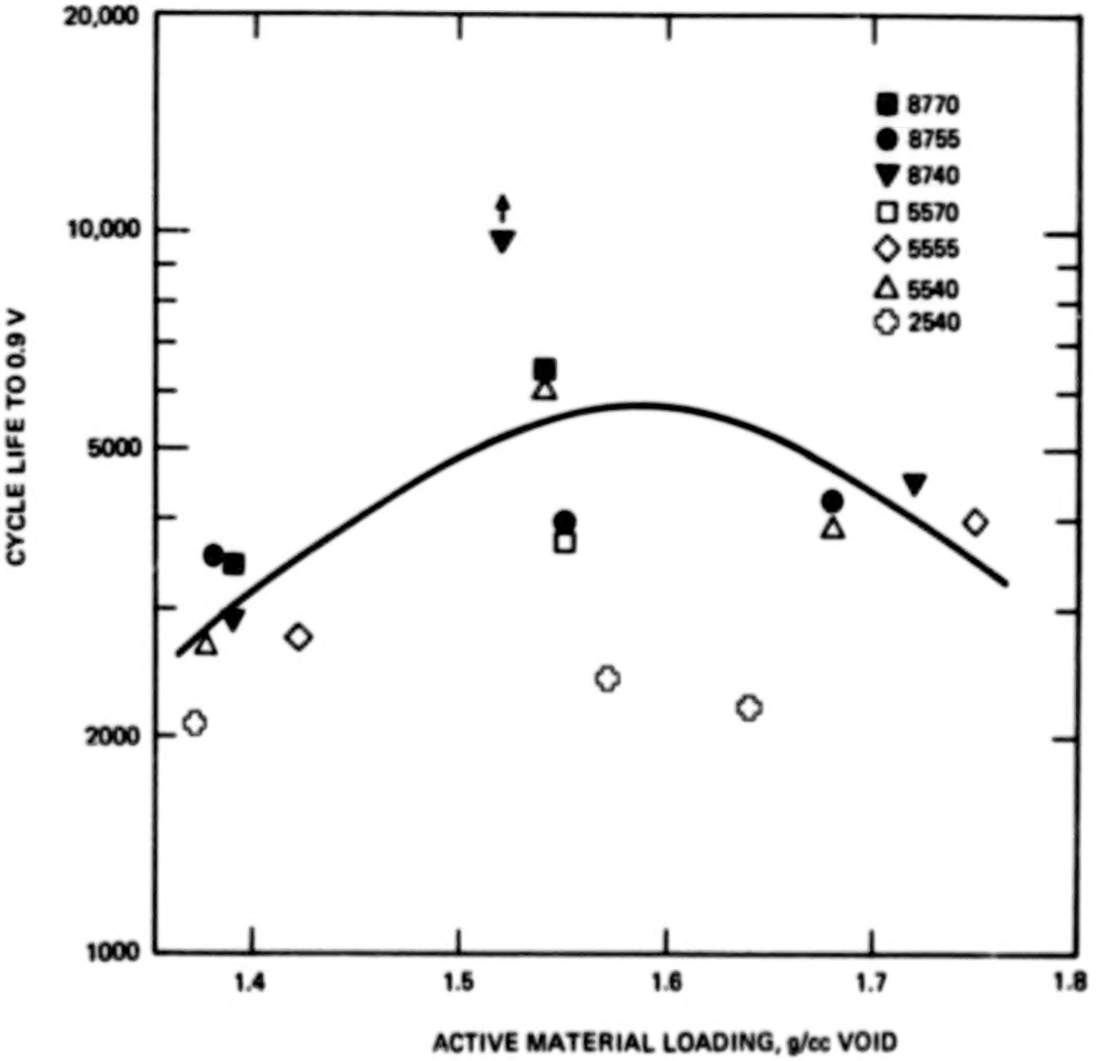

Figure 4. A plot of cycle life to 0.9V of EDOV vs. active material loading level.

ORIGINAL PAGE IS
OF POOR QUALITY

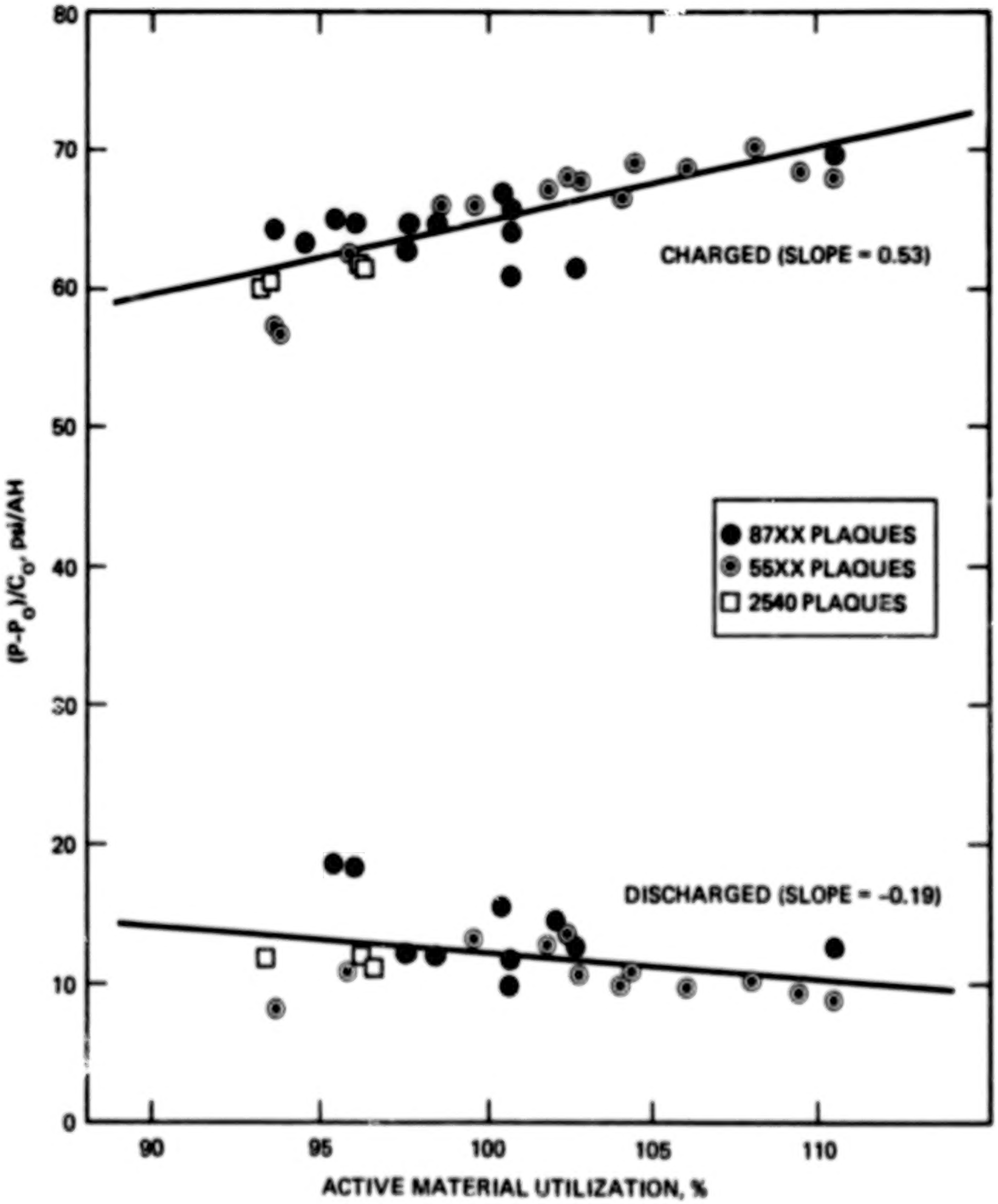

Figure 5. $(P-P_O)/C$ vs. active material utilization after 1700 cycles. Charged for 16 hours at 0.1C rate and discharged to 0.5V at 0.5C rate.

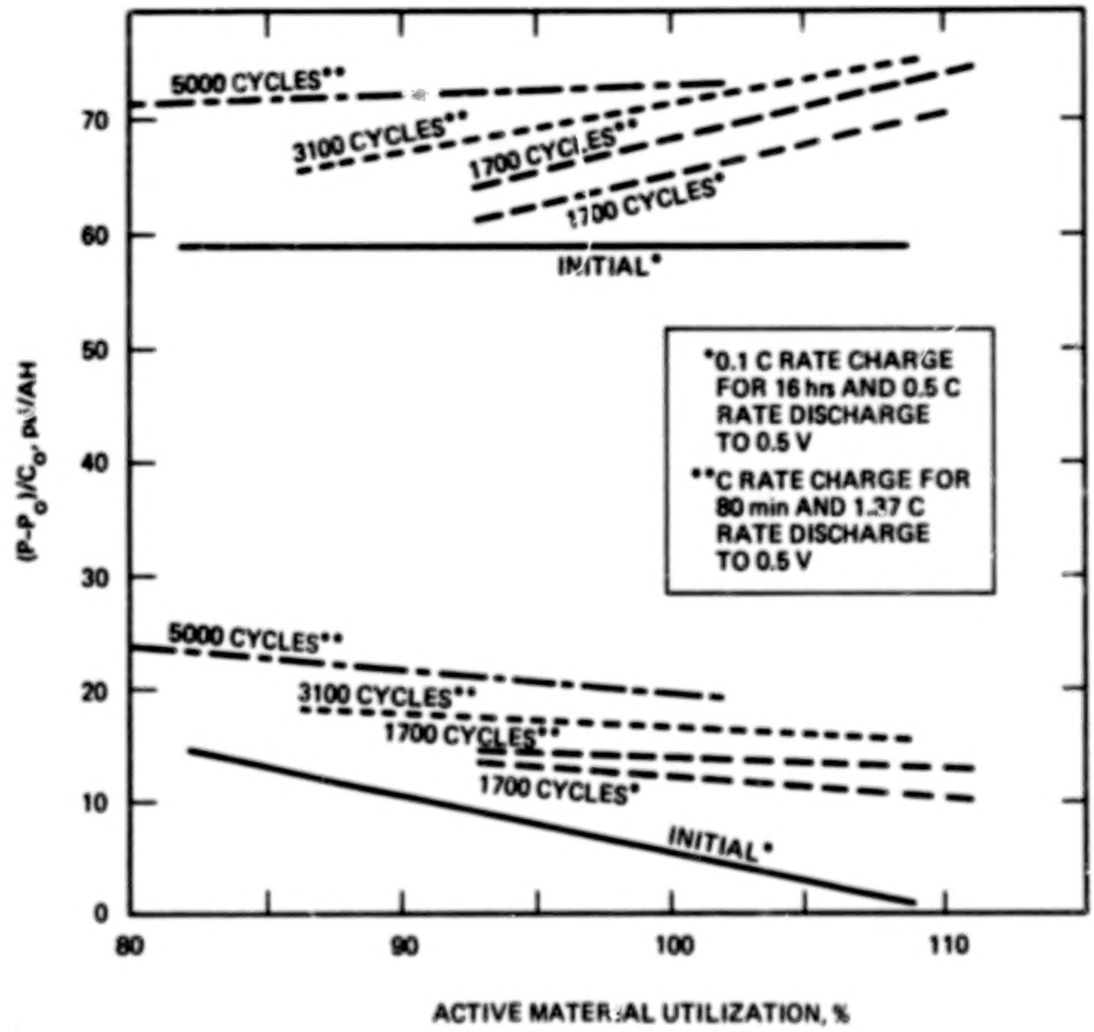

Figure 6. $(P-P_o)/C_o$ vs. active material utilization at various life cycles.

Q. Gross, Boeing: Based on the data you have taken so far how would you compare the best of your combinations with the performance of the existing nickel electrodes used for nickel hydrogen cells.

Q. Lim, Hughes Research Lab: The best combination appears to be the 87 excess plaques here which is 287 powder. We didn't see any strong effect of the mechanical trends so the mechanical trends in the range of 400 to 700 PSI didn't make that much of a difference.

Q. Gross, Boeing: Well how does that material compare in other respects with the existing nickel electrodes commercial.

A. Lim, Hughes Research Lab: I cannot speak it's all different types of nickel electrode presently available but this is very close to the Hughes Air Force standard electrode which is made of 287 nickel powder and the average pressure is around 550 PSI and the loading level is I understand close to 1.55 to 1.6 which is very close to the optimum.

Q. Edgar, Eagle Picher: Could you comment briefly on active material loss from these electrodes at the different cell sizes you investigated.

A. Lim, Hughes Research Lab: The active material loss we have reported earlier after the 200 cycle stress test the loss was I think it was around 2% overall except 25 to 40 plaque which has a medium size of 16 microns. The plaque I think it's loss was about twice as the other average and after this test we didn't measure the loss yet.

Q. Mallory, AT&T Bell Labs: Could you remind me what impregnation method you were using for these?

A. Lim, Hughes Research Lab: This was Dr. Pickett's method.

Q. Mallory, AT&T Bell Labs: And do you know what level the carbonate was in the cells?

A. Lim, Hughes Research Lab: We didn't analyze the carbonate level of this cell yet but I think we have a low initial carbonate content of the stock solution. I don't have the number with me. Maybe my co-worker Scott has it.

Q. Lim, Hughes Research Lab: Scott, do you remember? We had a very low value initially but after the test we didn't measure that yet.

N84
33699

UNCLAS

N84 33699 D31

FACTORS AFFECTING NICKEL-OXIDE ELECTRODE CAPACITY IN NICKEL-HYDROGEN CELLS

By

Paul F. Ritterman
COMSAT

The nickel-oxide electrode common to the nickel hydrogen and nickel cadmium cell is by design the limiting or capacity determining electrode on both charge and discharge. The useable discharge capacity from this electrode, and since it is the limiting electrode, the useable discharge capacity of the cell as well can and has been optimized by rate of charge, charge temperature and additives to electrode and electrolyte. Recent tests at COMSAT Labs with nickel hydrogen cells (Ref. 1) and tests performed almost 25 years ago with nickel cadmium cells (Ref. 2) indicate an improvement of capacity as a result of using increased electrolyte concentration.

The capacity attainable from the nickel oxide electrode and hence from the nickel-hydrogen (and nickel cadmium) cells depend on how effectively and extensively the electrode can be charged. Full charge or the conversion of all active material to a higher valence state is extremely difficult to achieve under spacecraft flight conditions where there are rate, time, and temperature constraints on charge. The difficulty in charging the nickel-oxide electrode is due to the occurance of a competing parasitic reaction involving the evolution of oxygen at approximately the same potential as that of the charging reaction of the nickel-oxide electrode. The two reactions and their open circuit potentials as well as the relative effect of current density and the temperature on potentials are shown in Figure 1.

At reversible (extremely low current densities) conditions a nickel hydrogen cell would never be charged because 81mv more voltage is required to charge the nickel-oxide electrode than to evolve oxygen in alkaline media. Because of the relative effect of temperature and charge current density on the potentials of there two reactions, it has been possible to combine these parameters so that the charge reaction predominates over the parasitic evolution of oxygen (Figure 1).

Within the practical limits of cell charging; between 1 and 10 ma/cm.^{2}; the voltage-current density curves favor the charging of the nickel electrode (Figure 2). The temperature-voltage coefficient for the oxygen evolution and that of nickel oxide charging reaction are both negative, however, that of the oxygen evolution is more negative (Figure 2). Therefore, a decrease in temperature would result in relative voltages favoring the charging of the nickel electrode. The effect of decreasing temperature and increasing charging rate to improve the efficiency of nickel hydrogen and nickel cadmium cells is well known and has been empirically applied by users of these alkaline systems for many years.

The thermodynamic effect of varying the KOH concentration is common to both the nickel electrode charging and the oxygen evolution reaction, nevertheless, a significant increase in available capacity has been noted as a result in increasing electrolyte concentration under constant condition of overcharge. (Ref. 1)

Figure 3 shows capacities obtained with nickel hydrogen cells at 0° and 20°C. The cells are identical except for their electrolyte concentrations. The capacities obtained at both temperatures are almost in linear proportion to electrolyte concentration.

The effect of increased electrolyte concentrations seems to be the same on the relative potentials of the nickel-oxide vs and parasitic oxygen evolution as that observed for decreasing temperature and increasing charge current. Thus there is an additional parameter which can be varied to create the most favorable conditions for nickel electrode cell charge acceptance.

Figure 4 shows plots of nickel hydrogen cell pressure vs. charge input for the cells whose capacities are shown in Figure 3. When the positive electrodes in a nickel hydrogen cell evolve oxygen, hydrogen and oxygen react causing a decrease in the slope of pressure vs. Ah input. When all of the charging current is used for oxygen evolution, all hydrogen evolved at the negative electrode is consumed and the cell pressure remains constant as charge continues.

As shown in Figure 4, the cells with the highest electrolytes concentration accept the most charge prior to pressure plateau indicating the greatest charge acceptance prior to predominant oxygen gassing.

The effect of electrolyte concentration on cell and electrode capacities may also have frequently been demonstrated by the capacity differences reported for flooded electrode tests and for the same electrodes as part of electrolyte starved cells. Flooded capacities have generally exceeded cell capacities by about 15 to 20%. It is widely accepted that nickel oxide electrodes absorbs KOH from the electrolyte during charge and at the same time yields water to the electrolyte. The equations shown in Figure 5 are only one representation of what is believed to occur during the charge of a nickel oxide electrode (Ref. 3). COMSAT Lab has developed data for nickel hydrogen cells which indicate a 10% decrease in electrolyte concentration when a cell is taken from complete discharge to full charge (Ref. 4).

The extent of decrease in electrolyte concentration as a result of charge is a function of ampere hours charged per unit volume of electrolyte. In a flooded condition the ampere hours of charge per unit volume of electrolyte is considerably smaller than that of a cell, therefore the decrease in KOH concentration will also be considerably less for electrodes charged in flooded electrolyte conditions than in case of the same electrodes contained in an electrolyte starved cell. Therefore, the electrodes in a flooded condition will accept more charge prior to gassing oxygen than the same electrode charged in a limited electrolyte volume cell as a result of the greater decrease in electrolyte concentration in the case of a cell.

The charge acceptance of a cell can be affected by both electrolyte concentration and volume. Electrolyte can therefore be considered a variable for improving charge efficiency and utilization in a Ni-H_2 cell and adds another dimension to charge management of these cells and batteries. By appropriate increase of electrolyte concentration and/or volume, a lower charge current and/or higher temperature, can be used resulting in smaller batteries and smaller charge arrays. This will impact weight and cost of a spacecraft. With respect to the effect of electrolyte concentration on life, data exists for geosynchronous orbit application, which indicates no adverse effects on battery life in the range of electrolyte concentrations investigated.

References:
(1) M. Earl - COMSAT Laboratories Technical Note PSD-83-029.
(2) L. Belove and I. M. Schulman - Proc. Ann Power Sources Conference 13, 82 1959.

(3) Bourgault and Conway - Can. J. Chem 38, 1557 (1960).

(4) J. F. Stockel - COMSAT Laboratories Technical Memo PSD-83-002.

C-6

ORIGINAL PAGE IS
OF POOR QUALITY

① $2\,Ni(OH)_2 \cdot + 2\,OH^- \rightarrow 2\,Ni\,OOH + 2\,H_2O + 2\ell^-;\ E_o = 0.490$

② $4\,OH^- \rightarrow O_2 + 2\,H_2O + 4\ell^-;\ E_o = 0.409$

$$\frac{\Delta E_2}{-\Delta T} > \frac{\Delta E_1}{-\Delta T}$$

$$\frac{\Delta E_2}{\Delta \ln i} > \frac{\Delta E_1}{\Delta \ln i}$$

Figure 1. Effect of temperature and current density on charging reaction (1) and parasitic reaction (2).

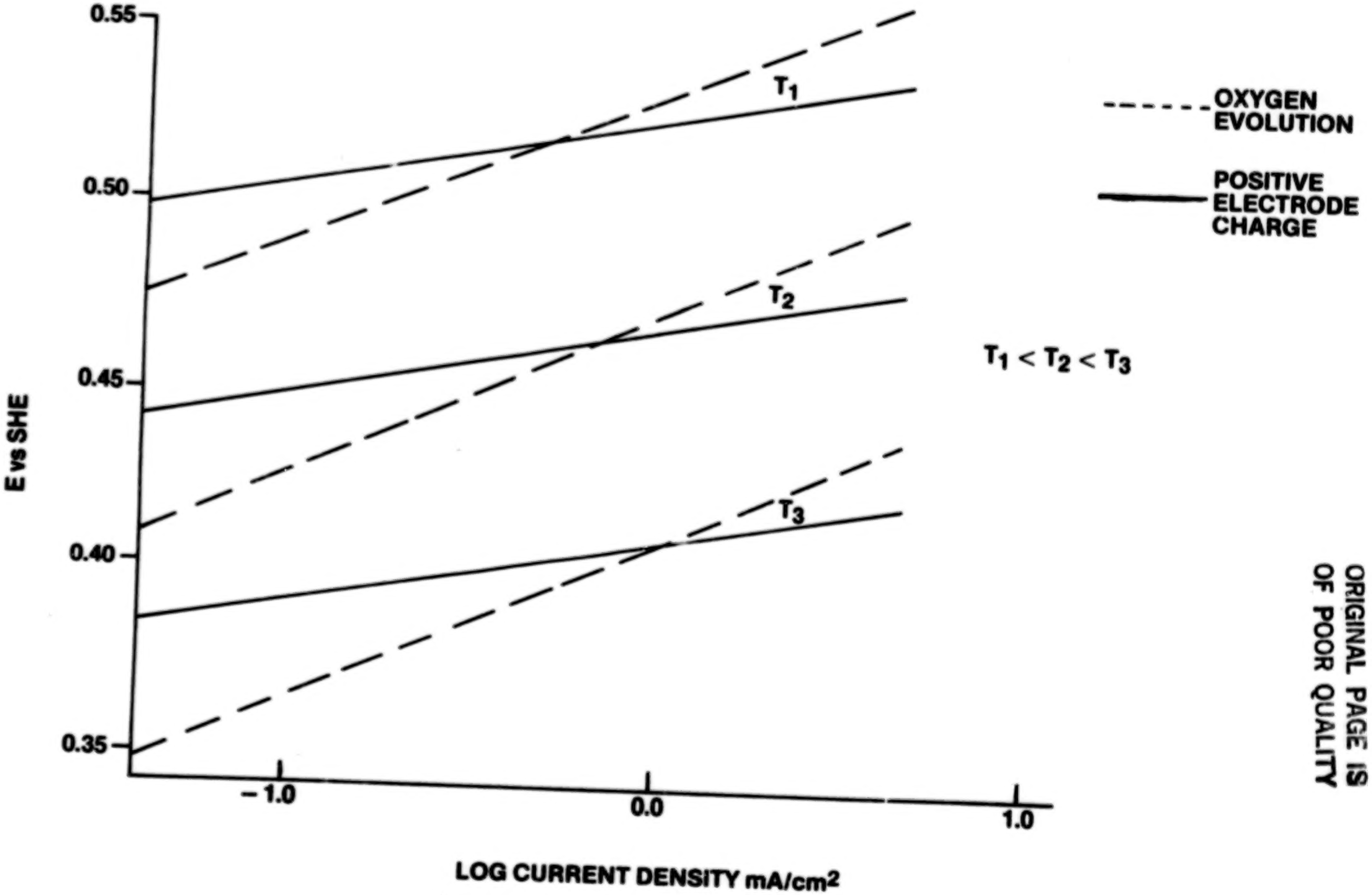

Figure 2. Charge efficiency as related to charge rate and temperature.

ORIGINAL PAGE IS
OF POOR QUALITY

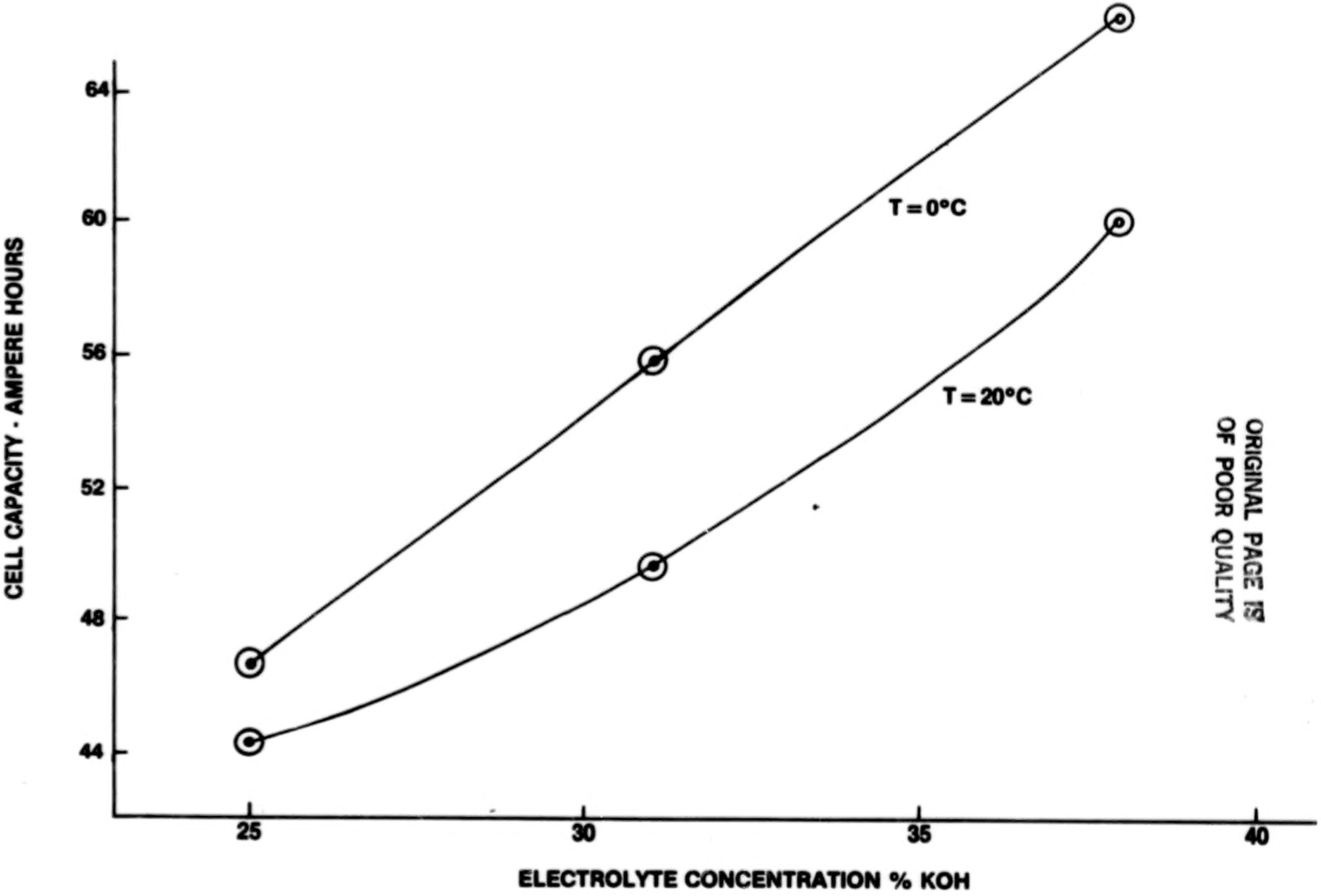

Figure 3. Nickel-hydrogen cell capacity vs. electrolyte concentration.

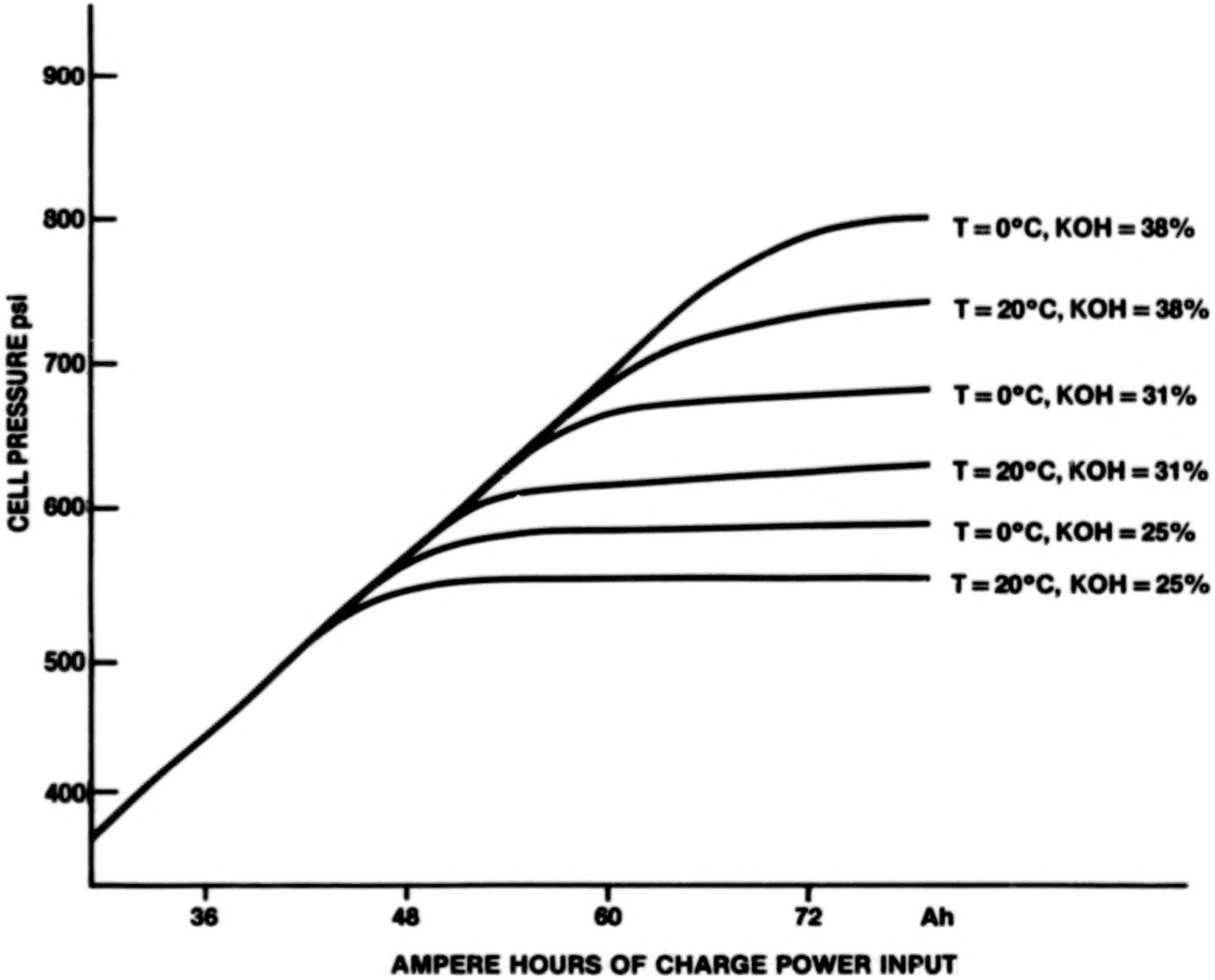

Figure 4. Nickel-hydrogen cell pressure vs. charge input as a function of electrolyte concentration and temperature.

THE CONCENTRATION OF KOH DECREASES AS THE STATE OF CHARGE OF A CELL INCREASES; AS A RESULT OF KOH ABSORBED BY THE CHARGED POSITIVE, AND H_2O RELEASED FROM THE DISCHARGED POSITIVE ACTIVE MATERIAL.

$$2\ \mathrm{Ni(OH)_2} \cdot 1.28\ \mathrm{H_2O} + 0.14\ \mathrm{KOH} + 2\ \mathrm{OH^-} \rightarrow 2\ \mathrm{NiOOH} \cdot 0.14\ \mathrm{KOH} + 4.56\ \mathrm{H_2O} + 2\ell^-$$

Figure 5. KOH concentration vs. state of charge.

A. Thaller, NASA/Lewis Research Center: I take it Paul that the benefits are related to using higher concentrations of KOH rather than using nickel hydrogen?

Q. Ritterman, Comsat: Beg your pardon?

Q. Thaller, NASA/Lewis Research Center: The benefits were they related to using higher concentrations of KOH or benefits of using nickel hydrogen?

Q. Ritterman, Comsat: I don't know why you are comparing concentration with system you can combine these. You can use these in both nickel hydrogen and nickel cadmium but I am talking primarily about nickel hydrogen because you have greater flexibility as far as current density and temperature goes. You are not limited by cadmium in nickel hydrogen.

Q. Green, RCA-Astro: Paul, would the life expectancy of the nickel hydrogen battery increase with the KOH concentration that you've described?

A. Ritterman, Comsat: Yes. Okay. There have been cells that have run for accelerated life test of 30 seasons at TRW with an end of discharge KOH concentration in excess of 38%. So within the range that I've talked about there has been reported no other problems in relation to life expectancy.

Q. Green, RCA-Astro: No problem?

A. Ritterman, Comsat: No problem.

Q. Milden, Aerospace Corporation: The choice of the 31 or 32% electrolytes was over the years an optimum or a trade off between voltage characteristics and everything else how would you suspect or expect the voltage on charge and discharge to vary with the increased concentration and also the effects of swelling and all other kinds of good stuff like that with a varied concentration. In other words, is this all good or is there a trade-off?

A. Ritterman, Comsat: So far it looks like all good. I guess some more specific test would have to be done to determine the effect on swelling. But I think life data shows that you can sustain certainly at the end of discharge with a concentration as high as 40%.

Q. Unidentified: What I'm saying Paul, when the current was higher the difference between the end of discharge voltages was higher?

Q. Ritterman, Comsat: Yeah. Was it all the way through on the discharge?

A. Unidentified: It was more pronounced toward the end. At the very beginning they were a little closer but they spread out as the discharge went on.

Q. Unidentified: For the same amp output?

A. Ritterman, Comsat: I can't answer that.

COMMENT

Unidentified: This is a comment. There are two points coming out of this session. One point is when you are talking about nickel cadmium or nickel hydrogen there are significant changes in the electrolyte concentration between charge and discharge. There are also significant differences in the variation in the KOH concentration of one to the other because the reaction that's taking place during that time of discharge. The other point is that there are different nickel hydrogen systems in operation using different levels of KOH concentration. And one other thing that Paul has pointed out very nicely in his paper is that there is a significant impact on cells performance as a result of KOH concentration.

Ritterman, Comsat: Yes I guess I didn't make my point clear about nickel cadmium and nickel hydrogen. In nickel hydrogen you really have no net change in hydroxide due to compound formulation but you do have a change in absorption of water and KOH concentration. But I didn't want to limit this to nickel hydrogen I think it's applicable to nickel cadmium cells.

Hendee, Telesat Canada: Basically the comment you made was the one I was going to make. You have to be careful about translating this into nickel cadmium as well. One of the reasons for the 31 to 32% was the nylon separator was it not? The degradation of the nylon separator was shown to be the least around a 31 or 32% KOH concentration. If you can change that you have a new ball game.

Q. Rogers, Hug Aircraft Corporation: Paul, I'm wondering the test data that you presented is that what we got after building the cells at Hughes or is additional data which is the same basically as what I remember we got?

A. Ritterman, Comsat: The initial data about the effective concentration was found sometime prior to the Hughes testing.

A. Ritterman, Comsat: Yes these cells are 48 amp per hour cells.

N84
33700

UNCLAS

N84 33700 D32

POSITIVE ELECTRODE FABRICATION FOR BI-POLAR NI-H_2 CELLS*

Tim A. Edgar
Eagle-Picher Industries, Inc.
Colorado Springs, CO

---

* Portions of this paper are based on work performed at Eagle-Picher Industries, Inc. under contract to NASA Lewis Research Center.

INTRODUCTION

Bi-Polar nickel hydrogen design studies (ref. 1) have indicated a potential improvement in energy density and specific energy if positive electrodes could be manufactured in configurations of twice or more of the present "normal" thickness. Such electrodes would have to achieve similar active material loading, utilization, and cycle life to conventional 0.8mm I.P.U. nickel hydrogen electrodes. Eagle-Picher's experience with D.O.E. near term nickel iron batteries (ref. 2) indicated that 2.0mm or greater thickness electrodes could be manufactured by the wet slurry process (ref. 3), loaded by electrochemical impregnation processes, and achieve useful capacities and cycle lives.

Both the dry sinter and wet slurry plaque processes are presently producing 0.8mm thin positive electrodes for nickel hydrogen flight programs. The slurry process is known to be capable of producing thick electrodes, but the dry sinter process used in many space applications had not yet demonstrated thick electrode capability.

The EPI/USAF electrochemical impregnation process (ref. 4) is utilized for flight quality thin electrodes (ref. 5) and was thought to be adaptable to impregnation of thicker electrodes. The reported high utilization, and limited swelling with electrochemical impregnation processes were seen as desirable qualities to achieve for thick electrodes. In addition a large data base incorporating formation, electrochemical characterization tests, accelerated high rate tests, and cell tests, exists for electrochemically loaded thin electrodes, that offers a good comparison to the thick electrode data generated in this test.

ELECTRODE PRODUCTION

FLOW CHART (fig. 1)

Nickel powder and wire plus binders and solvents for the slurry process are combined and sintered at high temperatures. Subsequently the nickel plaque is characterized for bend strength, porosity, thickness, and weight. Impregnation lots of forty plaque are selected through a weight sorting technique and process tabs are attached. The electrochemical impregnation system processes three lots at a time and individual lots may be independently controlled in terms of time, current density, etc. Following a short rinse in D.I. H_2O the plaque undergo a five and one half cycle formation procedure followed by scrubbing, rinsing, drying, and weight pickup calculation. Plaque lots are returned to the formation tanks for twenty-one cycles of electrochemical characterization testing which continues

ORIGINAL PAGE IS
OF POOR QUALITY

the active material formation and allows a plaque capacity determination. Following a second scrubbing, rinsing, and drying operation random plaques are selected to undergo an accelerated, high rate (10C) stress test consisting of two hundred cycles followed by five capacity measurement cycles.

SINTER PRODUCTION

Sintering process data is shown in figure 2. The dry sinter process utilizing I.N.C.O. 287 powder produced 1.03 mm thickness, 84.4% porosity and bend strength of 521.6 P.S.I. All properties are well within the tolerances set for this program. Plaque size is 11 x 14.5 in, and 150 plaque were produced for this program. The wet slurry process which incorporates I.N.C.O. 255 powder produced 1.52 mm thickness, 84.4% porosity, and 847 P.S.I. bend strength. Slurry plaque size is 11.25 x 12 in. and 160 plaque were manufactured.

ELECTROCHEMICAL IMPREGNATION

The EPI/USAF impregnation process (fig. 3) utilizes a mixed solvent consisting of 45% ethanol and balance water. Metal salt content is analyzed by Atomic Absorption prior to each run and adjusted to the range of 1.6 to 1.8 molar $Ni(NO_3)_2$ and 0.12 to 0.18 molar $Co(NO_3)_2$. pH is continuously monitored and held between 2.8 and 3.2 by the automatic addition of dilute nitric acid. Impregnation bath temperature is maintained between 70° and 80°C, near the solution boiling point. Current, voltage, and time of impregnation are microprocessor controlled functions. Three different current regimes and variable times between 140 and 320 minutes were employed to achieve a target loading level of 1.60 to 1.70 grams per cubic centimeter of plaque void. Plaque are cathodically protected during all phases of the impregnation procedure to assure minimal corrosion of the nickel sinter. Immediately following impregnation plaques are rinsed in D.I. water to remove bulk nitrates.

FORMATION

The formation procedure (fig. 4) employs five and one half cycles of charge/discharge starting with discharge. Formations are carried out in 20% KOH electrolyte against nickel sheet counterelectrodes. Current densities are calculated on the basis of surface area at 0.45 amps/in^2 through cycle 4, 0.10 amps/in^2 for cycle 5, and 0.07 amps/in^2 for the last half cycle. Currents were run for the larger size 1.03mm plaque which gave the higher rates shown for the smaller 1.52mm slurry plaque. Time of each half cycle is twenty minutes. Plaque are subsequently rinsed and scrubbed, dried under nitrogen, and weighed.

ELECTROCHEMICAL CHARACTERIZATION TEST

E.C.T. (fig 5) is again carried out in 20% KOH with nickel counterelectrodes. The test consists of twenty complete formation cycles at the nominal capacity rate. Charge is 120% of capacity and the plaque are discharged to -0.2 volts vs. a Hg/HgO reference electrode. The final charge is sixteen hours at a C/10 rate followed by discharge to -1.0 volts vs. Hg/HgO. The C rate for E.C.T. was a calculated average from the formation loading data for the three lots subjected to this test. Following E.C.T. plaque are rinsed, scrubbed, and dried. A final thickness and weight for each plaque are also taken. Capacities for each lot are calculated based on the time of the final discharge.

IMPREGNATION RESULTS

The results of six different impregnated lots are shown in table 1. Data is presented on lot sinter characterizatics followed by results after either formation, E.C.T., or both. Impregnation efficiency has been calculated in terms of ampere hours loaded divided by ampere hours input to the impregnation tanks.

$$\frac{\text{AH loaded}}{\text{AH Impreg. Input}} \times 100 = \text{Loading Efficiency}$$

Lot nos. 7023, 7024, and 7027 were loaded with the same current/voltage regime with impregnation time varied to achieve different loading levels or compensate for increased void volumes. Lot nos. 7025 and 7026 were loaded at reduced current densities, but at a similar number of total ampere hours to the above lots. Lot no. 7028 was loaded with an Eagle-Picher proprietary current/voltage regime with the same total ampere hour input as lot no. 7026. All loading levels were 1.60g/cm^3 void or greater. Thickness change after impregnation, formation, and E.C.T. was calculated on the basis of nine points per plaque averages. Weight loss during E.C.T. is shown for the three lots that went through this procedure.

STRESS TEST

Two plaque per lot were selected at random for the EPI/HAC accelerated stress test. From each plaque two test electrodes were taken as well as samples for chemical analysis and active material distribution testing. Stress test electrodes were sized on the basis of their parent

ORIGINAL PAGE IS
OF POOR QUALITY

plaque loading to give a theoretical capacity of 1.70 ampere hours per electrode. The stress test (fig. 6) incorporates a two cycle hot formation step to prepare electrodes for the test. Hot formation is carried out at 70°C in 20% KOH at the 5C rate. After formation, test electrodes are characterized for weight, thickness, and visual appearance. The actual stress test takes place in flooded, excess, 31% KOH against nickel counterelectrodes. An initial electrode capacity cycle is run consisting of 5C charge for 12 minutes followed by C/2 charge for 1 hour or 150% charge. Discharge is at the capacity rate to -1.0 volts vs. nickel sheet. The 200 stress cycles are 10C rate for 12 minutes of charge or 200% charge, and discharge at 10C for 8 minutes with the reverse voltage clamped to -1.0 volts vs. Ni. by individual cell bypass diodes. After stress, electrodes are subjected to five capacity cycles identical to the initial capacity above. When stressed electrodes are removed from the test fixture, they are examined for visual appearance then scrubbed, rinsed, and dried. Dried electrodes are characterized for weight loss, swelling, and other anomalies.

STRESS TEST RESULTS

ELECTRODE BASIS

Table 2 gives the test results for the twenty-four individual electrodes from six lots. Prestress and post stress capacities are indicated as well as individual weight and thickness changes. Electrode capacity increase during stress is given as a percentage.

LOT BASIS

In table 3 stress tests results have been compiled as lot averages. Utilization has been calculated using 1.70 ampere hours as the theoretical capacity.

DISCUSSION

Individual plaque lots of the same type exhibited remarkably uniform sinter characteristics, indeed all lots are quite similar in terms of porosity, and differ mainly in void volume and thickness. These plaque similarities accomodate relatively straightforward comparison of impregnation results. Lower current density impregnation appears to increase void volume loading in both types of plaque, while the Eagle-Picher proprietary current/voltage regime gave the highest loading results. Thickness change through impregnation, formation, and E.C.T. is quite small and with plaque visual appearance and weight change is indicative of little or no surface loading or plating of active material. Impregnation efficiencies are all quite similar, but interestingly are maintained at the higher void volume loadings.

Stress test results indicate low capacities prior to test especially on the thicker more highly loaded electrodes. The three dry sinter lots seem to show some benefit from the extended E.C.T. formation that two of them received, however, this correlation is not clear for the slurry plaque lots. Post stress utilization for all dry sinter lots is uniform and slightly high for that capacity regime, slurry lots demonstrated dramatic capacity improvement through stress although their utilization is still below expected values. Thickness increase follows a general trend upward with increased loadings and in conjunction with respective void loadings may indicate some support for the contentions of mcHenry (ref 6) concerning practical limits of loading.

CONTINUING INVESTIGATIONS

Eagle-Picher and Hughes Research Laboratories are pursuing thick electrode development and testing under the sponsorship of NASA Lewis Research Center. 0.86mm thick dry sinter plaque will serve as a baseline for this program which will look at the feasibility of producing 2.0mm thick dry sinter plaque with and without a supporting wire grid. Plaque characterization and electrochemical impregnation experimentation will take place as well as stress testing, electrode chemical tests, and cell testing. Reports of this work will be presented as it progresses.

SUMMARY

We have demonstrated a capability for producing 1.0mm dry sinter and 1.5mm slurry sinter structures on production processes and equipment. The EPI/USAF electrochemical impregnation process proved capable of loading thick electrodes to 1.60 g/cm^3 void or higher. Sample electrodes incurred 200 high rate stress cycles without significant structural or performance degradation. Formation regimes developed for thin plaque are not optimal for thick plaque and further investigation into electrode capacity build-up would seem warranted. Thick electrode technology development is continuing under other programs and shows promise of fulfilling the projected energy density and specific energy improvements.

REFERENCES

1. Adler, E.; and Perez, F.: Advanced Nickel Hydrogen Cell Configuration Study. Proceedings NASA/GSFC Battery Workshop, 1982, p. 496.

2. Research, Development, and Demonstration of Nickel-Iron Batteries for Electric Vehicle Propulsion. Annual Report, Argonne National Laboratory, 1980.

3. Edgar, T.: The Development of Multipurpose Slurry Sintered Structures for Use as Nickel Oxide and Cadmium Electrodes. Proceedings 30th Power Sources Symposium, June 1982, p. 105.

4. Pickett, D.F.: Preparation of Nickel Electrodes. U.S. Patent 3,827,911, 6, Aug. 1974.

5. Bleser, C.: Positive Electrode Processing For Hughes Ni-H_2 Cells. Proceedings NASA/GSFC Battery Workshop, 1979, p. 461.

6. McHenry, E.: The Practical Limit of Loading Nickel Hydrogen Electrodes. Proccedings NASA/GSFC Battery Workshop, 1979, p. 461.

Table 1
Impregnation/Formation Results

Lot Number	Original Thickness	Porosity	Void Volume	Plaque Loading	Void Loading	Thickness Change	E.C.T. Wt. Loss	Impregnation Efficiency
7023	0.0402 in.	84.2%	85.2 cm³	1.38.3 g	1.62 g/cm³	0.0005 in.	——	30.7%
7024	0.0404 in.	84.1%	85.4 cm³	138.3 g	1.62 g/cm³	——	−1.59	28.7%
7025	0.0405 in.	83.9%	85.5 cm³	147.4 g	1.72 g/cm³	0.0009 in.	+0.65	29.8%
7026	0.0582 in.	84.1%	105.6 cm³	187.5 g	1.77 g/cm³	——	−4.08	31.1%
7027	0.0588 in.	83.9%	106.4 cm³	170.7 g	1.60 g/cm³	0.0015 in.	——	29.1%
7028	0.0597 in.	83.9%	108.0 cm³	195.6 g	1.81 g/cm³	0.0027 in.	——	32.2%

Table 2

Stress Test Results: Electrode Basis

Lot/Electrode #	Pre-Stress Capacity	Weight Change	Thickness Change	Post-Stress Capacity	Capacity Increase
7023-36 A	1.42 AH	−0.11 g	+0.0011 in.	2.04 AH	144%
7023-18 A	1.19 AH	−0.086 g	+0.0017 in.	1.87 AH	157%
7023-36 B	1.36 AH	−0.277 g	+0.0021 in.	1.87 AH	138%
7023-18 B	1.36 AH	−0.099 g	+0.0021 in.	1.885 AH	139%
7024-66 B	1.56 AH	−0.107 g	+0.0002 in.	1.93 AH	124%
7024-66 A	1.50 AH	−0.069 g	+0.0003 in.	1.81 AH	121%
7024-49 B	1.62 AH	−0.067 g	+0.0004 in.	2.07 AH	128%
7024-49 A	1.53 AH	−0.072 g	+0.0002 in.	1.96 AH	128%
7025-113 A	1.50 AH	−0.031 g	+0.0016 in.	1.64 AH	109%
7025-93 A	1.50 AH	−0.070 g	+0.0004 in.	1.96 AH	131%
7025-113 B	1.56 AH	−0.101 g	+0.0010 in.	1.93 AH	124%
7025-93 B	1.45 AH	+0.011 g	+0.0010 in.	1.93 AH	133%
7026-15 B	1.16 AH	+0.031 g	+0.0029 in.	1.615 AH	139%
7026-34 B	0.96 AH	−0.117 g	+0.0034 in.	1.47 AH	153%
7026-15 A	0.79 AH	−0.042 g	+0.0037 in.	1.605 AH	203%
7026-34 A	0.65 AH	−0.188 g	+0.0047 in.	1.655 AH	255%
7027-44 A	0.99 AH	−0.216 g	+0.0025 in.	1.59 AH	161%
7027-44 B	0.99 AH	−0.137 g	+0.0018 in.	1.64 AH	166%
7027-68 B	0.62 AH	−0.418 g	+0.0078 in.	1.345 AH	217%
7027-68 A	1.02 AH	−0.181 g	+0.0046 in.	1.81 AH	177%
7028-86 A	0.96 AH	−0.402 g	+0.0097 in.	1.575 AH	164%
7028-114 B	0.57 AH	−0.360 g	+0.0045 in.	1.47 AH	258%
7028-114 A	0.71 AH	−0.393 g	+0.0072 in.	1.67 AH	235%
7028-86 B	0.57 AH	−0.375 g	+0.0060 in.	1.30 AH	228%

Table 3

Stress Test Results: Lot Basis

Lot Number	Wt. Change	Thickness Change	Pre-Stress Capacity	Pre-Stress Utilization	Post-Stress Capacity	Post-Stress Utilization	Capacity Increase
7023	0.143 g	0.0018 in.	133 AH	78%	1.92 AH	113%	123%
7024	0.079 g	0.0003 in.	1.55	91%	1.94 AH	114%	129%
7025	0.048 g	0.0010 in.	1.50	88%	1.87 AH	111%	125%
7026	0.079 g	0.0037 in.	0.89	52%	1.59 AH	93%	178%
7027	0.238 g	0.0042 in.	0.91	53%	1.60 AH	94%	177%
7028	0.383 g	0.0069 in.	0.70	41%	1.50 AH	88%	214%

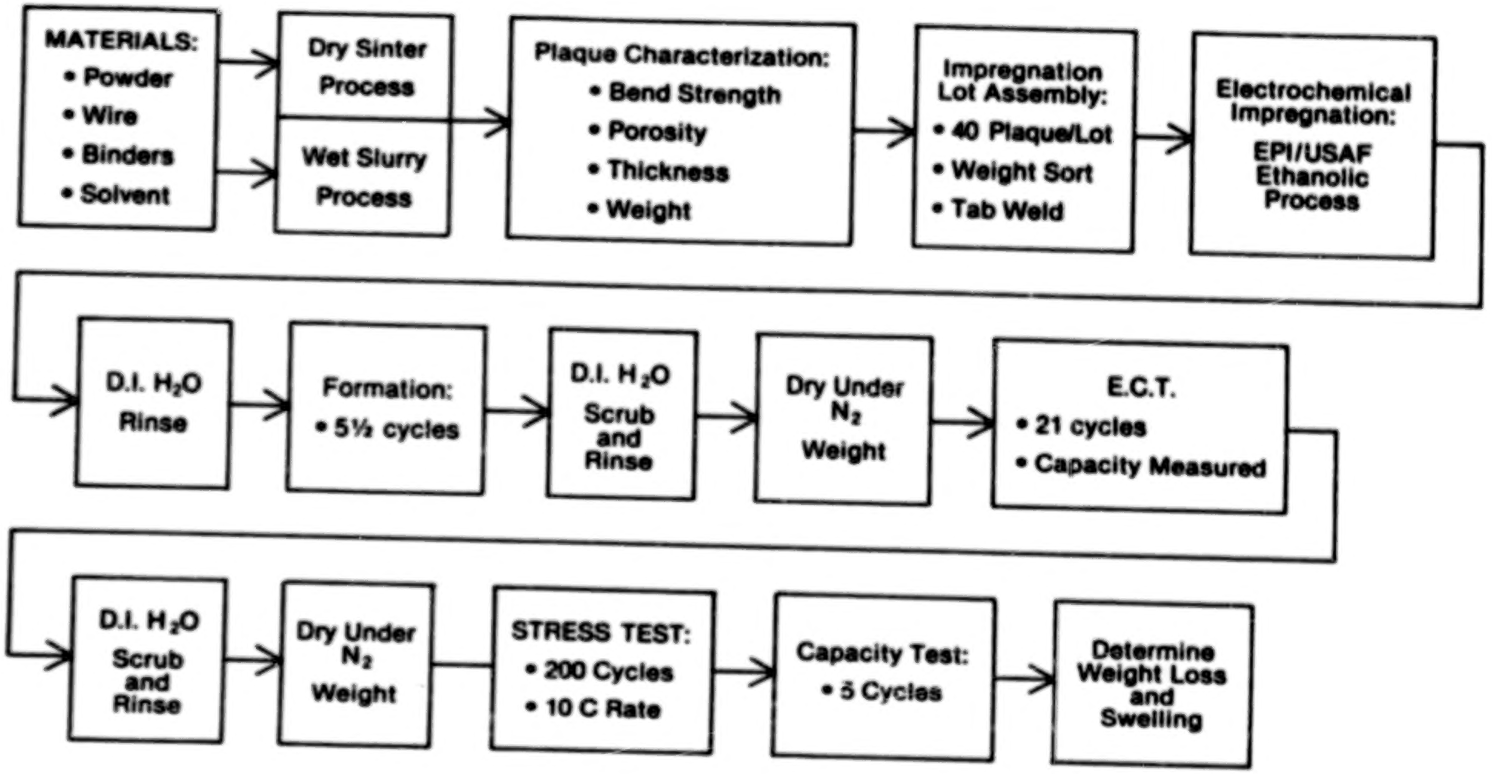
MATERIALS:
• Powder
• Wire
• Binders
• Solvent
Dry Sinter Process
Wet Slurry Process
Plaque Characterization:
• Bend Strength
• Porosity
• Thickness
• Weight
Impregnation Lot Assembly:
• 40 Plaque/Lot
• Weight Sort
• Tab Weld
Electrochemical Impregnation:
EPI/USAF Ethanolic Process
D.I. H2O Rinse
Formation:
• 5½ cycles
D.I. H2O Scrub and Rinse
Dry Under N2 Weight
E.C.T.
• 21 cycles
• Capacity Measured
D.I. H2O Scrub and Rinse
Dry Under N2 Weight
STRESS TEST:
• 200 Cycles
• 10 C Rate
Capacity Test:
• 5 Cycles
Determine Weight Loss and Swelling

Figure 1. Electrode production flow chart.

Dry Sinter Process	Wet Slurry Process
I.N.C.O. 287 Powder	I.N.C.O. 255 Powder
Thickness: .04 ± .002 In.	Thickness: .060 ± .003 In.
Actual .0406 In.	Actual .0619 In.
Sinter Porosity: Nominal 82-87%	Sinter Porosity: Nominal 82-87%
Actual Porosity: 84.41%	Actual Porosity: 84.35%
Bend Strength: 521.6 P.S.I.	Bend Strength: 847 P.S.I.
Plaque Size: 11 × 14.5 In.	Plaque Size: 11.25 × 12 In.
Substrate: Nickel Wire	Substrate: Nickel Wire
Lot Size: 150 Ea.	Lot Size: 160 Ea.

Figure 2. Sinter production.

- Concentration: 1.6 to 1.8 M $Ni(NO_3)_2$, 0.12 to 0.18 M $Co(NO_3)_2$
- Solvent: Ethanol 45% Balance H_2O
- pH: 2.8 to 3.2
- Temperature: 70° to 80° C
- Current Density: 3 different regimes
- Target Loading Level: 1.60 to 1.70 g/cm^3 void
- Time: Variable 140 to 310 minutes

Figure 3. E.P.I./USAF electrochemical impregnation.

- 5½ cycles beginning with discharge • Nickel Counterelectrodes
- 20% KOH

Cycle #	–/+	Amps/in.^{2} .040 Plaque	Rate .040 Plaque	Amps/in.^{2} .060 Plaque	Rate .060 Plaque	Time: Min.
1	–	0.45	1.8 C	0.53	1.35 C	20
	+	0.45	1.8 C	0.53	1.35 C	20
2	–	0.45	1.8 C	0.53	1.35 C	20
	+	0.45	1.8 C	0.53	1.35 C	20
3	–	0.45	1.8 C	0.53	1.35 C	20
	+	0.45	1.8 C	0.53	1.35 C	20
4	–	0.45	1.8 C	0.53	1.35 C	20
	+	0.45	1.8 C	0.53	1.35 C	20
5	–	0.10	C/2.5	0.12	C/3.5	20
	+	0.10	C/2.5	0.12	C/3.5	20
6	–	0.07	C/3.6	0.08	C/4.8	20

Figure 4. Formation procedure.

- [illegible] cycles at C Rate:
  120% Charge Discharge to -0.2V vs Hg/HgO
- 16 Hr. Charge at C/10 rate
- Discharge at C/2 rate to -1.0V vs Hg/HgO: Capacity Calculated
- 20% KOH
- D.I. H_2O Rinse and Scrub
- Final Weight and Thickness

Figure 5. Electrochemical characterization test.

- Hot Formation: 5C Rate, 70°C, 20% KOH, 2 Cycles
- Pre-Stress: Weight, Thickness, and Visual Appearance Characterization
- Initial Capacity: Charge 5C for 12 min. C/2 for 1 hr.
  Discharge C rate to – 1.0V vs Ni sheet
- 200 Cycles: Charge 10C for 12 min.
  Discharge 10C for 8 min. Diode Clamped to – 1.0V
- Ending Capacity: 5 Cycles Same as Initial Capacity
- Visual Appearance
- Scrub, Rinse, and Dry
- Weight Loss and Swelling

Figure 6. E.P.I./H.A.C. electrode stress test.

- Thick Electrodes offer Improved Energy Density and Specific Energy
- Thick Electrode Technology well established by E.P.I. for NI-FE Traction Batteries
- Both Dry Sinter and Wet Slurry Sintered Plaque processes Producing Flight Quality Thin Electrodes
- Automated, Ethanolic, Consumable Anode, Electrochemical Impregnation Process should be Adaptable to Thick Plaque Loading
- Formation, Electrochemical Characterization Test, and Stress Test offer Comparison to Large Data Base of Thin Electrodes

Figure 7. E.P.I./NASA-LeRC bi-polar positive electrodes.

- 0.034 In. Thick Dry Sinter Plaque with wire
- 0.080 In. Thick Dry Sinter Plaque with wire
- 0.080 In. Thick Dry Sinter Plaque without wire
- Plaque Characterization: Weight, Thickness, Porosity, Bend Strength, Pore Size
- Electrochemical Impregnation: Various Regimes to achieve 1.60 ± .05 g/cm^3 void
- Formation/E.C.T.
- Stress Test
- Electrode Chemical Tests
- Cell Testing

Figure 8. E.P.I./Hughes Research/NASA-LeRC Electrode Program.

- Demonstrated Capability of Producing 0.040 in. Dry Sinter, and 0.060 in. Slurry Plaque.
- EPI/USAF Impregnation Facility Flexible enough to load thick plaques to at least the 1.60 to 1.70 g/cm^3 void level.
- Sample Electrodes Subjected to Severe High Rate Test without Significant Degradation.
- Thick Electrode Capacity Buildup Through Formation and Stress Cycles Should be Investigated Further
- Thick Electrode Technology Undergoing Further Development with The Assistance of NASA, and Hughes Research Laboratories.

Figure 9. Summary.

Q. Hendee, Telesat Canada: Were these with dry powder or was it the slurry process?

A. Edgar, Eagle Picher Company: We used both. Most of the work has been done really with dry powder plaque although some of the later data you saw on the last sheet were with slurry process. Principally, I think for the aerospace type electrodes we would be looking to dry sooner at the moment.

Q. Hendee, Telesat Canada: Okay, any schedules?

A. Edgar, Eagle Picher Company: As I said we are following up the production equipment essentially right now for full-scale type production and then we are going to go into an evaluation phase on those electrodes and we are hoping to talk more about it this year and talk you guys into it a little bit.

Q. Hendee, Telesat Canada: Well when would you come out and say hey, Ed I've got something new for you?

A. Edgar, Eagle Picher Company: We are hoping for this year Ed. Really.

Q. Lim, Hughes Research Lab: You said the voltage against the reference electrode there is a kind of indication for the end of the loading. Is the loading after the voltage against reference an indication of surface loading?

A. Edgar, Eagle Picher Company: Yes, it seems typically to be surface loading if you stop the impregnation at the point of where you reach about -.65 volts you have a pretty good surface plaque that is fairly uniform appearance and if you continue beyond that point even under the same regime you get a considerable amount of thickening on the surface you get a very dark deposit of cadmium.

Q. Lim, Hughes Research Lab: The second question is the weight loss during the initial cycling is that related to a cadmium solubility in the KOH. If so, it should be related to the volume of KOH you used if you are using those conditions.

A. Edgar, Eagle Picher Company: I think the weight loss is principally cadmium that is lossely adhered to the surface of these plaques either loaded on the surface or in pores that are very close to the surface that the electrodes have typically been in a large excess of KOH and subsequent cycling of course is done in smaller amounts but I'm not sure that I really follow your question about the soluability of KOH.

Q. Maurer, AT&T Bell Labs: Have you measured the percent utilization or have you done a chemical analysis of the plates? One of the problems with comparing weight gains in several different processes is the possibility of a difference in nickel corrosion in various cases so you get a lot of nickel hydroxide precipitated you will get an artificially high weight gain.

A. Edgar, Eagle Picher Company: Right.

Q. Maurer, AT&T Bell Labs: One of the problems I was worried about is in the current reversal technique? We would be making a plaque more subceptible corrosion.

A. Edgar, Eagle Picher Company: Yeah we are quite aware of that problem and I agree with you. We have done some chemical analysis of the electrodes that hasn't been shown here. We intend to talk about that in the future as well as the utilization. We've experienced utilizations that reported in the literature by yourselves at Bell Labs and Dr. Pickett. The corrosion problem we considered early on to be a significant problem to worry about especially with the current reversal techniques. So we followed that in a couple of ways. One is by the traditional chemical analysis of the plates and utilization testing which indicated in fact that the sintered materials did corrode quite a bit and we got some loaded with nickel hydroxide and that showed up in the chemical analysis. You can also see it building up in your impregnation solution which is a real clear cut way of looking at it. That's one of the big driving reasons we went to the dry sinter plack and we experienced a significant reduction in corrosion by doing that and we intend to continue with that especially since we are using the current reveral techniques as you said.

Q. Ritterman, Comsat: You showed a viewgraph of impregnation time versus voltage against the counter reference at three different current densities and if memory serves me properly you had a significant increase in the impregnation time and evidently in the loading level when you went from .2 to .16. Did you do that for a whole bunch of plaques or is that data for one plaque?

A. Edgar, Eagle Picher Company: Those were data points for single runs but they are indicative of numerous runs that we made and essentially what we are doing there Paul is monitoring the impregnation with the potential and turning it off as the potential rose above a certain level.

Q. Ritterman, Comsat: It looks like you would get maybe two or three times as much impregnation going to .16. I gather you went below .16 in current densities.

A. Edgar, Eagle Picher Company: Yes.

Q. Ritterman, Comsat: Did you continue to get this increasing impregnation time or was there some sort of limit on the lower current density?

A. Edgar, Eagle Picher Company: Yeah, we did seem to encounter that you could in fact run for tremendously long periods of time without reaching the higher potentials but you didn't seem to get the benefit in terms of added loading.

N84
33701

UNCLAS

D33

N84 33701

BIPOLAR NICKEL-HYDROGEN BATTERIES FOR AEROSPACE APPLICATIONS

C. W. KOEHLER & G. VAN OMMERING
FORD AEROSPACE & COMMUNICATIONS CORP.
AND
N. H. PUESTER & V. J. PUGLISI
YARDNEY ELECTRIC CORPORATION

INTRODUCTION

Space platforms and many other future spacecraft are expected to operate at electrical power levels of 20 to 125 kW and beyond. To reduce distribution losses, the electrical power systems are likely to operate at higher bus voltages (150-250V) than commonly used today. Space qualified energy storage systems compatible with these high-power and high-voltage requirements do not exist and must be developed. An additional desirable characteristic of such systems is that they should lend themselves to rather straightforward installation and integration in orbit.

One energy storage system which has been identified as an excellent candidate for these applications is the bipolar nickel-hydrogen battery. Studies aimed at identifying design approaches for this battery system have been conducted by several organizations. Ford Aerospace & Communications Corporation and Yardney Electric Corporation have designed a bipolar nickel-hydrogen battery which effectively addresses all key requirements, including long-term reliability and low mass. In 1984 Ford Aerospace and Yardney will start development of this battery under NASA Lewis sponsorship. This paper discusses this design in the context of system requirements and nickel-hydrogen ($Ni-H_2$) battery technology in general.

SYSTEM DESIGN OBJECTIVES

To achieve the ultimate goal of an aerospace application of a bipolar $Ni-H_2$ battery several objectives must be met in the design and development of the system. These objectives include:

- Maximization of reliability and life
- High specific energy and energy density
- Reasonable cost of manufacture, test, and integration
- Ease in scaling for growth in power requirements

These basic objectives translate into a number of specific design requirements, which are discussed below.

BIPOLAR BATTERY REQUIREMENTS

Electrolyte Management

A key requirement for a practical bipolar Ni-H_2 battery is effective electrolyte management. A significant electrolyte path between two cells in a bipolar stack essentially shorts out these cells and any in between, leading to substantial performance problems. The requirement for electrolyte isolation between cells is more stringent in a bipolar battery than in a multiple, conventional stack common pressure vessel (CPV) design. In a CPV the height of the electrode stack and the required intercell distance can be used to advantage to prevent an electrolyte path from developing from cell to cell. Conversely, because the cell compartment containing the two electrodes of a bipolar cell requires very little height, it is possible to have high voltages across very short stack distances.

One of the most effective methods of dealing with potential electrolyte paths is to utilize hydrophobic materials and to provide long and tortuous electrolyte paths if the individual cells cannot be completely sealed. This can be accomplished by designing necessary gas vent openings so that the cell provides a lengthy path constructed of a material such as polytetrafluoroethylene through which the gases must pass.

Finally, the method of sealing the perimeter of each cell in the areas other than a vent opening must be reliable. Because of the creep characteristics of the potassium hydroxide electrolyte, any slight sealing flaws will be vulnerable to leakage. Therefore, redundant or permanent sealing features must be considered wherever possible.

Material Balance

Material balance management is a particularly critical issue in a bipolar battery design. Gases (H_2 and O_2) must be reacted in the cells where they were stoichiometricaly evolved; otherwise the drying out of one cell and the flooding of another may occur. This requires careful control of the flow of oxygen from the nickel electrode on overcharge so that it is directed to the recombination sites. These must be designed so that all oxygen is scavenged before it can reach the common gas space. Because of the relatively large size of the electrodes, material utilization gradients across the surface must be considered and minimized. This can be achieved by maintaining good thermal control, providing good electrolyte wicking and reservoir materials, and properly filling the cells initially with electrolyte.

Thermal Management

The heat dissipated as a result of stack resistive losses is minimized by the bipolar electrode approach. However, heat evolved because of charging/discharging inefficiencies (e.g., O_2 generation and electrode polarization) and the exothermic O_2-H_2 recombination reaction must still be removed from the stack. In fact, thermal control of a bipolar battery is more challenging than for a conventional stack individual pressure vessel (IPV) or CPV battery, because a single-electrode bipolar cell, of equivalent capacity, is substantial in size. Further, electrolyte isolation requires encasement of each cell, hindering heat transfer and eliminating electrode to pressure vessel wall proximity. Also, in a continuously operating bipolar battery, cell-to-cell temperature gradients must be eliminated to maintain long-term material balance.

Current state-of-the-art LEO or GEO cells, with an electrode size of approximately 3.5 inch diameter, can be adequately cooled by employing passive cooling. Because of the constraints imposed by a multiple, high capacity bipolar electrode stack configuration, the only viable approach to thermal control is an active cooling system.

Two possible physical arrangements for an active system are either to place cooling plates within the electrode stack, parallel to the electrodes, or to place cooling plates externally, in contact with the edges of the cell stack. Parallel cooling plates require heat transfer perpendicular to the stack components including the negative electrode and separator, which have a low coefficient of heat transfer. In addition, when the cooling plates are placed at intervals of several cells to minimize mass, a thermal gradient will exist from cell to cell. Furthermore, parallel cooling plates may require the battery current to flow through them. In this case extreme care must be taken so that the cooling loops do not electronically short out the bipolar stack via the conduits or ionically via the coolant. Lastly, the large number of fluid path connections raises serious concerns about the long term reliability.

Edge cooling, however, results in relatively even temperatures from cell to cell. Yet, the thermal gradient across each electrode could be greater than with parallel cooling plates. Therefore, in order to hold this gradient to a manageable level, the distance from any part of the electrode to the cooling plate must be reasonably small. Additionally an edge cooling system is electrically isolated from the cell stack.

A significant positive factor resulting from the need for active cooling is that it eliminates the requirement that the cell stack perimeter be adjacent to the pressure vessel wall. This allows the consideration of other than a circular cell configuration as is necessary with the multi-electrode IPV and CPV passive cooling systems.

BIPOLAR BATTERY DESIGN

Battery Configuration

The bipolar battery design which Ford Aerospace and Yardney will develop consists of 210 cells of 75 Ah capacity each. The battery will be a hermetically sealed pressure vessel containing the cell stack, an active edge cooling system, and support hardware. To minimize temperature gradients within each cell, the shape of the cell is rectangular, with an approximate electrode size of 12.7 x 96.0 cm (5 x 37.8 inches). The cell stack assembly is divided into three series-connected stacks of 70 cells each. Including the cell frames, the approximate size of the individual stacks will be 14.0 x 97.3 x 25.1 cm (5.5 x 38.3 x 9.9 inches) and with heat removal channels installed on each side 15.2 x 97.3 x 25.1 cm (6 x 38.3 x 9.9 inches). The three stacks, combined in a final stack assembly measuring 45.7 x 93.7 x 30.5 cm (18 x 38.3 x 12 inches), is installed in a cylindrical pressure vessel with the stack's long dimension parallel to the vessel longitudinal axis. Figure 1 illustrates the overall layout of the battery and bipolar cell stacks.

The decision to change electrode configuration from circular to a long, rectangular shape is initially difficult to accept because the natural shape which fits the pressure vessel is circular. However, extensive and intensive review of the implications of this change led Ford Aerospace and Yardney to the realization that it yields a number of significant benefits. One is essential to the successful long-term performance of bipolar Ni-H_2 batteries, namely the maintenance of the lowest cell-to-cell temperature gradients possible. Using an edge cooling system with long, narrow electrodes achieves the same level of thermal control within each electrode as in the case of the established IPV designs. Another advantage is that heat removal with a heat-pipe system becomes a practical option, which would control intra-electrode gradients even better.

A perceived disadvantage of rectangular electrodes is that they may not be as efficiently packaged in a pressure vessel. However, the required combined stack and gas volume will be independent of electrode configuration. With a practical maximum operating pressure of 41 to 48 atmospheres (600 to 700 psi), the volume impact is insignificant.

Stack Configuration

Each bipolar stack consists of 70 cells directly connected in series. These cells each consist of a group of active components and a bipolar conduction plate placed within a polymer frame in the following sequence:

- Bipolar conduction plate
- Metallic gas diffusion screen

- Hydrogen electrode
- Asbestos separator
- Nickel electrode
- Oxygen recombination site/electrolyte reservoir

The reservoir is placed against the back of the nickel electrode, a similar approach to that used in some recirculating stack designs. The reservoir, by choice of material properties and pore size distribution will readily yield most of its electrolyte content to the nickel electrode. However, during overcharge it will absorb and retain electrolyte displaced from the nickel electrode due to oxygen gassing. The pore size structures of the asbestos separator and the reservoir are such that the asbestos forms a much more effective gas barrier. As a result, oxygen is forced into the reservoir. The total cell electrolyte inventory should be chosen such that the reservoir is only partially filled with electrolyte during overcharge, so that the oxygen will pass through relatively easily to the recombination layer. This structure could be a metal screen or perforated metal sheet with platinum dispersed on it. Alternatively, a platinum impregnated reservoir type material could be used. On the back of the recombination layer a porous teflon sheet is placed to provide for hydrogen access to the recombination sites.

The cell seal is obtained by joining the frames of two adjacent cells. The frames are molded with sealing and alignment provisions to enhance the seal quality. Depending on material selection, the seal may be accomplished by mechanical compression, heat sealing (ultrasonic bonding), or adhesives. Gas access holes in the walls of the frame provide for adequate hydrogen flow during both charge and discharge.

The second major element in accomplishing individual cell sealing is the bipolar conduction plate molded in place in each frame. This provides both an effective cell-to-cell electrolyte barrier and an effective electronic cell-to-cell bipolar contact.

The heat conduction path through the cell frame is improved by extending the bipolar plate into the frame. The thermal path can be further improved by increasing the foil thickness, but this does entail a mass penalty.

The estimated mass breakdown for the 75 Ah bipolar Ni-H_2 battery is shown in Table I.

DEVELOPMENT PLAN

NASA Lewis Research Center has selected Ford Aerospace and Yardney to develop the 75 Ah bipolar Ni-H_2 battery under a program titled "Advanced Nickel-Hydrogen Battery Development". The three year program scheduled to start in January 1984, will consist of three overlapping phases: development, improvement, and optimization.

The Development Phase consists of the design, fabrication, and test activities associated with the development of an initial bipolar battery design. Two bipolar stacks of 10 cells will be fabricated and tested in boiler plate pressure vessels. Another design will be considered in parallel with the design described in the preceeding paragraphs. This design eliminates the bipolar plate and achieves the bipolar connection in a different manner. It has the advantage that it permits significant mass savings. The estimated specific energy for this configuration is 50.8 Wh/kg (23.1 Wh/lb) for a 75 Ah battery. Two stacks of 10 cells using this design will be assembled and tested. At the conclusion of the Development Phase of the program one of the two designs or a hybrid version will be selected to continue through the final two phases of the program.

The Improvement Phase has the objective to improve the initial design based on information generated in the Development Phase. Two more 10 cell stacks will be fabricated and evaluated based on the improved design.

Based on the experience with the initial and improved stacks, the Optimization Phase will result in a final design. Two optimized design cell stacks of 10 cells will be assembled and tested.

All cell stacks will undergo a characterization test followed by a LEO cycling test. Characterization testing will be performed at three charge rates (C, C/2, C/4) and four discharge rates (2C, C, C/2, C/4). The LEO regime consists of a one hour charge and a one-half hour discharge.

CONCLUSION

Ford Aerospace and Yardney have designed a bipolar Ni-H_2 battery capable of meeting the electrical power levels for spece platforms and other future spacecraft. The design achieves the system design objectives in a mass efficient way. Development of two designs will be sponsored by NASA Lewis Research Center beginning in early 1984. The design represents a significant improvement in bipolar Ni-H_2 technology. The development program provides the opportunity to achieve a space quality energy storage system for high power applications.

TABLE I

Mass Breakdown - 75 Ah Bipolar Ni-H_2 Battery

Component	Mass (Kg)	Mass (lbs)
Cell Stack:		
Bipolar Plate	78.6	173
Nickel Electrode	142.7	314
Separator	6.4	14
Hydrogen Electrode	9.5	21
Recombination Site/Reservoir	23.2	51
Electrolyte	46.8	103
Cell Frames	31.4	69
Miscellaneous Hardware	3.2	7
Total Cell Components	341.8	752
Battery:		
Cooling Channel Assembly	14.1	31
Coolant	14.5	32
Assembly Hardware	8.6	19
Stack Supports	4.1	9
Pressure Vessel	86.6	191
Miscellaneous	16.4	36
Total Battery	486.3	1070
Specific Energy (18,900 Wh)	38.9 Wh/kg	17.7 Wh/lb

ORIGINAL PAGE IS
OF POOR QUALITY

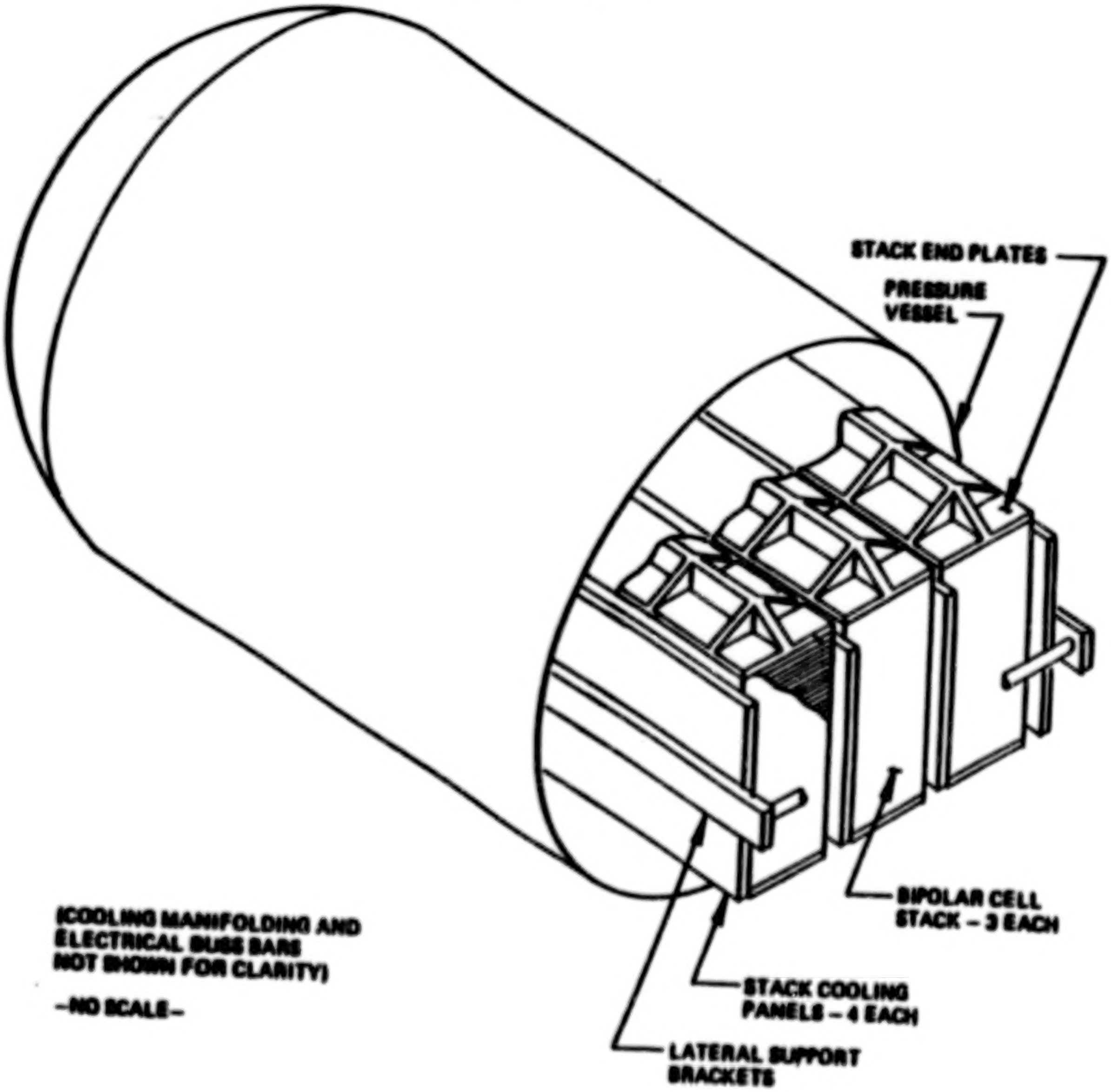
STACK END PLATES
PRESSURE VESSEL
BIPOLAR CELL STACK – 3 EACH
STACK COOLING PANELS – 4 EACH
LATERAL SUPPORT BRACKETS
(COOLING MANIFOLDING AND ELECTRICAL BUSS BARS NOT SHOWN FOR CLARITY)
–NO SCALE–

Figure 1. Ford Aerospace/Yardney Bipolar Battery.

Comment

Lackner, Defense Research Canada: You've got an awful lot of trouble when you are getting a specific energy at 17½ amp hours.

Koehler, Ford Aerospace Corporation: 17½ watt hours per pound.

Lackner, DND/DREO: There is a figure mentioned by Jim Dunlop something like 44 a little earlier and I'm wondering is all this trouble wroth what you are doing.

Koehler, Ford Aerospace Corporation: I'm not quite sure what assumptions Jim is using in his. Maybe I can hit on that again. The number was 389 watt hours per kilogram. I based that on a worst case end of life assumption of 1.2 volts per cell.

Q. Unidentified: What is the best you can get out of it?

A. Koehler, Ford Aerospace Corporation: I'm sorry.

Q. Unidentified: What is is the best potential you can get out of the system?

A. Koehler, Ford Aerospace Corporation: I think plateau voltages and discharge of at least 1.25 volts are conceivable.

Q. Ritterman, Comsat: Is your 38.4 based on 100% depth discharge or 80% depth discharge?

A. Koehler, Ford Aerospace Corporation: No that's all the way down. That's complete discharge.

Q. Unidentified: The potential you are talking about is voltage potential. I'm wondering about the energy density potential that you can possibly get out of it?

Q. Koehler, Ford Aerospace Corporation: The energy well it would be maybe you can help me Gert. The question is what would be the optimistic specific energy?

COMMENT

Unidentified: I think we have to look at bipolar batteries in a way that really doesn't concentrate completely on specific energy, there's a few other reasons why bipolar batteries are being pursued. I can answer the question directly and state that with the bipolar plate approach we can probably reach specific energies on the order of 21 hours per pound. If the other approach is successful that we are going to take a look at the, might reach 23 or 24 watt hours per pound. The lower specific energy system with the bipolar plate has a number of advantages through that in terms of overall cost effect of the system as it is applied they'll be very significant. One thing is that it has a pretty high current capability because of the very large cross section. That gives the system a very high pulse rate capability which for many future applications is a very important consideration. The other thing is that the cost effectiveness of integrating the large battery we are talking multi kilowatt hours into a work space station or other space systems. The cost of integrating a large battery is likely to be much less than the cost of integrating many individual cells. There are two of the reasons beyond specific energy that this system is being pursued so vigorously.

Q. Lim, Hugh Research Lab: I understand you have the cooling panel vertical to the bipolar rate?

A. Koehler, Ford Aerospace: Yes that's right.

Q. Lim, Hughes Research Lab: And if you have that the heat collection should be through the frame of the cell and I'm wondering if you have an advantage of collecting that way versus the heat collection parallel to the bipolar plate or incorporated inside a bipolar plate.

A. Koehler, Ford Aerospace: One thing that we are going to try to incorporate in the design is that the conduction plate will be incased in the cell frame and the conduction plate will actually stick into the cell frame almost to the very outside edge. There will be a very small layer of the frame covering the edge of the bipolar plate but it will be very close.

Q. Sperber, GTE: Is your design a constant compressive force on the stack design?

A. Koehler, Ford Aerospace: Yes that would be required that the compressant force over the stack area has to be very uniformed and the stack compressant plates will have to be designed accordingly to provide that function.

Q. Unidentified: Do you have some sort of spring arrangement to provide that?

A. Koehler, Ford Aerospace: The specific details of the design have not been set. The developmental phase of the program is approximately a year to a year and half project in itself and no specific type details will be identified at that point.

N84
33702

UNCLAS

D34

N84 33702

TEST RESULTS OF A TEN CELL BIPOLAR NICKEL-HYDROGEN BATTERY

Robert L. Cataldo

National Aeronautics and Space Administration
Lewis Research Center
Cleveland, Ohio 44135

INTRODUCTION

Space power systems of the future are projected to require power levels that extend far beyond those currently in the 1 KW range. High power systems will most likely utilize either higher battery voltages in the 200V-300V range or special power processing equipment to convert low battery voltage to high system voltage. This second option will demand batteries with high capacity (greater ampere-hours per cell or cells configured in parallel), and high discharge current capability. The energy storage for such large systems becomes a challenging battery engineering problem.

The two candidate battery systems for space power are nickel-cadmium and nickel-hydrogen. Presently, both these types are available in capacities ranging from 30 to 50 ampere-hours. The energy storage for a low-earth orbit mission requiring 35 KW of power would contain about 500 individual 50 ampere-hour cells, arranged in series and/or parallel. No battery of this magnitude has yet been constructed and tested, and there are serious concerns about the feasibility of such a system for the long lifetimes required in low earth orbit.

In light of this problem, a study was initiated in late spring of 1981 at the NASA Lewis Research Center to design and evaluate a new design concept for nickel-hydrogen cells. This concept involved constructing a battery in a bipolar stack with cells consisting of one plate for each nickel and hydrogen electrode. Preliminary designs at the system level of this concept promised improvements in both volumetric and gravimetric energy densities, thermal management, life extension, costs, and peak power capability over more conventional designs.(1)

To get an early confirmation of these encouraging design studies, a concept verification program was initiated. The first phase of the program was the design and assembly of a preprototype bipolar battery. The design incorporated hardware and components available from past programs along with some that were specially constructed. The size of the cell hardware (10 cm x 21 cm active area) allowed the use of a 6.5 ampere-hour capacity nickel electrode. Ten of these cells were assembled into a stack with the dimensions length - 35.4 cm, height - 15.2 cm, width - 10 cm. The second phase included a series of characterization and cycle tests.

PRECEDING PAGE BLANK NOT FILMED

The following discussion of oxygen, electrolyte and thermal management, convey the design philosophies incorporated into the bipolar concept as applied to nickel-hydrogen batteries. Use of these concepts offers a high probability of a successful design which theoretically would yield good performance and long-life.

OXYGEN MANAGEMENT

In prior designs, oxygen generated on overcharge has been allowed to combine with hydrogen at the hydrogen electrode. A separate electrode for recombination would prevent damage to the hydrogen electrode from the heat generated. The approach taken in this design was to have recombination occur behind the Ni electrode (1). Figure 1 depicts the methodology used. A high bubble pressure asbestos separator forces the 0_2 into a highly porous electrolyte reservoir plate. The recombination sites are strips of hydrogen electrodes 0.47 cm x 19 cm. They are encapsulated in a vapor permeable tubing to allow passage of gases in and water vapor out. The tubing also isolates the catalyst electrically, preventing parasitic reaction between the recombination sites and the nickel electrode. This method of oxygen management also benefits the overall electrolyte management scheme by keeping the recombined water from possibly flooding the hydrogen electrode.

ELECTROLYTE MANAGEMENT

Electrolyte management can have a significant effect on the cycle life of a nickel-hydrogen battery and should be a prime consideration of the overall battery design. The objective of electrolyte management is to prevent flooding of the hydrogen electrodes and drying of the nickel electrodes and separators. The approach taken to achieve this objective is through pore size selection of components such that each component has the optimum amount of electrolyte (2).

The electrolyte reservoir plate has a pore size that freely accommodates the water formed during the charge portion of the cycle and returns electrolyte by wicking to the nickel electrode and separator as required. The wicking action is created by choosing a reservoir plate with larger pores than the electrode and separator and maintaining physical contact. Flooding of the hydrogen electrode is also prevented by proper pore size selection as well as use of hydrophobic materials in the electrode.

THERMAL MANAGEMENT

In the present design, heat is primarily rejected from the stack by cooling fins which are that part of the bipolar plates that extend beyond the frame edges. Thus, the heat generated during cycling is transferred by a combination of conduction and convection to the test chamber wall. Cell temperatures did not exceed 29°C (84°F) at the end-of-discharge. Therefore, this method of cooling is adequate at the power levels being tested. However, larger power levels would require alternate heat rejection options such as heat pipes or cooling plates within the stack with gaseous or liquid recirculating coolant.

CELL COMPONENTS

The following paragraphs describe the composition, manufacture, and function of the components used in the cell.

GAS FLOW SCREEN

The flow screen for the hydrogen electrode was expanded nickel of 1.05 mm (0.042 in) thickness with approximately 95% open area.

NICKEL ELECTRODE

The nickel electrodes used in the battery are chemically impregnated, pressed powder sinter type electrodes remaining from a previous program. These electrodes have a screen grid and an average loading of 2.1 grams/cc of void volume. The electrodes for this application were cut slightly smaller than the frame dimensions to allow for electrode expansion. The electrode thicknesses ranged from 0.96 mm to 1.0 mm. The capacity of the electrode was calculated to be about 6.50 ampere hours with a surface area of 218 cm^2 (one side).

HYDROGEN ELECTRODE

The hydrogen electrode was a fuel cell type catalyzed porous screen electrode. Electrode dimensions were: 0.025 cm thick, 10.1 cm wide, and 21.6 cm long, with a surface area of 218 cm^2 (one side). Other electrode properties are proprietary to the manufacturer.

SEPARATOR

The separator material was a beater treated asbestos (BTA). BTA is a reconstituted blend of asbestos sheets with a 5% latex binder. The experimentally determined bubble pressure (pressure at which the first bubble passes through the separator) is 2.0 atmospheres. The dimensions of the separator are 11.9 cm wide by 23.3 cm long, making it larger than the electrodes. This extra separator area, along with six wick rings, forms a seal with the frame ledge to provide a barrier against oxygen passage to the hydrogen electrode (Figure 2). The uncompressed thickness of the separator is 0.053 cm (21 mils), while the average compressed thickness is designed to be 0.025 cm (10 mils).

ELECTROLYTE RESERVOIR PLATE

The electrolyte reservoir plate (ERP) was a foam nickel structure with a density of 10%. Each plate was compressed from 0.25 cm to 0.125 cm, followed by cutting with a rule die that cut out four slots 0.8 cm wide and 20.6 cm long to house the recombination strips. The average pore diameter is 0.025 cm (10 mils). This pore size allows the passage of hydrogen and oxygen gas through the ERP to the recombination sites. The water that is formed at the recombination sites during charge and overcharge is freely wicked out of the ERP by the separator and nickel electrode since these cell components have smaller pores.

BATTERY HARDWARE

The hardware used for the bipolar battery was originally a carbon dioxide removal unit for the life support system on the Apollo missions. The configuration of the unit was such that it could readily be utilized for verification testing of a bipolar nickel-hydrogen battery. The items used from the unit were ten polysulfone frames, eleven gold-plated nickel bipolar plates, two polysulfone insulation plates, and two stainless steel end plates.

The injection molded polysulfone frames were used to contain the cell components and electrolyte. The nominal frame thickness was 0.378 cm (.149 in) as shown in Figure 2. The inner frame ledge provides a means of sealing the separator around the nickel electrode, thus eliminating evolved oxygen passage to the hydrogen electrode. Hydrogen gas was channeled to the hydrogen electrode via slots connecting the inner frame to two manifolds. The 16 slots provide 0.515 cm^2 of area for hydrogen gas ingress/egress. These slots were in line with the gas flow screen (expanded nickel). Similar slots and manifolding were provided on the other side of the frame to supply hydrogen gas to the recombination sites. The total slot area for this side was 0.296 cm^2 and these slots align with the electrolyte reservoir plate.

The bipolar plates are thin gold-plate nickel sheets and were sandwiched between each frame. Each cell was enclosed between two bipolar plates. A neoprene gasket fit into a recess in the frame and seals against the bipolar plate, retaining the electrolyte within each cell. External current connections were made to the bipolar plates on each end. The interior bipolar plates conduct current from the positive electrode of one cell to the negative electrode of the next, thus no inter-cell electrical connectors were needed. However, electrical connections were made to each plate to monitor individual cell voltages. The bipolar plate was also used for heat rejection. Each plate extends beyond the frame on two opposite sides forming a set of cooling fins.

The stainless steel end plates and tie bolts compressed the cell components and gaskets. The cell compression was designed for a nominal 0.028 cm (.011 in), which compressed the separator from 0.053 cm to 0.025 cm. The manifolds formed by the cell frames and end plates allowed for vacuum electrolyte fill and drain.

Life Systems Inc. of Beechwood, Ohio, has loaned to NASA Lewis Research Center the following hardware: cell frames, stack end plates, insulation plates, tie bolts, and bipolar plates to help expedite the verification testing of the bipolar concept as applied to nickel-hydrogen batteries.

STACK ASSEMBLY

The following sequence was used to assemble the stack components:

1. The negative side end plate was placed in position.

2. The negative side insulation plate and "O" rings were positioned.

3. Six guide pins were inserted into bolt holes for alignment of subsequent parts.

4. The negative terminal bipolar plate was positioned.

5. The hydrogen side gasket was placed over the guide pins.

6. The polysulfone frame was positioned on the gasket.

7. The cell components were inserted in the frame cavity in the following order:

   a) hydrogen flow screen
   b) hydrogen electrode
   c) separator
   d) nickel electrode
   e) wick rings
   f) electrolyte reservoir plate
   g) recombination strips

8. The nickel side gasket was lowered over the guide pins.

9. The bipolar plate was positioned on the gasket.

Steps 5-9 were repeated for the next nine cells followed by the positive side insulation plate and end plate. The tie bolts were inserted from the negative side and threaded into the positive side end plate with 3 inch-pounds of torque.

The stack was then placed in a hydraulic press with an applied force of 5000 pounds. The tie bolts were retorqued to 10 inch-pounds. The press was readjusted to 5000 pounds and the tie bolts were torqued to 15 inch-pounds. This step was repeated once more.

ELECTROLYTE FILL AND DRAIN

Two acrylic plates were fitted to the stack end plates with gaskets and C-clamps. The acrylic plates had tube fittings adjacent to the manifold openings. After a vacuum was pulled on the stack, a 31% potassium hydroxide solution was valved into the stack. The stack remained filled overnight and was then drained of excess electrolyte over a period of several hours. The manifolds were then wiped clean of excess electrolyte and the stack inserted into the test chamber. The test chamber was evaluated, leak checked, and filled with hydrogen at 50 PSI. (The test chamber was an oversize pressure vessel and the pressure changes during cycling were negligible.)

TEST PROCEDURES

Initial testing was carried out in several phases. First, characterization tests were run to determine the performance of the bipolar nickel-hydrogen battery. Following the successful completion of this test matrix, the second phase of tests was initiated. Low-earth orbit (LEO) cycle tests were run with a depth-of-discharge of 80%. The third phase was to determine the peak power capability of the battery.

The characterization tests were carried out at three charge levels, C/4, C/2, and C rate. The capacity of the battery is designated as 6.5 ampere-hours based on a C/4. Discharge rates (constant current) used in the characterization matrix were C/4, C/2, C, and 2C. The recharge ampere-hours were the same (6.5 Ahr) for all conditions of the test matrix regardless of discharge rate. Therefore, the battery received an overcharge at conditions where discharge rates were high. The discharge was terminated when the voltage of the weakest cell in the stack fell to 0.5V.

LEO cycling tests were run at one hour charge and half-hour discharge intervals. (The battery was rated at 6.0 Ahr for the LEO testing, based on the 1.6C discharge rate to be used in this testing.) Constant current charge and discharge rates were employed for this phase of testing. The depth-of-discharge was set at 80%, giving a discharge current of 9.6 amperes. A recharge fraction of 1.10 of the rated capacity was necessary for end-of-discharge voltage stabilization. A peak power test was carried out at the end of 100 LEO cycles. Using a programmable load, the discharge current was increased until the power passed its maximum value.

After completion of the peak power tests, the test chamber was opened and the stack examined. Cell number one was removed from the stack solely for evaluation and analysis (no anomalies were evident in the data). This also would permit possible problem areas within the cell or stack to be discovered at an early date. The stack was then reassembled with nine cells and placed on LEO cycling tests to establish an operational data base.

INSTRUMENTATION

The individual cell voltages and the stack current were monitored and recorded. Cell temperatures were monitored, but not recorded. Temperatures were measured on the fin of the bipolar plate with an iron-constant thermocouple. Computer-generated data includes ampere-hours and watt-hours with integration intervals of every 18 seconds.

RESULTS

Characterization test results are shown in Figures 3 and 4. Figure 3 shows ampere-hour and watt-hour efficiencies at different charge and discharge levels.

The equations used to determine efficiencies are:

$$\frac{I_d \times T_d}{I_c \times T_c} \times 100 = \text{ampere hour eff.}$$

$$\frac{P_d \times T_d}{P_c \times T_c} \times 100 = \text{watt-hour eff.}$$

where: I - current (amps) c = charge
P = power (watts) d = discharge
T = time (hrs)

In general, the efficiencies increased as the charge rate is increased, which is consistent with nickel electrode behavior in other battery systems such as nickel-cadmium and nickel-zinc. Figure 3 further shows that efficiencies increase as the discharge rate decreases. This is expected; however, since a fixed recharge of 6.5 ampere-hours was returned each test, the highest rate discharges were penalized by being overcharged. Figure 4 shows a family of curves at the different discharge rates. An additional curve was added for the 10C (65 amperes) discharge rate. This data was obtained when the discharge equipment malfunctioned during LEO cycling. Five ampere-hours were withdrawn (83% DOD) in just under six minutes.

A LEO cycle regime of 60 min. charge, 30 min. discharge, 80% DOD with 1.10 recharge fraction would correspond to a 1.6C rate discharge and a 1.10 C rate charge and would be predicted to have amp-hour and watt-hour efficiencies of about 88 and 76 percent, respectively.

The peak power was determined following the 100th LEO cycle. The battery current and voltage was 165 amperes (about 27C) and 6.6 volts, respectively, supplying 1.1 KW of power. This is shown in Figure 5. The peak power would probably have been higher but the power leads were only two #14 AWG wires connecting the stack to the terminals that were mounted in the vessel. In addition, the slip-on type electrical connectors that attach to the end plates are rated for about 10 amperes. These factors contribute to a significant voltage drop.

Following the peak power test, one end cell was removed for evaluation and the physical appearance of the stack observed. The nickel electrode was measured for growth. A 10% increase in thickness and 2-3% increase in length and width were noted. The hydrogen electrode appeared as that of an unused electrode. The separator was wet and could be easily separated from the electrodes intact. The ERP was damp but not wet with electrolyte. The strips of hydrogen electrode used for recombination showed no evidence of burning.

Some evidence of corrosion was noted on the positive end bipolar plate inside the manifold. The substance was analyzed and found to be a nickel compound. It's greenish color suggests the substance was probably nickel carbonate or nickel nitrate. An electrolyte film probably remained on the inner surface of the manifold, even after a thorough cleaning, which most likely contributed to the corrosive actions. The bottom of the vessel was damp with electrolyte. Several causes were postulated; these being insufficient draining time, electrolyte forced out during vessel evacuation preceeding the hydrogen fill or electrolyte forced out during charge. If the electrolyte was due to the latter cause, it would have only occured during the early cycles, since such a process continuing over 2000 cycles would tend to cause resistive cells (high polarization voltage) which had not been observed.

The stack was refilled with electrolyte and drained. The nine-cell stack was again placed on LEO cycle testing. Initially, a minimum end-of-discharge voltage of 1.20 V per cell was obtained with a 1.10 recharge fraction, a charge of 5.3 ampere-hours and a 4.8 ampere-hour discharge. After 600 cycles, cell #4 would reach 0.50 volts prematurely, terminating the half-hour timed discharge. The battery was then deep-discharge reconditioned by placing a 10 ohm resistor across the terminals, followed by a short circuit overnight. The battery was then charged for two hours at a current of 6.5 amperes and placed on cycle test with a recharge fraction of 1.20. After 182 additional cycles, cells 3, 4, and 5 exhibited voltages in the 0.80 volt range at the end-of-discharge. Shunt currents were suspected, therefore the stack was removed from the pressure tank and wiped clean. Evidence of free electrolyte was found in the manifolds and a few drops between the bipolar plate fin area. When the stack was replaced into the test chamber more electrolyte came out. The stack was then cleaned in place.

After another 200 cycles at a recharge fraction of 1.20, cell #3 again had a low end-of-discharge voltage. After a complete charge, cell #3 was charged individually through the voltage data leads with an additional 3 ampere-hours. After 4 cycles, cell #3 had low voltage again. The whole stack was then deep-discharge reconditioned in the same manner as before. All weak cells recovered, maintaining 1.20 volts per cell after the half-hour discharge. The recharge fraction was varied over three levels, 1.20, 1.15, and 1.10. Figure 6 shows that a recharge fraction of 1.10 cannot maintain 1.2 volts per cell at end-of-discharge. Shunt currents formed by electrolyte paths between cells could be the cause for the need to increase the recharge fraction.

An open circuit self-discharge test was conducted to determine if any shunt currents existed. Figure 7 shows individual cell voltages on open circuit. Cell #3 went to zero volts after 53 hours. This corresponds to about a 120 milliampere average shunt current. Cells #4 and #5 also possess shunt currents, but of a lesser magnitude. The other cells have a normal self-discharge curve. Electrolyte bridges will divert a portion of the charge current, thus contributing to the need for larger recharge fractions when shunt currents are present. However, the battery is still operable, but at reduced efficiency.

Constant voltage charging was tested to provide some additional operational data, since many spacecraft use this mode of charging. Figure 8 shows a charge/discharge voltage profile of an early cycle. Original indications were that constant voltage charge method was a more efficient method, because charge voltages were lower than constant current voltages. However, over a few days of increasing the charge voltage to stabilize end-of-discharge voltage, a recharge fraction of 1.30 could not maintain a 1.2 volt end-of-discharge voltage.

CONCLUSIONS

Test results of the first NASA Lewis Research Center bipolar nickel-hydrogen battery are most encouraging. This preprototype battery, built with less than ideal components and hardware, exceeded expectations. A total of 2000 LEO cycles at 80 percent depth of discharge have been accrued. A cycle life goal of 30,000 cycles appears achievable with minor design changes. These improvements include advanced technology nickel electrodes, insulated bipolar plates and specifically designed frames to minimize shunt currents.

The discharge rate capability of this design exceeds 25C. At the 10C discharge rate, 80% of the battery capacity can be withdrawn in six minutes. This data shows that the bipolar design is well suited for those applications requiring high peak power pulses.

Deep discharge reconditioning improved end-of-discharge voltages on LEO cycling, while overcharge techniques were much less effective. Those cells with probable shunt currents had improved capacity performance following reconditioning.

Low polarization voltages, which result in a cyclic watt-hour efficiency of 76-80%, have been demonstrated an improvement over other more conventional nickel-hydrogen designs. This will result in reduced weight of the solar array and power processing components. Additional weight savings are realized with the battery itself. Thus, the high voltage bipolar stack within one common pressure vessel makes an ideal building block for large advanced energy storage systems for applications like the manned space station.

REFERENCES

1. Cataldo, R. L. and J. J. Smithrick, "Design of a 35-Kilowatt Bipolar Nickel-Hydrogen Battery for Low-Earth-Orbit Applications," in 17th IECEC Proceedings, Vol. 2, pp. 780-783, IEEE, New York (1982).

2. Abbey, K. M. and L. H. Thaller, "Pore Size Engineering Applied to Starved Electrochemical Cells and Batteries," in 17th IECEC Proceedings, Vol. 2, pp. 757-764, IEEE, New York (1982).

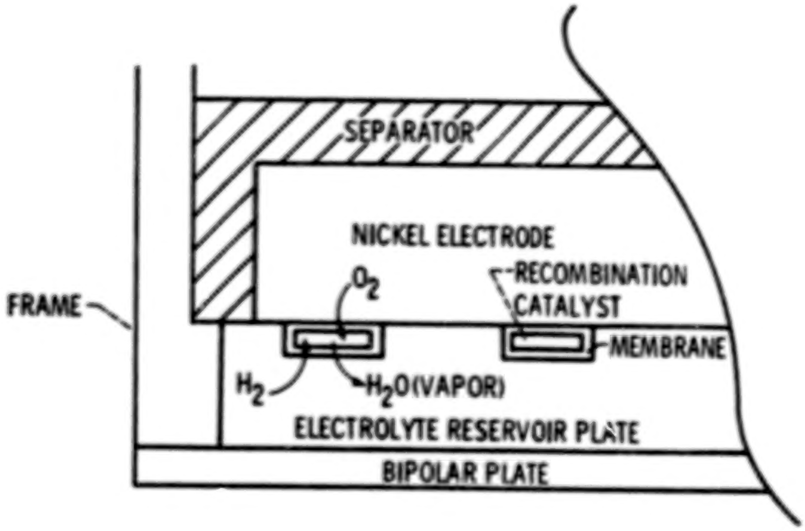
SEPARATOR
NICKEL ELECTRODE
O_2
RECOMBINATION CATALYST
FRAME
MEMBRANE
H_2
H_2O(VAPOR)
ELECTROLYTE RESERVOIR PLATE
BIPOLAR PLATE

Figure 1. Graphic representation of oxygen-hydrogen recombination.

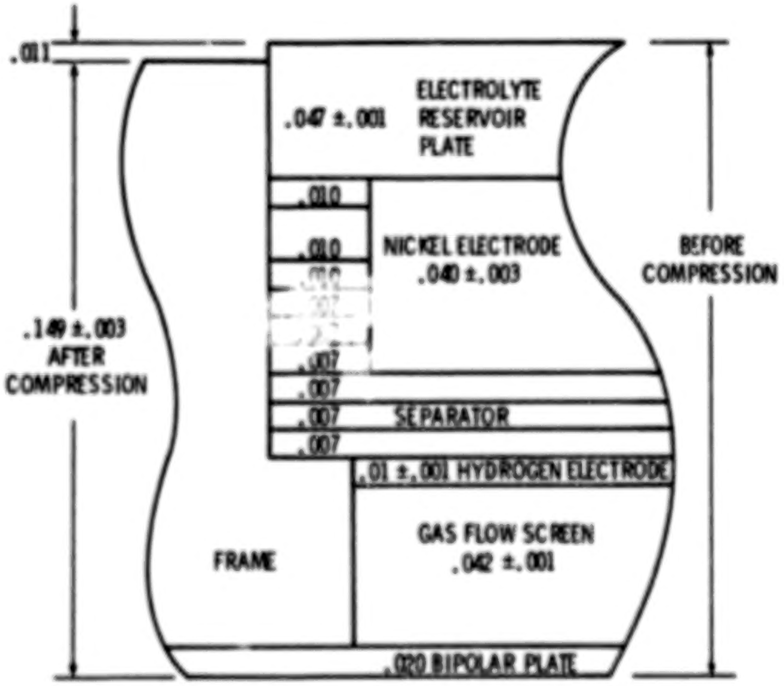
.011
.047 ±.001
ELECTROLYTE RESERVOIR PLATE
.010
.010
NICKEL ELECTRODE .040 ±.003
BEFORE COMPRESSION
.149 ±.003 AFTER COMPRESSION
.007
.007
.007
SEPARATOR
.007
.01 ±.001 HYDROGEN ELECTRODE
GAS FLOW SCREEN .042 ±.001
FRAME
.020 BIPOLAR PLATE

Figure 2. Cell cross section with dimensions of components, in.

CHARGE RATE	C/4		C/2		C	
DISCHARGE RATE	A-H	W-H	A-H	W-H	A-H	W-H
C/4	93.7	86	97	88	98.3	88
C/2	88.6	81	87	78	93	82
C	88	78	91	80	88	76
2C	86	73	90	76	90	75

Figure 3. Ampere hour and watt hour efficiencies at various charge and discharge rates.

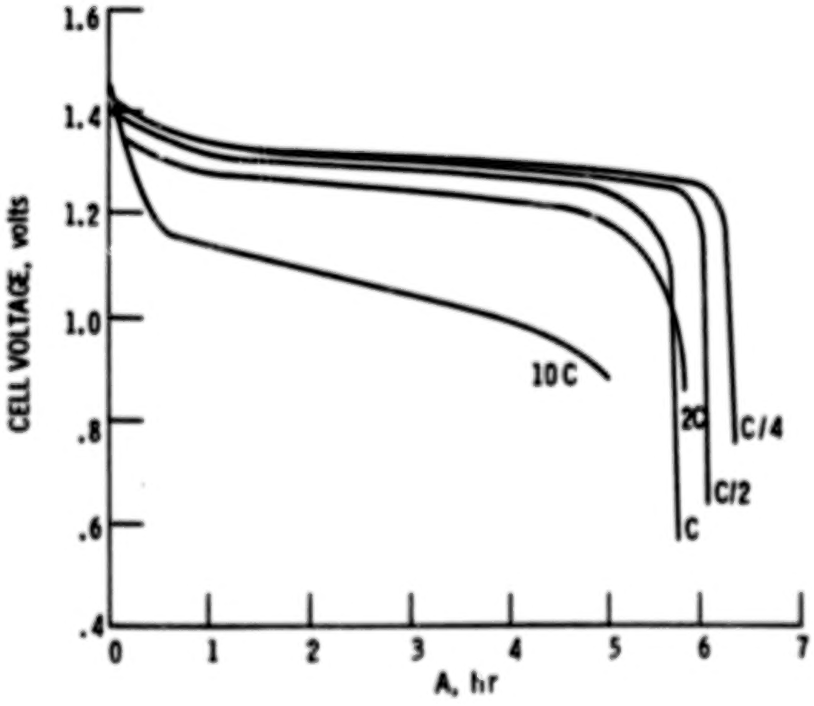

Figure 4. Discharge voltage versus ampere hours out at the C/4, C/2, C, 2C and 10C rate.

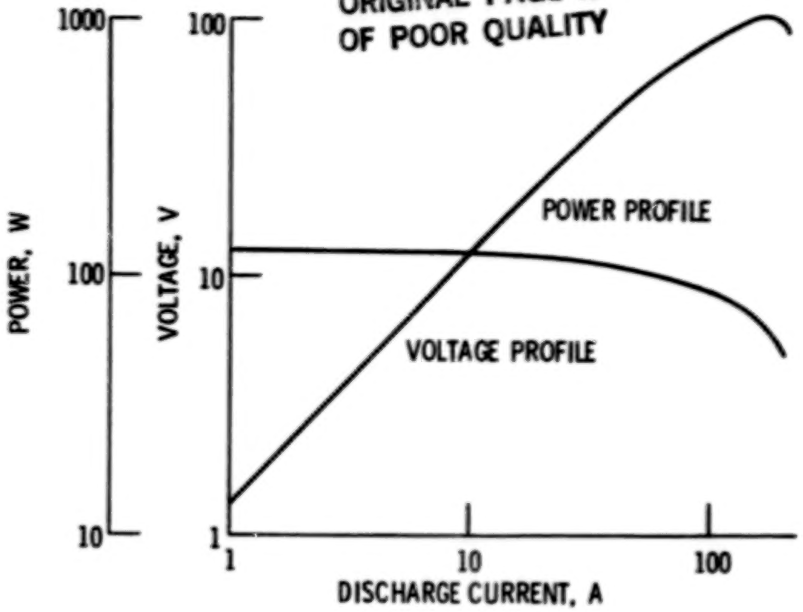

Figure 5. Voltage and power profiles for increasingly ramped discharge current.

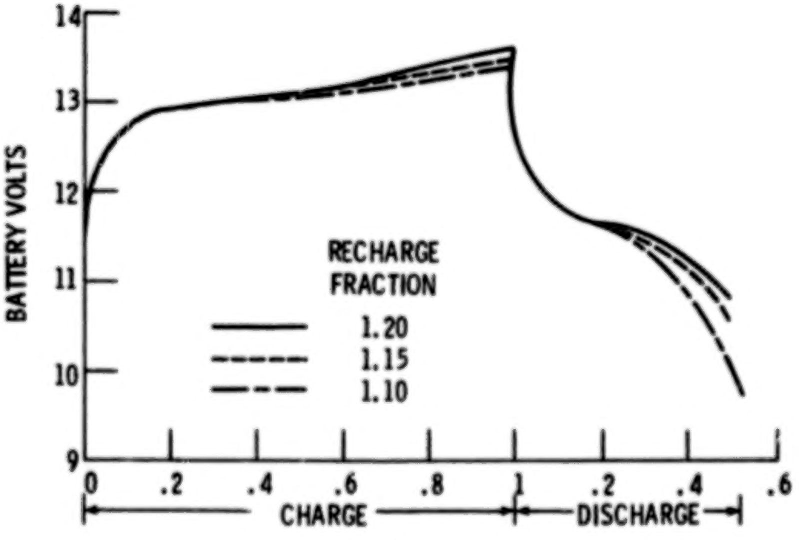

Figure 6. Cyclic battery voltage for recharge fractions of 1.20, 1.15 and 1.10.

ORIGINAL PAGE IS
OF POOR QUALITY

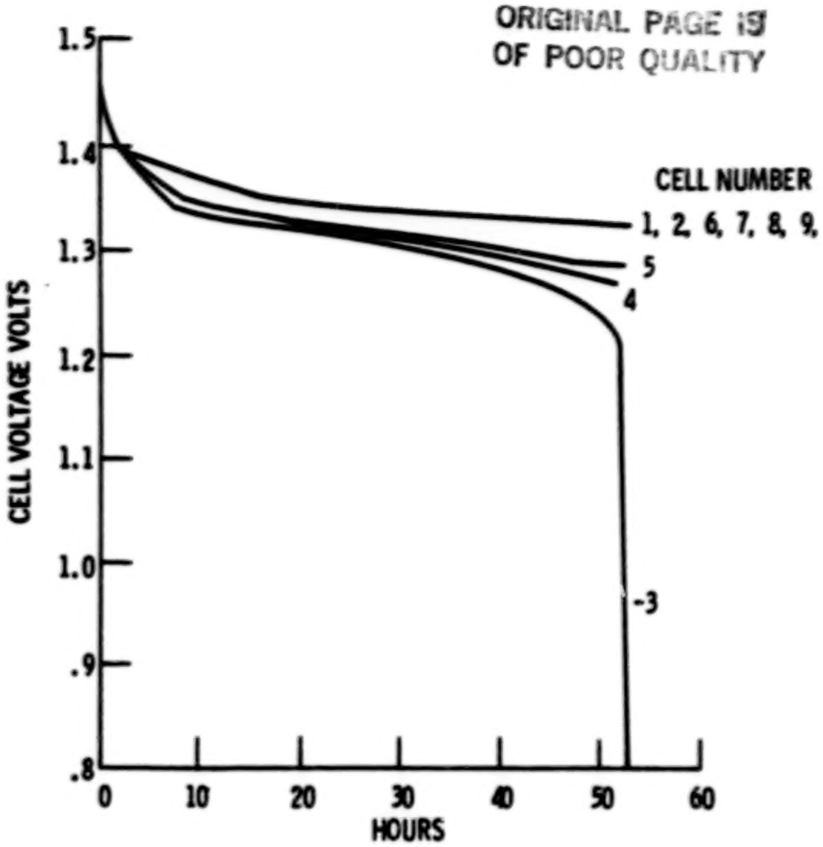

Figure 7. Individual cell voltages on open circuit stand.

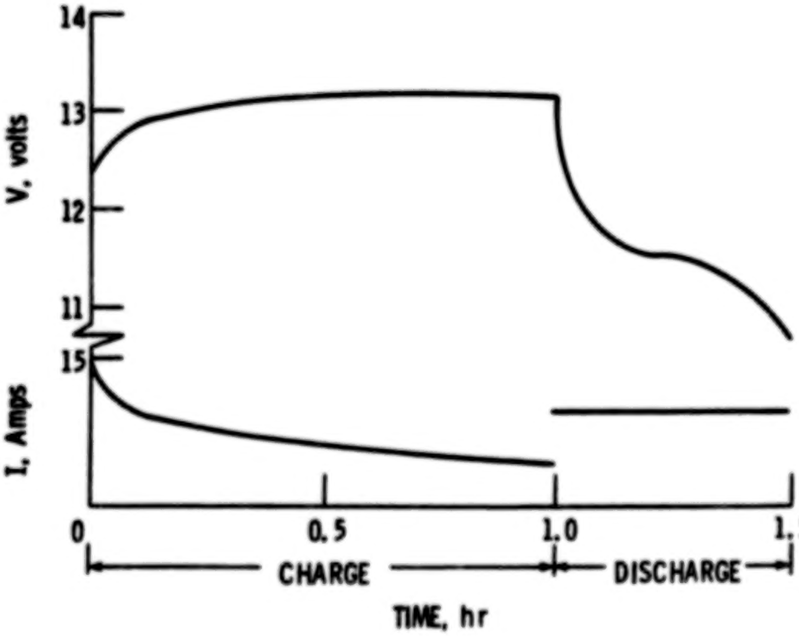

Figure 8. Battery voltage and current for LEO cycle employing constant voltage charging.

Q. Bell, Hughes Aircraft: The nickel hydrogen cell, the Hughes Air Force cell, that was compared there had a energy density of about 21 watt hours per pound. Does that imply that the 50 amp per hour cell was only 20 hours amp per hours useable capacity in the application?

A. Cataldo, NASA/Lewis Research Center: Mostly when people toss around numbers from IPB it says cell level. You can't compare bipolar batteries at a cell level because if you say it has so many watt hours of the cell.

A. Bell, Hughes Aircraft: I wasn't using the bipolar cell I was just inquiring as to the energy density over 50 amp per hour cell shown to have 20 watt hours per kilogram.

A. Cataldo, NASA/Lewis Research Center: That's what it says. I'm just comparing the end of charge voltage and then the discharge voltage on that.

A. Bell, Hughes Aircraft: Okay, thank you.

Q. Milden, Aerospace Corporation: Are you going to look for platinum throughout the cell or are you going to analyze for it as well as other materials in your corrosion products?

A. Cataldo, NASA/Lewis Research Center: We haven't.

A. Milden, Aerospace Corporation: Look for it. It might be going around.

COMMENT

Rogers, Hughes Aircraft: The data you showed didn't look terribly familiar to me but I should point out that we normally cycle at 1.05 to one CD ratio primarily to keep the positive electrode from being overcharged all the time. I would point out that 1.15 to 1 could be potentially dangerous to life even though it does give you better voltage performance. So that's one of the reasons you saw voltage difference. It wasn't simply the bipolar design, although that's certainly part of it.

Cataldo, NASA/Lewis Research Center: You've been charging at the 2C rate. It still does not get much over 1.15. It's just that the current density is so.

A. Rogers, Hughes Aircraft: What I'm saying is that the .15 part of it is oxygen off the positive electrode which isn't particularly good for it over a long term.

A. Cataldo, NASA/Lewis Research Center: There is no roll over voltage that we see on charge.

A. Rogers, Hughes Aircraft: You are getting an inefficiency somewhere and I don't really know where it would be other than oxygen.

Q. Edgar, Eagle Picher Company: I'd like to ask you a couple of questions about the expansion of the nickel electrode. Was some of that expansion taken up in the separator? You indicated that the separator looked very good when you took it apart but thickness growth of that kind must have gone somewhere. The second question is the nickel foam metal that you used as a reservoir appeared quite black in that last slide. Is that active materials from the nickel electrode?

A. Cataldo, NASA/Lewis Research Center: Yes but we haven't determined if that has any capacity. For the first question if our nickel electrode expanded 20 mills and we had only had 10 mills of separator and all the other components were the same thickness as we put in, I tend to think that some of the things expanded once we started to loosen the tie bolts. Because otherwise we wouldn't have any separator at all.

Q. Dudley, European Space Agency: A couple of questions. If I understand it you are aiming for battery which will have the full best voltage within one vessel so that you may have one or more modules in parallel? This leads to two immediate thoughts on my part. One is do you foresee the need to provide any extra components to insure that a failed cell in a large battery will not allow failure of the whole module, and do you regard having all of your battery as one pressure vessel as a significant single point failure problem and would that lead to choosing a number greater than one for an actual power system.

A. Cataldo, NASA/Lewis Research Center: I think if you were to compare a bipolar module you are going to compare it to some other system either 120 series or 120 nickel hydrogen series. If one nickel hydrogen cell IPV leaks you have a failure there of the whole strength if you have an open. As long as you have a short then if you can suffer the reduce voltage there's no problem.

Q. Question inaudible.

A. Cataldo, NASA/Lewis Research Center: Oh no we'll not. There is no external relay or by pass circuitry or any of that. Otherwise we would have to conduct a current out the sides through some leads and relays and then come back through again. That's something I don't think we are trying to eliminate number of connections, number of pressure vessels for extremely large systems. Three or four of these modules will replace upwards of 600 or 700 50 amp per hour cells of whatever nature.

N84
33703

UNCLAS

D35

N84 33703

FAILURE ANALYSIS OF NICKEL-HYDROGEN CELL SUBJECTED TO SIMULATED LOW EARTH ORBIT CYCLING

Vernon C. Mueller
McDonnell Douglas Astronautics Company - St. Louis Division

ABSTRACT

A nickel-hydrogen cell completed 10,080 simulated low earth orbit charge/discharge cycles at depths-of-discharge ranging from 50 to 80 percent prior to failure. The cell is of the Air Force design, rated at 50 ampere-hours, 8.9 cm (3.5 inches) in diameter. Upon disassembly, the end of the polysulfone core supporting the electrode stack was found to have fractured. This allowed the electrode stack to expand. A massive short was found at the inner diameter of the electrodes centered roughly at plate set 34 to 37 from the positive end of the electrode stack. The damaged area extended through approximately one third of the electrode stack, with the effect becoming progressively less with distance from plate set 34 to 37. Measured thicknesses of the positive plates were significantly greater than the initial specification values. The postulated cause of failure is: (1) Positive plate growth caused fracture of the shoulder from the end of the polysulfone core on which the electrodes are mounted, (2) The electrode stack relieved and pressure points were created at the area near the inner diameter of the plates at the tab attachment, and (3) A short occurred at a pressure point between opposing plates and propagated to other electrode sets due to thermal and mechanical stresses caused by the short.

INTRODUCTION

Nickel-hydrogen cell serial number 148 was provided to McDonnell Douglas Astronautics Company-St. Louis Division (MDAC-STL) by the Air Force Wright Aeronautical Laboratory (AFWAL) for parametric and simulated low earth orbit cyclic tests. The cell is rated at 50 ampere-hours and is 8.9 cm (3.5 inches) in diameter. Figure 1 shows the cell general arrangement. This cell was constructed with asbestos separators.

MDAC-STL mounted the cells horizontally during test in a fixture which gripped the cell about the cylindrical section and permitted heat to flow from the cell to the aluminum clamp and then to the supporting aluminum plate. Figure 2 shows three cells in the test fixture. The aluminum baseplate was cooled by a circulating liquid coolant bath to permit temperature control of the test cells. Insulation was applied around the cells such that all heat removed from them was by conduction through the mounting clamp to the temperature controlled baseplate.

PRECEDING PAGE BLANK NOT FILMED

~~PRECEDING PAGE BLANK NOT FILMED~~

The cell was cycled by discharging into a fixed resistor such that 25 ampere-hours were removed over a 35-minute period, followed by charging at approximately 50 amperes to a voltage limit, which was then held constant while the current tapered for the balance of the 55-minute charge interval. Nominal cell temperature was 23°C. Cycling was controlled automatically to permit unattended operation. In order to prevent cell damage due to equipment malfunction, alarms were provided to shut down the test (open-circuit the cell) for over/under voltage, excessive discharge current, overtemperature, overpressure, and loss of facility power. Approximately 5 minutes into the charge period of cycle 10,080, the cell exceeded the temperature limit, and on the next data-scan a few seconds later the voltage dropped below 0.5 volts. The system automatically shut down, open-circuiting the cell. Eighteen minutes later when the next data set was recorded, the highest temperature was 89.6°C, measured at the top of the cylindrical section furthest removed from the coolant bath. Intermediate data points were not recorded, and the peak temperature excursion is not known. After about an hour, the cell voltage dropped to zero. Later in the day, a charge current of 5 amperes was applied for one hour but the voltage did not exceed 8.3 millivolts. The cell was then disconnected electrically from the test system but physically left in the fixture for approximately 11 months before the failure analysis was done.

FAILURE ANALYSIS RESULTS

The cell was cut open with a lathe just below the weld toward the negative terminal (See Figure 1). Before any cutting operations, something loose could be heard rattling within the pressure vessel. When the negative end of the pressure vessel was removed, exposing the electrode stack, the ceramic insulating washer at the negative terminal was found broken into four pieces which accounts for the rattling noise. Also, the end plate, belleville washer, and the end of the polysulfone core were loose. These parts were captured by the negative leads, however, and not free to move within the pressure vessel. Figure 3 is a sketch of the electrode stack assembly showing component parts in greater detail. The end of the polysulfone core had fractured at the shoulder completely around the intersection with the central part of the core. Also, a plastic washer with a square opening and 2.69 cm (1.06 inches) outside diameter which was not identified on the drawing available to us, was found broken inside the cell. Figure 4 is a photograph of the shoulder of the core, broken ceramic insulating washer, end plate, unidentified washer, and belleville washer shown clockwise from the upper left. The electrode stack had relieved with the first negative roughly flush with the broken end of the polysulfone core. The reservoir had melted completely across the annular section in the area of the negative tab. Also, the electrode stack was indented in the area of the negative tab extending across the annular section of the plate. This may have been caused by the negative tabs which applied forces to the plates when the electrode stack relieved. Figure 5 is a photograph of the electrode stack prior to further disassembly, showing these features.

Referring to Figure 3, for purposes of identification the electrodes are numbered consecutively from the positive end (weld ring end). Therefore, negative plate number 41 is the first electrode encountered when disassembly proceeds from the fractured end of the polysulfone core. It was discovered during disassembly that this particular cell had been constructed with an additional reservoir between each set of plates rather than one at each end of the stack as shown in the artist's sketch of Figure 3. Mr. Don Warnock of AFWAL confirmed that some early cells had been constructed in this manner. The sequence of stack components was positive electrode, separator, negative electrode, gas screen, and reservoir. This sequence was repeated throughout the electrode stack. Another observation of general interest was that many of the positive plates had irregularly shaped depressed areas randomly dispersed over the surface. There appeared to be two distinct levels of material similar to looking over a broad plain with mesas protruding from it. Finally, the positive electrodes had grown in thickness considerably due to extended cycling.

Shorting of adjacent positive and negative plates was found at the inner perimeter of the plates in the area of the negative tab. In many cases, active material from the positive plate was embedded in the adjacent negative. The gas screen and reservoir between negative and positive plates had melted and shrunk and were fused to the teflon coated side of the negative electrodes. Figures 6 and 7 illustrate these conditions. Figure 6 is a photograph of positive plate 36 viewed from the negative end of the electrode stack. Note the missing active material and the burned area at the core where the tab attachment to the adjacent negative was located. Figure 7 is a photograph of the adjacent negative plate 37 viewed from the positive side of the electrode stack after removal. Note the active material from positive plate 36 adhering in the tab area, and the melting and shrinking of the gas screen and reservoir which adhere to the plate. Such damage was found to extend from the negative end of the electrode stack to plate set 27. The most massive damage appeared to occur in plate sets 34 to 37 with the effect becoming less pronounced on either side. Also, the plates became more planar as disassembly progressed toward the positive end of the electrode stack.

The heat pulse generated when the shorting occurred appeared to discolor and swell the polysulfone core, such that a ribbed appearance was created and a black deposit was left where the positive plates restricted this swelling. Figure 8 is a photograph illustrating this phenomenon at the fractured end of the core (negative end of electrode stack). The dimension from the end of the core to the first indentation caused by a positive plate is less than the combined thickness of the end plate and belleville washer, which implies that the end of the core fractured prior to the occurrence of the short.

CONCLUSIONS

The thicknesses of positive plates were measured during disassembly and are tabulated in Figure 9. As built positive electrodes have a thickness of of 0.762 mm (0.030 inches) to 0.813 mm (0.032 inches). Assuming that each positive electrode was fabricated at the maximum dimension, the electrode stack heighth increased by 1.00 cm (0.395 inches) due to positive plate growth during cycling. This growth is believed to have caused the fracture of the shoulder from the center of the polysulfone core. Examination of the failed area shows striations in the material which is typical of a fatigue failure in metals. Since the material properties of polysulfone are differen a similar conclusion can not be supported. Also, the angle that the tabs mak with the electrodes were acute angles in the case of negative electrodes and obtuse angles for positive electrodes. The effect is most pronounced at the negative end of the electrode stack where the greatest relative movement occurred. This is believed to have been caused when the electrode stack relieved, by the forces applied through the tab. The tabs are restricted in the center of the core and act as a column pushing on the attachment poin in the case of negative electrodes. In the case of positive electrodes, the tab pulls on the attachment point.

A chronological history of the failure can be postulated as follows:

- Positive plate growth during cycling causes fracture of the shoulder from the polysulfone core.
- Forces applied to the electrodes when the stack expands create pressure points between adjacent pairs of electrodes, most pronounced at the tab attachments.
- A short occurs at a pressure point after some period of time.
- The heat pulse and mechanical forces generated by the short cause the failure to propagate to adjacent plate sets.

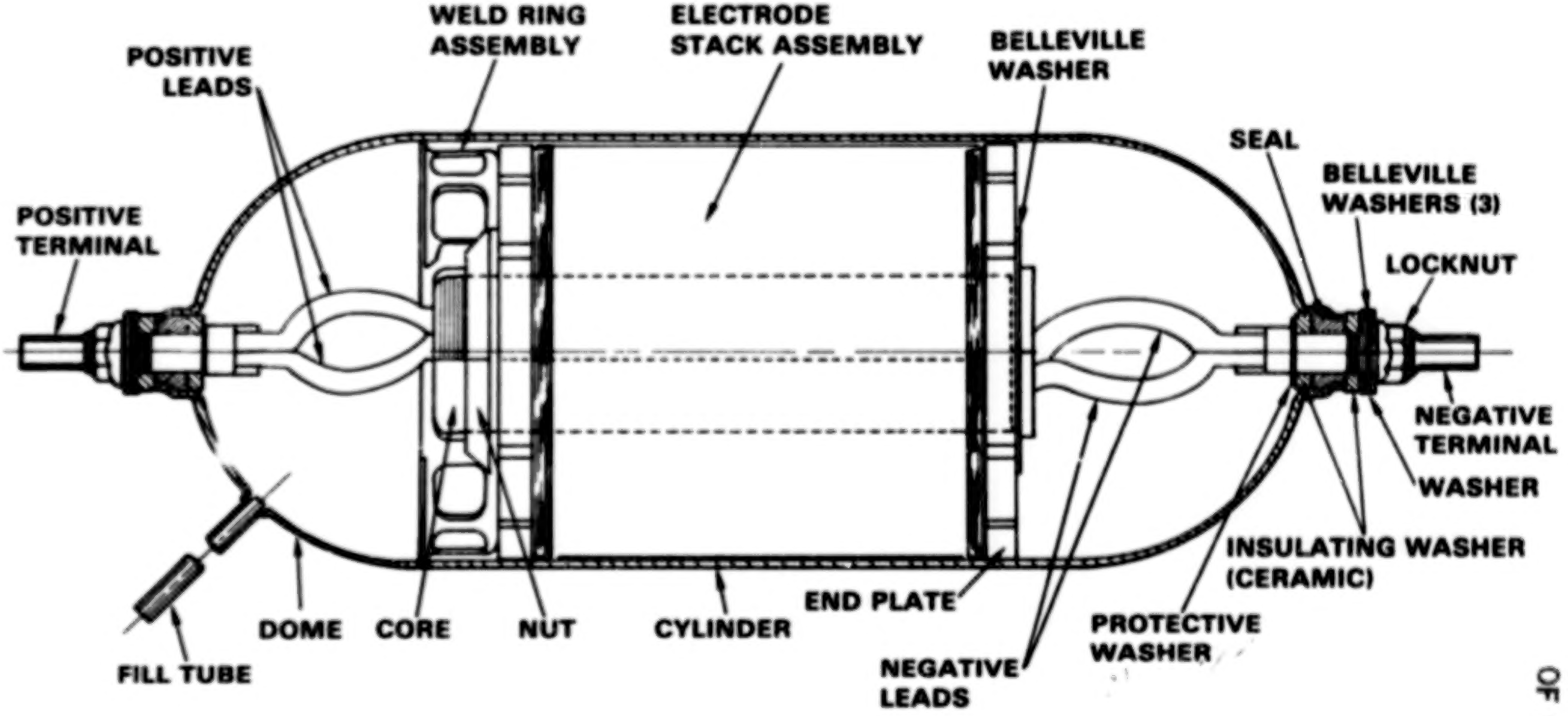
WELD RING
ASSEMBLY
ELECTRODE
STACK ASSEMBLY
POSITIVE
LEADS
BELLEVILLE
WASHER
SEAL
BELLEVILLE
WASHERS (3)
POSITIVE
TERMINAL
LOCKNUT
NEGATIVE
TERMINAL
WASHER
INSULATING WASHER
(CERAMIC)
DOME
CORE
NUT
CYLINDER
END PLATE
PROTECTIVE
WASHER
FILL TUBE
NEGATIVE
LEADS

Figure 1. 50 ampere-hour nickel-hydrogen cell.

ORIGINAL PAGE IS
OF POOR QUALITY

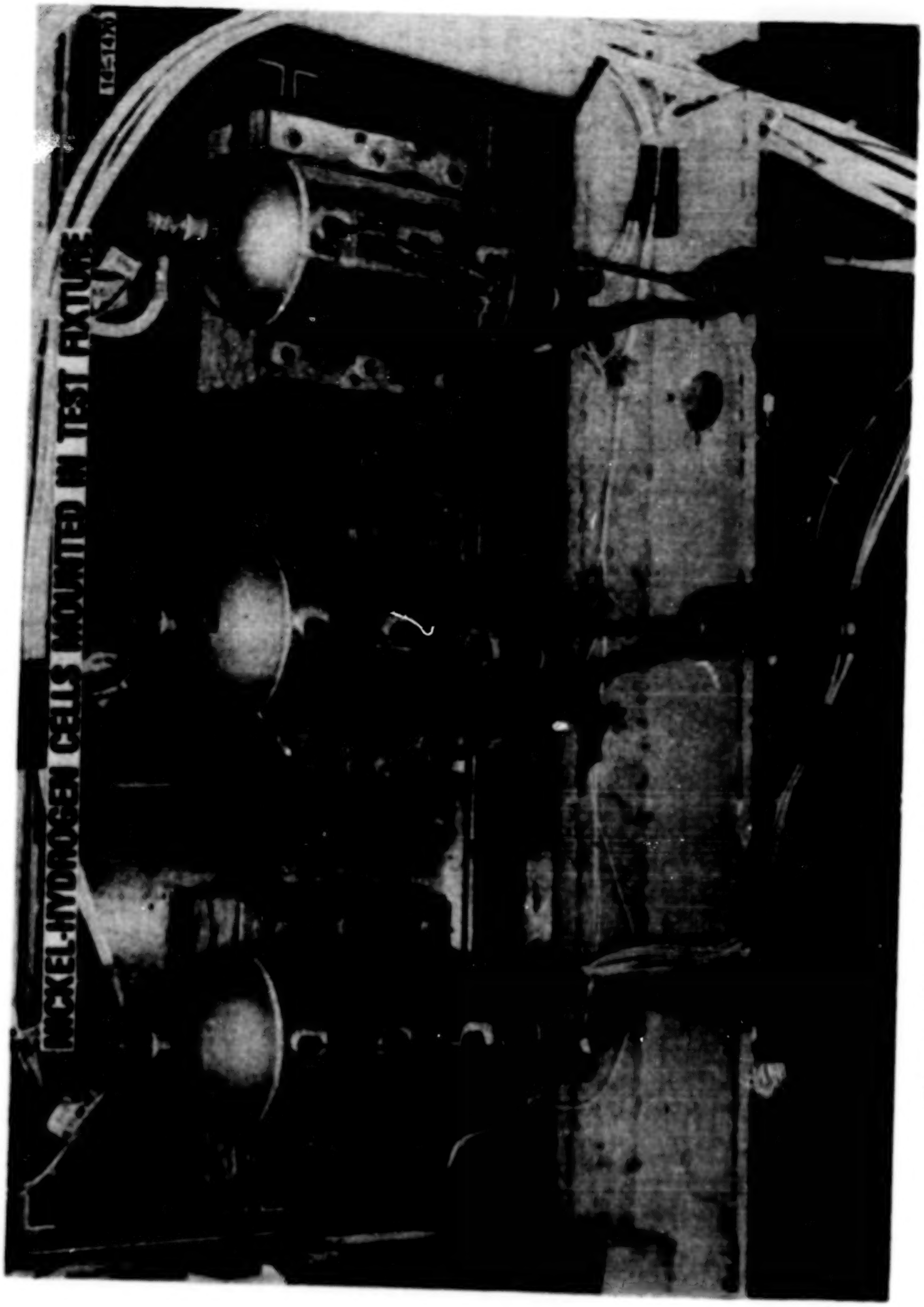
NICKEL-HYDROGEN CELLS MOUNTED IN TEST FIXTURE
C-75-1471

Figure 2. Nickel-hydrogen cells mounted in test figure.

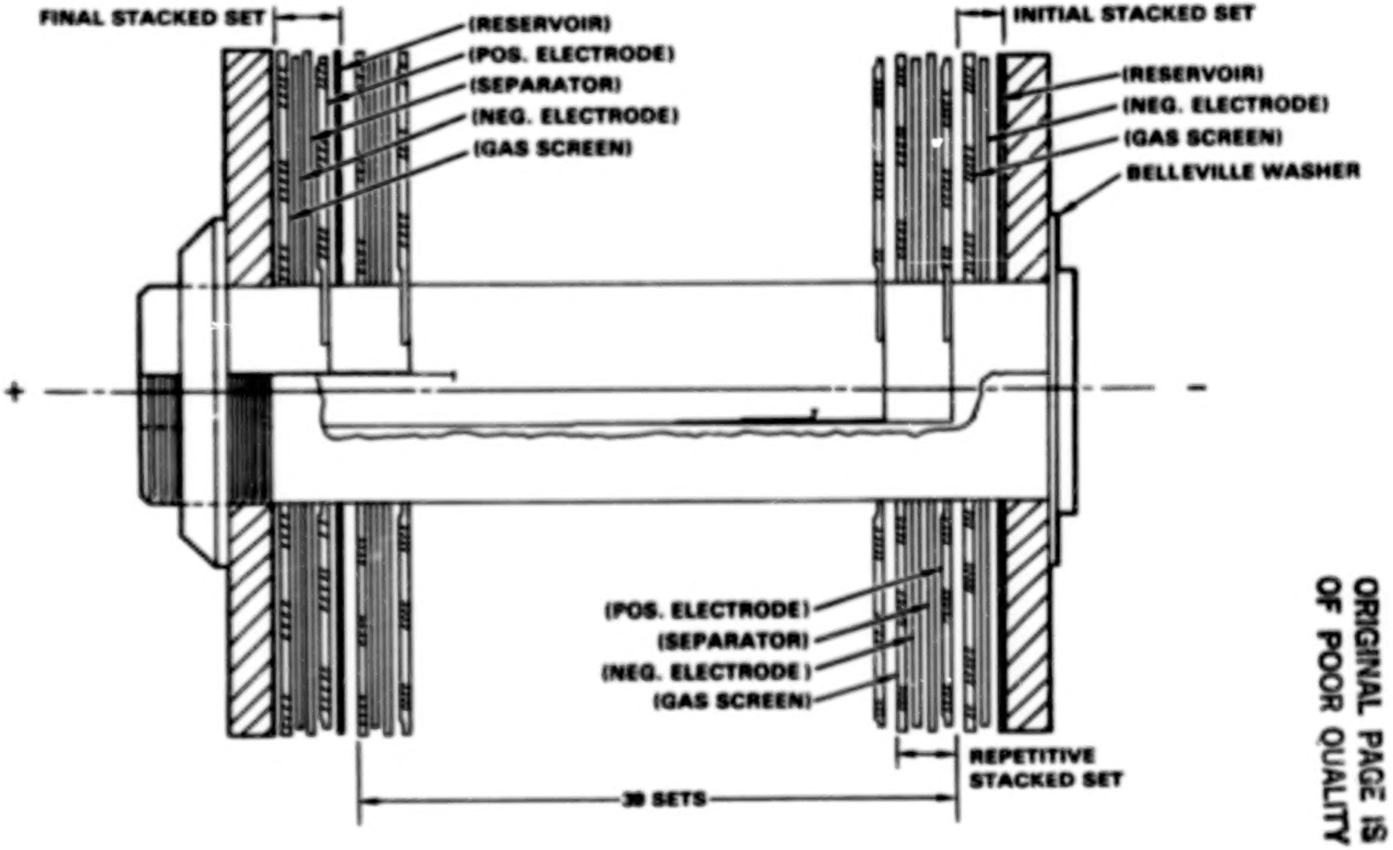
FINAL STACKED SET
(RESERVOIR)
(POS. ELECTRODE)
(SEPARATOR)
(NEG. ELECTRODE)
(GAS SCREEN)
INITIAL STACKED SET
(RESERVOIR)
(NEG. ELECTRODE)
(GAS SCREEN)
BELLEVILLE WASHER
(POS. ELECTRODE)
(SEPARATOR)
(NEG. ELECTRODE)
(GAS SCREEN)
REPETITIVE
STACKED SET
39 SETS

Figure 3. Electrode stack sketch.

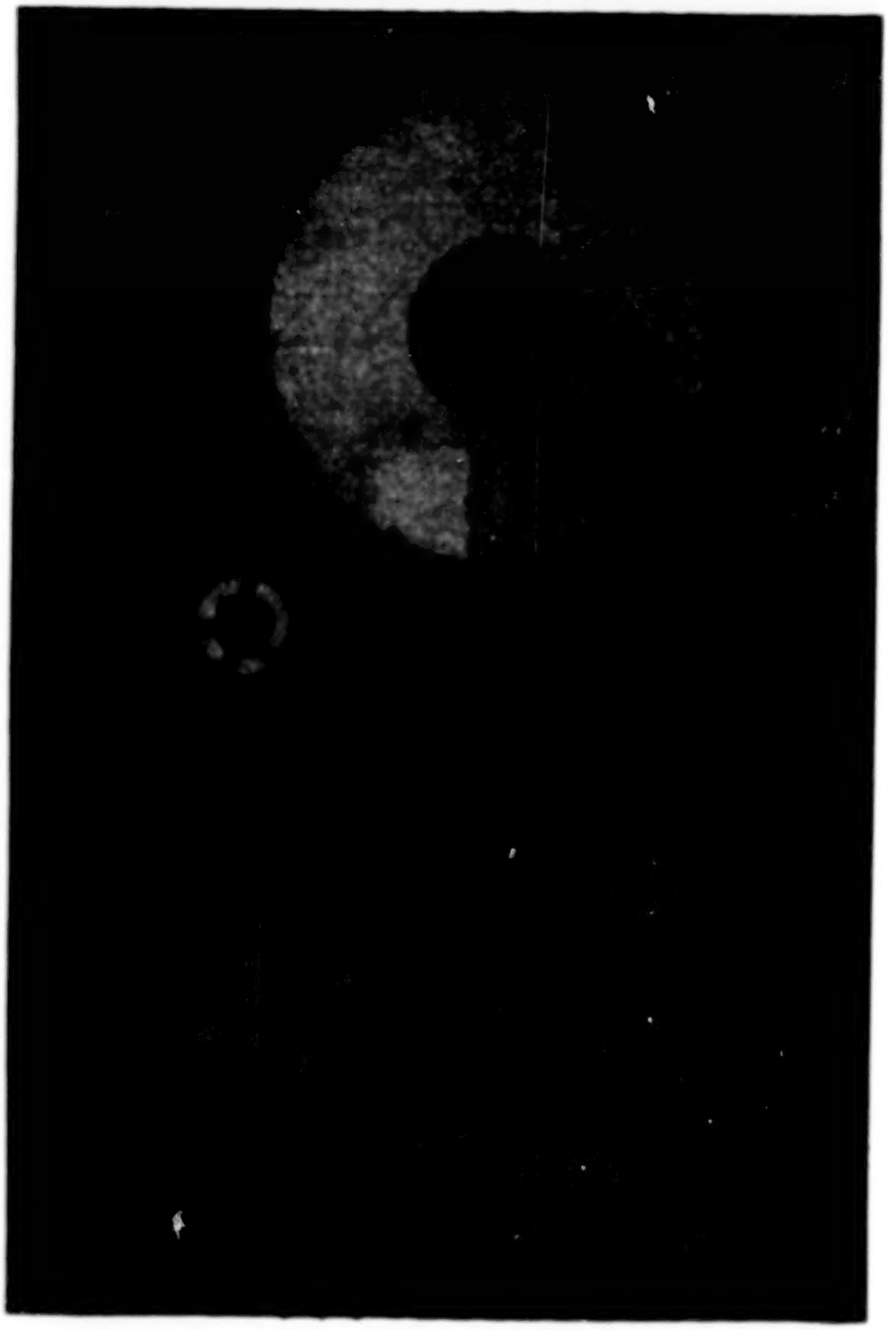

Figure 4. Loose parts/materials found within failed cell.

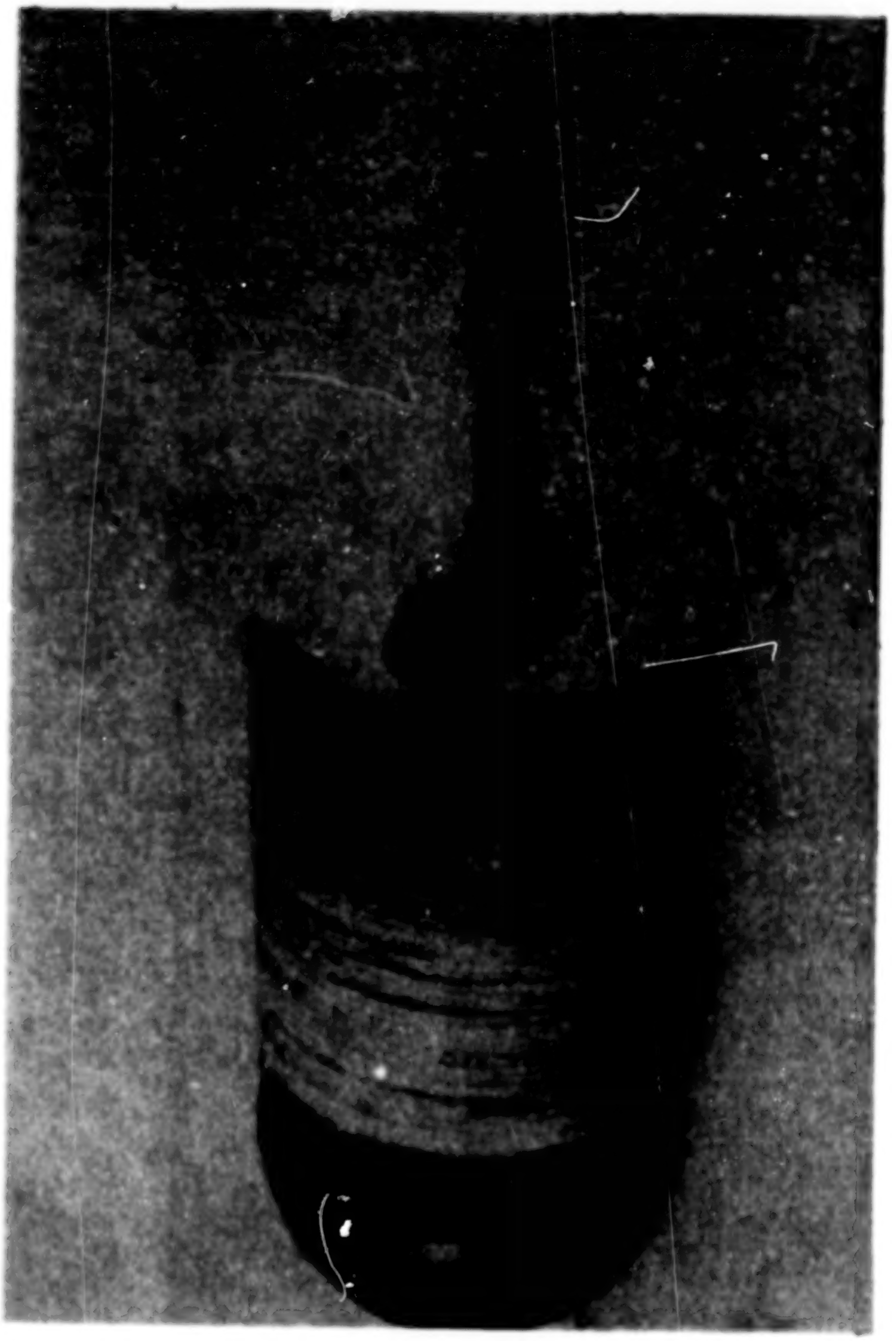

Figure 5. Electrode stack prior to disassembly.

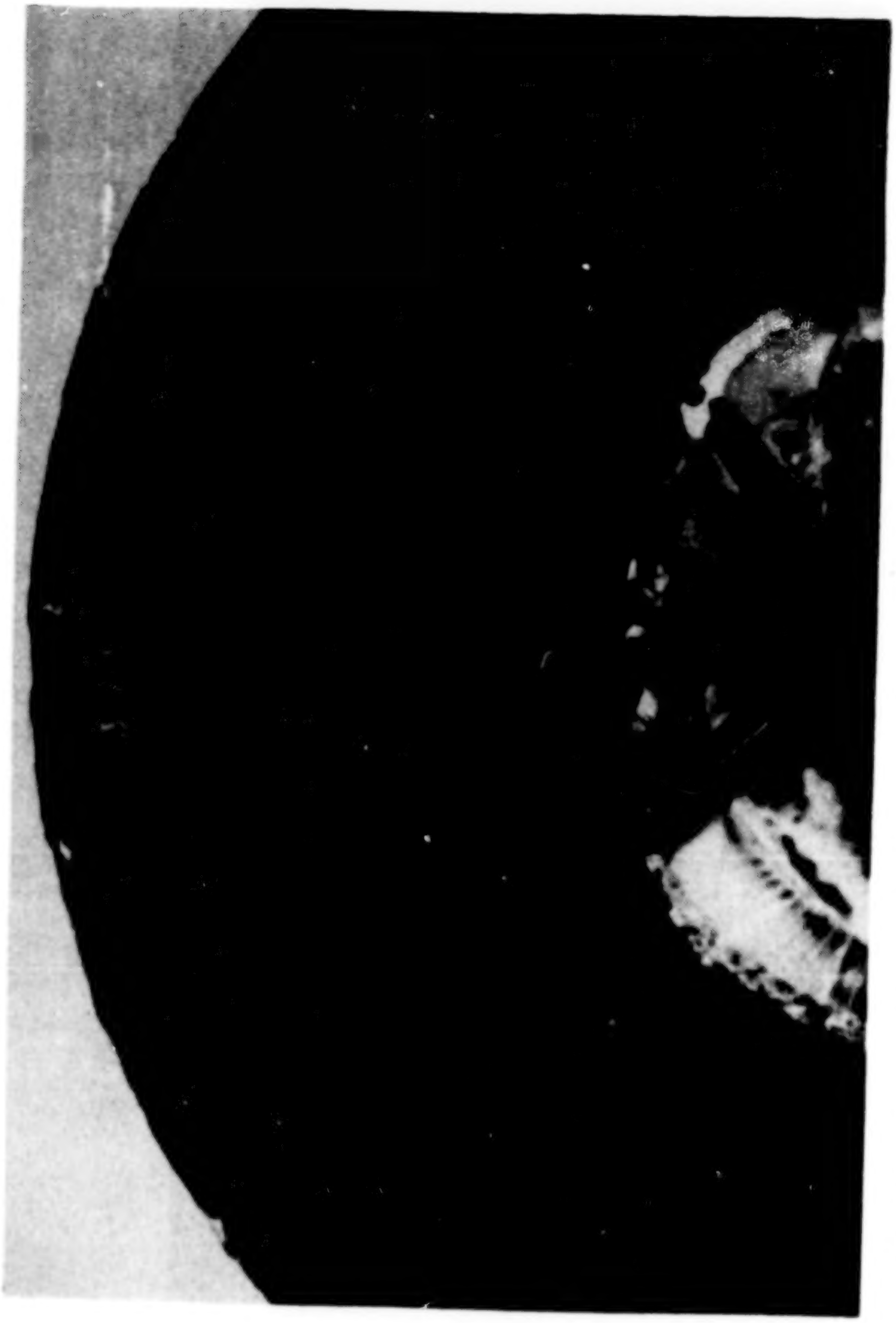

Figure 6. Typical positive plate showing active material loss.

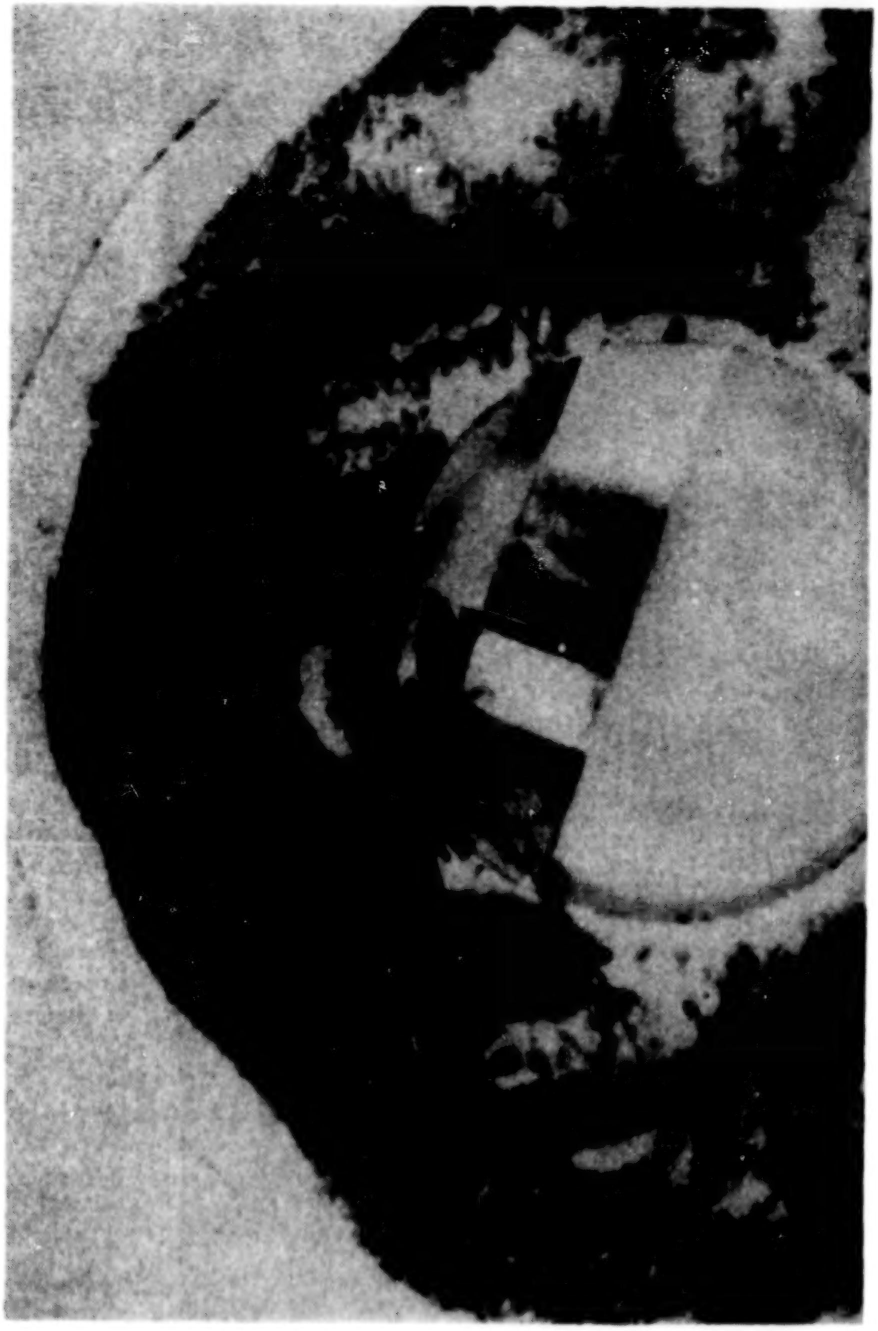

Figure 7. Typical negative plate showing adhesion of reservoir and gas screen.

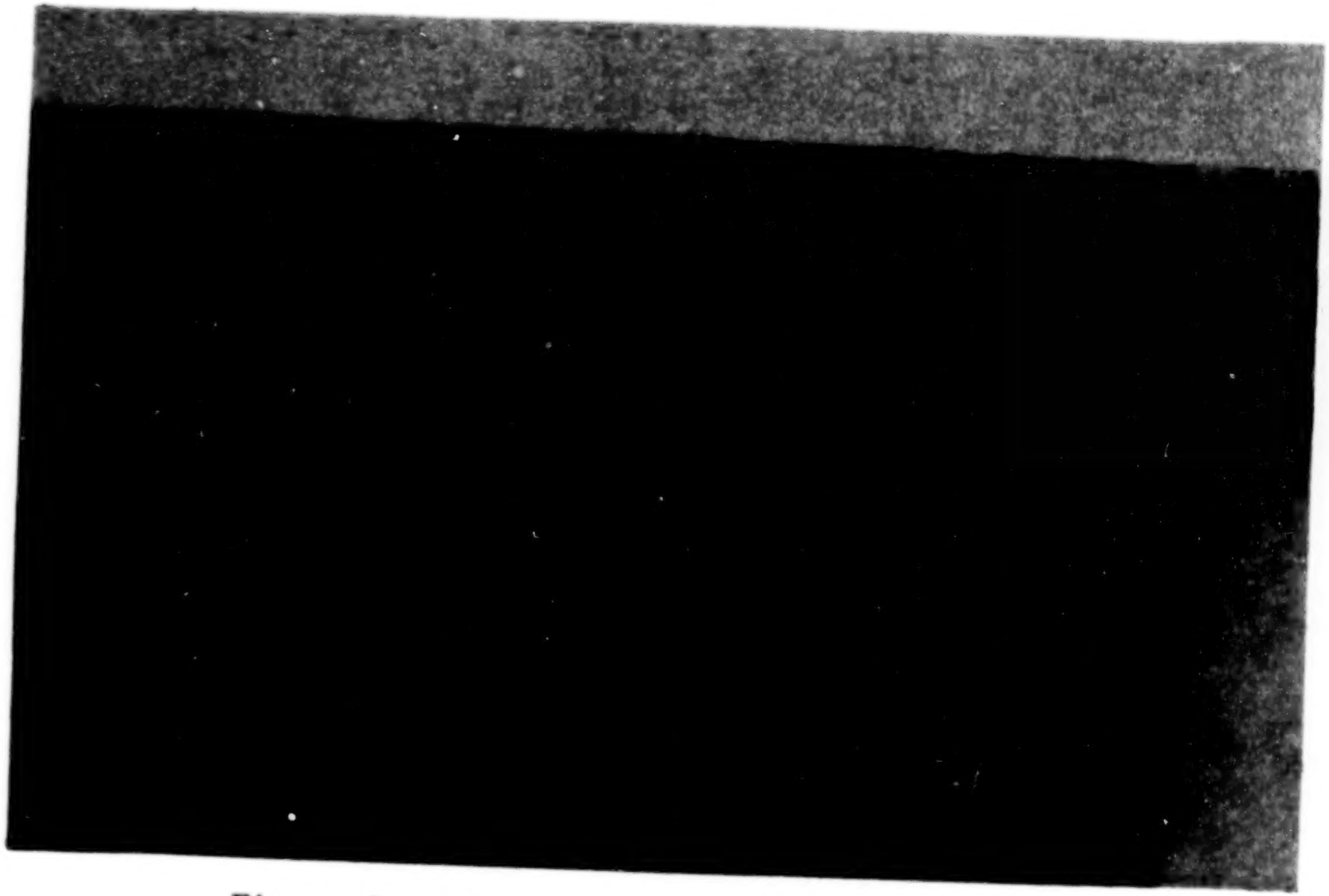

Figure 8. Fractured end of polysulfone core.

PLATE IDENTIFICATION	THICKNESS CENTIMETERS	THICKNESS (INCHES)	PLATE IDENTIFICATION	THICKNESS CENTIMETERS	THICKNESS (INCHES)
P1	0.097	0.038	P21	0.097	0.038
P2	0.102	0.040	P22	0.104	0.041
P3	0.107	0.042	P23	0.104	0.041
P4	0.109	0.043	P24	0.112	0.044
P5	0.104	0.041	P25	0.104	0.041
P6	0.109	0.043	P26	0.109	0.043
P7	0.094	0.037	P27	0.107	0.042
P8	0.107	0.042	P28	0.099	0.039
P9	0.109	0.043	P29	0.112	0.044
P10	0.117	0.046	P30	0.109	0.043
P11	0.112	0.044	P31	0.109	0.043
P12	0.102	0.040	P32	0.099	0.039
P13	0.117	0.046	P33	0.109	0.043
P14	0.117	0.046	P34	0.107	0.042
P15	0.122	0.048	P35	0.102	0.040
P16	0.102	0.040	P36	0.109	0.043
P17	0.104	0.041	P37	0.097	0.038
P18	0.114	0.045	P38	0.104	0.041
P19	0.107	0.042	P39	0.104	0.041
P20	0.112	0.044	P40	0.097	0.038

TOTAL THICKNESS OF ALL POSITIVES 4.255 CM (1.675 IN.)

Figure 9. Measured positive plate thicknesses-Cell S/N 148.

Q. Pickett, Hughes Aircraft: Could you tell me what year the cells were made?

A. Mueller, McDonnell Douglas Astronautics Company: No I can't. The serial number is 148 if that helps. I think we got them in about 1980.

COMMENT

Pickett, Hughes Aircraft: I just wanted to comment that these don't have the plates that we are currently making now.

Mueller, McDonnell Douglas Astronautics Company: No these have the old plates. I don't know. I talked to different people about this plate expansion problem or the plate expansion I saw they have told me that there is some test data available. I think they cited some at Lewis and one other location that shows that the plates that you have now expansion rates of less than 10% of what we see here.

Q. Lim, Hughes Research Lab: Do you have the plate loading data for this?

A. Mueller, McDonnell Douglas Astronautics Company: No I have not.

Q. Unidentified: You didn't mention much about the broken ceramic washer which is something that would concern me because it's going to be representative of cell failure. Did you find anything to tell you why that broke? Whether it broke earlier or at the same time as the core?

A. Mueller, McDonnell Douglas Astronautics Company: No. I theorized that broke at the same time and my theory is that it broke due to the mechanical shock which created the timely shorting. We had no indication we were leaking hydrogen and I do think that's a good indication that the end of the core broke before the cell shortage. I might mention also that the cell continued to work relatively well up until the cycle before the failure occurred.

Q. Green, RCA-Astro: Could you tell us anything about the history of the cells, what was done before you yourself put them on test.

A. Mueller, McDonnell Douglas Astronautics Company: Yes we got them from the Air Force and I assume that all that was done to them was normal exceptance testing. We did some characterization test where we tried different charge schemes and different charge rates probably about a month in duration. Then we went on to cycling and we did 10,000 cycles on this particular cell - 90 minute cycles.

COMMENT

Rogers, Hughes Aircraft: Just a comment on the ceramic washer. Had that failed prior to your main failure you would undoubtedly lost the hydrogen.

Mueller, McDonnell Douglas Astronautics Company: I would think so.

Rogers, Hughes Aircraft: It's clear that was associated with the other failure in the cell.

Mueller, McDonnell Douglas Astronautics Company: As I was saying before there was no indication of performance degradation other than normal graceful degradation before the failure occurred.

Q. Ritterman, Comsat: You had no pressure indicator on the cells as I saw.

A. Mueller, McDonnell Douglas Astronautics Company: Yes we did.

Q. Ritterman, Comsat: You did have pressure?

A. Mueller, McDonnell Douglas Astronautics Company: And we saw no loss of pressure.

COMMENT

Milden, Aerospace Corporation: I was at Hughes Aircraft when these were built and I was actually the guy who was building them and first the good news is the cell went 17,500 cycles at 23 degrees centigrade which is astounding.

Mueller, McDonnell Douglas Astronautics Company: That is the one that just failed yes this one went 10,000.

Milden, Aerospace Corporation: Considering that's a first generation of the first fifty that were produced in any quantity, it's astounding that they went that far. There have been a number of changes made in the design as a result of the learning experiences. One of them is that the positive electrode tabs are performed now so that there's not quite a sharp a edge there so that shorting path would be a little bit different. Also in one program that area has been redesigned and improved significantly. The electrodes were an early attempt and very very far from optimum in terms of lower orbit electrodes. And it's amazing that they went that far. So for first generation air force design production cells actually pre-production since they were advanced development it's astounding.

Q. Kunigahalli, Bowie State College: Could you please tell me what was the volume of the electrolyte in the cell?

A. Mueller, McDonnell Douglas Astronautics Company: I'm sorry I can't tell you any details about the cell construction.

Q. Kunigahalli, Bowie State College: What was the condition of the separator?

A. Mueller, McDonnell Douglas Astronautics Company: The separators toward the end of the stack were actually in very good condition and in fact they were not, did not adhere to the positives very much. In some cases they did adhere to the positives, but we were able to get them off usually in one piece, some shredding some adherence. But really not bad at all.

Q. Kunigahalli, Bowie State College: Because my experience of nickel cadmium cells you know most of the time the separator would be very strongly sticking to the negative due to the cadmium migration. So I was wondering what is the situation in nickel hydrogen?

A. Mueller, McDonnell Douglas Astronautics Company: I'm always sticking to the positives. The negatives have teflon coating on them.

Q. Kunigahalli, Bowie State College: Excuse me one last question. By any chance did you take the same pictures of the positives? Were there any crystal growth or anything like that?

A. Mueller, McDonnell Douglas Astronautics Company: All we did was a tear down of visual inspection. We did do a chemical analysis of the separator to verify it was asbestos. It was kind of amazing to us that it was hanging together so well if it was asbestos.

A. Kunigahalli, Bowie State College: Thank you very much.

Q. Unidentified: Vern, you did mention that they had a reservoir in the building stack. Did it have a wall wick also?

A. Mueller, McDonnell Douglas Astronautics Company: Well it had one the standard wick on wall yes. As I mentioned it was wet they must have had very good electrolyte retention.

N84
33704

UNCLAS

D36

N84 33704

COMPARATIVE PERFORMANCE ASSESSMENT

OF

INTELSAT V NICKEL HYDROGEN AND NICKEL CADMIUM BATTERIES

D. Cooper and A. Ozkul
International Telecommunications Satellite Organization
Washington, D.C.

ABSTRACT

The first Nickel Hydrogen battery deployment onboard a commercial geosynchronous communications satellite was realized with the launch of the INTELSAT V, Flight 6 spacecraft on 19 May 1983. The initial five spacecrafts in this series are equipped with Nickel Cadmium batteries. Based on the data available on both types of batteries, design and operational performance comparisons of INTELSAT-V Nickel Hydrogen and Nickel Cadmium batteries are presented. General characteristics of the INTELSAT-V spacecraft as related to electrical-power-subsystem functions and battery operations are summarized.

1.0 INTRODUCTION

INTELSAT (International Telecommunications Satellite Organization), with headquarters in Washington, D.C., is a global satellite communications system formed in 1964 by its member countries in two segments as space and earth segments. The space segment consists of 14 operational and spare satellites distributed among the three ocean regions as Atlantic (AOR), Indian (IOR), and Pacific Ocean Region (POR). The INTELSAT earth segment is formed by 678 ground stations (owned by 109 user countries) which are linked to those satellites operating in each region. Although the planning, procurement, launch, TTC&M functions, and operational management of the space segment are administered by the INTELSAT organization, the construction and operation of the individual earth stations are performed by the user countries under the guidelines and standards established by INTELSAT. INTELSAT's services include provision of capacity in telephone, data, and television communications to the world community in general, as well as lease services in maritime and regional/domestic communications to various organizations.

INTELSAT began operations in 1965 with INTELSAT I (Early Bird) and recently launched Flight 7 of the fifth generation satellites in the INTELSAT-V series. The next generation satellites of the INTELSAT-VI series are currently under procurement with planned commencement of service in mid-1986. The evolution of the INTELSAT space segment is shown in Figure 1.

In regards to INTELSAT's experience with in-orbit operation of spacecraft batteries, we experienced the first major problem with INTELSAT-IV batteries during the 1976-1978 period. The degraded performance of batteries on board INTELSAT-IV's resulted in five to six years of full capacity operations in contrast to seven years design life. During this period various attempts were made to make the optimum use of these batteries, among which powering half of the transponders onboard each malfunctioning spacecraft and thereby reducing the necessary depth-of-discharge helped to prolong the satellites' operational life. In addition, colocation of poorly performing satellites were initiated in early 1980 with two INTELSAT-IV's (F4-F5 at 179°E location) when neither spacecraft could provide full communications capability during eclipse periods due to insufficient power availability.

The Nickel-Cadmium batteries of INTELSAT-IVA satellites, which commenced service in 1974 with a seven-year design life, have performed exceptionally well. Current data indicate that there is no significant performance degradation on INTELSAT-IVA batteries even after nine years of service corresponding to 18 eclipse seasons. The minimum voltage on 14 batteries is approximately 28.8 Volts (1.15 Volts/cell), with measured capacity during reconditioning periods maintaining a minimum value of 30 Amp Hours (reconditioning voltage: 25 V). The measured capacity of INTELSAT-IVA batteries, which consist of 25 Nickel-Cadmium cells, is 26 Amp Hours (22 Amp Hour name-plate rating). The nominal depth-of-discharge of 14 operational batteries ranged between 26-43 percent of the measured capacity during the recent eclipse season of Fall 1983.

After having reasonably successful operational experiences with Nickel Cadmium batteries, especially during the INTELSAT-IVA and early INTELSAT-V era, the current INTELSAT-V and VA's (starting with Flight 6 launched in May 1983), and INTELSAT-VI satellites are equipped with Nickel-Hydrogen batteries. Aside from theoretically proven improvements and limited test/low orbit performance results available on Nickel-Hydrogen batteries, it can be expected that the long-term, practical benefits of using these batteries may be proven towards the end-of-life of INTELSAT-V satellites.

2.0 GENERAL DESIGN AND OPERATIONAL CHARACTERISTICS

The first INTELSAT-V spacecraft (Flight 506) equipped with a Ni-H2 battery was launched on 19 May 1983. Since the launch and during the recent eclipse season of Fall 1983, the batteries have been used during three inclination maneuver periods utilizing the electro-thermal thrusters (ETT). Both batteries of spacecraft 506 were reconditioned prior to the eclipse.

All INTELSAT-V's are three-axis-stabilized spacecraft with total end-of-life solar array power capability of approximately 1500 Watts. The Ni-H2 batteries of the later spacecraft (506 through 516) consist of two 27-cell modules located on the north and south panels. The battery temperature control is accomplished by means of optical solar radiators (OSR) and thermostatically controlled heaters. The modular design and location of batteries on all INTELSAT-V spacecraft are shown in Figure 2.

The Ni-H2 batteries were direct replacements for the Ni-Cad batteries of earlier spacecraft with nearly identical volume and shelf area requirements. The top view of each Ni-H2 battery assembly on the north and south panels of the INTELSAT-V support subsystem module is shown in Figure 3.

The INTELSAT Ni-H2 battery cell design is similar to that of NTS-2 (Navigation Technology Satellite) launched in June 1977 into low earth orbit with 12 hours orbit period. The experimental battery package onboard NTS-2, which was developed and manufactured under INTELSAT sponsorship, consists of fourteen 35-Amp Hour Ni-H2 cells with a design DOD of 60 percent and a total eclipse load of 350 Watts. A pictorial view of the INTELSAT-V battery assembly and the cell design diagram are shown in Figure 4. This figure also shows the typical temperature sensor (thermistor) locations on a single cell. Each battery assembly contains one cell with a thermistor and another with a strain gage bridge to provide pressure readouts in the telemetry data.

Table 1 shows the design characteristics of Ni-Cad and Ni-H2 batteries for comparison. The charge current characteristics on all INTELSAT-V spacecraft are listed in Table 2.

Figure 5 shows the simplified diagram of one bus of the INTELSAT-V electrical power subsystem. The other bus is identical to the one shown in this figure. The available telemetry data on the electrical power subsystem parameters are as follows:

Function	On Each Bus/Battery	On Both Busses/Batteries
Battery Volts	1	2
Cell Volts	27	54
Battery Temp	2	4
Battery Pressure	1	2
Discharge Current	1	2
Charge Current	1	2
Bus Current	1	2
Array Current	1	2
Shunt Current	1	2
Bus Voltage	1	2

The control relays shown in Figure 5 are used to configure the battery charge rates, cross strapping, and reconditioning. The battery sequencer is a five-minute OFF/ON switch which sequentially charges the north and south batteries for a period of five minutes each. Although there exists an override capability on sequential charging to switch to continuous charge, the latter charging mode is rarely used since the thermal and charge rate design of the spacecraft are based on sequential charging.

3.0 IN-ORBIT PERFORMANCE CHARACTERISTICS AND COMPARISON OF NICKEL-HYDROGEN AND NICKEL-CADMIUM BATTERIES

INTELSAT has had extensive experience in the operational aspects of Ni-Cad batteries. With the deployment of spacecraft 506, which represents the first Ni-H2 battery system on board a commercial geosynchronous communication satellite, we are in a position to make a comparative assessment of the performance of each type of battery. An attempt is made in this report to present such a comparison. It should be noted here that although our experience on the in-orbit performance of Ni-H2 batteries is limited to one eclipse season (Fall 1983) following the deployment of spacecraft 506 in June 1983, the comparative assessment as shown in the following diagrams is still of interest.

Comparative performance characteristics of a typical Ni-Cad (Spacecraft 503, Battery No. 1) and Ni-H2 battery during the eclipse season of Fall 1983 is shown in Figure 6. This figure indicates a nominal battery load of 11-11.5 Amps for both batteries, with corresponding minimum end-of-discharge voltages of 33.6 Volts and 32.7 Volts for Ni-Cad and Ni-H2, respectively. Among the five INTELSAT-V's equipped with Ni-Cad batteries, spacecraft 503, Battery No. 1 was selected for comparison with Battery No. 2 of spacecraft 506 because of similar loading characteristics during the eclipse season.

Shown in Figure 7 is the comparison of the voltage and temperature profiles of spacecraft 503, Battery No. 2 with those of Ni-H2 Battery No. 2 of spacecraft 506 during the 24 September 1983 eclipse. Notice here that DOD on both batteries are similar (35 percent), and that the steep voltage rise at the end of charging cycle of the Ni-Cad battery is not apparent in the case of the Ni-H2 battery.

The performance data on Ni-H2 batteries during the longest eclipse of the Fall 1983 season (23 September) is shown in Figure 8. This figure includes battery voltage, discharge current, pressure, and temperature profiles during a 24-hour cycle, as well as the pressure and temperature profiles with time scale of two hours to show the variation on these parameters during the discharge period in more detail. It should be pointed out here that spacecraft 506 is equipped with a Maritime Communications System (MCS), and this system was undergoing in-orbit testing during the time when this data was recorded. Hence, the battery current shown here increased from the nominal value of 11.5 - 12 Amps to approximately 17 Amps, resulting in a 66 percent DOD reference to 30 Amp Hour capacity. The corresponding battery and cell voltages are 31.4 Volts and 1.16 Volts, respectively.

The MCS payload operation as shown in Figure 8 represents a test case, and heavy loading of batteries as observed here usually does not occur during normal operations.

The comparative profiles in voltage, cell voltage, and temperature of a Ni-Cad (spacecraft 502, No. 2), and a Ni-H2 (spacecraft 506, No. 2) battery during reconditioning is shown in Figure 9. The reconditioning of both types of batteries was performed prior to the corresponding eclipse season by discharging through a 50 Ohm resistor until the first cell reached 0.9 Volt. At the reconditioning rates of C/44 (0.7 Amps) of Ni-Cad batteries, an average capacity increase of 3-4 Amp Hours is usually observed in comparison with the reconditioning rate of C/2 (15 Amps). The corresponding capacity differential in the case of Ni-H2 batteries, however, was measured to be ± 1 Amp Hour (reference to 37 Amp Hour overall capacity). This observation is attributed to the higher self discharging of Ni-H2 batteries and/or errors introduced in the processing of telemetry data.

Table 1

Battery Assembly Performance Characteristics

CHARACTERISTIC	VALUE (NI-HYD.)	VALUE (NI-CAD.)
TOTAL ELECTRICAL BUS LOAD	911 W	911 W
MAXIMUM DEPTH OF DISCHARGE	70%	55%
NOMINAL CELL CAPACITY	30 AH	34 AH
MEASURED CELL CAPACITY	37 AH	38 AH
NOMINAL DISCHARGE CURRENT	15 AH	15 AH
MAXIMUM DISCHARGE TIME	1.2 HOURS	1.2 HOURS
HIGH CHARGE CURRENT (BOL - EOL)	[1.42-1.25 C/21-C/24]	[1.42-1.25 C/24-C/27]
TRICKLE CHARGE CURRENT (BOL - EOL)	[0.48-0.43 C/63-C/70]	[0.48-0.43 C/71-C/79]
TOTAL CYCLES AND ECLIPSE (7 YEARS) (616 ECLIPSE CYCLES + 176 ETT FIRINGS)	791 CYCLES	791 CYCLES
ORBITAL LIFE	7 YEARS	7 YEARS
BATTERY CONFIGURATION (2 BATTERIES PER SPACECRAFT)	27 CELL ASSEMBLIES	28 CELL ASSEMBLIES
NOMINAL BATTERY HEAT OUTPUT DURING OVERCHARGE, AVERAGE	50 W (EQUIVALENT)	52 W (EQUIVALENT)
ALLOWABLE BATTERY TEMEPERATURE RANGE DURING ORBITAL OPERATION (THERMISTOR MEASUREMENT)	0° TO +25°C	0° TO +25°C

ORIGINAL PAGE IS
OF POOR QUALITY

Table 2

Battery Charge Array Current (In Amperes)

SEASON/LIFE	CHARGE CONTROL ARRAY MODULE		
	A,D (6P x 9S)	B,E (2P x 9S)	C,F (3P x 8S)
VERNAL EQUINOX			
BOL	1.89	0.64	0.95
EOL	1.68	0.57	0.86
AUTUMNAL EQUINOX			
BOL	1.86	0.63	0.94
EOL	1.65	0.56	0.85
SUMMER SOLSTICE			
BOL	1.66	0.56	0.84
EOL	1.46	0.50	0.75
WINTER SOLSTICE			
BOL	1.77	0.60	0.90
EOL	1.56	0.53	0.80

The charge arrays can be used in various combinations to provide rates in the range C/100 to C/5.

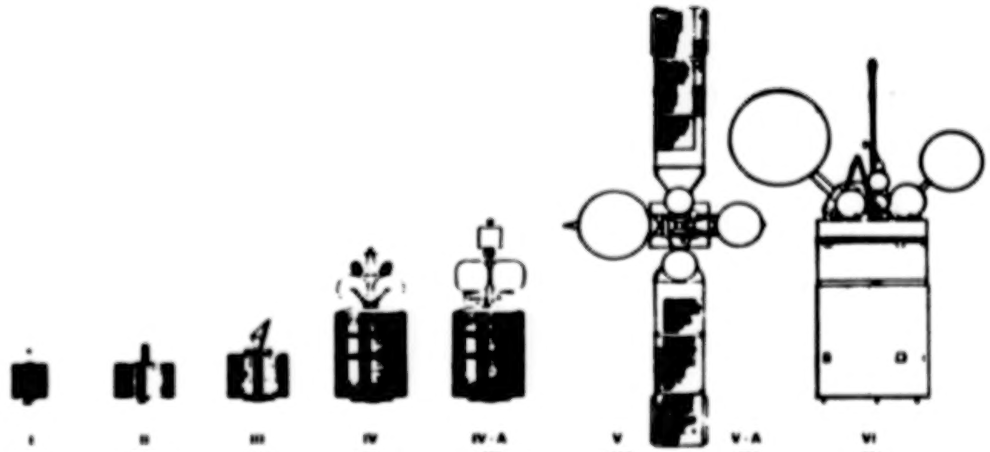

INTELSAT DESIGNATION	I	II	III	IV	IV - A	V	V - A	VI
YEAR OF FIRST LAUNCH	1965	1966	1968	1971	1975	1980	1983	1986
PRIME CONTRACTOR	HUGHES	HUGHES	TRW	HUGHES	HUGHES	FORD AEROSPACE	FORD AEROSPACE	HUGHES
DIMENSIONS (undeployed)								
WIDTH, m.	0.7	1.4	1.4	2.4	2.4	2.0	2.0	3.6
HEIGHT, m.	0.6	0.7	1.0	5.3	6.8	6.4	6.4	5.3
LAUNCH VEHICLES	THOR DELTA			ATLAS CENTAUR		ATLAS CENTAUR, OR ARIANE 1, 2		STS OR ARIANE 4
SPACECRAFT TRANSFER ORBIT MASS, Kg.	68	162	293	1,385	1,469	1,946	2,140	12,100/3,720
COMMUNICATIONS PAYLOAD MASS, Kg.	13	36	56	185	190	235	280	800
POWER EOL EQUINOX, Watts	40	75	134	400	800	1,270	1,270	2,200
DESIGN LIFETIME, YEARS	1.5	3	5	7	7	7	7	10
RATED VOICE CHANNEL CAPACITY IN AOR	480	480	2,400	8,000	12,000	25,000	30,000	80,000
BANDWIDTH, MHz	50	130	300	500	800	2,300	2,180	3,000
ANTENNA BEAM COVERAGES								
C - BAND	TOROIDAL NORTHERN ONLY	TOROIDAL ALMOST FULL EARTH	DESPUN EARTH COVER	DESPUN EARTH COV. AND 2 SPOTS STEERABLE	DESPUN EARTH COV. AND 2 HEMI	3 - AXIS EARTH COV., 2 HEMI, 2 ZONE	3 - AXIS DUAL POL. EARTH COV., 2 HEMI, 2 ZONE 2 SPOTS	DESPUN DUAL POL. EARTH COV., 2 HEMI, 4 ZONE
Ku - BAND	N.A.	N.A.	N.A.	N.A.	N.A.	2 SPOTS STEERABLE	2 SPOTS STEERABLE	2 SPOTS STEERABLE
L - BAND	N.A.	N.A.	N.A.	N.A.	N.A.	EARTH COV	N.A.	N.A.

Figure 1. Evolution of Intelsat satellites.

ORIGINAL PAGE IS OF POOR QUALITY

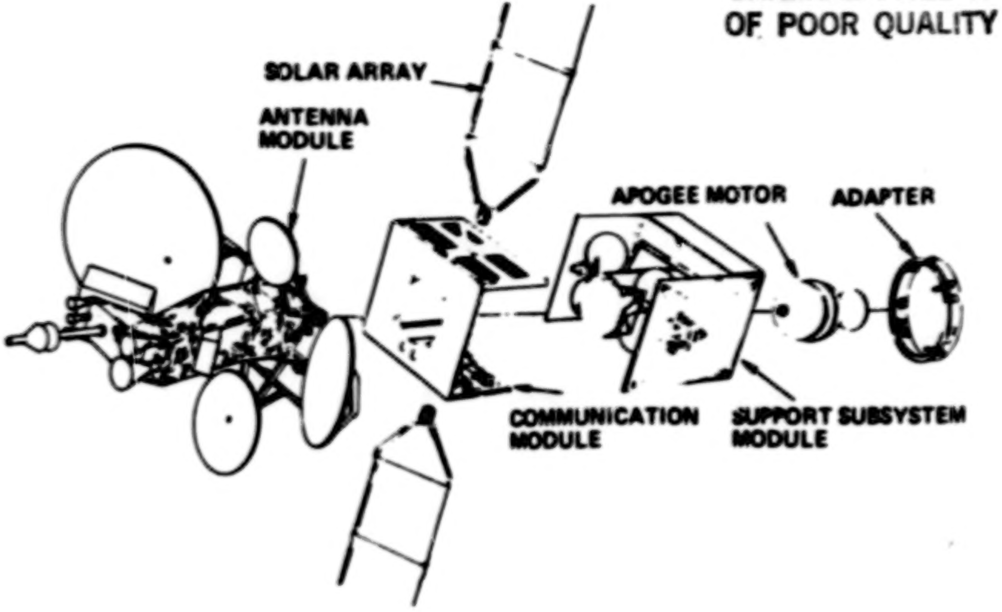
SOLAR ARRAY
ANTENNA MODULE
APOGEE MOTOR
ADAPTER
COMMUNICATION MODULE
SUPPORT SUBSYSTEM MODULE

INTELSAT - V Spacecraft Modular Design

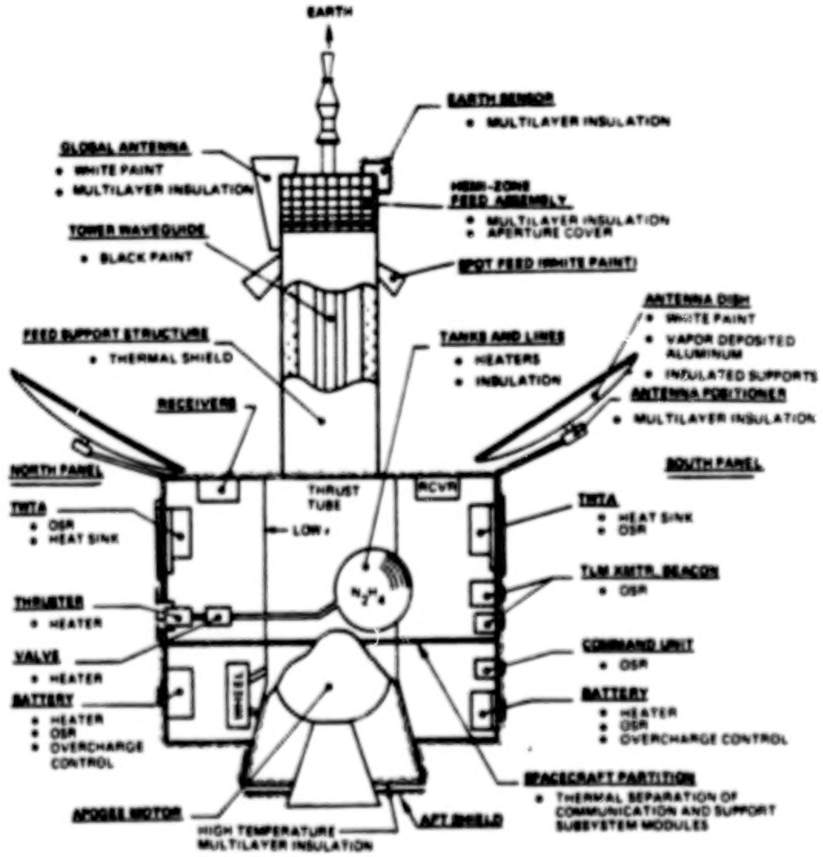
EARTH
EARTH SENSOR
• MULTILAYER INSULATION
GLOBAL ANTENNA
• WHITE PAINT
• MULTILAYER INSULATION
HEMI-ZONE FEED ASSEMBLY
• MULTILAYER INSULATION
• APERTURE COVER
TOWER WAVEGUIDE
• BLACK PAINT
SPOT FEED (WHITE PAINT)
ANTENNA DISH
• WHITE PAINT
• VAPOR DEPOSITED ALUMINUM
• INSULATED SUPPORTS
FEED SUPPORT STRUCTURE
• THERMAL SHIELD
TANKS AND LINES
• HEATERS
• INSULATION
ANTENNA POSITIONER
• MULTILAYER INSULATION
RECEIVERS
NORTH PANEL
SOUTH PANEL
THRUST TUBE
RCVR
LOW ε
N_2H_4
TWTA
• OSR
• HEAT SINK
TWTA
• HEAT SINK
• OSR
TLM XMTR, BEACON
• OSR
THRUSTER
• HEATER
COMMAND UNIT
• OSR
VALVE
• HEATER
BATTERY
• HEATER
• OSR
• OVERCHARGE CONTROL
WHEEL
BATTERY
• HEATER
• OSR
• OVERCHARGE CONTROL
SPACECRAFT PARTITION
• THERMAL SEPARATION OF COMMUNICATION AND SUPPORT SUBSYSTEM MODULES
APOGEE MOTOR
HIGH TEMPERATURE MULTILAYER INSULATION
AFT SHIELD

Thermal Subsystem Operation Configuration

Figure 2

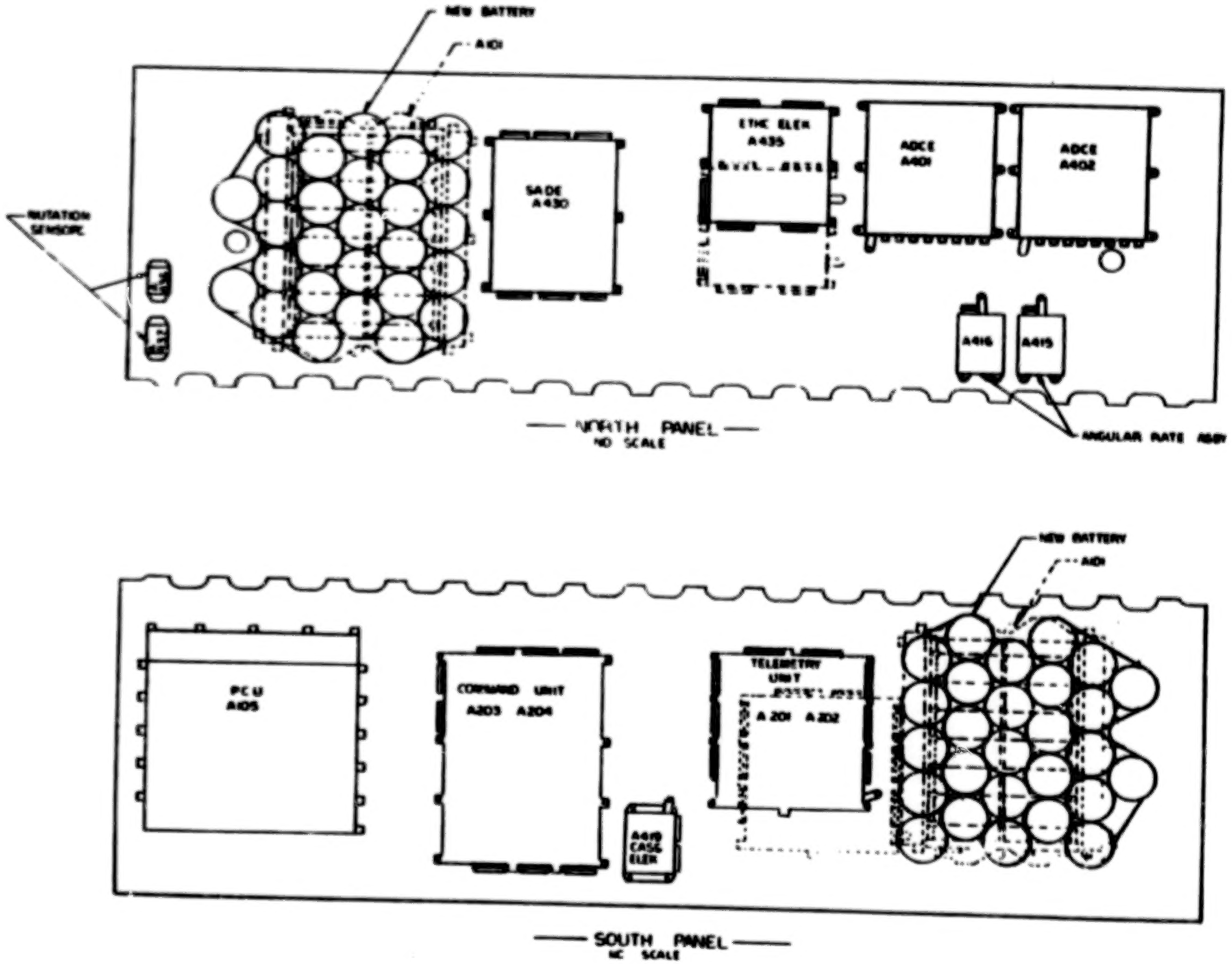
NEW BATTERY
A101
NUTATION SENSORS
SADE
A430
ETHC ELEK
A435
ADCE
A401
ADCE
A402
A416
A415
ANGULAR RATE ASSY
NORTH PANEL
NO SCALE
NEW BATTERY
A101
PCU
A105
COMMAND UNIT
A203 A204
A410
CASG
ELEK
TELEMETRY
UNIT
A 201 A 202
SOUTH PANEL
NO SCALE

Figure 3. Intelsat-V nickel-hydrogen battery location.

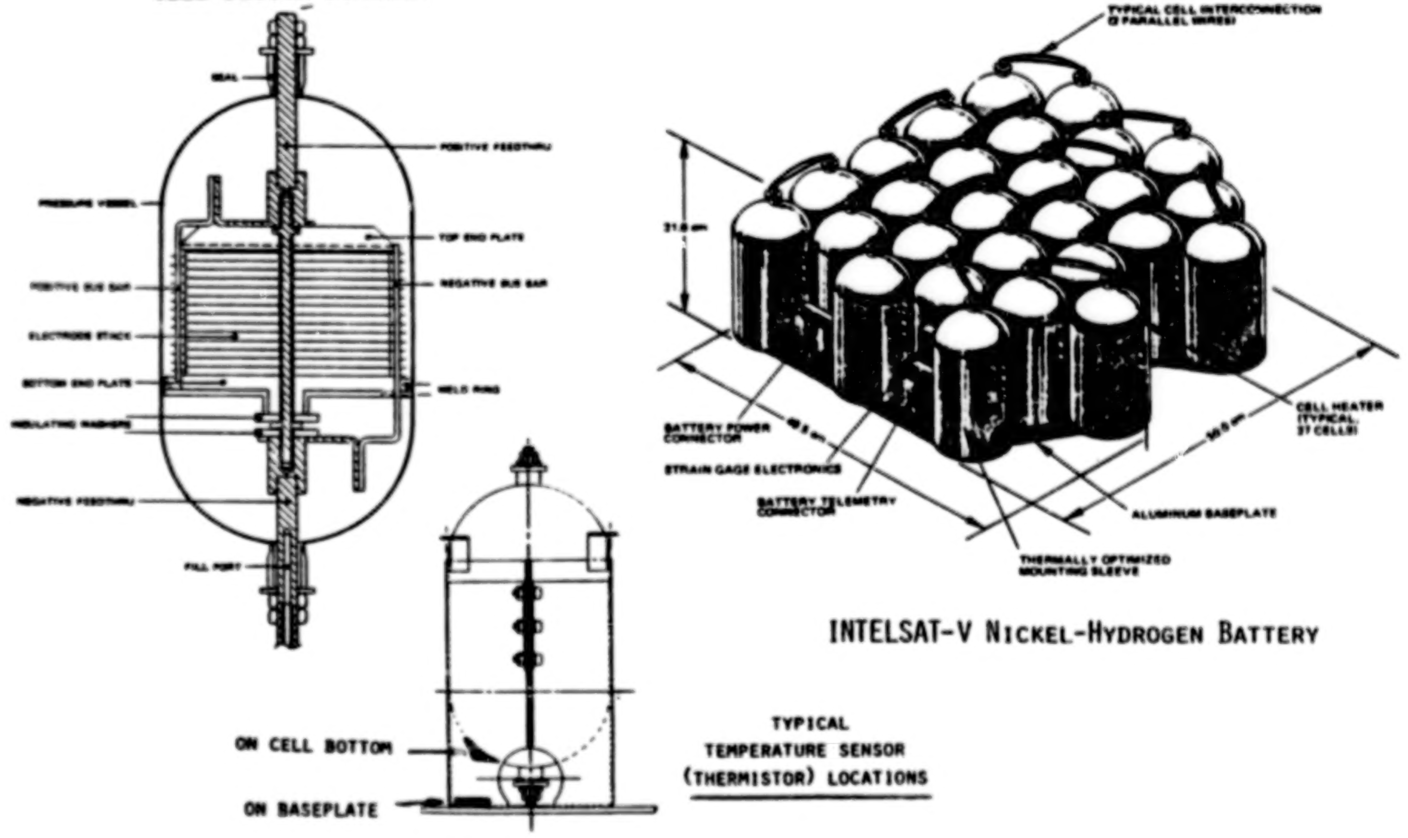
SEAL
POSITIVE FEEDTHRU
PRESSURE VESSEL
TOP END PLATE
POSITIVE BUS BAR
NEGATIVE BUS BAR
ELECTRODE STACK
BOTTOM END PLATE
WELD RING
INSULATING WASHERS
NEGATIVE FEEDTHRU
FILL PORT
TYPICAL CELL INTERCONNECTION (2 PARALLEL WIRES)
31.8 cm
BATTERY POWER CONNECTOR
STRAIN GAGE ELECTRONICS
BATTERY TELEMETRY CONNECTOR
THERMALLY OPTIMIZED MOUNTING SLEEVE
ALUMINUM BASEPLATE
CELL HEATER (TYPICAL, 27 CELLS)
ON CELL BOTTOM
ON BASEPLATE

INTELSAT-V NICKEL-HYDROGEN BATTERY
CELL DESIGN DIAGRAM

INTELSAT-V NICKEL-HYDROGEN BATTERY

TYPICAL
TEMPERATURE SENSOR
(THERMISTOR) LOCATIONS

Figure 4

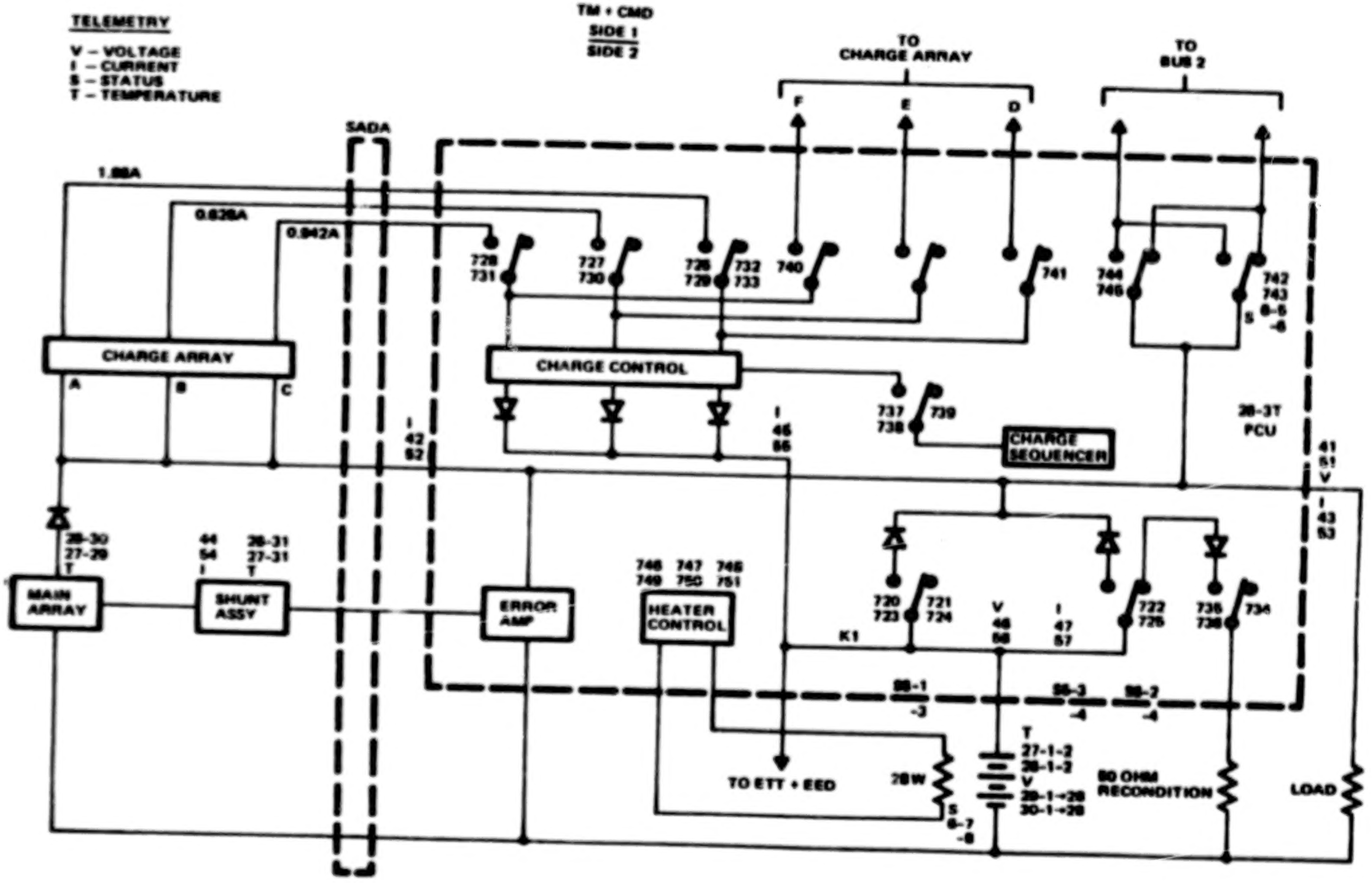
TELEMETRY
V – VOLTAGE
I – CURRENT
S – STATUS
T – TEMPERATURE
TM + CMD
SIDE 1
SIDE 2
TO CHARGE ARRAY
F
E
D
TO BUS 2
SADA
1.88A
0.828A
0.942A
728
731
727
730
725
729
732
733
740
741
744
745
742
743
S
6-5
-6
CHARGE ARRAY
A
B
C
CHARGE CONTROL
I
42
52
I
46
56
737
738
739
CHARGE SEQUENCER
28-37
PCU
41
51
V
I
43
53
28-30
27-29
T
MAIN ARRAY
44
54
I
28-31
27-31
T
SHUNT ASSY
ERROR AMP
746
749
747
750
748
751
HEATER CONTROL
720
723
721
724
V
46
56
I
47
57
K1
722
725
735
736
734
55-1
-3
55-3
-4
55-2
-4
TO ETT + EED
28W
S
6-7
-8
T
27-1-2
28-1-2
V
29-1→28
30-1→28
80 OHM
RECONDITION
LOAD

Figure 5. Intelsat-V electrical power subsystem simplified block diagram.

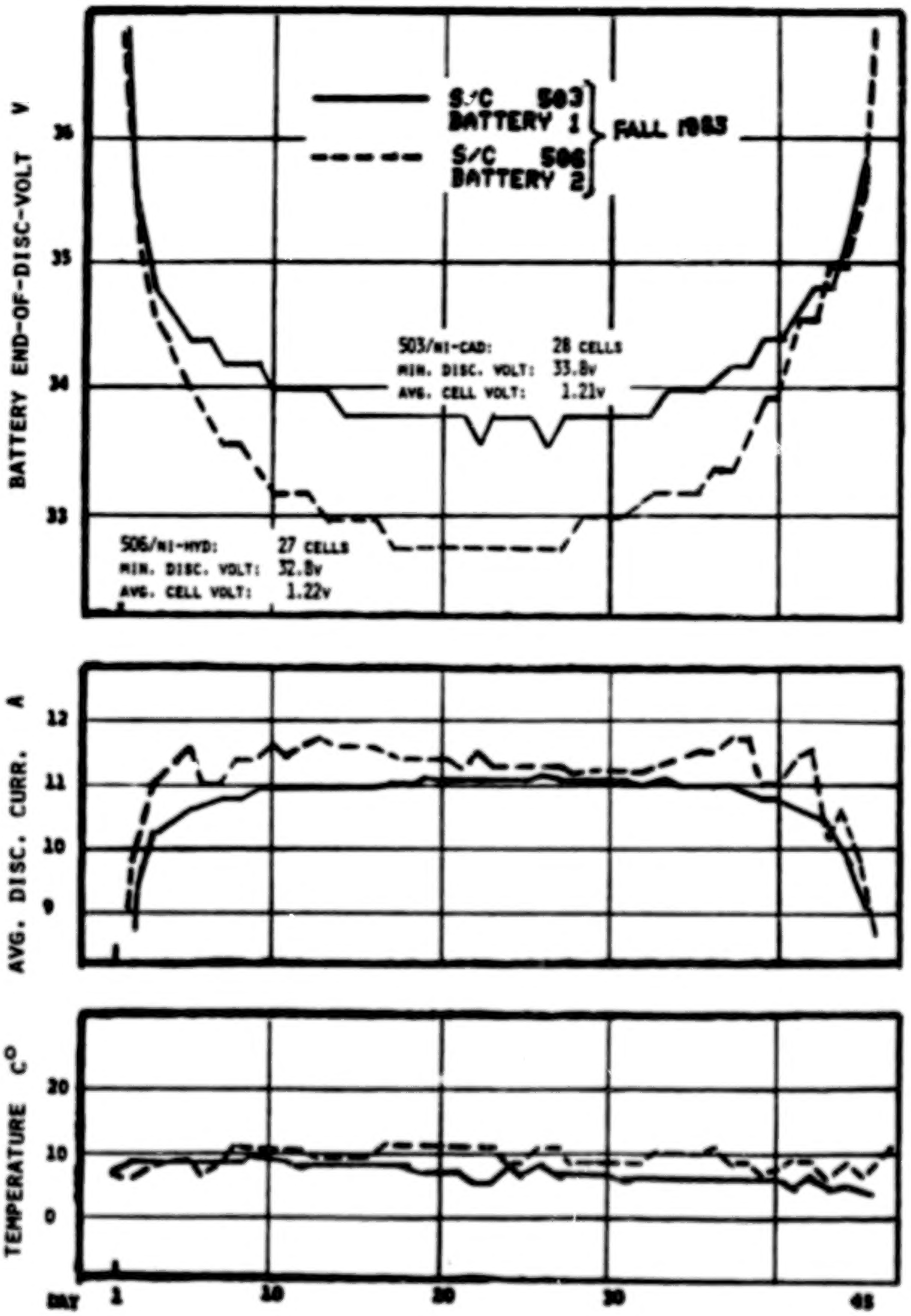

Figure 6. Performance comparison of nickel-cadmium and nickel-hydrogen batteries during eclipse season of fall 1983.

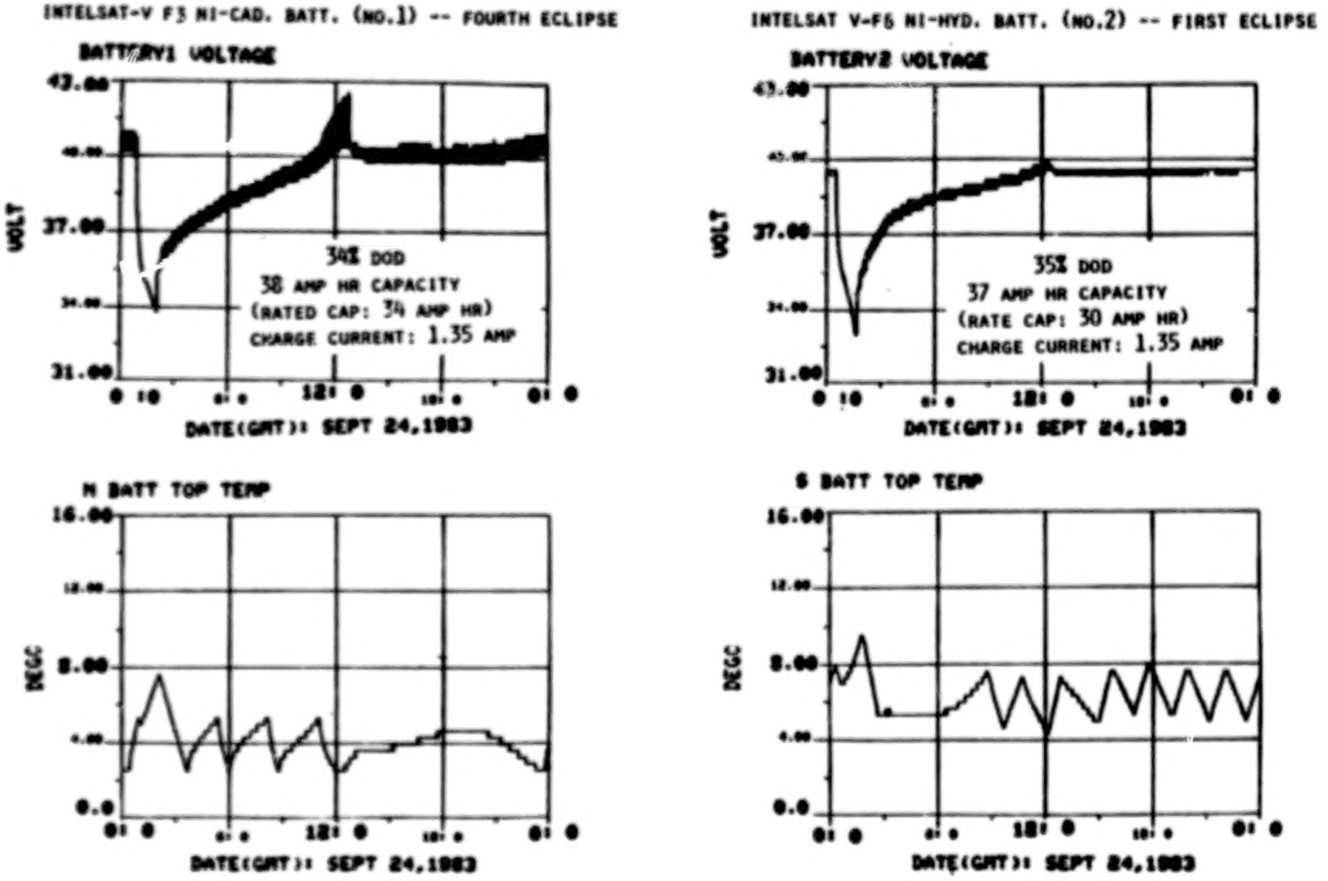

Figure 7. Performance comparison of nickel-cadmium and nickel-hydrogen batteries during longest eclipse of fall 1983.

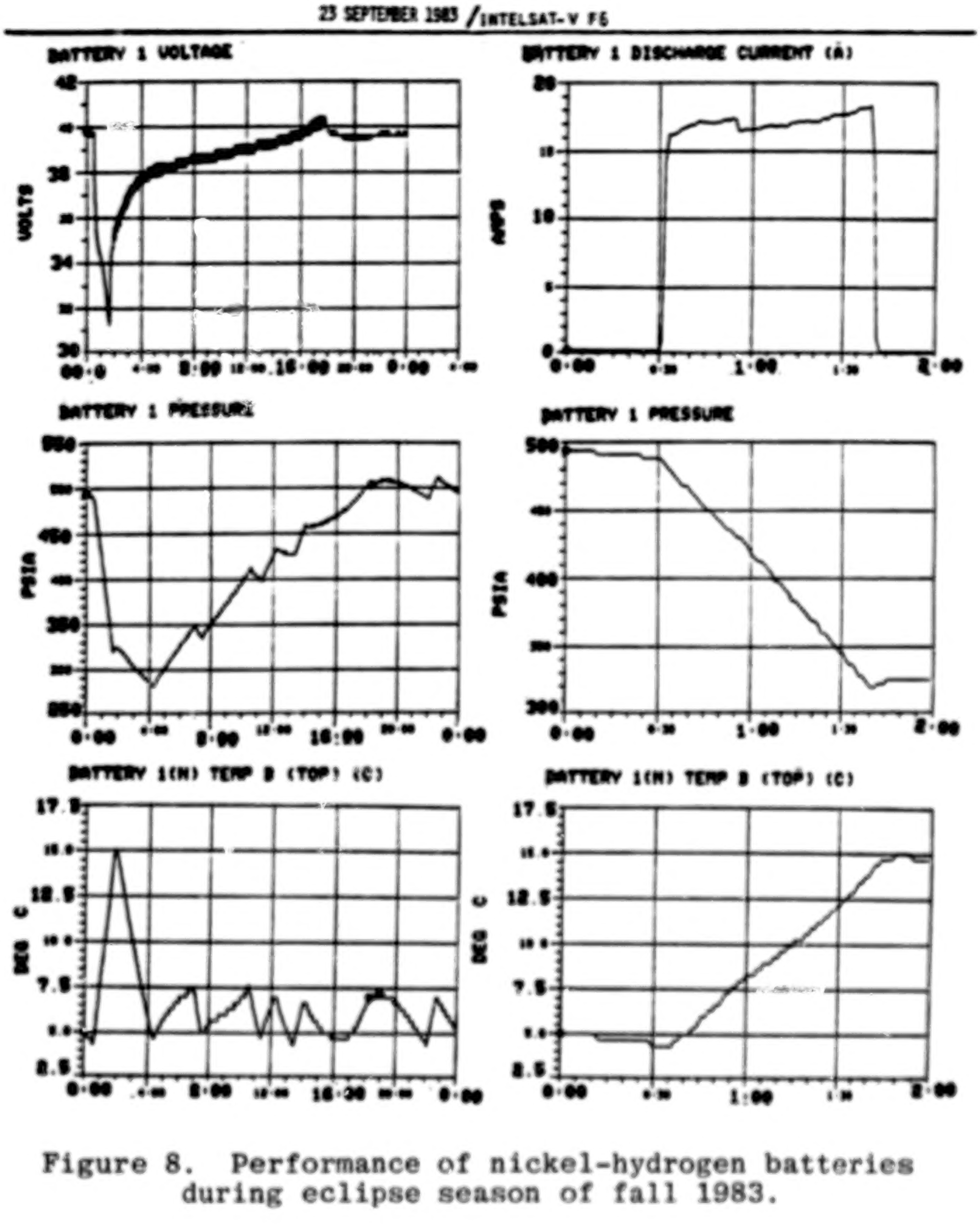

Figure 8. Performance of nickel-hydrogen batteries during eclipse season of fall 1983.

ORIGINAL PAGE IS
OF POOR QUALITY

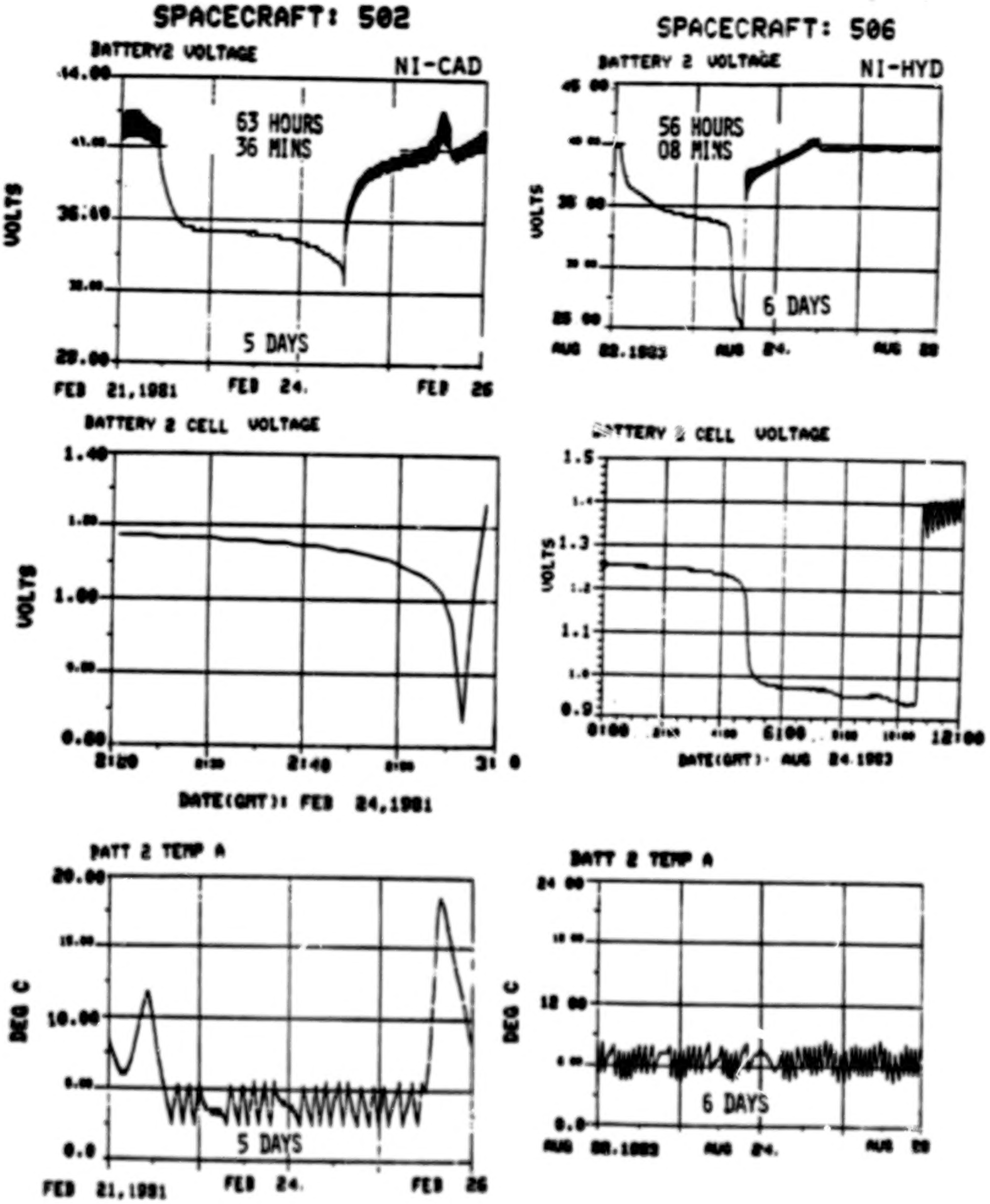

Figure 9. Comparison of nickel-cadmium and nickel-hydrogen batteries during reconditioning.

Q. Rogers, Hughes Aircraft: On the last curve you showed roughly of the .95 volts, is that per cell from a battery average?

A. Cooper, Intelsat: We have individual cell voltages on the spacecraft and we just picked one to show, just an arbitrary choice.

Q. Rogers, Hughes Aircraft: Oh I see. Is that, what is the discharge rate there?

A. Cooper, Intelsat: The discharge rate is about at that time .5 amps or whatever that works out to be. It's a 50 OHM resistor so we are discharging starting out at about .7 and we are down to maybe .5 at this time. Very low rate. That's C over 70.

A. Rogers, Hughes Aircraft: Okay. Low rate. Thank you

COMMENT

Unidentified: Dennis, just a comment. Isn't there one less cell in nickel hydrogen?

Cooper, Intelsat: Yeah we showed that on one of the first slides maybe I didn't point that out. It's 27 cells on the nickel hydrogen, 28 on the nickel cadmium which obviously makes that first slide like I said if you take the cell out, those numbers the nickel hydrogen would be slightly above the nickel cadmium. I think you can see it is essentially a one volt difference there.

Cooper, Intelsat: Did that answer your question Joe? By the way the measure capacity on the nickel hydrogen I don't know if I mentioned this 37 amp-hours and 38 on the nickel cadmium so they are very close compared to the name plate on the nickel cadmium is 34 and the name plate on the nickel hydrogen is 30 so we have been trying to sort out what C rates to use on all these things. We are having a difficulty presenting this as a matter of fact.

Dunlop, Comsat: A subject has come up a couple of times today so I'm just going to make a comment about the specific energy of these cells and the specific energy of this battery. Specific energy of these cells based on that measured capacity which he just mentioned of 36 is pretty close to 53, 54 watt hours per kilogram. And if you've made, that's a 36 amp-hour cell. If you made that cell bigger the energy per unit weight would go up somewhat because as the capacity increases the rest of the hardware doesn't go up correspondently. If you take those and put that in that battery that he showed there you would find the specific energy per unit weight is something like about 40 to 44 watt hours per killogram and again it depends on the average voltage and where you are talking about beginning life or end of life. But it's something like for the batteries, something like 40 to 44 watt hours per kilogram.

BATTERY WORKSHOP   LISTING OF ATTENDEES

NOVEMBER 15-17, 1983

George Allvey
Saft America Inc.
107 Beaver Court
Cockeysville, MD 21030
301-666-3200

Jon D. Armantrout
Lockheed Missiles & Space
Company
1111 Lockheed Way
Sunnyvale, CA 94086
408-742-5730

Charles Badcock
The Aerospace Corporation
M2-275
P.O. Box 92957
Los Angeles, CA 90009
213-648-5180

David Baer
NASA/GSFC
Greenbelt, MD 20771
301-344-6691

James A. Barnes
Code R-33
Naval Surface Weapons
Center
Silver Spring, MD 20910
301-394-1796

Wilbert L. Barnes
Naval Research Lab
4555 Overlook Ave., S.W.
Washington, D.C. 20375
202-545-6700

Jim Bell
Hughes Aircraft Company
MS S12/V330, Box 92919
Los Angeles, CA 90009

Gordon Bentley
Yardney Battery Division
82 Mechanic Street
Pawcatuck, CT 02891
203-599-1100 ext. 254

E. R. Berry
Aerospace Corporation
M4 986
P.O. Box 92957
Los Angeles, CA 90009
213-648-6273

Frederick E. Betz
Naval Research Lab
4555 Overlook Ave., S.W.
Code 7712
Washington, D.C. 20375
202-767-6626

Samuel Birken
Aerospace Corporation
P.O. Box 92957
M4-986
Los Angeles, CA 90009
213-648-6080

L. J. Blagdon
Honeywell Power Sources
Center
104 Rock Road
Horsham, PA 19044
215-674-3800

PRECEDING PAGE BLANK NOT FILMED

Carole Bleser
Eagle Picher Company
Electronics Division
3820 S. Hancock Expwy.
P.O. Box 5234
Colorado Springs,CO 80931

Lt. Christine Bonniksen
SB/YASB
P.O. Box 92960
World Way Postal Center
Los Angeles, CA 90009

William A. Boyd
Utah Research & Development
Co. Inc.
7915 South 1530 West
West Jordan, Utah 84084
801-561-9385

R. J. Broderick
GTE Satell Corporation
P.O. Box 800
M.S. 70B
Princeton, NJ 08540
609-426-3043

Michael Brookman
Saft America Inc.
107 Beaver Ct.
Cockeysville, MD 21030
301-666-3200

Robert Byrnes
Dept. of the Army
4316 San Carlos Drive
Fairfax, VA 22030
703-273-9583

Robert Carey
1000 Wehrle Drive
Clarence, NY 14031
716-759-6901 Ext. 441

Dennis Carr
Eagle Picher Industry
P.O. Box 47
Joplin, MO 64801
417-623-8000

Robert Cataldo
NASA Lewis Research Center
21000 Brookpark
MS-309-1
Cleveland, OH 44135
216-433-4000 Ext. 364

David L. Chua
Honeywell
104 Rock Road
Horsham, PA 19044
215-674-3000

Lee Christensen
Pellon Corporation
20 Industrial Avenue
Chelmsford, MA 01824
617-256-6588

James Ciesla
Electro-Chem Industries
1000 Wehrle Drive
Clarence, NY 14031
716-759-6901

Dr. Stewart Codosh
495 Boulevard
Elmwood Park, NJ 07407
201-796-4800

Dennis Cooper
Intelsat
Room 8031
490 L'Enfant Plaza S.W.
Washington, D.C. 20024
202-488-0176

Suzanne Crenshaw
Ford Aerospace
GSFC Code 435.7
Greenbelt, MD 20771

Glenn F. Cruze
Duracell U.S.A.
South Broadway
Tarrytown, NY 10591
914-591-7000

F. S. Cushing
Exide Corporation
19 W. College Avenue
Yardley, PA 19067
215-493-7189

Steven Dallek
Naval Surface Weapons
Center
Code R33
Silver Spring, MD 20910
202-394-1364

Ivan F. Danzig
U. S. Army
6812 Wild Rose Court
Springfield, VA 22152
202-695-3516

Patrick Davis
Code R-33
Naval Surface Weapons Ctr.
Silver Spring, MD 20910
301-394-1796

R. Dettling
Weapon Power Systems
Branch
Code 3275
Naval Weapons Center
China Lake, CA 93555

C. Tom Dils
Honeywell Power Sources
Center
104 Rock Road
Horsham, PA 19044
215-674-3800

M. J. Domeniconi
LMSC
Box 504
Sunnyvale, CA 94086
408-742-5720

Geoffrey J. Dudley
European Space Agency
Post Bus 299 2200 AG
Noordwijk Zh
Netherlands
+31-71983834

David Dwyer
Sanders Association
Mail Code HUD-2
95 Canal Street
Nashua, NH 03061

Martin W. Earl
Comsat Labs
22300 Comsat Drive
Clarksburg, MD
301-428-4503

Tim A. Edgar
Eagle Picher Company
Electronics Division
3820 S. Hancock Expwy.
P.O. Box 5234
Colorado Springs, CO 80931
303-392-4266

Robert R. Eliason
Lockheed Missiles & Space
Company
Org. 81-65 Bldg. 157-3E
P.O. Box 504
Sunnyvale, CA 94086
408-756-0171

Rolan Farmer
Eagle Picher Company
Electronics Division
3820 S. Hancock Expwy.
P.O. Box 5234
Colorado Springs, CO 80931
303-392-4266

H. Fechter
1201 Hub Street
Brookings, OR 97415

F. E. Ford
NASA/GSFC
Code 711.2
Greenbelt, MD 20771

P. G. Fougere
SAFT
156 Avenue de Metz
Romainville
France 93230
331-843-9361

Harvey A. Frank
Jet Propulsion Laboratory
4800 Oak Grove Drive
MS 198-220
Pasadena, CA 91109
213-354-4157

James Frawley
FBI
9th & Pennsylvania
Room 1B475
Washington, D.C. 20535
202-324-3000

A. K. Galassi
Hughes
7221 Calamo Street
Springfield, VA 22150

Steve Gaston
RCA Astro
P.O. Box 800
Princeton, NJ 08540
609-426-3052

Lawrence J. George
NASA/Marshall Space Flight Center
EB 12
MSFC, AL 35812
205-453-4362

Mark Glavach
Westinghouse
10210 Greenbelt Road
Seabrook, MD 20706
301-344-6974

Warren H. Glenn
NASA HQ/ET
600 Independence Avenue
Washington, D.C. 20546
202-453-1476

Olga Gonzalez
NASA/Lewis Research Center
21000 Brookpark Rd.
MS 309-1
Cleveland, OH 44135
216-433-4000 Ext. 764

H. R. Grady
Foote Mineral Company
Route 100
Exton, PA 19341
215-363-6500

Robert Green
RCA Astro
P.O. Box 800
Princeton, NJ 08540
609-426-3052

Sidney Gross
Boeing Aerospace Company
M.S. 8W-08
P.O. Box 3999
Seattle, WA 98124
206-773-1198

Douglas Hafen
Lockheed MSC
B/151A, D/62-16
P.O. Box 504
Sunnyvale, CA 94086
408-742-5720

John C. Hall
Altus Corporation
1610 Crane Court
San Jose, CA 95112
408-295-1300

Phil Hall
Motorola GEG
8220 E. Roosevelt
Scottsdale, AZ 85252
602-990-5458

Gerald Halpert
Jet Propulsion Laboratory
198-220
4800 Oak Grove Drive
Pasadena, CA 91109
213-354-5474

Lee Hansen
Thermochemical Institute
Brigham Young University
250 FB, BYU
Provo, Utah 84602
801-378-6043

Lt. Matthew E. Hanson
USAF Space Division
2400 E. Elsegundo Blvd.
El Segundo, CA 90009
213-643-1750

James D. Harkness
NWSC
Code 30531, Bldg. 2919
Crane, IN 47522

Albert F. Heller
The Aerospace Corporation
M4-988
P.O. Box 92957
Los Angeles, CA 90009
213-648-6858

E. A. Hendee
Telesat Canada
333 River Road
Ottawa, Canada K1L 8B9
613-746-5920

Thomas J. Hennigan
T. J. Hennigan, Associates
900 Fairoak Avenue
Hyattsville, MD 20783
301-559-0613

Gregg Herbert
JIJU/APL
3900 Blackburn Rd. #32
Burtonsville, MD 20866

James S. Herzau
NASA/Lewis Research Center
21000 Brookpark Rd.
M.S. 301-3
Cleveland, OH 44135
216-433-4000

Robert Higgins
Eagle Picher Company
C & Porter Streets
Joplin, MO 64802
417-623-8000

Jim Hill
Eagle Picher Company
Electronics Division
3820 S. Hancock Expwy.
P.O. Box 5234
Colorado Springs,CO 80931

H. Peter Hirschler
Vitro Laboratories
Bldg. 127
Naval Underwater Systems Center
Newport, RI 02840

Lt. Gary Hislip
Airforce Space Technology Center/YLV
Bldg. 434
Kirtland AFB, NM 87117
505-846-4851

Paul L. Howard
P.L. Howard Associates Incorporated
P.O. Box K
Millington, MD 21651
301-928-5101

Warren Hwong
The Aerospace Corporation
P.O. Box 92597
Los Angeles, CA 90009
213-648-5180

Lee Inscho
The Gates Corporation
P.O. Box 5887
999 S. Broadway
Denver, CO 80217
303-744-4633

James M. Jagiewski
GSFC
Code 711.1
Greenbelt, MD 20771
301-344-5541

S. D. James
Naval Surface Weapon
Center
Silver Spring, MD 20910
202-396-2948

D. H. Johnson
Union Carbide Corporation
P.O. Box 45035
Westlake, OH 44145
216-835-7619

James K. Johnson
The Gates Corporation
900 So. Broadway Box 5887
Denver, CO 80217
303-744-4006

Katherine Jung
Westinghouse Electric
Corporation
10210 Greenbelt Road
Suite 420
Seabrook, MD 20706
301-344-6974

Michael Paul Kimmey
Catalyst Research Corp.
1421 Clarkview Rd.
Baltimore, MD 21209
301-296-7000

Eddison W. Kipp
TRW, Space Technology
Group
One Space Park R4/1028
Redondo Beach, CA 90278
213-536-3503

Peter Kitchener
MIT Lincoln Lab
244 Wood Street
Lexington, MA 02173
617-863-5500

Charles W. Koehler
Ford Aerospace & Comm.
Corporation
3939 Fabian Way
M/S GA5
Palo Alto, CA 94303
415-852-5133

P. W. Krehl
Wilson Greatbatch Ltd.
10000 Wehrle Drive
Clarence, NY 14031
716-759-6901

Dr. Vasanth L. Kunigahalli
Bowie State College
Code 711, Bldg. 22
Rm. 341
Greenbelt, MD 20771
301-344-5751

Joseph L. Lackner
DND/DREO.
Shirley Bay
Ottawa, Canada K1A0Z4
613-596-9419

Robert C. LaFrance
The Aerospace Corporation
GPS Program Office M5/686
P.O. Box 92957
Los Angeles, CA 90009
213-648-5876

Ann H. Le
Naval Surface Weapons Ctr.
Code R33
Silver Spring, MD 21910
301-394-1364

Peter Lensi
Honeywell
104 Rock Rd.
Horsham, PA 19044
215-674-3800

Samuel Levy
Sandia National Lab
Division 2523
P.O. Box 5800
Albuquerque, NM 87185

Dr. C. C. Liang
Omnion Enterprises, Inc.
9460 Grenier Road
Clarence, NY 14031

Hong S. Lim
Hughes Research Lab
MS RL70
3011 Malibu Canyon Road
Malibu, CA 90265
213-456-6411

David Linden
78 Lovett Avenue
Little Silver, NJ 07739
201-741-2271

James M. Lohr
Fusite Division
Emerson Electric Company
6000 Fernview Avenue
Cincinnati, OH 45212
513-731-2020

Charles Lurie
TRW Space Technology Group
One Space Park R4-1028
Redondo Beach, CA 90278
213-536-3503

Gerald P. Lynas
Southern Avionics Company
P.O. Box 5345
Beaumont, TX 77706
409-842-1717

Dr. Tyler X. Mahy
CIA
Washington, D.C. 20505
703-351-3912

D. E. Mains
NWSC
Crane, IN 47522
812-854-1431

Balaraman Mani
Energy Conversion
Devices, Inc.
197 Meister Avenue
North Branch, NJ 08876
201-231-9060

Lynn Marcoux
Hughes Aircraft Company
Bldg. 512 M/S U330
P.O. Box 92919
Los Angeles, CA 90009
213-647-8213

Nikola Marincic
Hellesens Battery
Engineering, Inc.
1636 Hyde Park Ave.
Hyde Park, MA 02136
617-361-7555

Jean Marinkovich
Hughes Aircraft Company
MS S12/V330, Box 92919
Los Angeles, CA 90009

Dean W. Maurer
Bell Labs
Mountain Avenue
Room 1E207
Murray Hill, NJ 07974

Joe McDermott
Martin Marietta
P.O. Box 179
M/SS0550
Denver, CO 80201
303-977-5690

Gregory C. McDonald
Satellite Business Systems
P.O. Box 291
Clarksburg, MD 20734
301-428-3464

George G. McKhann Jr.
McDonnell Douglas
Astronautics Company
Mail Stop 14-3
5301 Bolsa Ave.
Huntington Beach, CA 92647
714-896-4669

Willard Menish
NASA Headquarters/ET
600 Independence Avenue
Washington, D.C. 20546
202-453-1477

W. C. Merz
Bedford Engineering Corp.
3B05 Mt. Vernon Avenue
Alexandria, VA 22305

George J. Methlie
2705 N. Jefferson St.
Arlington, VA 22207
703-351-3913

John Meyer
APL
John Hopkins Road
Laurel, MD
301-792-7800

Ronald P. Mikkelson
General Dynamics/Convair
MZ 41-6390
P.O. Box 85357
San Diego, CA 92138
619-277-8900 Ext. 1486

M. J. Milden
Aerospace Corporation
P.O. Box 92957
M4-988
Los Angeles, CA 90009

David Miller
Martin Marietta
Denver Aerospace
S0550
P.O. Box 179
Denver, CO 80201
303-977-3713

Richard Mills
Westinghouse Electric
Corporation
10210 Greenbelt Road
Suite 420
Seabrook, MD 20706
301-344-6974

Anthony J. Miserendino
GTE Power Systems
520 Winter Street
Waltham, MA 02254
617-466-3205

Malcolm H. Moody
Canadian Astronautics Ltd.
1024 Morrison Drive
Ottawa, Ontario K2H 8K7
513-820-8280

George W. Morrow
NASA/GSFC
Code 711.2
Greenbelt, MD 20771
301-344-6691

Harry Moses
Naval Research Lab
Code 7711
4555 Overlook Avenue
Washington, D.C. 20375
202-767-6529

Dr. Carl E. Mueller
Naval Surface Weapons
Center
Code R33
Silver Spring, MD 20910
202-394-2472

Vernon C. Mueller
Dept. E454 Bldg. 101
McDonnell Douglas
Astronautics Company
P.O. Box 516
St. Louis, MO 63166
314-234-0877

Lo Nguyen
Ovonic Battery Company
1826 Northwood
Troy, MI 48098
313-362-1750

Steve Nichols
Naval Electronics Systems
Command
PDE 106-6
Washington, D.C. 20363

Dr. Robert J. Nowak
Naval Research Lab
Code 6130
Washington, D.C. 20375
202-767-2631

Phillip D. Olbert
Ball Aerospace Division
P.O. Box 1086
Boulder, CO 80306
303-441-4401

Kathleen O'Neill
Naval Surface Weapons Ctr.
Silver Spring, MD 20910
202-394-2243

Hans W. Osterhoudt
Eastman Kodak Company
Building 82
Rochester, NY 14650
716-477-3358

L. T. Ostwald
Ball Aerospace Systems
Division
P.O. Box 1062
Mail Stop MP-4
Boulder, CO 80306
303-441-4443

Tom O'Sullivan
Bell Labs
Mountain Avenue
Room 1E207
Murray Hill, NJ 07974

Burton Otzinger
Rockwell International
SL-10
12214 Lakewood Blvd.
Downey, CA 90241
213-594-6349

Charles Palandati
NASA/GSFC
Code 711.2
Greenbelt, MD 20771
301-344-5379

Wendy A. Parkhurst
Naval Surface Weapons Ctr.
Code R33
Silver Spring, MD 20910
202-394-1364

Greg Patterson
Ballard Research Inc.
1164 W. 15th Street
North Vancouver
B.C. Canada V7P 1M9
604-986-4104

Leo Pessin
Fairchild Space Company
20301 Century Blvd.
Germantown, MD 20874
301-428-6000

Chester J. Petkiewicz
Pellon Corporation
221 Jackson Street
Lowell, MA 01852
617-454-0461

David F. Pickett, Jr.
Hughes Aircraft Company
M.S.-S12/N330
Box 92919 Airport Sta.
Los Angeles, CA 90009
213-648-2128

Mike Pollack
3E Labs
840 West Main Street
Lansdale, PA 19446

F. J. Porter
Applied Physics Lab
Johns Hopkins Rd.
Laurel, MD 20707
301-953-7100

William Price
FBI
9th & Pennsylvania
Room 1B475
Washington, D.C. 20535
202-324-2020

Hamid Rahnamai
Intelsat Corporation
L'Enfant Plaza, Box 33,S.E.
Washington, D.C. 20024
202-488-0177

Dalbir Rajoria
Energy Conversion Devices
197 Meisler Avenue
P.O. Box 5357
North Branch, NJ 08876
201-231-9060

N. Raman
Saft America Inc.
107 Beaver Ct.
Cockeysville, MD 21030
301-666-3200

George J. Rayl
GE Company
P.O. Box 8555
Philadelphia, PA 19101
215-962-4551

Edward Reiss
USA Eradcom
Delet-PB
Ft. Monmouth, NJ 07703
201-544-4211

Ken Richardson
General Electric
P.O. Box 114
Gainesville, FL 32602

Paul Ritterman
Comsat Corporation
999 N. Sepulveda
Suite 800
El Segundo, CA 90245
213-416-9106

G. E. Rodriguez
NASA/GSFC
Code 711.2
Greenbelt, MD 20771

Dr. Howard H. Rogers
Hughes Aircraft Corp.
S12/V330 P.O. Box 92919
Los Angeles, CA 90009

Gilbert L. Roth
NASA Headquarters
LB-4
Aerospace Safety Advisory Panel
Washington, D.C. 20546
202-755-8380

Theodore Russell
Space Communications Company
1300 Quince Orchard Rd.
Gaithersburg, MD 20878
301-258-6880

Douglas Rusta
TRW Science & Technology Group
One Space Park R4/1120
Redondo Beach, CA 90278
213-535-0723

Karl Salinas
TRW, Space Technology Group
One Space Park (R4/1028)
Redondo Beach, CA 90278
213-536-3503

Steven H. Samborn
Gates Corporation
999 S. Broadway
Denver, CO 80217
303-744-5360

S. Schiffer
RCA Astro
P.O. Box 800
Princeton, NJ 08540
609-426-3052

Charles Scuilla
U.S. Government
5501 Starboard Court
Fairfax, VA 22032
703-351-3912

Eddie T. Seo
The Gates Corporation
P.O. Box 5887
Denver, CO 80217
303-744-4614

Robert Siegler
10000 Wehrle Drive
Clarence, NY 14031
716-759-6901 Ext. 537

David E. Simm
OAO Corporation
1304 North Road
Severna Park, MD 21146
301-345-0750

Paul Skarstad
Medtronic Energy Tech.
6700 Shingle Creek Pkwy.
Minneapolis, MN 55430
612-574-6380

Jerry Smith
Office of Naval Research
Chemistry Division
Arlington, VA 22217
202-696-4410

Patricia Smith
NSWC
Code R-33
Silver Spring, MD 20910
202-394-1796

W. Andrew Somerville
The Aerospace Corporation
P.O. Box 9113
Albuquerque, NM 87119
505-846-0209

Dr. Robert Somoano
Jet Propulsion Laboratory
4800 Oak Grove Drive
Pasadena, CA 91011
213-354-2213

Wayne T. Stafford
Aerospace Corporation
P.O. Box 92957
Los Angeles, CA 90009
213-416-7302

Robert E. Stark
Ford Aerospace
3939 Fabian Way
Palo Alto, CA 94303

R. Stearns
General Electric Space
Systems Division
Box 8555
Philadelphia, PA 19101
215-962-2027

Irv Stein
Jet Propulsion Laboratory
4800 Oak Grove Drive
M.S. 198-220
Pasadena, CA 91109
213-354-6048

David B. Stewart
RCA American
Communications
400 College Road East
Princeton, NJ 08512
609-734-4122

J. A. Stiles
NPLI Energy, Ltd.
4010 Myrthe St.
Burnaby, British Columbia
Canada VYC462
604-437-6927

Ralph Sullivan
APL
Johns Hopkins Rd.
Laurel, MD 20707
301-953-7100

Martin Sulkes
USAERADCOM
Delet-PC
Fort Monmouth, NJ 07703
201-544-2458

David J. Surd
Catalyst Research Corp.
1421 Clarkview Rd.
Baltimore, MD 21209
301-296-7000 Ext. 206

Robert Taenaka
Hughes Aircraft
16318 Devonshire Street
Granada Hills, CA 91344
213-615-7224

H. Taylor
Duracell International
3rd Ave. N.W. Ind. Park
Burlington, MA 01803
617-272-4100

Lawrence Thaller
NASA/Lewis Research Ctr.
MS-301-3
21000 Brook Park Rd.
Cleveland, OH 44135

H. E. Thierfelder
General Electric Space
Systems Division
Box 8555
Philadelphia, PA 19101
215-962-2027

Stephen Thornell
ET & DL
Delet-PC, Bldg. 116
Ft. Monmouth, NJ 07703
201-544-2458

S. Tiller
NASA/GSFC
Code 711.2
Greenbelt, MD 20771
301-344-6489

Hari Vaidyanathan
COMSAT Laboratories
22300 Comsat Drive
Clarksburg, MD 20871
301-428-4507

Gert Van Ommering
Ford Aerospace & Comm.
Corporation
3939 Fabian Way, MS G45
Palo Alto, CA 94303
415-494-7400

Donald C. Verrier
Yardney Corporation
82 Mechanic Street
Pawcatuck, CT 02891
203-599-1100

Scott Verzwyvelt
Hughes Research Labs
MS RL70
3011 Malibu Canyon Rd.
Malibu, CA 90265
213-456-6411

Dallas B. Vowell
Martin-Marietta Corp.
P.O. Box 179
M/SS0550
Denver, CO 80201
303-977-5106

Charles R. Walk
Bedford Engineering Corp.
3805 Mt. Vernon Avenue
Alexandria, VA 22305
703-549-3932

Hubert C. Watton
General Dynamics
Convair Division
P.O. Box 85357
MZ 36-1015
San Diego, CA 92138
619-277-8900

Howard Weiner
The Aerospace Corp.
MS-M4-988
P.O. Box 92957
Los Angeles, CA 90009

James R. Wheeler
Eagle Picher Ind.
C & Porter Street
Joplin, MO 64801
417-623-8000

Douglas White
Countermeasures Research
Laboratories
Box 115
Ft. Belvoir, VA 22060
703-664-2243

Eileen Whitlock
5925 Quantrell Ave.
Alexandria, VA 22312
202-347-4342

Mark Williams
Catalyst Research
1421 Clarkview Rd.
Baltimore, MD 21209
301-296-7000

Alvin H. Willis
Boeing Aerospace Co.
M/S 8W-04
P.O. Box 3999
Seattle, WA 98124
206-773-1550

Thomas H. Willis
Western Electric
600 Mountain Avenue
Murray Hill, NJ 07974
201-582-3545

Edward L. Woodbury
COMSAT
950 L'Enfant Plaza S.W.
Washington, D.C. 20024
202-863-7477

Dr. Walter Wurster
Electro-Chem Industries
10000 Wehrle Drive
Clarence, NY 14031
716-759-6901 Ext. 453

I. David Yalom
AT & R Inc.
10813 East Nolcrest Dr.
Silver Spring, MD 20903
301-593-1973

Shiao-Ping Siao Yen
Jet Propulsion Laboratory
4800 Oak Grove Drive
Pasadena, CA 91109
213-354-3105

David Yeswab
ARDC LEWSL/LCN-6
Dover, NJ 07801
201-724-3058

END

DATE

FILMED

DEC 3 1984